Digitized by the Internet Archive
in 2023 with funding from
Kahle/Austin Foundation

https://archive.org/details/contributionsfro0010unse

Carnegie Institution of Washington

STEWARD OBSERVATORY
TUCSON, ARIZONA

CONTRIBUTIONS

FROM THE

MOUNT WILSON OBSERVATORY

VOLUME X

NOS. 200-227

WITH TEN PLATES

DECEMBER, 1920—FEBRUARY, 1922

UNIVERSITY OF ARIZONA
LIBRARY

C28
V.10

CONTENTS

NO. PAGE

200. CHARACTERISTIC BEHAVIOR OF THE BRIGHT LINES IN STELLAR SPECTRA OF CLASS Md. *Paul W. Merrill* 1

201. THE ORBITS OF SEVEN SPECTROSCOPIC BINARIES. *R. F. Sanford* . 17

202. WAVE-LENGTHS OF LINES IN THE IRON ARC FROM GRATING AND INTERFEROMETER MEASURES λ 3370–λ 6750. *Charles E. St. John and Harold D. Babcock* 41

203. MEASUREMENT OF THE DIAMETER OF α ORIONIS WITH THE INTERFEROMETER. *A. A. Michelson and F. G. Pease* . . . 81

204. PHOTOGRAPHIC DETERMINATION OF STELLAR PARALLAXES WITH THE 60-INCH REFLECTOR. *Adriaan van Maanen* 93

205. INVESTIGATIONS ON PROPER MOTION. THIRD PAPER: THE PROPER MOTIONS OF STARS IN AND NEAR THE DOUBLE CLUSTER IN PERSEUS. *Adriaan van Maanen* 125

206. OBSERVATIONS OF THE NEBULAR LINES IN THE SPECTRUM OF THE LONG-PERIOD VARIABLE STAR R AQUARII. *Paul W. Merrill* 155

207. IDENTIFICATION OF AIR LINES IN SPARK SPECTRA FROM λ 5927 TO λ 8683. *Paul W. Merrill, F. L. Hopper, and Clyde R. Keith* . 161

208. ON SYSTEMATIC DISPLACEMENTS OF LINES IN SPECTRA OF VENUS. *Charles E. St. John and Seth B. Nicholson* 163

209. BRIGHT AND DARK NEBULAE NEAR ζ ORIONIS PHOTOGRAPHED WITH THE 100-INCH HOOKER TELESCOPE. *John C. Duncan* . 175

210. THE RELATIONSHIP OF ABSOLUTE MAGNITUDE TO SPACE-VELOCITY. *W. S. Adams, G. Strömberg, and A. H. Joy* 181

211. THE ELECTRIC FURNACE SPECTRUM OF SCANDIUM. *Arthur S. King* 199

212. THE SPECTROSCOPIC BINARY BOSS 3644 VIRGINIS. *John C. Duncan* 217

213. INVESTIGATIONS ON PROPER MOTION. FOURTH PAPER: INTERNAL MOTION IN THE SPIRAL NEBULA MESSIER 51. *Adriaan van Maanen* 221

214. INVESTIGATIONS ON PROPER MOTION. FIFTH PAPER: THE INTERNAL MOTION IN THE SPIRAL NEBULA MESSIER 81. *Adriaan van Maanen* 231

215. ON THE ACCURACY WITH WHICH MEAN PARALLAXES CAN BE DETERMINED FROM PARALLACTIC AND PECULIAR MOTIONS. *Henry Norris Russell* 241

JM

174385

CONTENTS

NO. PAGE

216. On Majorana's Theory of Gravitation. *Henry Norris Russell* 247
217. Note on Cooling by Expansion in Sun-Spots. *Henry Norris Russell* 261
218. Studies Based on the Colors and Magnitudes in Stellar Clusters. Nineteenth Paper: A Photometric Survey of the Pleiades. *Harlow Shapley and Myrtle L. Richmond* 265
219. The Vacuum-Spark Spectra of the Metals. *Edna Carter* . 277
220. Systematic Corrections to Spectroscopic and Trigonometric Parallaxes. *Gustaf Strömberg* 281
221. The Orbits of the Spectroscopic Binaries 1 Hydrae and 75 Cancri. *R. F. Sanford* 291
222. The Wave-Length in Astronomical Interferometer Measurements. *J. A. Anderson* 297
223. An Investigation of the Constancy in Wave-Length of the Atmospheric and Solar Lines. *Charles E. St. John and Harold D. Babcock* 321
224. Investigations on Proper Motion. Sixth Paper: The Motions of 65 Stars in the Neighborhood of α Tauri. *Adriaan van Maanen* 333
225. The Theory of Ionization and the Sun-Spot Spectrum. *Henry Norris Russell* 341
226. The Masses and Densities of the Stars. *Frederick H. Seares* 367
227. On the Calculation of Masses from Spectroscopic Parallaxes. *Henry Norris Russell* 441

LIST OF PLATES

NO. FACING PAGE

I. INTERFEROMETER USED WITH 100-INCH HOOKER REFLECTOR . 82

II. REGION OF *h* and χ PERSEI, SHOWING STARS WHOSE RADIAL VELOCITIES HAVE BEEN DETERMINED 127

III. SPECTROGRAMS OF THE LONG-PERIOD VARIABLE STAR R AQUARII, SHOWING LINES CHARACTERISTIC OF GASEOUS NEBULAE . . 156

IV. PHOTOGRAPHS OF THE SPECTRA OF VENUS AND THE SKY . . 166

V. BRIGHT AND DARK NEBULAE SOUTH OF ζ ORIONIS . . . 176

VI. ζ ORIONIS AND THE NEBULAE ON THE EAST AND NORTH . . 176

VII. INTERNAL MOTIONS IN MESSIER 51 226

VIII. INTERNAL MOTIONS IN MESSIER 81 235

IX. SPECTRUM OF MAGNESIUM: (*a*) SPARK IN AIR; (*b*) VACUUM-SPARK; (*c*) ARC 279

X. SPECTRUM OF CADMIUM: (*a*) SPARK IN AIR; (*b*) VACUUM-SPARK; (*c*) ARC 279

Contributions from the Mount Wilson Observatory, No. 200
Reprinted from the *Astrophysical Journal*, Vol. LIII, pp. 185–200, 1921

CHARACTERISTIC BEHAVIOR OF THE BRIGHT LINES IN STELLAR SPECTRA OF CLASS Md

By PAUL W. MERRILL

ABSTRACT

Periodic changes in the emission lines of spectra of Class Md variables.—R Leonis, R Hydrae, R Serpentis, X Ophiuchi, χ Cygni, and T Cephei have been observed spectroscopically over a considerable part of their light periods, from two to twelve spectrograms having been made of each. The intensities of Hδ, Hγ, λ 4202 Fe, λ 4308 Fe, λ 4571 Mg, and some other bright lines at the different phases are recorded in Table IV. A compilation and discussion of past and present data referring to these lines shows that they appear after light minimum, in the order mentioned, in every long-period variable of Class Md whose spectrum has been adequately observed, and exhibit substantially the same remarkable behavior as in the type star *o* Ceti. There is strong evidence, therefore, that these spectral variations, shown in Figure 1, are characteristic of stars of this class. *The changes in relative intensity of the lines of the Balmer series of hydrogen and also of certain iron lines* are particularly interesting. A discussion of the physical interpretation of these variations is reserved until more data are available.

Although it has been known for many years, chiefly through the extensive labors of the Harvard College Observatory, that striking changes occur in the spectra of numerous long-period variable stars, practical difficulties have prevented the securing of satisfactory observations through the whole light cycle. It is therefore not yet possible to give a complete description of the spectroscopic changes which accompany the extraordinary fluctuations in brightness. Much valuable material has, however, already been gathered: the combined results of several observers have shown numerous salient features of the variations in the spectrum of *o* Ceti; some of the same phenomena have been observed in χ Cygni; and changes in other stars have been indicated by shorter series of observations.

The present discussion will be confined largely to the bright lines, as observations of the continuous spectrum and of the absorption lines and bands do not yet afford a reliable basis for a description of the characteristic changes.[1] The data for the bright lines are not so complete as might be desired, but certain features are definitely established, and the general course of the changes is indicated. Much remains to be determined, however, especially in regard to the behavior of the spectrum at minimum brightness.

---

[1] The available observational material bearing on the absorption spectrum is not extensive, owing to the faintness of the stars, except at maximum, and to other circumstances. It is, however, definitely known that variations do take place, but

The new observational material described here refers to the stars in Table I. These are among the best known of the long-period variables, and all possess spectra strongly resembling that of *o* Ceti.

TABLE I

STARS OBSERVED

Star	α 1900	δ 1900	Magnitude
R Leonis	$9^h42^m.2$	+11° 54′	4.6–10.5
R Hydrae	13 24.2	–22 46	4.0– 9.8
R Serpentis	15 46.1	+15 26	5.6–13
X Ophiuchi	18 33.6	+ 8 44	6.5– 9.0
χ Cygni	19 46.7	+32 40	4.0–13.5
T Cephei	21 8.2	+68 5	5.1–10.5

TABLE II

RESULTS OF HARVARD OBSERVATIONS

Star	Range	Period	$m-M$	Br.	Ft.
o Ceti	5.7 mags.	332 days	0.64	0.19	0.30
R Leonis	4.2	313	.55	.26	.28
R Hydrae	5.4	425	.57	.15	.32
R Serpentis	6.3	357	.61	.20	.28
X Ophiuchi	2.2	337	.45	.32	.44
χ Cygni	8.3	406	.54	.22	.17
T Cephei	3.9	387	0.46	0.23	0.27

Data from *Harvard Annals*, **57**, 202, showing the character of the light-variation, are given in Table II, in which *o* Ceti is included for convenient comparison. The fourth column, "$m-M$," shows

---

apparent discrepancies or, perhaps, real differences between different stars, make it difficult to know which variations should be considered as characteristic. For instance it is stated by Adams and Joy, *Publications of the Astronomical Society of the Pacific*, **32**, 163, 1920, and by Shane, *ibid.*, **32**, 234, 1920, in confirmation of previous observations, that in *o* Ceti the absorption bands of titanium oxide increase in strength as the star wanes, but, in the case of X Ophiuchi, observations by the writer from May to September, 1920, show that the bands grew decidedly weaker while the brightness was decreasing. Although there are several possible explanations of this apparent discrepancy their discussion will not be taken up here.

the fraction of the period during which the light decreases; the fifth, "Br.," gives the fraction of the period during which the light is more than one-half as great as at maximum, and the last column, "Ft.," that fraction during which the light is less than twice as great as at minimum.

All the observations in Table III were made with one-prism spectrographs. The column "Phase" is the only one requiring explanation. This indicates for each plate the fraction of the period before (−), or after (+), light maximum. The photometric data were kindly supplied by the Harvard College Observatory.

R LEONIS

Jan. 16, 1920. This observation was made about 110 days after minimum and 60 days before maximum. The light-curve rose gradually for 70 or 80 days after minimum, and then much more rapidly.

May 30, 1920. This last observation was about 60 days before minimum.

R HYDRAE

A minimum occurred on April 27, 1920, magnitude 9.5. The first plate, on May 31, was taken 34 days after minimum, but the star had brightened only half a magnitude. Two bright lines which are the last to appear during the decreasing phase are still in evidence. The bright hydrogen lines, which in Md stars are weak or absent at minimum, have not yet appeared. The continuous spectrum is weak but is visible from λ 4500 toward longer wavelengths, being interrupted by wide absorption bands of titanium oxide. The second plate, taken on July 8, when the increase in magnitude since minimum had been 1.7 magnitudes, shows more continuous spectrum due to a generally more effective exposure, but the band absorption is very strong; Hδ is a distinct emission line; Hγ is not seen, although continuous spectrum is visible in its neighborhood; λ 4308 is not seen; near λ 4571 the continuous spectrum is strong and the magnesium line of that wave-length, if present at all, is so blended with the background as to be indistinguishable.

TABLE III

OBSERVATIONS

Date	Mag.	Phase	Telescope	Camera	Exposure	Remarks
			R Leonis			
1920 Jan. 16	9.0	−0.19	100-inch	18-inch	164^{m}	
April 8	6.4	+ .08	100	18	30	
11	6.5	+ .09	60	18	140	
11	6.5	+ .09	60	18	40	
May 5	7.4	+ .16	60	18	152	
11	7.6	+ .18	60	18	150	Hubble observer
30	8.3	+0.24	100	18	80	
			R Hydrae			
1920 May 31	9.0	−0.33	100-inch	18-inch	214^{m}	
July 8	7.8	−0.25	100	7	50	
			R Serpentis			
1920 May 1	7.6	+0.13	100-inch	18-inch	106^{m}	
30	8.8	+ .20	100	18	184	
June 1	8.8	+ .21	100	18	184	
July 8	10.7	+0.32	100	7	160	
			X Ophiuchi			
1919 June 9	6.6	−0.03	60-inch	18-inch	24^{m}	
10	6.6	− .02	60	18	30	
1920 April 8	7.3	− .16	100	18	(70)	Clouds
May 1	6.9	− .09	100	18	62	
4	6.8	− .08	60	18	52	
31	6.6	.00	100	18	80	
July 5	7.0	+ .10	60	18	110	
6	7.0	+ .11	100	18	90	
31	7.5	+ .18	100	18	66	
Sept. 2	8.3	+ .28	100	18	110	
27	8.8	+ .35	100	18	180	
Oct. 27	9.0	+0.44	100	18	90	Clouds
			χ Cygni			
1920 May 30	8.2	−0.08	100-inch	18-inch	66^{m}	
June 1	8.1	− .07	100	18	40	
30	5.2	.00	60	18	125	Benioff observer
July 29	5.8	+ .07	100	18	90	
Sept. 3	6.5	+ .16	100	18	66	
26	8.1	+ .21	100	18	180	
Oct. 26	9.6	+0.29	100	18	180	

TABLE III—*Continued*

OBSERVATIONS

Date	Mag.	Phase	Telescope	Camera	Exposure	Remarks
			T Cephei			
1917 Nov. 3..	7.6	−0.19	60-inch	18-inch	50^m	Joy observer
Dec. 3..	6.8	− .11	60	18	80	Joy observer
1918 Jan. 2..	5.8	− .04	60	18	60	Joy observer
Oct. 24..	7.2	− .27	60	18	150	Joy observer
1920 June 3..	8.0	+ .20	60	18	240	
July 5..	8.9	+ .28	60	18	364	
28..	9.4	+ .34	60	18	508	
Sept. 5..	10.1	+0.44	60	7	520	

R SERPENTIS

Maximum occurred on March 16, 1920, magnitude 6.1. The facts concerning the following minimum are not available at present. It appears, however, that the minimum brightness was not above the fourteenth magnitude. The spectroscopic observations described in Table IV cover about the central third of the decreasing branch of the light curve.

X OPHIUCHI

Maximum light and the decreasing phase are well covered by the observations. The last plate, taken on October 27, was probably about 20 days before minimum. The magnitude at this time was not more than a few tenths above the minimum magnitude. On April 8, 1920, Hγ shows small contrast with the continuous spectrum; on May 1, this contrast is decidedly greater. On July 31, the titanium bands have a curious, blended appearance; the heads of the bands are not sharp, and as the absorption is less than on the preceding plates the bands are not so pronounced. The bands are still weaker in September. The decrease in intensity of Hγ from September 2 to September 27 is striking; this line is practically absent from the spectrum on the latter date. The only emission line observed on the plate of October 27 is λ 4571, just at the red edge of which there appears a well-defined and rather strong *dark* line. This has developed within a month, as no absorption was observed in this position on the preceding plate. A somewhat similar appearance of bright and dark portions of the same line has been observed by Stebbins[1] in *o* Ceti at λ 4308 and λ 4376, and by the writer in other stars in connection with the manganese line λ 4030. This phenomenon suggests that the well-known displacement of the dark lines with respect to the bright lines may be due in part to a reinforcement by a partially developed emission line of the continuous spectrum on the violet edge of the dark lines.

X Ophiuchi is a double star, Hu 198, with a measured separation of 0.″2. The small light-range and some of the spectral peculiarities may thus be due to exceptional circumstances. The motions and light-variations of the components are being investigated by Van Biesbroeck at the Yerkes Observatory.[2]

RÉSUMÉ OF OBSERVED CHANGES IN THE BRIGHT LINES

Upon combining the data of Table IV with those previously available for Md stars, it is found that certain phenomena shown by the bright lines appear in substantially the same form in several stars. We thus conclude that these phenomena are characteristic of the variation of Md stars and that they are, therefore, of great importance in the study of the problems presented by these remarkable objects.

The changes exhibited by some of the more conspicuous bright lines are outlined in the following pages. In most cases several illustrative instances are cited to indicate the character and extent of the data upon which each statement rests. This collection of references and quotations may prove useful to anyone desiring to review the observational evidence.

Hydrogen lines.—The bright hydrogen lines are such conspicuous and characteristic features of Md spectra that they have been the means in many instances of the discovery of long-period variables at the Harvard Observatory. The variations of these lines have accordingly attracted more notice than any of the other spectral modifications presented by Md stars. Notes in the

---

[1] *Lick Observatory Bulletins*, **2**, 93, 1903.

[2] December, 1920, meeting of the American Astronomical Society.

TABLE IV

INTENSITIES OF EMISSION LINES

Date	Phase	Hη	Hζ	3905	Hε	Hδ	4202	4308	Hγ	4373	4376	4571	Hβ
	R Leonis												
1920 Jan. 16...	−0.19	....	....	....	....	2	....	....	....	....	....	....	....
April 8...	+ .08	1	3	1	....	15	3	....	7	....	tr.	....	....
11...	+ .09	1−	3	0.5	....	15	4	....	7	....	0.5	....	....
May 5...	+ .16	1.5	3.5	1+	2	15	6	3	10	2	1.5	4	....
11...	+ .18	1.5	3.5	1	2	15	6	4	12	2	1	5	1
30...	+0.24	....	....	....	....	4	4	3+	6	2	1	5	tr
	R Hydrae												
1920 May 31...	−0.33	....	....	....	....	....	....	1	....	....	....	3	....
July 8...	−0.25	....	....	....	....	2	....	....	....	....	....	....	....
	R Serpentis												
1920 May 1...	+0.13	....	0.5	....	....	8	....	....	7	....	....	....	1
30...	+ .20	....	0.5	....	....	8	2+	2	7	1	0.5	2	2
June 1...	+ .21	....	0.5	tr	....	8	3	3	7	1	1	3	3
July 8...	+0.32	....	....	....	....	4+	3	4	4	0.5	1	4+	1.5
	X Ophiuchi												
1919 June 9...	−0.03	....	....	....	....	6	....	....	4	....	....	....	....
10...	− .02	....	....	....	....	7	....	....	4	....	....	....	....
1920 April 8...	− .16	....	....	....	....	7	....	....	2	....	....	....	....
May 1...	− .09	....	0.5	tr	....	9	....	....	4	....	....	....	....
4...	− .08	....	0.5	....	....	8	....	....	4	....	....	....	....
31...	.00	1−	2	1−	....	9	tr	....	6	....	....	....	....
July 5...	+ .10	....	....	....	....	6	1	....	4	....	....	....	....
6...	+ .11	0.5	1	0.5	....	7	2	....	6	....	....	....	....
31...	+ .18	....	....	....	....	2	1	....	4	....	....	....	....
Sept. 2...	+ .28	....	....	....	....	1	2−	1+	2	1−	....	2	....
27...	+ .35	....	....	....	....	....	tr	1	....	....	....	2	....
Oct. 27...	+0.44	....	....	....	....	....	....	....	....	....	....	1	....
	χ Cygni												
1920 May 30...	−0.08	....	2	....	....	7	....	....	2+	....	....	....	1
June 1...	.07	....	1	....	....	6	....	....	2	....	....	....	0.5
30...	.00	....	3	1−	....	15	tr	....	7	....	....	....	8
July 29...	+ .07	2	6	2	....	15	3	1	7	....	....	....	7
Sept. 3...	+ .16	1	3	1	....	15	3	3−	8	1	....	1	5
26...	+ .21	....	2	1	....	7	3	4	7	1	....	3	3
Oct. 26...	+0.29	....	....	tr	....	3	4	5	4	2	0.5	4	3
	T Cephei												
1917 Nov. 3...	−0.19	....	....	....	....	3	....	....	....	....	....	....	....
Dec. 3...	− .11	....	tr	....	....	15	....	....	4	....	....	....	....
1918 Jan. 2...	− .04	2−	5	1	....	15	1	....	8	....	....	....	2
Oct. 24...	− .27	....	....	....	....	4	....	....	1+	....	....	....	....
1920 June 3...	+ .20	....	....	....	....	2	2−	2+	4	0.5	....	4	0.5
July 5...	+ .28	....	....	....	....	....	2	4	2	0.5	....	6	0.5
28...	+ .34	....	....	....	....	....	1−	2	....	....	....	4	....
Sept. 5...	+0.44	....	....	....	....	....	0.5	1	....	....	....	2	....

Harvard publications show that in practically every Md star the relative intensities of Hγ and Hδ are subject to wide variations.

Although the bright hydrogen lines (referring particularly to Hγ and Hδ) are usually of very great intensity, nevertheless it appears that near the phase of minimum light they are weak or absent from the spectrum.

To avoid repetition certain references will hereafter be indicated by number as follows:

(1) Stebbins, "The Spectrum of *o* Ceti," *Lick Observatory Bulletins*, **2**, 78, 1903.
(2) Eberhard, "On the Spectrum and Radial Velocity of χ Cygni," *Astrophysical Journal*, **18**, 198, 1903.
(3) Merrill, "Spectroscopic Observations of Stars of Class Md," *Publications of the Astronomical Observatory, University of Michigan*, **2**, 45, 1916.
(4) Adams and Joy, "Note on the Identification of Certain Bright Lines in the Spectrum of *o* Ceti," *Publications of the Astronomical Society of the Pacific*, **30**, 193, 1918.
(5) Adams and Joy, "Changes in the Spectrum of Omicron Ceti," *Publications of the Astronomical Society of the Pacific*, **32**, 163, 1920.

ABSENCE OR WEAKNESS OF BRIGHT HYDROGEN LINES NEAR MINIMUM

o Ceti. 1902, Oct. 4, to 1903, Jan. 5. Phase, +0.36 to +0.64. Reference (1). Hydrogen lines weaker than other bright lines, or not observed at all. "On 58*A* and 59*A* (1903, Jan. 2 and 5) the continuous spectrum was visible in the Hγ and Hδ regions, but no trace of a bright line was seen in either case. The evidence furnished by these later plates therefore strengthens the conclusion that the bright lines disappeared at minimum."

R Hydrae. 1920, May 31. Phase, −0.33. Table IV. Hγ and Hδ not observed although other bright lines and some continuous spectrum are present.

X Ophiuchi. 1915, June 4. Phase, −0.38. Reference (3). Faint continuous spectrum; no bright lines.

1920, Sept. 27 and Oct. 27. Phase, +0.35 and +0.44. Table IV. Hγ and Hδ are very weak or absent.

T Cephei. 1920, July 28 and Sept. 5. Phase, +0.34 and +0.44. Table IV. Hγ and Hδ are not seen and are certainly much weaker than other bright lines.

Adams and Joy found that near the minimum of *o* Ceti the usual hydrogen lines were replaced by others having quite different characteristics. Whether this is typical behavior for long-period variables is not known.

HYDROGEN LINES AT MINIMUM

o Ceti. 1920, Jan. 15 to Feb. 6. Phase, +0.51 to +0.57. Reference (5). "The hydrogen lines appear very diffuse and greatly displaced toward the red. The brightest of the three hydrogen lines on this photograph is Hβ, Hγ being next and Hδ faint."

Shortly after minimum brightness the hydrogen lines Hγ and Hδ appear faintly as emission lines, Hγ being at first much the weaker, so that for a time Hδ may be seen alone. Both lines grow in intensity until maximum or after, but Hγ gains relatively to Hδ so that during the decreasing phase, before both lines disappear, Hγ may become much the stronger.

In a brief summary of the general features of the spectra of long-period variable stars[1] as photographed with objective-prism spectrographs by the Harvard Observatory, Miss Cannon says: "Changes occur in the class of spectrum during the light variation, and in the relative intensities of the bright lines. In some cases, Hδ appears first and becomes from ten to twenty times as bright as Hγ. At maximum light, Hγ often reaches equality with Hδ. The relative intensities of these two lines often vary at different maxima of the same star." The results from slit spectrograms, as noted below, are in harmony with Miss Cannon's observations.

CHANGES IN RELATIVE INTENSITIES OF Hγ AND Hδ

o Ceti. 1915, Nov. 5, 12. Phase, −0.2. Reference (3). "On Nov. 5, Hγ is so weak as not to be readily visible. It is easily seen on Nov. 12, but is not much stronger than the adjacent continuous spectrum. This is strikingly at variance with its appearance on my earlier plates and as observed by others."

1919, Autumn. Phase decreasing. Reference (5). "As the star grows fainter . . . . the relative intensity of the hydrogen lines changes, Hγ becoming stronger with reference to Hδ."

R Leonis. 1920, April 8 to May 30. Phase, +0.08 to +0.24. Table IV. Relative intensities of Hγ and Hδ changed from 7:15 to 6:4.

R Virginis. 1915, March 28 to May 7. Phase, −0.11 to +0.16. Reference (3). Relative intensities of Hγ and Hδ changed from 3:4 to 2−:1.

X Ophiuchi. 1920, April 8 to July 3. Phase, −0.16 to +0.18. Table IV. Relative intensities of Hγ and Hδ changed from 2:7 to 4:2.

---

[1] *Popular Astronomy*, **27**, 527, 1919.

χ Cygni. 1901, Aug. 2 to Nov. 23. Phase, −0.03 to +0.24. Reference (2). "From Aug. 2 until Sept. 19 Hδ was considerably brighter than Hγ; from Oct. 3 to 15 Hγ and Hδ differed little from each other; on Oct. 26 they were equal; and on Nov. 9 and 23 Hγ was brighter than Hδ."

1920, May 30 to Oct. 26. Phase, −0.08 to +0.29. Table IV. Relative intensities of Hγ and Hδ changed from 2+:7 to 4:3.

The foregoing are instances of considerable variation in the hydrogen lines occurring in a single light cycle. Many more examples can be found by comparing observations in different cycles, but deductions from such comparisons must be made with circumspection since it is not safe to assume that the behavior of the spectrum of a long-period variable is identically repeated in different cycles.

The relative intensities of the hydrogen lines near maximum are very different from laboratory values. The most striking discrepancies are the great strength of Hδ and of numerous ultra-violet lines, and the relative weakness of Hβ and Hϵ. Miss Maury[1] and C. D. Shane[2] have called attention to the relative weakness of Hκ, Hλ, and Hμ in *o* Ceti; the same phenomenon has been observed partially in other Md spectra through the fact that the hydrogen series appears to stop abruptly with Hι. Other peculiarities of the hydrogen series are described by Shane. By combining the results of several observers it appears that a bright Hα line may or may not be present in the spectrum of *o* Ceti. Unfortunately this line has not been observed systematically over any considerable period of time. The variation in Hβ is thought by Father Cortie[3] to be connected with the brightness of the maximum. According to him, at a bright maximum the titanium oxide bands are especially weak and Hβ especially strong. This same correlation between Hβ and the titanium bands appears also in comparing the average characteristics of different stars.[4] Hϵ (though seldom observed) may increase relatively to Hδ and Hζ during the decline in brightness.

---

[1] *Harvard Annals*, **28**, 45, 1897.

[2] *Publications of the Astronomical Society of the Pacific*, **32**, 234, 1920.

[3] *Scientific American Supplement*, **85**, 21, 1918.

[4] *Publications of the Astronomical Observatory, University of Michigan*, **2**, 63, 1916

CHANGES IN RELATIVE INTENSITY OF Hε

o Ceti. 1902, June 27 to Sept. 22. Phase, +0.07 to +0.33. Reference (1).
Relative intensities of Hδ, Hε, and Hζ changed from 420:4:30 to 40:10:7.

R Leonis. 1920, April 8 to May 11. Phase, +0.08 to +0.18. Table IV.
Relative intensities of Hδ, Hε, and Hζ changed from 15:–:3 to 15:2:3.5.

Observations by Shane[1] at the Lick Observatory have revealed the interesting fact that in variables of Class N the characteristic phenomena connected with the bright hydrogen lines are much the same as in variables of Class Md. It appears, however, that in Class N the bright hydrogen lines reach their greatest intensities earlier in the light cycle, and are less persistent after maximum light than in the Md stars.

Bright lines not due to hydrogen.—Besides the hydrogen series there are other bright lines subject to very great changes in intensity during the light cycle. The available data, though rather fragmentary, make clear a certain system in these changes which is undoubtedly followed by several, and probably by many or all, Md long-period variables. Accordingly an attempt will be made in the following paragraphs to indicate some of the phenomena connected with these various bright lines as typical of Md variation.

λ 3905.—This line, thought to be due to silicon (3905.51 I.A.), is (excepting hydrogen) one of the strongest and most persistent of the emission lines during the time that the star is bright. After maximum it seems to gain relatively to the hydrogen lines, but it is possible that this increase arises from the diminution of the latter. Its behavior near the minimum phase is not known for it has usually been photographed only when the continuous spectrum and the bright hydrogen lines are strong. It appears certain, however, that λ 3905 does not grow stronger toward minimum to any such degree as do λ 4308 and λ 4571 (see below). Further observations of this line are much to be desired.

λ 4202.—This iron line (4202.033 I.A.) has very frequently been observed as an emission line in Md spectra. Appearing about the time of maximum, it grows steadily stronger during the first part of the decline until it may equal or surpass Hγ and Hδ. This increase does not continue throughout the decreasing light phase, as toward minimum this line is in turn exceeded in intensity by λ 4308 and λ 4571.

---

[1] *The Spectra of Certain Class N Stars, Lick Observatory Bulletins,* 10, 79, 1920.

CHANGES IN RELATIVE INTENSITY OF λ 4202

o Ceti. 1902, June 27 to Oct. 6. Phase, +0.07 to +0.37. Reference (1). Relative intensities of Hγ, λ 4202, and Hδ varied from 420:10:420 to 13:40:13.

R Leonis. 1920, Jan. 16 to May 30. Phase, −0.19 to +0.24. Table IV. Relative intensities of Hγ, λ 4202, and Hδ varied from −:−:2 to 6:4:4.

χ Cygni. 1920, June 30 to Oct. 26. Phase, 0.00 to +0.29. Table IV. Relative intensities of Hγ, λ 4202, and Hδ varied from 7:−:15 to 4:4:3.

T Cephei. 1920, June 3 to July 28. Phase, +0.20 to +0.34. Table IV. Relative intensities of Hγ, λ 4202, and Hδ varied from 4:2−:2 through 2:2:− to −:1−:−.

λ 4308.—This line, apparently belonging to the iron spectrum (4307.909 I.A.), becomes bright at a later phase than the somewhat similar line λ 4202, and grows stronger than λ 4202 if the observations are continued a sufficient time past maximum. Near maximum λ 4308 is sometimes observed as an absorption line, usually of low intensity.

CHANGES IN RELATIVE INTENSITIES OF λ 4202 AND λ 4308

o Ceti. 1902, June 27 to Oct. 26. Phase, +0.07 to +0.43. Reference (1). Relative intensities of λ 4202, λ 4308, and Hγ varied from 10:−:420 through 19:12:190 to 40:60:13. λ 4308 appeared between July 22 and 29; phase, about +0.16.

R Leonis. 1920, April 8 to May 30. Phase, +0.08 to +0.24. Table IV. Relative intensities of λ 4202, λ 4308, and Hγ varied from 3:−:7 to 4:3+:6.

R Serpentis. 1920, May 30 to July 8. Phase, +0.20 to +0.32. Table IV. Relative intensities of λ 4202, λ 4308, and Hγ varied from 2+:2:7 to 3:4:4.

χ Cygni. 1901, Aug. 24 to Nov. 23. Phase, +0.02 to +0.17. Reference (2). "λ 4308 increased in brightness the fainter the star became."
1920, July 29 to Oct. 26. Phase, +0.07 to +0.29. Table IV. λ 4308 appeared as an emission line between June 30 and July 29. Relative intensities of λ 4202, λ 4308, and Hγ varied from 3:1:7 to 4:5:4.

T Cephei. 1920, June 3 to July 28. Phase, +0.20 to +0.34. Table IV. Relative intensities of λ 4202, λ 4308, and Hγ varied from 2−:2+:4 to 1−:2:−. Compare with plate of 1918, Jan. 2, on which the intensities were 8:−:1. Compare also with Hδ. Intensities of λ 4308 and Hδ on 1917, Dec. 3, 1918, Jan 2, were −:15 and on 1920, July 5, 4:−. The relative intensities of these two lines must have changed 250 or more times.

λ 4571.—This line, which is probably a low-temperature magnesium line (4571.114 I.A.), does not appear until a later epoch than λ 4202 and λ 4308, but gains in relative strength as minimum is approached. In several instances it has finally become the strongest line in the photographic spectrum. This is probably typical behavior. This line is usually observed near the maximum phase as a weak absorption line.

CHANGES IN RELATIVE INTENSITIES OF λ 4308, Hγ, AND λ 4571

o Ceti. 1902, July 22 to Oct. 26. Phase, +0.14 to +0.43. Reference (1). Relative intensities of λ 4308, Hγ, and λ 4571 changed from 12:190:– to 60:13:75.

1918, March 2. Phase, +0.44. Reference (4). "This line (λ 4571) is the most intense of any on the photograph with the exception of those due to hydrogen." This precise condition was not shown by any of Stebbins' photographs although it was approached on Aug. 11, Aug. 25, and Sept. 6, 1902.

R Leonis. 1920, May 5 to May 30. Phase, +0.16 to +0.24. Table IV. Relative intensities of λ 4308, Hγ, and λ 4571 changed from 3:10:4 to 3+:6:5.

R Hydrae. 1920, May 31. Phase, −0.33. Table IV. Only two bright lines are visible, λ 4308 and λ 4571. Compare with the observation of July 8, and with the Ann Arbor observations.

R Serpentis. 1920, May 30 to July 8. Phase, +0.20 to +0.32. Table IV. Relative intensities of λ 4308, Hγ, and λ 4571 changed from 2:7:2 to 4:4:4+.

χ Cygni. 1920, July 29 to Oct. 26. Phase, +0.07 to +0.29. Table IV. Relative intensities of λ 4308, Hγ, and λ 4571 varied from 1:7:– to 5:4:4.

T Cephei. 1920, June 3 to Sept. 5. Phase, +0.20 to +0.44. Table IV. Relative intensities of λ 4308, Hγ, and λ 4571 changed from 2+:4:4 to 1:–:2.

GENERAL DISCUSSION

It should not be inferred that the foregoing references represent all the known observational material bearing on each line. They have been selected as the most complete and reliable illustrations of the changes under discussion. Fragmentary observations indicate that the same course of spectral variation is followed in other stars, and in these same stars in other light cycles.

In Figure 1 an attempt has been made to display graphically the changes in the intensities of the lines Hγ, Hδ, and λ 4202, λ 4308, and λ 4571, as related to the light phase. The relationships depicted are believed to be typical of long-period variables of Class Md. It is clear that considerable differences exist between the spectra of different stars at any given phase, but all stars of the *o* Ceti type which have been adequately observed have shown, with no very great variations, the changes in spectrum indicated in Figure 1. The phases at which certain lines appear or disappear may vary somewhat in different stars. Figure 1 is intended to represent the average behavior of the small group of stars observed, and may require modification when more complete data become available.

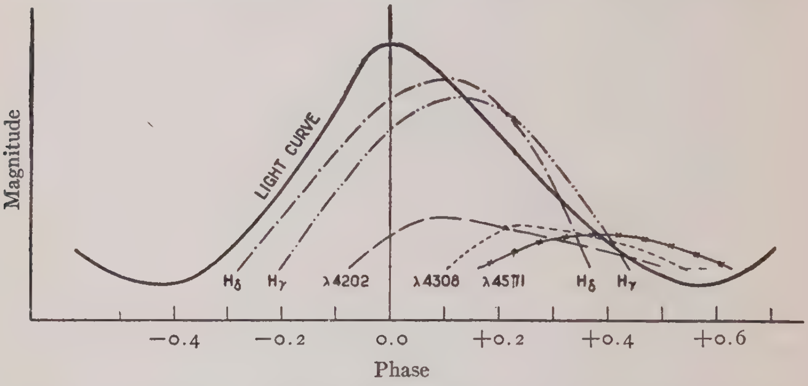

FIG. 1.—Intensities of bright lines in Md spectra in relation to the variation in total light. The light-curve, which is the mean curve for *o* Ceti, R Leonis, R Hydrae, χ Cygni, and T Cephei, has an amplitude of 5.3 magnitudes. The amplitudes of the other curves are not determined.

The method of comparing observations of different stars by referring them to the light phases counted from maximum to maximum is obviously but a first approximation. For an exact comparison of the behavior of different stars the light-curves cannot be assumed to be of the same shape, or to be identically repeated in different cycles. In a final discussion the circumstances of any particular cycle should be recognized either by counting the phase from maximum to *minimum* instead of from maximum to maximum, or by dropping the time relation and using instead the *magnitude* when observed, as compared with the magnitudes at the maximum and minimum of the same cycle.

In addition to the lines which have been discussed in the preceding pages a large number of other less conspicuous bright lines have been observed in Md spectra, including λλ 3852, 3967, 4007, 4030, 4102, 4138, 4178, 4215, 4233, 4373, 4376, and 4512, all of which appear subject to variation. The intensities of λ 4373 and λ 4376 are found in Table IV. After some further observations have been secured several of these lines can probably be grouped according to their behavior and compared with the stronger lines λ 4202, λ 4308, and λ 4571. They may thus prove useful aids in interpretation. It is hoped to discuss them in a future contribution.

Adams and Joy have pointed out that "the bright lines appearing in the spectrum of *o* Ceti near minimum of light are lines which are strengthened at low temperatures."[1] This is undoubtedly correct, but it appears that some other cause in addition to low temperature must be operative to produce the observed peculiarities. The magnesium line 4571 is indeed an extreme low-temperature line and its behavior strongly suggests low temperature as the prevailing condition near minimum. With λ 4202 and λ 4308 and some other lines, however, the case is not so clear. There is no apparent reason why certain of these lines should be so strongly accentuated as compared with other lines of the same elements in the same temperature class[2] and having comparable intensities in most sources. It will probably be well to reserve discussion of temperature and other physical conditions until the fainter emission lines mentioned in the foregoing paragraph have been more extensively observed.

It is believed that the spectral changes described in this paper have such intimate connection with the light variations of Md stars that a knowledge of them is quite essential to a correct general interpretation of the phenomena exhibited by stars of this class. More complete observations of the bright lines, of the dark lines and bands, and especially of the spectrum near minimum will be required as a basis for a satisfactory discussion of the conditions prevailing in these stars and of the causes of variation. The writer is inclined to favor the "veil theory" of variation as outlined a few years ago,[3] but even if this be correct much amplification will be needed.

---

[1] *Publications of the Astronomical Society of the Pacific*, **30**, 193, 1918.

[2] King, *Mt. Wilson Contr.*, No. 66; *Astrophysical Journal*, **37**, 309, 1913.

[3] *Publications of the Astronomical Observatory, University of Michigan*, **2**, 70, 1916.

o Ceti, the brightest of the long-period variables and having a period which differs appreciably from a year, offers the strategic point for an observational attack on the physical problems of Md variation, provided we are justified in assuming that the remarkable spectral features of this star and their variations are not isolated peculiarities but may be accepted as typical Md phenomena. One consequence of the present discussion may be increased confidence that this is the case.

MOUNT WILSON OBSERVATORY
December 1920

Contributions from the Mount Wilson Observatory, No. 201
Reprinted from the *Astrophysical Journal*, Vol. LIII, pp. 201–223, 1921

THE ORBITS OF SEVEN SPECTROSCOPIC BINARIES

By R. F. SANFORD

ABSTRACT

Seven spectroscopic binaries, Boss 373, OΣ 82, Lalande 29330, Companion to α Herculis, 205 Draconis, Boss 5591, Lalande 46867.—The elements of the orbits have been derived from 15 to 30 spectrograms of each, most of them made with an 18-inch camera and the 60-inch or 100-inch reflector. In the case of the first, fifth, and sixth binaries, both components were measured. The periods are each about 4 days except for the fourth and seventh, which are 51.6 and 6.72 days respectively. Radial-velocity diagrams are shown in Figures 1–7. The *spectroscopic parallax, proper motion, and absolute magnitude* of each, as furnished by Adams and Joy, are given in Table I. Lalande 29330 and 46867 are particularly interesting because of low luminosity, +6, and late spectral class, K. Lalande 46867 is very similar in spectroscopic peculiarities to σ Geminorum.

α Herculis and companion.—The *radial velocity* of the center of mass of the companion, −37.2 km/sec., and of α Herculis, −32.2 km/sec., when corrected for Campbell's K-term furnishes evidence in connection with their common proper motions of physical connections between the two.

Probable eclipsing variable star.—The data for *205 Draconis* suggest that it would be a favorable case to examine for variability caused by eclipse. Its magnitude is 7.2 and spectral class F2.

This paper deals with the derivation of the elements of the orbits of the seven spectroscopic binary stars listed in Table I.

TABLE I

Name	Mag.	α 1900	δ 1900	Spectral Class	Abs. Mag.	μ	$\pi_{sp.}$	No. Rev.
Boss 373 = Σ 145	6.3	1^h36^m	+25° 14′	F3–F3	+2.6	0.″135	0.″018	161
OΣ 82	7.0	4 17	+14 49	F9	+4.1	0.096	0.024	194
Lalande 29330	8.5	16 1	+10 57	K0	+6.0	0.491	0.032	350
Comp. α Herculis-Boss 4374	5.4	17 10	+14 30	F9	+1.7	0.032	0.018	7
205 Drac. = β 971	7.2	18 45	+49 19	F2–F2	+1.4	....	0.005	119
Boss 5591 = Pi. 267	6.9	21 40	+28 19	A9–A9	+2.3	0.061	0.009	103
Lalande 46867	7.3	23 50	+28 5	K2	+6.0	0.573	0.055	179

The last four columns of the table give, respectively, the absolute magnitude, proper motion, spectroscopic parallax, and number of revolutions of the binary in its orbit between the first and last observations. Six of the stars were announced as binaries in a note by Adams and Joy,[1] who have also furnished from manuscript the data for absolute magnitude, proper motion, and spectroscopic parallax.

---

[1] *Publications of the Astronomical Society of the Pacific*, 31, 41, 1919.

The spectroscopic parallaxes for the first, fifth, and sixth binaries may be considerably in error, since blends of the spectra of the two stars may affect the relative intensities of the lines used for the determination of the absolute magnitudes. The spectral class in these three cases is indicated for both components. The elements of three of the above binaries have been previously announced by the writer.[1]

The spectrograms upon which the orbits depend were obtained with spectrographs of one-prism dispersion and an 18-inch camera, the only exceptions being a few plates of Lalande 29330, noted in Table IV, which were obtained with a 7-inch camera. Both the 60-inch and the 100-inch reflector were used: in all cases the letter prefixed to the plate number indicates the telescope—a Greek γ for the 60-inch series, and the letter C for the 100-inch series. Except where noted in the remarks, Seed 30 plates were used.

An effort was made in each case to determine the period as soon as possible and thereafter to secure with the minimum number of plates a reasonably good distribution over the velocity-curve. In some cases this has led to the determination of the elements from rather fewer plates than has usually been the custom. But no great increase in accuracy would have been possible without the addition of a very considerable number of observations and it was considered better to spend the time in the investigation of other orbits rather than accumulate observations on a few binaries.

The tables of observations accompanying the individual discussions are similar, each giving the plate number, date, Greenwich mean time of mid-exposure, the phase from periastron, the measured velocity, the residuals from the final elements, the weights assigned when any distinction has been made among the plates of a binary, and finally such remarks as seemed necessary. When the spectra of both components have been measured on the same plate two columns for velocities and two sets of residuals are given in the tables.

A few general remarks will make clear the procedure which has been followed and will avoid unnecessary repetition.

Since, in every case but one, at least 100 revolutions of the stars in their orbits separate the first and last observations, it seemed justifiable to assume that the period already determined needed no correction. Except for Lalande 29330 and the companion to α Herculis, the preliminary period has, therefore, been taken as final. The freehand velocity-curves drawn through the plotted observations were used to determine preliminary elements by Russell's method.[1] When a velocity diagram included the curves of both components, the preliminary elements used were based upon both curves, excepting of course the semi-amplitude of velocity variation, K. For such binaries the elements were corrected by the method of least squares, using the equations of condition given by Harper,[2] in which a single set of normal equations is derived from the observed velocities of both primary and secondary. Assuming the period to be known and noting that the angles of periastron for primary and secondary differ by 180°, it is readily seen that there are six independent elements to be corrected, so that the normal equations involve six unknown quantities. For the binaries showing only one spectrum, the equations adapted by Schlesinger[3] were used to derive corrections to the preliminary elements.

---

[1] *Publications of the Astronomical Society of the Pacific*, **32**, 192, 1920.

In all cases where the elements are given for two components, those which are common to the two have not been repeated. Those which belong to the secondary alone are distinguishable by the subscript 1.

A radial velocity diagram has been drawn for each binary (Figs. 1–7). The zero for the abscissae corresponds to the epoch of periastron. The curves are based upon the elements adopted as final; the individual velocities are represented by circles with radii equal to the probable error of a velocity of unit weight; and a broken line indicates the velocity of the center of mass (γ).

The details for the individual stars are briefly as follows:

BOSS 373

This star is the brighter component of the double Σ 145. The fainter component is of the eleventh magnitude, 11″ distant, in p.a. 32°. Measures separated by 35 years show no evidence of orbital motion.

---

[1] *Astrophysical Journal*, **40**, 282, 1914.

[2] *Publications of the Dominion Observatory*, **1**, 327, 1914.

[3] *Publications of the Allegheny Observatory*, **1**, 33, 1908.

Table II gives the nineteen spectrograms available for the derivation of the elements, and three others subsequently obtained. Fifteen of these gave velocities for both components and showed

TABLE II

Observations of Boss 373

Plate No.	Date	G.M.T.	Phase	Velocity		O–C		Wt.
				Prim.	Second.	Prim.	Second.	
				km/sec.		km/sec.		
γ 7272...	1918 Aug. 27	23^h57^m	3^d880	−25.2	+44.9	+ 6.1	+ 1.4	0.5
7379...	Sept. 20	22 53	1.228	+68.9	−60.5	+ 5.1	− 0.7	1.0
7412...	23	22 37	4.217	+12.8		+ 0.5	+17.8	0.5
7448...	Oct. 17	21 26	1.560	+39.8	−28.4	+ 5.5	− 0.6	0.5
7582...	Nov. 21	18 43	0.969	+76.1	−74.0	− 5.0	+ 4.7	1.0
7596...	22	17 56	1.934	+10.2		+12.9	− 0.7	0.5
7603...	Dec. 11	17 22	3.181	−76.3	+90.6	− 3.1	+ 1.5	1.0
7618...	12	18 19	4.212	+10.4		− 1.2	+14.7	0.5
7628...	13	18 16	0.775	+79.5	−83.4	− 9.1	+ 3.4	1.0
7639...	14	16 30	1.702	+10.2		− 9.5	+23.2	0.5
7646...	15	19 22	2.820	−68.4	+78.4	− 2.1	− 3.1	1.0
7662...	18	16 34	1.269	+61.2	−67.0	+ 0.8	−10.8	1.0
7739...	1919 Jan. 11	16 48	3.106	−74.5	+87.2	− 1.4	− 1.8	1.0
7769...	15	18 05	2.724	−58.6	+78.1	+ 3.3	+ 1.4	1.0
7782...	17	16 20	0.217	+72.1	−68.5	+ 3.8	− 3.8	1.0
7850...	Feb. 8	15 45	0.018	+47.3	−47.6	+ 1.6	− 7.4	1.0
8942...	1920 Jan. 6	15 50	3.851	−35.1	+47.5	− 0.6	+ 0.4	0.5
8958...	9	16 07	2.429	−50.7	+55.6	− 7.1	− 1.3	0.5
8991...	Feb. 6	15 02	3.775	−44.8	+53.5	− 2.1	− 2.4	1.0
9428...	Aug. 3	23 48	1.315	+60.8	−44.2	+ 5.3	+ 7.7	.....
9502...	29	21 45	0.622	+81.7	−60.2	− 6.9	+27.7	.....
9519...	Sept. 1	22 24	3.657	−55.4	+64.3	− 1.0	− 3.2	.....

that both are of spectral class F3. On the other four plates the velocities of the two components differ so little that with the dispersion employed the lines could not be separately measured. Mr. Joy had obtained 4.4 days as an approximate period, which soon led to 4.43474 days as the best value for the assembly of the observations about a single epoch.

The following preliminary elements were found:

$P = 4.43474$ days $\quad K = 79$ km/sec.
$e = 0.12 \quad K_1 = 89$ km/sec.
$\omega = 270^\circ \quad T =$ J.D. 2,421,940.65
$\omega_1 = 90^\circ \quad \gamma = +5$ km/sec.

The four plates on which the lines of the two components are blended were combined into two normal places; otherwise each plate furnished a conditional equation for each component, thus giving a total of thirty-four equations. The weights depend upon the separation of the lines of the two components and refer equally to the velocities for primary and secondary. Two least-squares solutions were made with the corrections to six elements as unknowns. In the second solution the corrections were small for all except ω and T. A third solution was then made assuming all elements to be definitive except these two. This solution gave only slight corrections. The second solution (six unknowns) and the third (two unknowns) yield elements from which nearly identical residuals result. In either case the quantity Σpv^2 is little more than 50 per cent of its value for the preliminary elements. Applying the corrections obtained by the three solutions and deriving the probable errors from the second solution we have the following final elements:

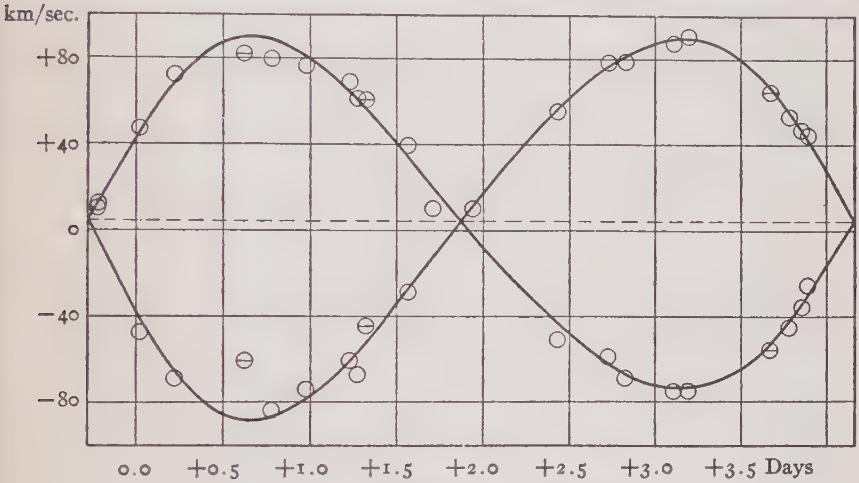

FIG. 1—Velocity-curves of Boss 373

$P = 4.43474$ days
$e = 0.108 \pm 0.011$
$\omega = 295^\circ.58 \pm 5^\circ.02$
$\omega_1 = 115^\circ.58 \pm 5^\circ.02$
$K = 81.5 \pm 1.3$ km/sec.
$K_1 = 88.6 \pm 1.3$ km/sec.
$T =$ J.D. $2{,}421{,}940.9865 \pm 0^d.0053$
$\gamma = +4.6$ km/sec.
$a \sin i = 4{,}942{,}100$ km
$a_1 \sin i = 5{,}371{,}800$ km
$m \sin^3 i = 1.16 \odot$
$m_1 \sin^3 i = 1.06 \odot$

The probable error of a radial velocity of unit weight based upon all the residuals, including those from the four plates with blended spectra, is ±3.5 km/sec. The three observations obtained after the elements were derived have been plotted upon the velocity diagram (Fig. 1) as barred circles. The velocity for the secondary star from γ 9502 is discordant. This plate is strongly exposed. The velocity derived from Hγ alone is −81 km/sec., which agrees fairly well with the curve.

OΣ 82

The star is a visual binary in comparatively rapid motion, the position angle having changed about 180° since discovery. The elements by different computers still differ widely, however, the periods ranging from 90 to 158 years. The last available observations of the visual pair were kindly furnished by Dr. Aitken. In 1916 the position angle was about 75° and the separation about 0ʺ.7. During the period covered by the spectrograms it was not possible to separate the brighter star from the fainter on the slit, even with the 100-inch reflector. Consequently light from both visual components entered the slit, but in the time needed to get a good spectrogram, component *B*, two magnitudes fainter than *A*, could produce no appreciable effect upon the photographic plate. Consequently the spectroscopic binary here studied is star A.

The data of the fifteen plates available are given in Table III. The five plates taken on successive nights showed the period to be close to four days, and a subsequent adjustment of all fifteen observations was best made by using $P=4.00000$ days.

Since the period is an exact number of days, it was impossible to observe all parts of the velocity-curve. Fortunately two of the regions that could be observed correspond to maximum and minimum radial velocity. Little would have been gained by multiplying observations of the four parts of the curve that can be represented, and it was therefore decided to derive the best elements possible from the fifteen plates available.

The curve resulting from an assembly of the observations about a single epoch gave the following provisional elements:

$P=4.00000$ days $K=35.0$ km/sec.
$e=0.15$ $T=$ J.D. 2,422,274.680
$\omega=0^\circ.00$ $\gamma=+37.4$ km/sec.

These were once corrected by the method of least squares applied to the equations of Schlesinger. The resulting elements and their probable errors are adopted as final for the data available:

$$P=4.00000 \text{ days} \qquad K=36.1\pm0.7 \text{ km/sec.}$$
$$e=0.060\pm0.020 \qquad T\doteq\text{J.D. } 2{,}422{,}274.8123\pm0^{\text{d}}.2400$$
$$\omega=+12^\circ.74\pm13^\circ.56 \qquad \gamma=+37.4 \text{ km/sec.}$$
$$a \sin i=1{,}980{,}000 \text{ km}$$
$$\frac{m_1^3 \sin^3 i}{(m+m_1)^2}=0.0193 \odot$$

TABLE III

Observations of OΣ 82

Plate No.	Date	G.M.T.	Phase	Velocity	O−C
				km/sec.	km/sec.
γ6511	1917 Dec. 30	$18^{\text{h}}43^{\text{m}}$	$2^{\text{d}}.968$	+45.0	+3.6
6655	1918 Jan. 30	15 44	1.844	+ 4.3	+0.9
6761	Mar. 22	15 45	0.844	+34.6	−1.5
7451	Oct. 18	0 08	2.194	+ 7.4	−0.3
8782	1919 Oct. 13	0 25	2.205	+ 7.4	−0.6
8850	Nov. 10	20 38	3.048	+43.2	−2.7
8858	11	22 13	0.114	+74.8	+2.4
8865	12	17 25	0.914	+31.5	−0.6
C 213	13	22 18	2.117	+ 1.0	−5.1
C 217	14	19 26	2.998	+42.5	−0.6
γ8908	Dec. 9	20 57	0.061	+73.8	+0.2
γ8922	13	16 49	3.889	+76.2	+0.7
C 244	1920 Jan. 12	19 07	1.985	+ 9.6	+5.4
C 245	13	15 30	2.833	+34.4	+0.4
C 282*	Feb. 11	15 06	3.817	+74.5	−0.9
γ3804†	1914 Oct. 26	22 10	2.110	+11.3	+5.4

* Seed 23.

† Not used for orbit.

The quantity Σpv^2 corresponding to these elements is less than 50 per cent of its value for the preliminary elements. The probable error of a velocity of unit weight is ±2.0 km/sec. The size of the probable error, the sum of the residuals, the small number of observations, and the uncertainties that enter because of the limited portions of the velocity-curve which can be observed, render further approximations inadvisable.

After the elements had been derived it was discovered that a spectrogram, listed at the end of Table III, had been taken on October 26, 1914. The velocity from this plate has been plotted in the diagram (Fig. 2) as a barred circle. Four hundred and sixty-one revolutions of the binary separate this plate from the epoch of the velocity diagram. If the period were lengthened by 0.00050 of a day, this velocity would fall upon the curve and the distribution of the other velocities would hardly be affected; but as it stands the representation is as good as for some of the other plates, and the period has been left as previously found. After the lapse of several years it will be possible to make any slight change in the period that may be necessary.

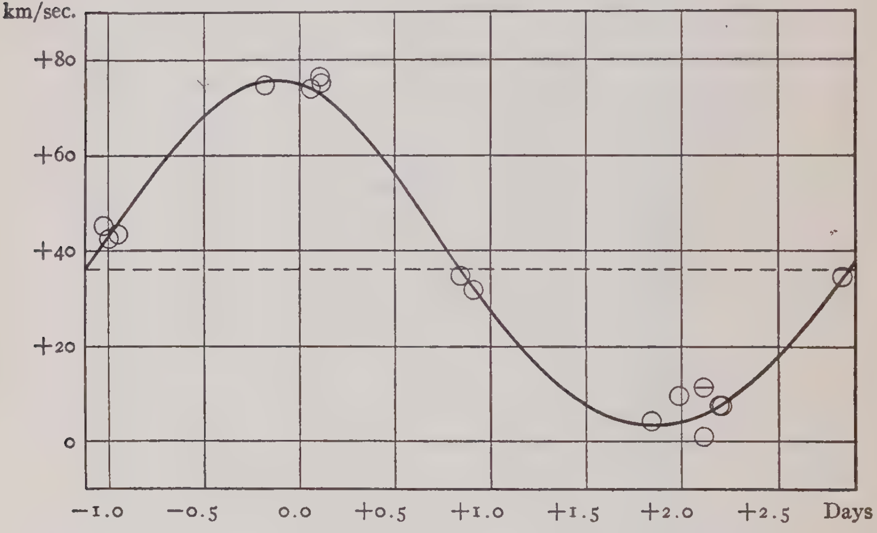

FIG. 2.—Velocity-curve of 0Σ 82

From spectrograms of 19 members of the Taurus stream, Adams, Joy, and Strömberg[1] find +39 km/sec. as the mean radial velocity of the group. The velocity of the center of mass of 0Σ 82 *A* found above for 1919 is +37.4 km/sec. Bearing in mind that the period of the visual binary is certainly more than 50 years and that the mass of the visual component *B* almost certainly is less than that of *A* (it is two magnitudes fainter), the radial velocity of component *A* (+37.4 km/sec.), the proper motion, and the position seem to designate the system as a member of the Taurus stream. The mean value of the parallax for the group from the determinations of Boss and of Kapteyn, and from the spectroscopic results, giving equal weight to each, is $+0''.023$. If we call M_A the mass of visual component A, and M_B the mass of visual component B, we can compute the value of M_A+M_B for each of the three orbits given by Hussey.[1] Further, if we assume the velocity of the center of mass of the visual binary to be $+39$ km/sec., the velocity of B can be derived from the velocity of A ($+37.4$ km/sec.) and the parallax, $+0''.023$. From the velocities of A, B, and the center of mass the ratio $\frac{M_B}{M_A}$ can be calculated for each set of elements. The values (M_A+M_B) and $\frac{M_B}{M_A}$ then give M_A and M_B corresponding to each orbit. The quantity $\frac{m_1^3 \sin^3 i}{(m+m_1)^2}$, derived from the spectroscopic observations, contains $m+m_1=M_A$; hence, if we substitute successively the values of i given for each of the three visual orbits, M_A may be split up into the two parts m and m_1. The results are as follows:

---

[1] *Publications of the Astronomical Society of the Pacific*, **32**, 195, 1920.

	Orbit by	Glasenapp		Gore		Hussey	
Unit is mass of sun	M_A m	1.94	1.17	4.45	3.44	6.19	5.04
	m_1		0.77		1.01		1.15
	M_B	0.78		0.68		0.93	

These values are given with the clear understanding that they are based upon the assumption that the radial velocity of the center of mass of OΣ 82 differs in nowise from the mean value for 19 other stars of the group. Furthermore no one of the three sets of visual elements is probably correct, nor does it follow that i has even approximately the same value in the spectroscopic orbit as in the visual orbit.

Note added February 17, 1921.—Exceptionally good conditions of seeing upon the night of November 23, 1920, made it possible to separate stars A and B of the visual binary OΣ 82 with the 100-inch telescope, and an attempt was made to secure the spectrum of star B separated from that of star A. As the position angle, 75°, is not favorable, guiding was difficult. The velocity derived from measurement of this plate is +38.6 km/sec. The velocity predicted from the elements of the spectroscopic binary, star *A*, is +5.0 km/sec. Hence there is no question but that the spectrum obtained is that of *B*. Furthermore this velocity is that of the Taurus stream which was used in the discussion of the probable masses. The spectral class of *B* is not greatly different from that of *A*, though probably slightly later.

---

[1] *Publications of the Lick Observatory*, 5, 60, 1901.

LALANDE 29330

This binary is of particular interest because of its low luminosity (abs. mag. = +6.0) and late spectral class, Ko. The twenty plates upon which its orbit is based are summarized in Table IV. Spectrograms upon five succeeding nights led to a trial of periods around four days. A smooth velocity-curve was obtained when $P=4.28495$ days was used. This yielded the preliminary elements:

$P=4.28495$ days $\qquad K=38.2$ km/sec.
$e=0.10$ $\qquad T=$ J.D. 2,422,418.619
$\omega=134^\circ$ $\qquad \gamma=-60.3$ km/sec.

TABLE IV

OBSERVATIONS OF LALANDE 29330

Plate No.	Date	G.M.T.	Phase	Velocity	O−C	Wt.
				km/sec.	km/sec.	
γ4886*	1916 June 18	$19^{h}09^{m}$	$4^{d}.095$	− 43.0	+0.1	0.5
4985*.....	Aug. 13	16 33	4.281	− 56.8	−1.8	0.5
5759*.....	1917 May 3	21 30	1.815	− 84.5	−4.8	0.5
5862*.....	June 9	20 54	0.225	− 67.8	+2.3	0.5
5918*.....	July 1	18 42	0.708	− 93.8	−0.2	0.5
6040*.....	Aug. 2	16 15	2.611	− 36.7	+6.8	0.5
6861*.....	1918 Apr. 25	23 26	3.240	− 20.8	+2.6	0.5
7231*.....	Aug. 21	16 18	0.962	− 94.8	+3.3	0.5
C 349......	1920 Apr. 3	23 15	0.917	− 99.0	−1.3	1.0
354......	4	23 42	1.936	− 75.3	−0.8	1.0
359......	5	21 28	2.843	− 31.7	+2.4	1.0
363......	6	22 26	3.884	− 29.9	+2.2	1.0
407......	May 6	20 57	3.826	− 31.0	−1.3	1.0
413......	7	21 32	0.565	− 85.1	+3.5	1.0
415......	8	18 45	1.450	− 88.9	+3.5	1.0
433......	26	18 57	2.317	− 59.6	−2.6	1.0
465......	June 4	22 14	2.885	− 35.9	−3.3	1.0
468......	5	18 30	3.729	− 26.5	0.0	1.0
471......	6	16 10	0.337	− 80.8	−3.8	1.0
492†.....	26	21 30	3.427	− 20.6	+1.5	0.5
557......	July 28	16 36	0.944	−101.1	−3.1	1.0

* 7-inch camera.

† Underexposed.

The first eight plates were secured with a camera of 7 inches focal length instead of the usual 18-inch camera. These and one of the later plates, which was much underexposed, were given half-weight, all the others unit weight. A least-squares solution with twenty-one conditional equations was made by Schlesinger's method for the correction of all six elements. The changes for P, K, and γ were small, while those for the other three elements were of sufficient size to require a second least-squares solution for these three unknowns. The deviations from an ephemeris based on the resulting elements showed satisfactory agreement with the residuals given by the conditional equations. These elements were therefore adopted as final. With their probable errors they are:

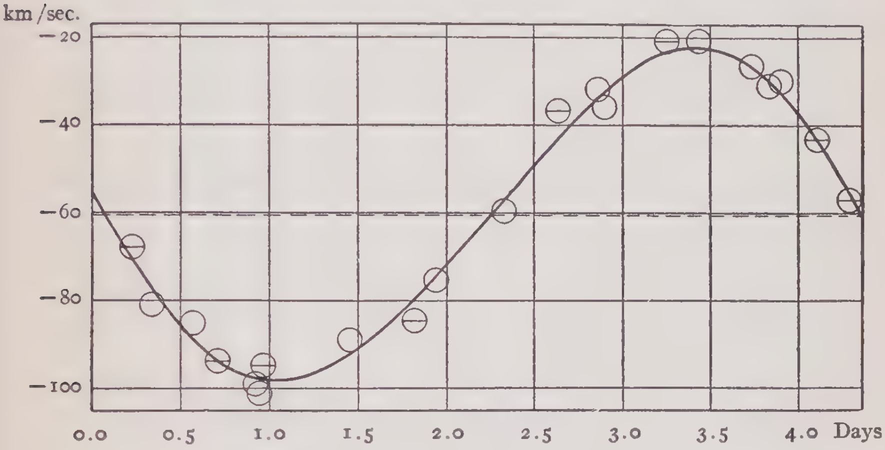

Fig. 3.—Velocity-curve of Lalande 29330

$P=4.28503\pm0.00016$ days $K=38.1\pm0.3$ km/sec.
$e=0.089\pm0.024$ $T=$ J.D. $2,422,418.0522\pm0^{d}\!.0221$
$\omega=82^{\circ}\!.49\pm13^{\circ}\!.40$ $\gamma=-60.6$ km/sec.

$a \sin i=2,238,160$ km

$$\frac{m_1^3 \sin^3 i}{(m+m_1)^2}=0.0244\ \odot$$

The corresponding value of Σpv^2 is one-half that from the preliminary elements.

Reference to the table of observations shows that the first eight spectrograms obtained with low dispersion give satisfactory residuals, whose mean is very little larger than that of the other residuals. This result tends to give one confidence in the observed velocities of faint stars of late spectral class, which must be obtained with low dispersion. In the velocity diagram (Fig. 3) barred circles represent the eight velocities derived with low dispersion.

It is noteworthy that we have here a star absolutely faint ($M=+6.0$) as the brighter member of a spectroscopic binary whose period is short and whose eccentricity is small for stars of its spectral class. Attention may also be called to the large velocity of the center of mass. The space motion derived from the radial velocity, proper motion, and parallax is 75.8 km/sec. with its apex at $A=116.^\circ7$, $D=-6.^\circ8$. The rectangular components, x, y, z, where x and y are parallel to the galactic plane, are $x=-72.2$, $y=-16.7$, $z=+12.8$ km/sec.; further $L=193^\circ$ and $B=10^\circ$, where L and B are the galactic longitude and latitude of the apex. These may be compared with the mean values found by Adams and Joy[1] for 29 stars with large radial velocities: $\bar{x}=-59.5$, $\bar{y}=-44.5$, $\bar{z}=-4.4$, $\bar{v}=74.4$ km/sec., $L=217^\circ$, $B=-3^\circ$.

The agreement with the stars used by Adams and Joy is seen to even better advantage when x, y, z are plotted upon their velocity diagram.

COMPANION TO α HERCULIS

This star, hereafter referred to as B, was found from measures of the first two plates to have a variable radial velocity. It is the companion to α Herculis, hereafter designated A, whose spectral class is Mb and whose magnitude varies between 3.1 and 3.9, with a period that is uncertain if not irregular. In the visual pair no certain evidence of orbital motion has been found. Boss gives a proper motion for A of $0.''030$ and for B of $0.''032$. The magnitude of B is 5.4 and its spectral class F9, forming, with A, a striking visual pair, apparently red and blue. Their separation, $5''$, makes it easily possible to obtain a pure spectrum of the fainter star with either the 60-inch or 100-inch telescope, provided the seeing is good.

Table V contains the data for the twenty-eight spectrograms available for the orbit. A period of 51.6 days gave a satisfactory assemblage of the velocities about a single epoch and furnished a velocity-curve from which the following preliminary elements were derived:

---

[1] *Mt. Wilson Contr.*, No. 163, 1919; *Astrophysical Journal*, **49**, 179, 1919.

$P=51.6$ days $K=31.8$ km/sec.
$e=0.08$ $T=$ J.D. 2,422,467.13
$\omega=15^\circ.5$ $\gamma=-37.2$ km/sec.

TABLE V

OBSERVATIONS OF THE COMPANION TO α HERCULIS

Plate No.	Date	G.M.T.	Phase	Velocity	O−C
				km/sec.	km/sec.
C 60*....	1919 Sept. 10	15^h23^m	$2^d.010$	− 9.2	+5.4
66†....	19	15 58	11.034	−43.4	+2.2
114.....	Oct. 12	15 03	33.996	−36.2	+4.1
350.....	1920 Apr. 4	0 48	2.042	−18.6	−3.9
408.....	May 6	22 28	34.947	−33.3	+3.7
416.....	8	21 04	36.887	−29.0	+1.1
422.....	10	23 20	38.980	−25.0	−1.9
430.....	25	23 35	2.400	−18.5	−2.9
442*....	28	23 39	5.405	−28.3	−3.2
470‡....	June 5	23 48	13.411	−48.2	+5.0
477‡§...	7	21 10	15.301	−55.8	+2.5
508.....	July 3	15 55	41.083	−17.7	−0.9
519.....	5	19 24	43.227	−10.1	+1.5
527.....	7	16 27	45.104	−16.8	−8.3
539*....	23	15 55	9.493	−45.6	−5.5
γ9404*....	30	16 13	16.505	−64.9	−4.0
C 573.....	Aug. 2	15 27	19.473	−64.3	+0.9
γ9431*....	4	17 50	21.572	−68.0	−2.0
C 622.....	30	15 07	47.460	− 6.9	−0.1
C 627.....	31	15 08	48.460	− 0.8	+6.0
γ9514*....	Sept. 1	14 58	49.452	−11.4	−4.0
γ9531.....	3	16 15	51.506	− 3.0	+7.5
C 647‖....	5	15 04	1.867	−13.7	+0.5
C 664.....	25	15 17	21.876	−65.3	+0.7
γ9573.....	26	15 07	22.870	−67.4	−1.7
γ9581.....	27	14 42	23.852	−64.2	+0.8
γ9591.....	28	14 58	24.863	−65.5	−1.6
γ9616§....	Oct. 3	14 51	29.858	−58.0	−4.5

* Overexposed.
† Focus poor.
‡ Seed 23.
§ Strongly exposed.
‖ Somewhat underexposed.

Since the interval between the first and the last observation covers but seven revolutions of the binary in its orbit, it seemed best to derive a correction for the period from the least-squares solution, together with corrections to the other five elements. As the table shows, *B*, which is really a very bright star for the one-prism spectrograph and 100-inch telescope, has given in several cases overexposed plates. It is assumed that the necessity of measuring upon such plates farther to the violet than usual has given the advantage of greater dispersion, which compensates for some falling off in focus. Hence all values of the radial velocity were given weight unity, and corrections derived from the set of six normal equations based upon the twenty-eight conditional equations. The resulting corrections proved to be moderate in size and effected a reduction of 25 per cent in the value of Σpv^2.

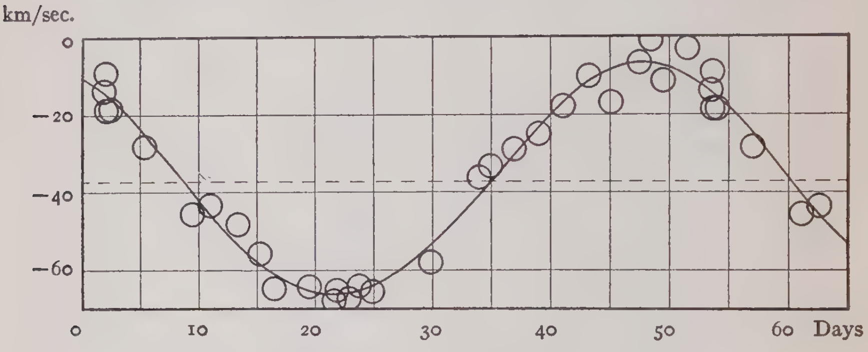

FIG. 4.—Velocity-curve of companion to α Herculis

Hence they have been adopted as final and with their probable errors are to be found below:

$P = 51.590 \pm 0.002$ days

$e = 0.028 \pm 0.026$

$\omega = 27\overset{\circ}{.}89 \pm 19\overset{\circ}{.}3$

$K = 29.64 \pm 0.77$ km/sec.

$T = \text{J.D. } 2{,}422{,}468.581 \pm 3\overset{d}{.}030$

$\gamma = -37.2$ km/sec.

$$\frac{m_1^3 \sin^3 i}{(m+m_1)^2} = 0.1395 \odot$$

$a \sin i = 2{,}102{,}700$ km

The probable error derived for a determination of velocity of weight unity is ±2.85 km/sec.

Attention is called to the fact[1] that the radial velocity of *A* is −32.2 km/sec., whereas that for the center of mass of *B* as here determined is −37.2 km/sec., showing a difference which disappears almost entirely if the velocity of A is corrected by an amount equal to the difference of Campbell's K-terms for the spectral classes of the two components, as Professor Russell kindly suggested to me. The radial velocity of A then becomes about −36.5 km/sec. These velocities and the proper motions of A and B are good evidence of physical connection between them. A previous statement to the contrary was ill considered even if the velocity of A were accepted unmodified, as has been pointed out in *Nature*, June 2, 1921.

---

[1] *Lick Observatory Bulletin*, 7, 113 (No. 229), 1913.

Coblentz'[1] radiometric measures of *B* led Burns[2] to conclude that light from *A* was probably involved in the measurement. This seems very probable in view of experience with the 100-inch and 60-inch telescopes whose focal lengths, in Cassegrain form, give a much greater linear separation of *A* and *B* in the focal plane than would be the case with the Crossley reflector used in Newtonian form. It may be pointed out, however, that the only indication of spectral class available to Coblentz, viz., the designation as a "blue" star, is not borne out by the spectrum, which is F9, hence the star is approximately "yellow." Although it is certain that the secondary member of the spectroscopic binary is photographically at least one magnitude fainter than the primary, for the spectrum is not recorded, its spectral class may be such as to help account for the discrepancy in Coblentz' measures.

205 DRACONIS

This binary is evidently the brighter component of the visual double β 971. The fainter component is of magnitude 8.5. Burnham says "it, β 971, is certainly a binary and in rapid motion. . . . . The measures indicate that the plane of the orbit is nearly in the line of sight. The period will probably be short." The last observation reported by him in which the two stars were resolved is by Aitken:

1905.29 p.a. 26°.6 dist. 0".37.

Thirty spectrograms were obtained between August 22, 1918, and November 14, 1919. The data are in Table VI. Both spectra show lines when the difference in velocity is sufficient, but the lines are so poor that considerable uncertainty attaches to the measured velocities, a difficulty increased at times by the blending of lines of the two spectra. Observations upon successive nights considered in connection with the results for pairs of plates upon the same night led to a trial of periods around four days. $P=3.76468$ days was found to represent the observations best and was adopted as final. When all the observations had been gathered about a single epoch with this period, the two resulting velocity-curves led to the following preliminary elements:

---

[1] *Lick Observatory Bulletin*, **8**, 104 (No. 266), 1914.

[2] *Publications of the Astronomical Society of the Pacific*, **27**, 110, 1915.

$P=3.76468$ days $K=96.5$ km/sec.
$e=0.10$ $K_1=102.5$ km/sec.
$\omega=166°$ $T=$ J.D. 2,422,161.597
$\omega_1=346°$ $\gamma=-14.0$ km/sec.

TABLE VI

OBSERVATIONS OF 205 DRACONIS

PLATE NO.	DATE	G.M.T.	PHASE	VELOCITY		O−C	
				Primary	Secondary	Primary	Secondary
				km/sec.		km/sec.	
γ7239...	1918 Aug. 22	18^h37^m	$0^d.299$	+ 83.9	−112.4	+16.9	− 7.3
7376...	Sept. 20	18 41	2.948	−23.3		(−24.7)	(+15.8)
7385...	21	17 50	0.149	+ 87.0	−116.0	+11.1	− 1.9
7395...	22	17 50	1.149	−15.1		(+36.9)	(−29.7)
7404...	23	17 01	2.115	−109.2	+ 77.1	0.0	+ 4.9
7523...	Oct. 26	15 05	1.154	−25.8		(+27.0)	(−41.2)
8328*..	1919 July 3	20 22	2.904	+ 28.7	− 53.7	(+34.4)	(−21.7)
8354...	9	23 17	1.495	− 83.6	+ 56.4	+13.2	− 3.3
8374...	13	18 22	1.525	−109.1	+ 79.4	− 9.5	+16.9
8411...	17	16 57	1.702	−111.0	+ 72.8	+ 1.1	− 2.3
8416...	17	23 39	1.981	−122.9	+ 88.7	− 7.7	+10.5
8417†..	18	16 50	2.697	− 68.1	+ 23.4	(−28.8)	(+21.6)
8435...	19	16 45	3.694	+ 60.6	−111.3	−17.6	+ 5.1
8438...	19	21 36	0.131	+ 83.9	−117.9	+ 7.3	− 3.1
8441...	Aug. 2	16 27	2.622	−27.2		(+23.8)	(−40.8)
8444...	2	21 22	2.827	−21.7		(− 3.5)	(− 2.3)
8447...	3	16 14	3.615	+ 77.4	−110.4	+ 1.5	+ 3.6
8458‡..	4	16 19	0.852	+ 15.7	− 56.0	(+20.0)	(−22.6)
8462...	4	21 55	1.085	−14.0		(+28.0)	(− 9.4)
8467...	5	15 55	1.835	−103.5	+ 77.1	+12.7	− 2.1
8471...	5	21 40	2.075	−117.9	+ 76.0	− 6.4	+ 1.5
8703...	Sept. 12	15 35	2.172	− 93.3	+ 42.7	+12.0	−25.5
8765§..	Oct. 11	15 13	1.042	− 51.5	+ 16.7	(−16.3)	(+19.0)
8776...	12	15 23	2.049	−111.3	+ 66.5	+ 1.4	− 9.2
C 118...	13	15 28	3.052	+ 29.8	− 55.7	+12.2	− 0.3
γ8786...	14	15 18	0.281	+ 63.7	−113.3	− 4.7	− 6.8
C 156‖..	Nov. 1	15 55	3.248	+ 35.3	− 83.5	− 9.5	− 0.7
171...	4	15 44	2.476	− 91.0	+ 44.2	−18.7	+ 9.1
210‖..	13	15 10	0.158	+ 76.5	−118.0	+ 1.0	− 4.3
215¶..	14	14 35	1.134	− 50.9	+ 15.2	(− 1.2)	(+ 2.9)

* First measured as single spectrum; vel. −10.1 km/sec.

† First measured as single spectrum; vel. −11.9 km/sec.

‡ First measured as single spectrum; vel. −22.0 km/sec.

§ First measured as single spectrum; vel. −15.6 km/sec.; Seed 23.

‖ Seed 23.

¶ First measured as single spectrum; vel. −18.6 km/sec.; Seed 23.

In deriving the corrections to the elements by the method of least squares only those spectrograms were used, nineteen in all, upon which both spectra had been measured. These were given equal weight and combined into twelve normal places which resulted in twenty-four conditional equations of the form given by Harper.

The correction found for e reduced it to zero, thus giving a circular orbit in which of course ω and T are arbitrary. The time of maximum positive velocity for the primary was adopted for T.

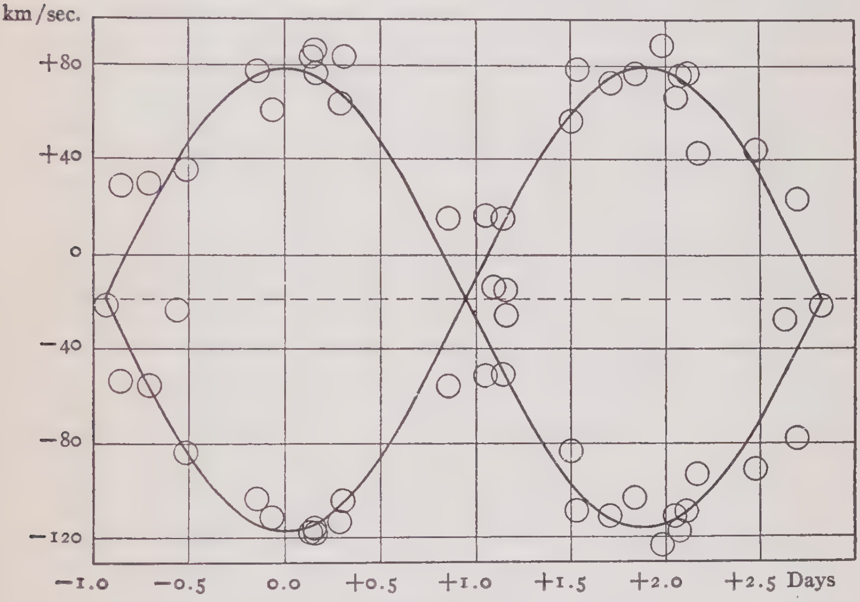

FIG. 5.—Velocity-curves of 205 Draconis

Since some of the corrections were rather large, a second least-squares solution, based upon the circular elements, was made. The quantity, Σpv^2, for the final elements is about 25 per cent of the value it had for the preliminary elements. The preliminary elements of this binary are somewhat less accurate than was the case for the others. Corrected as indicated by the two solutions they gave the following elements and probable errors:

$P=3.76468$ days
$K=97.7\pm2.0$ km/sec.
$K_1=98.3\pm2.0$ km/sec.
$T=$ J.D. $2,422,159.7691\pm0^{d}0178$
$\gamma=-18.8$ km/sec.

$a \sin i=5,058,000$ km
$a_1 \sin i=5,089,000$ km
$m \sin^3 i=1.48 \odot$
$m_1 \sin^3 i=1.47 \odot$

The probable error of a velocity of unit weight derived from the nineteen spectrograms whose spectra are separated is ±4.5 km/sec. In the table of observations the residuals for those plates which did not contribute to the normal places have been placed in parentheses. It will be seen from the velocities or from the remarks that in all cases they were first measured as single spectra. Later it was found that by going to the extreme violet end of the spectrum the increased dispersion gave some material for the velocities of both components, but in a region that has already departed from good focus. These measures have been given in the velocity columns, but the residuals indicate their relative inferiority.

The intensities of the absorption lines for the two components were so little different that they could not be used as a reliable criterion of phase. The results for K and K_1 and the similarity of the spectra are in accord with this lack of difference in intensity.

If Burnham's conclusion that the plane of the orbit of the visual double is nearly in the line of sight is correct, and if the inclination of the spectroscopic orbit should be nearly the same, this binary would be a favorable case to examine for variability caused by eclipse. The large amplitudes K and K_1 are likewise favorable to this possibility.

BOSS 5591

Table VII contains the data for the nineteen spectrograms which form the material for deriving the orbit. Sixteen of these gave velocities for both components. The phase could not be determined with certainty from differences in the intensities of the spectral lines of the two components, which seem to be identical in spectral class A9. As in the case of 205 Draconis, plates on successive nights, combined with pairs upon the same night (the latter to be sure that the period was not less than a day), resulted in a choice of 3.74860 days as best for grouping the observations about a single epoch. Preliminary elements were obtained as follows:

$P=3.74860$ days
$e=0.175$
$\omega=89\overset{\circ}{.}2$
$\omega_1=269\overset{\circ}{.}2$

$K=97.8$ km/sec.
$K_1=98.0$ km/sec.
$T=$ J.D. 2,422,175.243
$\gamma=+0.3$ km/sec.

In correcting the preliminary elements only the velocities from plates showing both spectra were used, sixteen in all. The period was assumed to need no correction. Three pairs of plates, taken in each case at nearly the same time and at favorable parts of the orbit, furnished three normal places. Otherwise each plate furnished a conditional equation for both primary and secondary star. All plates used were given unit weight.

Although corrections to the preliminary elements were twice derived by the method of least squares applied to the twenty-six conditional equations, the corrections from the second solution were so small that the elements adopted as final and their probable errors are based upon the results of the first solution. These are:

TABLE VII

OBSERVATIONS OF BOSS 5591

PLATE NO.	DATE	G.M.T.	PHASE	VELOCITY		O−C	
				Second.	Prim.	Second.	Prim.
				km/sec.		km/sec.	
γ 7408.....	1918 Sept. 23	$19^h 11^m$	$0^d.524$	− 63.4	+65.7	+12.9	−17.7
7577.....	Nov. 21	15 10	3.128	+ 94.7	−81.0	− 5.1	+ 9.1
7594.....	22	16 14	0.423	− 81.3	+81.4	−15.9	+ 8.7
7626.....	Dec. 13	15 16	2.641	+ 68.4	−77.4	− 6.4	−11.9
7636.....	14	14 55	3.627	+ 31.8	−33.9	−13.8	+ 2.8
7643.....	15	15 02	0.882	− 98.2	+97.8	−12.3	+ 4.9
8365.....	1919 July 11	23 14	3.051	+104.3	−86.4	+ 5.1	+ 3.2
8376.....	13	21 55	1.247	− 74.2	+76.0	− 8.2	+ 2.6
8413.....	17	20 38	1.445	− 50.0	+65.6	− 1.0	+ 8.9
8437.....	19	19 45	3.408	+ 94.5	−82.0	+11.9	− 8.9
8443.....	Aug. 2	19 57	2.421	+0.2			
8451.....	3	19 50	3.417	+ 87.1	−85.8	+ 5.7	−13.8
8456.....	4	0 05	3.594	+ 59.9	−52.5	+ 7.7	− 9.2
8460.....	4	20 06	0.680	− 76.3	+95.6	+ 9.1	+ 3.2
8469.....	5	18 40	1.620	+5.0			
8473.....	6	0 12	1.859	−0.4			
C 119*....	Oct. 13	16 22	3.041	+105.4	−80.0	+ 6.2	+ 9.5
123*....	14	16 56	0.326	− 50.8	+66.3	+ 0.2	+ 7.8
129*....	15	16 46	1.316	− 49.3	+60.7	+11.3	− 7.2

* Seed 23.

$P=3.74860$ days
$T=$ J.D. $2{,}422{,}175.1577 \pm 0^d.0880$
$e=0.189 \pm 0.021$
$\gamma=+4.2$ km/sec.
$\omega_1=82^\circ.66 \pm 9^\circ.00$
$a_1 \sin i=4{,}728{,}000$ km
$\omega=262^\circ.66 \pm 9^\circ.00$
$a \sin i=4{,}662{,}000$ km
$K_1=93.2 \pm 2.8$ km/sec.
$m_1 \sin^3 i=1.17 \odot$
$K=92.1 \pm 2.8$ km/sec.
$m \sin^3 i=1.19 \odot$

Attention is called to the fact that in giving the final elements, the order is the same as for the preliminary elements, but the subscripts have been changed, because the corrections to the elements have interchanged the two stars in respect to the semi-amplitudes, K and K_1, and hence to their masses.

Substitution of the unknowns derived from the first solution in the conditional equations gives residuals in substantial agreement with those derived from the final elements. Σpv^2 is 64 per cent of its value for the preliminary elements. The probable error of a velocity of unit weight for either component, on the basis of all residuals for plates with double spectra, is ±6.4 km/sec. This is larger than that for either of the other two spectroscopic binaries showing double lines, and is to be accounted for in part by the fact that all plates were given unit weight. The spectral class is somewhat earlier than that of the others, which involves a greater uncertainty in the measures.

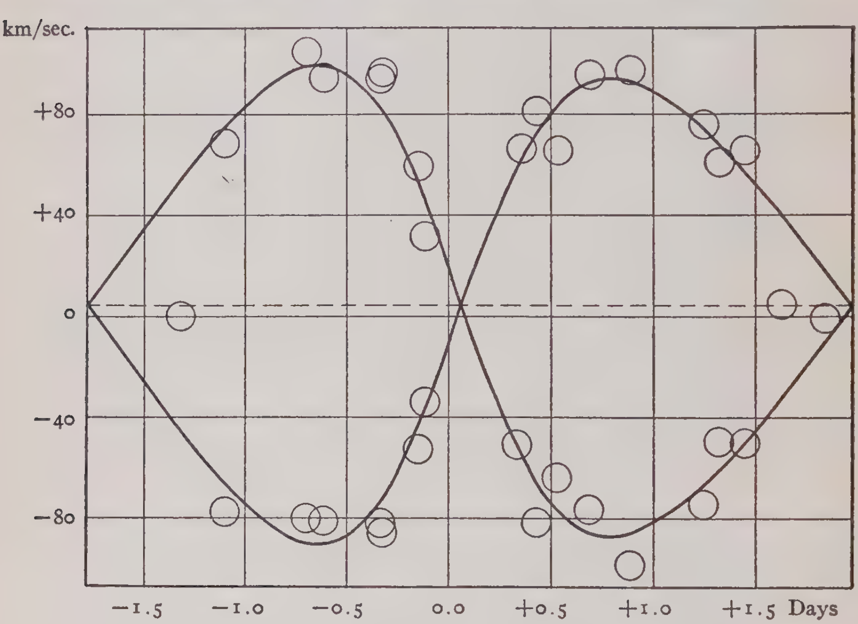

Fig. 6.—Velocity-curves of Boss 5591

LALANDE 46867

This spectroscopic binary shows only the spectrum of a single star of class K2 from which the absolute magnitude derived is +6.0. The twenty-five spectrograms available are listed in Table VIII. The velocity-curve, which proved satisfactory when all observations were assembled around a single epoch with $P=6.7217$ days, yielded the following preliminary results:

$P=6.7217$ days $\quad K=+39.2$ km/sec.
$e=0.08$ $\quad T=$ J.D. 2,422,220.768
$\omega=20\overset{\circ}{.}5$ $\quad \gamma=-20.2$ km/sec.

Plate γ9492, for which the preliminary elements give a residual far larger than for any other plate in the table and which was found to be in poor focus except in the region of the H and K lines, was omitted from the least-squares solution but retained in the table because the velocity derived from the emission lines H and K, to be referred to later, agrees fairly well with the velocity computed from the elements. The twenty-four remaining plates were given equal weight and the period was assumed to be known with the requisite accuracy, since the interval between the first and last spectrograms corresponds to one hundred and seventy-nine revolutions of the binary in its orbit. When the remaining five elements had been corrected by the method of least squares, the new elements were found to decrease the quantity Σpv^2 by only 3 per cent. Therefore, as so corrected, they are adopted as final and are given below with their probable errors:

$P=6.7217$ days $\quad \gamma=-19.8$ km/sec.
$e=0.059\pm0.019$ $\quad \frac{m_1^3 \sin^3 i}{(m+m_1)^2}=0.0125\odot$
$\omega=18\overset{\circ}{.}6\pm16\overset{\circ}{.}3$
$K=38.5\pm0.76$ km/sec. $\quad a \sin i=3,552,300$ km
$T=$ J.D. $2,422,220.7403\pm0\overset{d}{.}3005$

The probable error for a single determination of velocity of weight unity is ±2.8 km/sec.

Plate γ9671, obtained by Mr. Hoge on a partly cloudy night, is very strongly exposed and was noticed by him to have two emission lines in the violet. These proved to be H and K of calcium superposed upon their usual broad absorption lines. Thereafter an effort was made to expose plates strongly enough to show this feature of the spectrum. By using earlier plates which upon second examination showed this feature, velocities from these two emission lines were secured from twelve plates in all. They are listed in a separate column in Table VIII and placed in parentheses whenever they are derived from plates on which these lines are extremely feeble. Judging from the better-exposed plates, the H and K emission lines yield the same velocities as the lines of the absorption spectrum. No satisfactory measures of the H and K absorption lines could be made.

TABLE VIII

Observations of Lalande 46867

Plate No.	Date	G.M.T.	Phase	Velocity Abs. Lines	Velocity H and K	O−C Abs. Lines
				km/sec.	km/sec.	km/sec.
γ6036	1917 July 31	$23^h 28^m$	$0^d.916$	−11.1	....	− 3.3
6367	Nov. 23	16 38	1.401	−25.5	....	− 1.0
6499	Dec. 29	15 01	3.725	−46.5	....	+ 2.3
7214*	1918 Aug. 17	23 39	6.548	+28.5	....	+ 7.9
7271	27	22 47	3.067	−55.0	....	+ 1.0
7410	Sept. 23	21 10	3.114	−53.0	....	+ 2.9
8722*	1919 Sept. 14	22 40	2.927	−60.5	....	− 4.4
C 555	1920 July 27	20 36	3.921	−49.7	....	− 5.0
γ9434	Aug. 4	22 33	5.278	− 4.2	....	− 2.6
9492†	28	21 18	2.340	−36.7	−46.4	+14.0
9504	29	23 25	3.440	−48.6	(−62.4)	+ 4.6
C 626	31	0 13	4.463	−33.5	....	− 4.0
C 630	31	23 10	5.418	+ 5.9	....	+ 2.9
γ9518‡	Sept. 1	21 26	6.357	+15.4	+13.3	− 5.5
C 665	25	16 27	3.252	−58.1	....	− 3.0
γ9578	26	20 21	4.415	−27.9	....	+ 3.1
9587	27	21 00	5.442	+ 8.6	(+ 6.0)	+ 4.9
9595	28	19 43	6.389	+20.6	(+25.9)	− 0.3
9671	Oct. 26	19 01	0.750	+ 4.2	+ 2.1	+ 4.5
9678	27	20 15	1.802	−39.4	−29.6	− 1.5
9680	28	16 45	2.656	−55.0	−57.7	− 0.2
C 738	31	19 31	5.772	+ 9.7	+ 9.3	− 3.2
C 743	Nov. 1	17 32	6.689	+18.2	+ 7.7	− 1.1
γ9734	21	16 25	6.478	+18.8	+20.2	− 2.1
C 774	23	19 19	1.876	−35.8	(−34.6)	+ 4.2

* Underexposed.

† Best focus around H and K. Plate not used in least-squares solution.

‡ Focus poor.

In general the absorption lines of Lalande 46867 seem to be less sharp than for the general run of stars of spectral class K2.

The spectroscopic binary σ Geminorum, spectral class G9, abs. mag. +1.1,[1] has been noted both by H. M. Reese,[2] who announced its variable velocity, and by Harper,[1] who published its orbit, to have abnormally fuzzy lines. Schwarzschild[2] reports having observed H and K emission lines in objective-prism spectrograms of σ Geminorum. A plate of this star obtained by Mr. Duncan for the writer showed emission lines H and K but, relatively to the adjacent continuous spectrum, these were weaker than in Lalande 46867. The velocity derived from the emission lines was in close agreement with that for the absorption lines and agreed as well as could be expected with the velocity computed from Harper's elements. Hence these stars present several points of similarity: (*a*) spectral class; (*b*) character of absorption; (*c*) presence of emission lines for H and K; and (*d*) the fact that both are spectroscopic binaries with eccentricities smaller and periods shorter than the average for binaries of this spectral class. There is a notable difference in the absolute magnitude (σ Geminorum, +1.1, Lalande 46867, +6.0), associated with emission lines which are stronger relatively to the continuous spectrum in the case of the absolutely fainter star.

---

[1] *Mt. Wilson Contr.*, No. 142; *Astrophysical Journal*, **46**, 313, 1917.

[2] *Lick Observatory Bulletin*, **2**, 29 (No. 31), 1903.

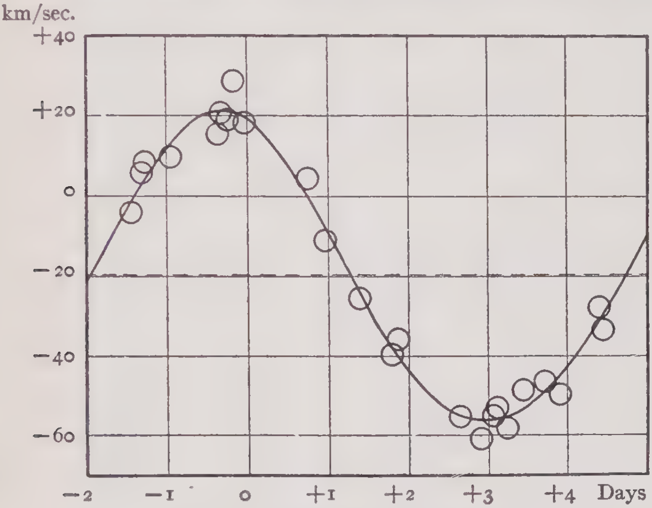

FIG. 7.—Velocity-curve of Lalande 46867

MOUNT WILSON OBSERVATORY
October 1920

---

[1] *Publications of the Royal Astronomical Society of Canada*, **5**, 200, 1911.

[2] *Astrophysical Journal*, **38**, 292, 1913.

Contributions from the Mount Wilson Observatory, No. 202
Reprinted from the *Astrophysical Journal*, Vol. LIII, 260–299, 1921

WAVE-LENGTHS OF LINES IN THE IRON ARC FROM GRATING AND INTERFEROMETER MEASURES λ 3370–λ 6750

By CHARLES E. ST. JOHN and HAROLD D. BABCOCK

ABSTRACT

Wave-lengths of iron-arc lines from λ3370 to λ6750; grating and interferometer measurements.—To avoid errors due to pole-effect a 12-mm, 5-amp. Pfund arc was used. This arc has also the advantage of yielding very sharp lines. To eliminate instrumental errors, spectrograms made with two Michelson and three Anderson gratings and with four pairs of interferometer plates were compared. Table III contains the mean *results for 1026 lines*, of which 976 were measured on each of from 1 to 62 grating spectrograms and 576 on each of from 1 to 39 etalon spectrograms. The agreement shown indicates that for most of the lines the weighted mean wave-length is accurate to 0.001 A. In the case of 250 stable lines, the agreement with Bureau of Standards measurements is good. But for 46 lines of groups *c*5 and *d*, the Bureau measurements are systematically greater, the mean difference being 0.007 A, due to *pole-effect in the 6-mm, 6-amp. arc.* Of 78 *International Secondary Standards* measured with the interferometer, 62 stable lines came out as follows: 53 within ±0.001, 8 within ±0.002, 2 within ±0.003, and 1 within 0.004 A of the adopted values; while in the case of 16 lines belonging to groups *c*5 and *d*, the International values are systematically greater, the mean difference being 0.007 A, due to pole-effect in the arcs used in the original determinations. Evidently these sources had the same order of pole-effect as the 6-mm, 6-amp. arc. *Ghosts and reversals* gave the same wave-lengths as those obtained from fine lines produced in the core of a lean arc. A comparison of readings from long and short exposures of the same lines showed no *intensity effect* in the case of interferometer measurements.

Spectroscopic measurements.—(1) *Method of reduction of interferometer spectrograms.* The elimination of a gauge plate over the slit and the introduction of a plate constant, $K\lambda$, which may be determined from measurements of the ring diameters alone, greatly reduce the labor of measurement and reduction, without decreasing the precision. (2) *Comparison of grating and interferometer.* The advantages and disadvantages of each are discussed.

I. INTRODUCTION

In a previous paper[1] we discussed the influence of pole-effect in the iron arc upon the measurement of the wave-lengths of certain lines in the lists of adopted secondary and suggested tertiary standards. It was shown that the arc 6 mm in length, carrying a current of 6 amperes, adopted at the Bonn meeting of the International Union for Co-operation in Solar Research, gave a pole-effect of +0.006 A even in its central plane, and that the wave-lengths of the secondary standards belonging to groups $c5$ and d were affected to approximately the same amount. This has been confirmed in the present investigation.

---

[1] *Mt. Wilson Contr.*, No. 137; *Astrophysical Journal*, 46, 138, 1917.

In the *Report of the Committee on Standards of Wave-Length* adopted at the Washington meeting of the American Section of the International Astronomical Union[1] the source to be used in the determination of iron standards of wave-length is defined as "the Pfund arc operated between 110 and 250 volts, as convenient, with 5 amperes or less, at a length of 12 millimeters, and used over a central zone at right angles to the axis of the arc not to exceed 1¼ millimeters in width." Under these specifications the iron arc yields wave-lengths that appear to be free from pole-effect and is easily workable for wave-lengths shorter than 6000 A. For longer wave-lengths the time of exposure is excessive and pole-effect is not entirely eliminated.

The committee also recommended that independent measurements be made with the grating and with the interferometer, "on the ground that the errors of these two instruments are largely complementary." In the determinations carried out by us, both methods have been employed.

II. APPARATUS AND METHODS

The apparatus used for the interference observations is in the main the same as that described in a previous paper.[2] It is now permanently installed in a double-walled, wooden case with convenient arrangements for projecting the light into it. Various etalons have been used, the plates being either of fused quartz or glass, and the separators of invar or fused quartz. The thickness varied from 2.5 mm to 15 mm; most of the photographs were taken with etalons of 5, 7.5, or 10 mm. The rings were projected upon the slit by a concave mirror having a focal length of 633 mm. No thermostat was used in connection with the interference apparatus, as efficient protection from temperature changes was afforded by the housing. On the longest exposures no loss of definition can be observed, and the results from these plates show no systematic deviations from those yielded by short exposures. The interferometer plates were several times resilvered by cathodic deposition. On account of the different ratio between its reflection and transmission coefficients, gold was occasionally used for one of the reflecting surfaces. The phase-change corrections have been evaluated in the usual manner by plotting the differences between observed and known wave-lengths for the standards occurring upon each plate. The correction-curves have always been straight lines. No correction for atmospheric dispersion has been applied, since the standards are distributed throughout the extent of each region photographed.

---

[1] *Proceedings of the National Academy of Sciences*, **6**, 367, 1920.

[2] *Mt. Wilson Contr.*, No. 137; *Astrophysical Journal*, **46**, 138, 1917.

Careful attention has been given throughout the investigation to the adjustment of each part of the apparatus, and no difficulty has been experienced from mechanical disturbances. The etalon was so located with respect to the mirror which projects the rings upon the slit as to bring an image of its diaphragm into focus upon the grating, in accordance with the remark of Buisson and Fabry in their important paper.[1] Furthermore, the size and shape of the diaphragm were so chosen that its image was much smaller than the grating, and the slit-width was so adjusted that diffraction never widened the image beyond the lateral boundaries of the ruled surface. These precautions and the use of large apertures in the projecting systems insured uniform illumination *upon the photographic plate* of several more rings for each line than were actually used for measurement.

As indicated in the paper already referred to, the method of reduction employed at Mount Wilson for interferometer plates is not the same as that described by Buisson and Fabry, Pfund,[2] Burns,[3] and others. These observers derived the fractional order of interference by means of an equation of the form

$$\epsilon=\frac{p\theta^2D^2}{8L^2},$$

---

[1] *Journal de physique*, **7**, 169, 1908.

[2] *Astrophysical Journal*, **28**, 197, 1908.

[3] *Bulletin of the Bureau of Standards*, **12**, 179, 1915.

where

ϵ=fractional order of interference for the ring whose linear diameter is D.
θ=angular distance of standard gauge marks in front of the slit, as seen from lens which projects the rings on the slit.
L=linear distance of photographed gauge marks for the same spectral line.
p=order of interference at center of ring system.

This requires, in addition to the photograph of the interference pattern, an exposure to the spectrum with the etalon removed and the gauge plate inserted in front of the slit, from which the value of L is obtained. The quantity θ has also to be determined from independent observations.

A simple transformation of this equation, however, makes possible a marked saving in labor and offers other advantages which are referred to below. If we define by m the magnification of the spectrograph for a given spectral line, and let F be the focal length of the lens or mirror which projects the rings upon the slit, it is readily seen that in the equation above θ^2/L^2 may be replaced by $1/m^2F^2$, giving

$$\epsilon=\frac{pD^2}{8F^2m^2}$$

or more generally, for the n^{th} ring, counting the innermost as the first,

$$n-1+\epsilon=KD_n^2\,,$$

where K is written for $p/8F^2m^2$. It is evident that both ϵ and K may be determined from this equation if two diameters are measured. For any two consecutive rings, for example the first and second, it is seen that

$$K\lambda=\frac{\lambda}{D_2^2-D_1^2}\,.$$

An increase in accuracy may be obtained, however, if the condition is imposed that m be constant for all spectral lines upon the plate. If e is the thickness of the etalon,

$$K\lambda=\frac{p\lambda}{8F^2m^2}=\frac{2e}{8F^2m^2}\,,$$

which is a constant for the plate considered. The determination of this plate-constant and its application to the problem will be understood from a description of the procedure followed.

Two measurements in reverse directions are made upon the diameters of each of the first two rings for every line upon the plate, except when the fractional order of interference is judged to be less than 0.3, in which case the measures are made upon the second and third rings instead. The two observations upon each diameter are then averaged, and the rough value of the wave-length is divided by the difference of the squares. The number thus derived, in which only four significant figures are retained, is a value of the plate-constant, $K\lambda$, the accuracy of which is then increased as desired by using a sufficient number of lines. The refined value of the plate-constant, divided by the rough wave-length and multiplied by the square of a ring diameter, yields the fractional order directly. The two fractional orders thus obtained from the two rings measured are averaged to produce the final fractional order. In practice it is found that the probable error of a single determination of the plate-constant is about 0.6 per cent, from which it follows that the mean of 35 or 40 values will have a probable error of one part in one thousand, the accuracy aimed at in these measurements. It may be remarked that no systematic difference appeared in the fractional orders yielded by individual rings for the same line.

The assumption of constant magnification in the spectrograph over the field used, while not rigorously true, is found in practice to be permissible in the case of the apparatus employed for this work and also for a plane-grating spectrograph of the Littrow type having a glass lens of 18 feet focal length. An extreme case is found in a quartz spectrograph wherein the normal to the photographic plate stands at an angle of 65° with the optical axis of the camera lens. In the ultra-violet the magnification for this instrument varies as the square root of the wave-length, and the plate-constant is $K\lambda^2$ instead of $K\lambda$. In general the method can be applied without difficulty for any type of spectrograph by a slight modification of the procedure described above.

In the course of the present investigation many determinations of the plate-constants have been made. It has been found that for the same adjustments of the spectrograph, $K\lambda$ for different plates is constant within the errors of observation when the etalon is the same, and that etalons of different thickness give plate-constants in the ratio of the thicknesses, as indicated by the equation above.

Furthermore, it may be pointed out that, when the interference rings are projected by a concave mirror upon the slit of a spectrograph of the type used for this work, it is easy to derive a fundamental instrument-constant from which the plate-constant, $K\lambda$, may be obtained directly from a knowledge of the setting of the spectrograph camera. As indicated above, however, the practice followed in this investigation has been to determine $K\lambda$ from each plate, in which case the instrument-constant serves as a valuable check.

An application of the laws of propagation of errors to the two equations stated above for deriving the fractional order of interference shows that in general the probable error of ϵ is larger for the method of Buisson and Fabry than for the Mount Wilson method. This is to be expected from the fact that in the first method auxiliary quantities θ and L must be observed, the effect of whose probable errors can only be to increase the probable error of the result. A comparison of the results of our interferometer measurements with those of other observers, as well as with values derived from gratings, strengthens the conclusion that the method used by us for deriving fractional orders involves no sacrifice of accuracy as compared to the procedure usually adopted. Furthermore, the simplicity and directness which characterize the new method, the lessening of the necessary photographic and microscopic observations, and the additional numerical checks which become available through its use combine to lend it weight and emphasize its value.

In the region λ 3370–λ 5662 the interferometer plates were measured and reduced for the most part by two observers independently; the weighted means of their results are given in Table I. Over the region of longer wave-lengths most of the measuring was done by one of them, but nearly all of the lines tabulated were measured and reduced by a third observer upon a selected list of plates. A comparison of the results shows that the various observers are in excellent agreement, no systematic differences of any significance being found between them. It is probable that effects dependent upon personal equation are too small to influence the final values.

The grating measures include only the stable lines from the list published by St. John and Ware,[1] but cover all the lines in the two new series of plates. The old series by St. John and Ware, λ 4118–λ 6500, was taken with the 30-foot Littrow spectrographs on Mount Wilson and in Pasadena, for which Michelson plane gratings with available ruled surfaces 37×114 mm were used in the second-order; scale, 0.88 A per mm. In the new laboratory series the 15-foot concave-grating spectrograph[2] was used in the third order for the region λ 3370–λ 4200. The grating, made by Anderson, has a ruled surface 50×106 mm; scale as used, 1.25 A per mm. From λ 4100 to λ 5658 the 30-foot Littrow spectrograph with an Anderson grating, ruled surface 63×72 mm, was used in the second order; scale, 0.88 A per mm. The new mountain series, λ 3600–λ 5500, was taken with the 30-foot spectrograph of the 60-foot tower telescope. The second order was employed; scale, 0.88 A per mm. The grating, ruled surface 114×160 mm, was made by Anderson and loaned by the Physical Laboratory of the Johns Hopkins University.

The comparators used were constructed in the observatory shop; the screws have been tested and found satisfactory. The standard measuring machines have screws 20 cm long; one specially designed machine with a screw 50 cm long furnished an excellent means for adjusting the reference lines, as its exceptionally long range allows the inclusion of many standards in a single run under constant conditions.

Two methods of reducing the grating data have been used. In one the interpolation between standards was made from a curve whose abscissae are the mean wave-lengths of adjacent secondary standards and whose ordinates are the scale-factors for the intervals. In the other, the wave-lengths were calculated from an empirical formula derived from three standards, of the form

---

[1] *Mt. Wilson Contr.*, No. 61; *Astrophysical Journal*, **36**, 14, 1912; *Mt. Wilson Contr.*, No. 75; *Astrophysical Journal*, **39**, 5, 1914.

[2] King, *Mt. Wilson Contr.*, No. 84; *Astrophysical Journal*, **40**, 205, 1914.

$$\lambda = a + bx + cx^2.$$

A curve of corrections was obtained for the deviations of the other standards from the calculated values.

III. THE REGIONS OF THE SPECTRUM COVERED

The interferometer measures extend from λ 3370 to λ 6750. The grating series cover the regions λ 3370–λ 5658 and λ 5975–λ 6500. The gap between λ 5658 and λ 5975, owing to the dearth of suitable standards in this region, is too wide to bridge with the grating. In both the grating and interferometer series all measurable lines were observed. The new laboratory series of grating plates were greatly varied in exposure time in order to obtain a wide range of line-intensity. When feasible, measurements were made upon lines reversed and unreversed and also upon clearly determined ghosts.

IV. SOURCES

For the region λ 3370–λ 6000 the interferometer photographs were taken from a horizontal zone, 1¼ mm wide, at right angles to the axis, of a 12-mm Pfund arc carrying 5 amperes or less. For the region λ 6000–λ 6750 the integrated light of a somewhat shorter Pfund arc was used, only stable lines being measured upon the plates.

In the early series by St. John and Ware no particular attention was at first given to the character of the arc, which in general was approximately 5 mm long, or to the portion from which the light was taken. For this reason only the wave-lengths of the lines not subject to pole-effect are retained. In the new grating series the wave-lengths are those given by a 12–14-mm arc with a current of 5 amperes. In the four grating series the wave-lengths of the stable lines are in excellent agreement. The wave-lengths of the lines showing pole-effect depend only upon observations made on the arc recommended by the American committee.

V. RESULTS

The wave-lengths with related data are entered in Table I. The third column gives the group and class. When both group and class are shown the allocation is taken from the paper by Gale and Adams.[1] When no entry appears, the line is practically free from pole-effect, but data are lacking for definite classification. Groups *c*5 and *d* contain all the lines with recognized positive pole-effect; as our data are insufficient to differentiate the two groups, the lines not in the list of Gale and Adams are provisionally assigned to the major group *d*. Lines with a negative pole-effect constitute group *e*.[2] An interrogation point indicates that the evidence for grouping is contradictory. "G" and "I" relate the remarks to grating and interferometer respectively. The dependence of the wave-lengths upon direct measurements, ghosts, or reversals is indicated by "direct," "g," and "r" in the corresponding combination. The other symbols are those suggested by Burns[3] and recommended in the *Report* of the American committee.[4] "A" indicates a probable error less than 0.0007 A; "B," 0.0007 A–0.0012 A, and "C," that the determination is poor; "h" = hazy; "l" = shaded to red; "v" = shaded to violet.

While the interferometer spectrograms were under the microscope, weights 1, 2, and 3 were assigned to the various lines, corresponding to poor, average, or excellent quality. This furnished the basis for combining the observations and also for grouping the final wave-lengths into three classes according to the total weights attached to them. The classes A, B, and C, equivalent to those recommended by the committee, have in general the following limits and numbers of lines:

A = weight from 10 to 159; number of lines 352.
B = weight from 4 to 9; number of lines 111.
C = weight from 1 to 3; number of lines 113.

---

[1] *Mt. Wilson Contr.*, No. 58; *Astrophysical Journal*, **35**, 10, 1912.

[2] St. John and Ware, *Mt. Wilson Contr.*, No. 75, p. 4; *Astrophysical Journal*, **39**, 8, 1914.

[3] *Lick Observatory Bulletin*, **8**, 29, 1913.

[4] *Proceedings of the National Academy of Sciences*, **6**, 367, 1920.

TABLE I

WAVE-LENGTHS OF LINES IN THE IRON ARC (λ 3370–λ 6750), INTERNATIONAL SYSTEM

λ		GROUP	GRATING		INTERFEROMETER		REMARKS
Grating	Interferometer		Plates	Probable Error	Plates	Probable Error	
3370.788	.788	......	8	A	5	B	
3378.684	......	......	7	A	......	......	
3379.022	......	......	8	B	......	......	
3380.115	......	......	8	B	......	......	
3382.409	......	......	6	B	......	......	
3383.697	......	......	6	A	......	......	
3383.982	.987	......	8	A	1	C	
3392.309	......	......	7	A	......	......	
3392.656	.656	......	10	A	2	C	
3394.595	.590	......	8	B	1	C	G, h
3396.980	.982	......	8	A	1	C	
3399.336	.337	......	12	A	8	A	
3401.520	.524	......	8	A	2	C	
3402.262	......	......	8	B	......	......	
3404.355	.351	......	3	C	4	B	G, v
3406.442	......	......	6	B	......	......	
3406.805	.803	......	8	A	1	C	
3407.464	.462	......	16	C	21	A	G, direct, g
3410.171	......	......	1	C	......	......	
3411.355	......	......	6	B	......	......	
3413.134	.135	......	12	A	12	A	
3415.537	......	......	7	A	......	......	
3417.	.274	*e?*	......	......	2	C	
3417.845	.845	......	12	A	14	A	
3418.508	.510	......	12	A	6	A	
3422.500	......	......	6	B	......	......	
3422.658	.665	......	8	A	3	C	Diff.>error
3424.287	.288	......	12	A	4	B	
3425.013	......	......	8	A	......	......	
3426.384	......	......	8	B	......	......	G, v
3426.638	......	......	8	A	......	......	
3427.003	......	......	6	A	......	......	
3427.123	.124	......	18	B	5	A	G, direct, g
3428.194	.197	......	8	A	6	A	⊙ Fe, Co
3431.816	......	......	1	C	......	......	
3440.611	.611	......	16	C	3	B	
3440.993	.988	......	12	B	3	C	Diff.>error
3442.673	......	......	7	A	......	......	
3443.881	.879	......	12	A	28	A	
3445.152	.152	......	12	A	13	A	

TABLE I—*Continued*

λ		Group	Grating		Interferometer		Remarks
Grating	Interferometer		Plates	Probable Error	Plates	Probable Error	
3445.763	......	*d*	1	C	......	......	
3447.282	.281	......	8	B	4	B	
3450.333	.331	......	8	A	5	A	
3451.	.629	......	......	......	1	C	
3451.917	.920	......	8	A	2	C	
3452.278	.281	......	8	A	1	C	
3453.023	......	......	6	A	......	......	
3458.305	......	......	6	A	......	......	
3459.915	......	......	6	A	......	......	
3461.	.654	......	......	......	2	C	
3462.	.354	......	......	......	1	C	
3465.866	.863	......	12	B	27	A	
3475.455	......	......	18	A	......	......	
3475.652	......	......	8	A	......	......	
3476.707	.706	......	11	B	27	A	
3476.854	......	......	5	A	......	......	
3483.008	.010.	......	6	A	1	C	
3485.340	.345	......	7	A	7	A	⊙ Fe Co
3489.667	.675	......	6	A	1	C	
3490.575	.576	......	17	B	26	A	G, direct, g
3492.	.959	......	......	......	5	B	
3495.286	.289	......	8	B	5	A	
3497.110	.111	......	7	B	1	C	G, l
3497.843	.843	......	11	A	29	A	G, direct, g
3500.563	......	......	1	C	......	......	
3506.499	.501	......	3	C	5	A	
3508.	.495	......	......	......	1	C	
3513.819	.820	......	18	B	30	A	
3515.	.056	......	......	......	3	B	
3521.264	.264	......	12	A	31	A	
3521.834	......	......	6	B	......	......	
3524.076	......	......	4	B	......	......	
3524.240	......	......	8	B	......	......	
3526.040	......	......	12	A	......	......	
3526.168	......	......	12	A	......	......	G, l
3526.378	......	......	8	B	......	......	
3526.466	......	......	8	A	......	......	
3526.674	......	......	8	B	......	......	
3527.793	.798	......	8	A	3	B	G, v
3529.821	.824	......	8	A	3	B	⊙ Fe–Co
3530.386	......	......	6	A	......	......	
3533.009	......	......	8	B	......	......	
3533.199	......	......	10	B	......	......	
3536.559	.559	......	12	A	14	A	
3537.492	......	......	1	C	......	......	

TABLE I—*Continued*

λ		Group	Grating		Interferometer		Remarks
Grating	Interferometer		Plates	Probable Error	Plates	Probable Error	
3537.730	......	......	6	A	......	......	
3537.897	......	......	8	A	......	......	
3540.126	.128	......	7	A	2	C	
3540.710	......	......	1	C	......	......	
3541.088	.088	......	12	A	20	A	
3542.080	.080	......	12	A	16	A	
3543.670	......	......	6	A	......	......	
3545.644	.641	......	8	A	4	B	
3547.204	......	......	1	C	......	......	
3549.869	......	......	1	C	......	......	
3552.837	.839	......	8	A	1	C	
3553.744	.747	......	8	A	1	C	
3554.122	.125	......	8	A	2	C	
3554.931	.928	......	16	A	22	A	Diff.>error
3556.889	.883	......	12	C	11	B	G, l, wgt very low; I, h
3558.522	.518	......	17	B	33	A	G, direct, g; diff.>error
3559.507	......	......	6	A	......	......	
3565.383	.381	......	16	C	23	A	G, h, direct, g
3565.584	......	......	8	A	......	......	
3568.978	......	......	6	A	......	......	
3570.103	.100	......	4	B	1	C	
3571.	.997	......	6	B	2	C	
3573.893	......	......	7	A	......	......	G, line on violet
3575.250	......	......	5	A	......	......	
3575.375	......	......	7	B	......	......	
3575.983	......	......	1	C	......	......	
3576.759	......	......	5	B	......	......	
3581.197	.196	......	6	A	18	A	G, r; I, r
3581.646	......	......	3	C	......	......	
3582.202	.201	......	7	A	1	C	
3583.338	......	......	5	B	......	......	
3584.664	.665	......	10	A	2	C	
3584.791	......	......	6	A	......	......	
3584.961	......	......	8	A	......	......	
3585.320	.322	......	5	A	10	A	G, g
3585.709	.710	......	15	B	1	C	G, direct, g
3586.114	......	......	8	A	......	......	
3586.987	.987	......	10	A	29	A	
3587.425	......	......	6	A	......	......	
3587.753	......	......	8	A	......	......	
3588.919	......	......	6	A	......	......	
3589.109	.106	......	10	B	2	C	
3589.455	......	......	8	A	......	......	
3594.636	.636	......	8	A	11	A	
3599.627	......	......	6	A	......	......	

TABLE I—*Continued*

λ		Group	Grating		Interferometer		Remarks
Grating	Interferometer		Plates	Probable Error	Plates	Probable Error	
3602.	.513	......	......	......	1	C	
3603.206....	.207	......	12	A	11	A	
3603.829....	......	......	3	C	......	......	G, l
3605.466....	.460	......	12	C	16	B	Diff.>error; I, h
3606.682....	.682	......	12	A	28	A	
3608.147....	......	......	6	A	......	......	
3608.862....	.861	*b*1	13	B	24	A	G, direct, g
3610.164....	.164	......	12	A	18	A	
3610.704....	......	......	1	C	......	......	
3612.074....	.073	......	8	A	4	A	
3612.941....	......	......	1	C	......	......	
3614.562....	......	......	1	C	......	......	
3616.573....	......	......	8	A	......	......	
3617.318....	......	......	6	A	......	......	
3617.790....	.789	......	12	A	9	A	
3618.393....	......	......	8	A	......	......	
3618.773....	.770	*b*1	6	A	22	A	G, g; I, r, direct
3621.465....	.463	......	18	B	13	A	
3622.009....	.009	......	15	B	11	A	
3623.190....	.188	......	11	B	5	A	
3625.	.148	......	......	......	4	A	
3630.353....	.354	......	6	A	1	C	
3631.104....	......	......	11	C	......	......	
3631.467....	.466	*b*1	6	B	22	A	G, g; I, r
3632.043....	.043	......	8	B	2	B	
3632.559....	......	......	11	B	......	......	
3632.980....	......	......	3	C	......	......	
3634.336....	......	......	11	B	......	......	
3636.996....	......	......	3	C	......	......	
3637.863....	......	......	3	C	......	......	
3638.300....	.300	......	23	A	14	A	
3640.392....	.392	......	23	A	21	A	
3643.628....	......	......	11	B	......	......	
3645.823....	......	......	15	A	......	......	
3647.428....	......	......	15	B	......	......	
3647.846....	.845	*b*1	4	B	22	A	G, r; I, r, direct
3649.305....	......	......	19	A	......	......	
3649.509....	.511	......	15	B	11	A	
3650.032....	......	......	15	C	......	......	
3650.281....	......	......	15	A	......	......	
3651.471....	.470	......	26	A	20	A	
3655.468....	.463	......	18	A	2	C	
3659.520....	.520	......	21	A	10	A	
3664.541....	......	*d*	6	A	......	......	
3667.265....	......	*d*	4	C	......	......	

TABLE I—*Continued*

λ		Group	Grating		Interferometer		Remarks
Grating	Interferometer		Plates	Probable Error	Plates	Probable Error	
3669.152	......	......	1	C	......	......	
3669.524	.524	......	10	A	9	A	
3670.	.072	......	......	......	1	C	
3674.	.767	......	......	......	1	C	
3676.313	.315	......	19	A	10	A	
3677.310	......	......	9	B	......	......	
3678.863	.865	......	11	A	1	C	
3679.916	.916	*a*1	10	B	32	A	G, g, r; I, r, direct
3682.226	.228	......	16	B	11	A	
3683.059	.059	......	12	A	7	A	
3684.113	.113	......	24	B	7	A	
3686.002	.001	*e*	23	B	7	A	
3686.261	......	......	1	C	......	......	
3687.101	......	......	15	B	......	......	
3687.460	.460	*b*1	8	B	32	A	G, g, r
3687.657	......	......	14	B	......	......	
3689.462	.463	......	18	B	11	A	
3690.731	.731	......	12	B	4	A	
3693.009	.009	......	19	C	14	A	
3695.055	.056	......	28	B	12	A	
3697.433	.433	*d*	16	A	6	A	
3698.613	......	......	5	C	......	......	
3699.149	......	......	2	C	......	......	
3701.091	.091	......	6	A	15	A	
3702.033	.037	......	14	A	1	C	
3702.502	......	*e*	2	C	......	......	
3703.558	......	......	9	B	......	......	
3703.699	......	*d*	10	C	......	......	
3703.826	......	......	9	C	......	......	
3704.465	.466	......	30	A	9	A	
3705.568	.568	*a*1	17	C	30	A	G, g, r; I, r, direct
3707.051	.051	......	20	A	3	B	
3709.251	.250	*b*1	26	A	30	A	
3709.537	......	......	4	C	......	......	
3711.227	.227	......	20	A	2	B	
3711.413	......	......	11	B	......	......	
3715.917	.914	......	7	B	3	B	
3716.449	.449	......	29	A	11	A	
3718.408	.410	......	20	A	1	C	
3719.939	.937	*a*1	23	A	23	A	G, r; I, r, direct
3722.030	......	......	2	B	......	......	
3722.564	.565	*a*1	18	A	31	A	G, direct, g, r; I, r, direct
3724.380	.380	......	8	A	18	A	
3725.500	......	......	1	C	......	......	
3726.929	......	*e*	18	A	......	......	

TABLE I—*Continued*

λ		Group	Grating		Interferometer		Remarks
Grating	Interferometer		Plates	Probable Error	Plates	Probable Error	
3727.098			22	A			
3727.622	.623	*b*1	10	A	30	A	G, g
3727.811			19	A			
3728.670			3	C			
3730.388	.391		19	A	1	C	
3730.947	.948		15	A	1	C	
3731.377	.375		13	A	1	C	
3732.400	.398		34	A	18	A	
3733.319	.321	*a*1	25	A	28	A	G, direct, g, r; I, r, direct
3734.870	.866	*b*1	13	A	19	A	Diff.>error; I, r, direct
3735.327			22	A			
3737.135	.134	*a*1	25	A	25	A	G, g, r; I, r, direct
3738.309	.309		20	A	9	A	
3739.122			2	B			
3739.529		*d*	15	A			
3740.248	.250	*d*	10	B	1	C	
3742.624	.622		5	B	1	C	
3743.365	.366	*b*1	41	A	32	A	G, direct, g
3743.470			3	B			
3744.108	.106	*e*	15	A	1	C	
3745.564	.562	*a*1	38	A	14	A	G, direct, g
3745.902	.904	*a*1	53	A	14	A	G, direct, g, r
3746.488			2	B			
3746.933		*e*?	18	A			
3748.264	.264	*a*1	49	A	22	A	G, direct, g, r; I, r, direct
3748.971		*e*	19	A			
3749.490	.489	*b*1	44	A	23	A	G, direct, g, r; I, r, direct
3751.061			3	C			
3751.822			2	C			
3752.422			2	B			
3753.156			2	C			
3753.615	.614		25	A	15	A	
3754.508		*e*	3	B			
3756.071			3	B			
3756.942	.941		17	A	2	B	
3757.461			6	B			
3758.238	.236	*b*1	48	A	22	A	G, direct, g, r; I, r, direct
3760.053	.054		24	A	12	A	
3760.534	.536		12	B	3	C	G, .524, h, v
3761.418			2	C			
3763.791	.791	*b*1	51	A	26	A	I, r, direct
3765.543	.543	*b*1	16	B	13	A	G, g near
3767.195	.195	*b*1	50	A	28	A	G, direct, g, r; I, r, direct
3768.	.032				1	C	
3773.701		*e*	1	C			

TABLE I—*Continued*

λ		Group	Grating		Interferometer		Remarks
Grating	Interferometer		Plates	Probable Error	Plates	Probable Error	
3774.827	.827	......	30	A	6	A	
3775.862	......	......	2	C	......	......	
3776.458	.458	......	20	A	6	A	
3777.063	......	......	1	C	......	......	
3777.450	......	......	6	B	......	......	
3778.511	......	......	8	A	......	......	
3778.699	......	......	4	B	......	......	
3779.488	.488	......	2	C	1	B	G, l
3781.189	.190	......	4	B	1	B	
3781.940	......	......	2	C	......	......	
3782.124	......	......	2	C	......	......	
3782.452	......	......	2	C	......	......	
3782.610	......	......	1	C	......	......	
3785.708	......	......	2	C	......	......	
3785.950	.949	......	34	A	5	A	
3786.178	......	......	11	C	......	......	
3786.679	.680	......	32	A	4	A	
3787.166	......	......	2	C	......	......	
3787.885	.885	*b1*	33	A	31	A	G, direct, r
3789.180	......	......	15	A	......	......	
3789.430	......	*d*	2	C	......	......	
3789.572	......	......	5	C	......	......	
3790.095	.097	......	33	A	16	A	
3790.658	......	......	3	C	......	......	
3790.758	......	......	10	B	......	......	
3791.506	......	......	3	C	......	......	
3792.158	......	......	7	B	......	......	
3793.480	......	......	9	B	......	......	
3793.874	......	......	11	C	......	......	
3794.342	.342	......	32	A	4	B	
3795.006	.005	*b1*	57	A	27	A	G, direct, r
3795.533	......	......	4	C	......	......	
3797.518	.519	......	37	A	7	A	
3797.950	......	......	2	C	......	......	
3798.515	.514	......	62	A	29	A	G, direct, g, r
3799.551	.551	......	60	A	31	A	G, direct, r
3801.683	.682	......	17	A	2	C	
3801.806	......	......	4	C	......	......	
3801.977	......	*e*	4	C	......	......	
3802.285	......	......	5	C	......	......	
3804.015	......	......	5	C	......	......	
3805.346	.346	......	36	A	18	A	
3806.205	......	*d*	19	C	......	......	
3806.700	.700	......	25	A	11	A	
3807.540	.541	......	32	A	13	A	

TABLE I—*Continued*

λ		GROUP	GRATING		INTERFEROMETER		REMARKS
Grating	Interferometer		Plates	Probable Error	Plates	Probable Error	
3808.288	......	......	4	C	......	......	
3808.733	.733	......	25	A	2	B	
3810.761	......	......	25	B	......	......	
3811.894	......	......	10	C	......	......	
3812.967	.968	......	37	A	32	A	G, direct, r
3813.061	......	......	10	C	......	......	
3813.640	......	......	17	C	......	......	
3814.527	.529	......	24	A	1	C	
3815.843	.843	*b*1	24	A	23	A	G, r; I, r, direct
3816.342	......	......	24	A	......	......	
3820.430	.429	......	53	A	21	A	G, direct, g, r; I, r, direct
3821.181	.183	......	41	A	11	A	
3821.836	......	......	22	B	......	......	
3824.076	......	......	8	B	......	......	
3824.444	.446	......	25	A	26	A	G, r
3825.406	......	......	3	C	......	......	
3825.884	.885	*b*1	40	A	24	A	G, g, r; I, r, direct
3826.838	......	......	3	C	......	......	
3827.574	......	......	10	B	......	......	
3827.826	.826	*b*1	28	A	27	A	G, g, r
3829.127	......	*d*	3	B	......	......	
3830.759	......	......	3	B	......	......	
3830.852	......	*d*	2	C	......	......	
3833.312	.314	......	39	A	7	A	
3834.224	.225	*b*1	32	A	25	A	G, g, r; I, r, direct
3836.334	.334	......	25	A	7	A	
3837.134	......	......	4	C	......	......	
3839.260	.259	......	23	A	9	A	
3840.439	.439	......	28	A	23	A	G, g, r
3841.051	.052	......	50	A	23	A	G, direct, g, r
3843.260	.260	......	26	A	16	A	
3845.694	......	......	4	C	......	......	
4846.414	......	......	12	B	......	......	
3846.805	.804	......	30	A	12	A	
3849.970	.971	......	32	A	28	A	G, direct, r
3850.821	.821	......	20	A	21	A	
3852.576	.576	......	32	A	9	A	
3855.848	......	*d*	3	C	......	......	
3856.372	.374	......	28	A	29	A	G, g, r; I, r, direct
3859.216	.215	......	30	A	7	A	G, direct, g, r
3859.915	.914	......	29	A	22	A	I, r, direct
3861.343	......	......	15	B	......	......	
3865.529	.527	......	31	A	32	A	G, direct, r
3867.221	.222	......	23	A	8	A	
3871.752	.751	......	14	B	2	C	

TABLE I—*Continued*

λ		Group	Grating		Interferometer		Remarks
Grating	Interferometer		Plates	Probable Error	Plates	Probable Error	
3872.506....	.505	......	34	A	29	A	G, direct, g, r
3873.764....	.765	......	21	A	8	A	
3876.045....	......	......	15	A	......	......	
3878.023....	.022	......	26	A	22	A	G, direct, r
3878.576....	.575	......	24	B	20	A	G, direct, g, r; I, r, direct
3883.284....	.284	......	11	B	1	C	
3884.363....	.358	*b*	17	B	3	C	
3885.512....	.514	*b*	24	C	4	B	
3886.286....	.285	*a*1	17	C	20	A	G, direct, r; I, r, direct
3887.052....	.055	*b*1	27	B	20	B	G, direct, g, r
3888.518....	.518	*b*1	23	B	29	A	G, direct, g, r
3890.846....	......	*b*	16	B	......	......	
3891.934....	.926	*b*	16	C	3	B	Diff.>error
3893.396....	.396	......	10	B	5	A	G, direct, g
3893.926....	......	......	6	B	......	......	
3894.007....	......	......	1	C	......	......	
3895.660....	.660	*a*1	17	B	30	A	
3897.451....	......	......	5	B	......	......	
3897.898....	......	*b*	10	B	......	......	
3899.039....	......	*e*	2	C	......	......	
3899.713....	.710	*a*1	14	B	28	A	G, direct, g
3900.521....	......	......	6	B	......	......	
3902.948....	.950	*b*1	4	A	21	A	G, g
3903.904....	......	*b*	16	A	......	......	
3906.486....	.484	*a*1	13	C	23	A	
3906.750....	......	......	12	A	......	......	
3907.466....	......	......	3	C	......	......	
3907.940....	.936	*b*	16	C	6	B	
3909.666....	......	......	7	B	......	......	
3909.	.832	*b*	......	......	2	B	
3910.848....	.847	......	8	B	2	C	
3913.637....	.637	*b*	13	A	5	A	
3916.737....	......	*b*	14	B	......	......	
3917.186....	.186	*a*	16	A	6	A	
3918.321....	......	......	14	B	......	......	
3918.420....	......	......	13	B	......	......	
3918.646....	......	*b*	14	B	......	......	
3919.071....	......	*b*	13	A	......	......	
3920.262....	.260	*a*1	11	B	19	A	
3920.841....	......	*d*	3	C	......	......	
3922.915....	.916	*a*1	11	C	17	A	
3925.648....	......	*b*	10	B	......	......	
3925.945....	.950	*a*1	15	B	5	C	
3927.923....	.924	*a*	18	B	16	A	
3928.087....	......	*d*	10	B	......	......	

TABLE I—*Continued*

λ		Group	Grating		Interferometer		Remarks
Grating	Interferometer		Plates	Probable Error	Plates	Probable Error	
3929.116....	......	......	3	C	......	......	
3929.210....	......	......	3	C	......	......	
3930.301....	.300	*a*1	18	C	16	A	G, direct, r
3931.124....	......	......	6	C	......	......	
3932.630....	.631	*b*	12	A	3	B	
3932.919....	......	......	2	B	......	......	
3933.608....	......	......	3	C	......	......	
3935.817....	.817	*b*	15	B	7	A	
3937.330....	.332	*b*	5	B	2	C	
3940.883....	.883	*a*	19	B	7	A	
3941.285....	......	*d*	6	C	......	......	
3942.445....	.444	*b*	10	B	8	A	
3943.341....	......	*b*	4	B	......	......	
3944.750....	......	......	2	C	......	......	
3944.892....	......	*b*	6	B	......	......	
3945.121....	......	*b*	7	B	......	......	
3947.004....	......	......	7	B	......	......	
3947.535....	......	*b*	12	B	......	......	
3948.107....	......	*d*	14	B	......	......	
3948.780....	.781	*b*	15	A	4	B	
3949.958....	.958	*b*	15	A	4	A	
3951.168....	.172	*b*	15	C	3	C	
3952.607....	.607	*b*	15	A	6	A	
3953.158....	......	*b*	9	B	......	......	
3955.354....	......	*d*	4	C	......	......	
3955.958....	......	*b*	2	C	......	......	
3956.463....	.459	*b*	9	B	4	B	
3956.681....	.682	*b*4	12	A	6	A	
3957.029....	......	*d*	12	A	......	......	
3960.286....	......	......	4	C	......	......	
3961.149....	......	......	4	C	......	......	
3963.110....	......	*d*	8	C	......	......	
3964.520....	.528	*b*	8	C	1	C	
3965.513....	......	*d*	2	C	......	......	
3966.067....	.067	*b*	14	A	7	A	
3966.632....	......	*e*	13	B	......	......	
3966.826....	......	*e*	2	C	......	......	
3967.424....	.424	......	4	B	2	B	
3967.966....	......	......	6	A	......	......	
3969.261....	.262	*b*1	27	B	11	A	G, direct, r
3969.630....	......	......	5	B	......	......	
3970.264....	......	......	2	C	......	......	
3970.393....	......	*b*	3	C	......	......	
3971.327....	.327	*b*	20	A	9	A	
3973.657....	......	*b*	5	B	......	......	

TABLE I—*Continued*

λ		Group	Grating		Interferometer		Remarks
Grating	Interferometer		Plates	Probable Error	Plates	Probable Error	
3974.399	......	......	2	C	......	......	
3976.617	.617	*d*	7	B	1	C	
3976.867	......	......	6	C	......	......	
3977.745	.745	*b*4	14	A	10	A	
3981.776	.777	*b*	16	B	5	B	
3983.963	.961	*b*	15	A	10	A	
3985.395	......	......	5	C	......	......	
3986.178	.178	*b*	11	B	1	C	
3989.861	......	......	5	C	......	......	
3990.381	......	*b*	7	B	......	......	
3994.119	......	*b*	7	C	......	......	
3995.201	......	*d*	2	C	......	......	
3995.998	......	*b*	5	B	......	......	
3996.970	......	*b*	7	C	......	......	
3997.396	.396	*b*4	14	A	11	A	
3998.058	.059	*b*	13	A	9	A	
4000.268	......	......	2	C	......	......	
4000.468	......	*b*	2	C	......	......	
4001.669	.666	*b*	8	C	4	B	
4003.766	......	*b*	4	B	......	......	
4004.834	......	*b*	2	C	......	......	
4004.978	......	*b*	2	C	......	......	
4005.247	.247	*b*1	16	B	13	A	G, direct, r
4006.316	......	*b*	7	C	......	......	
4006.633	......	*b*	5	C	......	......	
4007.279	......	*b*	14	B	......	......	
4009.717	.717	*a*	14	B	11	A	
4013.643	......	......	1	C	......	......	
4013.824	......	*b*	5	C	......	......	
4014.536	.536	*b*	14	A	9	A	
4017.157	.158	*b*	13	B	4	B	
4018.284	......	......	2	C	......	......	
4021.871	.872	*b*	8	A	12	A	
4024.111	......	......	2	C	......	......	
4024.738	.735	*d*	3	C	2	C	
4030.501	......	*d*	7	B	......	......	
4040.652	......	*e*	2	C	......	......	
4044.618	.615	*b*	2	C	3	C	
4045.816	.817	*b*1	7	B	5	A	G, .807 g
4051.925	......	......	2	C	......	......	
4052.314	......	......	2	C	......	......	
4062.448	.447	*b*	9	B	11	A	
4063.288	......	*d*	7	B	......	......	
4063.596	.599	*b*1	6	C	7	A	G, .587 g
4066.983	.983	*b*	7	B	5	B	

TABLE I—*Continued*

λ		Group	Grating		Interferometer		Remarks
Grating	Interferometer		Plates	Probable Error	Plates	Probable Error	
4067.276....	.275	*b*	6	C	3	C	
4067.987....	.985	*b*	7	B	3	B	
4070.	.768	......	......	......	2	C	
4071.740....	.743	*b*1	6	C	10	A	G, .733 g
4074.796....	......	......	3	C	......	......	
4076.234....	......	......	2	C	......	......	
4076.638....	.638	*b*	4	B	7	A	G, 3057 4th order coincides
4076.812....	......	......	2	C	......	......	
4078.367....	......	......	2	C	......	......	
4079.850....	......	*b*	3	C	......	......	
4080.228....	......	*b*	1	C	......	......	
4082.127....	......	......	2	C	......	......	
4083.782....	......	......	2	C	......	......	
4084.501....	.500	*d*	7	B	1	C	
4085.013....	......	*b*	4	B	......	......	
4085.314....	......	*b*	7	B	......	......	
4089.227....	......	......	2	C	......	......	
4091.563....	......	......	2	C	......	......	
4092.289....	......	......	2	C	......	......	
4095.980....	.975	*b*	7	C	10	A	
4097.101....	......	......	2	C	......	......	
4098.186....	.184	*b*	6	C	7	A	
4100.750....	.744	......	2	C	6	A	
4101.274....	......	*d*	2	C	......	......	
4107.495....	.494	*b*	9	A	16	A	
4109.072....	......	......	2	C	......	......	
4109.812....	.808	*b*	8	B	13	A	Diff.>error
4112.974....	......	*d*	2	C	......	......	
4114.454....	.450	*b*	6	C	11	A	
4114.959....	......	......	2	C	......	......	
4118.552....	.550	*b*	18	B	19	A	
4120.215....	.211	*b*	3	C	7	A	
4121.810....	.808	......	14	B	7	A	
4122.524....	.525	*b*	3	B	7	B	
4123.750....	......	......	3	B	......	......	
4125.624....	......	*d*	1	C	......	......	
4125.886....	......	......	2	A	......	......	
4126.193....	.194	*b*	3	B	1	C	
4127.615....	.614	......	20	B	12	A	
4127.809....	......	......	3	B	......	......	
4132.061....	.063	*b*1	21	B	17	A	
4132.905....	.906	*b*	6	B	9	A	
4133.871....	......	*d*	1	C	......	......	
4134.684....	.684	*b*4	19	A	18	A	
4136.514....	......	*d*	6	B	......	......	

TABLE I—*Continued*

λ		Group	Grating		Interferometer		Remarks
Grating	Interferometer		Plates	Probable Error	Plates	Probable Error	
4137.006....	.003	*b*	7	B	14	A	⊙ enh Mn
4139.935....	......	*a*	1	C	......	......	
4143.421....	.420	*b*	17	A	10	A	
4143.872....	.874	*b*1	11	B	14	A	
4147.676....	.675	*b*	26	A	14	A	
4149.374....	.374	*e*	8	A	5	B	
4150.260....	......	*d*	6	C	......	......	
4152.173....	.174	......	8	B	3	C	
4153.907....	.909	*d*	16	A	4	B	
4154.111....	......	......	2	C	......	......	
4154.505....	.504	*b*	36	A	5	B	
4154.813....	.815	*d*	16	A	1	C	
4156.805....	.804	*b*	32	A	15	A	
4157.792....	.788	*d*	15	B	2	C	
4158.801....	.800	*d*	8	B	4	B	
4170.907....	.906	*b*	31	A	1	C	
4171.698....	......	*d*	1	C	......	......	
4172.128....	......	......	7	A	......	......	
4172.751....	......	*a*	7	B	......	......	
4173.324....	......	*b*	6	B	......	......	
4173.928....	......	*a*	6	B	......	......	
4174.919....	......	*a*	18	A	......	......	
4175.642....	.642	*b*	43	A	13	A	
4176.574....	.572	*e*	10	B	7	B	⊙ Fe–Mn
4177.599....	.599	*a*	17	B	8	A	
4181.760....	.760	*b*	24	A	21	A	
4182.386....	......	*b*	4	A	......	......	
4184.897....	.896	*b*	35	A	17	A	
4187.047....	.045	*d*	12	A	11	A	
4187.804....	.805	*d*	12	A	11	A	
4191.439....	.438	*d*	12	A	11	A	
4191.687....	......	*e*?	4	C	......	......	
4195.340....	.338	*d*	10	A	4	B	
4195.617....	......	......	1	C	......	......	
4196.220....	......	*d*	6	C	......	......	
4198.312....	.312	*d*	3	C	11	A	
4198.647....	......	*d*	5	C	......	......	
4199.099....	.101	*b*	31	A	18	A	
4200.932....	......	*e*	4	C	......	......	
4202.033....	.034	*b*1	37	A	18	A	
4203.988....	.990	*b*3	24	A	12	A	
4205.548....	......	......	2	C	......	......	
4206.704....	.703	*a*	6	B	5	A	
4207.133....	.132	*b*	7	C	5	B	
4208.612....	......	*b*	7	B	......	......	

TABLE I—*Continued*

λ		Group	Grating		Interferometer		Remarks
Grating	Interferometer		Plates	Probable Error	Plates	Probable Error	
4210.355....	.352	*c5*	13	A	9	A	Diff.>error
4213.652....	.652	*b*	8	B	8	A	
4215.432....	......	*b*	4	C	......	......	
4216.188....	.188	*b3*	20	A	20	A	
4217.554....	.552	*d*	9	B	4	B	
4219.367....	.367	*b*	36	A	18	A	
4220.348....	.350	*b*	7	B	1	C	
4222.222....	.221	*d*	9	B	10	A	
4224.179....	.177	*e*	22	B	7	B	
4225.463....	.462	*d*	10	B	1	C	
4225.958....	......	*b*	7	B	......	......	
4226.428....	......	*b*	7	B	......	......	
4227.437....	.436	*d5*	10	A	11	A	
4229.518....	......	......	1	C	......	......	
4229.762....	......	......	1	C	......	......	
4233.142....	......	*d*?	2	C	......	......	⊙ Mn–Fe
4233.611....	.610	*d5*	10	B	11	A	
4235.	.945	*d5*	......	......	12	A	
4237.164....	......	......	2	C	......	......	
4238.029....	......	*d*?	6	B	......	......	
4238.818....	.819	*d*	10	B	4	B	
4239.849....	.849	*a*	1	C	1	C	
4240.374....	......	......	3	C	......	......	
4242.732....	......	......	2	C	......	......	
4245.264....	.261	*b*	10	C	2	B	
4246.092....	......	*b*	4	C	......	......	
4247.436....	.434	*d*	10	A	7	A	
4248.230....	......	*b*	7	B	......	......	
4250.128....	.126	*c5*	12	C	7	A	
4250.792....	.792	*b*	42	A	16	A	
4254.337....	.340	*d*	5	A	3	B	Cr
4258.322....	......	*a*	5	B	......	......	
4258.621....	......	......	1	C	......	......	
4258.958....	......	*e*	1	C	......	......	
4260.482....	.482	*c2*	8	B	15	A	
4264.211....	......	*d*	1	C	......	......	
4265.262....	......	......	1	C	......	......	
4266.970....	.971	*b*	7	B	3	B	
4267.831....	.832	*b*	6	A	3	B	
4268.	.746	*b*	......	......	1	C	
4271.163....	.159	*d*	7	C	5	C	
4271.766....	.766	*b1*	33	B	11	A	
4274.	.802	......	......	......	2	B	Cr
4276.686....	......	?	1	C	......	......	
4278.236....	......	?	1	C	......	......	

TABLE I—*Continued*

λ		GROUP	GRATING		INTERFEROMETER		REMARKS
Grating	Interferometer		Plates	Probable Error	Plates	Probable Error	
4279.866....	......	?	1	C	......	......	
4282.408....	.408	*b*1	30	A	20	A	
4285.448....	.449	*b*	6	B	4	B	
4288.150....	......	......	5	C	......	......	
4290.384....	......	......	3	C	......	......	
4290.872....	......	......	2	C	......	......	
4291.465....	......	*a*3	7	B	......	......	
4294.130....	.130	*b*2	8	C	19	A	
4298.044....	.042	......	6	A	4	B	
4299.243....	.242	*d*5	8	B	11	A	
4302.	.193	......	......	......	1	C	
4304.554....	......	......	2	C	......	......	
4305.454....	.459	*b*	2	C	3	C	Fe, Cr?
4307.908....	.908	*b*1	48	A	7	A	
4309.038....	......	?	1	C	......	......	
4315.090....	.090	*b*3	45	A	19	A	
4321.803....	......	......	3	C	......	......	
4325.766....	.767	*b*1	52	A	8	A	
4327.103....	.101	*b*	6	B	1	C	
4337.052....	.052	*b*3	47	A	19	A	
4338.262....	......	......	1	C	......	......	
4343.259....	......	*d*	4	B	......	......	
4343.701....	......	......	5	B	......	......	
4346.560....	.560	......	5	B	1	B	
4348.941....	......	?	1	C	......	......	
4351.551....	.551	*b*	6	C	6	A	
4352.739....	.740	*b*3	20	A	20	A	
4358.508....	.506	*b*	6	B	4	B	
4367.582....	.584	*b*	17	A	5	B	
4367.908....	......	*a*	6	B	......	......	
4369.776....	.777	*b*3	30	A	20	A	
4373.563....	.567	......	5	B	1	C	
4375.934....	.934	*a*3	40	A	26	A	
4383.550....	.550	*b*1	......	A	8	A	
4387.898....	.900	*b*	6	B	2	C	
4388.414....	.415	*d*?	10	B	2	C	
4389.247....	.246	*a*	7	B	1	C	
4390.955....	.957	*b*	6	B	5	A	
4401.295....	......	*d*	6	A	......	......	
4404.755....	.755	*b*1	45	A	12	A	
4407.715....	.716	*c*4	24	A	7	A	
4408.420....	.420	*c*4	30	A	18	A	
4409.125....	......	?	1	C	......	......	
4415.128....	.128	*b*1	53	A	18	A	
4422.573....	.573	*b*3	40	A	32	A	

TABLE I—*Continued*

λ		Group	Grating		Interferometer		Remarks
Grating	Interferometer		Plates	Probable Error	Plates	Probable Error	
4427.314....	.314	*a*3	36	A	38	A	
4430.621....	.620	*c*4	35	A	34	A	
4432.574....	......	......	7	B	......	......	
4433.225....	......	*e*	12	A	......	......	
4433.795....	......	*d*	6	C	......	......	
4435.153....	......	*a*	11	A	......	......	
4439.885....	......	......	7	B	......	......	
4442.345....	.345	*c*4	11	A	34	A	
4442.837....	......	......	9	B	......	......	
4443.197....	.200	*b*3	31	A	32	A	Diff.>error
4446.844....	......	*d*	9	B	......	......	
4447.136....	......	......	4	A	......	......	
4447.723....	.724	*c*4	32	A	37	A	
4450.323....	......	......	6	C	......	......	
4454.386....	.386	*b*3	12	B	28	A	
4454.658....	......	*d*	2	C	......	......	
4455.035....	......	?	2	C	......	......	Probably Mn
4456.334....	......	......	3	C	......	......	
4459.123....	.125	*c*4	27	A	39	A	
4461.656....	.656	*a*3	22	A	34	A	
4461.992....	......	*d*	1	C	......	......	
4466.556....	.557	*b*4	22	A	37	A	
4469.386....	.384	*d*	5	B	18	A	
4472.724....	......	?	3	C	......	......	
4476.026....	.023	*b*4	16	C	29	A	Double in vacuum. Cf. *Astrophysical Journal*, 44, 331, 1916.
4479.615....	......	......	4	A	......	......	
4480.145....	......	......	5	B	......	......	
4481.624....	......	......	3	C	......	......	
4482.	.174	*a*	......	......	14	A	G, too close; I, meas. at orders 22250, 32890
4482.	.260	*a*	......	......	14	A	
4484.231....	.229	*d*	4	B	13	A	
4485.681....	.682	*e*?	5	A	4	B	I, h
4488.143....	......	......	3	B	......	......	
4488.920....	......	......	2	C	......	......	
4489.745....	.744	*a*3	13	A	23	A	
4490.087....	.087	......	3	B	2	C	⊙ Mn–Fe; I, fringes poor
4490.776....	......	......	5	B	......	......	
4494.572....	.570	*c*4	40	A	38	A	
4495.569....	......	*d*	1	C	......	......	
4495.969....	......	......	3	B	......	......	
4504.841....	......	*d*	1	C	......	......	
4514.192....	.191	......	8	A	2	B	
4517.533....	.532	......	11	A	4	B	
4523.406....	......	......	3	A	......	......	
4525.148....	.146	*d*?	5	A	22	A	

TABLE I—*Continued*

λ		Group	Grating		Interferometer		Remarks
Grating	Interferometer		Plates	Probable Error	Plates	Probable Error	
4526.566....	......	......	1	C	......	......	
4528.622....	.620	*c*4	29	A	29	A	
4531.155....	.155	*b*3	28	A	31	A	
4531.636....	......	*d*	2	A	......	......	
4537.680....	......	......	1	C	......	......	
4547.025....	......	......	3	B	......	......	
4547.853....	.853	*b*	29	A	22	A	
4549.473....	......	......	5	B	......	......	
4550.788....	......	*d*	3	B	......	......	
4552.548....	.547	......	7	B	1	C	
4556.130....	.134	*e*?	24	A	22	A	⊙ Fe–Cr
4556.942....	......	......	1	C	......	......	
4558.111....	......	......	1	C	......	......	
4560.099....	......	*d*	1	C	......	......	
4566.523....	......	......	3	B	......	......	
4574.728....	.726	......	7	B	2	B	
4581.520....	.519	*d*	3	C	2	B	
4583.838....	......	......	3	B	......	......	
4587.135....	......	......	4	B	......	......	
4592.658....	.658	......	13	A	28	A	
4595.367....	.365	......	5	B	1	C	
4696.069....	......	......	5	B	......	......	
4598.125....	......	*d*	3	B	......	......	
4600.940....	......	......	2	C	......	......	
4602.009....	.007	......	5	A	4	A	
4602.947....	.947	......	17	A	39	A	
4607.659....	.657	*d*	5	A	7	A	
4611.289....	.288	*d*	5	A	14	A	
4613.212....	.214	*d*	3	B	2	B	
4614.219....	......	......	1	C	......	......	
4618.768....	......	......	4	A	......	......	
4619.297....	.297	......	5	A	10	A	
4625.057....	.055	*d*	5	B	10	A	
4630.127....	.128	......	5	A	10	A	
4632.917....	.918	......	5	A	14	A	
4635.849....	......	......	3	B	......	......	
4637.516....	.513	*d*	3	B	4	A	
4638.018....	.019	*b*	18	A	6	A	
4643.471....	.471	......	5	B	6	A	
4647.439....	.440	*b*	17	A	28	A	
4654.504....	.504	*b*	3	B	6	A	
4654.632....	.629	*d*	3	C	4	B	
4661.541....	......	......	1	C	......	......	
4661.978....	......	......	3	A	......	......	
4663.186....	......	......	1	C	......	......	

TABLE I—*Continued*

λ		Group	Grating		Interferometer		Remarks
Grating	Interferometer		Plates	Probable Error	Plates	Probable Error	
4667.462	.461	*b*	5	B	14	A	
4668.144	.145	*d*	5	A	10	A	I, h
4669.177	.177	......	5	A	2	C	I, h
4673.172	.171	......	5	A	4	B	
4678.856	.854	......	18	A	26	A	
4680.300	......	......	2	C	......	......	
4682.114	......	......	2	C	......	......	
4683.568	......	......	3	C	......	......	
4687.390	......	......	2	C	......	......	
4689.498	......	......	2	C	......	......	
4690.149	......	......	3	C	......	......	
4691.417	.417	......	18	A	22	A	
4700.174	......	*d*	1	C	......	......	
4701.055	......	......	6	C	......	......	
4704.962	.960	......	7	B	1	C	I, h
4705.467	......	?	4	C	......	......	
4707.283	.283	*d*	6	B	16	A	
4707.490	......	......	7	B	......	......	
4709.095	......	*d*	5	C	......	......	
4710.288	.288	*b*	22	A	16	C	
4721.000	......	......	5	C	......	......	
4727.408	......	*d*	6	B	......	......	
4728.	.558	......	......	......	6	B	
4729.031	......	*e*	1	C	......	......	
4731.494	......	......	6	C	......	......	
4733.598	.598	*a*	9	A	12	A	
4734.103	......	......	3	C	......	......	
4735.849	......	......	9	B	......	......	
4736.782	.782	*d*	7	B	20	A	
4737.636	......	......	4	C	......	......	
4740.346	......	......	4	B	......	......	
4741.084	......	......	3	C	......	......	
4741.534	.535	*b*	9	A	8	A	
4745.807	.809	*b*	4	B	6	A	
4757.585	......	......	7	A	......	......	
4771.705	......	......	2	C	......	......	
4772.818	.819	*b*	7	A	4	B	
4779.447	......	......	3	C	......	......	
4786.813	.812	*b*	28	A	12	A	
4788.760	......	......	6	B	......	......	
4789.656	.655	*b*	22	A	15	A	
4800.655	......	......	1	C	......	......	
4802.886	......	......	2	C	......	......	
4832.737	......	......	1	C	......	......	
4838.522	......	......	1	C	......	......	

TABLE I—*Continued*

λ		Group	Grating		Interferometer		Remarks
Grating	Interferometer		Plates	Probable Error	Plates	Probable Error	
4839.552....	......	......	2	C	......	......	
4843.158....	......	......	2	C	......	......	
4855.686....	......	......	2	C	......	......	
4859.750....	.750	*c*5	4	A	16	A	
4863.656....	......	......	2	C	......	......	
4871.327....	.327	*c*5	4	B	23	A	
4872.145....	.147	*c*5	3	A	18	A	
4878.220....	.220	*c*5	4	A	12	A	
4881.729....	......	......	2	C	......	......	
4882.154....	......	*d*	2	C	......	......	
4885.438....	......	......	3	B	......	......	
4886.338....	......	......	3	C	......	......	
4890.764....	.765	*c*5	3	B	23	A	
4891.503....	.501	*c*5	2	C	20	A	
4903.319....	.319	*d*	4	A	10	A	I, fringes poor
4909.390....	......	?	2	C	......	......	
4910.030....	......	?	3	C	......	......	
4910.331....	......	?	2	C	......	......	
4910.573....	......	?	2	C	......	......	
4918.998....	.001	*c*5	3	C	21	A	
4920.510....	.513	*c*5	2	B	23	A	
4924.776....	.775	*b*	16	A	2	B	
4938.820....	.823	*d*	5	B	5	B	
4939.247....	......	?	1	C	......	......	
4939.690....	.692	*a*	10	B	8	A	
4946.396....	.398	*d*	6	C	1	C	
4950.115....	......	*d*	2	C	......	......	
4957.305....	......	*c*5	3	C	......	......	
4957.603....	.605	*c*5	7	C	6	B	
4966.097....	.099	*d*	3	B	6	A	
4967.902....	......	*e*	2	C	......	......	
4969.930....	......	*d*	2	C	......	......	
4973.111....	......	*d*	2	C	......	......	
4978.609....	......	*d*	2	C	......	......	
4982.510....	......	*d*	3	B	......	......	
4983.261....	......	*d*	3	B	......	......	
4983.858....	......	*d*	3	B	......	......	
4985.264....	......	*d*	3	B	......	......	
4985.556....	......	*d*	4	C	......	......	
4988.966....	......	*d*	3	C	......	......	
4991.280....	......	*d*	2	C	......	......	
4994.135....	.136	*a*	50	A	10	A	
5001.873....	.873	*d*	8	B	6	A	
5002.802....	......	?	3	C	......	......	
5005.722....	.722	*d*	7	A	1	C	

TABLE I—*Continued*

λ		Group	Grating		Interferometer		Remarks
Grating	Interferometer		Plates	Probable Error	Plates	Probable Error	
5006.129	.128	*d*	7	A	8	A	
5007.291	......	*d*	4	A	......	......	
5012.074	.074	*a*	6	A	23	A	
5014.952	.953	*d*	7	B	3	B	
5018.440	......	......	6	B	......	......	
5022.247	.245	*d*	6	C	1	C	
5027.138	......	*d*	4	B	......	......	
5028.131	......	......	7	C	......	......	
5041.076	.077	*a*	24	A	6	B	
5041.761	.760	*a*	31	A	10	A	
5049.827	.827	*a*	30	A	14	A	
5051.640	.640	*a*	32	A	12	A	
5065.022	......	*e*	1	C	......	......	
5068.776	.775	*d*	4	B	5	B	
5074.759	......	*e*	4	B	......	......	
5079.228	......	*b*	19	A	......	......	
5079.744	......	*a*	23	B	......	......	
5083.344	.343	*a*	17	B	7	A	
5097.000	......	*e*	1	C	......	......	
5098.705	.705	*b*	42	A	3	B	
5107.454	......	*a*	22	A	......	......	
5107.647	......	*a*	22	A	......	......	
5110.415	.416	*a*	18	A	7	A	
5123.727	.725	*a*	20	B	5	B	
5125.132	.131	*d*	4	C	1	C	
5127.367	.365	*a*	21	B	4	B	
5131.477	......	*a*	2	C	......	......	
5133.696	.692	*e*	4	C	6	B	Pole-effect extreme; I, fringes poor
5137.390	......	*d*	3	C	......	......	
5139.262	......	*d*	5	C	......	......	
5139.470	......	*d*	5	C	......	......	
5142.543	......	......	3	C	......	......	
5142.935	.933	*a*	21	A	1	C	
5150.846	.844	*a*	30	A	5	B	
5151.918	.916	*a*	18	B	4	B	
5162.290	.290	*d*	5	C	2	B	Pole-effect extreme; I, fringes poor
5165.424	......	*d*	1	C	......	......	
5166.289	.288	*a*	7	B	2	B	
5167.492	.492	*a*	25	A	26	A	
5168.904	.902	*a*	4	C	1	C	
5171.601	.600	*a*	31	A	18	A	
5191.461	.463	*d*	5	A	12	A	
5192.351	.351	*d*	5	B	12	A	
5194.946	.946	*d*	6	A	11	A	
5195.479	......	*e*	7	C	......	......	

TABLE I—*Continued*

λ		GROUP	GRATING		INTERFEROMETER		REMARKS
Grating	Interfer-ometer		Plates	Proba-ble Error	Plates	Proba-ble Error	
5198.713	.716	*a*	4	B	4	B	
5202.340	.341	*a*	38	A	7	A	
5204.582	.586	*a*	2	C	1	C	Fe, Cr?
5208.601	.605	*d*	4	B	3	C	
5215.187	......	*d*	4	B	......	......	
5216.280	.280	*a*	35	A	3	B	
5217.397	......	*d*	4	C	......	......	
5226.870	......	*d*	4	B	......	......	
5227.192	.194	*a4*	36	A	8	A	
5229.859	......	*d*	4	C	......	......	
5232.946	.949	*d5*	4	B	21	A	
5242.497	.496	*a*	17	B	3	B	
5250.652	.652	......	15	A	3	B	
5263.316	.316	*d*	4	A	1	C	
5266.033	......	*d*	3	A	......	......	
5266.562	.564	*d5*	13	C	19	A	
5269.540	.541	*a1*	54	A	14	A	
5270.360	.362	*a4*	4	B	19	A	
5273.381	......	*b*	1	C	......	......	
5281.800	.800	*d*	4	B	7	A	
5283.627	.629	*d*	4	B	9	A	
5302.	.308	*d*	......	......	5	A	
5307.	.367	*a*	......	......	3	B	
5324.186	.188	*d5*	4	C	22	A	
5328.044	.044	*a1*	4	A	15	A	
5328.537	.535	*a4*	4	B	11	A	I, fringes poor
5329.996	......	*a*	1	C	......	......	
5332.906	.904	*a4*	15	C	3	B	
5339.938	.939	*d5*	3	B	6	A	
5341.029	.027	*a4*	4	B	17	A	
5364.881	......	*e*	3	B	......	......	
5365.405	......	*a*	3	B	......	......	
5367.475	.475	*e*	3	C	7	B	
5369.976	.967	*e*	3	B	8	B	Diff.>error
5371.495	.494	*a1*	20	A	18	A	
5379.582	......	*a*	1	C	......	......	
5383.378	.376	*e*	3	C	15	B	
5393.179	.176	*d5*	3	B	8	A	
5397.136	.133	*a4*	4	B	31	A	
5400.512	.510	*e*	3	C	1	C	
5404.149	.144	*e*	3	B	15	B	Diff.>error
5405.780	.780	*a4*	20	A	30	A	
5410.918	.916	*e*	3	B	13	B	
5415.208	.204	*e*	3	B	15	B	
5424.071	.072	*e*	3	B	16	B	

TABLE I—*Continued*

λ		Group	Grating		Interferometer		Remarks
Grating	Interferometer		Plates	Probable Error	Plates	Probable Error	
5429.702....	.701	*a*4	26	A	20	A	
5434.529....	.528	*a*4	20	A	32	A	
5445.048....	.046	*e*	3	C	3	B	
5446.920....	.921	*a*4	44	A	21	A	
5455.616....	.615	*a*4	4	C	22	A	
5462.972....	......	*e*	3	C	......	......	
5463.284....	......	*e*	3	C	......	......	
5466.406....	......	*d*	1	C	......	......	
5473.912....	.909	*d*	3	C	1	C	
5476.300....	......	*a*4	2	C	......	......	
5476.573....	.574	*d*5	3	A	5	B	
5497.522....	.521	*a*3	48	A	20	A	
5501.470....	.470	*a*3	48	A	17	A	
5506.784....	.783	*a*3	48	A	21	A	
5535.419....	......	*a*4	24	A	......	......	
5543.930....	......	*d*	1	C	......	......	
5554.894....	.893	*e*	3	C	1	C	
5563.605....	......	*d*	3	C	......	......	
5565.708....	.710	*e*	4	B	1	C	
5569.627....	.627	*d*5	3	C	20	A	
5572.849....	.851	*d*5	3	C	20	A	
5576.095....	.098	*d*5	3	C	12	A	
5586.765....	.765	*d*5	3	C	26	A	
5598.305....	.302	*e*	3	C	1	C	
5602.955....	.955	*d*5	3	C	9	A	
5615.653....	.653	*d*5	3	C	24	A	
5624.548....	.551	*d*5	3	C	17	A	
5638.269....	.269	*d*5	1	C	2	C	
5658.826....	.826	*d*5	3	C	8	A	
5662.	.523	*d*	......	......	5	B	
5701.	.553	?	......	......	2	C	
5731.	.771	?	......	......	2	C	
5752.	.043	?	......	......	1	C	
5753.	.136	*d*	......	......	4	B	
5775.	.090	*d*	......	......	2	C	
5956.	.702	*b*	......	......	2	C	
5975.354....	.356	*b*4	35	A	3	C	
6027.059....	.058	*b*4	35	A	10	A	
6042.	.092	*e*	......	......	4	B	
6065.492....	.491	*b*4	35	A	13	A	
6127.912....	.915	*b*	31	A	4	B	
6136.625....	.623	*b*4	40	A	22	A	
6136.999....	......	*b*	26	A	......	......	
6137.701....	.703	*b*4	20	A	22	A	
6157.731....	.736	*b*4	31	B	10	A	Diff.>error

TABLE I—*Continued*

λ		Group	Grating		Interferometer		Remarks
Grating	Interferometer		Plates	Probable Error	Plates	Probable Error	
6165.366....	.366	*b*	36	A	3	B	
6173.342....	.344	*b*4	38	A	10	A	
6191.568....	.568	*b*4	40	A	22	A	
6200.322....	.324	*b*4	30	A	8	A	
6213.438....	.440	*b*4	40	A	18	A	
6215.	.152	*b*4	......	......	3	B	
6219.289....	.291	*b*4	51	A	20	A	
6230.734....	.734	*b*4	40	A	20	A	
6240.	.656	?	......	......	2	C	
6252.568....	.566	*b*4	40	A	21	A	
6254.268....	.267	*b*4	40	A	20	A	
6256.	.373	*b*	......	......	17	A	
6265.145....	.145	*b*4	40	A	20	A	
6270.	.238	*b*	......	......	4	B	
6280.	.627	*a*	......	......	9	A	
6290.	.975	*e*?	......	......	3	C	
6297.801....	.807	*b*4	40	B	16	B	Diff.>error
6315.312....	.319	*b*	36	B	1	C	Diff.>error
6318.028....	.029	*b*4	40	A	22	A	
6322.694....	.698	*b*	40	B	11	B	Diff.>error
6335.341....	.344	*b*4	40	A	22	A	Diff.>error
6344.159....	.162	*b*	8	B	4	B	
6355.039....	.042	*b*	16	B	9	A	
6358.	.701	?	......	......	7	B	
6380.	.755	*b*	......	......	3	C	
6393.612....	.612	*b*4	40	A	2	A	
6421.363....	.361	*b*	30	A	21	A	
6430.859....	.859	*b*4	40	A	20	A	
6462.	.738	*b*	......	......	7	B	
6469.	.220	?	......	......	1	C	
6475.	.641	*b*	......	......	3	B	
6494.993....	.994	*b*4	40	A	23	A	
6518.	.383	*b*	......	......	3	B	
6546.	.253	*b*	......	......	22	A	
6569.	.236	?	......	......	2	C	
6575.	.030	*b*	......	......	2	C	
6592.	.927	*b*	......	......	20	A	
6609.	.125	*b*	......	......	3	B	
6663.	.457	*b*	......	......	11	A	
6678.	.003	*b*4	......	......	21	A	
6750.	.166	*b*	......	......	4	B	

VI. DISCUSSION

a) *Agreement with standards.*—Eighty-three secondary standards were measured with the interferometer, of which 64 belong to groups of stable lines and 19 to groups *c*5 and *d*. For the 64 stable lines the differences, secondary standards *minus* Mount Wilson, are as follows:

0.000 A for 24 lines; ±0.001 A for 29; ±0.002 A for 8; ±0.003 A for 2; +0.004 A for λ 4076.

The sum of the positive differences is +0.030 A, of the negative differences A −0.025. For the 19 standards of groups *c*5 and *d* the mean difference, secondary standards *minus* Mount Wilson, is +0.007 A, a difference due to pole-effect in the sources used in the original determinations of the secondary standards. It is unfortunate that such differences are involved in the adopted secondaries. It will lead to a series of iron standards and a series of iron wave-lengths differing from each other, unless revised values based on a source measurably free from pole-effect are soon substituted for those adopted.

b) *Questioned standards.*—Questions have been raised by different observers about the lines in the subjoined list. The difficulties encountered are in the majority of cases due to the characteristics of the 6-mm, 6-amp. arc which does not produce these lines fine and sharp enough for satisfactory measurement with the interferometer. With the exception of λ 3556 and λ 4076 for which the adverse criticism is general and apparently justified by the character of the lines or of their immediate surroundings, these lines are measurable with high precision in the 12-mm, 5-amp. arc, as they then permit the use of a satisfactory order of interference.

c) *Ghosts and reversals.*—The long exposures used in the grating series to obtain the weak lines brought out ghosts of the very strong lines. These were measured and the wave-lengths of the lines calculated from the positions of the ghosts, and when possible settings were made upon the primary line, "direct measure." The gratings were made on the Rowland ruling engine, whose spacing wheel has 750 teeth. All reversals were measured and for some lines the wave-lengths were found in all three ways. The wave-lengths from these separate determinations have been compared with the Mount Wilson interferometer wave-lengths, obtained from

	Remarks	Authority
λ 3513......	Not sharp in 6-mm, 6-amp. arc	Bureau of Standards
	Good in 12-mm, 5-amp. arc	Mount Wilson
	Discrepancy of 0.006 A	Viefhaus[*]
λ 3556......	Little wgt., poor in 6-mm, 6-amp. arc	Bureau of Standards
	Low wgt., p.e. large, shaded to red	Mount Wilson
	Meas. difficult, weak line to violet	Viefhaus
	Companion to red and violet	Goos[†]
λ 3677......	Poor in 6-mm, 6-amp. arc	Bureau of Standards
	Good in 12-mm, 5-amp. arc	Mount Wilson
λ 3850......	Not sharp in 6-mm, 6-amp. arc	Bureau of Standards
	Good in 12-mm, 5-amp. arc	Mount Wilson
λ 3865......	Very poor in 6-mm, 6-amp. arc	Bureau of Standards
	Broad in 6-mm, 6-amp. arc	Goos
	Good in 12-mm, 5-amp. arc	Mount Wilson
λ 3906......	Very poor in 6-mm, 6-amp. arc	Bureau of Standards
	Very discordant in grating measures	
	Good in 12-mm, 5-amp. arc	Mount Wilson
λ 4076......	Very poor in 6-mm, 6-amp. arc	Bureau of Standards
	Poor, λ 3057 4th order coincides in 3d	Mount Wilson
	Difficult, shaded to violet and red	Viefhaus
λ 4191......	Very poor in 6-mm, 6-amp. arc	Bureau of Standards
	d line good in 12-mm, 5-amp. arc	Mount Wilson
λ 4233......	Very poor in 6-mm, 6-amp. arc	Bureau of Standards
	d line good in 12-mm, 5-amp. arc	Mount Wilson
λ 4736......	No wgt. in 6-mm, 6-amp. arc	Bureau of Standards
	d line good in 12-mm, 5-amp. arc	Mount Wilson
λ 5167......	Poor in 6-mm, 6-amp. arc	Bureau of Standards
	Good in 12-mm, 5-amp. arc	Mount Wilson
λ 5266......	0.003 A > international value, 6-mm, 6-amp. arc	Bureau of Standards
	d line good in 12-mm, 5-amp. arc	Mount Wilson
λ 5371......	Not sharp in 6-mm, 6-amp. arc	Bureau of Standards
	Good in 12-mm, 5-amp. arc	Mount Wilson
λ 6678......	No wgt. in 6-mm, 6-amp. arc	Bureau of Standards
	Good in 12-mm, 5-amp. arc	Mount Wilson

[*] *Zeitschrift für wissenschaftliche Photographie*, **13**, 209, 245, 1914.

[†] *Astronomische Nachrichten*, **199**, 33, 1914.

weaker exposures upon the center of a somewhat leaner arc giving very fine lines. The results of the comparisons for some threescore lines are: mean difference, ghosts *minus* interferometer, −0.0004 A, reversals *minus* interferometer, −0.0002 A, "direct measures" *minus* interferometer, +0.0020 A.

From the close agreement of the wave-lengths given by reversals and ghosts with those from the interferometer it is evident that the reversals and ghosts correspond to the lines when produced in the core of a lean arc and hence that the absorbing centers in the cooler outer vapor producing the reversals have the same period as the emitting centers in the core of the arc, and that the maximum of the line, to which the ghosts correspond, is not displaced by the strong exposure. The excess of 0.002 A given by the direct measures indicates a slight unsymmetrical widening for such over-exposed lines, in general toward the red. This characteristic renders them of doubtful utility as standards when unreversed, unless produced in a lean arc. As under special circumstances strong lines only may be available for reference, the reliability of the wave-lengths given by ghosts or reversals may prove useful.

VII. COMPARISONS WITH BUREAU OF STANDARDS

a) *Stable lines as a whole.*—Approximately 250 stable lines are common to the interferometer measures[1] of the Bureau of Standards and the Mount Wilson lists. For the Mount Wilson interferometer measures *minus* the Bureau of Standards, the sum of the positive differences is +0.187 A, the sum of the negative differences −0.162 A, the mean difference ±0.0014 A, the systematic difference +0.0001 A. For the Mount Wilson grating measures *minus* the Bureau of Standards, the sum of the positive differences is +0.202 A, the sum of the negative differences −0.184 A, the mean difference ±0.0015 A, and the systematic difference again +0.0001 A.

b) *Stable lines by spectral regions.*—From Table II it is seen that for the interferometer measures there is good agreement except in the region to the red of λ 6200. Here the Mount Wilson wave-lengths average 0.001 A longer than the measures of the Bureau of

---

[1] Burns, Meggers, and Merrill, *Bulletin of the Bureau of Standards*, 13, 245, 1916.

Standards. This lack of agreement probably arises from the paucity of standards in the orange-red region and slight variations in drawing the correction-curves.

The Mount Wilson grating wave-lengths appear to be systematically too small for the region λ 3373–λ 3500 compared with both interferometer series. This, however, is due to the inclusion of a few lines showing large negative differences; and whenever the systematic difference approximates 0.001 A, it would fall well below that limit by omitting two or three lines of low weight.

c) *Unstable lines of groups c5 and d.*—There are 46 lines of groups *c*5 and *d* common to the Bureau of Standards and Mount Wilson interferometer series. For these the Bureau of Standards wave-lengths obtained with the central zone of the 6-mm, 6-amp. arc adopted at Bonn[1] are systematically longer than those made with the central zone of a 12-mm, 5-amp. arc. The average difference Bureau of Standards *minus* Mount Wilson is +0.007 A. There are 34 other lines of the same groups common to the Mount Wilson interferometer series and the grating measures by Burns.[2] For these lines the average difference Burns *minus* Mount Wilson is +0.008 A. From this it appears that the source adopted at Bonn exhibits nearly the same degree of pole-effect as the arc used originally by Burns. In their paper Burns, Meggers, and Merrill say: "The region λ 3500 A to λ 4200 A was observed with both 4 and 6 amperes, but no differences in wave-length were detected as a result of the increased current strength."[3] Unfortunately for such a test, unstable lines are relatively rare in this region, and they observed only one such line, viz., λ 4191. Of this they say[4] that it could be measured only with a low order of interference and had little weight in the final results. Their wave-length for it differs by 0.003 A from the international value. In saying that interferometer observations under the conditions used by them were found to be reasonably free from the effects of pole-shifts, they seem to have had in mind not absolute effects, but rather that the arc used by them did not differ greatly from the average arc with which the secondary standards were originally obtained. This agrees with the Mount Wilson observations which show that the secondary standards of groups *c*5 and *d* are contaminated by pole-effect to practically the same degree as the Bureau of Standards measurements of lines of these groups. That the measurement of these lines in the 6-mm, 6-amp. arc is difficult and relatively uncertain is shown by the Bureau of Standards measures; for 12 secondary standards belonging to groups *c*5 and *d* the mean difference, Bureau of Standards *minus* International, is +0.0012 A, while for stable standards it is 0.0000 A, and in their list of secondary standards differing by more than 0.001 A from International values, half of the lines belong to groups *c*5 and *d*, though they form only one-fifth of the total number of secondary standards.

---

[1] *Transactions of the International Union for Co-operation in Solar Research,* 4, 59, 1914.

[2] *Lick Observatory Bulletin,* 8, 27 (No. 247), 1913.

[3] *Loc. cit.*, p. 247.

[4] *Ibid.*, p. 261.

TABLE II

MOUNT WILSON *minus* BUREAU OF STANDARDS BY SPECTRAL REGIONS

Region	Interferometer		Grating	
	Number of Lines	Systematic Difference	Number of Lines	Systematic Difference
3370–3500..........	23	+0.0003 A	30	−0.0013 A
3500–3600..........	17	0.0000	18	+0.0006
3600–3700..........	16	+0.0005	15	+0.0006
3700–3800..........	13	+0.0001	16	+0.0003
3800–3900..........	12	−0.0004	12	+0.0001
3900–4000..........	11	−0.0005	13	−0.0003
4000–4200..........	18	−0.0006	19	+0.0010
4200–4400..........	18	−0.0006	18	−0.0003
4400–4600..........	22	−0.0001	23	+0.0002
4600–4800..........	15	−0.0003	18	−0.0003
4800–5200..........	19	+0.0006	22	+0.0009
5200–5700..........	22	0.0000	24	+0.0008
6000–6200..........	12	−0.0001	10	−0.0011
6200–6500..........	24	+0.0010	17	−0.0003
6500–6750..........	8	+0.0010	....	....

d) *Intensity effect.*—Burns, Meggers, and Merrill were of the opinion that for lines weaker than the standards the grating gives wave-lengths different from those obtained by the interferometer, but that the wave-lengths obtained by the latter instrument are free from an intensity effect. In the present series of grating measures an effort was made to obtain as many of the weaker lines as possible. The lines common to this series and the Bureau of Standards list have been compared in three groups, intensities 1–3, 4–5, and stronger than 6.

It is evident from results given in Table III that in the Mount Wilson grating series the wave-lengths of lines weaker than the standards show no systematic deviation from the Bureau of Standards interferometer values depending upon line-intensity. There is, moreover, no systematic difference between the Mount Wilson grating and interferometer measures for weak lines, or between the interferometer measures for strong and weak exposures.

e) *Grating and interferometer.*—As to the use of both grating and interferometer in obtaining relative wave-lengths as suggested by the American committee, we have found the practical advantage to be the detection of accidental errors, to which attention was directed by occasional marked disagreement between the results from the two methods, rather than the elimination of complementary errors. Even with optically perfect instruments each method has in practice both advantages and disadvantages.

TABLE III

BUREAU OF STANDARDS INTERFEROMETER *minus* MOUNT WILSON GRATING

	INTENSITIES					
	1–3		4–5		6 and Above	
Positive differences	+0.069	36 lines	+0.077	43 lines	+0.021	12 lines
Negative differences	−0.079	33 lines	−0.068	39 lines	−0.038	21 lines
Zero differences	0.000	17 lines	0.000	33 lines	0.000	12 lines
Mean differences	±0.0017	86 lines	±0.0013	115 lines	±0.0013	45 lines
Systematic differences	−0.0001	86 lines	+0.0001	115 lines	−0.0004	45 lines

For the interferometer the main points of superiority are: (1) the long range of spectrum on each plate, allowing the use of many standards or the bridging of wide gaps between standards; (2) the wide variation of resolving power without loss in extent of spectrum; (3) the moderate sensibility to instrumental disturbances; and (4) the less exacting character of the necessary microscopic measurements. The disadvantages are: (1) the integrating effect introduced by diaphragms with relatively large openings in front of the etalon; (2) the loss in separation of close lines due to coincidences and the low auxiliary dispersion usually employed; (3) the loss of light due to absorption in the metal film; and (4) the necessity of applying the correction for phase-change.

For the grating spectrograph the advantages are: (1) the easily obtained high dispersion combined with great resolution for spectral regions rich in lines; (2) the relative ease, in practice, with which faint lines may be obtained; (3) the simplicity of the instrumental equipment; and (4) the great analyzing power in forms free from astigmatism. Its disadvantages are: (1) the extreme sensitiveness to instrumental disturbances; (2) the difficulties involved in obtaining the necessary degree of perfection in the illumination; (3) the narrow spectral range under high dispersion, limiting the number of available standards; and (4) the higher precision required in the measurement of the spectrograms.

The theoretical advantages of the two instruments are well compared by Dr. Sparrow as follows:

> The defects of the gratings are fixed. If we have a good instrument we can make measurements as good as the best; if it is defective a definite limit is set to the accuracy of all our measurements. With the interferometer a good pair of plates may become defective through rotating one of them, or through tarnish or non-uniformity of the silver film; on the other hand, we may more or less average out the errors of a defective pair by this process, since each silvering or change of position makes virtually a new pair of plates.[1]

In the present investigation we have used three pairs of glass interferometer plates by Jobin and a pair of fused quartz by Hilger. The plates were several times resilvered with films of high uniformity, and were frequently changed in relative angular position. In no case was a plate used on which there appeared any evidence of tarnish or variable thickness of metal. Five high-quality gratings, two by Michelson and three by Anderson, were used in obtaining the grating series of spectrograms. As the apparent distribution of intensity in a spectral line depends upon the peculiarities of the ruling engine and the particular conditions under which each grating is produced, it is plainly an advantage in eliminating any resultant systematic errors to use gratings ruled upon two types of engine and under different circumstances for the two types. In view of the diversity of instrumental equipment employed, it is probable that defects inherent in the particular instruments, whether interferometers or gratings, play a minor rôle in both series of measures.

---

[1] *Astrophysical Journal*, **49**, 95, 1919.

Moreover, the absence of systematic effects depending upon line-intensity, the precautions taken to avoid errors due to pole-effect, and the substantial agreement shown by the wave-lengths in the two series lend weight to the results. It is perhaps not too much to hope that, for lines common to our two lists and having probable errors marked A or B, the weighted mean wave-length will be found accurate to one unit in the third decimal place.

Assistance in measurement and reduction has been given by Mrs. A. H. Joy, who as Miss Burns was formerly a member of the computing division, by Miss A. M. Brayton, by Miss A. L. Miller, and by Miss L. M. Keener. For their interested co-operation and efficient work we wish to express our appreciation.

MOUNT WILSON OBSERVATORY
November 1920

Contributions from the Mount Wilson Observatory, No. 203
Reprinted from the *Astrophysical Journal*, Vol. LIII, pp. 249–259, 1921

MEASUREMENT OF THE DIAMETER OF α ORIONIS WITH THE INTERFEROMETER

By A. A. MICHELSON and F. G. PEASE

ABSTRACT

Twenty-foot interferometer for measuring minute angles.—Since pencils of rays at least 10 feet apart must be used to measure the diameters of even the largest stars, and because the interferometer results obtained with the 100-inch reflector were so encouraging, the construction of a 20-foot interferometer was undertaken. A very rigid beam made of structural steel was mounted on the end of the Cassegrain cage, and four 6-inch mirrors were mounted on it so as to reduce the separation of the pencils to 45 inches and enable them to be brought to accurate coincidence by the telescope. The methods of making the fine adjustments necessary are described, including the use of two thin wedges of glass to vary continuously the equivalent air-path of one pencil. Sharp fringes were obtained with this instrument in August, 1920.

Diameter of α Orionis.—Although the interferometer was not yet provided with means for continuously altering the distance between the pencils used, some observations were made on this star, which was known to be very large. On December 13, 1920, with very good seeing, no fringes could be found when the separation of the pencils was 121 inches, although tests on other stars showed the instrument to be in perfect adjustment. This separation for minimum visibility gives the angular diameter as 0″.047 within 10 per cent, assuming the disk of the star uniformly luminous. Hence, taking the parallax as 0″.018, the linear diameter comes out 240×10^6 miles.

Interferometer method of determining the distribution of luminosity on a stellar disk.—The variation of intensity of the interference fringes with the separation of the two pencils depends not only on the angular diameter of the disk but also on the distribution of luminosity. The theory is developed for the case in which $I=I_0\,(R^2-r^2)^n$, and formulae are given for determining n from observations.

Table of values of $\int_0^1 (1-x^2)^{n+\frac{1}{2}}\cos kx\,dx$, for n equal to 0, $\frac{1}{2}$, 1, and 2, and for k up to 600°, is given.

It was shown in *Contributions* Nos. 184 and 185,[1] that the application of interference methods to astronomical measurements is not seriously affected by atmospheric disturbances, and indeed observations by these methods have proved feasible even when the seeing was very poor. The explanation of this apparent paradox lies in the fact that when the whole objective is effective, the atmospheric disturbances, being irregularly distributed over the surface, simply blur the diffraction pattern; but in the case of two isolated pencils too small to be affected by such an integrated disturbance, the resulting interference fringes, though in motion, are quite distinct, unless the period of the disturbances is too rapid for the eye to follow.

---

[1] *Astrophysical Journal*, **51**, 257, 263, 1920.

When it was found that the interference fringes remain at full visibility with the slits separated by the diameter of the 100-inch mirror, it was decided to build an interferometer with movable outer mirrors (Fig. 1) in order to make tests with separations as great as 20 feet.

The interferometer beam (Plate I*a* and Fig. 2) was made of structural steel, as stiff and rigid as circumstances of weight and operation would permit, for flexure causes a separation of the two pencils, and any vibration as great as one-thousandth of a millimeter blurs the fringes.

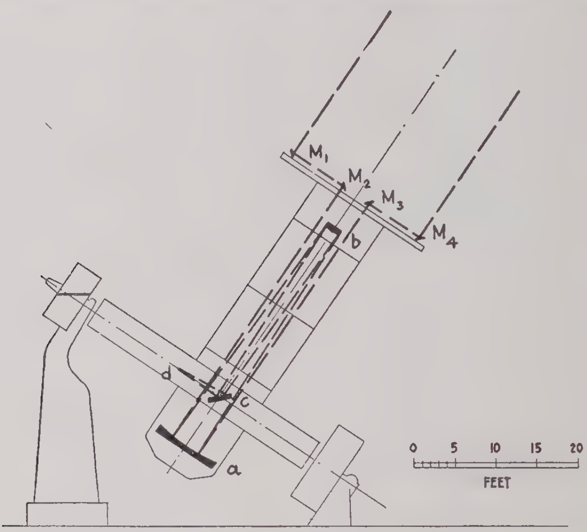

FIG. 1.—Diagram of optical path of interferometer pencils. M_1, M_2, M_3, M_4, mirrors; *a*, 100-inch paraboloid; *b*, convex mirror; *c*, coudé flat; *d*, focus.

The beam is constructed of two 10-inch channels with flanges turned inward, separated by pieces of 12-inch channel and covered on the bottom with $\frac{3}{16}$-inch (4.75 mm) steel plate (*C*, Fig. 2), all riveted securely together.

To reduce the weight holes were cut wherever the removal of metal would not cause a weakening of the structure. The inner edges of the top flanges were planed true to 0.001 of an inch

PLATE I

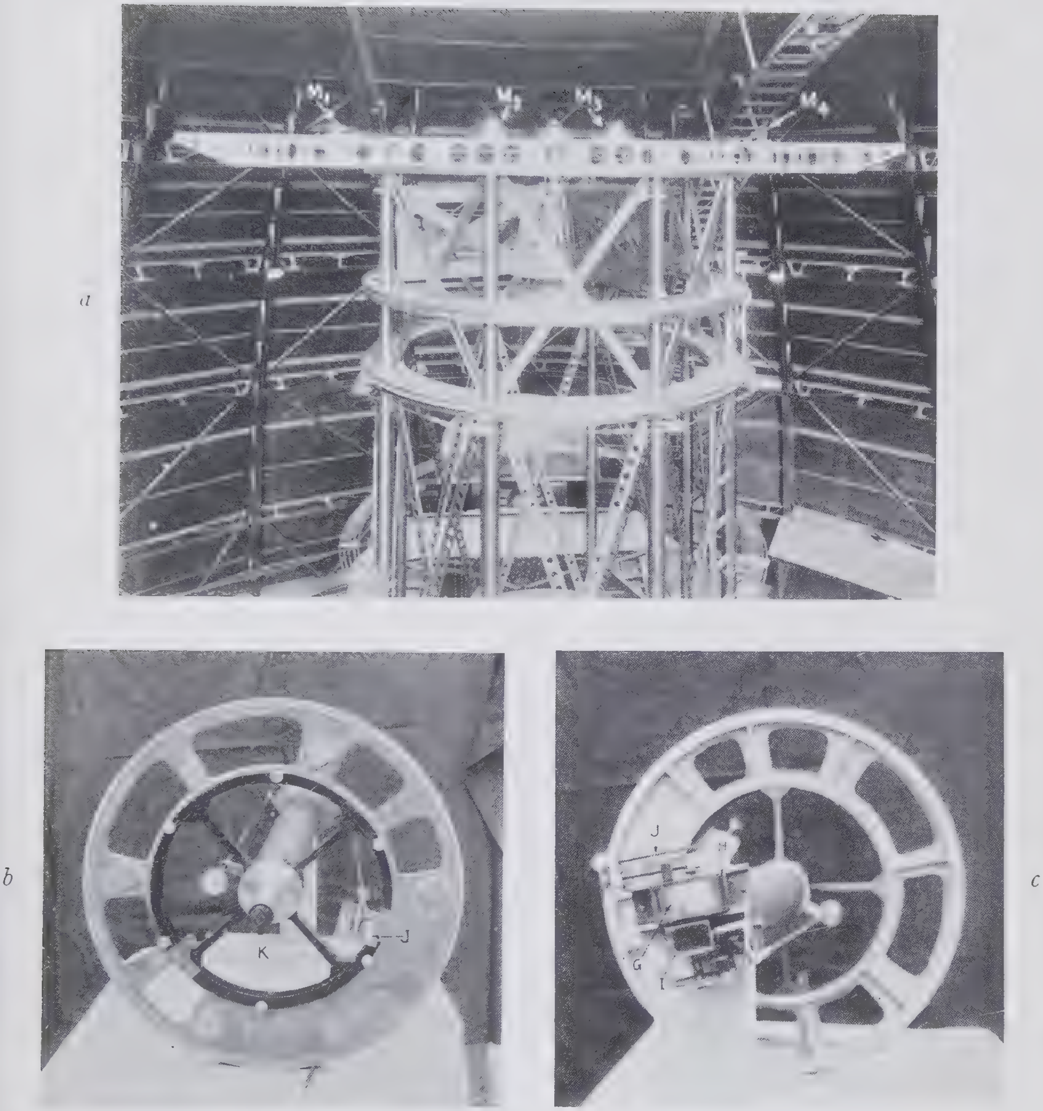

INTERFEROMETER USED WITH 100-INCH HOOKER REFLECTOR

a. *A*, 20-foot interferometer beam on end of telescope; M_1, M_2, M_3, M_4, mirrors.

b, *c*. Adapter at focus; *J*, rod to shift wedge; *K*, direct-vision prism; *G*, fixed wedge; *H*, movable wedge; *I*, plane-parallel compensator.

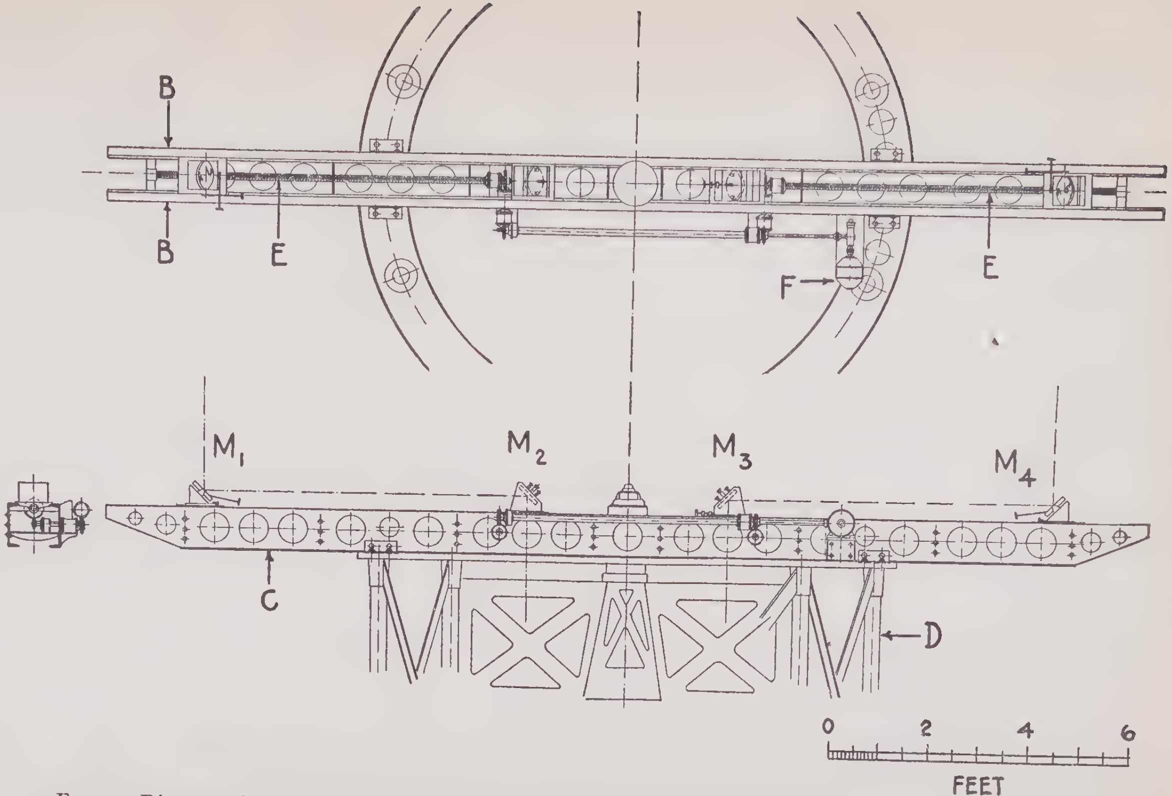

FIG. 2.—Diagram of 20-foot interferometer beam. M_1, M_2, M_3, M_4, mirrors; *B*, *B*, 10-inch channels; *C*, steel plate; *E*, *E*, screws to move outer mirrors; *F*, motor drive for screws; *D*, Cassegrain cage.

(0.025 mm), the beam being supported as it was to be mounted on the telescope.

Four mirrors, M_1, M_2, M_3, M_4 (Figs. 1 and 2 and Plate I*a*), about 6 inches (152 mm) in diameter, inclined 45° to the base, are mounted on slides; M_2 and M_3 are adjusted by three screws at the back, while M_1 and M_4 are adjustable about two horizontal axes by means of fine screws at the ends of 9-inch (228 mm) lever arms. The mirrors M_2 and M_3 are permanently fixed except that M_3 has a motion of several millimeters along its slide parallel to the beam.

The nearly constant separation of the mirrors M_2 and M_3 by about 45 inches (114.2 cm) gives the fringe pattern a fixed spacing equal to 0.02 mm, easily visible with a magnification of 1600. The mirrors M_1 and M_4 can be shifted along the beam; their distances from M_2 and M_3 must be equal, a condition satisfied as closely as possible by measurement with steel scales.

The beam is mounted on the end of the Cassegrain cage (Plate I*a* and Fig. 2), which is 11 feet (3.35 m) in diameter, and all observations are made at the Cassegrain focus corresponding to an equivalent focal length of 134 feet (40.84 m). Two pencils from the star are reflected from the outer mirrors M_1 and M_4 to mirrors M_2 and M_3, thence over the ordinary course in the telescope to the paraboloid (*a*, Fig. 1), the convex mirror (*b*, Fig. 1), the coudé flat (*c*, Fig. 1), and finally the focus (*d*, Fig. 1).

M_2 and M_3 are adjusted during the day and M_1 and M_4 on a star at night; and usually after the first setting of a run the image appears in the field of view of the telescope.

Coincidence of the two interferometer pencils at the focus is obtained by first adjusting the mirrors M_1 and M_4 and then tilting a plane-parallel glass plate, 15 mm thick (*I*, Fig. 3, and Plate I*c*), in the path of one of the pencils, which also serves to compensate the path of the double wedge mentioned below.

Equality of path in the two interferometer pencils is obtained by first setting the mirrors M_1 and M_4 symmetrically on the beam, as nearly as possible, and then adjusting the double wedge of glass (*G*, *H*, Fig. 3, and Plate I*c*, 2 feet within the focus) in the path of one of the pencils, the relative motion of the wedges altering the path slowly and continuously.

One of the wedges (*H*, Fig. 3), whose angles are about 10°, can be moved 25 mm either side of its mean position, parallel to the inclined surfaces. One turn of the rod (*J*, Plate I*b*) shifts this wedge 0.5 mm, thus introducing an equivalent air path of about 0.045 mm. Although fringes can be observed throughout one-third of a turn, corresponding to an air path of 0.015 mm, or about 26 light-waves, the finding of the fringes is notably facilitated by a direct-vision prism (*K*, Plate I*b*) placed in front of the eyepiece, which permits observation of interference bands with a path-difference of several hundred waves.

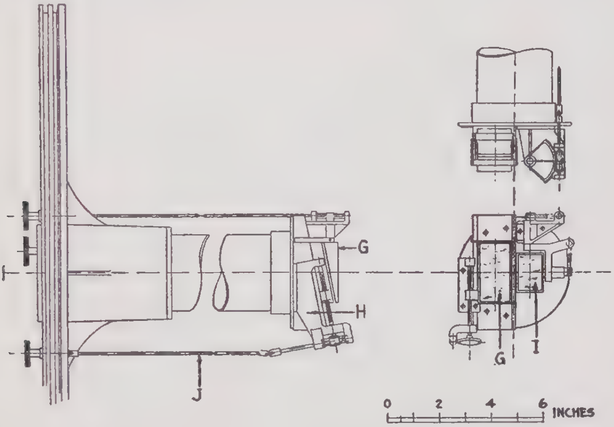

FIG. 3.—Diagram of adapter at focus. *G*, fixed wedge; *H*, movable wedge; *I*, plane-parallel compensator; *J*, rod to shift wedge.

To obtain a series of reference or "zero" fringes the end of the telescope tube is entirely covered, save for two apertures in the beam (in addition to those of mirrors M_2 and M_3), 6 inches (152 mm) in diameter. The pencils entering these apertures pass through the wedges and the compensating plate, respectively, and produce an image of the star in the field of view. When adjusted for coincidence and equality of path, these pencils interfere and produce the zero fringes which cross the reference image.

The interferometer images are next brought into the field of view of the eyepiece and made to coincide a short distance from the zero star, thus forming a second star in the field of view. Usually the adjustment of the mirrors M_1 and M_4 is sufficient to do this and the parallel plate compensator is used only for differential deflection of the steel beam. As soon as the wedge is moved to equalize the path-difference in the interferometer pencils, the zero fringes disappear and count is made of the turns of the rod required to bring the interferometer fringes into view. The mirror M_3 is then moved a small amount to compensate for this difference, and after several trials both sets of fringes are seen in the field of view crossing their respective images.

Differential refraction between air and glass limits the amount by which the effective thickness of the wedges may differ from that of the compensator, but interferometer fringes have been found with the wedge 20 mm from its mean position, corresponding to a 2-mm difference of air path.

Fringes were obtained with this apparatus in August, 1920, with the mirrors M_1 and M_4 at various distances apart, and, as there was no appreciable deterioration in their visibility at 18 feet (5.49 m) as compared with a separation of 6 feet (1.83 m), it seems reasonable to hope that this distance can be increased to 50 feet (15.24 m) or even to 100 feet (30.48 m). Work was discontinued after this series of experiments and again resumed in December, 1920.

Although provision is only just now being made for continuous alteration of the distance between the mirrors, as is essential in making accurate measurements, it was nevertheless decided to attempt a measurement of the angular diameter of α Orionis, for the calculations of Eddington, Russell, and Shapley, based on estimates of apparent surface brightness, had indicated that this star would be a promising subject for investigation.

The possibility of measuring the angular diameter of a distant object by interference methods depends upon the following considerations.

Let the distribution of light in the disk be represented by

$$I=I_0(R^2-r^2)^n,$$

r being the distance from the center, R the radius of the star, n the exponent of darkening at the limb. The visibility of the interference bands is

$$V=\frac{1}{P}\sqrt{C^2+S^2},$$

where

$$C=\int F(x)\cos kx\,dx,\qquad S=\int F(x)\sin kx\,dx,$$

$$P=\int F(x)\,dx,\qquad k=\frac{2\pi b}{\lambda d},$$

in which b is the distance between two pencils entering the interferometer, λ the mean length of the light-waves of the source, and d the distance of the source. $F(x)dx$ is the total intensity of a strip of the source whose width is dx. For a symmetrical source such as a star disk,

$$V=\frac{C}{P}.$$

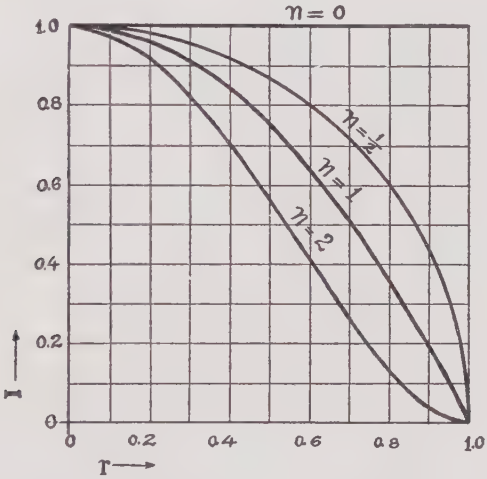

Fig. 4.—Distribution of light in various sources

If the illumination is uniform, $F(x)=\sqrt{R^2-x^2}$, whence

$$V=\frac{\int_0^R\sqrt{R^2-x^2}\cos kx\,dx}{\int_0^R\sqrt{R^2-x^2}\,dx},$$

tables for which[1] have been computed by Airy.

If the illumination can be represented as a function of the distance from the center, $I=(R^2-r^2)^n$, then

$$F(x)=\int_0^{\sqrt{R^2-x^2}}(R^2-x^2-y^2)^n dy$$

which, expanded in series and substituted in V, gives

$$V=\frac{\int_0^R (R^2-x^2)^{\frac{2n+1}{2}}\cos kx\,dx}{\int_0^R (R^2-x^2)^{\frac{2n+1}{2}}\,dx}\,.$$

This integral has been computed under the direction of Professor Moulton, the results being summarized in the accompanying table; and in Figure 4 is shown the distribution of light in the source for the values $n=0$, $\frac{1}{2}$, 1, and 2, and in Figure 5 the resulting visibility-curves.

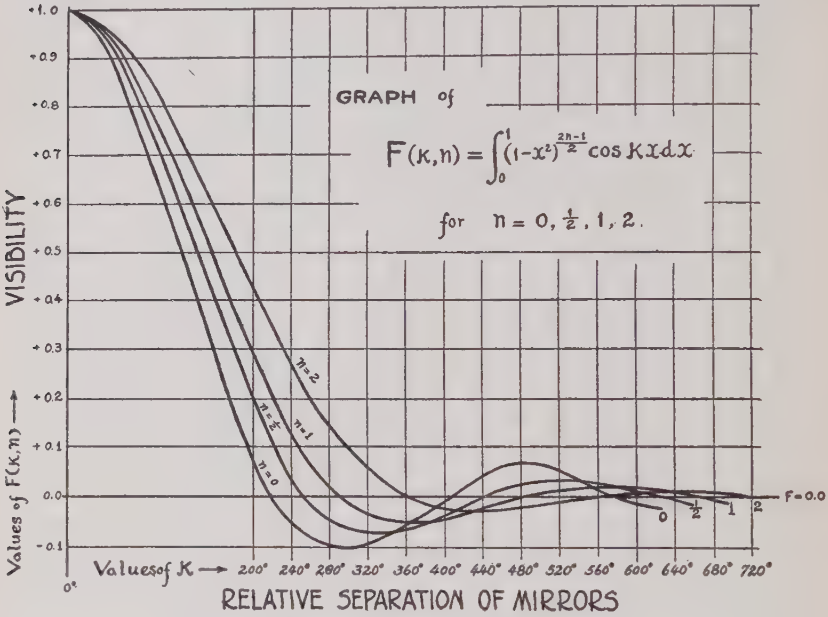

Fig. 5.—Visibility-curves for various sources

It will be noted that for $n=0$ the first disappearance of the fringes occurs at $k=220°$, while for $n=0.5$, the value is $k=257°$. For this value of n, the corresponding value of the diameter of Betelgeuse would be about 17 per cent greater than given below. (For the sun, the value of n is not far from 0.4.)

VALUES OF

$$F(k,n)=\int_0^1 (1-x^2)^{\frac{2n+1}{2}} \cos kx\,dx$$

$n=0$		$n=0.5$		$n=1$		$n=2$	
k	$F(k,n)$	k	$F(k,n)$	k	$F(k,n)$	k	$F(k,n)$
0°	+0.785	0°	+0.785	0°	+0.785	0°	+0.785
100	+0.507	30	+0.765	40	+0.746	40	+0.761
130	+0.378	60	+0.702	80	+0.663	80	+0.694
160	+0.243	90	+0.607	120	+0.536	120	+0.590
200	+0.065	120	+0.490	160	+0.383	160	+0.468
230	−0.024	150	+0.363	200	+0.237	200	+0.342
240	−0.050	180	+0.238	240	+0.112	240	+0.221
280	−0.100	210	+0.127	280	+0.024	280	+0.123
320	−0.095	240	+0.038	320	−0.029	320	+0.054
360	−0.053	257°27′	0.000	360	−0.045	360	+0.003
400	−0.007	270	−0.024	400	−0.039	400	−0.019
440	+0.036	300	−0.057	440	−0.020	440	−0.024
520	+0.042	330	−0.068	480	−0.001	480	−0.018
600	−0.011	360	−0.059	520	+0.012	520	−0.006
		390	−0.040	600	+0.013	560	0.000
		420	−0.016	640	+0.005	600	+0.005
		450	+0.005	680	−0.004	680	+0.005
		480	+0.019			720	+0.002
		510	+0.028				
		540	+0.026				
		570	+0.019				
		600	+0.009				
		630	−0.002				

While it may be too much to expect that we shall be able to deduce the actual distribution of the light in the source from observations of the visibility-curve itself, it may be worth while to point out that this is theoretically possible; and perhaps the case will not be entirely hopeless when the requisite skill in making the observations has been obtained by practice.

If b_1 and b_2 are the distances at which the fringes vanish for the first and second times, then the following formula will give a fair approximation to the value of n in the light-curve:

$$n=-1+75\left(\frac{b_1}{b_2}-\frac{1}{2}\right)^2 .$$

Or again, if V_m is the visibility at the first negative maximum (that at $b=0$ being unity),

$$n=0.22\left(\frac{1}{V_m}-7.8\right)^{0.7} .$$

It will be seen from this discussion that the measurement sought is that value of the separation of the outer mirrors M_1 and M_4 for which the fringes vanish. This corresponds to the point where the graphs (Fig. 5) cross the horizontal axis, that is, for the value $F(k,n)=0$. A preliminary investigation by Merrill, with the apparatus used by Anderson[1] in the measurement of Capella, revealed in fact a definite decrease in visibility of the fringes of α Orionis for the maximum separation of the slits (100 inches). This was true, moreover, for all position angles, which indicated that the star is not a binary and that the decrease in visibility is to be attributed to a measurable diameter.

On December 13, 1920, after preliminary settings on β Persei with the mirrors separated 81 inches (229 cm) and on β Persei and γ Orionis with a separation of 121 inches, thus insuring that the instrument was in perfect adjustment, it was turned on α Orionis and fringes across the interferometer image were sought for some time, but could not be found. The seeing was very good, and the zero fringes could be picked up at will.

When next turned on α Canis Minoris the fringes stood out on both images with practically no adjustment of the compensating wedge, which furnishes a check on the disappearance of the fringes for α Orionis.

It is clear from these observations that the disappearance of the fringes in the case of α Orionis cannot have been due to any disturbance of the mirrors caused by changes in the position of the telescope, for changes such as those here involved require only a few turns of the rod controlling the compensating wedge to counteract differences in atmospheric path and flexure and bring the fringes again into view. There is therefore no chance that they were simply overlooked in the case of α Orionis.

To observe the recurrence of the fringes near the second maximum for α Orionis, the mirrors were next separated a distance of 13 feet and the telescope turned on α Canis Minoris, fringes appearing across both star images as soon as the component pencils were brought into coincidence. On December 14 and the nights following, the seeing was very poor, the visibility of standard check stars being decidedly less than on the night of December 13; consequently no attempt was made to observe the second maximum and minimum of α Orionis, but attention was turned to other stars, and settings were made on α Ceti, α Tauri, and β Geminorum. The zero fringes were seen in every case, although with slightly decreased visibility; but it was only at rare intervals of better seeing that the interferometer fringes could be seen at all. From this fact it is presumed that there was an actual decrease of visibility for these stars and that some estimate of their diameters can be made with the 20-foot beam. Observations on these and other objects of presumably large diameter are being continued.

---

[1] *Mt. Wilson Contr.*, No. 185; *Astrophysical Journal*, **51**, 263, 1920.

Assuming that the effective wave-length for α Orionis is λ 5750, its angular diameter from the formula $\alpha=1.22\ \lambda/b$ proves to be 0″.047; and with a parallax[1] of 0″.018 its linear diameter turns out to be 240×10^6 miles, or slightly less than that of the orbit of Mars. This value corresponds to a uniformly illuminated disk, while for one darkened at the limb, this result, as mentioned above, would be increased by about 17 per cent. The uncertainty of the measurement of the angular diameter is about 10 per cent.

Cordial acknowledgment is tendered to Director George E. Hale for placing the resources of the Observatory at our disposal and for his enthusiastic co-operation in furthering the investigation.

Mr. J. A. Anderson was present on several occasions and we wish particularly to acknowledge his valuable assistance in checking the measures on December 13.

Mount Wilson Observatory
February 1921

---

[1] The weighted mean of Adams' spectroscopic parallax, 0″.012, and the trigonometric values of Elkin, 0″.030, and of Schlesinger, 0″.016.

Contributions from the Mount Wilson Observatory, No. 204

THE PHOTOGRAPHIC DETERMINATION OF STELLAR PARALLAXES WITH THE 60-INCH REFLECTOR

FIFTH SERIES

By ADRIAAN VAN MAANEN

The present publication is a continuation of the four previous series of parallaxes.[1] As the processes of taking, measuring, and reducing the plates are practically the same as in the former series, no details as to the derivation of the present results need be mentioned.

The necessary data for each field are collected in the tables, which are arranged as in the previous papers.

The results are collected in Table I, in which the successive columns give: (1) the name of the object; (2) and (3) the right ascension and declination for 1900.0; (4) the magnitude on the Harvard system; (5) the Mount Wilson estimated spectral type; (6) the relative parallax; (7) its probable error; and (8) the number of exposures.

The mean number of exposures is 16.4; the mean probable error of a final parallax, 0".0057.

An extensive discussion of the systematic error of the Mount Wilson trigonometric parallaxes was given in the fourth series.[2] A comparison with the spectroscopically determined parallaxes was then omitted, as they were at that time in process of revision. The results for seventy-nine stars common to both lists have since then been published by Adams and his collaborators in *Contribution* No. 199, the weighted mean difference $\pi_{\text{sp.}} - \pi_{\text{vM}}$ being $-0''.0032$. For the thirteen stars included in the present paper the difference is $-0''.0007$; for all ninety-two stars which have now been observed by both Adams and the author, it is $-0''.0029$. This result is in good agreement with the conclusions reached in *Contributions* Nos. 182 and 189.

[1] *Mt. Wilson Contr.*, Nos. 111, 1916; 136, 1917; 158, 1918; 182, 1920.

[2] *Ibid.*, No. 182, 1920.

Special note should be made of the following fields, of which it should be mentioned that the absolute parallaxes have been used after applying the systematic corrections found in *Contribution* No. 189.

TABLE I

Object	α 1900	δ 1900	Vis. Mag. Harvard	Mount Wilson Spectrum	Relative Parallax	P.E.	No. of Exp.
N.G.C. 40	$0^h\ 7^m 35^s$	$+71°58'$	11.6*	Pl. Neb.	+0″.003	0″.003	18
T Cassiopeiae	0 17 48	+55 14	Var.	Md	+0.027	0.003	18
Lalande 1966	1 3 18	+61 1	7.8	F5	+0.015	0.004	16
Boss 394	1 40 30	+63 22	5.74	K0	+0.118	0.007	16
Boss 500	2 6 57	+50 36	5.40	G5	+0.011	0.005	16
Boss 654	2 47 24	+37 56	5.32	F0	+0.027	0.009	16
Lalande 6888	3 40 12	+41 9	8.4	K0	+0.076	0.005	16
Lalande 6889			8.8	K2	+0.081	0.006	16
Anonymous	4 53 11	+39 13	13.2†	....	+0.010	0.005	16
RX Aurigae	4 54 28	+39 49	Var.	F9p	−0.001	0.005	16
N.G.C. 2022	5 36 37	+ 9 2	14.2*	Pl. Neb.	+0.008	0.004	16
N.G.C. 2371–2	7 19 18	+29 41	13.5*	Pl. Neb.	+0.011	0.005	16
W Ursae Maj	9 36 42	+56 25	Var.	F8p	+0.023	0.006	14
Boss 3145	11 57 24	+43 39	6.83	G7	−0.013	0.006	16
N.G.C.4051	11 58 7	+45 6	13.8*	Sp. Neb.	+0.001	0.005	16
Boss 3322	12 40 24	+45 58	5.53	N	−0.002	0.003	16
Boss 3554	13 42 0	+ 6 51	6.32	F9	+0.026	0.007	16
N.G.C. 6210	16 40 18	+23 59	11.7*	Pl. Neb.	−0.003	0.003	16
N.G.C. 6543	17 58 32	+66 38	11.3*	Pl. Neb.	+0.029	0.004	16
Nova Aquilae No. 3	18 43 49	+ 0 29	Var.	Nova	+0.019	0.006	16
17 Lyrae C	19 3 40	+32 21	11.00	Ma	+0.109	0.008	16
RR Lyrae	19 22 14	+42 36	Var.	F0p	+0.006	0.006	20
B.D+30°3639	19 30 54	+30 18	9.55	O	+0.005	0.009	16
Pi. 22^h214	22 40 54	+29 54	6.52	K0	+0.027	0.007	16
Boss 6020	23 18 52	+31 59	6.53	A9	+0.014	0.008	16
Pi. 23^h164	23 38 30	+57 31	7.3	G2	+0.028	0.009	20

* The magnitudes for the central stars of the nebulae are photographic, derived from counts of the number of stars of equal and brighter magnitudes and are based on Table IV of *Groningen Publications*, No. 27.

†This magnitude is photographic, determined in the same way as the magnitudes of the central stars of the nebulae.

a) **Planetary Nebulae.** The present series contains the results for five additional planetary nebulae. A summary of their parallaxes, together with the computed absolute magnitudes and diameters in light-years, is given in Table II.

In order to get an idea of the size of these remarkable objects, the mean absolute magnitude and the mean diameter have been computed for the eleven planetaries for which fairly reliable parallaxes are now available. The result is, for mean absolute magnitude,

+8.4; for mean diameter, 3740 astronomical units or 0.06 light-years.

TABLE II

N.G.C.	$\pi_{\text{abs.}}$	m	M	Diameter	
				Angular	Light-Years
40	+0″.003	11.6	+4.0	60″	0.32
2022	+0.008	14.2	+8.7	28	0.06
2371–2	+0.011	13.5	+8.7	60	0.09
6210	−0.003	11.7	....	43	....
6543	+0.029	11.3	+8.6	22	0.01

b) **T Cassiopeiae.** This is the first long-period variable for which a parallax has been determined at this observatory. For only one other star of this type is a trigonometric parallax available, viz., *o* Ceti, for which Russell gives $\pi_{\text{abs.}}$ +0″.160; Kostinsky, −0″.025; and Mitchell, +0″.064.

The parallax of +0″.027, found for T Cassiopeiae, gives for this star the absolute magnitudes +3.9 at maximum and +9.7 at minimum. Using the weighted mean value of the parallax for *o* Ceti, we find as corresponding values +0.1 and +8.0.

Several stars of this type are now under observation for parallax, and it therefore seems better to await further results before drawing any conclusions about these objects.

In securing parallax plates for these long-period variables, it is necessary to know the apparent magnitude at the different epochs with a fair degree of accuracy, in order that we may always secure photographic images of about the same brightness by the use of rotating sectors of different openings. Mr. Leon Campbell has had the extreme kindness to furnish me with the necessary data for most cases. I am also under obligation to Mr. Paul Merrill for several estimates of the brightness of the stars under observation.

c) **Lalande 1966.** This star was placed on the parallax program on account of the discordance between the existing values for its parallax. Other stars included for similar reasons are Lalande 6888–9, for which the parallax values range from −0″.161 to +0″.190, Pi. $22^{\text{h}}214$, and Pi. $23^{\text{h}}164$.

d) **Boss 500.** This star has a proper motion of 0″.400; its parallax, however, is extremely small; Yerkes gives $\pi_{\text{abs.}}$ +0″.003; Allegheny, +0″.014; Adams, +0″.012; van Maanen, +0″.011; the weighted mean is 0″.010. The motion at right angles to the line of sight is 190 km/sec. As its radial velocity is 30 km/sec., the space velocity is 192 km/sec., an extraordinary value for a star of absolute magnitude +0.4.

e) **Anonymous.** $\alpha=4^h53^m11^s$, $\delta=+39°13'$. This star was measured as a comparison star in deriving the parallax of Boss 1182, but was later rejected for this purpose on account of its large proper motion ($\mu=0''.377$ in p 114°.6) and presumably large parallax. The present measures yield a parallax of +0″.010±0″.005, indicating an absolute magnitude of +8.2 and a velocity at right angles to the line of sight of about 180 km/sec.

f) **RX Aurigae and RR Lyrae.** The parallaxes of these Cepheids show good agreement with the values found by Shapley, +0″.0006 and +0″.0030, respectively. For RR Lyrae, Adams finds the spectroscopic parallax to be +0″.004. The small value of the parallax found by three different methods is quite remarkable, as the star has a large proper motion, viz., 0″.221. Taking the mean of the three values, we find the absolute magnitude to be 0.0 at maximum and +0.9 at minimum. The velocity at right angles to the line of sight is 243 km/sec.; the radial velocity is 50 km/sec., thus giving a total velocity of nearly 250 km/sec., another example of a very luminous star with an extraordinarily high velocity.

g) **W Ursae Majoris.** For this eclipsing variable, three parallaxes are now known: Shapley, +0″.020; Yerkes, +0″.017; and van Maanen, +0″.023. The mean parallax, +0″.020, gives an absolute magnitude of +4.4 at maximum and +5.1 at minimum.

h) **N.G.C. 4051.** This is a spiral nebula described by Curtis as "a fine, rather bright spiral 4′×2′; very bright stellar nucleus. There are numerous almost stellar condensations. It is a two-branched spiral and each branch is bifid." On the 15-minute exposures taken at the 80-foot focus of the 60-inch reflector, the central part only is visible and in appearance its images are hardly different from the surrounding stars. The photographic magnitude is 13.8. For three spiral nebulae (N.G.C. 224, 4051, and 5194) parallaxes have now been determined at this observatory; all give positive parallaxes, but the values are too small to afford any reliable conclusions as to the distance of these objects.

i) **Boss 3322.** This is the only N-type star for which a trigonometric parallax has been determined. Its small negative value points to high luminosities for these stars, in agreement with Kapteyn's value for their mean parallax (0".0007), based on their proper motions.[1]

j) **Nova Aquilae No. 3.** The parallax of +0".019 derived here gives an absolute magnitude of −5.1 at maximum and +6.9 at minimum. The other results at present available are the preliminary value by Olivier, +0".007, and two values derived from meridian circle observations by Messrs. Philippot and Delporte,[2] who find +0".197 and +0".064, respectively. As the star is on the parallax programs of several observatories, we may expect before long a more reliable value for its distance.

k) **B.D.+30° 3639.** This is Campbell's hydrogen-envelope star. The nebulosity surrounding the star is not quite symmetrical and plates taken when the seeing is not of the best may easily vitiate the result. Great weight should not, in consequence, be attached to the present result. The series of plates will be continued until an extremely good set is available.

[1] *Astrophysical Journal*, **32**, 91, 1910.

[2] *Annales de l'Obs. Royal de Belgique*, **14**, 223, 237, 1918.

N.G.C. 40 $\alpha = 0^h 7^m 35^s$ $\delta = +71^\circ 58'$

Pl. No.	Date			t	Obs.	Qy	p	m	Remarks
1852_1..	1918	Aug.	11	−11.°7	Hum	fg	+0.641	+3.61	
1852_2..			11	− 7.2	vM	g	+0.641	+3.61	
1864_1..			12	− 9.0	Hum	g	+0.629	+3.62	
1864_2..			12	− 4.5	vM	g	+0.629	+3.62	
1989_1..		Oct.	27	+ 2.2	H	f	−0.479	+3.82	20^m exp.
1989_2..			27	+ 8.0	vM	f	−0.479	+3.82	20^m exp.
2023_1..		Nov.	10	−11.7	vM	g	−0.650	+3.86	
2023_2..			10	− 7.5	H	fg	−0.650	+3.86	
2040_1..			11	− 6.5	vM	fg	−0.659	+3.87	
2040_2..			11	− 2.0	H	fg	−0.659	+3.87	
2078...		Dec.	27	+12.5	vM	fg	−0.900	+3.99	
2095...			28	+14.0	vM	gas	−0.900	+3.99	
2300...	1919	July	31	+ 6.5	B	fg	+0.756	+4.58	
2326_1..		Aug.	19	− 5.0	B	fg	+0.547	+4.64	
2326_2..			19	− 0.5	H	fg	+0.547	+4.64	
2448...		Nov.	16	−10.0	Hum	g	−0.708	+4.88	
2810_1..	1920	Aug.	6	+ 1.5	vM	g	+0.690	+5.60	
2810_2..			6	+ 5.7	Hum	g	+0.690	+5.60	

Mor.-Ev.	Δp	Δm	M	v	Δt
1852_1–2023_1....	+1.29	−0.25	+13	+ 9	0.°0
1864_1–2448....	+1.34	−1.26	+17	+ 6	+ 1.0
1852_2–2023_2....	+1.29	−0.25	−10	−14	+ 0.3
2326_1–2040_1....	+1.21	+0.77	− 6	− 2	+ 1.5
1864_2–2040_2....	+1.29	−0.25	+ 2	− 2	− 2.5
2326_2–1989_1....	+1.03	+0.82	−12	− 8	− 2.7
2300 –1989_2....	+1.24	+0.76	− 7	− 4	− 1.5
2810_1–2078	+1.59	+1.61	−10	− 1	−11.0
2810_2–2095....	+1.59	+1.61	+ 2	+11	− 8.3

$+8.79\,\mu_\alpha + 5.18\,\pi = -55$ $\qquad \pi = +1.6 = +0''.003 \pm 0''.003$

$+5.18\,\mu_\alpha + 15.90\,\pi = -11$ $\qquad \mu_\alpha = -7.2 = -0''.012 \pm 0''.004$

Comp. Star	Br.	x	y	π	P.E.
1........	bf	+3′.0	+2′.3	−0″.002	±0″.011
2........	bf	+7.1	+0.5	−0.003	0.009
3........	f	+2.6	−1.8	−0.005	0.009
4........	f	−1.6	−4.1	−0.001	0.013
5........	b	−3.7	−4.1	+0.010	0.011
6........	f	−5.1	+1.9	−0.017	0.008
7........	f	−2.2	+3.0	+0.005	0.009
8........	f	−0.3	+3.4	+0.013	±0.012

T Cassiopeiae $\alpha = 0^h 17^m 48^s$ $\delta = +55^\circ 14'$

Pl. No.	Date	t	Obs.	Qy	p	m	Remarks
2488_1..	1919 Dec. 15	$+4^\circ.5$	vM	g	−0.882	+4.96	Thick, 20^m exp.
2488_2..	15	+10.0	H	gas	−0.882	+4.96	Thick, 20^m exp.
2500_1..	17	− 3.2	vM	fg	−0.889	+4.96	Clouds, 20^m exp.
2500_2..	17	+ 3.2	H	fg	−0.889	+4.96	Thick, 20^m exp.
2828_1..	1920 Aug. 19	+ 1.7	H	g	+0.574	+5.64	
2828_2..	19	+ 6.0	vM	fg	+0.574	+5.64	
2839_1..	20	− 8.5	vM	g	+0.561	+5.64	
2839_2..	20	− 4.0	H	g	+0.561	+5.64	
2853_1..	21	− 1.5	vM	g	+0.548	+5.64	
2853_2..	21	+ 2.2	H	g	+0.548	+5.64	
2868...	22	+12.5	H	g	+0.536	+5.64	
2879...	Sept. 7	+13.5	vM	fg	+0.313	+5.69	20^m exp.
2886...	8	+ 7.5	vM	g	+0.297	+5.69	
2962_1..	Nov. 3	+ 0.2	vM	g	−0.538	+5.84	
2962_2..	3	+ 4.2	Hum	g	−0.539	+5.84	
2975_1..	Dec. 3	+ 9.0	vM	gas	−0.830	+5.93	
2975_2..	3	+13.2	Hum	fg	−0.830	+5.93	
2989...	5	− 0.2	Hum	fg	−0.839	+5.93	Trail of Boss 71

Mor.-Ev.	Δp	Δm	M	v	Δt
2839_1–2500....	+1.45	+0.68	+25	+ 5	$-5^\circ.3$
2839_2–2989....	+1.40	−0.29	+20	− 6	−3.8
2853_1–2962_1....	+1.09	−0.20	+ 8	−11	−1.7
2828_1–2500_2....	+1.46	+0.68	+17	− 4	−1.5
2853_2–2962_2....	+1.09	−0.20	+11	− 8	−2.0
2828_2–2488_1....	+1.46	+0.68	+30	+ 9	+1.5
2886 –2975_1....	+1.13	−0.24	+36	+16	−1.5
2868 –2488_2....	+1.42	+0.68	+11	− 9	+2.5
2879 –2975_2....	+1.14	−0.24	+27	+ 7	+0.3

$$+2.12\,\mu_a + 2.55\,\pi = +31 \qquad \pi = +16.8 = +0''.027 \pm 0''.003$$

$$+2.55\,\mu_a + 15.30\,\pi = +242 \qquad \mu_a = -5.6 = -0''.009 \pm 0''.009$$

Comp. Star	Br.	x	y	π	P.E.
1........	bf	$+1'.8$	$+4'.9$	$-0''.001$	$\pm 0''.008$
2........	bf	+3.0	+1.6	+0.008	0.010
3........	f	+4.3	−4.8	+0.001	0.007
4........	bf	+1.4	−4.7	−0.007	0.007
5........	bf	−1.5	−1.9	+0.002	0.005
6........	b	−5.1	−2.5	−0.005	0.004
7........	b	−2.1	+2.6	+0.032	0.008
8........	f	−1.1	+4.9	−0.026	±0.009

Lalande 1966 $\alpha = 1^h 3^m 18^s$ $\delta = +61°1'$

Pl. No.	Date	t	Obs.	Qy	p	m	Remarks
1917_1..	1918 Sept. 4	−11°0	H	fg	+0.540	+3.68	
1917_2..	4	− 7.0	vM	fg	+0.540	+3.68	
1931_1..	5	−11.5	vM	g	+0.527	+3.68	
1931_2..	5	− 7.2	H	g	+0.527	+3.68	
2042_1..	Nov. 11	+ 1.0	vM	g	−0.477	+3.87	
2042_2..	11	+ 5.0	H	g	−0.477	+3.87	
2079_1..	Dec. 27	+ 4.2	H	fg	−0.888	+3.99	
2079_2..	27	+ 8.5	vM	fg	−0.888	+3.99	
2433_1..	1919 Nov. 15	− 2.7	vM	fg	−0.527	+4.88	
2433_2..	15	+ 1.5	Hum	fg	−0.527	+4.88	
2462_1..	17	− 8.7	vM	fg	−0.553	+4.88	Thick, 20^m exp.
2462_2..	17	− 3.5	H	fg	−0.553	+4.88	Thick, 20^m exp.
2811_1..	1920 Aug. 6	− 2.5	vM	g	+0.835	+5.60	
2811_2..	6	+ 1.5	Hum	g	+0.835	+5.60	
2829_1..	19	+ 0.7	H	g	+0.721	+5.64	
2829_2..	19	+ 5.0	vM	g	+0.721	+5.64	

Mor.-Ev.	Δp	Δm	M	v	Δt
1931_1–2462_1....	+1.08	−1.20	−458	−16	−2°8
1917_1–2462_2....	+1.09	−1.20	−443	− 1	−7.5
1931_2–2433_1....	+1.05	−1.20	−429	+13	−4.5
1917_2–2042_1....	+1.02	−0.19	− 49	+14	−8.0
2811_1–2433_2....	+1.36	+0.72	+275	− 9	−4.0
2829_1–2079_1....	+1.61	+1.65	+647	+11	−3.5
2811_2–2042_2....	+1.31	+1.73	+650	−13	−3.5
2829_2–2079_2....	+1.61	+1.65	+641	+ 5	−3.5

$$+13.31\,\mu_\alpha + 4.51\,\pi = +5054 \qquad \pi = +\ 9.3 = +0''015 \pm 0''004$$
$$+\ 4.51\,\mu_\alpha + 13.25\,\pi = +1822 \qquad \mu_\alpha = +376.6 = +0''614 \pm 0''004$$

Comp. Star	Br.	x	y	π	P.E.
1........	f	+1'2	+0'5	+0''007	±0''009
2........	bf	+4.0	+3.2	−0.005	0.004
3........	bf	+5.9	−0.7	0.000	0.006
4........	f	+1.4	−2.6	0.000	0.009
5........	bf	−4.1	−3.2	0.000	0.003
6........	bf	−4.0	−1.4	−0.003	0.004
7........	f	−2.6	0.0	0.000	0.007
8........	f	−1.5	+3.3	+0.002	±0.007

Boss 394 $\alpha = 1^h 40^m 30^s$ $\delta = 63°22'$

Pl. No.	Date	t	Obs.	Qy	p	m	Remarks
1933_1..	1918 Sept. 5	0°0	vM	g	+0.657	+3.68	
1933_2..	5	+ 4.0	H	fg	+0.657	+3.68	
2054_1..	Nov. 26	+ 1.2	H	f	−0.549	+3.91	20^m exp.
2080_1..	Dec. 27	+ 5.0	H	fg	−0.850	+3.99	
2080_2..	27	+ 9.2	vM	fg	−0.850	+3.99	
2096_1..	28	− 3.0	H	fg	−0.856	+3.99	
2096_2..	28	+ 1.0	vM	f	−0.856	+3.99	
2319_1..	1919 Aug. 18	+ 1.0	Hum	g	+0.834	+4.63	
2319_2..	18	+ 5.0	B	g	+0.834	+4.63	
2363_1..	Sept. 17	− 1.7	B	g	+0.511	+4.72	
2363_2..	17	+ 3.0	Hum	g	+0.511	+4.72	
2434_1..	Nov. 15	− 2.0	vM	fg	−0.395	+4.88	
2434_2..	15	+ 2.2	Hum	fg	−0.395	+4.88	
2528...	1920 Jan. 15	+10.0	vM	fg	−0.916	+5.04	
2830...	Aug. 19	+ 1.5	H	fg	+0.820	+5.64	Trail
2843...	20	+ 6.5	H	g	+0.812	+5.64	

Mor.-Ev.	Δp	Δm	M	v	Δt
2363_1–2434^1 ...	+0.91	−0.16	+ 18	+ 8	+0°3
1933_1–2096^1 ...	+1.51	−0.31	− 2	− 3	+3.0
2319_1–2096^2 ...	+1.69	+0.64	+345	− 2	0.0
2830 –2054....	+1.37	+1.73	+710	+ 4	+0.3
2363_2–2434^2 ...	+0.91	−0.16	− 34	−44	+0.8
1933_2–2080_1 ...	+1.51	−0.31	+ 23	+22	−1.0
2319_2–2080_2 ...	+1.68	+0.64	+331	−15	−4.2
2843 –2528....	+1.73	+0.60	+351	+15	−3.5

$+4.43\,\mu_\alpha + 4.33\,\pi = +1868$ $\pi = +72.6 = +0''.118 \pm 0''.007$

$+4.33\,\mu_\alpha + 16.77\,\pi = +2736$ $\mu_\alpha = +350.7 = +0''.572 \pm 0''.014$

Comp. Star	Br.	x	y	π	P.E.
1........	f	+0'.8	+5'.9	−0''.020	±0''.004
2........	f	+3.4	+2.5	+0.005	0.007
3........	b	+6.6	−2.1	−0.017	0.008
4........	ff	+1.0	−4.9	+0.008	0.006
5........	bf	−4.4	−6.5	−0.002	0.007
6........	f	−6.2	−0.3	−0.017	0.012
7........	f	−1.8	+3.4	+0.005	0.009
8........	bf	−0.3	+1.9	+0.038	±0.011

Boss 500 = Bu 1141 $\alpha = 2^h6^m57^s$ $\delta = +50°36'$

Pl. No.	Date	t	Obs.	Qy	p	m	Remarks
1934_1..	1918 Sept. 5	$+3°.5$	vM	g	+0.739	+3.68	
1934_2..	5	+ 7.5	H	fg	+0.739	+3.68	
2061_1..	Dec. 9	+ 1.0	vM	fg	−0.633	+3.94	
2081_1..	27	+ 8.5	H	fg	−0.812	+3.99	
2081_2..	27	+12.5	vM	fg	−0.812	+3.99	
2110...	1919 Jan. 23	+10.2	vM	fg	−0.925	+4.07	20^m exp.
2131...	25	+11.0	vM	fg	−0.925	+4.07	
2336_1..	Aug. 20	− 2.0	B	fg	+0.876	+4.64	
2336_2..	20	+ 2.0	H	fg	+0.876	+4.64	
2342...	Sept. 15	+ 1.0	B	g	+0.631	+4.71	
2343...	15	+ 5.7	H	g	+0.631	+4.71	
2353_1..	16	− 2.0	B	fg	+0.619	+4.71	
2353_2..	16	− 2.0	H	fg	+0.619	+4.71	
2489_1..	Dec. 15	−10.5	vM	fg	−0.697	+4.96	20^m exp.
2489_2..	15	− 4.7	H	fg	−0.697	+4.96	20 exp. Trail
2502...	17	− 6.2	H	gas	−0.718	+4.96	

Mor.-Ev.	Δp	Δm	M	v	Δt
2336_1–2489_1 ...	+1.57	−0.32	− 65	0	$+8°.5$
2353_1–2502....	+1.34	−0.25	− 66	−17	+4.2
2342 –2061....	+1.26	+0.77	+154	−34	0.0
2336_2–2081_1 ...	+1.69	+0.65	+179	+16	−6.5
2353_2–2110....	+1.54	+0.64	+167	+ 8	−8.2
1934_1–2489_2 ...	+1.44	−1.28	−296	− 7	+8.2
2343 –2131....	+1.56	+0.64	+165	+ 6	−5.3
1934_2–2081_2 ...	+1.55	−0.31	− 42	+20	−5.0

$$+3.73\mu_a + 0.90\pi = +877 \qquad \pi = +6.6 = +0''.011 \pm 0''.005$$
$$+0''.90\mu_a + 17.98\pi = +330 \qquad \mu_a = +233.5 = +0''.381 \pm 0''.011$$

The $10^M.2$ companion which is not physically connected with Boss 500 is Comparison Star 1.

Comp. Star	Br.	x	y	π	P.E.
1........	b	$+2'.1$	$+0'.8$	$+0''.009$	$\pm0''.009$
2........	f	+1.6	−0.8	−0.013	0.007
3........	f	−1.4	−2.3	+0.001	0.009
4........	bf	−1.4	−1.4	+0.016	0.007
5........	bf	−1.9	−0.7	−0.012	0.010
6........	f	−0.8	+1.9	−0.001	0.008
7........	f	+1.4	+2.6	0.000	±0.003

Boss 654 = Bu 1471 $\alpha = 2^h 47^m 24^s$ $\delta = +37°56'$

Pl. No.	Date			t	Obs.	Qy	p	m	Remarks
1947_1	1918	Sept.	28	−2°5	H	fg	+0.606	+3.75	Clouds, 20^m exp.
1947_2			28	+4.0	vM	fg	+0.604	+3.75	Clouds, 25^m exp.
1952			29	−13.5	vM	fg	+0.592	+3.75	Hazy, 25^m exp.
1965		Oct.	13	+2.0	vM	g	+0.394	+3.79	Clouds, 25^m exp.
2098_1		Dec.	28	+1.2	H	fg	−0.741	+3.99	
2098_2			28	+5.2	vM	fg	−0.741	+3.99	
2111_1	1919	Jan.	23	+6.7	H	fg	−0.922	+4.07	
2111_2			23	+11.0	vM	fg	−0.922	+4.07	
2132_1			25	+6.7	Hum	f	−0.927	+4.07	
2132_2			25	+11.0	vM	f	−0.927	+4.07	
2145_1			26	+2.2	vM	fg	−0.930	+4.07	
2145_2			26	+6.2	vM	fg	−0.930	+4.07	
2344		Sept.	15	+3.0	B	g	+0.758	+4.71	
2345			15	+8.0	H	g	+0.758	+4.71	
2364			17	−1.5	Hum	fg	+0.737	+4.72	
2378		Oct.	17	+9.0	Hum	g	+0.335	+4.80	20^m exp. Trail

Mor.-Ev.	Δp	Δm	M	v	Δt
$1952-2098_1$	+1.33	−0.24	−35	−58	−14°7
1947_1-2145_1	+1.54	−0.32	+32	+4	−4.7
$2364-2098_2$	+1.48	+0.73	0	−21	−6.7
$1965-2145_2$	+1.32	−0.28	+44	+21	−4.2
$2344-2111_1$	+1.68	+0.64	+51	+26	−3.7
1947_2-2132_1	+1.53	−0.32	+46	+18	−2.7
$2345-2111_2$	+1.68	+0.64	+36	+11	−3.0
$2378-2132_2$	+1.26	+0.73	+4	−13	−2.0

$$+2.22\mu_a + 2.49\pi = +30 \qquad \pi = +16.7 = +0''.027 \pm 0''.009$$

$$+2.49\mu_a + 17.64\pi = +281 \qquad \mu_a = -5.2 = -0''.008 \pm 0''.025$$

The principal star is a close double, with components about 0″2 distant; the images are all elongated and therefore difficult to measure.

The $10^M_.0$ companion, being covered by the sector, does not show measurable images on the plates.

Comp. Star	Br.	x	y	π	P.E.
1	f	+0′7	+0′5	−0″011	±0″007
2	bf	+1.5	+2.7	−0.002	0.003
3	f	+4.3	+0.1	+0.007	0.008
4	bf	0.0	−2.6	+0.002	0.007
5	b	−0.4	−5.6	−0.002	0.004
6	f	−2.3	−1.1	+0.001	0.006
7	bf	−4.1	+2.3	+0.004	0.006
8	f	−1.9	+3.6	0.000	±0.005

Boss 862 = B u 1854 $\alpha=3^h40^m12^s$ $\delta=+41°9'$

Pl. No.	Date	t	Obs.	Qy	p	m	Remarks
2099_1	1918 Dec. 28	− 2°0	H	g	−0.603	+3.99	
2099_2	28	+ 2.0	vM	fg	−0.603	+3.99	
2133_1	1919 Jan. 25	+ 3.7	Hum	f	−0.884	+4.07	
2133_2	25	+ 8.2	vM	fg	−0.884	+4.07	
2346	Sept. 15	+ 1.0	B	g	+0.887	+4.71	
2365_1	17	−10.0	B	fg	+0.873	+4.72	
2365_2	17	− 6.0	B	g	+0.873	+4.72	
2391_1	Oct. 18	−11.7	vM	fg	+0.525	+4.80	
2391_2	18	− 8.0	vM	fg	+0.525	+4.80	
2405_1	19	−10.7	vM	fg	+0.511	+4.80	
2405_2	19	− 7.0	vM	fg	+0.511	+4.80	
2425	20	+14.0	H	g	+0.495	+4.81	
2491_1	Dec. 15	− 6.5	vM	fg	−0.413	+4.96	Thick, 20^m exp.
2491_2	15	− 1.5	H	fg	−0.413	+4.96	Thick, 20^m exp.
2504_1	17	−15.5	H	g	−0.443	+4.96	Thick, 20^m exp.
2504_2	17	−10.2	vM	fg	−0.443	+4.96	Thick, 20^m exp.

Mor.-Ev.	Δp	Δm	M (862)	M (comp)	v (862)	v (comp)	Δt
2391_1–2504_1	+0.97	−0.16	+ 1	+ 4	+ 9	+11	+3°8
2405_1–2504_2	+0.95	−0.16	− 5	− 6	+ 4	+ 2	−0.5
2365_1–2491_1	+1.29	−0.24	− 41	− 33	−22	−15	−3.5
2391_2–2491_2	+0.94	−0.16	+ 9	− 11	+18	− 3	−6.5
2405_2–2099_1	+1.11	+0.81	+328	+338	+ 9	+ 5	−5.0
2365_2–2099_2	+1.48	+0.73	+308	+300	− 2	−24	−8.0
2346 –2133_1	+1.77	+0.64	+297	+322	+ 3	+14	−2.7
2425 –2133_2	+1.38	+0.74	+298	+330	−11	+ 8	+5.8

$$\left.\begin{array}{r}+2.29\,\mu_a+3.36\,\pi=+912\\+3.36\,\mu_a+12.83\,\pi=+1708\end{array}\right\}(862)\qquad\left.\begin{array}{r}+953\\+1789\end{array}\right\}(\text{comp.})$$

$$(862)\left\{\begin{array}{l}\pi=+46.8=+0''.076\pm0''.005\\\mu_a=+329.6=+0''.537\pm0''.013\end{array}\right\}(\text{comp.})\left\{\begin{array}{l}\pi=+49.=+0''.081\pm0''.006\\\mu_a=+343.5=+0''.560\pm0''.013\end{array}\right.$$

Comp. Star	Br.	x	y	π	P.E.
1	f	+0'.7	+3'.6	+0''.030	±0''.007
2	b	+5.6	+1.1	+0.010	0.008
3	ff	+1.5	−4.1	−0.017	0.011
4	ff	0.0	−2.5	−0.006	0.012
5	f	−1.4	−3.4	+0.005	0.014
6	f	−4.3	−2.5	+0.021	0.013
7	bf	−1.8	+3.7	−0.027	0.011
8	f	−0.7	+2.2	−0.016	±0.013

Anonymous $\alpha = 4^h 53^m 11^s$ $\delta = +39°13'$

Pl. No.	Date			t	Obs.	Qy	p	m	Remarks
2408_1..	1919	Oct.	19	+2°0	vM	fg	+0.747	+4.80	
2408_2..			19	+6.2	H	g	+0.747	+4.80	
2426_1..			20	+1.5	vM	g	+0.735	+4.81	
2426_2..			20	+5.7	H	vg	+0.735	+4.81	Trail of Boss 1182
2532_1..	1920	Jan.	15	−1.0	H	fg	−0.627	+5.04	20^m exp.
2532_2..			15	+4.5	vM	fg	−0.627	+5.04	20^m exp.
2545_1..			17	−0.7	H	f	−0.653	+5.05	25^m exp.
2545_2..			17	+6.0	vM	fg	−0.653	+5.05	25^m exp.
2558_1..		Feb.	11	+3.7	H	g	−0.904	+5.12	
2558_2..			11	+7.5	vM	g	−0.904	+5.12	
2573_1..			12	−4.5	H	g	−0.909	+5.12	
2573_2..			12	−0.5	vM	g	−0.909	+5.12	
2928_1..		Oct.	4	−7.0	vM	g	+0.886	+5.76	
2928_2..			4	−2.5	H	g	+0.886	+5.76	
2945_1..			5	−3.5	vM	fg	+0.878	+5.77	
2945_2..			5	+0.5	H	g	+0.878	+5.77	

Mor.-Ev.	Δp	Δm	M	v	Δt
2928_1–2573_1....	+1.80	+0.64	+163	+17	−2°5
2945_1–2532_1....	+1.51	+0.73	+157	− 7	−2.5
2928_2–2545_1....	+1.54	+0.71	+152	− 8	−1.8
2945_2–2573_2....	+1.79	+0.65	+145	− 3	+1.0
2426_1–2558_1....	+1.64	−0.31	− 58	− 3	−2.2
2408_1–2532_2....	+1.37	−0.24	− 43	− 1	−2.5
2426_2–2545_2....	+1.39	−0.24	− 73	−31	−0.3
2408_2–2558_2....	+1.65	−0.32	− 31	+26	−1.3

$$+2.18\,\mu_\alpha + 2.80\,\pi = +477 \qquad \pi = +6.3 = +0.''010 \pm 0.''005$$

$$+2.80\,\mu_\alpha + 20.31\,\pi = +718 \qquad \mu_\alpha = +210.7 = +0.''343 \pm 0.''015$$

Comp. Star	Br.	x	y	π	P.E.
1........	f	+1'5	+2'5	+0"002	±0"007
2........	f	+2.9	+3.2	+0.013	0.006
3........	bf	+5.5	−1.0	−0.013	0.007
4........	b	+1.9	−3.8	−0.008	0.003
5........	b	0.0	−3.2	+0.024	0.005
6........	f	−6.3	−0.1	−0.006	0.004
7........	bf	−5.2	+2.3	+0.001	0.005
8........	f	−1.0	+0.8	−0.015	±0.008

RX Aurigae $\alpha=4^h54^m28^s$ $\delta=+39°49'$

Pl. No.	Date	t	Obs.	Qy	p	m	Remarks
1992...	1918 Oct. 27	−13°0	vM	fg	+0.648	+3.82	20^m exp.
2015$_1$..	29	−11.0	vM	g	+0.621	+3.83	
2015$_2$..	29	− 6.5	H	g	+0.621	+3.83	
2045 ..	Nov. 11	− 4.0	vM	fg	+0.431	+3.87	
2148$_1$..	1919 Jan. 26	+ 6.2	vM	f	−0.759	+4.07	20^m exp
2148$_2$..	26	+11.2	Hum	f	−0.759	+4.07	20^m exp.
2155$_1$..	Feb. 21	+ 1.5	vM	fg	−0.957	+4.15	
2155$_2$..	21	+ 6.2	H	g	−0.957	+4.15	
2556 ..	1920 Feb. 11	−12.0	vM	g	−0.902	+5.12	
2557$_1$..	11	− 6.7	H	g	−0.902	+5.12	
2557$_2$..	11	− 3.0	vM	g	−0.902	+5.12	
2572...	12	−10.0	vM	fg	−0.911	+5 12	
2929$_1$..	Oct. 4	+ 4.0	vM	g	+0.888	+5.76	
2929$_2$..	4	+ 8.5	H	g	+0.888	+5.76	Trail of Boss 1182
2946$_1$..	5	+ 6.0	vM	g	+0.880	+5.77	
2946$_2$..	5	+10.2	H	g	+0.880	+5.77	

Mor.-Ev.	Δp	Δm	M	v	Δt
1992 −2556....	+1.55	−1.30	−11	− 8	−1°0
2015$_1$−2572....	+1.53	−1.29	+ 7	+10	−1.0
2015$_2$−2557$_1$....	+1.52	−1.29	− 2	+ 1	+0.2
2045 −2557$_2$....	+1.33	−1.25	−11	− 8	−1.0
2929$_1$−2155$_1$....	+1.85	+1.61	+ 9	+ 7	+2.5
2946$_1$−2155$_2$....	+1.84	+1.62	+35	+33	−0.2
2929$_2$−2148$_1$....	+1.65	+1.69	−23	−25	+2.3
2946$_2$−2148$_2$....	+1.64	+1.70	−17	−19	−1.0

$$+17.53\,\mu_a+\ 3.93\,\pi=+25 \qquad \pi\ =-0.7=-0''.001\pm0''.005$$

$$+\ 3.93\,\mu_a+21.04\,\pi=-\ 9 \qquad \mu_a=+1.6=+0''.003\pm0''.005$$

Comp. Star	Br.	x	y	π	P.E.
1........	bf	+0'.7	+4'.7	+0''.016	±0''.007
2........	bf	+5.2	+1.5	−0.013	0.007
3........	f	+3.7	−0.8	+0.002	0.004
4........	b	+3.8	−5.2	+0.007	0.006
5........	f	−3.6	−3.4	−0.011	0.008
6........	f	−3.4	−0.1	+0.008	0.009
7........	bf	−4.1	+0.5	+0.008	0.005
8........	f	−3.2	+3.7	−0.016	±0.008

N.G.C 2022 $\alpha=5^h36^m37^s$ $\delta=+9^\circ2'$

Pl. No.	Date	t	Obs.	Qy	p	m	Remarks
1598...	1917 Nov. 7	−0°.2	H	g	+0.629	+2.85	
1614...	8	−5.0	H	g	+0.615	+2.86	
1615...	8	+3.2	vM	fg	+0.615	+2.86	
1686_1..	1918 Feb. 2	−0.5	vM	fg	−0.741	+3.09	
1686_2..	2	+8.2	H	f	−0.741	+3.09	Hazy
1705...	3	+14.5	vM	g	−0.754	+3.10	Thick, 40^m exp.
1723_1..	4	+0.5	H	fg	−0.764	+3.10	
1723_2..	4	+8.7	vM	fg	−0.764	+3.10	Hazy
2031...	Nov. 10	−8.0	H	g	+0.590	+3.86	
2114...	1919 Jan. 23	+2.0	H and vM	f	−0.624	+4.07	40^m exp.
2115...	23	+12.5	H and vM	fg	−0.624	+4.07	40^m exp.
2149...	26	+10.7	vM and Hum	f	−0.650	+4.07	40^m exp.
2381...	Oct. 17	+6.7	vM and Hum	fg	+0.868	+4.80	50^m exp.
2395...	18	+8.2	H	fg	+0.860	+4.80	40^m exp.
2409...	19	+3.7	vM	g	+0.850	+4.80	Trail of Boss 1404
2428...	20	+14.2	H	fg	+0.841	+4.81	

Mor.-Ev.	Δp	Δm	M	v	Δt
2031–2114.....	+1.21	−0.21	+15	+9	−10°.0
1614–1686_1....	+1.36	−0.23	−9	−15	−4.5
1598–1723_1....	+1.39	−0.25	0	−7	−0.7
1615–1686_2....	+1.36	−0.23	+15	+9	−5.0
2409–1723_2....	+1.61	+1.70	+4	−5	−5.0
2381–2149.....	+1.52	+0.73	+22	+14	−3.0
2395–2115.....	+1.48	+0.73	+5	−3	−4.3
2428–1705.....	+1.60	+1.71	+7	−2	−0.3

$$+7.07\,\mu_\alpha+6.45\,\pi=+35 \qquad \pi=+4.7=+0''.008\pm0''.004$$
$$+6.45\,\mu_\alpha+16.74\,\pi=+83 \qquad \mu_\alpha=+0.7=+0''.001\pm0''.005$$

Comp. Star	Br.	x	y	π	P.E.
1.......	f	+1′.0	+1′.4	+0″.015	±0″.011
2.......	f	+2.3	+2.6	−0.009	0.008
3.......	f	+4.5	+1.0	+0.001	0.008
4.......	f	+1.6	−3.2	−0.009	0.008
5.......	f	+1.0	−2.5	+0.015	0.009
6.......	f	−0.4	−1.6	−0.013	0.006
7.......	f	−2.5	−2.6	+0.009	0.008
8.......	f	−3.6	−2.1	−0.003	0.012
9.......	f	−3.3	+1.1	−0.010	0.011
10.......	f	−2.5	+4.3	+0.007	±0.007

Boss 3145 $\alpha=11^h57^m24^s$ $\delta=+43°39'$

Pl. No.	Date	t	Obs.	Qy	p	m	Remarks
2197_1..	1919 Apr. 21	$+2°.2$	H	fg	−0.482	+4.31	
2197_2..	21	+6.0	vM	fg	−0.482	+4.31	
2208_1..	22	−2.0	vM	fg	−0.495	+4.31	Hazy, 20^m exp.
2208_2..	22	+3.7	H	fg	−0.495	+4.31	Hazy, 20^m exp.
2539_1..	1920 Jan. 15	−2.5	H	f	+0.814	+5.04	20^m exp.
2539_2..	15	+2.7	vM	fg	+0.814	+5.04	20^m exp.
2567_1..	Feb. 11	−15.7	H	g	+0.547	+5.12	
2567_2..	11	−12.0	vM	g	+0.547	+5.12	
2580_1..	12	−18.5	H	fg	+0.534	+5.12	
2580_2..	12	−12.0	vM	g	+0.534	+5.12	
2596_1..	13	+9.7	vM	g	+0.521	+5.12	
2596_2..	13	+14.0	H	g	+0.521	+5.12	
2653_1..	Apr. 25	−9.0	vM	g	−0.545	+5.32	
2653_2..	25	−5.0	H	g	−0.545	+5.32	Trail
2664...	May 14	−5.5	vM	fg	−0.755	+5.37	
2677...	15	−6.5	vM	fg	−0.764	+5.38	

Mor.-Ev.	Δp	Δm	M	v	Δt
2580_1–2653_1....	+1.08	−0.20	+ 32	0	$-9°.5$
2567_1–2677....	+1.31	−0.26	+ 48	+ 6	−9.2
2580_2–2664....	+1.29	−0.25	+ 40	− 1	−6.5
2567_2–2653_2....	+1.09	−0.20	+ 22	−10	−7.0
2539_1–2208_1....	+1.31	+0.73	−168	− 8	−0.5
2539_2–2197_1....	+1.30	+0.73	−138	+22	+0.5
2596_1–2208_2....	+1.02	+0.81	−200	−27	+6.0
2596_2–2197_2....	+1.00	+0.81	−161	+12	+8.0

$$+2.59\mu_\alpha+2.45\pi=-548 \qquad \pi=-8.1=-0''.013\pm0''.006$$
$$+2.45\mu_\alpha+11.19\pi=-590 \qquad \mu_\alpha=-203.9=-0''.332\pm0''.012$$

Comp. Star	Br.	x	y	π	P.E.
1........	ff	$+3'.0$	$+5'.2$	$+0''.017$	$\pm0''.013$
2........	f	+6.2	+2.3	−0.001	0.005
3........	ff	+6.5	+0.5	−0.010	0.007
4........	f	+1.0	−2.9	−0.004	0.014
5........	f	−1.8	−6.3	−0.022	0.008
6........	f	−6.3	−6.9	+0.019	0.005
7........	f	−6.0	+8.4	−0.022	0.007
8........	b	−1.9	+2.7	+0.023	±0.017

N.G.C. 4051 $\alpha = 11^h 58^m 7^s$ $\delta = +45°6'$

Pl. No.	Date			t	Obs.	Qy	p	m	Remarks
1714...	1918	Feb.	3	$-8°.0$	vM	g	$+0.639$	$+3.10$	
1767_1..		May	3	$+3.7$	H	g	-0.634	$+3.34$	
1767_2..			3	$+8.0$	vM	g	-0.634	$+3.34$	
1768...			3	$+12.2$	H	g	-0.634	$+3.34$	
1781_1..			4	-3.5	vM	fg	-0.646	$+3.34$	25^m exp.
1781_2..			4	$+3.7$	H	fg	-0.646	$+3.34$	25^m exp.
2094_1..		Dec.	27	-6.0	vM	g	$+0.895$	$+3.99$	
2094_2..			27	-2.0	H	g	$+0.895$	$+3.99$	
2526_1..	1920	Jan.	14	-2.2	H	fg	$+0.822$	$+5.04$	
2526_2..			14	$+2.0$	vM	fg	$+0.822$	$+5.04$	
2568_1..		Feb.	11	-5.5	H	g	$+0.548$	$+5.12$	
2568_2..			11	-1.5	vM	g	$+0.548$	$+5.12$	
2582...			12	$+10.7$	H	g	$+0.536$	$+5.12$	
2654_1..		Apr.	25	$+2.2$	vM	fg	-0.544	$+5.32$	
2654_2..			25	$+6.7$	H	fg	-0.544	$+5.32$	Trail of Boss 3145
2665...		May	14	$+1.2$	H	g	-0.753	$+5.37$	

Mor.-Ev.	Δp	Δm	M	v	Δt
1714 -1781_1....	$+1.29$	-0.24	-32	-34	$-4°.5$
2094_1-2665....	$+1.65$	-1.38	$+18$	$+10$	-7.2
2568_1-2654_1....	$+1.09$	-0.20	$+5$	$+3$	-7.7
2526_1-1767_1....	$+1.46$	$+1.70$	-10	-3	-5.9
2094_2-1781_2....	$+1.54$	$+0.65$	$+22$	$+24$	-5.7
2568_2-2654_2....	$+1.09$	-0.20	-4	-6	-8.2
2526_2-1767_2....	$+1.46$	$+1.70$	-8	-1	-6.0
2582 -1768....	$+1.17$	$+1.78$	-11	-3	-1.5

$$+11.41\,\mu_\alpha + 5.01\,\pi = -54 \qquad \pi = +0.6 = +0''.001 \pm 0''.005$$
$$+5.01\,\mu_\alpha + 14.76\,\pi = -16 \qquad \mu_\alpha = -5.0 = -0''.008 \pm 0''.006$$

Comp. Star	Br.	x	y	π	P.E.
1........	f	$+0'.7$	$+3'.8$	$0''.000$	$\pm 0''.006$
2........	f	$+2.5$	$+1.2$	-0.031	0.008
3........	f	$+5.1$	-0.1	$+0.019$	0.006
4........	f	$+4.5$	-8.6	-0.005	0.006
5........	b	-2.2	-0.7	$+0.036$	0.015
6........	f	-4.8	-0.8	-0.018	0.007
7........	f	-6.9	$+3.6$	0.000	± 0.010

Boss 3145 $\alpha = 11^h57^m24^s$ $\delta = +43°39'$

Pl. No.	Date	t	Obs.	Qy	p	m	Remarks
2197_1..	1919 Apr. 21	$+2\overset{\circ}{.}2$	H	fg	−0.482	+4.31	
2197_2..	21	+6.0	vM	fg	−0.482	+4.31	
2208_1..	22	−2.0	vM	fg	−0.495	+4.31	Hazy, 20^m exp.
2208_2..	22	+3.7	H	fg	−0.495	+4.31	Hazy, 20^m exp.
2539_1..	1920 Jan. 15	−2.5	H	f	+0.814	+5.04	20^m exp.
2539_2..	15	+2.7	vM	fg	+0.814	+5.04	20^m exp.
2567_1..	Feb. 11	−15.7	H	g	+0.547	+5.12	
2567_2..	11	−12.0	vM	g	+0.547	+5.12	
2580_1..	12	−18.5	H	fg	+0.534	+5.12	
2580_2..	12	−12.0	vM	g	+0.534	+5.12	
2596_1..	13	+9.7	vM	g	+0.521	+5.12	
2596_2..	13	+14.0	H	g	+0.521	+5.12	
2653_1..	Apr. 25	−9.0	vM	g	−0.545	+5.32	
2653_2..	25	−5.0	H	g	−0.545	+5.32	Trail
2664...	May 14	−5.5	vM	fg	−0.755	+5.37	
2677...	15	−6.5	vM	fg	−0.764	+5.38	

Mor.-Ev.	Δp	Δm	M	v	Δt
2580_1–2653_1....	+1.08	−0.20	+32	0	$-9\overset{\circ}{.}5$
2567_1–2677....	+1.31	−0.26	+48	+6	−9.2
2580_2–2664....	+1.29	−0.25	+40	−1	−6.5
2567_2–2653_2....	+1.09	−0.20	+22	−10	−7.0
2539_1–2208_1....	+1.31	+0.73	−168	−8	−0.5
2539_2–2197_1....	+1.30	+0.73	−138	+22	+0.5
2596_1–2208_2....	+1.02	+0.81	−200	−27	+6.0
2596_2–2197_2....	+1.00	+0.81	−161	+12	+8.0

$+2.59\mu_a + 2.45\pi = -548$ $\pi = -8.1 = -0\overset{''}{.}013 \pm 0\overset{''}{.}006$

$+2.45\mu_a + 11.19\pi = -590$ $\mu_a = -203.9 = -0\overset{''}{.}332 \pm 0\overset{''}{.}012$

Comp. Star	Br.	x	y	π	P.E.
1........	ff	$+3\overset{'}{.}0$	$+5\overset{'}{.}2$	$+0\overset{''}{.}017$	$\pm 0\overset{''}{.}013$
2........	f	+6.2	+2.3	−0.001	0.005
3........	ff	+6.5	+0.5	−0.010	0.007
4........	f	+1.0	−2.9	−0.004	0.014
5........	f	−1.8	−6.3	−0.022	0.008
6........	f	−6.3	−6.9	+0.019	0.005
7........	f	−6.0	+8.4	−0.022	0.007
8........	b	−1.9	+2.7	+0.023	±0.017

N.G.C. 4051 $\alpha = 11^h 58^m 7^s$ $\delta = +45°6'$

Pl. No.	Date			t	Obs.	Qy	p	m	Remarks
1714...	1918	Feb.	3	− 8°9	vM	g	+0.639	+3.10	
1767_1..		May	3	+ 3.7	H	g	−0.634	+3.34	
1767_2..			3	+ 8.0	vM	g	−0.634	+3.34	
1768...			3	+12.2	H	g	−0.634	+3.34	
1781_1..			4	− 3.5	vM	fg	−0.646	+3.34	25^m exp.
1781_2..			4	+ 3.7	H	fg	−0.646	+3.34	25^m exp.
2094_1..		Dec.	27	− 6.0	vM	g	+0.895	+3.99	
2094_2..			27	− 2.0	H	g	+0.895	+3.99	
2526_1..	1920	Jan.	14	− 2.2	H	fg	+0.822	+5.04	
2526_2..			14	+ 2.0	vM	fg	+0.822	+5.04	
2568_1..		Feb.	11	− 5.5	H	g	+0.548	+5.12	
2568_2..			11	− 1.5	vM	g	+0.548	+5.12	
2582...			12	+10.7	H	g	+0.536	+5.12	
2654_1..		Apr.	25	+ 2.2	vM	fg	−0.544	+5.32	
2654_2..			25	+ 6.7	H	fg	−0.544	+5.32	Trail of Boss 3145
2665...		May	14	+ 1.2	H	g	−0.753	+5.37	

Mor.-Ev.	Δp	Δm	M	v	Δt
1714 −1781_1....	+1.29	−0.24	−32	−34	−4°5
2094_1−2665....	+1.65	−1.38	+18	+10	−7.2
2568_1−2654_1....	+1.09	−0.20	+ 5	+ 3	−7.7
2526_1−1767_1....	+1.46	+1.70	−10	− 3	−5.9
2094_2−1781_2....	+1.54	+0.65	+22	+24	−5.7
2568_2−2654_2....	+1.09	−0.20	− 4	− 6	−8.2
2526_2−1767_2....	+1.46	+1.70	− 8	− 1	−6.0
2582 −1768....	+1.17	+1.78	−11	− 3	−1.5

$$+11.41\,\mu_\alpha + 5.01\,\pi = -54 \qquad \pi = +0.6 = +0''.001 \pm 0''.005$$
$$+5.01\,\mu_\alpha + 14.76\,\pi = -16 \qquad \mu_\alpha = -5.0 = -0''.008 \pm 0''.006$$

Comp. Star	Br.	x	y	π	P.E.
1........	f	+0'.7	+3'.8	0''.000	±0''.006
2........	f	+2.5	+1.2	−0.031	0.008
3........	f	+5.1	−0.1	+0.019	0.006
4........	f	+4.5	−8.6	−0.005	0.006
5........	b	−2.2	−0.7	+0.036	0.015
6........	f	−4.8	−0.8	−0.018	0.007
7........	f	−6.9	+3.6	0.000	±0.010

Boss 3322 $\alpha = 12^h 40^m 24^s$ $\delta = +45°58'$

Pl. No.	Date	t	Obs.	Qy	p	m	Remarks
1752_1..	1918 May 2	− 8°.2	vM	fg	−0.476	+3.34	Clouds, 25^m exp.
1752_2..	2	− 1.5	H	fg	−0.476	+3.34	Hazy, 20^m exp.
1784...	31	+ 1.0	vM	fg	−0.797	+3.42	
1798...	June 1	+ 2.0	vM	fg	−0.807	+3.42	
2122_1..	1919 Jan. 23	− 9.0	vM	fg	+0.838	+4.07	
2122_2..	23	− 4.5	H	fg	+0.838	+4.07	
2142...	25	− 0.7	vM	f	+0.830	+4.07	
2162 ..	Feb. 21	+ 1.0	vM	fg	+0.566	+4.15	
2570_1..	1920 Feb. 11	+ 5.5	H	fg	+0.681	+5.12	
2570_2..	11	+10.0	vM	g	+0.681	+5.12	
2583...	12	+ 6.5	vM	fg	+0.673	+5.12	
2607...	14	−12.2	vM	g	+0.651	+5.13	
2667_1..	May 14	+ 8.2	vM	fg	−0.634	+5.37	
2667_2..	14	+12.5	H	g	−0.634	+5.37	
2678_1..	15	−11.0	H	g	−0.644	+5.37	
2678_2..	15	− 7.0	vM	g	−0.644	+5.37	Trail

Mor.-Ev.	Δp	Δm	M	v	Δt
2607 −2678_1....	+1.29	−0.24	− 7	− 5	−1°.2
2122_1−1752_1....	+1.31	+0.73	+13	+14	−0.8
2122_2−2678_2....	+1.48	−1.30	+ 4	+ 8	+2.5
2142 −1752_2....	+1.31	+0.73	− 2	− 1	+0.8
2162 −1784....	+1.36	+0.73	−10	− 9	0.0
2570_1−1798....	+1.49	+1.70	+ 3	+ 2	+3.5
2583 −2667_1....	+1.31	−0.25	−14	−12	−1.7
2570_2−2667_2....	+1.32	−0.25	+ 1	+ 3	−2.5

$$+6.35\mu_a + 2.55\pi = +7 \qquad \pi = -1.4 = -0''.002 \pm 0''.003$$

$$+2.55\mu_a + 14.82\pi = -16 \qquad \mu_a = +1.7 = +0''.003 \pm 0''.005$$

Comp. Star	Br.	x	y	π	P.E.
1........	f	+0′.4	+6′.6	+0″.016	±0″.007
2........	f	+4.4	+5.1	−0.017	0.010
3........	b	+3.6	+1.8	+0.019	0.010
4........	ff	+1.9	+0.7	−0.002	0.010
5........	b	+3.0	−4.3	−0.016	0.005
6........	bf	−1.2	−6.9	+0.016	0.007
7........	f	−6.5	−2.2	−0.001	0.007
8........	f	−4.1	+0.1	−0.015	±0.008

Boss 3554 $\alpha = 13^h 42^m 0^s$ $\delta = +6°51'$

Pl. No.	Date	t	Obs.	Qy	p	m	Remarks
2230_1..	1919 June 4	0°0	vM	g	−0.679	+4.43	
2230_2..	4	+ 4.0	H	g	−0.679	+4.43	
2242_1..	5	+ 1.0	vM	fg	−0.690	+4.43	
2242_2..	5	+ 5.2	H	fg	−0.690	+4.43	
2584_1..	1920 Feb. 12	− 1.2	H	fg	+0.831	+5.12	20^m exp.
2584_2..	12	+ 5.0	vM	fg	+0.831	+5.12	25^m exp.
2597...	13	− 6.5	vM	g	+0.824	+5.12	
2609_1..	14	−13.5	vM	g	+0.817	+5.13	
2609_2..	14	− 9.5	Hum	g	+0.817	+5.13	
2621...	Mar. 12	− 4.0	vM	g	+0.534	+5.20	
2632_1..	15	−13.5	H	fg	+0.501	+5.21	20^m exp.
2632_2..	15	− 8.0	vM	fg	+0.501	+5.21	20^m exp.
2693_1..	May 24	−11.5	vM	g	−0.557	+5.40	
2693_2..	24	− 7.0	H	g	−0.557	+5.40	
2694...	24	− 3.0	vM	fg	−0.557	+5.40	
2703...	June 9	− 2.5	vM	fg	−0.739	+5.44	Clouds, 20^m exp. Trail

Mor.-Ev.	Δp	Δm	M	v	Δt
2609_1–2693_1....	+1.37	−0.27	+116	+15	−2°0
2632_1–2693_2....	+1.06	−0.19	+ 88	+15	−6.5
2609_2–2694....	+1.37	−0.27	+ 86	−15	−6.5
2632_2–2703....	+1.24	−0.23	+ 68	−19	−5.5
2597 –2230_1....	+1.50	+0.69	−193	−14	−6.5
2621 –2242_1....	+1.22	+0.77	−232	−25	−5.0
2584_1–2230_2....	+1.50	+0.69	−144	+35	−5.2
2584_2–2242_2....	+1.52	+0.69	−175	+ 4	−0.2

$$+2.26\,\mu_a + 2.84\,\pi = -619 \qquad \pi = +15.7 = +0''.026 \pm 0''.007$$
$$+2.84\,\mu_a + 14.75\,\pi = -602 \qquad \mu_a = -293.6 = -0''.479 \pm 0''.019$$

Comp. Star	Br.	x	y	π	P.E.
1........	bf	+5′5	+4′8	+0″001	±0″005
2........	f	+1.6	+2.2	−0.006	0.005
3........	f	+1.5	+0.7	−0.004	0.007
4........	f	+2.9	0.0	+0.009	0.009
5........	f	−0.4	−5.2	+0.010	0.005
6........	bf	−4.5	−2.5	−0.018	0.009
7........	bf	−1.5	−0.4	−0.010	0.006
8........	f	−4.9	+1.4	+0.019	±0.005

N.G.C. 6210 $\alpha = 16^h 40^m 18^s$ $\delta = +23^\circ 59'$

Pl. No.	Date	t	Obs.	Qy	p	m	Remarks
1430_1..	1917 June 26	$-6\overset{\circ}{.}5$	vM	g	−0.397	+2.49	
1430_2..	26	− 2.0	H	g	−0.397	+2.49	
1455_1..	July 11	+ 1.2	H	fg	−0.613	+2.53	
1455_2..	11	+ 5.0	vM	fg	−0.613	+2.53	
1774...	1918 May 3	− 4.0	vM	g	+0.480	+3.34	
2201_1..	1919 April 21	−16.5	H	g	+0.648	+4.31	
2201_2..	21	−12.0	vM	g	+0.648	+4.31	Trail of Boss 4262
2219...	23	− 2.7	vM	f	+0.623	+4.31	Clouds, 20^m exp.
2625...	1920 Mar. 12	− 7.0	vM	fg	+0.969	+5.20	Hazy, 20^m exp.
2636...	15	−10.0	vM	f	+0.956	+5.21	20^m exp.
2648_1..	Apr. 12	+ 0.2	vM	fg	+0.746	+5.28	
2648_2..	12	+ 4.5	H	g	+0.746	+5.28	
2754_1..	July 8	−11.7	H	fg	−0.576	+5.52	
2754_2..	8	− 7.2	vM	fg	−0.576	+5.52	
2764_1..	9	−15.0	vM	fg	−0.588	+5.52	
2764_2..	9	−11.0	H	g	−0.588	+5.52	

Mor.-Ev.	Δp	Δm	M	v	Δt
2201_1–2764_1....	+1.24	−1.21	−23	− 9	$-1\overset{\circ}{.}5$
2201_2–2754_1....	+1.22	−1.21	− 6	+ 8	−0.3
2636 –2764_2....	+1.54	−0.31	− 4	+ 2	+1.0
2625 –2754_2....	+1.55	−0.32	− 1	+ 5	+0.2
1774 –1430_1....	+0.88	+0.85	−11	−17	+2.5
2219 –1430_2....	+1.02	+1.82	+12	− 3	−0.7
2648_1–1455_1....	+1.36	+2.75	+36	+13	−1.0
2648_2–1455_2....	+1.36	+2.75	+18	− 5	−0.5

$$+22.27\,\mu_a + 6.13\,\pi = +199 \qquad \pi = -2.1 = -0\overset{''}{.}003 \pm 0\overset{''}{.}003$$

$$+6.13\,\mu_a + 13.31\,\pi = +31 \qquad \mu_a = +9.5 = +0\overset{''}{.}015 \pm 0\overset{''}{.}003$$

Comp. Star	Br.	x	y	π	P.E.
1........	bf	$+1\overset{'}{.}8$	$+2\overset{'}{.}5$	$-0\overset{''}{.}021$	$\pm 0\overset{''}{.}008$
2........	b	+4.0	+2.3	+0.017	0.010
3........	bf	+1.2	−2.5	−0.008	0.011
4........	f	+1.2	−5.6	−0.003	0.012
5........	bf	−3.4	−3.0	+0.002	0.014
6........	f	−2.1	+0.1	+0.019	0.010
7........	ff	−2.5	+2.7	−0.015	0.010
8........	ff	−0.3	+3.2	+0.005	±0.017

N.G.C. 6543 $\alpha = 17^h 58^m 32^s$ $\delta = +66°38'$

Pl. No.	Date			t	Obs.	Qy	p	m	Remarks
1480...	1917	July	29	+8°.2	H	fg	−0.608	+2.58	
1496...		Aug.	11	−4.5	H	g	−0.767	+2.61	
1513...			12	−3.7	H	vg	−0.778	+2.62	
2203$_1$..	1919	Apr.	21	−18.0	vM	fg	+0.855	+4.31	
2203$_2$..			21	−14.0	H	fg	+0.855	+4.31	
2221$_1$..		May	21	−1.2	H	fg	+0.497	+4.39	
2221$_2$..			21	+3.0	vM	f	+0.497	+4.39	
2293...		July	31	−2.0	B	fg	−0.628	+4.58	
2309$_1$..		Aug.	18	+2.0	B	g	−0.834	+4.63	
2309$_2$..			18	+6.7	Hum	g	−0.834	+4.63	
2673$_1$..	1920	May	14	−9.0	vM	fg	+0.586	+5.37	
2673$_2$..			14	−5.0	H	fg	+0.586	+5.37	Trail of Boss 4555
2689$_1$..			15	+10.5	vM	vg	+0.571	+5.37	
2689$_2$..			15	+15.0	H	g	+0.571	+5.37	
2801...		Aug.	6	−7.7	Hum	g	−0.713	+5.60	
2812...			7	−12.0	vM	fg	−0.724	+5.60	

Mor.-Ev.	Δp	Δm	M	v	Δt
2203$_1$–2812....	+1.58	−1.29	+20	−18	−6°.0
2203$_2$–2801....	+1.57	−1.29	+40	+2	−6.3
2673$_1$–1496....	+1.35	+2.76	−13	−15	−4.5
2673$_2$–1513....	+1.36	+2.75	+7	+4	−1.3
2221$_1$–2293....	+1.13	−0.19	+43	+22	+0.8
2221$_2$–2309$_1$....	+1.33	−0.24	+23	−3	+1.0
2689$_1$–2309$_2$....	+1.41	+0.74	+32	+13	+3.8
2689$_2$–1480....	+1.18	+2.79	+1	+2	+6.8

$$+26.93\,\mu_\alpha + 7.20\,\pi = -82 \qquad \pi = +17.9 + 0''.029 \pm 0''.004$$

$$+7.20\,\mu_\alpha + 15.06\,\pi = +213 \qquad \mu_\alpha = -7.8 - 0''.013 \pm 0''.003$$

Comp. Star	Br.	x	y	π	P.E.
1........	f	+1′.9	+5′.4	−0″.019	±0″.006
2........	b	+3.8	+3.6	+0.007	0.006
3........	bf	+7.1	−0.4	−0.005	0.004
4........	f	+4.0	−1.9	+0.001	0.009
5........	bf	−4.4	−6.9	+0.012	0.010
6........	f	−2.6	−3.6	−0.018	0.009
7........	bf	−5.1	−1.1	−0.016	0.008
8........	bf	−2.1	+4.4	+0.003	0.005
9........	f	−1.2	+1.8	+0.035	±0.008

Nova Aquilae No. 3 $\alpha=18^h43^m49^s$ $\delta=+0^\circ29'$

Pl. No.	Date	t	Obs.	Qy	p	m	Remarks
1843...	1918 Aug. 11	−15°5	Hum	g	−0.627	+3.61	
1856...	12	− 6.7	Hum	g	−0.641	+3.62	
1870...	13	− 4.5	vM	fg	−0.653	+3.62	
1882...	Sept. 2	+ 1.5	vM	fg	−0.871	+3.67	
2227...	1919 May 22	− 0.5	H	fg	+0.636	+4.39	Fog, 18^m exp.
2236_1..	June 4	−11.0	vM	fg	+0.454	+4.43	
2236_2..	4	− 6.5	H	fg	+0.454	+4.43	
2237...	4	− 2.0	vM	fg	+0.454	+4.43	Trail
2249_1..	5	− 9.7	H	g	+0.439	+4.43	
2249_2..	5	− 5.5	vM	g	+0.439	+4.43	
2250_1..	5	0.0	H	g	+0.438	+4.43	
2250_2..	5	+ 4.0	vM	g	+0.438	+4.43	
2329_1..	Aug. 20	− 6.5	B	fg	−0.735	+4.64	
2329_2..	20	− 2.0	H	fg	−0.735	+4.64	
2358_1..	Sept. 17	+ 7.2	B	fg	−0.960	+4.71	
2358_2..	17	+12.2	Hum	fg	−0.963	+4.71	

Mor.-Ev.	Δp	Δm	M	v	Δt
2236_1–1843....	+1.08	+0.82	+56	+31	+4°5
2249_1–1856....	+1.08	+0.81	+ 5	−19	−3.0
2236_2–2329_1....	+1.19	−0.21	+ 4	− 7	0.0
2249_2–1870....	+1.09	+0.81	+27	+ 3	−1.0
2237 –2329_2....	+1.19	−0.21	+21	+10	0.0
2227 –1882....	+1.51	+0.72	+14	−14	−2.0
2250_1–2358_1....	+1.40	−0.28	+16	+ 4	−7.2
2250_2–2358_2....	+1.40	−0.28	+10	− 2	−8.2

$$+2.75\,\mu_a+\ 2.45\,\pi=+\ 70 \qquad \pi\ =+11.4=+0.''019\pm0.''006$$
$$+2.45\,\mu_a+12.57\,\pi=+181 \qquad \mu_a=+15.3=+0.''025\pm0.''012$$

Comp. Star	Br.	x	y	π	P.E
1........	ff	+1.′8	+5.′2	−0.″014	±0.″008
2........	f	+6.2	−0.7	−0.031	0.012
3........	bf	+7.5	−1.2	+0.049	0.008
4........	bf	+4.1	−6.6	−0.014	0.009
5........	bb	−3.4	−3.6	−0.015	0.012
6........	bf	−5.9	−5.4	+0.019	0.009
7........	bf	−5.4	+5.2	+0.008	0.011
8........	b	−3.4	+3.8	−0.004	0.011
9........	f	−1.2	+3.4	+0.004	±0.005

17 Lyrae C = Bu 9053 $\alpha = 19^h3^m40^s$ $\delta = +32^\circ21'$

Pl. No.	Date	t	Obs.	Qy	p	m	Remarks
1923$_1$..	1918 Sept. 5	−8°0	vM	g	−0.848	+3.68	
1923$_2$..	5	−4.2	H	fg	−0.848	+3.68	
2222$_1$..	1919 May 21	−6.0	H	f	+0.704	+4.39	
2222$_2$..	21	−1.0	vM	f	+0.704	+4.39	Clouds, 20^m exp.
2238$_1$..	June 4	+3.0	vM	g	+0.521	+4.43	
2238$_2$..	4	+7.0	H	g	+0.521	+4.43	
2251$_1$..	5	+4.7	H	g	+0.506	+4.43	
2251$_2$..	5	+9.0	vM	g	+0.506	+4.43	
2330$_1$..	Aug. 20	+1.0	B	g	−0.677	+4.64	
2330$_2$..	20	+5.0	H	g	−0.677	+4.64	
2676...	1920 May 14	+6.2	vM	fg	+0.775	+5.37	
2690...	15	+5.0	vM	fg	+0.764	+5.37	Trail of 17 Lyrae
2804$_1$..	Aug. 6	+4.0	vM	g	−0.497	+5.60	
2804$_2$..	6	+8.2	Hum	g	−0.497	+5.60	
2815...	7	+9.2	vM	fg	−0.511	+5.60	Hazy, 20^m exp.
2821...	19	+0.2	vM	fg	−0.674	+5.64	

Mor.-Ev.	Δp	Δm	M	v	Δt
2222$_1$−1923$_1$....	+1.55	+0.71	+620	−14	+2°0
2222$_2$−1923$_2$....	+1.55	+0.71	+677	+43	+3.2
2238$_1$−2821....	+1.20	−1.21	−801	+22	+2.8
2251$_1$−2804$_1$....	+1.00	−1.17	−789	+17	+0.7
2690 −2330$_1$....	+1.44	+0.73	+639	− 2	+4.0
2676 −2330$_2$....	+1.45	+0.73	+610	−32	+1.2
2238$_2$−2804$_2$....	+1.02	−1.17	−810	− 5	−1.2
2251$_2$−2815....	+1.02	−1.17	−833	−28	−0.2

$$+7.63\,\mu_\alpha - 0.69\,\pi = +5647 \qquad \pi = +\ 66.9 = +0''.109 \pm 0''.008$$
$$-0.69\,\mu_\alpha + 13.49\,\pi = +\ 388 \qquad \mu_\alpha = +746.2 = +1''.216 \pm 0''.010$$

Comp. Star	Br.	x	y	π	P.E.
1........	ff	+1′.1	+2′.2	+0″.014	±0″.006
2........	bf	+3.3	+2.7	+0.003	0.005
3........	f	+4.8	−1.9	0.000	0.004
4........	f	+1.6	−1.4	−0.008	0.008
5........	bf	0.0	−2.2	−0.014	0.009
6........	f	−3.4	−3.7	+0.015	0.005
7........	f	−3.4	+2.5	−0.003	0.010
8........	bf	−2.5	+1.6	−0.010	±0.010

RR. Lyrae $\alpha = 19^h 22^m 14^s$ $\delta = +42°36'$

Pl. No.	Date			t	Obs.	Qy	p	m	Remarks
1858_1	1918	Aug.	12	+0°.5	vM	g	−0.508	+3.62	
1858_2			12	+4.7	Hum	g	−0.508	+3.62	
1871_1			13	−2.5	vM	fg	−0.523	+3.62	
1871_2			13	+1.5	H	fg	−0.523	+3.62	
2322	1919	Aug.	19	0.0	B	g	−0.602	+4.64	
2700_1	1920	May	24	−11.5	vM	g	+0.714	+5.40	
2700_2			24	−7.7	H	fg	+0.714	+5.40	
2701			24	−3.5	vM	fg	+0.714	+5.40	
2711_1		June	9	+2.5	vM	fg	+0.504	+5.44	20^m exp.
2711_2			9	+9.0	H	fg	+0.503	+5.44	25^m exp.
2737_1			11	+5.5	vM	f	+0.474	+5.45	
2737_2			11	+9.7	H	f	+0.474	+5.45	
2738			11	+14.0	vM	fg	+0.474	+5.45	
2750_1			12	+0.7	H	fg	+0.460	+5.45	
2750_2			12	+5.5	vM	fg	+0.460	+5.45	
2820		Aug.	19	−14.0	vM	g	−0.611	+5.64	
2822			19	+3.2	H	g	−0.612	+5.64	Trail of 17 Lyrae
2833			20	+0.7	H	fg	−0.625	+5.64	
2847			21	+5.5	vM	fg	−0.638	+5.64	
2891		Sept.	9	−5.2	H	g	−0.847	+5.69	

Mor.-Ev.	Δp	Δm	M	v	Δt
2700_1–2820	+1.33	−0.24	+19	−4	+2°.5
2700_2–2891	+1.56	−0.29	+26	0	−2.7
2701 –1871_1	+1.24	+1.78	−107	+19	−1.0
2750_1–2322	+1.06	+0.81	−89	−34	+0.7
2711_1–1858_1	+1.01	+1.82	−115	+15	+2.0
2750_2–2833	+1.09	−0.19	+22	+4	+4.8
2737_1–1871_2	+1.00	+1.83	−136	−5	+4.0
2711_2–2822	+1.11	−0.20	+9	−10	+5.8
2737_2–1858_2	+0.98	+1.83	−142	−11	+5.0
2738 –2847	+1.11	−0.19	+40	+22	+8.5

$$+14.10\,\mu_\alpha + 7.12\,\pi = -1007 \qquad \pi = +3.4 = +0''.006 \pm 0''.006$$
$$+7.12\,\mu_\alpha + 13.49\,\pi = -474 \qquad \mu_\alpha = -73.1 = -0''.119 \pm 0''.006$$

Comp. Star	Br.	x	y	π	P.E.
1	f	+0′.3	+1′.4	−0″.021	±0″.010
2	bf	+0.5	+3.8	+0.021	0.011
3	f	+3.6	+1.0	0.000	0.009
4	f	+3.3	+0.4	−0.011	0.006
5	f	+0.7	−4.8	+0.012	0.010
6	f	−1.9	−3.8	+0.006	0.008
7	f	−0.7	−1.6	−0.003	0.008
8	f	−4.4	−0.3	−0.012	0.004
9	f	−3.2	+2.7	+0.010	±0.007

B.D.+30° 3639 $\alpha = 19^h30^m54^s$ $\delta = +30°18'$

Pl. No.	Date	t	Obs.	Qy	p	m	Remarks
1925_1..	1918 Sept. 5	+5°7	vM	g	−0.778	+3.68	
1925_2..	5	+10.0	H	g	−0.778	+3.68	
2223_1..	1919 May 21	−0.7	H	f	+0.777	+4.39	
2223_2..	21	+3.5	vM	pf	+0.777	+4.39	
2239_1..	June 4	+6.5	vM	g	+0.611	+4.43	
2239_2..	4	+10.7	H	fg	+0.611	+4.43	
2252...	5	+8.7	H	g	+0.598	+4.43	
2261...	19	−5.0	vM	g	+0.397	+4.47	
2311_1..	Aug. 18	+5.0	B	g	−0.559	+4.63	
2311_2..	18	+9.0	B	g	−0.559	+4.63	
2347_1..	Sept. 16	−5.0	B	gas	−0.877	+4.71	
2347_2..	16	−1.0	H	fg	−0.877	+4.71	
2382_1..	Oct. 18	+11.5	vM	fg	−0.982	+4.80	
2382_2..	18	+15.7	H	f	−0.982	+4.80	Trail of Boss 5000
2702_1..	1920 May 24	+0.5	H	fg	+0.748	+5.40	
2702_2..	24	+4.5	vM	f	+0.748	+5.40	

Mor.-Ev.	Δp	Δm	M	v	Δt
2261 −2347_1....	+1.27	−0.24	+25	+25	0°0
2223_1−2347_2....	+1.65	−0.32	+38	+38	+0.3
2702_1−2311_1....	+1.31	+0.77	+21	+6	−4.5
2223_2−1925_1....	+1.56	+0.71	−21	−36	−2.2
2702_2−2311_2....	+1.31	+0.77	+9	−6	−4.5
2239_1−1925_2....	+1.39	+0.75	+48	+33	−3.5
2252 −2382_1....	+1.58	−0.37	−42	−42	−2.8
2239_2−2382_2....	+1.59	−0.37	−11	−11	−5.0

$+2.68\mu_\alpha + 2.17\pi = +46$ $\pi = +3.2 = +0''.005 \pm 0''.009$

$+2.17\mu_\alpha + 17.16\pi = +86$ $\mu_\alpha = +14.6 = +0''.024 \pm 0''.023$

Comp. Star	Br.	x	y	π	P.E.
1........	f	$+3'.6$	$+2'.7$	$-0''.013$	$\pm 0''.014$
2........	f	+1.6	+0.3	+0.015	0.006
3........	f	+1.8	−0.5	−0.022	0.007
4........	f	+2.3	−3.0	+0.028	0.017
5........	f	−0.7	−2.3	−0.001	0.006
6........	f	−2.1	−1.8	−0.025	0.019
7........	f	−1.6	−1.1	+0.001	0.010
8........	bf	−4.0	+2.1	+0.012	0.009
9........	f	−1.9	+4.4	+0.007	±0.014

Pi. 22^h214 $\alpha = 22^h40^m54^s$ $\delta = +29°54'$

Pl. No.	Date	t	Obs.	Qy	p	m	Remarks
2021_1..	1918 Nov. 10	−12°0	vM	g	−0.856	+3.86	
2021_2..	10	− 8.0	H	fg	−0.858	+3.86	
2038...	11	− 1.2	H	fg	−0.861	+3.87	
2051...	26	+ 9.2	vM	f	−0.909	+3.91	
2298_1..	1919 July 31	+ 3.0	B	g	+0.481	+4.58	
2298_2..	31	+ 7.0	H	g	+0.481	+4.58	
2367...	Sept. 25	− 9.5	vM	fg	−0.367	+4.74	
2762_1..	1920 July 8	−10.0	vM	g	+0.743	+5.52	
2762_2..	8	− 6.0	H	g	+0.743	+5.52	
2773_1..	9	− 9.0	vM	g	+0.733	+5.52	
2773_2..	9	− 5.0	H	g	+0.733	+5.52	
2807_1..	Aug. 6	− 9.0	vM	g	+0.388	+5.60	
2807_2..	6	− 4.2	Hum	g	+0.388	+5.60	
2920_1..	Oct. 4	− 5.2	H	gas	−0.503	+5.76	
2920_2..	4	− 1.2	vM	fg	−0.504	+5.76	
2936...	5	− 1.0	vM	fg	−0.516	+5.77	

Mor.-Ev.	Δp	Δm	M	v	Δt
2762_1–2021_1....	+1.60	+1.66	−285	−32	+2°0
2773_1–2367....	+1.10	+0.78	−108	+ 5	+0.5
2807_1–2021_2....	+1.25	+1.74	−251	+20	−1.0
2762_2–2920_1....	+1.25	−0.24	+ 48	−13	−0.8
2773_2–2038....	+1.59	+1.65	−245	+ 7	−3.8
2807_2–2920_2....	+0.89	−0.16	+ 59	+17	−3.0
2298_1–2936....	+1.00	−1.19	+221	+ 4	+4.0
2298_2–2051....	+1.39	+0.67	− 89	+ 1	−2.2

$$+11.08\,\mu_\alpha + 7.62\,\pi = -1742 \qquad \pi = +16.6 = +0''.027 \pm 0''.007$$
$$+7.62\,\mu_\alpha + 13.14\,\pi = -1069 \qquad \mu_\alpha = -168.6 = -0''.275 \pm 0''.008$$

Comp. Star	Br.	x	y	π	P.E.
1........	f	+3'.8	+6'.7	−0''.010	±0''.006
2........	f	+5.8	+2.1	+0.007	0.007
3........	f	+4.3	+0.4	−0.012	0.009
4........	bf	+5.8	−5.2	+0.010	0.008
5........	f	−4.3	−4.7	−0.009	0.010
6........	b	−6.3	−2.5	−0.002	0.007
7........	bf	−6.5	−0.1	+0.003	0.009
8........	bf	−3.0	+3.8	+0.014	±0.005

Boss 6020 $\alpha=23^h18^m52^s$ $\delta=+31°59'$

Pl. No.	Date	t	Obs.	Qy	p	m	Remarks
1484_1..	1917 July 29	− 0°5	vM	fg	+0.628	+2.58	
1484_2..	29	+ 3.5	H	fg	+0.628	+2.58	
1491_1..	Aug. 10	−13.0	vM	g	+0.470	+2.62	
1491_2..	10	− 8.5	H	g	+0.470	+2.62	
1603...	Nov. 8	−15.7	vM	fg	−0.765	+2.86	Clouds, 25^m exp.
1604...	8	− 8.2	H	fg	−0.765	+2.86	Hazy, 20^m exp.
1962...	1918 Oct. 13	− 6.2	H	fg	−0.472	+3.79	Clouds, 25^m exp.
1963...	13	+ 1.0	vM	fg	−0.472	+3.79	Clouds, 25^m exp.
1964...	13	+10.2	H	fg	−0.472	+3.79	Clouds, 25^m exp.
1970...	14	− 6.5	vM	fg	−0.486	+3.79	Clouds, 20^m exp.
1971...	14	+ 5.2	vM	f	−0.486	+3.79	Hazy, 18^m exp.
1988...	27	+ 5.5	vM	f	−0.644	+3.82	20^m exp.
2290...	1919 July 30	+ 7.5	B	fg	+0.624	+4.58	
2763_1..	1920 July 8	−10.5	vM	fg	+0.828	+5.52	
2763_2..	8	− 6.2	H	g	+0.828	+5.52	
2774...	9	− 9.5	vM	fg	+0.820	+5.53	Trail

Mor.-Ev.	Δp	Δm	M	v	Δt
1491_1–1603....	+1.24	−0.24	− 2	+22	+2°7
2763_1–1604....	+1.59	+2.66	+396	− 6	−2.3
2774 –1962....	+1.29	+1.74	+260	− 5	−3.3
1491_2–1970....	+0.96	−1.17	−205	−42	−2.0
2763_2–1963....	+1.30	+1.73	+251	−13	−7.2
1484_1–1971....	+1.11	−1.21	−154	+13	−5.7
1484_2–1988....	+1.27	−1.24	−169	+ 1	−2.0
2290 –1964....	+1.10	+0.79	+155	+31	−2.7

$$+18.15\,\mu_a+\ 5.26\,\pi=+2697 \qquad \pi\ =+\ \ 8.6=+0''.014\pm0''.008$$

$$+\ 5.26\,\mu_a+12.39\,\pi=+\ 876 \qquad \mu_a=+146.1=+0''.238\pm0''.006$$

Comp. Star	Br.	x	y	π	P.E.
1........	bf	+1′5	+4′8	0″000	±0″009
2........	bf	+1.9	+3.0	+0.006	0.010
3........	bf	+3.2	+1.4	−0.002	0.004
4........	f	+5.8	−2.9	+0.002	0.008
5........	bf	+0.7	−6.2	−0.013	0.008
6........	f	+0.1	−3.6	+0.017	0.004
7........	b	−5.1	−2.9	−0.013	0.010
8........	bf	−8.0	+0.3	+0.014	0.007
9........	bf	−1.9	+5.4	−0.014	±0.004

Pi. 23^h164 $\alpha=23^h38^m30^s$ $\delta=+57°31'$

Pl. No.	Date			t	Obs.	Qy	p	m	Remarks
2307_1..	1919	Aug.	1	$0°0$	B	fg	+0.662	+4.59	
2307_2..			1	+ 4.5	H	fg	+0.662	+4.59	
2373_1..		Oct.	17	− 9.0	vM	fg	−0.448	+4.80	
2373_2..			17	− 4.2	Hum	fg	−0.449	+4.80	Hazy, 20^m exp.
2385_1..			18	−15.0	vM	f	−0.462	+4.80	
2385_2..			18	−10.5	H	fg	−0.462	+4.80	
2401_1..			19	+ 2.5	vM	fg	−0.476	+4.80	
2401_2..			19	+ 7.0	H	g	−0.476	+4.80	
2808_1..	1920	Aug.	6	−12.5	vM	fg	+0.595	+5.60	
2808_2..			6	− 7.7	Hum	fg	+0.595	+5.60	
2818_1..			7	− 2.7	vM	g	+0.584	+5.60	Clouds, 20^m exp.
2818_2..			7	+ 3.5	Hum	g	+0.584	+5.60	Clouds, 20^m exp.
2826_1..			19	− 9.0	vM	g	+0.427	+5.64	
2826_2..			19	− 5.0	vM	g	+0.427	+5.64	
2852_1..			21	− 1.0	vM	g	+0.401	+5.64	
2852_2..			21	+ 3.0	H	g	+0.401	+5.64	
2960_1..		Nov.	3	−11.5	vM	fg	−0.665	+5.84	
2960_2..			3	− 7.5	Hum	g	−0.665	+5.84	Trail
2973_1..		Dec.	3	− 2.0	vM	gas	−0.881	+5.93	
2973_2..			3	+ 3.0	Hum	gas	−0.881	+5.93	

Mor.-Ev.	Δp	Δm	M	v	Δt
2808_1–2385_1....	+1.06	+0.80	+211	− 1	$+2°5$
2826_1–2960_1....	+1.09	−0.20	− 9	+21	+2.5
2808_2–2385_2....	+1.06	+0.80	+251	+39	+2.8
2818_1–2373_1....	+1.03	+0.80	+234	+22	+6.3
2826_2–2960_2....	+1.09	−0.20	− 7	+23	+2.5
2852_1–2373_2....	+0.85	+0.84	+189	−30	+3.2
2852_2–2401_1....	+0.88	+0.84	+179	−40	+0.5
2818_2–2973_2....	+1.47	−0.33	− 44	+11	+0.5
2307_1–2973_1....	+1.54	−1.34	−313	−13	+2.0
2307_2–2401_2....	+1.14	−0.21	− 71	−40	−2.5

$$+5.37\mu_\alpha+0.74\pi=+1318 \qquad \pi=+17.2=+0''.028\pm0''.009$$

$$+0.74\mu_\alpha+13.00\pi=+404 \qquad \mu_\alpha=+243.1=+0''.396\pm0''.015$$

Comp. Star	Br.	x	y	π	P.E.
1........	f	$+1'.6$	$+2'.6$	$+0''.010$	$\pm0''.007$
2........	f	+2.2	+4.1	−0.002	0.006
3........	bf	+2.2	−1.5	+0.002	0.025
4........	b	+3.4	−4.1	−0.005	0.011
5........	bb	−0.5	−2.9	−0.003	0.014
6........	f	−2.3	−1.0	+0.010	0.009
7........	f	−2.9	+0.5	−0.003	0.005
8........	bf	−2.9	+2.9	−0.009	±0.006

I wish to express my acknowledgment to Mr. Hoge and Mr. Humason for their valuable aid in securing the plates, and to Miss Coral Wolfe and Mrs. Marsh, of the Computing Division, who have performed a large share of the necessary computations.

I am also under great obligation to Mr. Hugo Benioff, who during three months in the summer of 1919 took charge of the parallax program, while the writer was in Europe.

Mount Wilson Observatory
January 1920

Contributions from the Mount Wilson Observatory, No. 205

INVESTIGATIONS ON PROPER MOTION

THIRD PAPER: THE PROPER MOTIONS OF STARS IN AND NEAR THE DOUBLE CLUSTER IN PERSEUS

BY ADRIAAN VAN MAANEN

This investigation began in 1909 with the measurement of the proper motions of 1418 stars in the neighborhood of *h* and χ Persei.[1] In several respects, however, difficulties were met in the discussion which could not at that time be overcome: it was then impossible to decide with certainty whether any star was a member of the cluster or not; the reduction from relative to absolute motion was based on very scanty material and was accordingly far from certain; and finally it was not easy to correct the proper motions for a possible error depending on magnitude.

In all these particulars much has been gained by later observational material, due to several observers who have kindly placed the necessary data at my disposal. Professor Philip Fox and Mr. Max Peterson have reobserved, with the meridian circle of the Dearborn Observatory, 130 stars for which older observations were available. To them I wish to express my most sincere gratitude. The large amount of work involved in the reduction of these observations could not have been carried out without the help of a grant from the Gould Fund of the National Academy of Sciences, which enabled me to use a computer for about three months.

The discovery by Adams and van Maanen in 1912[2] of several stars in the neighborhood of the cluster, showing the same radial velocity, permitted an improved treatment of the material. The work was later extended to the fainter stars by Adams and his collaborators, and the number showing common velocity, all of which are probably members of the group, is now 27.

---

[1] Van Maanen, *Recherches astronomiques de l'Observatoire d'Utrecht*, **5**, 1911. For brevity this investigation is referred to in the text as *Utrecht*, **5**.

[2] *Astronomical Journal*, **27**, 187, 1913.

The present investigation is divided into five parts:

I. THE RADIAL VELOCITIES OF THE CLUSTER STARS

The results for the radial velocities of stars in the neighborhood of the cluster *h* and χ Persei are collected in Table I; of the 38 stars observed, 28 have velocities of about −40 km/sec. Nearly all these probably belong to the cluster. One of the 28 stars of common velocity, B.D.+56°449, has a large proper motion, viz., 0″.334,

TABLE I

Current No.	B.D. No.	Rev. D.C. Vis. Mag.	α 1900	δ 1900	Spectrum	*V*
1	+53°439	4.94	$1^h55^m38^s$	+54° 0′	B9	+12
2	57 494	5.96	2 1 41	57 57	A2	−37
3	56 438	6.19	2 4 31	57 11	B8	−36
4	56 443	9.0	2 5 10	56 51	B6	+ 9
5	56 445	9.4	2 5 32	56 50	B8	−55
6	56 449	7.61	2 5 54	56 45	G1	−36
7	57 521	9.9	2 7 8	57 27	G5	−21
8	55 547	9.0	2 7 17	56 2	B5	−44
9	57 525	8.3	2 8 38	57 18	B4	−44
10	55 554	7.77	2 8 51	55 32	B7	−39
11	57 526	7.8	2 8 52	57 50	A0	−48
12	56 469	8.4	2 9 41	56 16	B6	−32
13	56 470	6.99	2 9 47	56 34	B2	−40
14	56 471	6.20	2 9 52	56 35	B2	−41
15	56 475	7.5	2 9 59	56 15	B2	−46
16	56 480	8.2	2 10 27	56 54	A0	−11
17	57 533	8.1	2 10 30	57 34	F0	− 9
18	55 564	8.4	2 10 48	56 11	B6	−34
19	57 535	7.09	2 10 55	57 26	K0	+ 1
20	56 486	7.15	2 11 2	57 3	G3	− 9
21	56 498	8.5	2 11 22	56 33	B6	−58
22	56 500	8.5	2 11 27	56 55	B3	−32
23	56 522	6.42	2 12 3	56 40	B3	−43
24	56 527	8.4*	2 12 9	56 40	B6	−39
25	56 530	6.42	2 12 12	56 42	B3	−45
26	56 543	8.0	2 12 53	56 48	A0	−31
27	55 588	6.82	2 13 45	55 27	B9	−44
28	56 555	8.7	2 14 9	56 24	B3	−42
29	56 568	6.60	2 14 51	56 47	A0	−46
30	56 570	8.4	2 14 57	56 41	B3	−40
31	55 598	5.28	2 15 23	55 23	B9p	−15
32	56 591	7.46	2 15 49	56 47	A2p	−51
33	56 593	6.90	2 15 55	56 56	B8	−51
34	57 554	8.8	2 16 45	57 24	B9	−12
35	55 612	6.05	2 18 12	56 9	B3	−46
36	57 566	7.82	2 18 13	57 44	A0	−12
37	56 621	7.42	2 19 11	56 47	A0	−42
38	+57 568	7.10	2 19 36	+57 14	B1	−39

* Magnitude from the B.D.

PLATE II

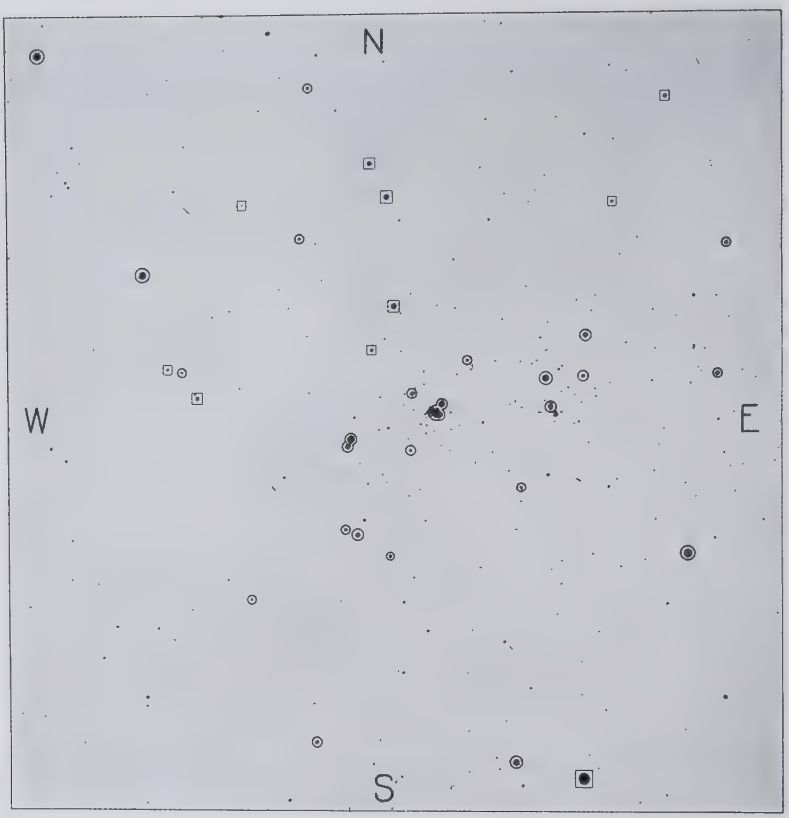

Region of *h* and χ Persei, showing stars whose radial velocities have been determined. Those enclosed in circles are probably members of the clusters; those in squares are non-members.

while the cluster stars, as is known from *Utrecht*, 5, have small proper motions. There is another reason for supposing that B.D. $+56°449$ is not a member of the group: its spectral type is G1, while all other stars with common velocity show spectra between B1 and A2. In discussing the motion of the cluster this star was accordingly excluded. It seems worth mentioning here that Adams, in measuring the spectra, found among the 27 members of the group only very few stars which may be binaries. Another curious fact is the lack of any appreciable change of spectrum with decreasing magnitude of the group stars. In other clusters, for instance in the Pleiades and Hyades, the fainter stars are of a more advanced spectral type than the brighter stars; in the present group we find for the four groups of 7, 7, 7, and 6 stars, respectively, arranged according to magnitude:

Mean Magnitude	Mean Spectrum
6.2	B6
7.2	B6
8.1	B7
8.6	B5

Besides the numbers and positions of the stars, Table I gives the visual magnitude from the *Revised Draper Catalogue*, the spectrum and the radial velocity as determined by Adams. The stars observed for radial velocity are indicated in Plate II, with the exception of No. 1 of Table I, which is too far off to be inserted. The group stars are surrounded by a circle, the other stars for which radial velocities have been determined, by a square.

II. THE COMMON PROPER MOTION OF THE GROUP

For the determination of the proper motion of the group it was supposed that the 27 stars showing the same radial velocity belong to the clusters and, therefore, have a common μ_α and μ_δ. Thanks to the large number of recent meridian observations in right ascension by Fox and Peterson, it was possible to derive a good value of μ_α. These observations include all but one of the stars observed between 1860 and 1862 by Krüger,[1] and nearly all those measured by Miss Young[1] on Rutherford plates taken in 1874. For the declination the material is less satisfactory, as but few stars have recently been observed in declination.

---

[1] *Catalog der Astronomischen Gesellschaft* (*Helsingfors-Gotha*, 1890), p. 8.

To derive the values of μ_α and μ_δ for the clusters the following process was used: A right ascension or declination as given by any observer and reduced to the epoch 1900 may be affected by a systematic error, by an accidental error, and by proper motion. Supposing the systematic error to be constant for each observer or catalogue, we may write for each co-ordinate:

$$\alpha = \alpha_0 + c + m\mu_\alpha$$
$$\delta = \delta_0 + c' + m\mu_\delta$$

where α_0 and δ_0 are the most probable values of right ascension and declination of the star, c and c' the systematic error of each observer in α and δ, and m the number of years between the time of observation and 1900. Nine of the stars with common radial velocity are not included in any of the sources used, and one appears only in Young and Fox. These stars cannot therefore be used for the derivation of the proper motion of the clusters.

We therefore have for the determination of μ_α, 82 equations of conditions with 27 unknown quantities, viz., μ_α, 18 values of α_0 and 8 systematic errors c. For declination we have 64 equations of condition with 25 unknown quantities, viz., μ_δ, 17 values of δ_0, and 7 systematic corrections c'.

The eight sources used are collected in Table II. Under n and n' are given the number of stars observed in α and δ respectively.

At first glance it may seem an endless task to solve equations of condition with so large a number of unknowns; but owing to their peculiar form, each containing but three unknown quantities, the 27 and 25 normal equations are easily reduced to 9 and 8 equations, respectively, involving only the unknown quantities μ_α or μ_δ and the systematic corrections. These were solved by a process of approximation. The resulting proper motion for the cluster is:

$$\mu_\alpha = +0''.003$$
$$\mu_\delta = +0''.003$$

---

[1] *Contributions from the Observatory of Columbia University*, No. 24, 1906.

The corrections to the catalogues, together with the weights used, are collected in Table III.

TABLE II

Observer	Abbreviation	Equinox	n	n'	Published
Krüger	K	1861	8	8	*A.G. Catalog, Helsingfors-Gotha*
Boss	B	1871	5	5	*Preliminary General Catalogue*
Young	Y	1874	15	15	*Contr. from the Obs. of Columbia Univ.*, No. 24
Bronsky and Stebnitzky	BS	1891	17	16	*Mem. de l'Ac. de St. Pétersbourg, Série VIII*, 2
Schur	S	1894	6	6	*Astr. Mitt. der K. Sternwarte in Göttingen*, 6
Leiden	L	1910	7	7	Communicated respectively by Professor E. F. van de Sande Bakhuyzen, Professor Küstner, and Professor Fox
Bonn	Bn	1910	7	7	
Fox and Peterson	F	1913	17	0	

TABLE III

Observer	Wt. α	Corr. α	Wt. δ	Corr. δ
Krüger	1.0	$-0^{s}.006$	1.0	$-0''.04$
Boss	3.0	+0.010	2.0	−0.07
Young	2.0	+0.017	1.4	−0.08
Bronsky and Stebnitzky	2.0	−0.023	1.4	+0.05
Schur	1.0	+0.027	1.0	+0.04
Leiden	3.0	+0.016	1.4	+0.15
Bonn	1.5	−0.004	1.2	−0.21
Fox	1.0	+0.014	....	....

III. POSITIONS AND PROPER MOTIONS OF STARS REOBSERVED AT THE DEARBORN OBSERVATORY

The corrections found above were next applied to the observations of all the stars appearing in *Utrecht*, 5, which were measured by any of the observers in Table II. If observed by more than one authority the proper motions were also derived. The results are collected in Table IV, which gives the current number in Young, Krüger, Bronsky and Stebnitzky, and *Utrecht*, 5. (The current numbers for Boss, Schur, Leiden, and Bonn are given in a supplementary Table, IV*a*, together with the corresponding numbers in

TABLE IV

Y	K	BS	*Utrecht,* 5	Pg. Mag.	α 1900	δ 1900	μ_α	P.E.	μ_δ	P.E.
3	....	......	1413	9.5	$2^h\ 8^m\ 8^s.748$	$+56°27'32''.82$	$+0''.021$	....	....	....
4	....	......	1353	8.7	37.676	57 17 47.87	+ 13	....	....	....
5	....	......	1301	10.2	47.115	56 57 14.82	− 6	....	....	....
7	....	15	1295	9.7	9 11.369	57 9 1.08	+ 6	$\pm 0''.009$	$+0''.033$	....
8	....	44	1275	10.2	31.236	56 1 21.13	+ 16	6	− 24	....
9	....	58	1262	8.7	41.057	56 16 19.97	+ 6	2	− 40	....
10	19	65	1247	7.5	47.007	56 33 50.21	+ 19	16	− 30	$\pm 0''.007$
11	18	76	1243	6.8	52.033	56 35 25.22	− 11	5	+ 27	7
12	....	81	1253	10.4	54.092	56 24 20.65	− 22	22	− 19	....
13	34	85	1164	9.5	57.690	56 39 54.80	+ 7	3	+ 9	2
14	....	86	1264	7.8	59.284	56 15 13.69	+ 7	8	+ 2	....
15	....	88	1170	10.9	10 0.383	56 38 4.51	+ 33	14	− 27	....
17	....	100	1184	10.3	5.035	56 30 13.64	− 8	8	− 1	....
18	....	109	1202	9.1	9.627	56 18 17.53	+ 22	0	− 23	....
19	32	119	1193	9.6	16.301	56 26 0.35	+ 1	4	+ 5	1
20	....	142	1154	8.5	26.501	56 54 5.61	+ 21	2	− 29	....
21	29	157	1082	10.8	34.837	56 37 17.04	+ 13	6	− 15	2
22	30	163	1066	9.8	38.290	56 44 6.99	0	9	+ 12	3
23	33	176	1100	10.0	45.032	56 26 9.40	+ 2	8	− 19	7
24	....	181	1061	10.4	46.461	56 56 24.57	− 10	6	+ 5	....
25	....	188	1115	8.6	47.791	56 10 39.10	+ 6	17	+ 8	....
26	28	189	1079	9.1	49.027	56 37 35.69	+ 2	1	− 6	3
27	....	199	1042	7.4	54.960	57 26 9.37	+ 57	6	− 29	17
28	....	216	1057	7.3	11 2.179	57 3 10.01	− 26	5	− 7	10
29	....	232	1125	9.2	6.530	56 0 57.12	− 8	3	− 15	....
30	....	254	929	10.8	11.563	56 53 42.91	0	12	+ 9	....
31	....	257	920	10.1	12.684	57 1 40.87	+ 15	3	− 5	....
32	....	264	909	9.4	13.911	56 42 27.71	− 5	8	− 22	....
33	27	265	964	10.6	14.102	57 21 14.76	+ 70	12	− 55	6
34	42	269	960	11.2	15.763	56 44 43.25	+ 12	6	− 6	0
38	....	290	1024	9.4	21.832	56 6 12.04	+ 356	2	− 239	....
....	20	......	990	10.8	22.298	56 34 34.76	+ 10	8	− 7	....
39	5	293	992	8.8	22.476	56 32 49.15	+ 2	6	− 15	11
40	4	311	959	8.7	26.672	56 44 43.58	+ 6	8	+ 11	3
41	....	315	928	11.2	27.749	56 54 12.47	+ 25	17	− 25	....
42	14	319	972	9.8	28.586	56 41 15.99	+ 12	9	− 18	5
43	....	322	918	10.7	29.064	57 5 44.20	+ 33	22	− 5	....
44	15	329	955	10.0	31.212	56 44 53.05	0	3	− 6	4
46	6	353	982	10.0	39.090	56 38 17.25	− 9	6	0	0
48	....	365	1014	9.6	42.105	56 17 54.79	− 7	9	− 14	....
49	24	379	778	9.8	45.958	56 49 22.31	+ 5	14	− 13	8
50	9	381	829	10.0	46.438	56 40 22.02	+ 33	10	+ 30	8
51	25	382	783	10.8	46.454	56 46 39.05	− 14	17	− 30	10
52	13	385	870	9.9	46.808	56 36 17.07	+ 2	4	+ 6	2
53	23	391	860	10.6	48.166	56 38 4.92	− 7	2	+ 1	2
54	8	416	822	10.0	52.292	56 40 37.38	− 20	17	− 4	4
55	....	418	804	11.1	52.714	56 41 44.66	+ 7	....	− 5	....
56	17	437	815	10.6	57.337	56 40 57.14	− 13	11	− 27	8
57	16	442	814	10.8	58.595	56 40 59.80	− 5	26	− 10	1
58	....	446	869	11.2	58.986	56 36 43.11	− 32	22	− 9	....
60	1	462	830	7.1	12 2.830	56 40 24.10	+ 2	1	+ 4	5
61	10	472	839	9.5	4.776	56 39 50.26	− 12	9	+ 10	5
62	3	487	831	10.3	7.526	56 40 22.86	− 7	5	0	3
63	*d*1	496	837	9.7	8.585	56 39 54.02	− 20	8	− 4	0
64	*d*2	497	833	9.1	8.757	56 40 7.21	− 1	9	+ 16	7
65	22	498	874	10.7	9.432	56 33 46.32	+ 26	2	− 7	1
66	36	503	836	10.8	11.865	56 40 0.37	− 30	18	+ 1	4
67	2	504	798	7.3	12.054	56 42 26.60	+ 6	5	+ 28	12
....	43	......	721	11.4	22.521	56 32 34.75	+ 31	2	− 26	....
....	37	......	706	11.6	24.401	56 39 9.89	+ 11	....	− 13	....
69	11	546	710	10.1	24.884	56 36 59.67	+ 10	2	− 20	2
70	7	549	704	10.0	25.557	56 40 35.44	+ 7	2	− 7	1
71	....	579	674	9.5	36.416	56 48 31.46	− 6	15	− 28	....
72	35	581	687	11.4	36.562	57 12 45.05	+ 31	1	− 2	4
73	....	583	679	10.3	37.020	57 2 27.10	+ 27	12	+ 3	....
74	21	589	709	10.5	38.229	56 37 49.92	+ 9	12	− 10	3
75	....	597	742	10.6	41.035	56 15 17.42	+ 16	12	− 11	....
76	44	599	726	11.2	41.421	56 31 4.85	+ 62	11	− 11	3
78	12	630	685	8.6	53.057	56 48 25.91	− 9	6	− 3	3
79	....	641	647	10.3	13 2.617	56 7 50.43	+ 14	12	− 36	....
80	....	648	612	10.9	6.538	57 0 19.54	+ 6	1	− 18	....
81	....	658	642	11.4	12.758	56 16 45.38	+ 13	8	− 23	....

TABLE IV—*Continued*

Y	K	BS	*Utrecht*, 5	Pg. Mag.	α 1900	δ 1900	μ_α	P.E.	μ_δ	P.E.
82..	26	662	630	9.6	2ʰ13ᵐ13ˢ.396	+56°38′16″.92	+0″.012	±0″.004	+0″.005	±0″.003
.....	31	......	635	10.9	27.038	56 31 58.02	+ 21	1	− 14	....
83..	....	692	547	9.6	33.138	57 20 49.94	− 25	2	+ 8	....
84..	....	696*a*	656	9.5	34.830	55 52 11.13	+ 1	4	+ 5	....
85..	....	697	561	10.1	35.504	56 51 6.38	+ 9	8	+ 2	....
86..	....	716	553	10.2	48.382	56 59 51.60	+ 16	2	+ 35	....
87..	....	723	582	9.8	50.863	56 27 57.70	+ 13	2	+ 11	....
88..	....	737	568	10.0	14 4.369	56 42 26.45	− 12	13	+ 2	....
89..	....	743*a*	587	9.9	7.561	56 21 26.13	+ 8	6	− 15	....
90..	....	744*a*	585	9.0	8.526	56 24 22.66	+ 41	8	+ 6	....
91..	....	746*a*	586	10.1	9.713	56 23 40.46	+ 30	3	+ 1	....
92..	....	754	571	11.8	13.753	56 41 9.84	+ 7	11	+ 28	....
93..	....	755	480	10.7	14.018	56 50 48.92	− 21	11	+ 1	....
94..	....	791	468	10.7	27.326	57 6 34.96	− 21	9	− 3	....
95..	....	796	482	10.4	31.543	56 50 15.72	+ 7	3	+ 13	....
96..	....	809	476	10.7	38.587	56 50 59.09	− 8	11	− 15	....
97..	....	817	505	10.2	39.931	56 40 1.85	+ 18	11	+ 8	....
98..	....	825	522	11.5	43.158	56 30 25.70	+ 45	12	− 9	....
99..	....	831	347	9.6	45.969	56 55 41.40	− 27	16	+ 15	....
100..	....	839	380	10.7	49.144	56 42 28.63	+ 20	14	+ 6	....
102..	....	840	429	9.1	49.734	56 26 47.84	+ 12	12	− 1	11
103..	....	843	358	7.3	51.248	56 47 4.48	+ 6	2	− 8	7
104..	....	847	349	11.7	52.806	56 52 51.71	+ 36	14	0	....
107..	....	859	388	8.7	56.721	56 41 12.09	− 7	10	− 6	....
108..	....	862	392	9.9	57.044	56 40 45.24	− 35	18	+ 35	....
109..	....	867	389	10.5	58.923	56 40 55.70	− 13	16	+ 14	....
112..	....	884	406	9.4	15 3.619	56 39 13.54	+ 5	7	+ 27	....
113..	....	890	398	9.8	4.741	56 39 59.65	− 1	9	+ 11	....
115..	....	896	404	9.9	5.857	56 39 33.44	− 12	10	+ 5	....
116..	....	916	353	9.1	12.433	56 48 50.36	+ 23	6	− 15	....
118..	....	919	400	10.1	13.690	56 39 56.76	− 24	11	+ 26	....
119..	....	928	351	10.2	18.007	56 49 37.50	− 15	15	+ 11	....
120..	....	942	285	10.2	25.416	56 45 2.15	+ 9	9	+ 38	....
121..	....	959	310	10.5	32.315	56 37 27.45	− 2	10	− 8	....
122..	....	972	308	10.3	39.403	56 37 46.23	− 12	9	− 5	....
123..	....	978	264	10.1	43 766	57 3 16.64	− 6	0	+ 10	....
124..	....	979	298	10.7	44.523	56 41 48.76	+ 1	7	+ 32	....
125..	....	982	281	8.8	48.561	56 47 17.63	0	0	+ 29	....
126..	....	989	327	10.1	52.083	56 9 59.02	+ 22	12	+ 6	....
127..	....	991	318	10.9	52.722	56 33 23.41	− 12	6	+ 15	....
128..	....	993	273	7.8	54.791	56 55 48.34	− 1	2	+ 3	4
129..	....	1000	228	11.2	59.682	56 40 14.41	+ 3	13	+ 11	....
130..	....	1007	189	9.7	16 5.554	57 0 55.42	− 24	13	− 2	....
131..	....	1009	220	10.1	6.825	56 42 55.81	+ 6	12	− 4	....
132..	....	1012	188	10.6	12.717	57 4 4.30	+ 2	11	+ 12	....
133..	....	1032	247	9.1	20.348	56 23 52.84	+ 2	2	− 6	2
134..	....	1049	215	10.5	29.211	56 45 41.79	+ 12	3	− 15	....
135..	....	1054	252	10.0	32.949	56 7 5.91	+ 10	9	− 14	....
136..	....	1056*a*	245	10.0	33.386	56 25 26.93	+ 43	17	− 45	....
137..	....	1070	124	8.8	44.807	57 23 35.52	+ 5	8	+ 28	....
138..	....	1079	144	10.7	51.761	56 46 54.09	− 7	2	+ 3	....
139..	....	1086*a*	140	10.5	55.560	56 50 4.31	− 1	7	− 4	....
140..	....	1088	135	10.1	56.005	56 53 54.55	+ 6	2	+ 5	....
141..	....	1103	175	10.0	17 9.254	56 8 22.15	+ 11	12	+ 54	....
142..	....	1116	82	9.9	21.036	57 15 53.14	+ 31	0	+ 14	....
143..	....	1131*a*	99	10.2	33.043	56 45 43.24	+ 15	6	− 26	....
145..	....	1142	87	10.1	39.086	57 0 35.38	+ 19	7	+ 18	....
.....	....	1183	39*	6.9	18 12.188	56 9 22.24	+ 10	4	+ 10	5

Bronsky and Stebnitzky.) The fifth column gives the photographic magnitude, derived from *Utrecht*, 5, corrected as indicated on page 9 of the present paper; the sixth and seventh columns give the right ascension and declination for 1900, the eighth and ninth columns the proper motion in right ascension and the probable error, the tenth and eleventh columns the corresponding values for declination.

All stars of Table IV with the exception of Young 55 and Krüger 37 were observed by Fox and Peterson. The probable errors in α, δ, μ_α, and μ_δ differ, of course, greatly with the number of observations available. In the mean they are:

TABLE IV*a*

DESIGNATION OF STARS

Bronsky and Stebnitzky	Boss	Schur	Leiden and Bonn
76	507	a	....
119	....	b	....
199	513	....	2057
216	515	....	2061
293	....	c	2071
311	....	d	....
462	519	....	2088
504	....	e	2093
630	....	f	2113
662	....	g	....
840	....	k	....
843	533	l	2150
993	535	m	2177
1032	....	o	....
1183	544	....	2217

P.E. in $\alpha = 0^{s}.019$ P.E. in $\mu_\alpha = 0''.008$
P.E. in $\delta = 0''.075$ P.E. in $\mu_\delta = 0''.005$

IV. REDUCTION OF THE PROPER MOTIONS IN UTRECHT 5 TO THE PRESENT SYSTEM

The proper motions derived in the last section are based on the weighted mean system of the eight observers used. A comparison between these motions and the corresponding values of *Utrecht*, 5, will enable us to reduce the latter to the same system. In doing this, new magnitudes were derived for the stars in *Utrecht*, 5. In the original paper the magnitudes were based on the diameters of the stars on one of the plates and were reduced to the Harvard visual scale. (See *Utrecht*, 5, pp. 38–42.) But as the results are derived from photographic plates, it is preferable to use photographic magnitudes. With the aid of *Publications of the Astro-*

nomical Laboratory at Groningen, No. 27, the following corrections to the original magnitudes were derived:

Mag. in *Utrecht*, 5.	Correction
< 7.5	+0.4
7.6–10.4	+0.5
10.5–12.3	+0.6
>12.4	+0.7

The results of the comparison between the motions in Table IV and in *Utrecht*, 5, are given in Table V.

Except for the fainter stars, where the meridian observations have less weight, the differences are fairly constant for μ_α; for μ_δ on the other hand there is a decided change with the magnitude.

A check on the result that the difference in motion is constant for μ_α, but a function of the magnitude for μ_δ, can be derived in the following way: On the plates measured in *Utrecht*, 5, there is a very strong concentration of stars toward the centers of the two clusters. The plates show 54 and 35 stars in regions of 25 square minutes, while in the absence of the clusters there would be only 2 or 3. Practically all these stars must therefore be members of the group. We have further the 27 members of the clusters, discussed in section 1; for the cluster stars we found $\mu_\alpha = +0''.003$, $\mu_\delta = +0''.003$. Comparing this proper motion with the motions for the same stars in *Utrecht*, 5, we find the differences as given in Table VI, in which the first two lines refer to the stars of the common velocity of −40 km/sec. and the others to the stars in the central regions.

TABLE V

Limits of Mag.	Mean Mag.	n	μ_α C$-\mu_\alpha$ *U*5	μ_δ C$-\mu_\delta$ *U*5
6.8– 7.8	7.3	10	+0″.0053	+0″.0065
7.9– 8.8	8.7	10	+ 55	+ 79
8.9– 9.8	9.5	29	+ 85	+ 37
9.9–10.8	10.3	64	+ 54	+ 16
10.9–11.8	11.3	17	+0.0191	−0.0089

The differences are plotted as ordinates in Figure 1, with the magnitudes as abscissae. The dots represent the values from Table V, the crosses the values from the first two lines of Table VI, the circles the other values from Table VI. All these results together indicate a constant correction of +0″.007 to the proper motions in right ascension in *Utrecht*, 5. For the proper motion in declination a correction which is a linear function of the magnitude is used. Its value is +0″.013 for magnitude 7.0 and −0″.008 for magnitude 15.0.

TABLE VI

Limits of Mag.	Mean Mag.	*n*	μ_α C−μ_α *U* 5	μ_δ C−μ_δ *U* 5
6.7– 7.9	7.2	8	+0″.0094	+0″.0159
8.0– 9.1	8.8	12	+ 62	+ 105
7.1– 7.8	7.2	2	+ 90	+ 175
7.9– 8.8	8.7	1	− 10	+ 90
8.9– 9.8	9.5	4	+ 62	+ 42
9.9–10.8	10.4	12	+ 116	+ 32
10.9–11.8	11.5	12	+ 60	+ 26
11.9–12.8	12.2	19	+ 57	+ 25
12.9–13.8	13.4	24	+ 29	− 44
13.9–14.7	14.3	15	+0.0065	−0.0075

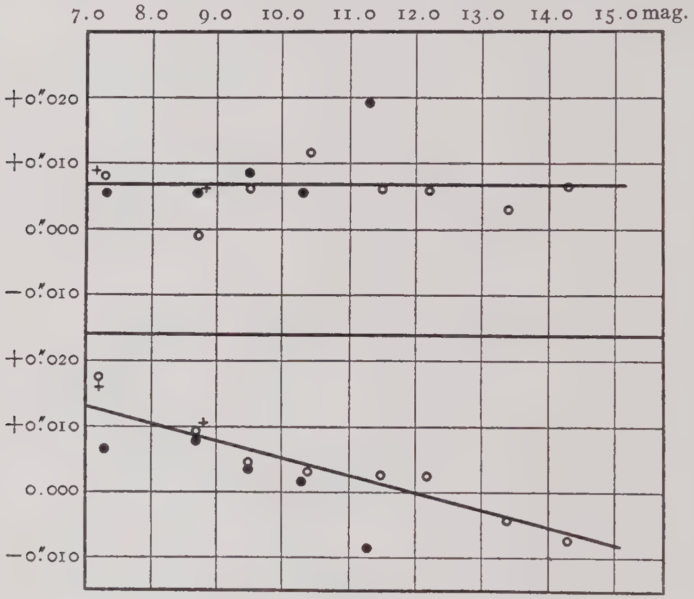

FIG. 1.—Corrections to the proper motions in *Utrecht*, 5

TABLE VII

No.	Pg. Mag.	μ_α	μ_δ	No.	Pg. Mag.	μ_α	μ_δ
1	12.5	+0″.019	−0″.024	47	11.9	+0″.009	−0″.012
2	12.9	+33	−35	48	12.2	−7	−10
3	11.6	−2	−2	49	11.9	+11	−13
4	11.9	+2	−2	50	12.6	−3	+3
5	8.2	+9	−3	51	12.9	−7	−13
6	12.7	−40	−4	52	11.8	+4	−8
7	9.2	−6	−5	53	11.9	−1	+7
8	12.8	−35	−4	54	12.3	+2	−6
9	9.7	+22	−21	55	13.7	+11	−5
10	11.5	−26	+4	56	13.8	+7	+1
11	12.2	+78	−33	58	11.4	+25	−2
12	8.9	+15	−12	59	14.1	−3	−13
13	11.5	+2	−10	60	13.7	−19	−10
14	12.2	−5	−16	61	12.8	−4	+5
15	10.6	+11	−13	62	13.8	−8	+12
16	11.5	+13	−30	63	10.8	+42	−7
17	12.3	+28	−38	64	12.9	−9	−11
18	12.7	−6	−16	65	12.9	−15	+1
19	9.4	+4	−12	66	11.2	+9	+9
20	10.1	+6	−6	67	12.9	−26	+13
21	12.2	−11	−3	68	10.0	+3	+6
22	11.7	+3	−8	69	12.4	−3	+12
23	10.2	+8	−5	70	12.5	−16	+5
24	12.9	−13	−14	71	13.1	−21	+17
25	12.1	0	+1	72	12.8	+12	+1
26	10.6	+6	−5	73	13.2	−23	+3
27	11.2	+20	−8	75	13.2	−18	+4
28	10.1	+4	−3	76	13.3	−19	+11
29	10.6	+2	+6	77	13.9	−26	+20
30	13.6	−29	+4	80	13.5	+1	−1
32	12.9	−29	+7	81	12.5	−5	−9
33	11.8	+18	+25	82	9.9	+51	−17
34	11.2	−18	0	83	11.6	+7	+1
35	12.3	−47	+6	84	11.5	+6	−15
36	12.4	−29	+3	85	13.8	+6	−20
37	12.9	−24	−2	86	12.5	0	−26
38	13.1	−38	−19	87	10.1	+8	−7
39	13.7	−33	+3	88	12.9	0	−18
39*	6.9	−2	−13	89	11.7	−23	−18
40	10.8	+12	−3	90	12.3	+14	−1
42	13.8	+4	−10	91	11.5	+17	+1
43	12.6	+8	−7	92	10.6	−3	−13
44	12.8	0	−2	93	12.7	+25	−2
45	13.6	−17	−15	94	13.8	+1	−3
46	13.2	−10	−7	95	12.5	+13	−12

TABLE VII—*Continued*

No.	Pg. Mag.	μ_α	μ_δ	No.	Pg. Mag.	μ_α	μ_δ
97......	13.3	+0″.008	+0″.005	145.....	13.9	+0″.015	−0″.008
98......	12.3	+ 8	+ 4	146.....	12.2	+ 3	− 1
99......	10.2	+ 17	+ 3	147.....	11.3	+ 11	− 6
100......	12.5	0	− 4	148.....	12.5	+ 10	+ 4
101......	12.3	+ 6	+ 10	149.....	12.5	+ 17	− 7
102......	12.8	− 3	+ 2	150.....	10.6	+ 8	− 1
103......	11.6	+ 11	+ 5	151.....	13.6	+ 9	0
104......	10.7	+ 4	+ 11	152.....	11.7	+ 4	+ 1
105......	12.4	+ 2	− 1	154.....	13.6	− 7	− 2
106......	10.9	+ 7	+ 2	155.....	12.4	+ 2	+ 9
107......	13.4	0	+ 3	156.....	12.7	+ 8	+ 7
108......	11.4	− 9	+ 3	157.....	12.8	− 4	− 3
109......	12.0	− 12	+ 8	158.....	14.4	− 17	− 12
110......	12.7	− 8	+ 12	159.....	12.9	+ 6	− 1
111......	12.4	− 1	− 3	160.....	12.3	+ 6	+ 7
112......	12.3	+ 2	+ 13	161.....	13.1	− 1	+ 5
113......	13.8	− 15	+ 28	164.....	12.4	− 2	+ 8
115......	13.5	− 17	+ 5	165.....	12.0	− 14	+ 15
116......	12.4	− 14	+ 9	166.....	11.4	− 4	+ 4
117......	12.0	+ 27	+ 4	167.....	11.7	+ 7	0
118......	12.9	− 9	+ 1	168.....	12.7	+ 4	+ 7
119......	12.4	− 2	− 3	169.....	11.9	− 2	+ 8
120......	13.7	− 13	− 2	171.....	12.7	− 12	+ 3
121......	12.8	+ 12	− 1	172.....	13.1	+ 11	+ 13
122......	11.5	− 25	− 11	173.....	11.8	− 9	+ 1
124......	8.8	− 4	+ 3	174.....	12.4	+ 5	+ 14
125......	12.1	+ 16	+ 10	175.....	10.0	− 15	+ 28
126......	11.9	+ 17	0	176.....	10.8	+ 1	− 3
127......	11.4	+ 16	+ 8	177.....	12.0	+ 10	+ 3
128......	10.6	+ 25	− 25	178.....	13.4	− 8	+ 3
129......	11.3	+ 16	− 13	179.....	12.3	− 13	0
130......	13.7	+ 17	− 13	181.....	12.5	+ 14	+ 14
131......	12.4	+ 8	+ 1	182.....	11.9	+ 12	+ 12
132......	12.3	+ 6	+ 2	183.....	11.4	+ 9	+ 22
134......	12.2	+ 3	+ 1	184.....	12.7	+ 21	+ 30
135......	10.1	+ 7	0	186.....	12.3	+ 22	− 7
136......	12.9	+ 10	− 7	187.....	12.6	+ 15	− 7
137......	12.5	+ 5	+ 1	188.....	10.6	+ 13	− 14
138......	12.9	+ 10	0	189.....	9.7	+ 7	− 3
139......	12.8	+ 9	+ 14	190.....	13.5	+ 16	− 11
140......	10.5	+ 17	0	191.....	12.9	+ 27	− 5
141......	12.9	+ 13	+ 10	192.....	12.3	+ 15	+ 1
142......	12.3	+ 25	+ 3	193.....	12.8	+ 4	− 10
143......	13.4	− 4	− 2	194.....	12.9	− 2	− 10
144......	10.7	+ 11	+ 12	195.....	12.1	+ 20	− 7

TABLE VII—*Continued*

No.	Pg. Mag.	μ_α	μ_δ	No.	Pg. Mag.	μ_α	μ_δ
196	13.8	+0″.016	−0″.012	245	10.0	+0″.056	−0″.012
197	11.1	+ 11	+ 7	246	11.5	+ 14	+ 8
198	13.8	+ 20	− 5	247	9.1	+ 24	+ 8
199	11.4	+ 11	− 5	248	12.0	0	+ 12
200	13.5	+ 7	− 20	249	13.8	− 2	+ 11
201	13.2	+ 18	− 5	250	13.4	+ 6	+ 16
202	12.1	+ 24	+ 3	251	13.5	− 7	+ 12
203	13.2	+ 6	− 12	252	10.0	+ 5	− 9
204	11.4	+ 11	− 5	253	14.4	+ 12	+ 14
205	12.1	+ 3	+ 1	254	11.1	+ 8	− 6
207	13.5	+ 13	0	255	14.2	+ 7	− 18
208	13.1	+ 10	− 2	256	13.9	+ 10	0
209	14.3	+ 10	− 10	257	12.3	+ 11	+ 2
210	11.8	+ 8	− 5	258	12.1	− 10	− 17
211	12.2	+ 9	− 4	259	11.9	+ 8	− 9
212	13.5	+ 13	− 12	260	13.4	+ 11	+ 6
213	13.1	+ 22	+ 9	261	11.4	+ 6	+ 10
214	12.9	− 7	+ 7	262	13.3	+ 12	− 8
215	10.5	+ 6	+ 10	263	12.4	+ 12	− 1
216	11.6	+ 11	+ 6	264	10.1	+ 8	− 14
217	11.3	+ 1	+ 12	265	12.1	+ 6	− 16
218	10.9	− 3	+ 7	266	11.8	+ 22	− 24
219	13.2	− 6	+ 3	267	12.2	+ 8	− 11
220	10.1	+ 1	+ 14	268	11.5	+ 1	− 9
221	13.3	− 4	− 11	269	12.0	+ 7	− 9
222	13.1	+ 10	+ 1	270	12.9	+ 7	− 3
223	13.4	+ 7	− 18	271	10.9	+ 13	+ 3
225	13.5	+ 13	+ 9	272	13.2	+ 3	− 2
226	13.2	+ 13	− 6	273	7.8	+ 15	+ 2
227	11.7	+ 9	+ 13	274	14.3	+ 13	− 1
228	11.2	+ 7	+ 11	275	11.5	+ 22	+ 3
229	12.3	+ 8	+ 4	276	11.2	+ 8	+ 2
231	13.3	+ 8	+ 4	277	12.4	+ 7	− 6
232	10.8	+ 3	− 3	278	12.6	+ 5	− 3
233	14.0	+ 3	− 2	279	13.3	+ 7	− 2
234	11.6	+ 22	+ 9	280	12.4	+ 6	+ 9
235	12.9	− 4	+ 8	281	8.8	+ 12	+ 16
236	12.7	− 8	+ 5	282	11.9	+ 8	− 2
237	13.4	+ 1	+ 11	283	12.4	+ 14	+ 12
238	12.1	+ 7	+ 4	284	13.4	+ 10	+ 9
240	14.3	− 16	+ 7	285	10.2	+ 13	− 2
241	13.3	+ 18	+ 7	286	12.8	+ 5	− 1
242	12.5	+ 1	+ 13	287	11.3	+ 11	+ 2
243	13.2	+ 12	+ 3	289	12.7	0	+ 5
244	13.2	+ 23	+ 6	290	11.1	+ 9	+ 5

TABLE VII—*Continued*

No.	Pg. Mag.	μ_α	μ_δ	No.	Pg. Mag.	μ_α	μ_δ
291......	12.9	+0″.013	+0″.006	338.....	11.6	+0″.009	+0″.012
292......	11.9	+ 3	+ 7	339.....	13.5	− 5	− 1
293......	12.1	+ 8	+ 14	340.....	12.3	+ 4	+ 2
294......	13.9	+ 75	− 28	341.....	10.7	− 7	+ 5
295......	12.2	+ 2	+ 1	342.....	11.1	+ 41	− 10
296......	12.6	+ 8	+ 6	343.....	12.9	+ 2	− 12
298......	10.7	+ 6	− 1	344.....	13.3	+ 22	− 21
299......	14.5	+ 14	− 2	345.....	12.4	+ 9	− 5
300......	12.7	+ 3	+ 1	346.....	12.4	+ 9	− 1
301......	12.6	+ 7	+ 5	347.....	9.6	+ 4	− 10
302......	13.5	+ 12	+ 8	348.....	14.5	+ 14	− 8
303......	11.5	+ 5	+ 3	349.....	11.7	+ 3	0
304......	....	− 18	....	350.....	12.8	+ 5	+ 6
305......	12.7	+ 16	− 1	351.....	10.2	+ 7	+ 7
306......	13.8	+ 19	− 2	352.....	13.8	+ 7	+ 2
307......	11.7	+ 4	+ 5	353.....	9.1	+ 1	+ 8
308......	10.3	+ 8	+ 12	354.....	12.6	0	+ 4
309......	....	+ 24	....	355.....	12.9	+ 6	+ 7
310......	10.5	− 2	+ 13	357.....	13.6	+ 16	+ 2
311......	12.6	+ 3	+ 1	358.....	7.3	+ 11	+ 9
312......	11.8	+ 8	+ 8	359.....	14.2	+ 4	0
313......	13.9	+ 4	+ 4	362.....	12.4	+ 11	+ 12
314......	11.5	+ 13	+ 3	363.....	13.1	0	− 6
315......	11.5	+ 6	+ 5	364.....	12.9	+ 8	+ 2
316......	13.9	+ 5	− 4	365.....	14.2	+ 21	− 4
317......	11.6	+ 6	+ 10	366.....	....	− 11	....
318......	10.9	+ 3	0	367.....	12.3	+ 9	+ 3
319......	13.4	+ 1	+ 13	368.....	13.1	+ 14	− 4
320......	11.4	+ 12	+ 4	369.....	12.3	0	+ 4
321......	12.8	+ 1	+ 13	370.....	14.4	+ 11	0
322......	13.6	+ 8	+ 11	371.....	11.9	+ 4	+ 11
323......	11.2	+ 10	+ 10	372.....	13.6	+ 7	+ 3
324......	14.1	+ 7	− 2	373.....	11.4	+ 2	− 5
325......	11.8	+ 12	+ 2	374.....	11.2	+ 12	+ 4
327......	10.1	− 2	− 6	376.....	13.7	+ 8	0
328......	13.9	+ 11	− 8	377.....	13.9	− 1	+ 4
329......	13.7	− 19	+ 1	378.....	13.9	+ 17	+ 8
330......	10.3	0	− 18	379.....	14.4	+ 8	+ 8
331......	12.3	− 17	− 19	380.....	10.7	+ 3	+ 5
332......	12.8	− 5	− 27	380*....	....	+ 15	....
333......	13.6	− 15	− 16	381.....	12.5	+ 7	− 1
334......	12.6	− 18	+ 1	382.....	11.8	+ 7	− 3
335......	12.6	+ 4	+ 16	383.....	12.8	+ 2	− 2
336......	12.2	+ 5	+ 7	384.....	11.6	+ 3	+ 7
337......	12.1	+ 12	+ 12	385.....	12.0	+ 7	− 7

TABLE VII—*Continued*

No.	Pg. Mag.	μ_α	μ_δ	No.	Pg. Mag.	μ_α	μ_δ
386	13.5	+0″.008	0″.000	431	13.1	+0″.010	+0″.004
387	13.7	+ 13	+ 3	432	13.3	+ 5	+ 8
388	8.7	+ 11	+ 2	433	12.9	+ 21	+ 6
389	10.5	+ 8	+ 7	435	11.5	+ 20	− 10
390	13.1	0	0	436	11.5	+ 19	− 15
391	13.6	− 3	+ 5	437	13.3	+ 13	− 1
392	9.9	− 2	+ 8	438	11.9	+ 9	+ 3
393	14.6	+ 6	+ 14	439	14.2	+ 7	+ 4
394	12.3	+ 8	+ 13	440	10.4	− 1	− 1
395	14.7	+ 16	+ 5	441	13.9	+ 16	+ 6
396	13.1	+ 4	+ 8	442	10.6	+ 10	+ 3
397	11.8	+ 10	+ 6	443	13.4	− 1	+ 5
398	9.8	+ 7	+ 10	444	12.6	+ 7	− 1
399	13.6	+ 49	+ 22	445	13.1	+ 22	− 2
400	10.1	+ 1	+ 3	446	10.2	+ 9	− 3
401	13.7	− 1	− 6	447	10.6	+ 5	− 5
402	12.8	+ 11	− 12	448	11.2	+ 5	− 21
403	14.7	+ 7	+ 2	449	12.4	− 5	− 1
404	9.9	− 6	+ 12	450	13.2	+ 13	− 40
405	12.1	+ 1	+ 10	451	12.6	− 1	− 13
406	9.4	+ 4	+ 6	452	14.0	+ 8	+ 10
407	13.7	+ 17	+ 3	453	11.7	− 6	− 29
408	11.1	+ 8	+ 3	454	12.2	+ 28	− 36
409	13.6	− 1	+ 2	455	12.6	− 5	− 4
410	13.6	+ 16	+ 1	456	13.5	+ 4	+ 9
411	13.2	+ 8	+ 3	457	10.7	− 3	+ 7
412	14.0	+ 3	+ 10	458	13.5	− 4	+ 7
413	11.8	+ 8	+ 10	459	13.1	+ 4	+ 5
414	10.7	0	+ 9	460	12.7	− 7	+ 9
415	14.0	+ 6	+ 9	461	11.3	+ 1	+ 11
416	13.6	0	+ 11	462	13.6	+ 5	+ 5
417	12.8	+ 7	+ 6	464	12.8	+ 2	+ 1
418	13.2	+ 21	+ 6	465	12.9	− 11	− 2
419	13.3	+ 1	+ 1	466	13.2	− 12	− 15
420	13.8	+ 3	− 3	467	12.4	+ 8	− 4
421	14.0	+ 9	− 6	468	10.7	− 5	− 8
422	13.6	+ 8	+ 8	469	13.1	+ 3	− 3
423	13.7	+ 24	+ 3	470	13.6	− 1	− 6
424	11.9	+ 5	− 4	471	13.2	+ 16	− 13
425	14.7	+ 19	− 13	472	13.7	+ 16	− 4
426	13.7	+ 18	0	473	13.9	+ 16	− 25
427	12.8	+ 4	+ 2	474	11.2	− 15	− 10
428	12.6	+ 10	+ 3	475	12.9	+ 23	− 11
429	9.1	+ 2	− 13	476	10.7	+ 9	− 6
430	13.8	+ 14	+ 16	477	13.2	+ 17	− 11

TABLE VII—*Continued*

No.	Pg. Mag.	μ_α	μ_δ	No.	Pg. Mag.	μ_α	μ_δ
478......	14.0	+0″.024	−0″.008	528.....	11.8	+0″.007	+0″.002
480......	10.7	− 4	− 4	529.....	11.9	+ 12	+ 8
481......	14.6	+ 22	+ 2	530.....	14.5	+ 16	+ 7
482......	10.4	+ 6	+ 6	531.....	14.1	+ 11	+ 7
483......	12.8	+ 3	− 3	532.....	14.6	+ 9	+ 4
484......	14.0	+ 16	− 29	533.....	12.6	− 5	− 3
485......	12.9	+ 18	+ 1	535.....	13.1	0	− 3
486......	14.1	+ 17	− 6	536.....	12.4	+ 6	+ 4
487......	12.5	+ 17	− 4	537.....	14.7	+ 3	+ 16
488......	11.3	+ 6	+ 2	538.....	13.5	+ 16	− 14
489......	12.7	+ 13	− 15	539.....	11.8	+ 14	+ 7
490......	11.2	+ 3	+ 1	540.....	12.6	+ 12	− 4
491......	13.4	+ 9	+ 8	541.....	13.3	+ 5	+ 2
492......	14.3	+ 23	+ 1	542.....	14.5	+ 14	+ 7
493......	12.6	+ 4	− 4	543.....	12.3	+ 11	+ 1
494......	12.5	+ 6	− 2	544.....	9.9	− 19	− 2
495......	13.7	+ 13	− 1	545.....	10.3	+ 3	+ 21
497......	12.9	+ 9	− 6	546.....	13.2	− 6	− 7
498......	13.2	+ 5	− 10	547.....	9.6	− 8	+ 6
499......	12.9	+ 5	− 2	548.....	13.8	− 10	+ 15
500......	13.1	+ 5	+ 4	549.....	13.7	+ 8	− 10
501......	10.6	+ 14	− 8	550.....	11.7	− 21	+ 11
502......	13.3	− 2	− 4	552.....	13.5	+ 1	− 3
503......	11.7	+ 5	+ 5	553.....	10.2	+ 1	+ 5
504......	13.1	+ 6	0	554.....	13.5	− 3	− 3
505......	10.2	+ 5	− 1	555.....	13.6	− 9	− 8
506......	11.9	+ 8	− 4	556.....	12.2	+ 11	− 28
508......	13.7	+ 7	− 12	557.....	11.7	+ 4	− 15
509......	12.7	− 7	+ 6	558.....	12.7	+ 16	− 13
510......	12.0	0	+ 11	559.....	12.2	+ 10	− 11
511......	12.1	+ 11	0	560.....	14.1	+ 11	− 13
512......	13.5	+ 7	+ 10	561.....	10.1	+ 11	− 4
514......	12.8	+ 8	+ 21	562.....	13.5	− 5	− 11
516......	12.2	+ 12	+ 6	563.....	12.5	+ 6	0
517......	13.1	+ 8	+ 7	565.....	13.3	− 1	+ 6
518......	13.8	+ 21	+ 7	566.....	12.4	+ 5	+ 6
519......	12.1	+ 1	+ 11	568.....	10.0	+ 4	− 2
520......	13.6	+ 24	+ 18	569.....	10.6	+ 1	+ 3
521......	13.4	+ 73	− 62	570.....	13.4	+ 12	+ 14
522......	11.5	+ 17	+ 6	571.....	11.8	− 6	+ 9
523......	12.6	+ 7	− 1	572.....	12.5	+ 11	+ 1
524......	12.9	+ 22	+ 8	573.....	12.5	+ 14	+ 6
525......	13.2	+ 3	− 2	574.....	12.9	+ 23	0
526......	12.7	+ 9	+ 3	576.....	13.2	+ 42	− 14
527......	12.0	+ 4	+ 9	577.....	11.8	+ 12	+ 5

TABLE VII—*Continued*

No.	Pg. Mag.	μ_α	μ_δ	No.	Pg. Mag.	μ_α	μ_δ
578......	12.1	+0″.003	+0″.003	628.....	13.5	+0″.008	+0″.003
578*.....	....	+ 28	....	629.....	12.5	+ 6	+ 17
579......	14.1	− 9	+ 4	630.....	9.6	− 3	+ 3
580......	13.9	+ 10	+ 8	631.....	13.9	+ 8	+ 7
581......	12.9	+ 6	+ 4	632.....	12.4	+ 1	+ 16
582......	9.8	+ 17	0	633.....	13.9	0	− 3
583......	14.3	+ 8	+ 5	634.....	12.7	− 1	+ 5
584......	13.2	+ 9	+ 7	635.....	10.9	− 1	+ 12
585......	9.0	+ 8	+ 1	636.....	13.5	+ 5	− 1
586......	10.1	+ 14	+ 10	637.....	14.1	+ 11	+ 3
587......	9.9	+ 16	− 1	639.....	13.1	+ 12	+ 5
588......	11.6	+ 7	+ 3	640.....	13.9	+ 9	− 3
589......	12.8	+ 24	− 3	642.....	11.4	+ 9	− 2
590......	13.6	+ 18	0	643.....	13.9	+ 21	+ 3
591......	13.9	+ 22	+ 24	644.....	14.3	0	+ 8
592......	14.4	+ 14	+ 4	645.....	14.5	+ 23	− 10
593......	11.3	+ 11	− 7	646.....	12.5	+ 15	− 1
594......	13.7	+ 2	− 15	647.....	10.3	+ 37	− 6
595......	13.2	+ 12	+ 6	648.....	13.9	+ 21	+ 1
596......	13.2	+ 14	+ 3	649.....	13.8	+ 23	+ 1
599......	12.2	+ 6	− 14	650.....	13.3	+ 21	− 8
600......	9.9	− 34	− 37	651.....	14.3	+ 7	− 18
601......	11.1	− 3	+ 13	652.....	11.4	+ 19	− 18
602......	12.3	− 9	+ 16	653.....	14.0	+ 58	− 67
603......	14.3	− 1	− 15	654.....	13.8	+ 21	+ 1
604......	13.2	− 2	+ 5	655.....	13.9	+ 21	+ 20
605......	13.1	− 1	+ 11	656.....	9.5	+ 23	− 11
606......	13.9	− 11	− 1	658.....	14.0	+ 18	+ 7
607......	13.1	+ 25	− 6	660.....	13.7	+ 36	+ 19
608......	13.9	+ 23	− 22	661.....	13.4	+ 24	− 2
609......	12.5	+ 1	+ 10	662.....	11.4	+ 29	− 17
610......	13.4	− 4	+ 7	663.....	13.4	− 15	− 22
612......	10.9	+ 2	− 4	664.....	12.6	+ 1	+ 6
613......	12.8	+ 8	+ 6	667.....	13.7	+ 8	+ 22
615......	13.8	+ 8	− 17	668.....	12.7	− 2	+ 14
616......	13.1	− 2	− 11	669.....	11.8	+ 3	+ 20
617......	13.5	+ 4	+ 1	670.....	12.8	− 8	+ 23
618......	14.0	+ 9	+ 2	671.....	12.6	+ 43	− 18
619......	12.9	+ 30	0	672.....	12.5	+ 8	− 13
621......	11.6	+ 9	0	673.....	13.2	− 11	+ 3
623......	11.8	+ 10	− 3	674.....	9.5	+ 23	− 11
624......	13.4	+ 19	+ 9	675.....	10.9	− 8	− 6
625......	14.6	+ 10	+ 4	676.....	13.6	− 9	0
626......	12.2	+ 8	+ 6	677.....	13.7	+ 3	+ 2
627......	13.1	+ 10	+ 6	678.....	14.6	− 4	+ 13

TABLE VII—*Continued*

No.	Pg. Mag.	μ_α	μ_δ	No.	Pg. Mag.	μ_α	μ_δ
679	10.3	−0″.006	−0″.002	727	14.2	+0″.016	−0″.006
680	11.9	− 7	+ 3	728	14.1	+ 17	+ 5
682	14.2	− 2	0	729	13.1	+ 12	+ 1
683	13.7	+ 15	+ 3	730	12.9	+ 8	+ 6
684	13.5	+ 3	− 17	731	13.6	− 1	+ 1
685	8.6	+ 5	− 16	732	13.5	+ 5	− 4
686	14.1	+ 4	− 1	733	11.8	+ 5	+ 10
687	11.4	+ 1	− 3	734	12.9	+ 10	− 8
688	13.8	+ 24	+ 9	735	11.4	+ 7	− 8
689	13.6	+ 14	− 1	736	13.3	+ 5	− 14
690	14.0	+ 4	+ 13	737	11.7	+ 5	0
691	14.6	+ 10	− 12	738	13.4	+ 15	+ 3
692	12.9	+ 4	− 3	739	12.3	0	− 8
693	12.8	+ 5	+ 10	740	11.8	+ 16	− 7
694	12.6	+ 17	+ 4	741	14.1	+ 3	− 3
695	13.2	+ 1	+ 7	742	10.6	+ 9	− 7
696	12.4	+ 3	+ 5	743	11.4	+ 5	− 2
697	14.0	+ 9	+ 4	745	13.3	+ 7	− 1
699	12.5	+ 12	− 2	746	13.7	− 3	− 5
700	13.5	+ 9	− 1	747	12.0	+ 1	− 3
701	12.7	+ 7	− 2	748	12.6	+ 9	− 14
702	14.4	+ 7	+ 6	749	13.4	+ 10	− 8
703	14.0	+ 17	+ 14	750	12.6	+ 11	− 18
704	10.0	+ 9	+ 7	751	11.8	− 16	+ 6
705	11.8	+ 7	+ 11	752	12.0	+ 36	− 11
706	11.6	+ 1	+ 6	753	10.5	+ 26	− 26
707	11.9	+ 4	+ 8	754	12.4	− 13	− 31
708	13.4	+ 1	+ 7	755	11.1	+ 21	− 14
709	10.5	0	+ 7	756	10.7	+ 29	− 22
710	10.1	+ 2	+ 4	757	11.1	+ 20	− 19
711	14.0	+ 7	+ 4	758	11.4	+ 28	− 13
712	12.9	+ 3	+ 4	760	12.4	....	+ 12
713	13.6	+ 8	+ 4	761	13.1	− 25	+ 3
714	13.7	+ 8	− 8	762	13.2	− 11	+ 29
715	12.5	0	+ 1	763	12.4	+ 14	+ 27
716	11.4	+ 5	− 3	765	12.9	− 3	+ 8
717	12.9	+ 23	+ 2	766	13.4	+ 9	− 15
718	12.0	+ 10	+ 17	768	10.8	+ 3	+ 4
719	13.6	+ 10	+ 6	770	13.4	+ 3	+ 15
721	11.4	+ 25	+ 3	772	12.9	+ 5	+ 12
722	12.3	+ 3	− 10	774	12.6	+ 33	− 16
723	13.3	+ 4	0	775	11.8	+ 8	+ 12
724	13.4	+ 46	− 18	776	13.3	+ 2	+ 4
725	13.2	+ 21	0	777	12.5	+ 5	− 15
726	11.2	+ 6	+ 6	778	9.8	+ 6	− 11

TABLE VII—*Continued*

No.	Pg. Mag.	μ_α	μ_δ	No.	Pg. Mag.	μ_α	μ_δ
780......	10.7	+0″.005	+0″.007	827.....	13.5	+0″.006	−0″.011
781......	12.4	+ 4	− 2	828.....	12.3	+ 2	+ 9
782......	12.8	− 4	+ 2	829.....	10.0	+ 7	− 4
783......	10.8	− 2	+ 5	830.....	7.1	+ 2	− 4
784......	13.4	+ 3	− 17	831.....	10.3	− 11	− 7
785......	12.5	+ 1	− 5	832.....	14.7	− 5	+ 16
786......	13.7	+ 3	− 12	833.....	9.1	+ 7	− 5
787......	14.5	− 11	− 1	834.....	13.9	+ 6	+ 24
788......	12.1	+ 8	+ 7	835.....	13.7	+ 12	+ 19
789......	13.2	+ 14	+ 12	836.....	10.8	− 13	+ 13
791......	12.0	+ 8	− 2	837.....	9.7	− 3	+ 2
792......	13.6	0	− 4	838.....	11.9	+ 8	+ 10
793......	11.7	− 3	− 5	839.....	9.5	+ 4	+ 12
794......	11.9	+ 2	− 5	840.....	12.9	+ 5	+ 5
795......	11.4	+ 7	− 1	841.....	13.6	+ 9	+ 2
796......	14.4	+ 1	− 13	842.....	13.7	+ 13	+ 1
797......	13.3	+ 3	+ 4	843.....	13.6	+ 7	− 3
798......	7.3	0	0	844.....	13.2	+ 10	+ 1
799......	14.4	+ 15	− 6	845.....	14.1	− 2	− 2
801......	12.7	− 2	− 2	846.....	11.5	+ 2	+ 4
802......	13.2	0	− 4	847.....	14.2	+ 4	+ 3
803......	13.1	+ 10	+ 5	848.....	14.5	+ 4	− 7
804......	11.1	+ 3	− 2	849.....	13.4	+ 2	+ 12
805......	11.7	− 7	− 1	850.....	12.4	+ 3	− 2
806......	13.9	− 2	+ 2	851.....	11.9	+ 7	+ 5
807......	14.7	− 5	− 8	852.....	13.4	+ 18	− 1
808......	10.8	+ 2	+ 6	853.....	13.9	+ 9	+ 14
809......	11.3	+ 2	− 5	855.....	13.2	+ 3	+ 6
810......	11.9	+ 2	− 3	856.....	14.6	+ 6	− 4
811......	11.9	+ 4	− 3	857.....	14.1	+ 10	+ 7
812......	12.3	− 7	0	858.....	14.0	+ 21	− 2
813......	13.1	+ 1	+ 1	859.....	13.7	+ 12	+ 2
814......	10.8	− 1	− 8	860.....	10.6	− 2	+ 8
815......	10.6	− 5	+ 4	861.....	12.8	+ 9	+ 12
816......	11.7	+ 10	+ 8	862.....	13.6	+ 2	+ 3
817......	14.1	− 19	+ 8	863.....	12.0	− 9	− 2
818......	13.3	+ 1	+ 34	864.....	13.7	+ 10	− 8
819......	12.4	+ 12	− 22	865.....	13.6	+ 4	+ 2
820......	12.2	+ 7	+ 8	866.....	13.2	+ 16	+ 6
821......	13.6	+ 1	+ 8	867.....	13.1	+ 13	+ 8
822......	10.0	− 2	+ 7	868.....	14.7	+ 6	− 4
823......	12.4	+ 11	+ 4	869.....	11.2	+ 1	+ 3
824......	12.2	0	− 6	870.....	9.9	+ 5	0
825......	11.8	+ 2	+ 10	871.....	13.6	+ 10	0
826......	13.2	+ 7	− 3	872.....	13.4	+ 9	− 7

TABLE VII—*Continued*

No.	Pg. Mag.	μ_α	μ_δ	No.	Pg. Mag.	μ_α	μ_δ
873......	13.1	+0″.004	+0″.013	926.....	11.9	−0″.003	+0″.008
874......	10.7	− 4	+ 9	927.....	12.8	0	+ 7
875......	12.6	+ 23	− 4	928.....	11.2	+ 2	+ 1
876......	12.6	+ 20	+ 11	929.....	10.8	− 5	+ 4
877......	13.6	+ 5	+ 8	930.....	14.1	+ 4	− 12
878......	11.4	+ 10	+ 9	931.....	11.7	− 1	+ 1
879......	13.6	+ 5	+ 7	932.....	14.1	+ 3	− 23
880......	11.9	+ 8	+ 18	933.....	12.1	− 5	− 29
881......	13.3	+ 7	+ 8	934.....	13.9	− 4	− 14
882......	13.9	+ 8	+ 2	935.....	11.9	+ 2	− 4
883......	11.6	+ 7	+ 6	936.....	14.3	+ 8	− 22
884......	12.9	0	− 11	937.....	13.1	+ 5	− 15
885......	13.5	+ 17	− 7	938.....	14.0	+ 12	+ 8
886......	12.2	+ 9	− 8	939.....	14.5	+ 21	− 13
887......	12.6	+ 12	− 1	941.....	12.6	+ 4	− 3
889......	12.1	0	− 1	942.....	12.0	0	− 5
890......	13.9	+ 15	− 4	943.....	12.7	− 1	− 4
891......	11.4	+ 4	− 22	944.....	12.3	+ 120	− 42
892......	13.3	+ 10	− 11	945.....	13.5	+ 6	− 7
893......	14.1	+ 1	− 1	946.....	11.9	+ 3	− 5
894......	13.2	+ 6	+ 4	947.....	13.6	− 1	− 5
895......	13.7	+ 14	+ 1	948.....	13.6	+ 5	− 18
896......	12.7	+ 9	− 17	949.....	12.1	+ 6	− 4
897......	12.1	+ 5	− 4	950.....	11.4	+ 2	− 7
898......	13.3	+ 8	− 10	951.....	11.8	+ 4	− 9
899......	13.6	+ 7	+ 18	952.....	14.7	− 6	− 20
901......	13.4	− 8	− 6	953.....	13.2	0	− 8
902......	13.4	− 8	− 2	954.....	12.7	− 2	− 9
903......	13.8	0	− 1	955.....	10.0	− 5	− 7
904......	14.1	− 17	− 6	956.....	13.9	+ 18	+ 7
905......	12.0	+ 14	+ 10	957.....	12.9	+ 3	− 10
907......	12.2	+ 1	+ 32	958.....	12.5	+ 3	− 14
908......	12.8	+ 3	+ 19	959.....	8.7	− 6	− 8
909......	9.4	+ 37	− 41	960.....	11.2	+ 2	− 1
910......	11.7	+ 7	+ 13	961.....	13.2	+ 4	− 7
914......	12.8	0	+ 12	962.....	11.3	+ 3	− 4
915......	13.3	+ 2	+ 1	963...	12.8	− 3	− 9
916......	13.1	+ 8	+ 9	964.....	10.6	− 5	− 5
918......	10.7	+ 1	+ 10	965.....	13.8	− 4	− 9
919......	12.9	− 2	+ 2	966.....	11.4	− 9	0
920......	10.1	+ 1	+ 27	967.....	11.3	0	− 2
922......	13.5	+ 9	+ 16	969.....	11.3	− 3	+ 1
923......	12.1	+ 4	+ 8	970.....	11.8	0	− 3
924......	11.6	0	+ 10	972.....	9.8	− 6	+ 12
925......	13.1	+ 30	+ 8	974.....	12.8	− 5	− 8

TABLE VII—*Continued*

No.	Pg. Mag.	μ_α	μ_δ	No.	Pg. Mag.	μ_α	μ_δ
975.....	13.8	+0″.009	−0″.004	1026....	12.6	+0″.037	−0″.001
976.....	13.8	+ 15	+ 4	1027....	11.1	− 10	− 6
977.....	13.7	− 3	+ 10	1028....	11.9	− 4	− 15
978.....	13.1	+ 4	+ 3	1029....	9.1	− 11	− 1
979.....	12.9	− 6	+ 4	1031....	12.6	− 2	− 12
980.....	12.8	+ 4	+ 4	1032....	11.2	+ 14	− 40
981.....	14.6	− 9	− 8	1033....	11.4	− 2	− 23
982.....	10.0	+ 4	0	1035....	13.1	− 5	− 15
983.....	13.1	+ 4	+ 5	1036....	12.9	+ 5	− 7
984.....	11.3	− 1	+ 1	1037....	10.9	+ 55	− 17
985.....	13.9	+ 10	0	1038....	7.8	− 6	+ 5
986.....	13.5	+ 5	+ 1	1040....	12.6	− 16	+ 20
987.....	13.8	+ 9	+ 1	1041....	12.7	+ 5	+ 10
988.....	12.9	− 12	+ 6	1042....	7.4	+ 62	+ 28
989.....	11.3	− 4	+ 8	1045....	14.7	+ 15	+ 3
990.....	10.8	− 4	− 8	1047....	10.6	+ 4	+ 3
991.....	11.6	− 9	0	1050....	12.9	− 1	− 3
992.....	8.8	0	− 1	1051....	12.4	− 1	+ 8
993.....	13.5	− 34	+ 25	1055....	12.0	+ 10	+ 16
994.....	11.4	+ 3	+ 9	1056....	13.6	+ 27	− 8
995.....	13.2	+ 5	0	1057....	7.3	− 8	+ 11
996.....	13.6	− 1	− 6	1058....	11.8	+ 4	+ 10
997.....	12.4	+ 4	0	1059....	12.9	+ 7	+ 9
999.....	13.2	+ 9	+ 8	1060....	11.7	+ 3	+ 3
1000.....	13.2	− 1	− 2	1061....	10.4	+ 5	+ 9
1001.....	13.4	+ 3	+ 2	1062....	13.8	+ 13	+ 7
1003.....	12.9	− 1	+ 7	1063....	13.3	+ 16	+ 3
1004.....	12.7	− 2	− 3	1064....	12.2	+ 29	− 23
1005.....	13.2	− 3	0	1065....	12.9	− 6	− 9
1006.....	10.3	− 5	+ 2	1066....	9.8	0	+ 3
1009.....	10.4	+ 1	+ 1	1067....	12.7	− 1	− 4
1010.....	12.3	0	+ 8	1068....	12.4	+ 2	− 7
1011.....	10.0	+ 5	+ 7	1069....	12.7	+ 35	+ 3
1013.....	13.4	− 11	− 7	1071....	13.6	+ 11	− 11
1014.....	9.6	+ 1	− 4	1072....	13.8	+ 14	− 3
1015.....	13.7	+ 4	− 3	1073....	12.5	− 1	− 3
1016.....	11.1	− 5	− 12	1074....	13.5	+ 6	− 1
1017.....	11.5	− 3	− 8	1075....	12.2	− 1	+ 3
1018.....	11.6	− 2	− 13	1076....	14.1	+ 13	+ 4
1019.....	13.1	− 5	− 5	1077....	12.5	0	− 5
1020.....	13.1	+ 11	0	1078....	11.8	+ 7	+ 4
1022.....	13.4	− 5	− 12	1078*...	....	+ 26	....
1023.....	11.9	− 3	− 5	1079....	9.1	0	+ 3
1024.....	9.4	+ 331	− 216	1080....	13.6	− 3	− 1
1025.....	12.8	− 5	− 5	1081....	13.2	− 5	− 1

TABLE VII—*Continued*

No.	Pg. Mag.	μ_α	μ_δ	No.	Pg. Mag.	μ_α	μ_δ
1082.....	10.8	+0″.002	+0″.003	1130....	11.7	−0″.015	−0″.010
1083.....	13.2	+ 6	− 2	1131....	13.9	− 1	− 1
1084.....	13.3	+ 25	+ 11	1132....	12.1	0	− 22
1085.....	11.9	0	+ 2	1133....	14.5	− 11	+ 1
1086.....	14.1	− 6	+ 3	1134....	9.3	− 25	− 3
1087.....	13.9	+ 2	− 11	1135....	12.5	− 8	+ 1
1088.....	14.4	+ 7	− 7	1136....	12.9	− 16	+ 5
1089.....	12.2	+ 10	+ 6	1137....	11.2	+ 30	+ 12
1090.....	14.4	+ 5	+ 6	1138....	12.2	+ 8	− 10
1091.....	14.0	0	+ 4	1140....	12.5	+ 7	+ 2
1092.....	13.8	+ 3	+ 1	1141....	12.7	+ 35	+ 5
1093.....	13.9	+ 2	− 6	1142....	13.1	+ 14	+ 2
1094.....	11.3	− 12	+ 7	1143....	12.9	+ 12	− 4
1095.....	13.3	+ 6	− 4	1144....	13.6	+ 24	− 5
1096.....	12.5	− 1	+ 10	1145....	14.6	+ 17	+ 7
1097.....	13.3	− 8	+ 6	1146....	12.7	+ 5	+ 1
1098.....	13.8	+ 9	+ 10	1148....	12.6	+ 2	+ 10
1099.....	13.3	− 9	+ 5	1150....	12.0	+ 9	− 5
1100.....	10.0	− 4	+ 12	1151....	13.5	+ 5	+ 4
1101.....	12.4	+ 4	− 1	1152....	11.8	+ 15	+ 4
1102.....	12.3	− 1	− 3	1153....	11.8	+ 8	+ 13
1103.....	13.7	+ 6	+ 9	1154....	8.5	+ 20	− 18
1104.....	14.0	+ 15	+ 2	1155....	11.1	− 20	− 39
1105.....	11.7	+ 1	+ 9	1156....	14.4	+ 4	− 17
1106.....	13.5	− 5	+ 9	1157....	12.8	− 10	− 27
1107.....	13.4	+ 19	− 4	1158....	13.8	− 4	− 16
1108.....	14.2	+ 4	− 14	1159....	12.3	− 8	− 22
1110.....	12.4	− 2	0	1160....	13.2	+ 7	− 11
1111.....	14.0	+ 7	+ 3	1162....	12.8	+ 2	− 3
1112.....	13.3	0	− 11	1163....	13.4	− 1	− 10
1113.....	13.8	+ 13	+ 5	1164....	9.5	− 7	+ 7
1114.....	12.6	+ 1	− 10	1165....	13.5	+ 2	+ 1
1115.....	8.6	+ 4	+ 5	1166....	13.1	+ 165	− 14
1117.....	12.7	− 3	− 16	1167....	12.5	− 10	− 9
1118.....	13.9	− 3	− 6	1168....	14.4	+ 5	− 4
1119.....	13.9	− 5	− 5	1169....	12.3	− 9	+ 5
1120.....	14.0	− 13	− 22	1170....	10.9	− 3	+ 11
1121.....	14.0	− 1	− 2	1171....	14.4	+ 11	+ 5
1122.....	14.5	− 5	0	1173....	14.1	+ 9	+ 2
1123.....	12.4	− 6	− 9	1174....	14.1	− 5	− 5
1124.....	13.5	− 2	− 7	1175....	13.9	+ 7	+ 17
1125.....	9.2	− 38	− 5	1176....	13.4	+ 10	+ 11
1126.....	14.5	− 12	− 18	1177....	12.7	+ 3	+ 6
1127.....	13.5	− 23	− 9	1178....	13.6	− 3	− 2
1129.....	13.5	− 94	− 63	1179....	12.6	+ 14	+ 6

TABLE VII—*Continued*

No.	Pg Mag.	μ_α	μ_δ	No.	Pg. Mag.	μ_α	μ_δ
1180.....	12.0	−0″.004	−0″.003	1232....	11.3	+0″.008	−0″.002
1181.....	13.2	+ 3	− 2	1233....	13.2	0	+ 7
1182.....	14.7	0	+ 8	1235....	13.9	+ 7	− 26
1183.....	12.3	+ 1	+ 9	1236....	11.9	+ 39	− 26
1184.....	10.3	− 3	+ 3	1237....	13.2	+ 13	+ 1
1185.....	13.8	0	0	1238....	13.2	+ 10	− 13
1186.....	14.0	+ 1	− 8	1239....	13.1	+ 8	− 4
1187.....	13.7	+ 5	+ 5	1240....	12.4	− 7	− 4
1188.....	14.5	+ 2	+ 4	1241....	13.1	+ 11	+ 1
1190.....	13.3	+ 3	− 2	1242....	14.5	+ 3	− 7
1191.....	10.8	+ 1	+ 10	1243....	6.8	+ 10	+ 11
1192.....	14.1	+ 6	+ 8	1244....	13.4	+ 2	− 10
1193.....	9.6	− 3	+ 8	1245....	13.2	+ 2	+ 2
1195.....	14.7	+ 19	+ 20	1246....	12.3	+ 6	− 7
1196.....	13.9	− 3	− 9	1247....	7.5	+ 3	+ 17
1197.....	13.9	+ 8	− 12	1248....	12.7	+ 9	+ 12
1198.....	13.8	+ 8	+ 12	1251....	12.6	+ 1	+ 8
1199.....	12.8	+ 4	− 8	1252....	14.3	+ 15	− 7
1200.....	13.2	+ 2	0	1253....	10.4	− 9	+ 8
1201.....	11.3	+ 2	+ 6	1254....	12.7	− 1	+ 4
1202.....	9.1	− 18	+ 7	1256....	13.1	− 10	+ 4
1203.....	12.1	− 8	+ 18	1257....	13.1	+ 11	+ 4
1205.....	14.0	+ 4	− 10	1258....	12.2	− 6	+ 1
1206.....	13.6	+ 14	+ 10	1259....	14.3	+ 45	− 34
1207.....	13.1	− 25	− 5	1260....	14.1	+ 6	− 8
1208.....	13.9	+ 5	− 1	1261....	12.4	− 3	+ 6
1209.....	14.3	+ 7	− 10	1262....	8.7	− 1	+ 4
1210.....	10.9	− 8	− 4	1263....	11.5	+ 7	− 3
1211.....	13.4	+ 1	− 3	1264....	7.8	− 7	− 4
1214.....	14.4	+ 5	+ 2	1265....	14.0	+ 5	− 8
1215.....	11.5	− 7	− 9	1266....	12.8	+ 2	− 1
1216.....	12.7	+ 1	− 14	1267....	14.2	+ 5	− 18
1217.....	11.6	+ 3	− 18	1268....	12.7	+ 10	− 19
1218.....	12.7	0	− 33	1269....	13.3	+ 2	− 16
1219.....	12.7	+ 23	+ 39	1270....	12.6	+ 10	− 20
1220.....	11.4	+ 12	+ 21	1271....	14.4	+ 7	− 8
1221.....	13.9	+ 22	+ 18	1272....	13.9	− 1	− 14
1222.....	12.7	+ 21	+ 15	1273....	14.3	+ 18	+ 4
1223.....	12.9	+ 1	− 14	1275....	10.2	+ 5	− 10
1224.....	11.6	+ 13	+ 10	1277....	14.0	+ 10	− 8
1225.....	11.9	+ 11	+ 13	1278....	12.1	+ 19	− 11
1226.....	13.4	+ 23	+ 9	1279....	12.3	+ 7	+ 1
1229.....	10.3	+ 4	+ 14	1280....	12.8	+ 15	+ 1
1230.....	12.5	+ 9	− 4	1281....	14.2	+ 24	− 24
1231.....	13.1	+ 5	+ 8	1282....	12.3	+ 4	− 10

TABLE VII—*Continued*

No.	Pg. Mag.	μ_α	μ_δ	No.	Pg. Mag.	μ_α	μ_δ
1284.....	11.4	+0″.001	−0″.017	1339....	13.9	+0″.006	−0″.005
1285.....	11.2	+ 3	− 16	1340....	14.3	+ 7	− 8
1286.....	13.5	− 2	− 3	1341....	14.5	+ 11	− 7
1288.....	13.5	+ 4	+ 3	1342....	14.2	+ 23	+ 8
1289.....	11.6	+ 23	+ 30	1343....	12.9	+ 13	− 17
1290.....	12.1	+ 22	+ 28	1344....	14.0	+ 48	− 9
1291.....	12.0	+ 21	+ 1	1346....	12.4	+ 23	+ 27
1292.....	9.4	+ 19	+ 19	1347....	12.1	− 4	+ 5
1294.....	12.2	+ 27	− 18	1348....	14.3	+ 3	+ 6
1295.....	9.7	+ 13	+ 8	1349....	13.9	+ 18	+ 1
1296.....	13.8	+ 10	− 11	1351....	13.2	+ 14	0
1297.....	13.5	+ 28	− 9	1353....	8.7	+ 17	+ 12
1298.....	11.4	+ 2	− 2	1354....	12.3	+ 11	− 3
1300.....	12.7	+ 5	− 22	1355....	12.6	+ 19	− 9
1301.....	10.2	− 6	− 23	1356....	14.7	+ 86	− 73
1302.....	13.1	− 1	− 23	1357....	9.9	+ 84	− 28
1303.....	11.4	− 6	− 29	1358....	11.3	+ 12	− 6
1304.....	13.7	+ 9	− 36	1359....	13.6	+ 1	− 6
1305.....	12.1	+ 14	− 27	1360....	12.9	+ 14	+ 2
1306.....	12.7	0	− 20	1361....	13.3	− 2	− 18
1307.....	13.9	+ 14	− 23	1362....	12.1	+ 10	− 10
1308.....	11.5	+ 28	− 38	1363....	14.1	+ 6	− 40
1309.....	13.9	− 4	− 17	1364....	14.6	+ 14	− 23
1310.....	13.7	+ 8	− 12	1366....	13.3	+ 22	− 3
1312.....	13.5	+ 49	− 43	1367....	12.5	+ 12	− 1
1313.....	13.6	+ 10	− 8	1368....	13.4	− 12	− 4
1314.....	12.4	+ 7	− 6	1369....	12.3	− 6	+ 3
1315.....	13.4	− 10	+ 9	1370....	10.8	− 74	− 64
1317.....	11.3	+ 24	+ 9	1371....	13.9	− 6	0
1318.....	14.5	+ 8	− 20	1372....	10.8	+ 22	+ 9
1319.....	11.4	0	− 1	1373....	13.1	+ 20	+ 6
1320.....	11.4	+ 4	+ 12	1374....	12.9	+ 5	+ 11
1321.....	14.4	+ 9	+ 10	1375....	13.1	− 1	+ 9
1322.....	13.1	− 3	+ 8	1376....	12.8	0	+ 8
1323.....	12.9	− 7	+ 4	1377....	12.9	0	− 3
1324.....	13.2	− 2	+ 4	1378....	13.4	− 1	+ 10
1325.....	11.6	0	+ 6	1379....	12.2	− 1	+ 5
1327.....	13.2	+ 12	+ 12	1380....	12.3	+ 45	− 2
1329.....	11.5	− 5	0	1381....	13.7	+ 6	− 1
1330.....	12.0	− 4	− 5	1382....	12.8	+ 53	− 32
1331.....	14.1	+ 2	+ 2	1383....	11.7	− 1	+ 7
1335.....	13.1	− 2	− 14	1384....	13.5	+ 30	+ 4
1336.....	11.3	+ 2	− 4	1385....	12.6	+ 8	+ 6
1337.....	14.2	+ 14	− 10	1386....	12.6	+ 23	− 5
1338.....	12.9	+ 4	− 3	1387....	13.4	− 12	− 26

TABLE VII—*Continued*

No.	Pg. Mag.	μ_α	μ_δ	No.	Pg. Mag.	μ_α	μ_δ
1391.....	12.4	+0″.023	−0″.002	1440....	12.6	+0″.006	−0″.015
1392.....	14.3	+ 36	− 9	1441....	11.3	+ 1	− 11
1393.....	12.2	+ 19	− 5	1442....	11.6	+ 6	− 8
1394.....	13.6	+ 16	+ 3	1443....	12.7	+ 3	− 3
1396.....	10.8	+ 3	+ 3	1444....	12.8	+ 17	+ 2
1398.....	13.2	+ 6	− 20	1445....	12.7	+ 18	− 5
1399.....	13.9	+ 12	− 5	1447....	12.6	+ 20	− 4
1400.....	12.0	0	+ 3	1448....	14.3	+ 28	− 3
1401.....	10.5	− 4	− 7	1449....	11.3	+ 2	− 6
1402.....	11.5	− 11	+ 1	1450....	11.9	+ 3	− 4
1403.....	14.3	− 1	− 36	1451....	13.4	− 3	+ 8
1404.....	13.7	− 1	− 15	1452....	13.2	+ 6	+ 13
1405.....	11.8	− 2	− 18	1454....	14.2	+ 7	− 4
1406.....	12.2	+ 76	− 21	1455....	14.5	+ 2	+ 11
1407.....	11.4	− 1	− 1	1456....	11.8	+ 3	+ 16
1408.....	10.1	− 14	− 6	1457....	12.4	+ 25	+ 17
1409.....	12.1	− 5	+ 4	1458....	12.7	+ 24	+ 5
1410.....	13.3	+ 8	− 1	1459....	14.6	− 16	+ 16
1411.....	12.7	− 1	+ 12	1460....	14.7	+ 22	− 30
1412.....	13.3	− 5	+ 14	1461....	12.5	+ 9	+ 6
1413.....	9.5	− 8	+ 7	1462....	13.4	+ 16	+ 28
1414.....	13.3	+ 10	+ 6	1463....	12.6	+ 16	+ 14
1415.....	11.1	− 3	+ 14	1464....	9.0	+ 1	+ 7
1416.....	10.5	− 1	+ 7	1465....	14.0	+ 20	+ 19
1417.....	11.3	+ 3	+ 3	1466....	13.3	+ 21	0
1418.....	13.6	+ 6	− 11	1468....	12.1	− 7	− 24
1419.....	13.6	+ 4	+ 10	1469....	13.1	− 10	− 8
1421.....	10.6	+ 25	− 18	1470....	14.6	− 47	− 18
1422.....	11.8	+ 11	− 1	1471....	12.3	− 15	− 17
1423.....	12.9	+ 28	+ 8	1472....	11.8	− 20	− 30
1424.....	13.7	+ 5	+ 5	1474....	12.0	+ 15	− 4
1425.....	11.9	+ 11	+ 6	1475....	12.0	− 10	− 28
1426.....	13.5	+ 5	− 13	1476....	10.7	− 5	− 16
1427.....	12.7	+ 18	+ 4	1477....	9.6	− 16	− 10
1428.....	12.0	+ 3	0	1479....	12.2	0	− 20
1429.....	11.1	+ 9	− 8	1480....	11.1	+ 17	− 16
1431.....	9.0	+ 58	− 61	1481....	13.6	− 3	+ 1
1432.....	12.0	+ 15	− 9	1482....	13.2	+ 1	− 6
1433.....	10.3	− 26	− 25	1483....	13.5	+ 22	+ 10
1434.....	10.8	− 21	− 20	1484....	11.1	− 4	+ 7
1435.....	11.6	− 28	− 23	1485....	12.6	+ 12	+ 21
1436.....	11.6	− 17	− 27	1486....	14.7	+ 9	+ 4
1437.....	10.1	− 14	− 24	1487....	12.9	+ 14	+ 11
1438.....	12.1	− 1	− 8	1488....	12.7	+ 30	+ 22
1439.....	11.7	+ 28	− 28	1489....	10.3	+ 11	+ 14

TABLE VII—*Continued*

No.	Pg. Mag.	μ_α	μ_δ	No.	Pg. Mag.	μ_α	μ_δ
1490.....	13.1	+0".028	+0".025	1527....	11.9	−0".002	−0".009
1491.....	13.7	+ 9	+ 28	1528....	12.8	− 5	− 3
1492.....	9.6	+ 8	+ 8	1529....	10.5	− 14	− 1
1493.....	14.2	+ 39	+ 13	1530....	11.9	+ 147	− 100
1495.....	10.3	+ 2	+ 13	1531....	13.9	− 8	+ 4
1496.....	9.5	− 15	− 21	1532....	....	− 3	....
1497.....	11.7	− 6	− 16	1533....	10.9	− 15	− 7
1498.....	12.8	− 2	− 9	1534....	12.8	− 6	− 4
1499.....	13.2	+ 14	− 23	1535....	8.7	+ 1	+ 3
1500.....	13.4	+ 23	− 13	1536....	12.2	+ 2	− 1
1501.....	13.4	− 28	− 17	1537....	9.0	− 4	+ 7
1502.....	12.4	+ 26	+ 15	1538....	13.1	+ 11	+ 7
1503.....	10.4	− 20	− 11	1539....	13.9	+ 17	− 9
1504.....	13.3	+ 9	− 10	1540....	14.0	+ 29	− 5
1506.....	13.8	+ 28	0	1541....	13.5	+ 18	+ 10
1507.....	13.8	+ 56	− 14	1542....	10.9	+ 75	+ 18
1508.....	9.5	+ 138	+ 16	1543....	13.7	+ 21	+ 5
1509.....	7.9	+ 264	− 203	1544....	12.3	+ 19	+ 22
1510.....	12.8	+ 4	+ 7	1545....	11.2	+ 12	+ 21
1511.....	13.6	+ 4	− 5	1546....	10.5	+ 8	+ 9
1512.....	13.4	+ 24	+ 9	1547....	14.0	+ 33	+ 16
1513.....	13.5	+ 15	+ 4	1548....	11.9	+ 26	+ 19
1514.....	12.6	+ 25	+ 20	1549....	13.8	+ 15	+ 12
1515.....	11.3	+ 21	+ 19	1551....	12.9	+ 17	+ 7
1516.....	10.7	+ 20	+ 24	1552....	11.9	+ 30	+ 22
1517.....	....	+ 23	....	1553....	11.6	+ 15	+ 24
1518.....	11.1	+ 10	+ 18	1554....	13.4	+ 43	+ 5
1519.....	12.5	+ 35	+ 23	1556....	13.2	+ 19	+ 9
1520.....	13.3	+ 60	+ 38	1557....	10.9	+ 5	+ 10
1521.....	11.3	+ 15	+ 21	1558....	9.9	− 3	+ 14
1522.....	12.9	+ 26	+ 10	1560....	11.6	+ 34	− 9
1523.....	13.2	+ 32	+ 18	1561....	10.2	− 4	+ 14
1524.....	13.5	+ 16	− 5	1563....	6.7	− 12	− 18
1525.....	11.9	+ 8	− 21	....	....	....	....
1526.....	10.1	− 15	− 9	....	....	....	....

Table VII gives the absolute motions of the 1418 stars of *Utrecht*, 5. For convenience we have kept the original numbering, although several numbers are missing which originally had been assigned to stars visible only on the first plate measured. The second column gives the photographic magnitude; the last two columns give the final values of μ_α and μ_δ.

V. THE DISTRIBUTION OF THE PROPER MOTIONS OF THE NON-MEMBERS OF THE GROUP

Even now we cannot decide with certainty whether any individual star belongs to the cluster or not. The best evidence that a star is a member of the group is a small proper motion and a radial velocity of about −40 km/sec. The velocities, however, are known only for the brighter stars. The condensation of the stars near the two clusters is so large that many of them must belong to the group.

If, however, we exclude stars which on account of their radial velocities are probably members of the cluster, and also all stars within an area of 1° in right ascension and 35′ in declination including the two centers, we have 768 left, of which probably only a small percentage are members of the group. The numbers in *Utrecht*, 5, for these 768 stars are given in Table VIII.

TABLE VIII

1 to 4
6 to 39
40 to 130
164 to 192
248 to 269
322 to 343
432 to 469
536 to 554
584
586 to 612
637 to 680
734 to 772
882 to 920
1009 to 1059
1102 to 1114
1117 to 1152
1195 to 1242
1244 to 1246
1248 to 1261
1263
1265 to 1463
1465 to 1536
1538 to 1561

For these we first derive the mean μ_α and μ_δ for different intervals of magnitude. The results are collected in Table IX.

TABLE IX

Pg. Mag.	μ_α	μ_δ	n	μ parall.	μ_τ
<− 7.9	+0″.078	−0″.040	4	+0″.084	+0″.021
8.0− 8.9	+0.007	+0.001	4	+0.004	+0.005
9.0− 9.9	+0.024	−0.012	28	+0.026	+0.007
10.0−10.9	+0.004	−0.003	73	+0.005	0.000
11.0−11.9	+0.007	−0.004	135	+0.008	+0.002
12.0−12.9	+0.004	−0.002	234	+0.004	+0.001
13.0−13.9	+0.005	−0.001	221	+0.004	+0.003
14.0−14.9	+0.011	−0.006	69	+0.012	+0.003

From the mean values of μ_α and μ_δ for the different magnitudes we can derive the amount of the motion in the direction of the antapex and that at right angles to it (μ_τ).

In *Utrecht*, 5, page 46, the statement was made that the stars seemed to have a preference of motion in the direction of the apex. By improving the data through additional observations we have been able to get rid of this abnormal result. Table IX gives in the last two columns the values of the parallactic motion and of μ_τ. It is clear that the mean motions are practically all in the direction of the sun's antapex.

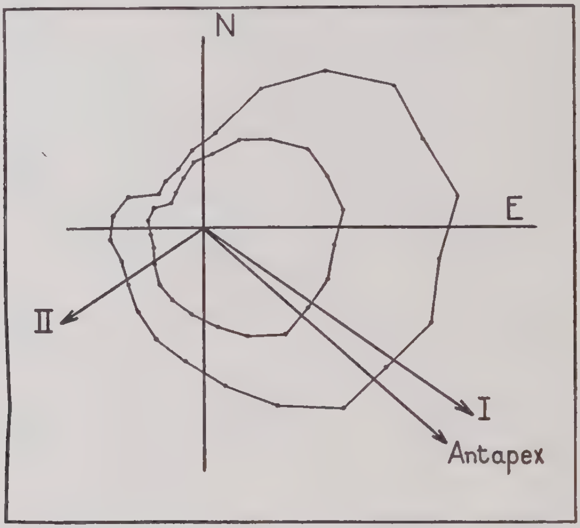

FIG. 2.—Distribution of proper motions of stars near *h* and χ Persei. Distances of points on the outer curve from the origin indicate the total motion in different directions; corresponding distances for the inner curve represent the numbers of stars having proper motions in these directions.

The distribution of the proper motions is shown in Figure 2. To construct this the number of stars and the total motion were determined for sectors of 15°; then, to smooth the curves, overlapping means for three successive sectors were formed. In order to avoid the influence of the large proper motions, stars with $\mu \geqq 0\overset{''}{.}050$ were excluded. The inner curve shows the numbers of stars having motions in each sector, and the outer curve the total motion in the different directions.

Finally we may derive for these 768 stars, which most likely do not belong to the clusters, a table showing the distribution of the numbers of stars between certain limits of magnitude and proper motion. The results are given in Table X.

TABLE X

MAGNITUDE AND PROPER MOTION—NUMBERS OF STARS

μ	6.9–7.9	8.0–8.9	9.0–9.9	10.0–10.9	11.0–11.9	12.0–12.9	13.0–13.9	14.0–14.9	Total
0″.000–0″.009	1	2	3	26	38	67	60	15	212
0.010–0.019	1	1	11	28	47	95	94	31	308
0.020–0.029	0	1	5	7	28	42	46	11	140
0.030–0.039	0	0	2	8	15	19	13	5	62
0.040–0.049	0	0	0	1	5	9	4	3	22
0.050–0.059	0	0	3	1	0	0	1	2	7
0.060–0.069	1	0	0	0	0	1	1	0	3
0.070–0.079	0	0	0	1	0	1	1	0	3
0.080–0.089	0	0	2	0	0	1	0	1	4
0.090–0.099	0	0	0	1	0	0	0	0	1
0.100–0.149	0	0	1	0	0	0	1	1	3
0.150–0.199	0	0	0	0	1	0	0	0	1
0.200–0.249	0	0	0	0	0	0	0	0	0
0.250–0.299	0	0	0	0	0	0	0	0	0
0.300–0.349	1	0	0	0	0	0	0	0	1
0.350–0.399	0	0	1	0	0	0	0	0	1
Total	4	4	28	73	134	235	221	69	768

In *Utrecht*, 5, attention was called to the fact that in the corresponding table of distribution (p. 43), the largest number of proper motions was found, not between the limits 0″.000 and 0″.009, but between 0″.010 and 0″.019. The effect is less evident in the present table. This result is not unexpected, however, since it is probably due to the influence of the accidental errors in the proper motions, as was shown in *Mount Wilson Contribution*, No. 168, page 12.

MOUNT WILSON OBSERVATORY
November 15, 1920

Contributions from the Mount Wilson Observatory, No. 206
Reprinted from the *Astrophysical Journal*, Vol. LIII, pp. 375-79, 1921

OBSERVATIONS OF THE NEBULAR LINES IN THE SPECTRUM OF THE LONG-PERIOD VARIABLE STAR R AQUARII

By PAUL W. MERRILL

ABSTRACT

Discovery of nebular lines in the spectrum of R Aquarii.—This star has a typical Md spectrum similar to that of about 85 per cent of all long-period variable stars. In October, 1919, the bright nebular lines λλ 4363, 4658, 4959 N_2, and 5007 N_1, and the helium line λ 4471, which also occurs in nebulae, were found to be superposed on the Md spectrum. Later observations have shown that these lines do not share in the changes of intensity exhibited by the light of the variable star, although they appear to emanate from the same object.

Intensities and *displacements* of the Md and nebular lines are given in Table I.

R Aquarii (R.A. 1900 = $23^h38^m.6$, Dec. 1900 = $-15°50'$) has been known as a variable star since 1811. The photometric data, according to the Harvard College Observatory, are as follows: maximum magnitude 6.2; minimum magnitude 11.0; period 385.5 days. The same authority states that R Aquarii has the broadest minimum of 75 long-period variables whose light curves were carefully studied. Its mean light-curve has a broad, flat minimum and a very rapid rise to maximum.

The Harvard objective-prism photographs have shown the spectrum to be of the same class as that of 85 per cent of the long-period variables, namely, Md. Spectra of this class are marked by bright hydrogen lines superposed upon a continuous spectrum which is notched by numerous absorption bands of titanium oxide. Variations in the relative intensities of the bright Hγ and Hδ lines are common in Md spectra, and have been found in the spectrum of R Aquarii.

So far as known, the first slit spectrogram of this object was secured on October 16, 1919, with a single-prism spectrograph attached to the 100-inch Hooker telescope. This showed, in addition to the usual Md spectrum, several bright lines characteristic of gaseous nebulae. Three such lines were conspicuous, namely, λ 5007 N_1, λ 4959 N_2, and λ 4363, while λ 4658 and λ 4471 He were faintly visible.

On this date the star was of magnitude 8.3; during the next fifteen days it brightened rapidly, and then remained nearly constant at magnitude 6.9 for about two months, after which a rapid decline took place.[1] This maximum appears to have been unusually broad and flat. The spectrographic observations following October 16, 1919, showed that the nebular lines did not share in the increase in intensity exhibited by the bright lines of the Md spectrum. No well-exposed plate was secured in the short interval *after* maximum before the star was lost in the evening sky, but such plates as were obtained indicated that the nebular lines had begun to regain their previous intensities with respect to the Md spectrum. By the time observations could be resumed in the morning sky in June, 1920, the star had faded to the tenth magnitude and was not much above its minimum brightness. Nevertheless, the chief nebular lines could be photographed with about the same exposure times as at maximum, although the continuous spectrum was practically absent, even with considerably longer exposures. Plate III reproduces four spectrograms.

The approximate relative intensities of the emission lines as photographed with a single dense flint prism on Seed 30 plates are given in Table I.

The Md spectrum of R Aquarii near maximum light contains the bright hydrogen lines Hβ, Hγ, and Hδ, which are superposed upon corresponding bright lines associated with the nebular spectrum. This is made clear by a study of the manner in which the intensities and displacements of these lines vary during the light cycle. At maximum the Hγ and Hδ lines of the Md spectrum are many times as strong as the corresponding nebular Hγ and Hδ lines, but at minimum they appear to be of negligible strength compared with these nebular lines. The relative intensities of the hydrogen lines in the Md spectrum of R Aquarii at maximum and the disappearance of these lines at minimum are not at all unusual for this type of spectrum. The bright magnesium line

---

[1] Mr. Leon Campbell, of Harvard College Observatory, has kindly supplied the photometric data.

PLATE III

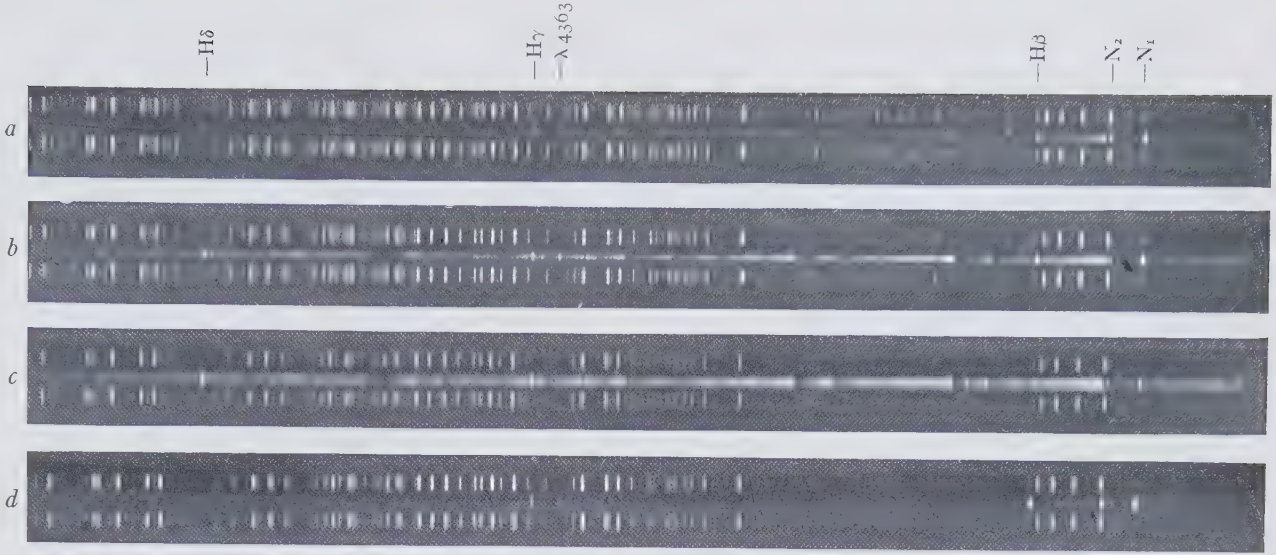

SPECTROGRAMS OF THE LONG-PERIOD VARIABLE STAR R AQUARII, SHOWING LINES CHARACTERISTIC OF GASEOUS NEBULAE

Secured with a one-prism spectrograph of 18-inch camera-focus attached to the 100-inch Hooker telescope.

(*a*) October 16, 1919; 43 days before maximum; magnitude 8.3.

(*b*) October 19, 1919; 40 days before maximum; magnitude 8.2. Strömberg, observer.

(*c*) November 1, 1919; 27 days before maximum; magnitude 7.0. Adams, observer.

(*d*) September 4, 1920; 281 days after maximum, 47 days after minimum, and 109 days before the next maximum. Magnitude 10.2.

λ 4571, which was observed in the spectrum of R Aquarii at minimum, is characteristic of Md stars at this phase.[1]

The relative intensities of the lines in the nebular spectrum do not appear to be precisely matched in any nebula observed by Wright[2] although there are several objects in his list that are similar in some particulars. The decrease in intensity in the Balmer series of hydrogen in passing from Hγ to Hδ is rapid as compared with the nebulae. Other noteworthy features are the strength of λ 4363, the presence of λ 4658, and the absence (or relative weakness) of λ 4686. An additional nebular line, λ 3869, was observed in the spectrum of R Aquarii by Moore[3] at the Lick Observatory on November 3, 1919. Light of this wave-length is strongly absorbed by the dense flint glass of the Mount Wilson spectrographs, but faint traces of the line appear to be present on spectrograms taken here on October 17 and December 14, 1919, and September 2, 1920. Wright has made some very interesting comments[4] on the absence of the companion line λ 3967, and on some other features of this spectrum.

TABLE I

INTENSITIES AND DISPLACEMENTS OF LINES IN THE SPECTRUM OF R AQUARII

WAVE-LENGTH I A	IDENTIFICATION	INTENSITIES		DISPLACEMENTS (km/sec.)	
		Nebular	Md (max.)	Nebular	Md
4101.74	Hδ	1	60	(− 6)	−32
4340.47	Hγ	5	30	−12	−33
4363.21*	Nebular	4	....	−25	....
4471.48	He	1	....	(−10)	....
4571.11	Mg	....	....	....	(−34)
4658.2*	Nebular	1	....	(−15)	....
4861.33	Hβ	10	5	−10	....
4958.91†	Nebular (N_2)	11	....	− 7	....
5006.84†	Nebular (N_1)	20	....	− 7	....
Absorption lines	....	....	....	....	−19

* Wright, *Publications of the Lick Observatory*, **13**, 183, 1918.

† Campbell and Moore, *Lick Observatory Bulletins*, **9**, 9, 1916.

---

[1] *Mt. Wilson Contr.*, No. 200; *Astrophysical Journal*, **52**, 185, 1921.

[2] *Publications of the Lick Observatory*, **13**, 183, 1918.

[3] *Publications Astronomical Society of the Pacific*, **31**, 309, 1919.

[4] *Ibid.*

In spite of the extraordinary nature of this combination spectrum, various observations appear to show that the nebular lines and the Md spectrum both emanate from the same star. Notes on these observations have been published[1] and need not be repeated here. Radial-velocity data bear on this question, but the measurements made at Mount Wilson and given in Table I do not as yet afford conclusive evidence concerning the nature of the connection between the two spectra. The values in the table, with the exception of those in parentheses, depend upon from seven to eighteen one-prism plates, and should not be much in error. Hβ and the chief nebular lines are in a part of the spectrum which is somewhat unfavorable for accurate measurement, but tests on N.G.C. 7027 and on bright-line stars show that no considerable systematic error is to be expected. All the lines associated with the nebular spectrum probably give the same displacement within errors of measurement, except λ 4363, which is shifted toward the violet by 0.2 A. It is improbable that Wright's value of the wave-length (4363.21 I A) is in error by so large an amount. The lines of the Md spectrum exhibit perfectly typical behavior, the same relative displacement of about 14 km between bright and dark lines having been found in *o* Ceti and in many other Md stars.

The principal facts concerning the line displacements in the spectrum of R Aquarii may be summarized as follows:

Md bright lines	−33 km/sec.
λ 4363, nebular	−25
Md absorption lines	−19
Nebular lines, except λ 4363	−10

The displacements are expressed in kilometers per second merely for convenience. The cause of the differences is not obvious; they may or may not be due to relative motion. One does not readily believe that the object is a long-period binary with an Md star for one component and a planetary nebula for the other.

The question as to whether in Md stars in general the bright lines, or the dark lines, or neither, yield the correct radial velocity of the star is an important one. It is hoped that a statistical investigation, observations for which are now being secured, will indicate the solution. Perhaps the behavior of the nebular lines in R Aquarii will throw a side light on this puzzling phenomenon.

---

[1] Wright, *Publications Astronomical Society of the Pacific*, **31**, 309, 1919; Merrill, *ibid.*, **31**, 305, 1919, and **32**, 247, 1920.

It would be of great interest to know whether the nebular lines have been present in the spectrum of R Aquarii for many years past, or whether they are the results of some recent outburst. The Harvard record, consisting of objective-prism spectrograms of small dispersion, dates from 1893. The fact that the nebular lines are not observable on the Harvard plates, even on those made at minimum light when the continuous spectrum would be very weak, tends to show that they have not been so strong at all times as they have been recently; but the evidence is perhaps not quite conclusive.

At present we have so little knowledge of the chemical and physical interpretation of the nebular lines that the meaning of their presence in R Aquarii cannot be stated. Since the Md spectrum probably arises under low-temperature conditions, the possibility of the production of the chief nebular lines N_1 and N_2 and of λ 4363 without intense conditions of excitation is suggested. It may be of significance in this connection that λ 4686, which in the laboratory requires high excitation for its production, has not been observed in R Aquarii. Laboratory experiments on long columns of gases under low excitation might not be amiss.

Mount Wilson Observatory
March 1921

Contributions from the Mount Wilson Observatory, No. 207
Reprinted from the *Astrophysical Journal*, Vol. LIV, pp. 76–77, 1921

IDENTIFICATION OF AIR LINES IN SPARK SPECTRA FROM λ 5927 TO λ 8683

By PAUL W. MERRILL, F. L. HOPPER, AND CLYDE R. KEITH

ABSTRACT

Spectrum of condensed spark in air and in oxygen, λ 5927 to λ 8683.—By operating the spark alternately in oxygen and in air, the lines due to oxygen have been identified. The remaining air lines, except a few *argon* lines, are ascribed to *nitrogen*. The work confirms numerous identifications made by other observers using vacuum tubes, and adds some identifications not previously available.

Experiments in continuation of those previously performed by one of the authors[1] have been carried out to determine the chemical identifications of the air lines from λ 5927 to λ 8683 in spark spectra.

The spark chamber, consisting of a glass bulb, was connected with an air pump and an oxygen apparatus in such a way that it could be filled either with air or with oxygen. The oxygen was generated by heating potassium permanganate and was purified by passage through caustic potash, calcium chloride, and phosphorus pentoxide. The photographic exposures were so arranged that the spectrum of the spark in air appeared on the negative close beside that of the same spark in oxygen, thus facilitating a comparison of the relative intensities of the lines. The pressure in the spark chamber was equal to one atmosphere in all cases. Several sets of comparisons were made with copper electrodes, and one with carbon (Acheson graphite) electrodes. All gave accordant indications of the identification of the air lines.

The second and fifth columns in Table I give our observations of the changes in relative intensities of the lines produced by the spark in oxygen as compared with the spark in air, *w* and *s* indicating weakened and strengthened, respectively. Of lines for which other identifications are available, those due to argon and nitrogen are weakened, while those due to oxygen are strengthened. Among the remaining lines, those weakened are believed to be due to nitrogen, and those strengthened to oxygen.

---

[1] *Contributions from the Mount Wilson Observatory*, No. 183; *Astrophysical Journal*, **51**, 211, 1920.

One line, λ 6370.92, should be removed from the previous list,[1] as it is probably due to silicon, while a nitrogen line at about 6341.5 A should be added, as it is observable in air. It undoubtedly corresponds to a line observed at 6340.84 A by Porlezza in a nitrogen tube.

TABLE I

RELATIVE INTENSITIES OF SPARK LINES IN AIR AND IN OXYGEN

λ in Air, I A	Oxygen	Vacuum Tubes	λ in Air, I A	Oxygen	Vacuum Tubes
5927.83.....	*w*	N*	7424.04.....	*w*	....
5931.78.....	*w*	N*	7442.70.....	*w*	....
5941.54.....	*w*	N*	7468.72.....	*w*	....
5952.33.....	*w*	N*	....	*s*	O 7476.58‡
6158.	*s*	O†	....	*s*	⎧O 7479.23‡
6171.0	*w*	....	....		⎩O 7481.27‡
6284.22.....	*w*	N*	7635.70.....	*w*	A
(6341.5).....	*w*	N 6340.84*	7772.07.....	*s*	O
6358.13.....	*w*	N*	7774.33.....	*s*	O
(6370.92)....	....	See note	7775.60.....	*s*	O
6379.52.....	*w*	N*	7947.83.....	*s*	O 7947.58‡
6456.	*s*	O†	7951.10.....	*s*	O 7950.84‡
6482.054....	*w*	N*	7952.3	*s*	O 7952.22‡
6610.39.....	*w*	N*	8185.26.....	*w*	....
6640.7	*s*	....	8188.42.....	*w*	....
6654.78.....	*s*	....	8200.72.....	*w*	....
6721.25.....	*s*	....	8211.12.....	*w*?	....
6887.61.....	*w*	....	8216.72.....	*w*	....
6950.	*w*?	....	....	*s*	O 8221.84‡
6965.95.....	*w*	A	8223.48.....	*w*	....
(7007)	*s*	O 7002†	8230.20.....	*s*	O 8230.05‡
7067.6	*w*	A	....	*s*	O 8233.05‡
7157.36.....	*s*	O?†	8242.80.....	*w*	....
....	*s*	O 7254†	8446.84.....	*s*	O
7384.53.....	*w*	A	8630.02.....	*w*?	....
			8680.63.....	*w*	....
			8683.70.....	*w*?	....

* Porlezza, *Atti R. Accademia dei Lincei*, Serie 5, **20**, 584, 1911.

† Runge and Paschen, *Annalen der Physik*, **61**, 641, 1897; **27**, 562, 1908.

‡ Kiess, *Popular Astronomy*, **29**, 18, 1921.

NOTES

λ 6158 Very broad, probably double or triple; includes λ 6160.72.

6171.0 Broad, probably double or triple.

6370.92 Not an air line; probably Si.

7007 Very, very hazy.

MOUNT WILSON OBSERVATORY
February 1921

---

[1] *Loc. cit.*

Contributions from the Mount Wilson Observatory, No. 208
Reprinted from the *Astrophysical Journal*, Vol. LIII, pp. 380–391, 1921

ON SYSTEMATIC DISPLACEMENTS OF LINES IN SPECTRA OF VENUS

By CHARLES E. ST. JOHN and SETH B. NICHOLSON

Systematic displacements of the solar lines in spectra of Venus.—Under certain conditions of observation there are line displacements to the violet of a few thousandths of an angstrom when comparison is made with the position of the lines in the spectrum of integrated skylight. Other conditions remaining constant, the displacements are greater at low than at high altitudes.

Atmospheric refraction.—The correlation with the altitude at the time of observation points to refraction as the controlling factor rather than to a repulsive "earth-effect" acting on the solar vapors as suggested by Evershed. The altitude correlation is represented by $\Delta\lambda 10^{-3}=1.4-1.0 \cot h$. The residuals, after removing the effect depending upon altitude, correlate equally well with the semidiameter D of Venus, the phase angle i, or the angle VSE. The observations are satisfactorily represented by the relation $\Delta\lambda 10^{-3}=1.3-\frac{8.5 \cot h}{D}$ which is deduced from the assumption that the observed displacements are caused by unsymmetrical illumination of the slit due to the separation of the visual and photographic images by atmospheric refraction, and that the unequal illumination is a function of the diameter of the image and the width of the slit.

Superposed skylight.—Spectroscopic observations of Venus beginning at sunset or ending at sunrise are not measurably affected by superposed skylight.

I. INTRODUCTION

Evershed and Royds have proposed an interpretation of the differences between terrestrial and solar wave-lengths[1] based solely on radial velocity. They assume that the solar gases at all points on the sun are receding from the earth. This means, they say, an "earth-effect"—an actual repulsion of the solar gases by the earth, and not by other planets. Through such earth-induced movements of the solar vapors Evershed has attempted to explain displacements of the Fraunhofer lines at the center, over the disk, and at the limb of the sun, discarding interpretations involving pressure-effects, radial convection currents, anomalous dispersion, and the Einstein gravitational shift.[2] No explanation of an "earth-effect" is suggested and the arbitrary and extraordinary nature of

[1] *Kodaikanal Observatory Bulletin*, No. 39, 1916.

[2] *Observatory*, **43**, 153, 1920.

the assumption is recognized; yet Evershed is so convinced of its reality that he says,[1] "Whether we like it or not, it seems necessary to admit that the Earth *does* affect the Sun, causing a movement of the gases analogous to that taking place in a comet." This view he believes is confirmed by his observations upon the spectrum of Venus. The idea of an apparent "earth-effect" upon solar phenomena is not new. Sykora[2] in 1897 called attention to a predominance of eastern prominences, and in 1907 Mrs. Maunder's paper "An Apparent Influence of the Earth on the Numbers and Areas of Sun-Spots in the Cycle 1889–1901" was communicated to the Royal Astronomical Society.[3]

According to Evershed's assumption, the displacements observed in the light from the earth-facing hemisphere of the sun should differ from those observed in the light from any other hemisphere; for example, from the hemisphere facing Venus.

He finds that when the angle Venus-sun-earth is small the wave-lengths in the spectrum of Venus are slightly shorter than those in direct sunlight; that this difference increases as the angle *VSE* increases; that when the angle is 90° the shortening equals the difference, sun *minus* arc, the wave-lengths from Venus and in the terrestrial source then becoming equal; and that for larger angles the displacements relative to the arc are to the violet; that is, in the light from the earth-facing hemisphere of the sun the Fraunhofer lines are displaced toward longer wave-lengths, while in the light from the opposite hemisphere the displacements are toward the violet when compared with the terrestrial source.[4] In order to obtain independent observational data bearing upon these extraordinary results, we have carried out two series of observations, the first in 1919 with Venus east of the sun, and the second in 1919–1920 with Venus west of the sun.

II. INSTRUMENTS AND METHODS

The observations were made with the Snow telescope of 60-foot focus in connection with a Littrow grating-spectrograph, focus

---

[1] *Observatory*, **42**, 52, 1919.

[2] *Memorie della Società degli Spettroscopisti Italiani*, **26**, 161, 1897.

[3] *Monthly Notices*, **67**, 451, 1907.

[4] *Observatory*, **43**, 156, 1920.

18 feet. The horizontal beam from the 2-foot concave mirror is directed downward by a 45° flat upon the slit of the spectrograph installed in the constant-temperature pit recently added to the equipment of the Snow telescope. The diameter of the image of Venus varied from 1.3 to 3.3 mm. The slit was 0.05 mm wide, its position being, in general, approximately normal to the terminator. The grating was ruled by Anderson and kindly loaned by Professor R. W. Wood, of the Johns Hopkins Physical Laboratory. The ruled surface is 95 mm × 170 mm; it is very bright in the first order and, as used, gives a linear dispersion of 3 A per mm. The collimating lens has an aperture of 6 inches.

Exposures were made upon the iron arc simultaneously with exposures upon Venus, the sky, or the center of the sun. In 1919 the center of an enlarged image of the arc was projected upon the slit, the intensity being controlled by a rotating sector and ray filter. In the second series a ground glass was placed in front of the arc, and the integrated light was used. Any errors in the wave-lengths of the reference lines would affect the measurements of Venus and of the sky in the same way, leaving the relative wave-lengths dependable. The iron lines in Table I were used as standards of reference.

TABLE I

REFERENCE LINES—INTERNATIONAL SYSTEM

4375.934 A	4466.557 A	4592.658 A
4407.716	4494.570	4625.054
4427.314	4525.146	4647.440
4447.724	4547.854	4667.461

The wave-lengths of 30 lines were measured in the spectra of the center of the sun, of skylight, and of Venus. The spectrograms were measured red right and red left and reduced by identical methods. In all, 56 spectrograms of Venus were secured, 41 of the sky, and 9 of the sun. It early became evident that the center of the sun and the integrated skylight give the same wave-lengths, the contribution of the limb-displacements to the red being inappreciable in the integrated light. The sky *minus* center for the 30 lines is +0.0001 A. The lines measured are given in Table II.

These lines were selected irrespective of whether they are blends or not, as they were to be used for relative wave-lengths only.

The data for the individual plates are given in Tables III and IV. The time of observation has been taken as the mean of the beginning and the end of the exposure, except in a few cases where clouds interrupted. No attempt has been made to obtain the mean time of the effective exposure, which would be somewhat different from that used on account of the change in atmospheric absorption. The third column gives the difference between the measured wave-lengths in the spectrum of Venus and those of the same lines in the spectra of the sky, corrections for velocity having been applied in both cases. The difference between the heliocentric longitudes of Venus and the earth was used as the angle *VSE*. The quantity *h* is the true altitude of Venus. The phase angle of Venus is indicated by *i* and the semi-diameter by *D*.

TABLE II

Lines Measured in Spectra of Venus and the Sky

Rowland λ	Int.	Element	Limb-Center	Rowland λ	Int.	Element	Limb-Center
4376.107...	6	Fe	+0.005	4527.101...	3	Ca?	+0.007
4422.741...	3	Fe, Y	....	34.953...	4	Ti	+0.004
35.851...	4	Ca	+0.006	48.024...	3	Fe	+0.008
42.510...	6	Fe	+0.006	54.211...	8	Ba	+0.008
43.976...	5	Ti	+0.008	63.939...	4	Ti	+0.008
47.892...	6	Fe	+0.005	71.275...	5	Mg	+0.007
51.752...	3	Mn	....	84.018...	4	Fe—	+0.012
56.030...	5	Mn2,Ca3	....	4602.183...	3	Fe	....
68.663...	5	Ti—	+0.007	03.126...	6	Fe	....
76.214...	7	Fe4, Ag3	....	25.227...	5	Fe	....
82.376...	8	Fe5, Fe3	+0.004	26.358...	5	Cr	....
84.392...	4	Fe	....	29.521...	6	Ti-Co	....
85.846...	3	Fe	....	30.306...	4	Fe	....
94.738...	6	Fe	+0.010	51.461...	4	Cr	....
4508.455...	4	Fe?,—	+0.011	52.343...	5	Cr	....

The velocity of Venus relative to the earth was obtained from the hourly variation in the logarithm of the geocentric distance. The relative velocity of Venus and the sun was calculated in the same way from the variation in the logarithm of the radius vector of Venus. The velocity of the observer due to the diurnal rotation

PLATE IV

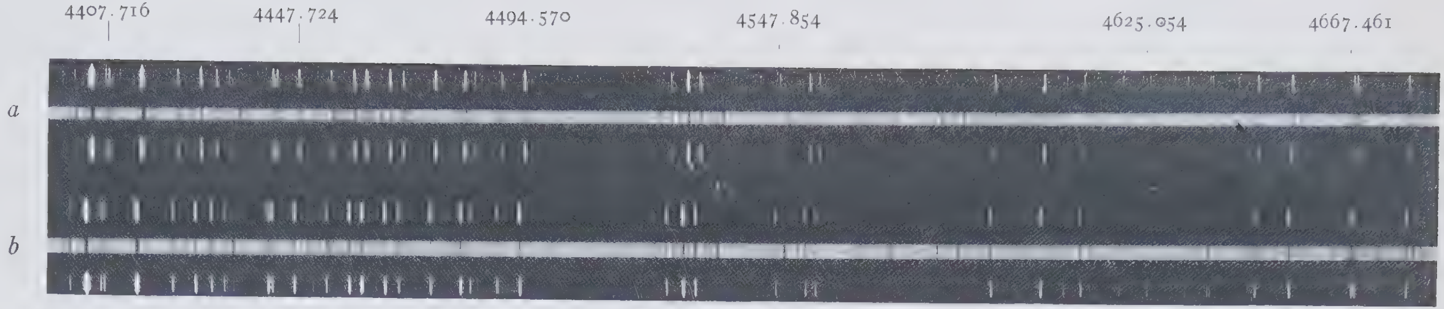

Photographs of the Spectra of Venus and the Sky

a. Venus, Plate V119, 1919, November 21, $17^h\ 17^m$—$18^h\ 21^m$ P.S.T.
b. Sky, Plate V115, 1919, November 20, 19 45 —20 45 P.S.T.
The comparison spectra are of the iron arc. Enlargement 2.

TABLE III

Observational Data, Venus East of the Sun

Date		Exposure P.S.T.	Δλ V−Sky	h	D	Angle VSE	i	Velocity in Line of Sight				Q	Sunset P.S.T.	Plate No.	Measurer
								V−E	Rot. E	V−S	Total				
			A					km	km	km	km				
1919 April	3..	6h43m–8h 3m	−0.007	14°	6″.3	103°	46°	− 9.48	+0.37	−0.16	− 9.27	4°	6h13m	V19	S
	7..	7 0 −8 15	−0.004	14	6.4	101	47	− 9.81	+0.36	−0.13	− 9.58	5	6 16	24	S
	8..	6 20 −7 20	−0.004	24	6.4	100	48	− 9.88	+0.35	−0.13	− 9.66	5	6 17	25	S
	20..	6 35 −8 5	−0.007	22	6.8	93	53	−10.80	+0.35	−0.05	−10.50	77	6 27	30	S, N
	21..	6 36 −8 6	+0.003	22	6.8	92	53	−10.88	+0.35	−0.05	−10.58	78	6 27	31	S, N
May	5..	6 48 −8 18	−0.005	24	7.3	82	59	−11.90	+0.34	+0.05	−11.51	264	6 38	38	N
	5..	8 30 −9 25	−0.006	8	7.3	82	59	−11.90	+0.35	+0.05	−11.50	264	6 38	39	N
	6..	6 38 −8 8	−0.002	27	7.4	81	60	−11.96	+0.33	+0.05	−11.58	84	6 39	40	S
	6..	8 16 −9 16	+0.002	11	7.4	81	60	−11.97	+0.35	+0.06	−11.56	84	6 39	41	S
	8..	6 48 −7 48	−0.002	28	7.5	80	60	−12.10	+0.33	+0.07	−11.70	265	6 40	49	S
	8..	7 51 −9 3	−0.004	15	7.5	80	60	−12.10	+0.35	+0.07	−11.68	265	6 40	50	S
	11..	7 3 −7 53	−0.004	27	7.6	79	62	−12.29	+0.33	+0.09	−11.87	87	6 43	61	N
	11..	7 58 −9 13	−0.004	13	7.6	79	62	−12.29	+0.35	+0.09	−11.85	87	6 43	62	N
	12..	6 53 −7 43	0.000	29	7.7	78	62	−12.36	+0.33	+0.09	−11.94	87	6 43	66	S
	12..	7 47 −9 8	−0.004	16	7.7	78	62	−12.36	+0.35	+0.09	−11.92	87	6 43	67	S
	31..	7 6 −8 6	−0.001	29	8.8	66	72	−13.36	+0.33	+0.19	−12.84	96	6 57	68	M
	31..	8 12 −9 12	−0.005	15	8.8	66	72	−13.36	+0.35	+0.19	−12.82	96	6 57	69	M
June	1..	7 5 −8 5	+0.005	29	8.8	65	72	−13.40	+0.33	+0.20	−12.87	277	6 58	70	N
	1..	8 11 −9 11	0.000	15	8.8	65	72	−13.40	+0.35	+0.20	−12.85	277	6 58	71	M
	2..	6 40 −7 41	+0.003	34	8.9	64	72	−13.44	+0.32	+0.20	−12.92	97	6 58	72	N
	2..	7 58 −9 1	−0.001	17	8.9	64	72	−13.45	+0.35	+0.20	−12.90	97	6 58	73	M
	3..	7 0 −8 0	+0.001	30	9.0	64	73	−13.48	+0.33	+0.20	−12.95	278	6 58	77	M
	3..	8 10 −9 15	+0.001	15	9.0	64	73	−13.49	+0.35	+0.20	−12.94	278	6 58	78	N
	4..	7 3 −7 59	−0.002	30	9.0	63	73	−13.52	+0.33	+0.21	−12.98	98	6 59	79	M
	4..	8 7 −9 17	+0.005	16	9.0	63	73	−13.53	+0.35	+0.21	−12.97	98	6 59	80	N
	22..	7 34 −8 20	−0.002	24	10.7	51	84	−13.99	+0.35	+0.24	−13.40	105	7 6	83	N, M
July	2..	7 36 −8 24	−0.006	21	11.9	45	90	−14.05	+0.36	+0.23	−13.46	203	7 7	87	M
	3..	7 56 −8 56	−0.002	15	12.0	44	90	−14.05	+0.37	+0.23	−13.45	102	7 7	89	S, N
	4..	7 36 −8 26	−0.006	21	12.1	44	91	−14.05	+0.36	+0.23	−13.46	89	7 7	90	S, M
	20..	7 14 −8 16	−0.005	18	14.8	34	102	−13.61	+0.36	+0.17	−13.08	93	7 2	96	S, M
	21..	7 19 −8 29	−0.003	15	15.1	33	103	−13.56	+0.36	+0.17	−13.03	273	7 2	99	S, N

TABLE IV

OBSERVATIONAL DATA, VENUS WEST OF THE SUN

Date	Exposure P.S.T.	Δλ V−Sky	h	D	Angle VSE	i	Velocity in Line of Sight				Q	Sun-rise P.S.T.	Plate No.	Meas-urer
							V−E	Rot. E	V′−S	Total				
		A					km	km	km	km				
1919 Nov. 3..	17^h10^m–17^h57^m	−0.003	34°	15″.8	32°	103°	+12.64	−0.29	−0.20	+12.15	270°	18^h14^m	V104	N
4..	15 56 −16 56	+0.011	21	15.6	33	102	+12.69	−0.35	−0.20	+12.14	270	18 14	107	N, M
4..	17 10 −18 12	+0.007	36	15.6	33	102	+12.69	−0.28	−0.20	+12.21	270	18 14	108	S
20..	16 21 −17 21	+0.001	24	12.8	42	90	+13.03	−0.32	−0.12	+12.59	266	18 29	113	N
20..	17 28 −18 28	−0.001	36	12.8	42	90	+13.03	−0.25	−0.12	+12.66	266	18 29	114	N
21..	16 10 −17 11	−0.001	22	12.7	43	90	+13.03	−0.33	−0.11	+12.59	270	18 30	118	S
21..	17 17 −18 21	−0.004	35	12.7	43	90	+13.03	−0.26	−0.11	+12.66	270	18 30	119	S
23..	16 55 −17 45	−0.001	30	12.4	44	89	+13.03	−0.29	−0.10	+12.64	90	18 32	124	S
23..	17 52 −18 37	0.000	39	12.4	44	89	+13.03	−0.22	−0.10	+12.71	90	18 32	125	N
Dec. 8..	17 25 −18 35	−0.001	32	10.7	54	81	+12.91	−0.24	0.00	+12.67	79	18 46	129	S
9..	16 5 −18 20	+0.010	21	10.6	54	80	+12.90	−0.32	0.00	+12.58	80	18 46	131	N
26..	16 32 −17 33	−0.010	17	9.2	64	72	+12.44	−0.31	+0.11	+12.24	88	18 56	133	S
26..	17 37 −18 39	−0.006	27	9.2	64	72	+12.43	−0.24	+0.11	+12.30	88	18 56	134	N
27..	16 45 −17 40	+0.007	18	9.1	65	71	+12.40	−0.30	+0.12	+12.22	269	18 57	137	N
27..	17 45 −18 43	+0.008	28	9.1	65	71	+12.40	−0.23	+0.12	+12.29	269	18 57	138	S
28..	16 42 −17 38	−0.005	18	9.0	65	70	+12.37	−0.30	+0.12	+12.19	269	18 57	141	S
28..	17 43 −18 47	−0.002	28	9.0	65	70	+12.37	−0.23	+0.13	+12.27	269	18 57	142	N
1920 Jan. 29..	18 0 −18 45	−0.003	19	7.2	85	57	+11.10	−0.25	+0.24	+11.09	89	18 51	151	S
31..	16 50 −17 55	−0.015	9	7.1	86	57	+11.02	−0.31	+0.24	+10.95	90	18 50	152	N, M
31..	17 56 −18 46	+0.001	18	7.1	86	57	+11.02	−0.26	+0.24	+11.00	90	18 50	153	N
Feb. 10..	17 40 −18 40	+0.001	14	6.8	92	53	+10.58	−0.28	+0.23	+10.53	96	18 42	155	N
11..	17 25 −18 35	−0.004	13	6.7	92	52	+10.52	−0.29	+0.23	+10.46	276	18 42	157	S
12..	17 20 −18 35	+0.002	12	6.7	93	52	+10.47	−0.30	+0.23	+10.40	277	18 41	159	N
13..	17 38 −18 46	−0.011	14	6.7	93	51	+10.47	−0.28	+0.23	+10.42	97	18 40	161	S
Mar. 11..	17 18 −18 14	−0.004	10	5.9	109	42	+ 9.04	−0.34	+0.12	+ 8.82	110	18 8	166	S

of the earth has been derived in the usual way. Q is the angle between the line joining the cusps and the slit of the spectrograph, measured from the north cusp in the direction of the illuminated portion of the disk to the end of the slit nearest the plate holder. In the first series the red end of the spectrum was on the right as one looked at the slit from the plate holder. In the second series the red was on the left until the end of 1919, when the grating was again reversed. The measurers are identified by the initials S, N, M, indicating St. John, Nicholson, and Miller, respectively.

We take this opportunity to express our appreciation of the assistance given us by Miss Miller in the work of measurement and reduction and by Mr. Edison Hoge in making the observations.

III. DISCUSSION

1. *Correlations.*—Evershed correlated his observations with the angle *VSE* and adopted an interpretation based upon the "very incredible hypothesis"[1] that an "earth-effect" is driving the solar vapors from the earth-facing hemisphere of the sun. Our observations are better correlated with the altitude of Venus at the time of observation. The natural tendency is to use as high an altitude as possible, with the result that the altitude of Venus at the time of observation varies with the angle *VSE*. Our observations, therefore, can apparently be correlated with the angle *VSE* nearly as well as with altitude, but on 18 nights spectrograms were taken at both high and low altitudes: mean high altitude 29°2, mean low altitude 16°1, which give $\Delta\lambda$ low $-\Delta\lambda$ high $=-0.0014$ A. Among the low altitude plates are four at mean altitude 24°2. Pairs in which the low-altitude plates had relatively high altitudes contribute little, on the basis of the correlation with altitude, to the difference shown by the plates at low and high altitudes. On omitting these plates the difference $\Delta\lambda$ low $-\Delta\lambda$ high for the 14 remaining pairs rises to -0.0021 A. As there was no change in the angle *VSE* between the plates of each pair or in the instrumental adjustments, this difference between plates at low and high altitudes is definite evidence of an effect depending in some way on the altitude of the planet, which

---

[1] *Observatory*, **43**, 156, 1920.

shortened the wave-lengths in the spectrum of Venus observed at low altitude, and indicates that the altitude of Venus is the controlling factor in our observations.

An effect depending on low altitude is naturally associated with refraction, and hence with cot h. To obtain a relation independent of the angle VSE and dependent only upon altitude the coefficient of cot h in the equation

$$\Delta\lambda_1 - \Delta\lambda_2 = A(\cot h_1 - \cot h_2)$$

was derived from each of the 18 pairs of plates. Its value closely approximated 0.001 A. By means of this relation the influence of altitude was eliminated from the 56 original observations. The residual displacements showed a slight variation with the relative position of the earth, sun, and Venus. It should be noted, however, that the angle VSE is only one of the variables dependent upon the relative positions of the three bodies which may be used in seeking such correlations. A satisfactory correlation is made by assuming that the observed displacements are fundamentally due to conditions arising from low altitude, and that the effect is greatest when the image of Venus is smallest. This would be the case if the systematic discrepancies were attributable to unsymmetrical illumination of the slit arising from atmospheric refraction and from the small and varying diameter of the image in relation to width of slit. This is the simplest interpretation of our observations, in that it refers the entire effect to a single rational cause. A solution by least squares for this correlation gives

$$\Delta\lambda 10^{-3} = 1.3 - 8.5 \frac{\cot h}{D},$$

where D is the semidiameter of Venus in seconds of arc.

If the angle VSE is used, the observations may be represented by

$$\Delta\lambda 10^{-3} = 3.0 - 1.0 \cot h - 3.0(1 - \cos VSE).$$

By introducing the phase angle i, the following equation may be used:

$$\Delta\lambda 10^{-3} = 2.3 - 1.0 \cot h - 3.5 \cos i.$$

As far as the observations are concerned, these three equations represent them equally well, but the first offers the most reasonable and probable explanation.

In the computation of the velocity corrections the value 8.″80 was used for the solar parallax, and the velocity displacements due to rotation of the planet were assumed to be negligible, as would be the case for the long rotation period shown by Slipher's observations.[1] An error in either of these assumptions would not affect the correlations, since deviations due to either of these causes would appear with opposite signs in the two series and be eliminated in the correlations which combine them both. It may be remarked that when the observations are corrected for the systematic displacements to the violet discussed above, the difference between morning and evening series, viewed in the light of the probable error of the observations, is not of an order that would indicate a divergence from the assumed parallax or a rate of rotation higher than that found by Slipher.

2. *Superposed skylight.*—Venus can be seen on the slit of the spectrograph at any time during the day, and some preliminary plates indicate that it may be possible to secure reliable observations in full daylight, provided the relative velocity of Venus and the earth is large enough to separate completely the absorption lines in the spectra of Venus and the sky. When the angle *VSE* is large, however, the displacement due to the relative velocity is less than the width of a line, and wave-lengths measured under such conditions are affected by an error depending on the brightness of the sky and the amount of displacement. This error appears as a shift to the violet when Venus is west of the sun, and to the red when Venus is east of the sun. Tests were made with superposed spectra having different exposures and a relative displacement of 0.120 A. They showed that a superposed spectrum having 5 per cent of the intensity of the primary spectrum was sufficient to produce measurable shifts.

When the angle *VSE* is large, the time available is short, and therefore it is necessary, with Venus east of the sun, to begin the exposures as early as possible and, with the planet west of the sun, to continue them until the brightness of the sky reaches the permissible limit. To examine our observations for possible effects due to superposed skylight near twilight and dawn, we have selected groups of observations in which the components have approximately equal altitudes but begin at unequal intervals after sunset or end at unequal intervals before sunrise. The effect of altitude is by this arrangement of the observations the same for each group. An examination of the data in Table V reveals no measurable effect due to superposed skylight, even when the exposures were begun at sunset or ended at sunrise, as is shown by the agreement between the components of each group.

---

[1] *Lowell Observatory Bulletin*, **1**, 9, 1903.

TABLE V

Absence of Effect of Superposed Skylight

1919				1919–1920			
Begun after Sunset	No. Plates	h	$\Delta\lambda$	Ended before Sunrise	No. Plates	h	$\Delta\lambda$
min.				min.			
36	5	17°	−0.005	6.3	3	15°	−0.002
15	2	16.5	−0.004	− 1.5	4	14	−0.003
14	6	26	−0.002	13	6	31	−0.001
1.6	8	26	−0.001	− 1	3	37	+0.002

3. *The effects of altitude.*—The spectroscopic conditions arising from low altitude are complex, and the following considerations show that further investigation is required to determine the rôle played by the various factors in producing the observed displacements. The atmospheric dispersion at low altitude displaces the photographic image relative to the visual image very appreciably. When the guiding is done upon the visual image, as in these observations, this relative displacement may produce dissymmetry in the illumination of the slit. At 8° altitude the dispersion between λ 4500 and λ 5700 is 8″, a third of the diameter of the planet at maximum elongation. Campbell found large differences in the radial velocity of Venus when he compared the values obtained by placing the slit just inside the terminator with those obtained

when the slit was just inside the limb.[1] These differences, which he attributed to non-uniform illumination of the slit, reversed in sign when the spectrograph was rotated through 180°. In observations such as ours non-uniform illumination of the slit due to guiding on the visual image would depend not only upon the atmospheric dispersion at low altitude but also upon the diameter of the image relative to the width of the slit. This source of error we hope to eliminate in our next series of observations upon Venus by using a blue screen in the observing telescope, thus making it possible to keep the photographic image symmetrically placed on the slit. We have not yet found a satisfactory reason why rotation of the spectrograph did not reverse the sign of the displacements, as was expected if they are due entirely to non-uniform illumination of the slit.

The refraction, moreover, requires compensation in both right ascension and declination, involving systematic corrective movements of the image on the slit. We were obliged to overcome the drift in declination by a progressive tilt of the concave mirror, a faulty procedure, as the angle of incidence at the grating is very sensitive to changes in the direction of the beam from the concave mirror. This possible source of error will be eliminated from our next observations as motor controls on the second flat now enable the observer to guide by it.

4. *Kodaikanal observations.*—The following Kodaikanal observations are collected from the reports and papers by Evershed:[2]

TABLE VI

RESIDUALS (VENUS—SKY) FROM KODAIKANAL OBSERVATIONS

VSE	45°	62°	67°	75°
V−Sky	+0.0026[3]	−0.0034	−0.0024	−0.0068
VSE	95°	102°	135°	140°
V−Sky	−0.0009	−0.0052	−0.014	−0.007 A

---

[1] *Lick Observatory Bulletin*, **9**, 30, 1916.

[2] *Kodaikanal Observatory Report*, p. 2, 1917; p. 2, 1918; p. 3, 1919; *Monthly Notices*, **78**, 278, 1918; **79**, 257, 1919; **80**, 395, 1920; *Observatory*, **43**, 156, 1920.

[3] *Kodaikanal Observatory Report*, 1918. Four excellent plates give orbital velocity 3.5 per cent low. *Monthly Notices*, **78**, 279, 1918: 0.45 km/sec. less than orbital velocity. A displacement of +.0067 A is deduced from these statements and averaged with that of the 1918 series.

Observations when the angle *VSE* is 135°–140° are necessarily made with Venus at altitudes of about 10°; near maximum elongation they would most naturally be made at high altitudes; and with *VSE* near 90°, at intermediate altitudes. The altitudes for the Kodaikanal observations are not available, but, if they are near the values suggested as probable, Evershed's observations of V−Sky may also be correlated with altitude. The question is then one of interpretation; plates at high and low altitudes with the same value of *VSE*, and at low altitude with large and small *VSE*, will eventually furnish a definite answer. As far as present observations have a bearing on the question, they indicate that the main factors producing the displacements are those depending upon the low altitude of Venus at the time of observation. When this effect is eliminated, the remaining residuals, which seem to vary with the relative position of earth, Venus, and sun, are more reasonably correlated with the varying diameter of the planet than with the angle *VSE*.

MOUNT WILSON OBSERVATORY
March 1921

Contributions from the Mount Wilson Observatory, No. 209
Reprinted from the *Astrophysical Journal*, Vol. LIII, pp. 392–96, 1921

BRIGHT AND DARK NEBULAE NEAR ζ ORIONIS PHOTOGRAPHED WITH THE 100-INCH HOOKER TELESCOPE

By JOHN C. DUNCAN

Photographs made with the 100-inch Hooker telescope of the Mount Wilson Observatory are reproduced in two plates. They exhibit the following features: the *bright nebulae N.G.C. 2024* and *2023* and *I.C. 431*, *432*, and *434:* the *dark cosmic cloud Barnard 33*, which indents or overlies the nebula I.C. 434; the *great disparity in the number of faint stars* on opposite sides of a line passing nearly north and south through ζ Orionis; and a *striated appearance* in the faint nebulosity west of I.C. 434.

Evidence is given of the existence of *four distinct types of extended masses* in the neighborhood, and suggestions made in explanation of the aspect of the region as presented by the photographs.

The region surrounding the star ζ, at the southeastern end of the Belt of Orion, has been studied on account of its remarkable nebulae by several observers, the first of whom was W. Herschel, who listed it as No. 25 of his fifty-two regions that contain diffuse nebulosity.[1] Six of its nebulae are included by Dreyer in the *New General Catalogue* or the first *Index Catalogue*. Photographs showing many of its interesting features have been published and discussed by W. H. Pickering,[2] Roberts,[3] Wolf,[4] Keeler,[5] Barnard,[6] and Curtis.[7]

During the past winter I have made photographs of this region at the principal focus of the 100-inch Hooker telescope, and the great focal length, light-gathering power, and resolving power of this instrument have brought out certain remarkable features with great distinctness. Two of these photographs are reproduced in Plates V and VI. The original negatives are 8×10 inches in size, but in making the reproductions only the central parts were used and these were reduced in scale. The excellence of the reproductions is due largely to the skill of Mr. Ellerman, who increased the intensity of the images of faint nebulosities by successive copying on slow plates.

---

[1] *Philosophical Transactions*, **101**, 276, 1811.

[2] *Annals of Harvard College Observatory*, **32**, 66, and Plate III, Fig. 3, 1895.

[3] *Astrophysical Journal*, **17**, 74, and Plate IV, 1903; also, *Monthly Notices*, **63**, 31, and Plate 1, 1903.

[4] *Monthly Notices*, **63**, 304, and Plate 11, 1903.

[5] *Publications of the Lick Observatory*, **8**, Plate XIII, 1908.

[6] *Astrophysical Journal*, **38**, 500, and Plate XX, Fig. 1, 1913; also *Publications of the Lick Observatory*, **11**, Plate XX, 1913.

[7] *Publications of the Astronomical Society of the Pacific*, **30**, 66, and Plate IV, Fig. 1, 1918; *Publications of the Lick Observatory*, **13**, 23, and Plate II, Fig. 5, 1918.

PLATE V.—Center of plate (1920.0), $\alpha=5^h37^m.0$, $\delta=-2^\circ31'$. 1920, November 13. Exposure three hours. Seeing good, but figure of mirror somewhat imperfect. Seed 23 plate.

The bright star ζ Orionis is just off the north side of the plate, and a bright ray, produced by diffraction of its light by one of the steel supports of the secondary mirror, extends from it toward the south and east. The brightest star shown is D.M. $-2^\circ1337$, 19 mm from the bottom of the plate and 42 mm from the right side. Its visual magnitude, as given by the *Durchmusterung*, is 7.5.

Almost vertically through the middle of the plate lies the nebula I.C. 434, which was discovered photographically at the Harvard Observatory in 1887.[1] It here appears as the bright fringe of a diffuse nebulosity that fills the western half of the field. This diffuse nebulosity is remarkably striated, the striae lying in a direction approximately east and west. The fringe has numerous branches and irregularities and is suggestive of the edge of a relatively thin sheet that is crumpled and turned edgewise to the observer. Earlier observers have noted the scarcity of faint stars east of the nebulous fringe as contrasted with their great abundance on the west. The effectiveness of the Hooker telescope in photographing faint stars makes this contrast very conspicuous.

In the northeastern corner of the field is the nebula N.G.C. 2023, which surrounds a star of magnitude 8.5, not shown on the plate because of overexposure of the nebula. It is terminated rather abruptly on the west side, and shows a clearly defined dark marking on the east. The existence of spiral rays, noted by the Harvard observers,[2] is not here confirmed.

---

[1] *Annals of Harvard College Observatory*, **18**, 115, 1890.

[2] *Ibid.*, 116, 1890.

PLATE V

N

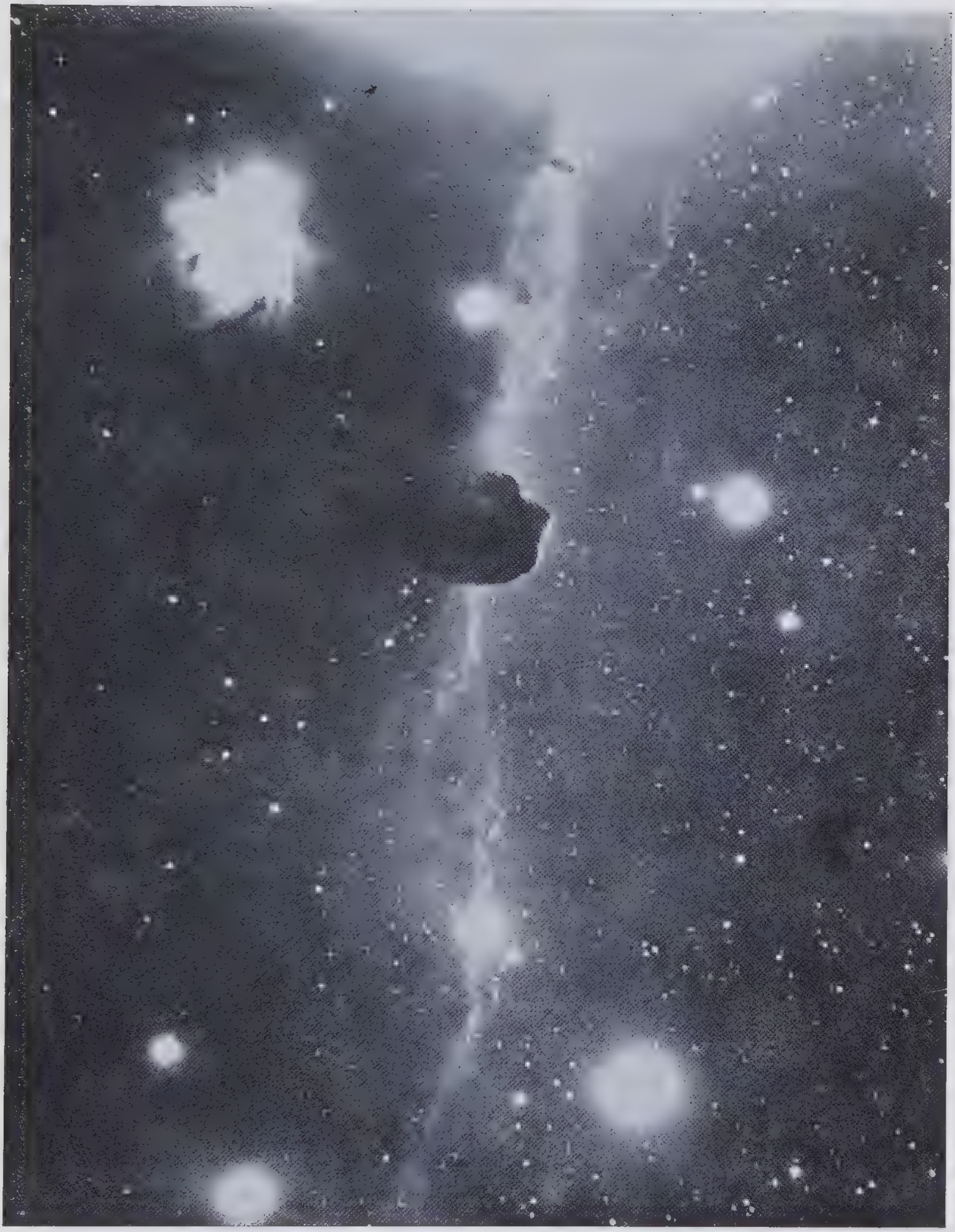

E

W

Bright and Dark Nebulae South of ζ Orionis
Scale: 1 mm = 14″0 (0.89 that of original negative)

PLATE VI

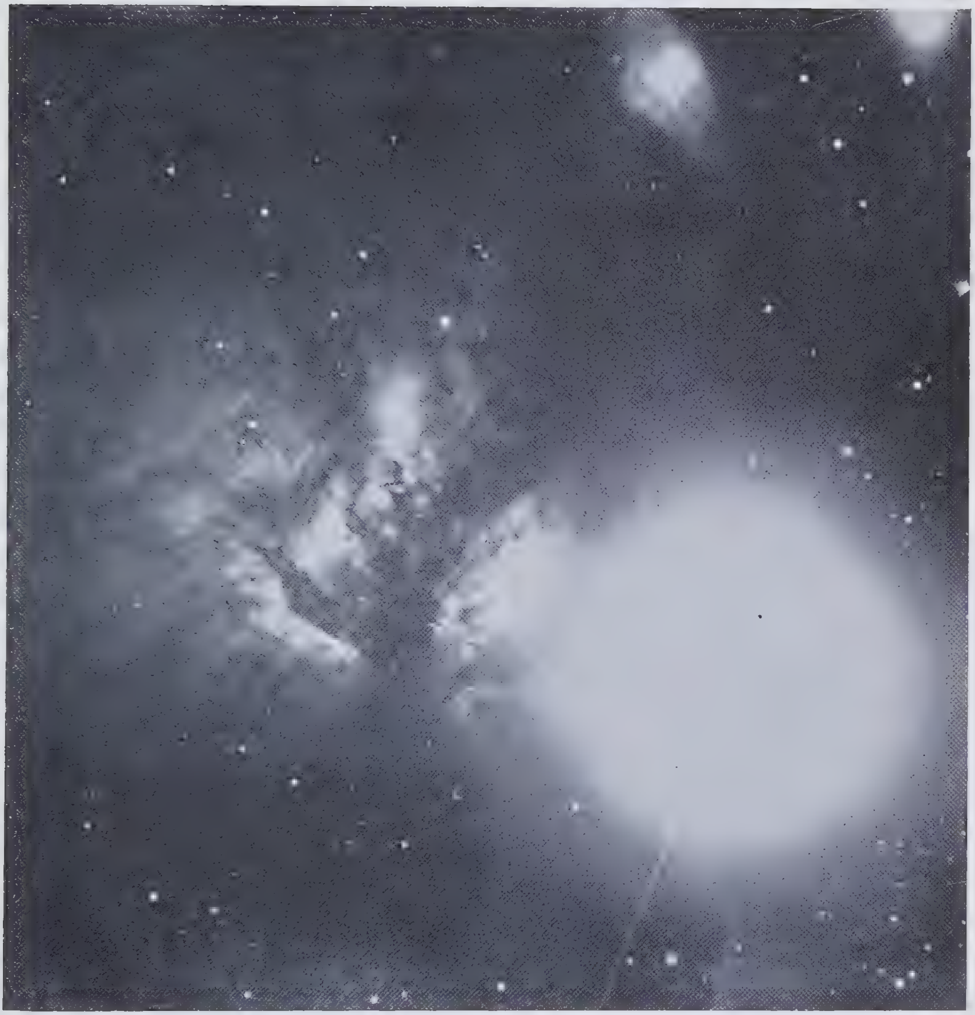

ζ Orionis and the Nebulae on the East and North
Scale: 1 mm = 12″.8 (0.81 that of original negative)

By far the most interesting object shown on the plate is the dark cloud near the center, which forms a bay in the bright nebula and which has attracted attention since the earliest photographic observations of the region. It is listed by Barnard as No. 33 of his dark markings of the sky.[1] On the present plate, faint lights appear within the cloud, and a notable silver lining is shown along its western edge. On the original negative the eastern boundary can be traced on the faint background of the sky, and is seen to extend north and east nearly to N.G.C. 2023. An aid to tracing its position is found in the diffracted ray from ζ Orionis, which seems to have been too faint to affect the plate perceptibly by its own light but is plainly visible where the plate has been brought to its threshold by the nebulous background, so that the ray is interrupted where it crosses the dark cloud. A second and much smaller and paler dark bay lies about 15′ north of Barnard 33, near the 8.5 magnitude star D.M. $-2^\circ1343$, and a third about 6′ still farther north.

PLATE VI.—Center of plate (1920.0), $\alpha=5^h37^m.3$, $\delta=-1^\circ53'$. 1920, December 8. Exposure, 5 hours, 35 minutes. Sky somewhat hazy. Seed 30 plate.

ζ Orionis is near the west side of the plate, where irradiation has spread its light into a great blot. The star may be located accurately at the intersection of the rays produced by the mirror supports. At the extreme northwest corner of the plate is the nebula I.C. 431, and 10′ east of this is I.C. 432. These nebulae surround the stars D.M. $-1^\circ1001$ and $-1^\circ1005$ respectively, stars of about 8.5 visual magnitude. A few of the stars that lie near the north edge of Plate V appear also near the south edge of Plate VI. The continuation of the nebula I.C. 434 toward ζ may be seen on Plate VI, which shows also that the disparity in the number of faint stars on the east and west sides of the nebulous fringe continues some distance north of ζ, where the line of division seems to turn somewhat toward the west.

The greater part of Plate VI is occupied by the remarkable nebula N.G.C. 2024, discovered in 1786 by W. Herschel, who described it[2] as a "remarkable nebulosity, divided in 3 or 4 large patches including a dark space." The brightest parts cover a space some 25′ in diameter, and there are faint extensions, one of which reaches as far as I.C. 432 on the northwest. Both this nebulosity and that of I.C. 434 can be traced on the original plate to within 5′ of ζ Orionis, where they are concealed in the glare about the bright star. The irregularities of the bright and dark markings of N.G.C. 2024 are such as to defy description, which fortunately is unnecessary, as they are well shown in the illustrations. The character of this nebulosity appears to be different from either that of I.C. 434 or that of the neighboring nebulous stars.

---

[1] *Astrophysical Journal*, **49**, 14, 1919.

[2] *Philosophical Transactions*, **79**, 248, 1789.

A study of the photographs of this region tends to the conviction that we have here to do with extended masses of not less than four distinct types: (1) the ropy, branching nebulosity of I.C. 434; (2) the nebulosity of N.G.C. 2024; (3) the nebulous stars N.G.C. 2023 and I.C. 431, 432, and 435;[1] (4) dark nebulosities, best exemplified by the cloud Barnard 33.

The phenomena shown suggest the following speculations: Perhaps the fringe of I.C. 434 represents the common boundary of a dense, dark mass on the east and a body of thin, luminous nebulosity on the west. These two masses may have a relative motion toward each other, which results in a concentration of the bright nebulosity along the line of contact, this concentrated nebulosity being the fringe. The faint nebulosity west of the fringe must be sufficiently transparent to transmit the light of the starry background, while the dark material on the east obscures all the stars behind it. The bright nebula N.G.C. 2024 seems to be of the nature of a bright outcropping of the dark nebula, which indeed is probably nowhere absolutely non-luminous unless it be so in the darkest part of Barnard 33. Perhaps the four stars that show nebulous burs—D.M. −1°1001, −1°1005, −2°1345, and −2°1350—are imbedded in the dark nebula and illuminate that part of it which lies immediately around them, the nebulosities of the third type being due in part to this cause and in part to the same cause as those of the second type. We may suppose the non-nebulous stars that appear east of I.C. 434 to lie between the observer and the dark nebula.

---

[1] The nebula I.C. 435 is some 20′ east of N.G.C. 2023 and is not shown in the illustrations. It surrounds the 8.5 magnitude star D.M. −2°1350.

Mr. E. P. Hubble has kindly loaned me a plate made by him with the Hooker telescope 1920, November 18, which shows the region immediately north of ζ Orionis. The line of cleavage between the regions of few and of many stars is clearly marked on this plate, and passes in a zigzag fashion northwest of ζ nearly to I.C. 431, where it bends toward the west and returns, forming a bay about 15′ deep, and then passes northeastward to a point near the sixth-magnitude star −1°1004, about 1° north of ζ and near the north edge of the plate. There is on this plate no hint of a nebulosity similar to I.C. 434, and the line of cleavage has not here the regularity that is noticeable in that part of it lying south of ζ. Long-exposure photographs of the Orion region made with the 10-inch Cooke refractor of this observatory by Mr. Hubble and Mr. Pettit indicate that the obscuring mass east of ζ Orionis is only a part of a much larger region that extends several degrees toward the northeast, enveloping the bright nebula Messier 78, and also, though less plainly, some distance toward the south. The general outlines of this dark region can be traced on the Franklin-Adams chart.

Mount Wilson Observatory
March 1921

Contributions from the Mount Wilson Observatory, No. 210
Reprinted from the *Astrophysical Journal*, Vol. LIV, pp. 9–27, 1921

THE RELATIONSHIP OF ABSOLUTE MAGNITUDE TO SPACE-VELOCITY

By W. S. ADAMS, G. STRÖMBERG, and A. H. JOY

ABSTRACT

Variation of the velocity of stars with absolute magnitude.—A statistical study of the radial, tangential, and space-velocities of 1350 stars, mostly of types F, G, K, and M, shows a marked correlation with absolute magnitudes. The results are given in the form of equations and tables. The increase in average space-velocity for a decrease of one magnitude in brightness varies with the type, but is of the order of 3 km/sec. The greater homogeneity of the giant stars as a class and their comparative freedom from large individual motions are indicated by the results. As would be expected for a random distribution of velocities as to direction, the average radial velocities are about half the corresponding average space-velocities.

Frequency of the space-velocities of stars cannot be represented by a distribution according to Maxwell's law, for there is a large excess of stars with high velocities, but a type of *frequency function* based upon the assumption of a normal error-distribution in the logarithms of the velocities is found to represent the observations much more closely. The function is proportional to $e^{-h^2(\log v-\log \underline{v})^2}$, where $\underline{v}$ is the geometrical mean space-velocity.

In a communication published in 1915, Kapteyn and Adams[1] showed that the radial velocities of a considerable number of stars depended upon proper motion and mean parallax in such a way as to indicate that the intrinsically brighter stars move more slowly than the fainter stars. More extensive investigations by Adams and Strömberg[2] in 1917, and by Strömberg in 1918,[3] based upon 1300 stars of spectral types F, G, K, and M, gave similar results. For this purpose the absolute magnitudes derived by the spectroscopic method were used, and not only the radial velocities but also the components at right angles to the direction of the sun's apex were included in the discussion. An average change in radial velocity of about 1.3 km for each unit of absolute magnitude was indicated by these investigations.

The subject had already been discussed by Eddington[4] on the basis of stars with parallaxes determined by the trigonometric method, and some of the important consequences of such a relationship had been pointed out by Eddington, Russell, Halm, and others. Additional evidence will therefore be of especial value for investigations dealing with the motions of stars in our Galaxy and their connection with spectral type and mass.

---

[1] *Mt. Wilson Communications*, No. 1; *Proceedings of the National Academy of Sciences*, **1**, 14, 1915.

[2] *Mt. Wilson Contr.*, No. 131; *Astrophysical Journal*, **45**, 293, 1917.

[3] *Mt. Wilson Contr.*, No. 144; *Astrophysical Journal*, **47**, 7, 1918.

[4] *Stellar Movements*, p. 52, 1914.

Previous studies of the subject have been limited to components of the stellar motions either in the line of sight or at right angles to it. With the rapid accumulation of parallax observations, both trigonometric and spectroscopic, and a similar increase in determinations of radial velocities, we can extend the investigation to the actual motions of the stars in space. In the pages which follow we shall compute the space-motions of the stars in our list, derive the frequency-law representing their distribution, and study the relationship of these motions to absolute magnitude.

The velocity-components of a star relative to the sun are computed from the following equations:

$$x = V \cos\alpha \cos\delta - \frac{k}{\pi}(\mu_\alpha \sin\alpha \cos\delta + \mu_\delta \cos\alpha \sin\delta)$$

$$y = V \sin\alpha \cos\delta + \frac{k}{\pi}(\mu_\alpha \cos\alpha \cos\delta - \mu_\delta \sin\alpha \sin\delta)$$

$$z = V \sin\delta + \frac{k}{\pi}\mu_\delta \cos\delta$$

where x, y, and z are the velocity-components in the equatorial system, expressed in kilometers per second, V is the radial velocity relative to the sun, α and δ are right ascension and declination, μ_α and μ_δ the corresponding proper motions, π is the parallax, and k is a constant equal to 4.737 km/sec.

If x_0, y_0, and z_0 are the velocity-components of the sun referred to the centroid of a large number of stars, we can obtain the components x_1, y_1, and z_1 of the star relative to this centroid from the equations

$$x_1 = x + x_0, \qquad y_1 = y + y_0, \qquad z_1 = z + z_0.$$

The space-velocity v of the star, corrected for the sun's motion, is therefore

$$v = \sqrt{x_1^2 + y_1^2 + z_1^2}.$$

The parallaxes used in this investigation are those obtained by the spectroscopic method and published recently.[1] In a few instances where the parallaxes are large the trigonometric values have been used instead. The proper motions are from the *Catalogue* of Boss or *Cincinnati Publications*, No. 18, with the addition of a few values determined by Kapteyn, Roy, and others. The radial velocities have been taken from Campbell's list in *Lick Observatory Bulletin*, No. 229, from the Mount Wilson lists published

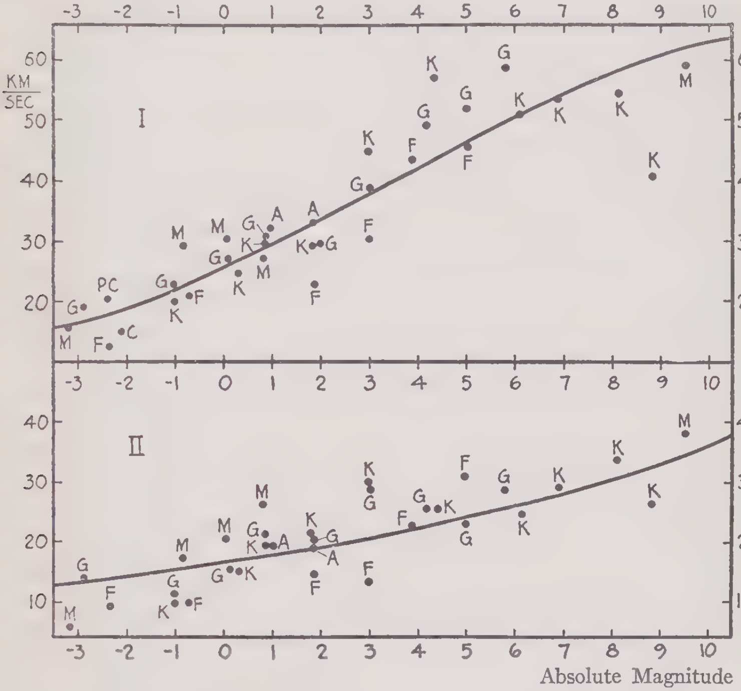

FIG. 1.—Curves showing the relationship of space-velocity to absolute magnitude for the various spectral types.

Curve I. Abscissae, average absolute magnitudes; ordinates, geometrical means of space-velocities. The continuous curve alone is shown.

Curve II. Abscissae, average absolute magnitudes; ordinates, average radial velocities.

---

[1] *Mt. Wilson Contr.*, No. 199; *Astrophysical Journal*, 53, 13, 1921.

in *Contributions*, Nos. 79 and 105,[1] and from unpublished Mount Wilson results.

Since many of the stars observed at Mount Wilson were selected on the basis of small proper motion, it is evident that there may be too large a proportion of stars with velocity-components in a plane perpendicular to the line of sight, which are nearly equal in direction and amount to the sun's velocity projected on this plane. For this reason we have omitted from the discussion 101 stars, this number being based on the distribution of proper motions given by Kapteyn in *Groningen Publications*, No. 30.

The detailed results based upon the values derived from the individual stars are given in Table I. The symbols in this table have the following meaning:

$\overline{M}$ = mean absolute magnitude
$\bar{v}$ = average space-velocity
$\overline{T}$ = average tangential velocity not corrected for the sun's motion. This is equal to $k\left(\frac{\mu}{\pi}\right)$
θ = average radial velocity
$\underline{v}$ = geometrical mean of space-velocities
$\underline{T}$ = geometrical mean of tangential velocities
r_1 and r_2 = probable deviations of $\log v$ and $\log T$ for a single star from the mean values $\log v$ and $\log T$

All of these quantities have been computed from the individual values of v, T, $\log v$, $\log T$ and V', the last being the radial velocity corrected for the sun's motion. The probable errors in $\log \underline{v}$ and $\log \underline{T}$ have been converted into corresponding errors in v and $\underline{T}$. The values used for the solar motion are those derived in 1917.[2]

$$A_0 = 270\overset{\circ}{.}9;\quad D_0 = +29\overset{\circ}{.}2;\quad V_0 = 21.48 \text{ km/sec.}$$

The use of the values $A_0 = 270°$, $D_0 = +30°$, $V_0 = 20.0$ km would in general affect $\bar{v}$ and $\underline{v}$ by less than 0.1 km.

The values for the A-type stars in Table I are based almost wholly upon stars of types A7 to A9, and the uncertainty in the determination of the absolute magnitudes may be larger than for

---

[1] *Astrophysical Journal*, **39**, 341, 1914; **42**, 172, 1915.

[2] *Mt. Wilson Contr.*, No. 144; *Astrophysical Journal*, **47**, 7, 1918.

TABLE I

Absolute Magnitude and Space-Motion

M	No.	$\overline{M}$	$\bar{v}$	$\overline{T}$	θ	$\underline{v}$	$\underline{T}$	r_1	r_2
	Type A (A7 to A9)								
			km	km	km	km	km		
−0.1 to +1.5....	11.5	+1.0	34.2	23.2	19.3	32.2± 2.4	19.4±2.6	±0.108	±0.201
+1.5 to +2.5....	14.5	1.9	36.6	31.8	19.6	32.9± 2.6	24.7±3.6	0.129	0.244
	Type F (F0 to F9)*								
−3.5 to −1.5....	9	−2.3	16.5	20.3	9.5	12.3± 2.6	15.2± 3.0	±0.271	±0.258
−1.5 to +0.5....	21	−0.6	43.7	44.6	11.7	23.7	19.8	....	....
	20†	−0.7	32.2	33.7	9.8	20.9± 3.7	17.4± 3.9	0.338	0.427
+0.5 to +2.5....	54.5	+1.9	28.1	26.9	14.6	22.8± 1.4	18.5± 1.7	0.198	0.286
2.5 to 3.5....	90	3.0	52.4	49.1	22.3	34.1± 1.7	30.3± 1.8	0.198	0.241
	85.5‡	3.0	34.5	33.4	13.4	30.1± 1.1	26.8± 1.4	0.150	0.205
3.5 to 4.5....	109	3.9	77.4	73.3	29.0	51.5± 2.8	47.6± 2.6	0.246	0.246
	99.5‡	3.9	54.5	51.9	22.5	43.6± 2.1	40.3± 2.0	0.208	0.211
4.5 to 5.7....	8.5	5.0	143.5	125.4	74.4	76.9±20.6	67.1±17.8	0.336	0.331
	6.5‡	5.0	54.0	47.4	31.0	45.5±10.4	39.7± 9.6	0.249	0.266
	Type G (G0 to G9)								
−4.5 to −1.5....	22	−2.9	30.1	27.0	13.7	21.7± 2.9	17.9± 2.5	±0.271	±0.288
	20	−2.9	25.6	21.7	14.0	19.2± 2.5	15.4± 2.0	0.255	0.263
−1.5 to −0.5....	25.5	−1.0	27.8	25.9	11.0	22.7± 1.9	19.4± 2.0	0.187	0.222
−0.5 to +0.5....	62.5	+0.1	35.7	32.2	15.5	27.2± 1.5	22.4± 1.5	0.193	0.233
+0.5 to +1.5....	72.5	0.9	37.8	31.8	21.0	30.2± 1.5	23.6± 1.5	0.186	0.230
1.5 to 2.5....	35.5	1.9	35.9	29.0	19.8	29.6± 2.0	22.7± 1.8	0.181	0.210
2.5 to 3.5....	18	3.0	45.4	39 0	29.4	38.8± 3.2	33.2± 3.4	0.154	0.189
3.5 to 4.5....	42.5	4.2	59.7	57.2	25.6	49.4± 3.4	47.6± 3.2	0.198	0.189
4.5 to 5.5....	73.5	5.0	58.7	58.2	23.1	51.9± 2.4	48.6± 2.5	0.168	0.187
5.5 to 6.6....	51	5.8	88.3	88.0	34.0	61.9± 3.4	63.4± 3.4	0.174	0.166
	50§	5.8	70.3	70.7	28.7	58.6± 3.0	60.0± 2.9	0.157	0.148
	Type K (K0 to K9)								
−4.0 to 0.0....	14	−0.8	44.4	42.2	11.9	26.6± 5.5	21.8± 5.0	±0.333	±0.372
	12	−1.0	28.0	23.6	9.9	20.0± 3.2	15.7± 3.2	0.276	0.312
0.0 to +0.5....	74.5	+0.3	29.4	22.8	14.6	24.4± 1.2	14.8± 1.1	0.182	0.289
+0.5 to +1.5....	186.5	0.9	36.5	28.6	19.5	29.6± 1.0	20.4± 0.8	0.190	0.248
1.5 to 2.5....	47	1.9	34.6	24.6	21.1	29.4± 1.7	17.0± 1.5	0.173	0.269
2.5 to 3.5....	11.5	3.0	48.8	37.6	29.8	45.9± 3.6	29.4± 4.6	0.116	0.231
3.5 to 5.5....	12.5	4.4	62.6	53.5	25.8	57.2± 4.6	32.7± 5.1	0.125	0.242
5.5 to 6.5....	67.5	6.1	67.3	70.4	24.3	50.9± 2.5	59.8± 2.8	0.177	0.162
6.5 to 7.5....	36	6.9	59.3	56.4	29.3	53.5± 2.8	52.8± 2.2	0.136	0.105
7.5 to 8.5....	12.5	8.1	58.7	54.8	33.7	54.2± 5.0	50.9± 4.3	0.143	0.130
8.5 to 9.7....	8	8.8	47.3	41.0	26.5	40.6± 6.7	36.2± 5.4	0.202	0.182
	Type M (Ma to Md)								
−3.8 to −2.7....	2	−3.2	16.4	11.2	5.6	15.8± 3.4	11.0± 1.7	±0.131	±0.095
−1.5 to −0.5....	13.5	−0.8	36.4	33.1	17.4	29.6± 2.7	21.4± 4.8	0.142	0.350
−0.5 to +0.5....	67.5	+0.1	36.5	28.2	20.4	30.2± 1.5	19.5± 1.4	0.174	0.249
+0.5 to +1.5....	31	0.8	32.0	26.3	26.3	27.2± 1.8	21.3± 1.8	0.154	0.203
8.5 to 10.0....	7	9.5	61.3	53.9	38.3	58.8± 4.7	49.3± 6.2	0.093	0.143
10.0 to 13.4....	11	10.9	62.3	50.0	37.5	51.4± 7.6	41.2± 5.8	0.214	0.203

* *Cin.* 560 (Sp. = A8, $M = 2.8$, $v = 557$, $V' = +327$) included in F type.

† RR Lyrae ($v = 274$, $V' = -49$) omitted.

‡ Stars with $v > 180$ omitted. These appear to form a separate group.

§ *Cin.* 2019 ($v = 986$) omitted.

TABLE I—*Continued*

M	No.	$\overline{M}$	$\bar{v}$	$\overline{T}$	θ	$\underline{v}$	$\underline{T}$	r_1	r_2
	CEPHEID VARIABLES ‖								
			km	km	km	km	km		
−3.4 to −2.1....	7	−2.6	19.9	24.6	10.1	12.2± 3.5	21.2± 3.3	±0.327	±0.178
−2.0 to −1.1....	8	−1.8	20.5	21.9	12.4	17.8± 2.4	19.9± 2.5	0.166	0.156
Sum and means	15	−2.1	20.2	23.2	11.3	14.9± 2.3	20.5± 1.9	0.255	0.159
	PSEUDO-CEPHEIDS								
−4.2 to −2.8....	14	−3.6	28.2	24.4	9.8	21.4± 3.7	15.6± 3.2	±0.277	±0.334
−2.7 to −0.1....	14	−1.2	30.6	22.4	19.3	19.0± 4.1	12.9± 2.5	0.353	0.308
Sum and means	28	−2.4	29.4	23.4	14.6	20.1± 2.7	14.2± 2.0	0.309	0.315

‖ RR Lyrae ($\overline{M}=0.3$, $v=274$ km, $V'=-49$) omitted.

stars of the succeeding types. Occasionally stars with absolute magnitudes falling on the limit between two groups are included with half-weight in each of the groups. Thus among the A-type spectra a star of absolute magnitude +1.5 is accountable for the fractional values appearing in the column giving the number of stars.

The use of the geometrical mean in this investigation has been found desirable for two reasons. In the first place it is influenced much less than the arithmetical mean by the inclusion of stars of exceptionally high velocities. In the second place, as will be shown later, the form of frequency-function representing most closely the observed distribution of the space-velocities is one in which the logarithm of the geometrical mean of the velocities is one of the fundamental constants. The conversion of the geometrical into the arithmetical mean may be made readily through multiplication by a factor dependent upon the dispersion in the logarithms of the space-velocity around the mean value. This has been found to be fairly constant for all the groups of stars.

Attention should be called to two points bearing on the results of Table I. The first is that of the effect of the selection of the stars. Reference has already been made to the omission of a number of stars of small proper motion in order to equalize the proportion of such stars. The effect of the selection of stars of large proper motion would no doubt have been very marked had all stars of the same spectral type been included in one group. The division according to absolute magnitude should, however, eliminate to a large extent the effect of selection, since most of the stars of large proper motion may be assumed to have been selected on account of their nearness and hence their low intrinsic brightness. A slight excess of rapidly moving stars of high luminosity might, however, be expected from a selection of stars of large proper motion, and this would tend to increase slightly the mean values of the giant stars in Table I.

A second point has to do with the stars of the very highest luminosity. This group contains some stars which have erroneously been estimated as too bright, and as there is a tendency toward an accumulation of such errors, the mean space-velocity and the mean tangential velocity are too large. In order to reduce this effect a special computation has been made for the very brightest G and K stars, omitting a few of the largest space-velocities. This result is given in the second line of the G and K subdivisions of Table I.

From the results of Table I it appears that the values of r_1, although somewhat larger for the brighter stars, do not show any very great range. Accordingly we may with sufficient accuracy adopt its mean value for all absolute magnitudes and spectral types. This value is

$$r_1 = 0.171 \pm 0.0033.$$

As will be shown in connection with the discussion of the frequency-law, the arithmetical mean of the space-velocities $\bar{v}$ and the most frequent velocity v_p can be computed from the geometrical mean by aid of the equations

$$\bar{v} = 10^{2.530 r_1^2} \underline{v}, \quad v_p = 10^{-5.061 r_1^2} \underline{v}.$$

Hence

$$\bar{v} = 1.186 \underline{v}, \qquad v_p = 0.7113 \underline{v}.$$

The values of $\overline{T}$ and $\underline{T}$ have been computed because of their importance in the derivation of mean parallaxes. Since

$$\overline{T} = k \overline{\left(\frac{\mu}{\pi}\right)},$$

we have approximately

$$\bar{\pi} = k\frac{\bar{\mu}}{T}\,.$$

Furthermore

$$\underline{T} = k\underline{\left(\frac{\mu}{\pi}\right)} = k\frac{\mu}{\underline{\pi}}\,,$$

or

$$\underline{\pi} = k\frac{\mu}{\underline{T}} = 10^{0.2(\bar{M}-\bar{m})-1}.$$

With the aid of the data given in Table I we can now compute the general relationship between absolute magnitude and velocity. The geometrical means of the space-velocities and the tangential velocities have been used, since these can be obtained with a higher degree of accuracy than the arithmetical means, but the average radial velocity has been used directly. The tangential velocities are not corrected for the solar motion.

Two different solutions have been made. In the first solution we assume for each type the relationship

$$\log \underline{v} = a + bM,$$

with similar expressions for log $\underline{T}$ and log θ, and use these equations under the assumption that they are constant for each spectral type over the entire range of absolute magnitude. In the second solution a discontinuity is assumed for the K and M stars at the point of division between the giants and dwarfs. The evidence afforded by Table I appears on the whole to be favorable to such a discontinuity, since the velocities of the dwarf stars of these types show little if any variation with absolute magnitude.

Tables II and III give the values of the coefficients and their probable errors in the equations of the form

$$\log \underline{v} = a + bM$$

for the two solutions. Further, all the types are discussed together, and a term involving the square of M has then been included in the first solution, the form being

$$\log \underline{v} = a + bM + cM^2$$

with similar expressions for the tangential and radial velocities.

TABLE II

Equations Connecting Absolute Magnitude with Velocity
First Solution: Continuous Variation

Type	$\log v$	$\log T$	$\log \theta$
F.	$1.356+0.0553\,M$ $\pm0.032\pm0.0111$	$1.248+0.0690\,M$ $\pm0.033\pm0.0113$	$1.149+0.0257\,M$ $\pm0.044\pm0.0154$
G.	$1.415+0.0605\,M$ $\pm0.008\pm0.0021$	$1.313+0.0768\,M$ $\pm0.016\pm0.0043$	$1.214+0.0412\,M$ $\pm0.021\pm0.0067$
K.	$1.428+0.0410\,M$ $\pm0.018\pm0.0038$	$1.224+0.0649\,M$ $\pm0.030\pm0.0063$	$1.232+0.0338\,M$ $\pm0.017\pm0.0036$
M.	$1.456+0.0302\,M$ $\pm0.013\pm0.0026$	$1.300+0.0402\,M$ $\pm0.019\pm0.0037$	$1.306+0.0282\,M$ $\pm0.025\pm0.0049$

ALL TYPES

Space-Velocity $\log \underline{v}=+1.408+0.0632M-0.00240M^2$
$\pm0.011\pm0.0067 \quad \pm0.00085$

Tangential Velocity $\log \underline{T}=+1.256+0.0870M-0.00303M^2$
$\pm0.017\pm0.0098 \quad \pm0.00124$

Average Radial Velocity $\log \theta=+1.219+0.0321M+0.00020M^2$
$\pm0.017\pm0.0103 \quad \pm0.00131$

TABLE III

Second Solution: Separate Equations for Giants and Dwarfs of Types K and M

Type	$\log \underline{v}$	$\log \underline{T}$	$\log \theta$
	$M<2.5$		
K.	$1.398+0.0531\,M$ $\pm0.024\pm0.0206$	$1.232+0.0281\,M$ $\pm0.052\pm0.0446$	$1.164+0.1062\,M$ $\pm0.028\pm0.0239$
M.	$1.455+0.0320\,M$ $\pm0.016\pm0.0213$	$1.298+0.0440\,M$ $\pm0.014\pm0.0191$	$1.304+0.1480\,M$ $\pm0.012\pm0.0165$
All (F to M)	$1.422+0.0282\,M$ $\pm0.010\pm0.0062$	$1.275+0.0417\,M$ $\pm0.013\pm0.0082$	$1.232+0.0113\,M$ $\pm0.022\pm0.0135$
	$M>2.5$		
K.	1.710 ±0.012	1.700 ±0.012	1.431 ±0.014
M.	1.734 ±0.031	1.645 ±0.040	1.578 ±0.012
All (F to M)	$1.640+0.0126\,M$ $\pm0.024\pm0.0042$	$1.549+0.0234\,M$ $\pm0.053\pm0.0089$	$1.271+0.0271\,M$ $\pm0.030\pm0.0051$

TABLE IV

ABSOLUTE MAGNITUDE AND VELOCITY: COMPUTED VALUES

M	F	G	K		M		All Types	
			1	2	1	2	1	2
	$\underline{v}$ = GEOMETRICAL MEAN OF SPACE-VELOCITIES							
− 2	17.6	19.7	22.2	19.6	24.9	24.6	18.7	23.2
− 1	20.0	22.6	24.4	22.1	26.7	26.5	22.0	24.8
0	22.7	26.0	26.8	25.0	28.6	28.5	25.6	26.4
+ 1	25.8	29.9	29.4	28.2	30.6	30.7	29.4	28.2
2	29.3	34.4	32.4	31.9	32.8	33.0	33.5	30.1
3	33.3	39.4	35.6	51.3	....	....	37.7	47.6
4	37.8	45.4	39.1		....	....	41.9	49.0
5	42.8	52.2	43.0		....	....	46.1	50.5
6	....	60.0	47.2		....	....	50.2	52.0
7	....	....	51.9		....	....	54.1	53.5
8	....	....	57.0		49.9	54.2	57.5	55.1
9	....	....	....	....	53.5		60.5	56.6
+10	....	....	....	....	57.3		63.1	58.3
	$\underline{T}$ = GEOMETRICAL MEAN OF TANGENTIAL VELOCITIES							
− 2	12.9	14.4	12.4	15.0	16.6	16.2	11.8	15.6
− 1	15.1	17.2	14.4	16.0	18.2	18.0	14.7	17.1
0	17.7	20.6	16.8	17.1	20.0	19.9	18.0	18.8
+ 1	20.8	24.6	19.4	18.2	21.9	22.0	21.9	20.8
2	24.3	29.3	22.6	18.4	24.0	24.3	26.2	22.8
3	28.5	34.9	26.2	50.1	....	....	30.9	41.6
4	33.4	41.7	30.5		....	....	36.0	44.0
5	39.2	49.8	35.3		....	....	41.2	46.3
6	....	59.4	41.0		....	....	46.7	48.9
7	....	....	47.6		....	....	52.0	51.6
8	....	....	55.3		41.9	44.2	57.3	54.4
9	....	....	....		45.9		62.2	57.5
+10	....	....	....	....	50.4		66.5	60.7
	θ = AVERAGE RADIAL VELOCITY							
− 2	12.5	13.6	14.6	9.0	17.8	10.2	14.3	16.2
− 1	13.3	14.9	15.8	11.4	19.0	14.3	15.4	16.6
0	14.1	16.4	17.1	14.6	20.2	20.1	16.6	17.1
+ 1	15.0	18.0	18.4	18.6	21.6	28.3	17.8	17.5
2	15.8	19.8	20.0	23.8	23.8	39.8	19.2	18.0
3	16.8	21.8	21.5	27.0	....	....	20.8	22.5
4	17.9	23.9	23.3		....	....	22.4	23.9
5	19.0	26.3	25.2		....	....	24.2	25.5
6	....	28.9	27.2		....	....	26.2	27.2
7	....	....	29.4		....	....	28.4	28.9
8	....	....	31.8		34.0	37.8	30.8	30.8
9	....	....	....	....	36.3		33.4	32.7
+10	....	....	....	....	38.7		36.3	34.8

From the equations of Tables II and III we obtain the values given in Table IV. The columns marked 1 and 2 under K, M, and All Types give the results derived from the two solutions, the first representing a continuous and the second a discontinuous variation.

The geometrical means of the space-velocities may be converted into arithmetical means by multiplication with the factor 1.186. The results are given in Table V, the values used being those derived from the first solution, based on the assumption of a continuous variation with absolute magnitude.

TABLE V

ARITHMETICAL MEAN OF SPACE-VELOCITY AND CORRECTED AVERAGE RADIAL VELOCITY

M	$\bar{v}$					θ				
	F	G	K	M	All	F	G	K	M	All
− 2	20.9	23.4	26.3	29.5	22.2	11.9	12.9	13.9	16.9	13.6
− 1	23.7	26.8	28.9	31.7	26.1	12.6	14.2	15.0	18.0	14.6
0	26.9	30.8	31.9	33.9	30.4	13.4	15.6	16.2	19.2	15.8
+ 1	30.6	35.5	34.9	36.3	34.9	14.2	17.1	17.5	20.5	16.9
2	34.7	40.8	38.4	38.9	39.7	15.0	18.8	19.0	21.8	18.2
3	39.5	46.8	42.2	......	44.7	16.0	20.7	20.4	......	19.8
4	44.8	53.8	46.4	......	49.7	17.0	22.7	22.1	......	21.3
5	50.8	61.9	51.0	......	54.7	18.0	25.0	23.9	......	23.0
6	......	71.2	56.0	......	59.5	......	27.5	25.8	......	24.9
7	......	......	61.6	......	64.2	......	......	27.9	......	27.0
8	......	......	67.6	59.2	68.2	......	......	30.2	32.3	29.3
9	......	......	......	63.5	71.8	......	......	......	34.5	31.7
+10	......	......	......	68.0	74.8	......	......	......	36.8	34.5

The average radial velocities θ are derived from stars north of $-30°$ declination with absolute magnitudes determined at Mount Wilson. Consequently, on account of the effect of stream-motion, the values of θ require a slight systematic correction if they are to be compared with values obtained from stars distributed over the whole sky. Allowance is made for the omission of stars in the area south of $-30°$ by multiplication with a factor 0.95 and the results of θ corrected in this way are also given in Table V.

The mean velocities for the giants and dwarfs separately have been computed for each spectral type and are given in Table VI.

It is of interest to compare the results for θ, the average radial velocity corrected for stream-motion, with those given by Campbell.[1] His values are:

F	G	K	M
14.4	15.9	16.9	17.1 km/sec.

The agreement is excellent if we assume the following mean absolute magnitudes for the stars of Campbell's list:

F, +1; G, 0; K, 0 to +1; M, −2.

These values of the mean absolute magnitudes for the stars observed by Campbell appear quite reasonable, except perhaps in the case of the stars of the M type. For these stars it seems probable that the systematic motions differ somewhat from those of other types, and hence our values of θ need a special correction in order to make them comparable with those obtained from stars distributed over the whole sky.

TABLE VI

SUMMARY OF RESULTS

		F	G	K	M
Giants	No.	152	216	320	114
$M<2.5$	$\overline{M}$	0.1	0.3	0.8	0.1
	$\underline{v}$	21.7	27.0	27.9	29.0
	v	25.7	32.0	33.1	34.4
	$\underline{T}$	18.0	21.7	18.2	20.0
	θ	14.1	17.4	18.2	21.4
Corrected	θ	13.4	16.5	17.3	20.3
Dwarfs	No.	191	184	148	18
$M>2.5$	$\overline{M}$	3.5	4.8	6.2	10.3
	$\underline{v}$	37.0	51.5	51.3	54.2
	$\bar{v}$	43.9	61.1	60.8	64.3
	$\underline{T}$	33.6	49.3	50.1	44.2
	θ	18.7	25.8	27.0	37.8
Corrected	θ	17.8	24.5	25.6	35.9

---

[1] *Lick Observatory Bulletin*, **6**, 125 (No. 196), 1911.

It has been shown by Campbell[1] that, if equal numbers of stars move in all directions, the average radial velocity should be exactly half the average space-velocity. This is strictly true only if stream-motion is neglected. A comparison of the results in Table V shows a remarkably close approach to this ratio among the giant stars. Thus for absolute magnitudes < 2 we find for the ratio of space-velocity to radial velocity the values:

F	G	K	M	All Types
2.02	1.98	1.96	1.77	1.92

In view of the uncertainties introduced by possible differences in the systematic motions not allowed for in the determination of the average radial velocity, these results are rather surprising.

For the dwarf stars the relationship holds much less closely, especially in types F and G. These stars in general have very high space-velocities, and, as will be shown in connection with an investigation of the directions of stellar motions, they exhibit very marked differences from the giants in their systematic motions.

The variation of velocity with spectral type among the giant stars is fully confirmed by these results, the space-velocities showing it quite as well as the radial motions. The latter values, as already noted, are in good agreement with those of Campbell, except possibly for the M-type stars where the difference from those of type K is somewhat larger. Among the dwarf stars, the existence of such a relationship is very doubtful and there even appears to be a tendency toward a reversal of the effect found for the giants, the F and G stars moving more rapidly than the K and M stars. As already stated, the largest space-velocities are found among the F and G types. In view of the peculiar character of the motions of the rapidly moving dwarf stars it seems very doubtful if we can distinguish a relationship dependent upon absolute magnitude without a further great addition to our observational material.

The values of the radial velocities shown in Table I among the very brightest stars of spectral types F and K and the Cepheid variables are quite comparable with those of stars of type B, and suggest that there is little variation with spectral type among such stars. The material, however, is insufficient for a definite conclusion. The space-velocities of these stars cannot well be compared, since they are affected systematically by any accumulation of errors in their parallaxes or proper motions.

---

[1] *Siellar Motions*, p. 215, 1914.

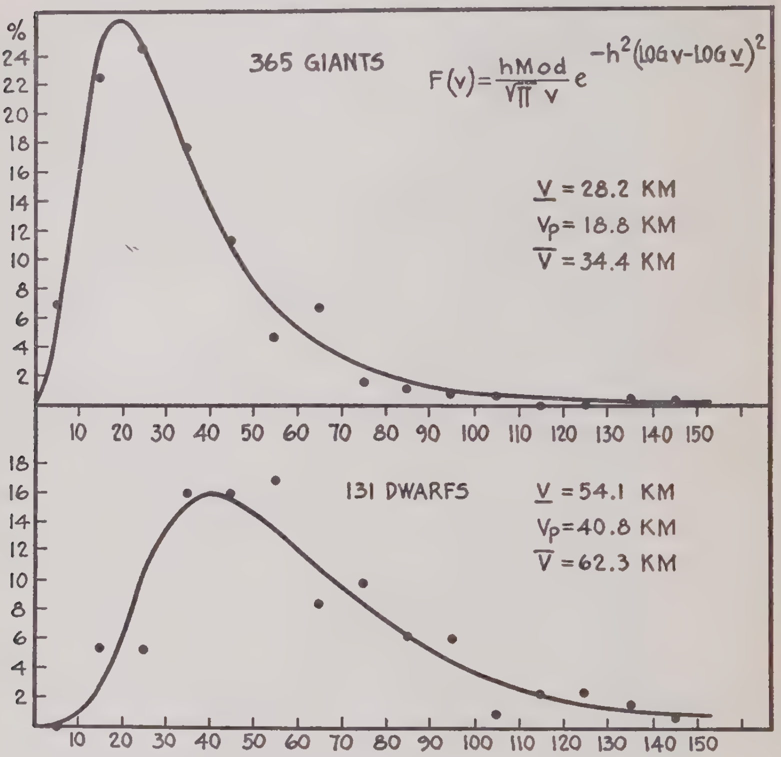

FIG. 2.—Frequency-curves for space-velocities of stars of spectral type K. Upper curve is based on 365 giant stars, lower curve on 131 dwarfs. Abscissae are space-velocities, ordinates are numbers of stars expressed in percentages of the whole within the limits of every 10 kilometers of space-velocity.

It is clear from the results of this investigation that the giant stars as a whole are much more homogeneous in character than the dwarf stars and show more clearly the effects of variation of velocity with absolute magnitude and spectral type. The latter show a much wider dispersion of velocities and are subject to systematic motions differing from those of the giant stars. This is perhaps to be expected if the masses of the giant and dwarf stars differ to any considerable extent.

THE FREQUENCY-LAW OF SPACE-VELOCITIES

It is of interest to compare the observed distribution of these space-velocities with that given by Maxwell's law. This assumes a random distribution in direction and contains a single constant, the modulus *h*, in the equation

TABLE VII

Comparison of Frequency of Space-Velocities with That Given by Maxwell's Law

v	F Type $M=2.5$ to 5.7		G Type $M=-1.5$ to $+2.5$		G Type $M=3.5$ to 6.6		K Type $M=-4.0$ to $+2.5$		K Type $M=5.5$ to 9.7		M Type $M=-3.8$ to $+1.5$	
	N_o	N_c	N_o	N_c	N_o	N_c	N_o	N_c	N_o	N_c	N_o	N_c
km/sec.												
0–20....	33	33	55	55	14	14	107	107	7	7	30	30
20–40....	90	90	101	101	39	39	154	154	28	28	57	57
40–60....	41	39	30	20	45	17	58	19	43	27	23	13
60–80....	16	5	17	1	33	2	30	0	24	11	7	1
>80....	47	0	12	0	49	0	16	0	29	2	6	0
Total..	227	167	215	177	180	72	365	280	131	75	123	101
h......	0.0352		0.0428		0.0351		0.0472		0.0263		0.0417	
Excess in per cent..	36		22		151		30		76		22	

$$F(v)dv=\frac{4h^3}{\sqrt{\pi}}e^{-h^2v^2}v^2\,dv\,.$$

Determining the value of *h* from the numbers of velocities between 0 and 20 km and 20 and 40 km, we obtain the results shown in Table VII. N_o and N_c denote the numbers of observed and computed velocities within the limits given.

This comparison at once shows a large excess in the number of observed high velocities over that required by Maxwell's law. It is especially marked among the dwarf stars and is probably due to the fact that a strong correlation exists among the three components of space-velocities, a large component along one axis being in general related to large components along the other two axes. Maxwell's function is based upon the assumption that the three components are independent of one another.

A type of frequency-function which represents much better the observed distribution of space-velocities is one based upon the assumption of a normal error-distribution of the logarithms of the velocities.[1] If we transform such a function into one expressing the frequencies of the velocities themselves instead of their logarithms, we obtain the form

$$F(v)dv=\frac{h\,\mathrm{Mod}}{\sqrt{\pi}\,v}e^{-h^2(\log v-A)^2}dv\,,$$

the logarithms here having the base 10.

This function contains two constants, h and A, the former of which is related to the probable error in the difference $\log v-A$ by the equation

$$r=\frac{0.6745}{\sqrt{2}\,h}\,.$$

The quantity A is the algebraic mean of the logarithms of the space-velocities, or,

$$A=\overline{\log v}=\log \underline{v}\,,$$

where $\underline{v}$ represents the geometrical mean of the velocities.

The arithmetical mean $\bar{v}$ and the most probable value v_p are related to $\underline{v}$, h, and r by the expressions

$$\log \bar{v}=\log \underline{v}+\frac{1}{4h^2\,\mathrm{Mod}}=\log \underline{v}+2.530\,r^2,$$

$$\log v_p=\log \underline{v}-\frac{1}{2h^2\,\mathrm{Mod}}=\log \underline{v}-5.061\,r^2.$$

Hence

$$v_p<\underline{v}<\bar{v}.$$

---

[1] Another type of frequency-function, involving only one constant, which represents the distribution nearly as well as the logarithmic one, is

$$F(v)dv=\frac{h^3}{2}v^2e^{-hv}dv\,.$$

This gives

$$\bar{v}=\frac{3}{h}\,,\quad v_p=\frac{2}{h}\,.$$

Table VIII shows how this frequency-function represents the observed velocities. The stars have been grouped according to spectral type and absolute magnitude. In the case of the F-type stars it was found necessary to use the sum of two frequency-functions, since there exists in this type a special group of stars of absolute magnitudes between 3 and 5 with velocities ranging from 160 to nearly 1000 km.

TABLE VIII

FREQUENCY OF SPACE-VELOCITIES ACCORDING TO LOGARITHMIC FUNCTION

v	F Type $M=2.5$ to 5.7		G Type $M=-1.5$ to $+2.5$		G Type $M=3.5$ to 6.6		K Type $M=-3.5$ to $+2.5$		K Type $M=5.5$ to 9.7		M Type $M=-3.8$ to $+1.5$	
	N_o	N_c	N_o	N_c	N_o	N_c	N_o	N_c	N_o	N_c	N_o	N_c
km												
0– 10......	3	3.7	16	8.4	3	0.7	25	18.6	0	0.1	6	3.8
10– 20......	30	31.7	39	49.2	11	9.9	82	88.7	7	3.8	23.5	26.8
20– 30......	53	44.9	59	54.0	17	20.7	89	89.4	7	13.5	37.0	31.8
30– 40......	37	38.7	42	38.7	21.5	24.9	65	62.5	21	19.9	20.5	23.1
40– 50......	29	28.2	17	24.5	22.5	23.4	41	39.4	21	20.5	14	14.6
50– 60......	12	19.2	13	15.0	23	20.1	17	24.1	22	17.8	9	8.9
60– 70......	10	12.9	7	9.1	18.5	16.6	24	14.9	11	14.3	5	5.3
70– 80......	6	8.7	10	5.8	14.5	13.1	6	9.2	13	10.8	2	3.2
80– 90......	9	5.8	1	3.4	16	10.6	4	6.2	8	8.2	1	1.9
90–100......	8	3.9	1	2.4	10	8.1	3	3.6	8	5.9	2	1.3
100–110......	2	2.7	2	1.5	7	6.3	2	2.6	1	4.3	0	0.7
110–120......	2	1.8	0	0.8	4	5.1	0	1.8	3	3.1	0	0.6
120–130......	1	1.3	2	0.7	3	4.1	0	1.1	3	2.4	0	0.3
130–140......	1	1.1	1	0.4	2	3.1	1	0.7	2	1.6	0	0.2
140–150......	2	0.7	4	0.2	1.5	2.5	1	0.7	1	1.3	1	0.1
150–200......	9	2.5	1	0.9	5.5	10.8	5	1.5	3	3.5	2	0.4
200–250......	0	2.6										
250–300......	2	3.4										
300–350......	2.5	3.4										
350–400......	2.5	3.0										
400–450......	2	2.2										
450–500......	1	1.7										
>500........	3	2.9										
Totals....	227	227.0	215	215.0	180	180.0	365	365.0	131	131.0	123	123.0

The constants of the frequency-function $\underline{v}$ and r, together with the arithmetical mean $\bar{v}$ and the most probable velocity v_p, are given in Table IX.

The marked difference in space-velocity between the giant and dwarf stars is shown clearly in the results of Table IX.

The principal results of this investigation may be summarized as follows:

1. The average space-velocities of the stars of types F, G, K, and M vary with absolute magnitude to a marked degree. The increase of velocity with decreasing brightness is most regular

among the giant stars. Among the fainter dwarf stars, if the effect is present, it is concealed in large measure by the individual peculiarities of motion.

2. The tangential and radial velocities show results similar to those obtained from the space-velocities.

3. The increase in average space-velocity is about 3 km/sec. for a decrease of one magnitude in brightness. In the radial velocity the increase is 1.2 km/sec.

TABLE IX

CONSTANTS OF LOGARITHMIC FREQUENCY-FUNCTION

Type	m	$\underline{v}$	r	v_p	$\bar{v}$	No.
		km		km	km	
F..........	+2.5 to +5.7	35.6	0.178	24.6	42.8	207
F..........	+2.5 to +5.7	346.0	0.104	306.0	368.0	20
G..........	−1.5 to +2.5	29.1	0.178	20.1	35.0	215
G..........	+3.5 to +6.6	55.0	0.190	36.2	67.7	180
K..........	−3.5 to +2.5	28.2	0.185	18.8	34.4	365
K..........	+5.5 to +9.7	54.1	0.156	40.8	62.3	131
M..........	−3.8 to +1.5	29.7	0.171	21.1	35.2	123

4. The average space-velocity of the giant stars is very nearly twice the average radial velocity, a result which would follow strictly if equal numbers of stars moved in all directions.

5. The variation of velocity with spectral type is well marked among the giant stars, but is much less certain among the dwarfs.

6. The very brightest stars intrinsically of all the spectral types appear to have nearly equal radial velocities.

7. The greater homogeneity of the giant stars as a class and their comparative freedom from large individual motions are indicated by these results. The dwarf stars show a very wide dispersion in motions.

8. The frequency of the space-velocities cannot be represented adequately by a distribution according to Maxwell's law, there being a large excess of high velocities. A type of frequency-function based upon the assumption of a normal error-distribution in the logarithms of the velocities is found to satisfy the observations in a much better way.

MOUNT WILSON OBSERVATORY
April 1921

Contributions from the Mount Wilson Observatory, No. 211
Reprinted from the *Astrophysical Journal*, Vol. LIV, pp. 28–44, 1921

THE ELECTRIC-FURNACE SPECTRUM OF SCANDIUM

By ARTHUR S. KING

ABSTRACT

Spectrum of scandium in arc and in electric furnace, λ 3015 to 6559 A.—A highly purified sample of scandia, prepared by Sir William Crookes, was placed in a graphite boat in the tube-resistance furnace operated as usual at low pressures. The relative *intensities* of 307 lines on grating spectrograms, obtained with the furnace at a temperature of 2000, 2250, or 2600° C. and with a carbon arc containing scandia, are recorded in Table I, together with the *classification* of each according to its behavior in furnace and arc. About 25 lines enhanced in the spark and 150 lines enhanced in the furnace are indicated by E and A respectively. The 29 arc-flame lines are all A lines but are scattered through temperature classes I to III; they cannot be due to oxidation, since none took place in the furnace. On the other hand, since the band lines are practically absent from furnace spectra, they are probably due to the oxide. These results are of great interest in *relation to solar and sun-spot spectra.* The A lines and low temperature furnace lines are absent or very weak in the solar spectrum but are prominent in the sun-spot spectrum.

Zeeman effect for scandium lines in sun-spot spectra is large and apparently uniform. Laboratory observations are lacking at present.

Observations as to chemical properties of scandium.—The scandia fused in the furnace seemed to form a carbide with the graphite boat. The shining black residue turned to a gray-brown powder after exposure to the air, presumably from the reabsorption of oxygen.

Scandium occurs in small amounts in a number of the rare-earth minerals, but its extraction in a fair degree of purity is an exceedingly difficult matter, and, as its separation has not been stimulated by any commercial application, the substance is extremely scarce. The late Sir William Crookes[1] described his examination of a large number of minerals in a search for those containing scandium. Wiikite, found in Finland, proved to contain over 1 per cent of scandium oxide (scandia) and was used by him to furnish pure scandia. The final difficulty in the tedious process of separation was the elimination of the closely related elements yttrium and ytterbium.

The spectrum of scandium is especially interesting on account of the peculiar intensity relations, to be discussed presently, among the scandium lines in the solar spectrum. An examination of the behavior of the lines at various temperatures of the electric furnace was therefore desirable, in order to determine the part which temperature may play in bringing about the peculiarities observed.

---

[1] *Philosophical Transactions*, A, **209**, 15, 1909.

Through the good offices of Professor Fowler, I have been able recently to obtain a sufficient amount of highly purified scandia to carry out the examination of the furnace spectrum. This scandia was prepared by Sir William Crookes. His former assistant, Mr. J. H. Gardiner, very kindly placed the material at my disposal through Professor Fowler.

In the earlier solar investigations in which the spot spectrum was studied it was noted that certain lines intensified in the spot coincided with lines in the scandium arc, while other strong arc lines were absent in the spot, though present in the solar spectrum and prominent in the chromosphere. Fowler[1] explained this phenomenon by producing, besides the regular arc spectrum, the spectrum of the arc in hydrogen, which approaches that of the spark, and the spectrum of the flame of the arc, in which certain lines are given a high intensity. His results showed clearly that the lines prominent in the spot spectrum are those given by the flame of the arc and probably result from a reduced temperature in the spot, while the scandium lines missing from the spot spectrum are enhanced lines, though present often with considerable intensity in the arc. The occurrence of three distinct types, enhanced, arc, and flame lines, in the scandium arc is a feature shown by some other elements, notably titanium, the low-temperature lines of which have been selected by the furnace,[2] while many lines prominent in the arc are much enhanced in the spark.

EXPERIMENTAL METHOD

The tube-resistance furnace was operated as usual, the chamber being pumped out to a few millimeters' pressure. To avoid scattering of the scandia in the tube, the powder was put in a small combustion boat of graphite, which was placed at the middle of the furnace-tube. The image of the space above this boat was focused on the slit of the spectrograph. The scandia fused in the boat, entering to some extent into the graphite as if a carbide were formed. The fused residue was a shining black when removed from the tube, but after exposure to the air for some time turned to a gray-brown powder, presumably from the reabsorption of oxygen.

---

[1] *Philosophical Transactions*, A, **209**, 47, 1909.

[2] *Mt. Wilson Contr.*, No. 76; *Astrophysical Journal*, **39**, 139, 1914.

The spectrograms were made with a 15-foot concave-grating spectrograph, the second order with a dispersion of 1 mm = 1.86 A being used for the ultra-violet, and the first order for the region from λ 3800 into the red.

EXPLANATION OF THE TABLE

The method followed in the study of the furnace spectrum of scandium was the usual one of selecting three temperature stages, the lowest of which gives a small number of distinctive lines. These lines are of two kinds, some remaining practically unchanged or even losing in strength as the temperature is increased, while others strengthen with rising temperature and frequently show wide reversals. These two kinds of lines are given in Table I as belonging to Class I and Class II respectively.

A higher stage, designated as medium temperature, brings out a large number of lines, placed as a rule in Class III, while a still higher temperature gives the lines of Class IV. Still other lines, which are absent or very faint in the high-temperature furnace, go into Class V. The furnace temperatures required to bring out lines of these various classes differ with different elements. For scandium the three stages selected were 1900° to 2000° C. for the low, 2250° for the medium, and 2600° for the high temperature.

In Table I, the wave-lengths in the first column are those of Exner and Haschek[1] for the arc spectrum. The arc wave-lengths measured by Fowler[2] cover the visible spectrum beginning at λ 3934 and include some lines not measured by Exner and Haschek. The wave-lengths, according to Fowler, of such lines are denoted by a dagger. The enhanced lines of scandium form an important class. I have taken Fowler's selection of these and designated them by "E" after the class-number. Finally, a large proportion

---

[1] *Spektren der Elemente bei normalem Druck*, Leipzig, 1911.

[2] *Loc. cit.*

TABLE I

TEMPERATURE CLASSIFICATION OF SCANDIUM LINES

λ Exner and Haschek	Arc Intensity	Furnace Intensities			Class
		High Temperature	Medium Temperature	Low Temperature	
3015.50*....	8	5r	3	2	II
3019.48*....	10	5r	3	2	II
3030.87*....	3	2	2	1	II
3040.03*	....	1	1	....	III A
3056.37.....	1	1	....	....	IV
3251.43.....	1	1	....	....	IV
3255.81.....	6	15r	10r	10	I A
3270.08......	15	40R	30R	15	II A
3273.79.....	20	50R	50R	20	II A
3333.67.....	1	5	2	....	III A
3343.42*....	1	4	1	....	III A
3349.36.....	1	4	1	....	III A
3351.34.....	1	3	....	....	IV A
3352.19.....	2	1	....	....	IV
3353.90.....	10	8	8	1	III
3359.84.....	6	6	4	....	III
3361.48.....	6	6	4	....	III
3362.12.....	6	6	4	....	III
3365.01.....	1	5	2	....	III A
3369.13.....	8	8	6	....	III
3372.33.....	12	10	10	1	III
3386.02.....	1	2	tr	....	IV A
3416.80.....	2	4	2	....	III A
3429.34......	3	8	5	....	III A
3429.61.....	3	8	5	....	III A
3431.50.....	3	8	6	....	III A
3435.68.....	5	12	10	....	III A
3439.55.....	1	3	1	....	III A
3440.31.....	1	5	2	....	III A
3444.13.....	1	4	1	....	III A
3448.62.....	1	4	1	....	III A
3457.56.....	3	8	5	....	III A
3462.30.....	2	5	3	....	III A
3469.76.....	1	4	2	....	III A
3469.84.....	1	3	1	....	III A
3499.05.....	2	6	4	....	III A
3535.89.....	6	7	6	....	III
3558.69*....	7	8	8	3	II
3567.89.....	6	6	4	2	II
3572.73.....	20	20	20	10	II
3576.53.....	8	10	10	4	II
3581.11.....	7	8	10	4	II
3589.81.....	6	6	5	2	II
3590.67.....	6	6	5	2	II
3614.00.....	30	25	25	15	II
3630.93.....	12	12	15	8	II
3635.45*....	1	?	1	....	III
3642.99.....	25	20	20	7	II
3645.50.....	10	15	8	2	III
3647.05.....	1	4	1	....	III A

TABLE I—*Continued*

λ Exner and Haschek	Arc Intensity	Furnace Intensities			Class
		High Temperature	Medium Temperature	Low Temperature	
3652.01	7	8	6	2	III
3657.75	tr	3	1	...	III A
3666.68	2	3	1	...	III
3895.11	1	2	tr	...	IV A
3907.69	75	75R	60	15	II
3912.03	100	100R	80	15	II
3915.09	tr	1	...	...	IV A
3933.59	20	25r	15	10	II
3952.43	1	2	...	...	IV A
3996.79	30	30r	20	20	I
4014.68	5	3	tr	...	IV E
4020.60	75	75R	60	40	II
4023.36*	2	5?	1	...	III A
4023.88	100	100R	80	40	II
4031.51	2	5	3	...	III A
4034.35	2	4	1	...	III A
4036.98	2	1	...	...	IV
4043.97	2	6	3	...	III A
4046.64	2	7	3	...	III A
4047.98	25	25r	25	20	I
4050.09	2	5	2	...	III A
4052.00	1	2	tr	...	IV A
4054.71	35	40R	40	40	I
4056.72	4	8	4	...	III A
4067.15	2	6	3	...	III A
4075.13	2	7	3	...	III A
4078.70	2	6	3	...	III A
4082.60	40	30R	40	50	I
4086.15	1	3	1	...	III A
4086.80	4	5	3	...	III
4087.28	8	7	5	...	III
4095.03	1	4	1	...	III A
4133.10	8	8	7	...	III
4140.42	10	8	7	...	III
4152.51	12	10	8	...	III
4165.39	12	10	10	...	III
4171.92	1	3	2	...	III A
4218.43	2	6	2	...	III A
4219.90	2	7	2	...	III A
4222.07†	1	3	tr	...	IV A
4225.76*	2	5?	2	...	III A
4232.13	2	5	1	...	IV A
4233.83	3	8	2	...	III A
4237.96	2	3	tr	...	IV
4238.21	6	10	5	...	III
4239.72	2	5	1	...	IV A
4246.27	1	5	1	...	IV A
4247.02	75	10	10	...	III E
4259.86†	1	1	...	...	IV
4283.71	2	6	1	...	IV A
4286.71	1	5	tr	...	IV A
4294.94	10	2	...	...	IV E

TABLE I—*Continued*

λ Exner and Haschek	Arc Intensity	Furnace Intensities			Class
		High Temperature	Medium Temperature	Low Temperature	
4305.89	10	2	....	....	IV E
4314.31	100	10	5	....	III E
4320.98	75	9	4	....	III E
4325.22	50	8	3	....	III E
4348.67	tr	2	....	....	IV A
4352.28	tr	2	....	....	IV A
4354.79	8	....	....	....	V E
4358.85	4	10	3	....	III A
4359.25	2	4	1	....	III A
4359.81	1	2	tr	....	IV A
4365.08	1	3	2	....	III A
4374.69	60	8	3	....	III E
4375.32	1	4	1	....	III A
4381.41	tr	3	1	....	III A
4384.98*	8	?	?	....	IV E ?
4389.76	2	6	1	....	IV A
4400.63	50	7	2	....	III E
4415.78	40	7	2	....	III E
4431.52	4	....	....	....	V E
4542.74	2	8	3	....	III A
4544.86*	5	10	4	....	III A
4557.45	5	7	2	....	III
4574.20	6	8	3	....	III
4579.13	1	6	1	....	IV A
4593.15	3	3	tr	....	IV
4598.32	1	3	tr	....	IV A
4598.63	3	5	1	....	IV
4604.89	(1)	6	1	....	IV A
4609.69	(0)	6	2	....	III A
4610.15	(0)	4	1	....	III A
4670.60*	15	?	....	....	IV E
4709.51	5	4	2	....	III
4721.00	(0)	6	3	....	III A
4728.98	5	8	8	tr	III
4729.40	30	20	25	3	III
4732.48*	2	5 ?	?	....	IV A
4734.30	15	15	20	4	III
4737.83	20	18	20	6	III
4741.23	30	30	30	8	III
4744.03	40	40	40	10	III
4746.31	(1)	3	tr	....	IV A
4749.15	(1)	2	....	....	IV A
4753.34	15	20	60	150	I A
4759.15	(1)	4	1	....	III A
4763.30	(3)	7	1	....	IV A
4771.67	(1)	2	....	....	IV A
4779.59	20	25	80	200	I A
4791.74	4	20	20	20	I A
4793.10	(0)	tr	....	....	IV
4827.48	4	12	3	....	III A
4833.86	2	10	3	....	III A
4839.63	10	20	8	....	III A

TABLE I—*Continued*

λ Exner and Haschek	Arc Intensity	Furnace Intensities			Class
		High Temperature	Medium Temperature	Low Temperature	
4840.65	2	6	tr	....	IV A
4841.04*	tr	4	2?	....	III A
4847.88	3	10	3	....	III A
4852.88	2	10	3	....	III A
4859.35†	(0)	2	....	....	IV A
4878.32	(2)	4	tr	....	IV
4880.93	(1)	5	tr	....	IV A
4890.54	(1)	3	....	....	IV A
4893.20	(1)	4	tr	....	IV A
4906.87	(2)	15	3	....	III A
4909.95	3	25	6	....	III A
4923.03	(2)	20	5	....	III A
4934.30*	(1)	5?	1	....	IV A
4935.95	(1)	4	1	....	III A
4941.51	2	10	3	....	III A
4951.46†	(1)	7	1	....	IV A
4951.84	(1)	6	1	....	IV A
4954.22	5	30	7	....	III A
4973.84	3	12	4	....	III A
4980.51	4	15	4	....	III A
4983.60*	2	20	3	....	III A
4992.14	5	15	3	....	III A
4995.24	(1)	7	1	....	IV A
5018.56	(2)	8	2	....	III A
5020.31	(2)	3	....	....	IV
5021.70	(2)	5	....	....	IV A
5031.23	10	1	....	....	V E
5032.90	(1)	2	....	....	IV
5064.51	10	15	5	tr	III
5069.05	2	2	1	....	III
5070.42	40	30	10	1	III
5076.00	10	10	4	tr	III
5081.80	125	40	40	20	II
5083.93	80	30	30	12	II
5085.75	40	15	15	6	II
5087.18*	40	?	15	6	II
5087.32*	10	?	1	....	IV?
5090.10	8	5	1	....	IV
5092.63*	1	3?	....	....	IV A?
5096.92	30	15	4	1	III
5099.41*	40	30?	8	2	III
5101.30*	20	25?	5	1	III
5109.25*	3	?	1	....	III
5113.05*	4	?	1	....	III
5116.89*	10	?	2	....	III
5210.70	20	15	1	....	IV
5211.50	(0)	2	....	....	IV A
5219.06†	(0)	1	....	....	IV
5219.79	10	10	1	....	IV
5240.00	2	1	....	....	IV E
5258.51	15	15	1	....	IV
5285.15	tr	2	....	....	IV A

TABLE I—*Continued*

λ Exner and Haschek	Arc Intensity	Furnace Intensities			Class
		High Temperature	Medium Temperature	Low Temperature	
5285.91	10	10	1	....	IV
5302.15	2	60	20	12	II A
5314.91†	tr	2	....	....	IV A
5315.77†	tr	2	....	....	IV A
5318.53	1	tr	....	....	IV E
5323.26†	tr	3	....	....	IV A
5323.94†	(0)	tr	....	....	IV
5331.95	3	10	1	....	IV A
5334.40	tr	1	....	....	IV A
5339.56	8	12	2	....	IV
5341.20	8	12	2	....	IV
5343.13	10	50	40	30	II A
5349.49	50	20	5	....	III
5349.88	15	70	50	40	II A
5350.45	4	10	1	....	IV A
5355.92	8	10	2	....	III
5356.26	60	30	6	1	III
5375.52	20	20	4	....	III
5392.28	30	30	5	tr	III
5416.32	2	2	1	....	III
5425.76	2	3	1	....	III
5429.65	2	3	1	....	III
5433.45	2	2	1	....	III
5438.50	1	2	1	....	III A
5439.24	2	3	1	....	III
5442.80	2	3	1	....	III
5446.41	20	20	4	....	III
5447.66†	1	1	....	....	IV
5451.55	6	12	2	....	III A
5455.50	1	2	1	....	III A
5465.44	tr	1	....	....	IV A
5468.63	2	2	1	....	III
5472.42	3	3	1	....	III
5482.20	100	40	15	3	III
5484.80	80	30	10	2	III
5514.41	80	30	10	2	III
5520.71	100	40	15	3	III
5527.04	10	....	....	....	V E
5541.19	3	3	....	....	IV
5546.63†	1	1	....	....	IV
5565.10	4	10	2	....	III A
5591.55	15	30	3	....	IV A
5604.35	1	1	....	....	IV
5624.08†	1	1	....	....	IV
5631.23*	1	3?	....	....	IV A?
5641.18	2	....	....	....	V E
5646.58	4	5	1	....	IV
5647.78†	1	2	....	....	IV A
5649.75	6	10	1	....	IV
5658.13	15	tr	....	....	V E
5658.56	2	....	....	....	V E
5661.86†	tr	1	....	....	IV A

TABLE I—*Continued*

λ Exner and Haschek	Arc Intensity	Furnace Intensities			Class
		High Temperature	Medium Temperature	Low Temperature	
5667.38......	2	....	....	....	V E
5669.26.....	2	2	....	....	IV E
5672.05.....	200	200	200	60	II
5684.41.....	8	tr	....	....	V E
5687.06.....	150	125	125	40	II
5691.55†....	(0)	tr	....	....	IV
5700.35.....	100	100	100	30	II
5708.81.....	15	100	10	3	III A
5711.99.....	100	200	150	20	III A
5717.51.....	15	100	10	3	III A
5721.20†....	tr	tr	....	....	IV
5724.30.....	15	100	10	3	III A
5739.53†....	2	4	tr	....	IV A
5741.56†....	1	5	1	....	IV A
5894.83†....	(2)	3	tr	....	IV
5919.21†....	tr	5	tr	....	IV A
5961.65†....	4	4	tr	....	IV
5969.37†....	3	3	tr	....	IV
5988.71.....	20	30	3	....	IV
6021.92†....	(0)	1	....	....	IV
6026.37.....	15	20	2	....	IV
6146.50†....	(3)	20	2	....	IV A
6193.94†....	(3)	100	100	40	II A
6198.69.....	(2)	10	1	....	IV A
6210.85.....	200	500	500	800	I A
6239.64*....	20	500	500	200	II A
6240.00.....	100	200	200	500	I A
6245.83.....	8	tr	....	....	V E
6250.15.....	15	20	1	....	IV
6259.20.....	100	300	300	400	I A
6262.50.....	10	15	1	....	IV
6273.37†....	(0)	tr	....	....	IV
6276.52.....	15	300	200	100	II A
6284.66†....	5	5	tr	....	IV
6293.30.....	(2)	4	tr	....	IV
6298.00†....	(0)	tr	....	....	IV
6305.94.....	400	500	600	1500	I A
6306.26*....	20	100	100	100	I A
6332.48.....	(1)	2	tr	....	IV
6345.06.....	5	100	75	50	II A
6379.07.....	40	300	300	300	I A
6396.62.....	2	2	tr	....	IV
6403.35.....	2	2	....	....	IV
6408.67.....	(1)	1	....	....	IV
6413.57.....	50	400	400	400	I A
6448.42†....	1	100	50	20	II A
6486.56†*...	(0)	2 ?	....	....	IV A ?
6525.84†*....	(3)	1 ?	....	....	IV ?
6558.28†*....	15	3 ?	tr	....	IV

λ	REMARKS
3015–3040.	Weakened at high temperature through incipient absorption and appear readily in absorption when continuous ground is present. λ 3040 is faint in arc, given intensity 1 by Exner and Haschek.
3343.	Probably double.
3559.	Blend Ti. Probable intensity of Ti line subtracted.
3635.	Blend with impurity line at high temperature.
4023.36.	Blend with λ 4023.88 at high temperature.
4226.	Blend with impurity line at high temperature.
4385.	Blend V. Very faint in furnace.
4545.	Blend Ti. Probable intensity of Ti line subtracted.
4671.	Blend V. Faint if present in furnace.
4732.	Disturbed by carbon.
4841.	Blend Ti at medium temperature.
4934.	Slightly affected by Ba blend.
4984.	Probably double.
5087–5117.	Disturbed by carbon.
5631.	Disturbed by carbon.
6239.64.	Measured in low-temperature furnace.
6306.26.	Measured in low-temperature furnace.
6487, 6526, 6558.	Disturbed at high temperature by band lines probably due to carbon.

of the scandium lines are found to be relatively strong in the furnace, at least at high temperatures, as compared with the arc. These are indicated by "A" after the class-number. The large number of these lines results in a measure from the choice of standard intensities in the arc and furnace spectra, but is chiefly due to the fact that there is less contrast among the scandium lines in the furnace than in the arc. Consequently faint arc lines often come out distinctly in the furnace, and if such lines were given the same intensity in arc and furnace very high values would have to be assigned to the stronger lines in the arc. The general meaning of "A" after the class-number then is that the furnace conditions are relatively favorable for the line in question.

The arc intensities entered in the second column were estimated from photographs taken with scandia in the carbon arc. Not desiring to use much scandia for a minor part of the investigation, I made but one set of arc spectrograms; consequently there was no variation of the arc conditions. Some of the fainter arc lines measured by Exner and Haschek and by Fowler did not show in my arc spectra, usually on account of disturbance by the prominent flutings. In such cases the arc values, usually from Fowler's list, are entered in parentheses.

An asterisk adjacent to the wave-length in Table I refers to a note among the "Remarks" at the end of the table. When a trace only of a line is to be seen, the intensity is denoted by "tr."

DISCUSSION

1. *Noteworthy lines of scandium.*—The temperature of approximately 2000°, designated as "low" for scandium, is about the same as has been employed as a medium temperature for several elements previously studied, so that the occurrence of low-temperature lines at wave-lengths as short as λ 3000 presents no anomaly. λ 2980.87 is probably to be classed with λλ 3015.50 and 3019.48, as it appeared at 2000°, but it is too near the end of the plates to show on those taken at higher temperature. λλ 3255.81, 3270.08, 3273.79 are strong and easily reversible lines. They maintain about the same relative strength except at low temperature, when the persistence of the first of the group justifies placing it in Class I. In this region, and throughout the spectrum, many lines remain about as strong at 2300° as at 2600°. Plates taken at 2100° showed lines of this type just appearing. Their absence in most cases at 2000° causes them to be placed in Class III.

Several strong lines occur in the violet, from λ 3908 to λ 4083. These are strong in the arc and reverse in the furnace at high temperature, retaining a considerable intensity at lower temperatures. From λ 4100 to λ 4700, the furnace gives no strong lines, and such lines as appear do not show at low temperature. The strong lines given in this region by the arc are uniformly classed as enhanced lines. Near λ 4750 a prominent group occurs, including the remarkable Class I lines λλ 4753.34 and 4779.59. These are not notably strong at high temperature, though their low density is caused partly by the beginning of reversal. At low temperature, however, they are much the strongest lines of the region, indeed, of the whole visible spectrum, with the exception of the very strong lines in the red.

Through the green and yellow the prominent lines are mostly arc lines which diminish gradually in strength with decreasing furnace temperature.

The region from λ 6146 to λ 6448 contains some very noteworthy lines. The stronger ones are relatively stronger in the furnace than in the arc. Two of them, λλ 6240 and 6306, have faint companions in the arc which have not previously been measured. These weak companions attain high intensities in the furnace and were measured on low-temperature furnace plates as λ 6239.64 and λ 6306.26. The lines in this red group are of three types, Class II and two varieties of Class I lines, some of the latter having about equal strength at all temperatures, and others being very strong at low temperature. A contrast between these two kinds of Class I lines is offered in the close pair λ 6305.94 and λ 6306.26, the former becoming three times as strong at low temperature as at high, while the latter retains the same strength at all the three temperatures. Especially notable is λ 6448.42. This has been measured in the arc only by Fowler. I have found it as a very faint line on a strong arc spectrum. In the furnace it is strong at all temperatures, but shows the behavior usually associated with strong arc lines, falling off rapidly with decreasing temperature. Fowler does not include it among the lines strong in the flame of the arc. It is difficult to account for a line of this type on the basis of dependence on intensity of excitation, as the arc conditions are distinctly unfavorable for it and it is relatively weak also at the low furnace temperatures. There being no reason to ascribe the line to an impurity, it must for the present be regarded as especially sensitive to some feature peculiar to the furnace radiation. λ 6345.06 shows a similar, though less pronounced, behavior in arc and furnace.

In addition to this type we have all gradations of intensity at different furnace temperatures for lines which are faint in the arc. Those of Class I A may be regarded as responding especially to low temperature. The many lines belonging to Class IV A, which, while faint in the arc, are strong at high furnace temperature, appear to respond only to a limited range of excitation.

2. *Enhanced lines.*—In the scandium spectrum we find the furnace able to produce with considerable intensity a number of enhanced lines. Of those given by Fowler in the visible region, and sufficiently strong in the arc to be entered in my list, 10 are in

Class V, 8 in Class IV, and 7 in Class III. This means that at 2250° some enhanced lines are given distinctly by the furnace. In most cases these are much stronger at 2600°, though λ 4247 is an exceptional line showing about the same strength at both temperatures. In every case the relative intensity in the arc as compared with the furnace is much greater than that of the regular arc lines.

In the furnace data given here and previously we have a confirmation of the view regarding enhanced lines expressed by Fowler in his paper on the scandium spectrum.[1] He called attention to the fact that in the spectra of titanium, calcium, strontium, and barium, as well as of scandium, the arc gives strong lines which have all the characteristics of enhanced lines. The furnace results show the relation among the enhanced lines of these several elements. Those of titanium[2] are just visible in the high-temperature furnace and are placed in Class V. Some of the scandium enhanced lines appear at medium temperature and go into Class III, while the H and K lines of calcium and the homologous pairs of strontium and barium[3] persist with considerable strength at temperatures as low as 1650°, and on account of their rapid increase at higher temperatures and in the arc are assigned to Class II.

Enhanced lines of different elements thus differ greatly as to the excitation required for their initial appearance. When given at all by the furnace, they agree in their rapid strengthening with increase of temperature and in the arc and finally in the great intensification shown in the spark. The last feature distinguishes them from the large group of high-temperature lines which in laboratory sources reach their maximum intensity in the arc and are unaffected or even weakened in the spark.

3. *Comparison of arc-flame and low-temperature furnace lines.*—By proper manipulation of the arc, a spectrum from the outer vapors can often be obtained which differs materially from that of the vapor in the direct path between the electrodes. The lines relatively strong in this "arc flame" are usually considered as the low-temperature lines, though in the arc the action of temperature

---

[1] *Op. cit.*, p. 52.

[2] *Mt. Wilson Contr.*, No. 76; *Astrophysical Journal*, **39**, 139, 1914.

[3] *Mt. Wilson Contr.*, No. 150; *Astrophysical Journal*, **48**, 13, 1918.

may be complicated by the vigorous oxidation taking place in the enveloping vapor.

Fowler[1] lists 29 of the principal arc-flame lines of scandium for the visible region and compares them with the corresponding sun-spot lines. All of these are strong in the furnace, usually at low temperature, though some belong in Class III. These lines, however, are strong also in the regular spectrum of the arc, in which the radiation of flame and core are superposed. In the same region the furnace gives 13 strong furnace lines not in Fowler's list. These are often stronger at low temperature than some of the arc-flame lines. All of them, however, are relatively weak in the arc, being lines with "A" after the class-number. This comparison shows how far the arc flame may be used to select low-temperature lines and also its limitation in this respect, in that it does not bring out with any notable intensity those lines which are faint in the core of the arc and, for some reason at present obscure, are strong in the furnace spectrum.

In the iron spectrum, the degree of extension into the flame of the arc of the various classes of furnace lines was studied by the writer[2] and it was then remarked that lines of Class I A appear to be radiated almost entirely by the outer vapors but are inherently very faint. For the study of such lines the furnace conditions are very advantageous.

The fact that the low-temperature furnace in a partial vacuum gives all of the lines prominent in the scandium arc flame, and a number besides, is evidence that the oxidation in the arc flame is not influential in producing the lines observed, but that they are due to the reduced temperature in this region of the arc.

4. *Band spectrum.*—The flutings prominent in the scandium arc burning in air were usually entirely absent in the furnace photographs. Only on some long exposures at low temperature was the head of the orange band at λ 6036 visible, and but one of these showed any development of structure. This evidence, as far as it goes, favors the view that the bands are due to the oxide, since, although the material was initially in the oxide form, it

---

[1] *Op. cit.*, p. 69.

[2] *Mt. Wilson Contr.*, No. 66; *Astrophysical Journal*, **37**, 239, 1913.

appeared to be reduced at once with the formation of a carbide, in which case the oxygen would unite with the carbon of the tube. The prolonged exposures in some cases may have allowed a little oxygen from the residue of air in the chamber to combine sufficiently with the scandium vapor to show the one band observed. If the flutings were due to scandium itself they should have appeared at one of the temperatures used, since in general the vacuum furnace is very effective in producing a banded spectum when this is due to the metal being vaporized.

5. *Comparison with solar and sun-spot spectra.*—The data now available furnish an extension of the observations of Fowler in regard to the scandium lines occurring in solar and spot spectra. In the first place a comparison of the lines in Table I with Rowland's "Table of Solar Spectrum Wave-Lengths" shows that, though only a few are identified by Rowland as belonging to scandium, and these in almost all cases enhanced lines, a large proportion of the scandium wave-lengths agree closely with those of solar lines. A number of these probable coincidences are listed by Lockyer and Baxendall.[1] The strength of scandium lines in the sun bears a rather close relation to the degree of electrical excitation in the laboratory, the strongest, graded 3, 4, or 5 on the Rowland scale, being enhanced lines or those strong in both arc and spark. Those showing no marked response to electrical excitation, but often strong in both furnace and arc, are faint in the sun, usually below intensity 1; while lines relatively strong in the furnace, designated by "A" after the class-number, are uniformly either of intensity 000 or 0000 in the sun, or entirely absent from Rowland's table. In this latter class the pronounced low-temperature lines λλ 4753 and 4780 have no counterparts in the solar spectrum and such powerful furnace lines as λλ 6194, 6259, 6306, 6379, 6413 are either lacking or just at the limit of visibility.

A comparison with the sun-spot spectrum showed a decided prominence of the lines which are strong in the furnace. For this purpose the lines in Table I of intensity 10 or higher in the furnace spectrum were selected. While some of them are indistinct or disturbed by blends, there is little question that these lines are very generally present in the spot spectrum, and a striking increase appears regularly over the intensities in the solar disk.

---

[1] *Proceedings of the Royal Society*, **74**, 538, 1905.

The material available was used in two ways. First, a comparison was made with a list of spot lines compiled several years ago from spectrograms of moderate dispersion. In these the effect of the magnetic field in the spot was usually simply to widen the line, so that intensity estimates were more easily made than when the lines are resolved into magnetic doublets. In this list low-temperature scandium lines not visible in the solar spectrum often appeared in the spot with a value of at least 00 on the Rowland scale, while λ 6413.57 of this type reaches an intensity of 2 in the spot. Lines with a solar strength of 0000 or 00 usually strengthen to 2 or higher in the spot.

The second comparison was with the more recent large-scale spectra in which, by means of a nicol prism and compound quarter-wave plate, the intensity of the line and also its response to the magnetic field are recorded across the spot and over a portion of the disk on each side. In these spectrograms the relatively high intensity in the spot of the scandium furnace lines is very pronounced, and many fine cases of magnetic separation occur. Lines faint or invisible in the solar spectrum appear with considerable strength in the spot, even when resolved into two components. Some of these magnetic doublets are very wide, notable among them being the strong furnace lines λλ 5717, 6194, 6240, 6259, 6276, 6306.26, 6345, 6414. As is usual with magnetic resolutions, the average width decreases as we proceed toward shorter wavelengths, though low-temperature lines such as λλ 4753 and 4780 are notable both for strength in the spot and for sensitiveness to the magnetic field. Judging from the spot spectrum, since there are no laboratory observations of the Zeeman effect for scandium, a uniformly strong response to the magnetic field characterizes this spectrum.

CONCLUSION

The varying response of spectrum lines to temperature change, observed in the study at different temperatures of the furnace spectrum of scandium, has concerned itself especially with the conditions of appearance and development of the three main types—

enhanced, arc, and low-temperature lines—which make up the spectrum. The scandium enhanced lines, as regards degree of excitation required, stand between the enhanced lines of titanium and those of the type of H and K of calcium. For the lines appearing in the arc spectrum the regular temperature classification is carried out. The group of arc lines given by the arc flame consists of prominent low-temperature lines, but, since many lines strong in the furnace are relatively weak in all parts of the arc, additional data on this type of line are supplied by the furnace spectrum.

The explanation advanced by Fowler as to the relative strength of the different types of scandium lines in the solar and sun-spot spectra is fully confirmed by their varying response to the furnace excitation. The strong low-temperature lines, faint or lacking in the disk, are distinctly brought out in the spot, and, especially in the red, show high sensitiveness to the magnetic field. A comparison of the Zeeman effect for scandium in the laboratory with that shown in spot spectra and a fuller listing of the scandium lines present in the sun are needed to give this element its due place among those on which solar studies are based.

Mount Wilson Observatory
May 1921

Contributions from the Mount Wilson Observatory, No. 212
Reprinted from the *Astrophysical Journal*, Vol. LIV, pp. 226–228, 1921

THE SPECTROSCOPIC BINARY BOSS 3644 VIRGINIS

By JOHN C. DUNCAN

ABSTRACT

Spectroscopic binary Boss 3644, Virginis.—The elements of the orbit of this sixth-magnitude star of type F2 have been determined from eighteen spectrograms. P is 2.6960 days, K is 24.3 km/sec., γ is 17.6 km/sec., and e is 0.00. A velocity-curve is given.

The radial velocity of the star Boss 3644 ($\alpha = 14^{h}8^{m}.5$, $\delta = -22°25'$; 1900.0) was found to be variable by Miss A. M. Brayton from her measures of three spectrograms made with the 60-inch reflector and single-prism spectrograph early in 1920. During the current

TABLE I

Observations of Boss 3644

Plate	Date, G.M.T.	J.D. 2422000+	Days after Maximum Velocity	Observed Velocity	O−C
8990.........	1920 Feb. 5 1h 06m	360.046	1.471	− 3.2	+ 2.6
9092.........	Mar. 31 21 57	415.915	0.724	+10.6	− 4.2
9239.........	May 31 20 20	476.847	2.344	+34.2	0.0
9881.........	1921 Jan. 29 1 02	719.043	1.900	+11.7	+ 0.9
9903.........	Feb. 17 23 18	738.971	0.260	+48.0	+10.4
9912.........	Feb. 19 1 14	740.051	1.340	− 2.7	+ 4.0
9925.........	Feb. 20 1 07	741.047	2.336	+41.8	+ 7.9
9930.........	Feb. 20 22 23	741.933	0.526	+28.8	+ 3.0
9943.........	Feb. 23 23 11	744.966	0.863	+ 3.6	− 3.7
9959.........	Feb. 25 22 31	746.938	0.139	+34.9	− 5.8
9972.........	Feb. 26 23 35	747.983	1.184	− 5.6	− 0.6
10017.........	Mar. 19 21 55	768.913	0.546	+21.4	− 3.3
10025.........	Mar. 20 19 38	769.818	1.451	−11.0	− 5.0
10027.........	Mar. 20 22 09	769.923	1.556	− 3.8	+ 0.1
10030.........	Mar. 22 20 17	771.845	0.782	+13.2	+ 1.7
10034.........	Mar. 23 0 30	772.014	0.951	+ 5.2	+ 2.2
10062.........	Mar. 27 19 16	776.803	0.348	+32.8	− 1.6
10096.........	Apr. 17 22 43	797.947	2.620	+35.5	− 6.1
10134.........	Apr. 27 19 31	807.813	1.702	+ 0.2	− 0.9
10142.........	Apr. 28 19 12	808.800	2.689	+39.9	− 2.0
10143.........	Apr. 28 19 36	808.817	0.010	+41.0	− 0.9

year, eighteen additional plates have been secured by various observers with the same equipment. All the plates are listed in Table I, in which the column headed "Observed Velocity" gives for each plate the mean result of Miss Brayton's measures and mine. The numbers in the fourth and last columns are derived from the circular elements given below.

The star is of the sixth magnitude and of spectral type F2. From eight to twelve lines were measured on each plate, those chosen being of iron and occasionally of hydrogen. Preliminary elements were derived by the method of Lehmann-Filhés as follows:

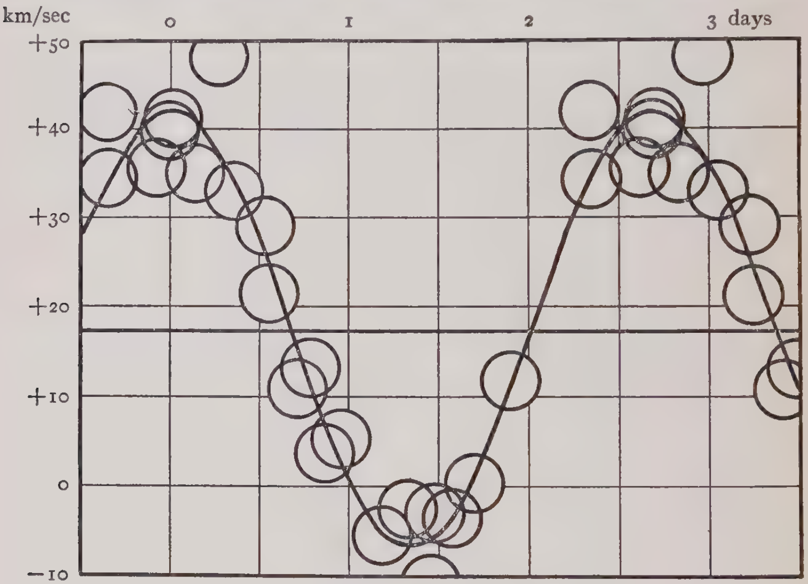

Velocity-curve of Boss 3644

$P = 2.6960$ days
$K = 25.0$ km/sec.
$\omega = 320^\circ$
$e = 0.08$
$T =$ J.D. 2422746.45
$\gamma = +17.47$ km/sec.

A least-squares solution was based on these elements, using only the eighteen plates of 1921 and omitting the period. As the resulting correction to the eccentricity was −0.11±0.06, this element was assumed to be 0.00 and a second solution was made with T, K, and γ as the only variables. By the first solution Σvv was reduced from 443 to 338, and by the second it was further diminished to 333. The circular elements from the second solution and the period originally found are:

$$
\begin{aligned}
P&=2.6960 \text{ days}\\
K&=24.34\pm1.08 \text{ km/sec.}\\
e&=0.00\\
T_{\Omega}&=\text{J.D. } 2422744.103\pm0.023\\
\gamma&=+17.60\pm0.85 \text{ km/sec.}\\
a \sin i&=902{,}300 \text{ km}\\
\frac{m_1^3 \sin^3 i}{(m+m_1)^2}&=0.00404 \odot
\end{aligned}
$$

T_{Ω} indicates the epoch of maximum positive velocity. In the accompanying velocity-curve the radius of the circles representing the observations is equal to the probable error of a single plate, ±3.18 km/sec.

Mount Wilson Observatory
June 1921

Contributions from the Mount Wilson Observatory, No. 213
Reprinted from the *Astrophysical Journal*, Vol. LIV, pp. 237–45, 1921

INVESTIGATIONS ON PROPER MOTION

FOURTH PAPER: INTERNAL MOTION IN THE SPIRAL NEBULA MESSIER 51

By ADRIAAN VAN MAANEN

ABSTRACT

Spiral nebula Messier 51.—A comparison of a plate taken by Mr. Duncan on April 8, 1921, with one taken by Mr. Ritchey on February 7–8, 1910, both at the 25-foot focus of the 60-inch reflector, enabled the *proper motion of the nebula* and the relative motion of its parts to be determined. Measurements of 80 points of the nebula compared with those of 20 stars give for the nebula an annual proper motion of +0″.006 in right ascension and +0″.001 in declination. The *internal proper motion* is not a pure rotation since the mean radial component is outward and is 42 per cent of the mean tangential component which is 0″.019 ENWS; rather it is a spiral motion out along the arms at the rate of 0″.021 per year together with a slight outward radial motion of 0″.003.

Two sixteenth magnitude stars with large proper motions, about 0″.15 per year, were found *near Messier 51*. They are called *f* and *r*.

Five years have elapsed since the first evidence of internal motion in a spiral nebula, as derived from direct photographs, was announced in this *Journal*.[1] The time interval between the old and new plates taken at the 25-foot focus of the 60-inch reflector has now been doubled, thus quadrupling the weight of the annual motions derived from them; it was accordingly thought worth while to investigate several objects of this class.

The first spiral nebula for which two plates with a ten-years' interval became available was M 33. A note concerning the preliminary measures for 51 points of this nebula has appeared elsewhere.[2] These results show a decided internal motion, which, as in the case of M 101,[1] can be explained either as a rotation combined with a radial motion outward, or as an outward motion along the streamers of the nebula. More elaborate measures of this object await the securing of another plate. If, as is hoped, we can measure several hundred points in this object, some light may be thrown on the laws that govern the motions.

---

[1] *Astrophysical Journal*, **44**, 210, 1916.

[2] *Proceedings of the National Academy of Sciences*, **7**, 1, 1921.

In the meantime Mr. Duncan secured a plate of the spiral nebula M 51, of which Mr. Ritchey had previously taken several photographs. Duncan's plate, taken April 8, 1921, compares most favorably with one secured by Ritchey on February 7 and 8, 1910. Both plates were exposed 3 hours and 55 minutes and are of good quality. Eighty points, presumably belonging to the nebula, were measured, while for comparison purposes 23 stars were selected. Further, two photographs taken by Mr. Seares, one with and one without a yellow color-screen, enabled me to see if objects were included in either category which probably did not belong there. Of the 80 nebulous points only one, No. 27, was decidedly red, and may therefore not be a part of the nebula. In the discussion of the internal motions this point was on this account excluded. Among the comparison stars, on the other hand, one object, *j*, was found to be decidedly blue. As for this reason it may be a part of the nebula, it was excluded for comparison purposes. A rough reduction of the measures showed, moreover, that two of the comparison stars, *f* and *r*, have large proper motions. These were also excluded, leaving 20 comparison stars in all.

The plates were measured with the new stereocomparator—which will be described in another article[1]—in four positions, with the directions east, west, north, and south successively coinciding with that of increasing readings of the micrometer screw.

In order to deal with smaller values in the computations, the mean measured displacements in right ascension and declination, expressed in parts of the micrometer screw, were reduced to displacements in 0″.001 per year by multiplication of the factor

$$q=\frac{27200}{31890\times 11.16}=0.0764,$$

in which 27200 is the number of thousandths of a second of arc per millimeter on the plates, 31890 the number of the parts of the micrometer screw per millimeter on the plates, and 11.16 the interval in years between the two plates. The resulting values, m_α and m_δ, may be reduced to annual proper motion by

$$\left.\begin{aligned} m_\alpha &= a+bx+cy+dx^2+exy+fy^2+\mu_\alpha, \\ m_\delta &= a'+b'x+c'y+d'x^2+e'xy+f'y^2+\mu_\delta, \end{aligned}\right\} \qquad (1)$$

---

[1] *Mt. Wilson Contr.*, No. 224, 1922.

TABLE I

Co-ordinates and Measured Annual Displacements

No.	x	y	μ_α	μ_δ
a	+0′.4	+1′.6	−0″.036	−0″.006
b	+3.4	+4.3	+ 22	− 4
c	+4.9	+2.7	− 6	+ 8
d	+3.4	+1.3	− 14	− 14
e	+3.7	−3.1	+ 9	+ 15
f	+3.6	−8.1	− 140	+ 38
g	−0.3	−7.3	− 9	− 7
h	+0.6	−3.1	+ 9	− 5
i	+1.2	−2.2	0	− 9
j	+0.5	−2.2	+ 17	0
k	−3.1	−2.4	+ 6	+ 30
l	−2.4	−1.9	+ 10	+ 6
m	−3.9	−0.5	− 32	− 28
n	−1.9	−0.2	+ 28	+ 4
o	−1.1	+0.3	+ 19	− 2
p	−1.2	+0.9	− 14	+ 10
q	−1.5	+2.4	− 8	0
r	−2.5	+2.5	− 159	− 34
s	−4.3	+2.2	+ 12	− 4
t	−0.8	+3.0	+ 9	+ 4
u	−0.8	+4.0	− 3	+ 11
v	+3.7	+1.3	0	− 1
w	+2.5	+0.4	0	− 5
1	+0.5	0.0	+ 28	+ 10
2	+0.6	−0.2	− 21	+ 6
3	+0.5	−0.7	− 13	+ 6
4	+0.6	−0.9	− 12	+ 14
5	0.0	−0.9	+ 4	+ 9
6	0.0	−1.0	+ 9	+ 3
7	−0.1	−1.2	− 25	+ 9
8	−1.0	−0.9	− 1	− 1
9	−1.5	+0.3	− 3	− 19
10	−1.5	+1.3	− 16	− 22
11	−1.3	+1.7	+ 36	− 18
12	−1.0	+2.1	− 8	− 24
13	−0.5	+2.0	+ 16	− 9
14	−0.3	+1.6	+ 23	− 7
15	−0.5	+1.0	+ 23	− 28
16	0.0	+1.0	+ 8	− 9
17	+1.2	+0.5	+ 11	+ 10
18	+1.5	+0.5	+ 22	+ 17
19	+1.4	0.0	+ 28	+ 19
20	+1.9	−0.6	+ 24	+ 16
21	+2.1	−0.7	+ 43	+ 29
22	+1.6	−1.6	− 6	+ 17
23	+1.6	−2.1	− 11	+ 28
24	+1.2	−1.9	− 26	+ 7
25	+1.0	−2.1	− 20	+ 23
26	+1.1	−2.1	− 25	+ 24
27	−2.1	+0.9	+ 8	− 45
28	−2.2	+0.9	− 7	− 21
29	+0′.9	+2′.5	+0″.025	−0″.003

TABLE I—*Continued*

No.	x	y	μ_α	μ_δ
30	+1'.3	+2'.2	+0".014	+0".008
31	+1.6	+1.9	+ 12	+ 24
32	+1.6	+1.8	− 10	+ 3
33	+1.8	+1.5	+ 21	+ 23
34	+2.5	+0.3	+ 7	+ 23
35	+2.4	+0.2	+ 18	+ 30
36	+2.7	−1.1	+ 19	+ 18
37	+2.4	−2.5	− 8	+ 22
38	+2.1	−3.8	− 1	+ 34
39	+1.9	−4.0	− 9	+ 21
40	+2.0	−4.2	− 6	+ 18
41	+1.6	−5.2	− 25	+ 26
42	+0.6	−0.9	+ 20	+ 5
43	−0.8	−0.9	− 10	− 21
44	−0.9	−0.9	− 5	− 13
45	−1.2	−0.7	+ 5	− 28
46	−2.1	−0.2	+ 16	− 6
47	−1.8	0.0	+ 3	− 33
48	−2.5	+0.6	+ 3	− 17
49	−2.7	+0.3	+ 10	− 24
50	−1.8	+0.5	+ 6	− 29
51	−2.8	+2.4	+ 8	− 25
52	−3.1	+2.1	+ 9	− 16
53	−0.6	+2.4	+ 23	− 25
54	−0.6	+2.4	+ 38	+ 3
55	−0.3	+2.4	+ 34	− 8
56	−0.2	+2.5	+ 40	− 14
57	0.0	+3.1	− 9	− 5
58	0.0	+3.0	+ 18	− 17
59	−0.8	+1.2	+ 22	− 33
60	+1.5	+0.6	+ 11	+ 10
61	+2.0	−0.5	+ 12	+ 34
62	+1.9	−0.8	+ 31	+ 23
63	+1.8	−0.9	+ 6	+ 15
64	+1.7	−2.4	+ 4	+ 39
65	+0.8	−2.2	− 19	+ 9
66	+0.2	−1.9	− 31	− 2
67	0.0	−2.2	− 34	+ 9
68	−2.0	−1.3	− 24	− 12
69	+0.6	+2.8	+ 30	− 17
70	+1.8	+1.9	+ 8	+ 12
71	+2.1	+2.0	+ 14	+ 15
72	+2.1	+1.9	+ 29	+ 15
73	+2.4	+1.8	+ 17	+ 4
74	+2.4	+0.8	+ 44	+ 21
75	+2.4	−0.6	+ 32	+ 27
76	+2.5	−0.6	+ 10	+ 33
77	+2.2	−1.1	+ 4	+ 13
78	+2.5	−2.4	− 27	+ 9
79	+2.4	−2.7	− 11	+ 25
80	+1'.6	−3'.8	0".000	+0".020

in which a, b, ... f' are the plate-constants, x and y the coordinates of the objects measured, and μ_α and μ_δ the annual proper motions, expressed in thousandths of a second of arc.

The plate-constants were derived by a least-squares solution from the twenty pairs of equations of the form (1) for the 20 comparison stars. For these objects the usual supposition was made that μ_α and μ_δ are in the mean zero and are not functions of x and y. The constants $a, b, \ldots . f'$ thus found were substituted in the equations of condition (1) of all the objects measured. The resulting annual proper motions are given in the fourth and fifth columns of Table I. The second and third columns of this table contain the co-ordinates in x and y, expressed in minutes of arc with a precision sufficient for identification.

The motions thus derived for the nebular points include the motion of the nebula as a whole with respect to the 20 comparison stars as well as the internal motions of the individual points. To derive the motion of the nebula as a whole, the same process was followed as for M 101.

a) The mean for all of the 79 points gives:

$$\mu_\alpha = +0''.006 \quad \mu_\delta = +0''.004.$$

b) Dividing the points into four groups, corresponding to the four quadrants, the means of the two groups in opposite quadrants should give a good agreement. We find:

$$\text{Means for I and III} \begin{cases} \mu_\alpha = +0''.004 \\ \mu_\delta = +0''.001 \end{cases}$$

$$\text{Means for II and IV} \begin{cases} \mu_\alpha = +0''.006^5 \\ \mu_\delta = 0''.000 \end{cases}$$

The four quadrants combined give:

$$\mu_\alpha = +0''.005 \quad \mu_\delta = +0''.000^5 .$$

c) In order to avoid points far from the center, which have an asymmetrical distribution, we may use only those within a radius of 3′. We then find:

$$\text{Means for I and III} \begin{cases} \mu_\alpha = +0''.004^5 \\ \mu_\delta = +0''.001^5 \end{cases}$$

$$\text{Means for II and IV} \begin{cases} \mu_\alpha = +0''.008^5 \\ \mu_\delta = -0''.001 \end{cases}$$

The four quadrants combined give:

$$\mu_\alpha = +0\overset{''}{.}006^5 \quad \mu_\delta = 0\overset{''}{.}000.$$

Giving equal weight to each of the three methods used, we derive as the final motion of the nebula as a whole

$$\mu_\alpha = +0\overset{''}{.}006 \quad \mu_\delta = +0\overset{''}{.}001.$$

If now we subtract these quantities from the values of μ_α and μ_δ for the nebular points, we obtain results which represent the internal motions. These are given in the second and third columns of Table II and are plotted in Plate VII. The plate also shows the motions of the 23 stars as given in Table I. The 20 comparison stars are surrounded by a circle, while for the stars *f*, *j*, and *r*, which, for the reasons mentioned on page 222, were excluded for comparison purposes, the motions are represented by broken lines. The scale of the motions is indicated in the lower left-hand corner. The arrows represent the motions in about 1100 years.

The plate indicates motions analogous to those found for M 101 and M 33. They may be interpreted either as a rotation combined with a radial motion outward, or as a motion along the streamers outward. Both possibilities are briefly discussed.

a) *Rotational motion.*—In order to discuss the results from the standpoint of rotation, the internal motions of the 79 points (excluding No. 27) were analyzed into components perpendicular to and along the radius. The values are given in the fourth and fifth columns of Table II, the positive sign being used for rotation in the direction ENWS and for outward radial motion. For the rotational component we find 74 positive and 5 negative values; for the radial component 59 positive and 19 negative values, while one is zero. The mean rotational component is $+0\overset{''}{.}019$; the mean radial component, $+0\overset{''}{.}008$. As the mean distance from the center is $2\overset{'}{.}3$, the rotational motion of $0\overset{''}{.}019$ annually would indicate a rotation period of about 45,000 years. The radial component is so large, however, that we can hardly believe the motion to be one of rotation only. Similar results have been found in all three cases discussed so far. For M 101 the radial component is 32 per cent of the rotational component; for M 33, 48 per cent; for M 51,

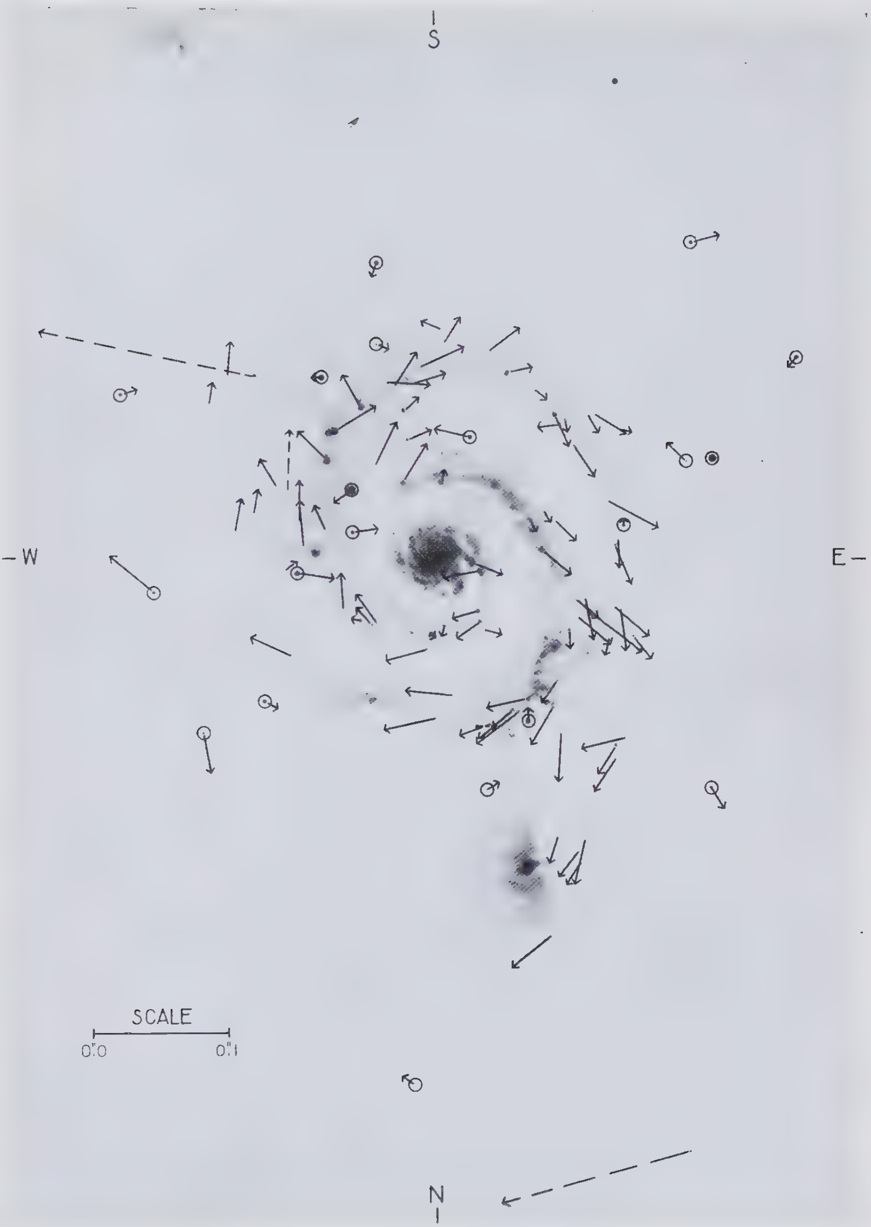

INTERNAL MOTIONS IN MESSIER 51

The arrows indicate the direction and magnitude of the mean annual motions. Their scale (0.″1) is indicated on the illustration. The scale of the nebula is 1 mm = 6.″2. The comparison stars are inclosed in circles.

TABLE II

Annual Internal Motions

No.	μ_α	μ_δ	Rotational	Radial	Stream	Transverse
1	+0″.022	+0″.009	+0″.007	+0″.022	+0″.011	+0″.019
2	−27	+5	+12	−24	+1	−27
3	−19	+5	+18	−7	+16	−9
4	−18	+13	+21	+2	+21	+2
5	−2	+8	+3	+8	+4	+7
6	+3	+2	−3	+2	−2	+3
7	−31	+8	+30	+12	+31	+7
8	−7	−2	+6	+4	+7	+2
9	−9	−20	+17	+14	+20	+8
10	−22	−23	+3	+31	+14	+28
11	+30	−19	+34	−4	+33	+9
12	−14	−25	−1	+28	+5	+28
13	+10	−10	+12	+8	+14	+4
14	+17	−8	+19	+3	+19	+1
15	+17	−29	+27	+20	+32	+10
16	+2	−10	+2	+10	+5	+9
17	+5	+9	+10	+1	+10	−2
18	+16	+16	+20	+11	+21	+8
19	+22	+18	+20	+21	+20	+21
20	+18	+15	+7	+22	+21	+9
21	+37	+28	+13	+44	+41	+19
22	−12	+16	+20	+4	+20	−1
23	−17	+27	+30	+10	+31	+7
24	−32	+6	+30	−11	+26	−19
25	−26	+22	+33	+8	+34	+3
26	−31	+23	+38	+6	+38	0
27	+2	−46	....	....	....	....
28	−13	−22	+14	+20	+25	+3
29	+19	−4	+16	+10	+16	+11
30	+8	+7	+10	−2	+11	0
31	+6	+23	+20	−14	+21	−11
32	−16	+2	−12	−11	−8	−13
33	+15	+22	+27	−3	+26	+5
34	+1	+22	+22	−2	+22	−4
35	+12	+29	+29	+10	+31	+5
36	+13	+17	+11	+18	+18	+12
37	−14	+21	+26	+7	+25	−7
38	−7	+33	+22	+27	+33	+6
39	−15	+20	+20	+14	+24	−7
40	−12	+17	+18	+10	+20	−4
41	−31	+25	+38	+14	+35	−20
42	+14	+4	−10	+11	−9	+12
43	−16	−22	+27	−5	+25	−10
44	−11	−14	+17	−2	+17	−2
45	−1	−29	+25	−13	+23	−16
46	+10	−7	+6	−10	+3	−12
47	−3	−34	+34	+5	+34	−3
48	+3	−18	+19	+1	+17	−8
49	+4	−25	+25	−1	+24	−7
50	0	−30	+29	+8	+30	−1
51	+2	−26	+21	+16	+26	0
52	+0″.003	−0″.017	+0″.016	+0″.007	+0″.017	−0″.003

TABLE II—*Continued*

No.	μ_α	μ_δ	Rotational	Radial	Stream	Transverse
53	+0″.017	−0″.026	+0″.024	+0″.020	+0″.026	+0″.018
54	+ 32	+ 2	+ 30	− 10	+ 28	− 13
55	+ 28	− 9	+ 30	+ 5	+ 30	0
56	+ 34	− 15	+ 35	+ 12	+ 37	+ 3
57	− 15	− 6	− 14	+ 7	− 11	+ 12
58	+ 12	− 18	+ 11	+ 19	+ 16	+ 14
59	+ 16	− 34	+ 32	+ 18	+ 34	+ 14
60	+ 5	+ 9	+ 10	+ 1	+ 10	− 1
61	+ 6	+ 33	+ 30	+ 14	+ 32	− 8
62	+ 25	+ 22	+ 9	+ 31	+ 31	+ 9
63	0	+ 14	+ 12	+ 6	+ 14	− 1
64	− 2	+ 38	+ 23	+ 30	+ 32	+ 18
65	− 25	+ 8	+ 26	0	+ 25	+ 2
66	− 37	− 3	+ 36	− 7	+ 37	0
67	− 40	+ 8	+ 40	+ 7	+ 36	+ 18
68	− 30	− 13	+ 29	+ 17	+ 29	+ 16
69	+ 24	− 18	+ 19	+ 24	+ 23	+ 20
70	+ 2	+ 11	+ 9	− 5	+ 10	− 3
71	+ 8	+ 14	+ 16	− 4	+ 16	+ 1
72	+ 23	+ 14	+ 26	+ 7	+ 24	+ 13
73	+ 11	+ 3	+ 10	+ 7	+ 7	+ 10
74	+ 38	+ 20	+ 32	+ 30	+ 25	+ 34
75	+ 26	+ 26	+ 18	+ 32	+ 27	+ 24
76	+ 4	+ 32	+ 30	+ 14	+ 32	+ 6
77	− 2	+ 12	+ 12	+ 3	+ 11	− 6
78	− 33	+ 8	+ 29	− 16	+ 18	− 28
79	− 17	+ 24	+ 29	+ 7	+ 28	− 8
80	−0″.006	+0″.019	+0″.013	+0″.015	+0″.020	+0″.002

42 per cent. It is on the basis of this cumulative evidence against a purely rotatory motion that we feel more inclined to believe that the motions are in general along the arms.

b) *Motion along the arms of the spirals.*—Considering the motion as following the arms of the spiral, we find the mean motion to be +0″.021, with an additional perpendicular component outward of +0″.003. In the case of M 101, we found a small additional motion inward. In M 33 there is a slight indication of motion outward. But in all cases the mean deviations from the direction of the arms are very small. Definite conclusions as to the real meaning of these motions must, however, await further measurements. The best evidence may be expected from several hundred points to be measured in M 33, as soon as another plate can be secured.

Among the stars selected originally for comparison purposes, *f* and *r* require comment. Although their photographic magnitudes cannot be brighter than 16, they show annual proper motions of 0ʺ145 and 0ʺ163, respectively.

I wish to express my thanks to Mrs. Marsh of the computing division, who has performed all the duplicate computations necessary for the derivation of the present results.

Mount Wilson Observatory
June 1921

Contributions from the Mount Wilson Observatory, No. 214
Reprinted from the *Astrophysical Journal*, Vol. LIV, pp. 347–56, 1921

INVESTIGATIONS ON PROPER MOTION

FIFTH PAPER: THE INTERNAL MOTION IN THE SPIRAL NEBULA MESSIER 81

By ADRIAAN VAN MAANEN

ABSTRACT

Spiral nebula Messier 81.—Two plates taken at Mount Wilson, one by Ritchey in 1910 and the other by Duncan in 1921, were measured with the new stereocomparator, and from the shifts of 104 points in the nebula with reference to 14 comparison stars, the *proper motion of the nebula* as a whole was found to be: $\mu_{\alpha}=+0''.014$ and $\mu_{\delta}=-0''.005$. In addition, when the displacements of the points with reference to the nebula as a whole were corrected for the fact that the *inclination of the plane of the nebula* to the celestial sphere is about 49°, the *internal motion* was found to be, in general, a spiral motion out along the arms, of 0".039 per year NWSE, combined with a slight outward transverse motion of about 0".007 per year. The rotational component of the motion is 0".038 and corresponds to a period of rotation of 58,000 years.

Formation of spiral nebulae.—The four nebulae whose internal motions have been studied, M 33, 51, 81, and 101, all have internal spiral motions such as Jeans described in his *Problems of Cosmogony and Stellar Dynamics.* This fact *suggests* that the nebulous masses were rotating and had reached a lenticular shape when the arms began to be formed by matter being thrown off at antipodal points.

In a previous paper[1] it was mentioned that measures of two photographs of M 81 taken by Mr. Ritchey in 1910 and 1916 gave preliminary evidence of internal motion, similar to that revealed in the case of M 101. Another plate of M 81 was obtained in 1921 by Mr. Duncan which made it advisable to examine the additional evidence made available by the longer interval. The photographs used for the present paper are of 1910, February 5, and 1921, April 7; both received exposures of 4 hours and 15 minutes and are of good quality. Since no plates taken with a color screen were available, the choice of nebular points and comparison stars was necessarily based on the appearance of their images. Six of the 58 points included in the former discussion on account of their coincidence with the streamers of the nebula were excluded from the present discussion in advance of measurement because of their starlike appearance; they were, however, again included in the measures. Their numbers are 4, 28, 40, 42, 51, and 54.

---

[1] *Mt. Wilson Contr.*, No. 118, 17, 1916; *Astrophysical Journal*, **44**, 210, 1916.

Although the brighter stars were avoided, the comparison stars, as a whole, are somewhat brighter than the nebular points. For this reason a magnitude error may have vitiated the relative motions of the latter. While this may have affected the total motion of the nebula, it cannot have influenced the internal motion, since the magnitudes of the nebular points have a nearly symmetrical distribution around the center of the nebula. For the present investigation 14 comparison stars (the same as before) and 110 nebular points were selected for measurement.

As in the case of M 51,[1] the plates were measured with the new stereocomparator, with the directions east, west, north, and south coinciding successively with that of increasing reading of the micrometer screw.

The means of the two sets of measures in right ascension and in declination, which are expressed in parts of the micrometer screw for the interval of 11.17 years, were reduced to annual displacements in thousandths of a second of arc by multiplying them by the factor 0.0764. The resulting quantities m_α and m_δ were then reduced by the formulae:

$$\left.\begin{aligned} m_\alpha &= a+bx+cy+dx^2+exy+fy^2+\mu_\alpha \\ m_\delta &= a'+b'x+c'y+d'x^2+e'xy+f'y^2+\mu_\delta \end{aligned}\right\} \qquad (1)$$

in which $a, b, \ldots . a', b', \ldots . f'$ are the plate constants, x and y the co-ordinates of each point measured, and μ_α and μ_δ the annual proper motions, expressed in thousandths of a second of arc. For the derivation of the constants $a \ldots . f'$, the two sets of equations (1) for the comparison stars were solved by least squares, after making the usual supposition that the motions of the comparison stars are in the mean zero and are not functions of their position on the plates. Substitution of the constants thus determined into the equations (1) for all the objects measured yields the annual proper motions. These are given in the fourth and fifth columns of Table I; the second and third columns of this table give the co-ordinates of each object measured. The proper motions thus derived are relative to the group of comparison stars. To separate the motion of the nebula as a whole from the

---

[1] *Astrophysical Journal*, **54**, 237, 1921; *Mt. Wilson Contr.*, No. 213, 1921.

TABLE I

Co-ordinates and Measured Annual Displacements

No.	x	y	μ_α	μ_δ
a	+1′.7	+0′.6	+0″.005	−0″.007
b	+4.6	+2.0	+5	+14
c	+5.5	+3.9	+2	−1
d	+4.0	+7.1	−2	−2
e	−2.9	+8.0	−5	+1
f	−5.5	+2.1	+17	+3
g	−1.6	+1.3	−2	−6
h	−3.7	−0.2	−12	+1
i	−1.5	−0.5	−5	−8
j	−0.9	−3.2	−10	+10
k	−7.1	−6.0	−4	−1
l	+1.0	−6.6	+21	+2
m	+5.2	−6.3	−11	−3
n	+4.0	−1.3	0	−3
1	+2.5	+0.3	+23	+20
2	+2.5	0.0	+22	+26
3	+2.8	−0.3	+11	+27
4	+3.1	−0.2	−1	+15
5	+3.2	−2.5	+52	+11
6	+0.3	−4.0	+38	−31
7	+0.6	−4.2	+32	−37
8	+0.6	−4.3	+43	−22
9	+1.2	−4.7	+42	−21
10	+1.7	−4.6	+59	−25
11	+1.9	−4.8	+53	−19
12	+2.1	−5.0	+27	−31
13	+2.2	−5.1	+62	−39
14	+2.2	−4.9	+58	−6
15	+2.3	−5.1	+51	−12
16	+2.4	−4.7	+25	+20
17	+2.7	−4.9	+40	−30
18	+3.0	−5.6	+45	0
19	+2.9	−5.9	+60	−20
20	+3.4	−5.1	+51	+11
21	+4.5	−4.8	+52	+40
22	+3.9	−0.6	+20	+14
23	+4.0	−0.5	+52	+67
24	+4.1	+0.4	+43	+20
25	+3.1	+1.2	+16	+31
26	+3.9	+1.7	+12	+29
27	+3.9	+2.2	+20	+14
28	+4.3	+2.5	−5	+5
29	+2.2	+5.0	−4	+17
30	−0.2	+7.9	−37	+12
31	−2.9	+9.0	−28	+19
32	+1.2	+1.8	−12	+19
33	+1.0	+3.3	−7	+11
34	+0.3	+3.5	−16	+14
35	+0.1	+3.6	−34	+5
36	−0.3	+3.7	−22	+15
37	−0.2	+3.8	−35	+9
38	−0.8	+4.2	−16	+10

TABLE I—*Continued*

No.	x	y	μ_α	μ_δ
39	−1′.6	+5′.0	−0″.016	+0″.015
40	−2.3	+5.8	− 4	− 2
41	−3.5	+5.5	− 15	− 22
42	−3.8	+5.2	0	+ 17
43	−3.7	+4.9	− 5	− 16
44	−3.3	+4.9	− 3	− 24
45	−3.2	+4.8	− 5	− 19
46	−4.0	+2.9	+ 5	− 24
47	−4.0	+2.0	− 2	− 28
48	−5.3	+1.9	+ 29	− 12
49	−4.9	+1.5	+ 19	− 19
50	−4.8	+1.3	+ 14	− 38
51	−4.7	+0.8	+ 16	+ 10
52	−4.8	+0.6	+ 13	− 25
53	−4.7	+0.1	+ 28	− 37
54	−4.6	−0.4	+ 30	− 11
55	−4.1	−0.6	+ 22	− 35
56	−1.7	−6.5	+ 36	− 22
57	−0.5	−5.2	+ 36	− 20
58	−1.6	−1.2	0	− 24
59	+2.2	+0.8	− 4	+ 39
60	+2.4	+0.6	+ 19	+ 8
61	+3.3	−0.7	+ 21	+ 27
62	+3.2	−0.8	+ 23	+ 34
63	+3.8	+1.7	+ 8	+ 17
64	+3.2	+3.3	+ 4	+ 35
65	+3.4	+3.9	− 7	+ 32
66	+2.3	+5.2	− 29	+ 4
67	+0.8	+6.3	− 11	+ 21
68	+0.6	+7.1	− 23	+ 44
69	−0.8	+8.3	− 30	+ 42
70	−0.8	+9.2	− 45	+ 52
71	−2.8	+6.9	− 21	+ 4
72	−2.1	+5.3	− 10	+ 1
73	−1.0	+5.9	− 27	+ 23
74	−1.7	+5.2	− 38	+ 8
75	−1.7	+5.0	− 14	− 18
76	−1.4	+4.5	− 30	+ 32
77	0.0	+4.0	− 17	+ 11
78	0.0	+4.5	− 23	+ 17
79	+1.0	+4.0	− 44	+ 11
80	+1.8	+3.4	0	+ 21
81	+1.7	+1.7	− 15	+ 25
82	−2.2	+3.2	− 9	− 19
83	−2.9	+3.1	− 4	− 36
84	−2.9	+3.4	− 8	− 32
85	−3.5	+3.7	− 1	− 42
86	−5.1	+2.7	0	− 22
87	−4.8	+1.0	+ 18	− 5
88	−4.9	+1.1	+ 25	− 11
89	−4.7	+0.4	+ 4	− 18
90	−4.6	+0.4	+ 30	− 11
91	−4.6	−0.5	+ 27	− 36
92	−4.0	−1.7	+ 12	− 36

PLATE VIII

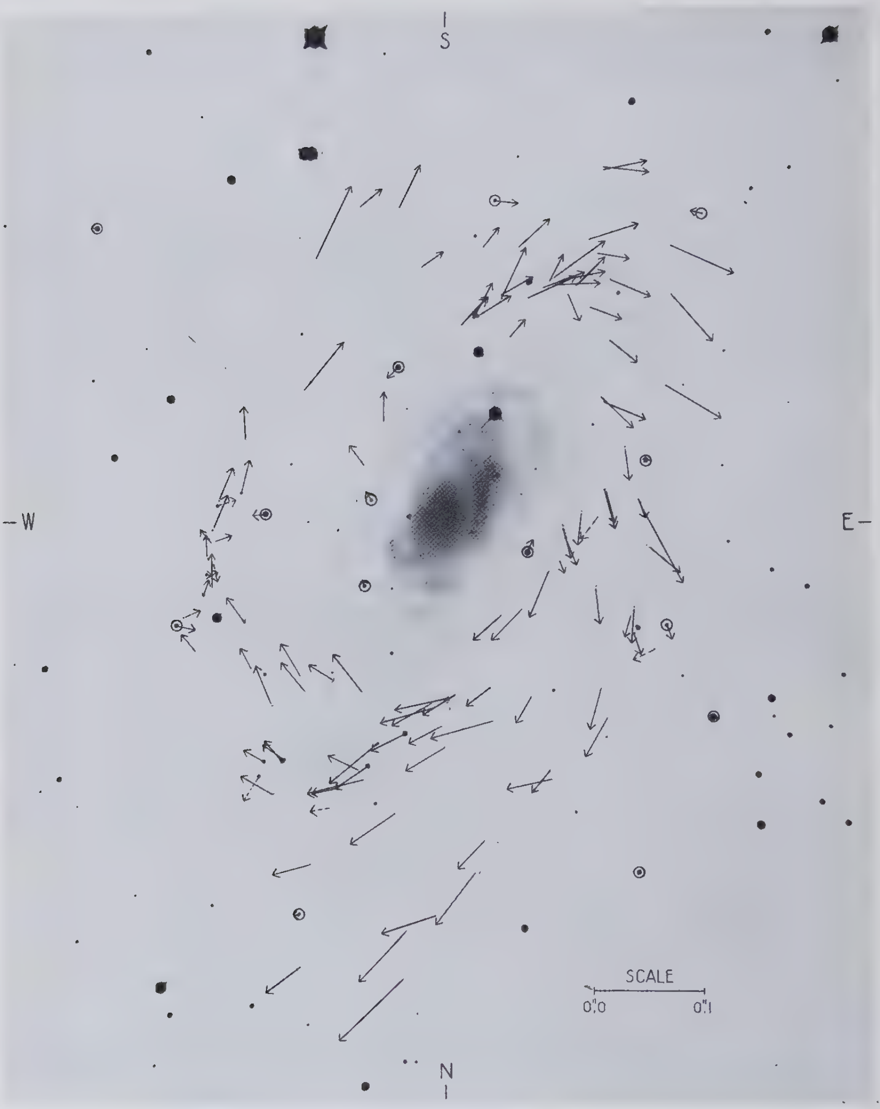

Internal Motions in Messier 81

The arrows indicate the direction and magnitude of the mean annual motions. Their scale (0.″1) is indicated on the illustration. The scale of the nebula is 1 mm = 9.″3. The comparison stars are inclosed in circles.

TABLE I—*Continued*

No.	x	y	μ_α	μ_δ
93	−2′.9	−2′.8	+0″.051	−0″.050
94	−2.7	−5.4	+ 47	− 73
95	−0.9	−6.5	+ 33	− 45
96	−1.2	−2.0	+ 14	− 32
97	+0.6	−4.3	+ 25	− 20
98	+0.7	−5.7	+ 29	− 24
99	+1.2	−4.6	+ 36	− 52
100	+1.3	−3.8	+ 30	− 23
101	+1.5	−5.7	+ 43	− 32
102	+2.9	−4.5	+ 44	+ 6
103	+4.6	−5.7	+ 74	+ 22
104	+3.4	−3.8	+ 39	+ 16
105	+3.2	−2.6	+ 44	+ 25
106	+3.7	−1.6	+ 18	+ 26
107	+4.5	−2.9	+ 66	+ 27
108	+3.1	−7.4	+ 57	0
109	+3.2	−7.3	+ 55	− 13
110	−1.7	+3.4	− 13	− 40

internal motion, the same process was used as previously in the case of M 101 and M 51, with the following results:

a) The mean motion of the 104 nebular points (excluding Nos. 4, 28, 40, 42, 51, and 54 for reasons given on page 231) is $\mu_\alpha = +0''.014$, $\mu_\delta = -0''.002$.

b) Combining the mean motions in quadrants I and III, we have $\mu_\alpha = +0''.017^5$, $\mu_\delta = -0''.005$; while for quadrants II and IV, $\mu_\alpha = +0''.012^5$, $\mu_\delta = -0''.008$. All four quadrants combined give $\mu_\alpha = +0''.015$, $\mu_\delta = -0''.006^5$.

c) Excluding points outside a circle with radius 5′.5, we find for quadrants I and III $\mu_\alpha = +0''.017$, $\mu_\delta = -0''.006$; for quadrants II and IV $\mu_\alpha = +0''.011^5$, $\mu_\delta = -0''.006$. For all four quadrants $\mu_\alpha = +0''.014$, $\mu_\delta = -0''.006$.

For the motion of the nebula as a whole the mean result from the three methods is

$$\mu_\alpha = +0''.014, \qquad \mu_\delta = -0''.005.$$

Subtracting these values from the annual motions given in Table I, we derive the internal motions, which are given in the second and third columns of Table II. These motions are plotted in Plate VIII. For the comparison stars, which are surrounded by circles, the

TABLE II

Annual Internal Motions

No.	μ_α	μ_δ	Rotational	Radial	Stream	Transverse
1	+0″.009	+0″.025	+0″.024	+0″.025	+0″.017	+0″.030
2	+ 8	+ 31	+ 32	+ 25	+ 25	+ 32
3	− 3	+ 32	+ 35	+ 6	+ 33	+ 12
4	− 15	+ 20	....	....	....	....
5	+ 38	+ 16	+ 35	+ 31	+ 15	+ 45
6	+ 24	− 26	+ 30	+ 21	+ 36	+ 8
7	+ 18	− 32	+ 17	+ 34	+ 28	+ 26
8	+ 29	− 17	+ 35	+ 14	+ 38	+ 3
9	+ 28	− 16	+ 34	+ 15	+ 37	+ 6
10	+ 45	− 20	+ 57	+ 21	+ 57	+ 20
11	+ 39	− 14	+ 48	+ 20	+ 50	+ 14
12	+ 13	− 26	+ 2	+ 30	+ 4	+ 30
13	+ 48	− 34	+ 45	+ 45	+ 50	+ 40
14	+ 44	− 1	+ 59	+ 12	+ 60	+ 3
15	+ 37	− 7	+ 50	+ 13	+ 51	+ 2
16	+ 11	+ 25	+ 35	− 18	+ 33	− 20
17	+ 26	− 25	+ 16	+ 34	+ 14	+ 35
18	+ 31	+ 5	+ 45	+ 9	+ 45	+ 42
19	+ 46	− 15	+ 52	+ 31	+ 55	+ 20
20	+ 37	+ 16	+ 58	+ 10	+ 59	0
21	+ 38	+ 45	+ 85	+ 10	+ 85	+ 8
22	+ 6	+ 19	+ 22	+ 14	+ 25	+ 1
23	+ 38	+ 72	+ 82	+ 76	+ 91	+ 65
24	+ 29	+ 25	+ 23	+ 53	+ 30	+ 50
25	+ 2	+ 36	+ 33	+ 38	+ 32	+ 39
26	− 2	+ 34	+ 32	+ 21	+ 35	+ 14
27	+ 6	+ 19	+ 14	+ 23	+ 18	+ 19
28	− 19	+ 10	....	....	....	....
29	− 18	+ 22	+ 28	+ 8	+ 29	+ 1
30	− 51	+ 17	+ 63	− 2	+ 55	− 31
31	− 42	+ 24	+ 46	+ 28	+ 54	− 6
32	− 26	+ 24	+ 35	+ 1	+ 35	− 3
33	− 21	+ 16	+ 27	+ 3	+ 27	− 4
34	− 30	+ 19	+ 38	+ 5	+ 37	− 13
35	− 48	+ 10	+ 61	− 11	+ 52	− 34
36	− 36	+ 20	+ 45	+ 10	+ 45	− 9
37	− 49	+ 14	+ 63	− 2	+ 58	− 25
38	− 30	+ 15	+ 36	+ 12	+ 37	− 7
39	− 30	+ 20	+ 32	+ 22	+ 39	0
40	− 18	+ 3	....	....	....	....
41	− 29	− 17	+ 51	+ 1	+ 51	0
42	− 14	+ 22	....	....	....	....
43	− 19	− 11	+ 33	+ 4	+ 33	+ 4
44	− 17	− 19	+ 36	− 6	+ 36	− 2
45	− 19	− 14	+ 36	+ 1	+ 36	0
46	− 9	− 19	+ 25	− 3	+ 25	− 4
47	− 16	− 23	+ 34	+ 16	+ 35	+ 13
48	+ 15	− 7	+ 2	− 19	0	− 19
49	+ 5	− 14	+ 14	− 6	+ 13	− 8

TABLE II—*Continued*

No.	μ_α	μ_δ	Rotational	Radial	Stream	Transverse
50	0″.000	−0″.033	+0″.036	+0″.002	+0″.036	−0″.002
51	+ 2	+ 15	....	....	....	....
52	− 1	− 20	+ 24	+ 6	+ 24	+ 3
53	+ 14	− 32	+ 35	− 8	+ 32	− 15
54	+ 16	− 6	....	....	....	....
55	+ 8	− 30	+ 35	+ 5	+ 35	− 4
56	+ 22	− 17	+ 30	+ 3	+ 30	− 3
57	+ 22	− 15	+ 29	+ 3	+ 29	− 2
58	− 14	− 19	+ 7	+ 31	+ 12	+ 30
59	− 18	+ 44	+ 45	+ 5	+ 44	+ 10
60	+ 5	+ 13	+ 11	+ 14	+ 8	+ 15
61	+ 7	+ 32	+ 44	+ 20	+ 33	+ 36
62	+ 9	+ 39	+ 39	+ 17	+ 29	+ 31
63	− 6	+ 22	+ 26	+ 8	+ 27	+ 5
64	− 10	+ 40	+ 35	+ 27	+ 38	+ 22
65	− 21	+ 37	+ 40	+ 13	+ 40	+ 11
66	− 43	+ 9	+ 48	− 28	+ 38	− 41
67	− 25	+ 26	+ 36	+ 19	+ 39	+ 7
68	− 37	+ 49	+ 49	+ 37	+ 60	+ 13
69	− 44	+ 47	+ 50	+ 41	+ 64	+ 6
70	− 59	+ 57	+ 68	+ 48	+ 82	+ 9
71	− 35	+ 9	+ 41	+ 15	+ 38	− 20
72	− 24	+ 6	+ 28	+ 9	+ 30	+ 4
73	− 41	+ 28	+ 48	+ 23	+ 50	− 17
74	− 52	+ 13	+ 64	+ 16	+ 65	− 3
75	− 28	− 13	+ 43	− 12	+ 38	− 25
76	− 44	+ 37	+ 44	+ 41	+ 55	+ 25
77	− 31	+ 16	+ 39	+ 7	+ 37	− 15
78	− 37	+ 22	+ 47	+ 8	+ 43	− 19
79	− 58	+ 16	+ 69	− 26	+ 62	− 40
80	− 14	+ 26	+ 26	+ 15	+ 28	+ 9
81	− 29	+ 30	+ 43	− 2	+ 42	− 8
82	− 23	− 14	+ 40	+ 4	+ 40	+ 1
83	− 18	− 31	+ 49	− 4	+ 49	− 7
84	− 22	− 27	+ 49	− 4	+ 49	− 6
85	− 15	− 37	+ 51	− 10	+ 52	− 5
86	− 14	− 17	+ 29	+ 13	+ 28	+ 15
87	+ 4	0	− 2	− 6	− 2	− 6
88	+ 11	− 6	+ 2	− 14	+ 1	− 14
89	− 10	− 13	+ 16	+ 16	+ 16	+ 16
90	+ 16	− 6	+ 5	− 21	+ 2	− 21
91	+ 13	− 31	+ 34	− 4	+ 32	− 13
92	− 2	− 31	+ 28	+ 23	+ 32	+ 17
93	+ 37	− 45	+ 58	− 4	+ 58	− 9
94	+ 33	− 68	+ 64	+ 40	+ 71	+ 25
95	+ 19	− 40	+ 31	+ 33	+ 34	+ 29
96	0	− 27	+ 16	+ 28	+ 25	+ 20
97	+ 11	− 15	+ 12	+ 17	+ 19	+ 7
98	+ 15	− 19	+ 17	+ 16	+ 18	+ 15
99	+ 22	− 47	+ 13	+ 51	+ 35	+ 40
100	+ 16	− 18	+ 13	+ 21	+ 20	+ 15

TABLE II—*Continued*

No.	μ_α	μ_δ	Rotational	Radial	Stream	Transverse
101	+0".029	−0".027	+0".032	+0".028	+0".033	+0".026
102	+ 30	+ 11	+ 46	+ 9	+ 45	+ 14
103	+ 60	+ 27	+ 94	+ 28	+ 95	+ 21
104	+ 25	+ 21	+ 48	+ 8	+ 39	+ 28
105	+ 30	+ 30	+ 59	+ 23	+ 45	+ 44
106	+ 4	+ 31	+ 36	+ 6	+ 34	+ 14
107	+ 52	+ 32	+ 70	+ 53	+ 62	+ 62
108	+ 43	+ 5	+ 62	+ 5	+ 62	− 6
109	+ 41	− 8	+ 50	+ 17	+ 51	+ 8
110	− 27	− 35	+ 57	− 30	+ 62	− 18

motions of Table I are used. The scale of the motions is indicated in the lower right-hand corner. The arrows represent the motions during an interval of about 1,300 years.

As in the case of M 101, 33, and 51, there is a question as to whether the displacements are best represented by a rotation or by a motion along the arms of the spiral. To investigate this, the motions were resolved into (*a*) rotational and radial components; (*b*) components along and perpendicular to the arms of the spirals (stream and transverse components). In order to do this, a diagram was made in which the foreshortening of the nebula was corrected. This was necessary because M 81 is decidedly elliptical in appearance, due undoubtedly to an inclination of the plane of the nebula to the tangential plane of the celestial sphere. It was estimated that the intersection of the two planes is in position angle 149° and that the inclination is 49°. Hence, the positions and components of the measured objects in the direction of position angles 149° and 329° were made the same in the diagram as on the photographs, while distances and components at right angles to this direction were increased in the ratio $1/\cos 49° = 1.5$. The results for individual points derived from the diagram are in the last four columns of Table II, where, as before, the positive sign is used for motions in the directions north, west, south, east, and outward.

The mean rotational component is +0".038; the mean radial component, +0".013, which is 34 per cent of the rotational vector. Since the mean distance of the nebular points from the center is

5′.8, the rotational component would correspond to a hypothetical period of about 60,000 years. The mean stream component is +0″.039, with a transverse component of +0″.007.

The evidence on internal motions derived from the four nebulae which have been measured, viz., M 101, 33, 51, and 81, is summarized briefly in Table III, in which the second column gives the focal length used, the third column the interval in years. The next four columns give the mean rotational, radial, stream, and transverse components of the annual motions derived, while the last column gives the number of nebular points measured.

TABLE III

SUMMARY OF INTERNAL MOTIONS IN SPIRAL NEBULAE

(Unit for motions and their probable errors is 0″.001)

Object	Focus in Feet	Interval in Years	Rotational	Radial	Stream	Transverse	*n*
M 101*...........	25	5	+21±1	+ 5±1	+21±1	0±1	87
M 101†...........	18	9	+20±2	+ 6±2	+22±2	− 3±2	69
M 101†...........	18	15	+12±2	+ 7±2	+14±2	+ 2±2	46
M 33.............	25	10	+20±3	+ 6±2	+24±3	− 2±2	30
M 33.............	80	5	+14±4	+12±3	+18±4	+ 4±3	21
M 51.............	25	11	+19±1	+ 8±1	+21±1	+ 3±1	79
M 81.............	25	6	+20±4	+17±3	+25±3	+16±3	52
M 81.............	25	11	+38±1	+13±1	+39±1	+ 7±1	104

* Including the measures by Mr. Nicholson, *Mt. Wilson Contr.*, No. 118, 18, 1916.

† Photographs taken with the Crossley reflector of the Lick Observatory. All others were taken with the 60-inch reflector at Mount Wilson.

All pairs of plates show the same type of motion, and when we keep in mind the different numbers of points measured, the agreement in the values of the motion for each nebula derived from different pairs of plates is as satisfactory as could be expected.

The rotational components would correspond to the following periods: for M 101, 85,000 years; for M 33, 160,000 years; for M 51, 45,000 years; for M 81, 58,000 years.

For M 101 there is no appreciable change in the measured rotational component with distance from the center, but for M 33, 51, and 81 there appears to be some increase of motion with distance.

All four nebulae show a large outward radial component, which for M 101 is 32 per cent of the rotational component; for M 33, 48 per cent; for M 51, 42 per cent; for M 81, 34 per cent.

The transverse components are in general very small and well within the limits of error, although the positive value for M 81 may be real. In all cases, however, the measured displacements agree better with the hypothesis of outward motion along the arms of the spiral than they do with an assumed rotation of the nebulae as a whole.

The close agreement of the displacements in direction with the spiral arms suggests that we have here a realization of the motions described by Jeans in *Problems of Cosmogony and Stellar Dynamics*, from which I quote freely.

If so, we must then suppose that before the formation of the spiral arms the nebular masses were rotating and had reached a lenticular shape. The formation of Laplace's ring requires perfect symmetry of mass about the axis of rotation. The distances of adjacent masses in space are in general so great that their gravitational influence will be extremely small, but even the slightest external gravitational field will be sufficient to preclude the formation of a ring; instead of this, the matter will be thrown off at two antipodal points. The masses first thrown off at the antipodal points form in themselves a tide-generating system which concentrates the region of ejection more and more at two points. The result is an extension farther and farther into the equatorial plane as the evolution of the nebula proceeds. The determination of the shape of the arms seems at present to be beyond the reach of mathematical analysis, but the long streams of gaseous matter must become longitudinally unstable and will tend to break up into condensations or nuclei.

MOUNT WILSON OBSERVATORY
July 1921

Contributions from the Mount Wilson Observatory, No. 215
Reprinted from the *Astrophysical Journal*, Vol. LIV, pp. 140–45, 1921

ON THE ACCURACY WITH WHICH MEAN PARALLAXES CAN BE DETERMINED FROM PARALLACTIC AND PECULIAR MOTIONS

By HENRY NORRIS RUSSELL[1]

ABSTRACT

Accuracy of mean parallaxes determined from parallactic and peculiar motions.—Assuming that the stars in the group are all at practically the same distance and that the velocities are distributed according to Maxwell's law, it is shown theoretically that the probable errors in the mean parallaxes determined by the two methods are, respectively, $\pm 1.035\ \pi\bar{V}/V_0\sqrt{n}$ and $\pm 0.721\ \pi/\sqrt{n}$. The ratio is $1.44\ \bar{V}/V_0$ and depends only upon the average value of the peculiar velocities, $\bar{V}$, since V_0 is the velocity of the sun. It follows that for Cepheids, stars of types A and B, and others with peculiar velocities less than 14 km, the parallactic motions give the better result, while for stars moving faster the peculiar motions should be used. The formulae also show that results of value may be obtained from rather small groups.

Statistical study of 180 stars of types B0 to B5.—The *mean peculiar velocities*, radial and tangential, are 6.5 km and 0ʺ.0076; the *mean parallax* computed from parallactic motions is 0ʺ.0083 (π_1), and from peculiar motions 0ʺ.0058 (π_2). From π_1 and the *mean visual magnitude*, 4.08, the *mean absolute magnitude* comes out −1.38. The probable errors for the determinations of parallax agree closely with those to be expected from the foregoing theory. The lower value of π_2 compared with π_1 is partly due to the inclusion of unknown binaries for which the observed peculiar motions are too large, but this does not fully explain the discrepancy.

If the proper motions and radial velocities are known for a group of stars the mean parallax may be found in two ways. Resolving the proper motions into two components, υ toward the solar apex, and τ at right angles to this, and clearing the radial velocities of the solar motion so as to get the peculiar velocities V, we have the familiar equations

$$\bar{\pi}_1 = -\frac{\overline{\upsilon\ \sin\lambda}}{V_0\ \overline{\sin^2\lambda}}, \qquad \bar{\pi}_2 = \frac{\bar{\tau}}{\bar{V}} \tag{1}$$

where as usual the horizontal bars denote mean values, and where the means for τ and V are taken regardless of sign while V_0 is the velocity of the sun's motion in space, and, like V, is expressed in astronomical units per year.

To examine the accuracy of the two methods we may suppose that we are dealing with a group of stars which are all at substantially the same distance (so that we have to consider only the statistical errors resulting from the fact that the "law of averages" does not apply exactly to small groups) and that the velocities of the stars are distributed according to Maxwell's law, so that the components in the directions of v, τ, and V obey the Gaussian law of errors, the probable errors defining the distribution being 0.845 $\overline{V}$ for the velocities and 0.845 $\overline{V}\,\overline{\pi}$ for the proper motions. Let n be the number of stars. The ordinary formula gives for the probable error of $\overline{\pi}$ as derived from the first equation

---

[1] Research Associate of the Mount Wilson Observatory.

$$r_1 = \pm \frac{0.845\,\overline{\pi}\,\overline{V}}{V_0\sqrt{n\,\overline{\sin^2\lambda}}}$$

If the stars are distributed uniformly over the celestial sphere the value of $\overline{\sin^2\lambda}$ is $\frac{2}{3}$; if they are close to the Galaxy, it will be approximately $\frac{1}{2}$. Taking the former value, we have

$$r_1 = \pm \frac{1.035}{\sqrt{n}}\,\frac{\overline{V}}{V_0}\,\pi_1 \tag{2}$$

For the second equation, the statistical error arises from the fact that the individual average values of τ or V, for groups of n stars, will not be identical with the averages for an indefinitely large number of cases.

The formula in this case is long established, but hardly familiar, and the proof is so simple that it is worth giving. Let $v_1, v_2, \ldots\ldots v_n$ be any set of n quantities (all positive), selected at random from a great number, distributed according to the law of errors, whose arithmetical mean is η and whose mean square value is ϵ. It is well known that

$$\epsilon^2 = \frac{\pi}{2}\eta^2.$$

The square of the deviation between the mean of these particular quantities and the mean for an infinite number is

$$\frac{1}{n^2}(v_1 + v_2 \ldots\ldots + v_n - n\eta)^2.$$

In the individual case this may have any value; but suppose we take the means for a great number of trials. The result may be obtained by expanding, substituting ϵ^2 for each squared term in the result, such as v_1^2; η for v in each term of the first degree, and η^2 for each product such as v_1v_2 (since in these terms large and small values of v occur indiscriminately and the large ones do not multiply themselves as in the case of v^2). We thus find for the mean of the squares of the deviations:

$$\epsilon_n^2 = \frac{1}{n^2}(n\epsilon^2 + n(n-1)\eta^2 - 2n^2\eta^2 + n^2\eta^2) = \frac{1}{n}(\epsilon^2 - \eta^2) = \frac{\pi-2}{2n}\eta^2$$

Although the distribution of these deviations for individual stars does not at all follow the Gaussian law, that of the means of a group of six or more will probably do so very closely.[1] We may, therefore, use the ordinary formulae for computing the probable error of deviation of an individual mean of n quantities from the standard value η.

$$r = \pm 0.675\sqrt{\frac{\pi-2}{2n}}\eta = \pm\frac{0.510}{\sqrt{n}}\eta \tag{3}$$

The statistical probable error of $\bar{\tau}$ will therefore be $\pm\frac{0.510}{\sqrt{n}}\bar{\tau}$, while that of $\bar{V}$ will be $\pm\frac{0.510}{\sqrt{n}}\bar{V}$. Since the errors are independent of one another and proportional to the whole quantities concerned, the probable error of their quotient, $\bar{\pi}_2$, will be

$$r_2 = \pm\frac{0.721}{\sqrt{n}}\bar{\pi}_2 \tag{4}$$

Comparing this with (2), we have

$$\frac{r_1}{r_2} = 1.44\frac{V}{V_0} \tag{5}$$

The relative precision of the two methods depends only upon the average magnitude of the peculiar velocities (assuming, to be sure, that the sun's motion relative to the stars under consideration is accurately known). If the average peculiar velocity of the stars is less than 14 km, the parallactic motion gives the better result; otherwise the peculiar motions do so.

The actual law of distribution of velocities is not Gaussian, large velocities being in excess. This will operate to increase somewhat the numerical coefficients in (1) and (2) but should not greatly affect their ratio.

Similarly, in any actual group of stars, there will be real differences in parallax between the members, which will also introduce a statistical error into the determination of the typical mean from small samples, even though the individual parallaxes are exactly known; but this again operates to increase the probable errors given by both methods without much effect on their relative accuracy.

---

[1] Compare Schlesinger, *Astron. Journal*, **30**, 185, 1917.

It follows that the parallactic motion affords the best means of determining the mean parallaxes of stars of spectra A and B, of Cepheids, and of other slow-moving stars. For the general run of naked-eye stars of the "later" types the two methods are about equally good, while for planetary nebulae, long-period variables, and other rapidly moving objects, the peculiar velocities afford the best solution. Results of value should be obtainable from rather small groups; thus the peculiar motions of ten stars give the mean parallax with a probable error of 23 per cent of its own value (so far as the statistical errors go); and the parallactic motions for slow-moving stars should give a considerably better value. It should further be noticed that the accidental errors of observation of both radial velocities and proper motions will increase the arithmetical mean values $\overline{V}$ and $\bar{\tau}$, while their influence upon the algebraic mean used in finding $\bar{\pi}$ will be much diminished. This is not, however, a serious matter, for, if the magnitude of the errors of observation is known, their effect may be removed from both $\overline{V}$ and $\bar{\tau}$ by well-known methods, and, in any case, both are increased, and the errors tend to compensate one another in their quotient $\bar{\pi}_2$.

As an example of these principles, the 180 stars of spectra B0 to B5 for which the quantities V and τ are given by Campbell[1] were divided into equal groups of ten stars each. To secure a random distribution, the first, nineteenth, and thirty-seventh stars, etc., were combined to form one group; the second, twentieth, and thirty-eighth were in the next, and so on. The results are given in Table I.

Each line of this table (except the last three) gives mean values for one of the eighteen groups of ten stars. The first column gives the mean of the visual magnitudes; the second, that of the spectral classes; the third, that of the peculiar radial velocities (corrected for the solar motion and K-term according to Campbell's solution III); and the fourth, that of the τ components. In the fifth column are the mean parallaxes $\bar{\pi}_2$ computed from the peculiar motions by equation (1); in the sixth, the values $\bar{\pi}_1$ found from the parallactic motions; and in the last column, the absolute magnitudes corresponding to the parallaxes in the preceding column and the apparent magnitudes in the first.

---

[1] *Lick Observatory Bulletin*, **6**, 101–124, 1911.

The last three lines of the table give, respectively, the means of the quantities in the columns above, the probable error of one of those quantities computed in the usual way from the deviations from the mean, and the ratio of the probable error to the general mean in the cases where this is significant.

TABLE I

Mean Magnitude	Mean Spectrum	$\bar{V}$	$\bar{\tau}$	$\bar{\pi}_2$	$\bar{\pi}_1$	Abs. Mag.
4.19.......	B3.5	5.0	0″.0096	0″.0091	0″.0087	−1.1
4.38.......	3.4	6.2	43	33	66	−1.5
4.24.......	2.1	7.4	49	31	69	−1.6
3.98.......	2.8	10.4	68	31	94	−1.1
4.00.......	2.2	6.8	122	92	93	−1.2
3.22.......	2.7	6.4	55	41	90	−2.1
3.83.......	2.4	4.6	84	87	103	−1.1
4.71.......	3.6	9.0	73	38	71	−1.0
3.76.......	2.4	6.9	52	36	72	−1.9
4.09.......	3.2	4.6	72	74	51	−2.4
4.09.......	3.7	6.4	68	50	65	−1.8
4.19.......	3.9	5.0	77	74	101	−0.8
4.05.......	3.0	7.0	105	71	93	−1.1
4.35.......	3.9	7.3	94	61	96	−0.8
4.11.......	2.0	6.1	56	43	62	−1.9
4.41.......	3.4	5.8	79	65	88	−0.9
3.75.......	3.0	5.9	97	78	100	−1.3
4.01.......	3.3	6.6	64	46	90	−1.2
Means.........4.08	B3.0	6.5	0″.0076	0″.0058	0″.0083	−1.38
P.E. one entry ±0.22	±0.41	±1.0	±0.00155	±0.00144	±0.00105	±0.32
Ratio.........	....	±0.15	±0.20	±0.25	±0.13	....

The "probable errors" for the mean magnitude and spectral type indicate only the degree of statistical similarity between the various groups, which is fairly high; but those for the next four quantities afford a practical test of the applicability of the theory developed above. From equation (3) the ratio of the probable error of one of the tabular values of $\bar{V}$ or $\bar{\tau}$ to the average value of these quantities should be ±0.16. This is substantially the case for $\bar{V}$. The greater variability found for τ may reasonably be attributed to real differences in the mean parallaxes of the various groups (which were assumed to be the same in deriving the formulae). Equation (4) gives ±0.23 as the value to be expected for

π_2, and equation (2), ±0.11 as the expectation for $\bar{\pi}_1$. The agreement in both cases is remarkably close.

There is, however, a remarkable difference between the means of $\bar{\pi}_1$ and $\bar{\pi}_2$, the latter being only 70 per cent of the former. Only three of the twenty values of $\bar{\pi}_2$ are greater than the mean for $\bar{\pi}_1$, and only one value of $\bar{\pi}_1$ is smaller than the mean for $\bar{\pi}_2$. The discordance must therefore arise from some real cause, and there can hardly be a doubt regarding its origin. Campbell calls attention[1] to the fact that the observed values of $\bar{V}$ must be systematically too great on account of the inclusion in the lists of some undetected spectroscopic binaries for which the greater part of the observed velocity is due to orbital and not to systematic motion,[2] and of the probable variability of the K-term from one star to another; and Kapteyn[3] has pointed out that the accidental error of observation, which he finds to correspond to a probable error of ±2.1 km for the well-observed stars, must also operate to increase them.

Campbell adopts the value 6 km instead of 6.5 for $\bar{V}$, which would raise $\bar{\pi}_2$ to 0."0063.

To obtain full accordance with $\bar{\pi}_1$, it would be necessary to reduce $\bar{V}$ to 4.5 km, which seems too large an allowance for these corrections, especially when it is considered that Boss,[4] from more than twice as many stars of the same spectral class, finds that the τ components correspond to a peculiar velocity of 6.3 km.

It is obvious, however, that the parallactic motions give much the better result in the case of the B-stars, irrespective of this uncertainty; and Kapteyn has based his classical work almost entirely upon them.

For rapidly moving stars, however, the peculiar motions are relatively much less influenced by such minor sources of error as have just been described, and by their use reliable values for the mean parallax can be obtained from groups of stars of moderate number.

MOUNT WILSON OBSERVATORY
July 2, 1921

---

[1] *Op. cit.*, p. 121.

[2] There are 53 of Campbell's 180 stars for which his notes indicate that the radial velocities are of inferior accuracy. The mean $\bar{V}$ for these is 7.5 km; for the remainder, 6.1 km. Hence the effect of this correction is small.

[3] *Astrophysical Journal*, **40**, 71, 1914.

[4] *Astronomical Journal*, **26**, 198, 1911.

Contributions from the Mount Wilson Observatory, No. 216
Reprinted from the *Astrophysical Journal*, Vol. LIV, pp. 334–46, 1921

ON MAJORANA'S THEORY OF GRAVITATION

By HENRY NORRIS RUSSELL[1]

ABSTRACT

Majorana's theory of gravitation.—As a result of carefully executed experiments, Majorana has suggested that gravitational force is weakened by passing through matter. In this paper certain *astronomical consequences* of this assumption are presented. The true masses of the planets according to this theory are computed and it is shown (1) that the inertial masses cannot be equal to these true masses, and (2) that if we assume them equal to the apparent gravitational masses we are led to such discrepancies in the case of the tides that we are forced to conclude that the absorption of gravitational force cannot exceed 1/5000 of the value assigned by Majorana.

Possible influence of one body on the mass of another body.—The interpretation of Majorana's positive experimental result, assuming it to be real, must be that the mass of a body is actually changed by the presence of another body.

Professor Majorana, in a very interesting series of papers,[2] has proposed a new theory of gravitation, with experimental evidence supporting it. The present communication deals with certain astronomical consequences of the theory, in the form in which he presents it, and suggests a modification which will remove the resulting discrepancies.

1. The law which Majorana proposes[3] is that the force of attraction between any two material particles is directed along the line joining them, but that its intensity is less than that given by Newton's law whenever this line traverses matter, being diminished in accordance with the "law of progressive absorption" which holds good for radiation.

If M_1 and M_2 are the masses of the particles, r their distance apart, and k the ordinary constant of gravitation, the attractive force will be

$$f=k\frac{M_1M_2}{r^2}e^{-\int h\theta dr}, \tag{1}$$

---

[1] Research Associate of the Mount Wilson Observatory.

[2] *Philosophical Magazine*, **39**, 488, 1920. *Atti della Reale Accademia dei Lincei*, **28**, 160, 221, 313, 416, and 480, 1919, and **29**, 23, 90, 163, and 235, 1920. Further citations refer to the detailed account in Italian.

[3] *Op. cit.*, p. 170.

where h is a second universal constant, that of absorption of gravitation, and θ the density of matter at any point on the line joining the particles, and the integral is taken over the whole length of this line.

In consequence of this absorption the attraction of any large body upon objects outside it will be diminished, and its "apparent mass," measured by means of its attraction, will be less than the true mass. For spherical bodies of uniform density Majorana shows[1] that the attraction will still be exactly proportional to the inverse square of the distance, while the apparent mass m will be connected with the true mass M by the equations

$$m=\psi M, \tag{2}$$

$$\psi=\tfrac{3}{4}\left[\frac{1}{p}-\frac{1}{2p^3}+e^{-2p}\left(\frac{1}{p^2}+\frac{1}{2p^3}\right)\right], \tag{3}$$

$$p=hR\theta, \tag{4}$$

where R is the radius of the mass, and θ the *true* density.

For small values of p we find, expanding in series,

$$\psi=1-\tfrac{3}{4}p+\tfrac{2}{5}p^2-\tfrac{1}{6}p^3+\ .\ .\ .\ .\ . \tag{5}$$

For large values of p, ψ approaches asymptotically to the value $3/4p$ and m to the value $\pi R^2/h$. The apparent mass of a homogeneous sphere has therefore, according to this theory, a superior limit, depending only upon its superficial area and the universal constant h. Majorana gives no calculations for bodies not of uniform density; but an easy calculation shows that the attraction of any spherical mass in which the density depends only upon the distance from the center, upon an external particle, is inversely proportional to the square of the distance from the center, as in the Newtonian case. The difference between the true and apparent masses will be greater, the greater the central condensation. For example, if the density at the distance r from the center is proportional to $(R^2-r^2)^n$, it is easy to show[2] that

$$\psi=1-\frac{(2n+3)^2}{12n+12}p+\ .\ .\ .\ .$$

---

[1] *Op. cit.*, p. 420. The notation is slightly changed here.

[2] See the appendix to this paper.

(where the *true mean density* is to be used in calculating p). For $n=1$, $\psi=1-\frac{25}{24}p\ \ldots\ldots$; for $n=2$, $\psi=1-\frac{49}{36}p.\ \ldots\ldots$ The former value corresponds to a central condensation greater than in the case of the earth, and the latter to a central density more than four times the mean density.

Majorana's conclusion, based upon qualitative reasoning, that condensation toward the center will not radically change the amount of absorption of gravitation, is therefore justified; but the numerical effects of such condensation appear to be somewhat greater than he has estimated.

2. We may now proceed to calculate the effects of absorption of gravitation in various bodies belonging to the solar system, using the value determined by Majorana[1] for the constant of absorption ($h=6.73\times10^{-12}$ in c.g.s. units) and assuming the bodies to be of uniform density. It must be remembered that, if ρ is the mean density derived from observation on the Newtonian theory, we will have $p=\psi\theta$, and hence $p\psi=hR\rho$. Knowing this, ψ may be determined by successive approximations, or, if p is small, by the equation

$$\psi=1-\tfrac{3}{4}p\psi-\tfrac{13}{80}p^2\psi^2-\tfrac{53}{480}p^3\psi^3\ \ldots\ldots \tag{6}$$

obtained by "reversion" from (5).

TABLE I

GRAVITATIONAL ABSORPTION ACCORDING TO MAJORANA

	R	p	$p\psi$	ψ
Sun	6.95×10^{10} cm	1.41	0.660	0.33
Jupiter	7.23×10^{9}	1.33	0.065	0.951
Saturn	5.90×10^{9}	0.72	0.029	0.978
Earth	6.37×10^{8}	5.53	0.024	0.981
Mars	3.39×10^{8}	3.95	0.0090	0.993
Moon	1.74×10^{8}	3.40	0.0040	0.997
Eros	2×10^{6}	3	0.00004	1.0000

The results are given in Table I. The data for the sun are from Majorana's paper. The diameter and density given for the asteroid Eros are rough estimates, but doubtless correct as regards order of magnitude.

---

[1] *Op. cit.*, **29**, 236.

It is evident that the absorption of gravitation within the larger planets is by no means negligible.

3. The changes which such an absorption would introduce into the planetary theory are remarkable. The attraction between two spherical bodies of masses M_1 and M_2 at a distance r is kM_1M_2/r^2 according to Newton. According to Majorana, we must substitute $kM_1M_2\psi_1\psi_2/r^2$ (since the force is weakened in traversing both bodies).

Nothing in Majorana's discussion suggests that any change would occur in the inertial masses. If these remain the same, the acceleration of M_1 will be $kM_2\psi_1\psi_2/r^2$, or $km_2\psi_1/r^2$. Similarly that of M_2 will be $km_1\psi_2/r^2$, and the relative acceleration of the bodies toward one another will be $k(m_1\psi_2+m_2\psi_1)/r^2$.

The expression in parenthesis takes the place of the sum of the masses, M_1+M_2, in the Newtonian theory. Let M_1 represent the sun and M_2 the planet. We will have, by Kepler's Third Law,

$$\frac{a_2^3}{T_2^2}=\frac{k}{4\pi^2}(m_1\psi_2+m_2\psi_1), \tag{7}$$

where a_2 and T_2 are the mean distance and periodic time of the planet. Comparing this with another planet, M_3, we find:

$$\left(\frac{a_2}{a_3}\right)^3=\left(\frac{T_2}{T_3}\right)^2\frac{m_1\psi_2+m_2\psi_1}{m_1\psi_3+m_3\psi_1}.$$

The masses of the planets are all less than a thousandth part of the sun's, and the factor ψ_1 is also small. We may therefore write with high approximation:

$$\frac{a_2}{a_3}=\left(\frac{T_2}{T_3}\right)^{\frac{2}{3}}\left(\frac{\psi_2}{\psi_3}\right)^{\frac{1}{3}}.$$

The error committed by disregarding the planetary masses is at most one part in ten thousand. This equation differs from the ordinary form of Kepler's law by the presence of the factor involving ψ_1 and indicates that a massive planet should be considerably nearer the sun than a planet of small mass and identical period.

Applying it first to Jupiter and the earth, we have $\psi_2/\psi_3=0.969$, so that, taking the earth's mean distance as unit, the mean distance of Jupiter should be less than that computed on the ordinary theory by 1.04 per cent.

This is utterly inadmissible. When Jupiter is in quadrature with the sun, its annual parallax (the angle at the planet between lines drawn to the sun and earth) is approximately 11° 5′, and the suggested change would increase this angle by 6′ 56″. The planet's longitude would then deviate from the ordinary ephemerides, which are computed on the Newtonian theory, by this amount every time that Jupiter was in quadrature, but in opposite directions according as it was east or west of the sun. Any actual deviation of this sort cannot at most exceed 1/500 of the predicted amount, and to avoid conflict with observation, Majorana's constant *h* would have to be correspondingly diminished.

The case of Eros is even more striking. Taking the earth again as standard, we find that $\psi_2/\psi_3 = 1.019$, and the distance of the asteroid should be greater by 0.63 per cent. When it is in perihelion and at the same time in quadrature, its distance from the sun is 1.13 astronomical units and from the earth 0.55. The suggested change in its mean distance would displace it by 39′ in geocentric longitude. With the planet in perihelion, but nearer to opposition (in about the position which it occupied in 1901, when it was very carefully observed), the discordance would exceed 1°—which is fully five thousand times as much as is allowable.

The most conspicuous case of all is provided by the moon. On Majorana's theory, the attraction of the sun should produce in the moon an acceleration greater by 1.6 per cent than that experienced by the earth at the same distance. This would be equivalent to a continually acting disturbing force, directed toward the sun, and amounting to 1/60 of its whole attraction on the moon, or 1/30 of the earth's attraction. This is three times the maximum disturbing force due to the sun on the Newtonian theory, and its introduction would play utter havoc with the whole lunar theory. The admissible magnitude of such an unrecognized disturbing force is probably less than one ten-thousandth as great.

Yet again, the tides on the earth's surface would be radically altered. In addition to the usual tidal forces depending on the variations in the magnitude and direction of the attraction of the sun and moon, there would be a force depending on the difference of the screening action for the earth as a whole and for a water particle on its surface. Over the hemisphere facing the sun this force would be directed toward the sun and amount to 1.9 per cent of the sun's attraction. In the opposite hemisphere it would rapidly diminish, changing sign for points such that the absorption along the "gravitational ray" from the sun was equal to the average value for the earth as a whole. Beyond this the force would be directed away from the sun and reach a maximum at the point opposite it, where it would be 2.9 per cent of the sun's whole attraction (assuming, as elsewhere, a homogeneous earth).

The tides are produced by the horizontal component of this force, which will evidently be a maximum when the sun (or moon) is on the horizon, and amount to 0.019 times the whole attraction of the body. The ordinary tide-raising force vanishes when the sun is on the horizon, is greatest when it is 45° above or below it, and amounts to 0.025 of the moon's whole attraction and 0.000064 of the sun's.

The additional tide-raising force demanded by Majorana's theory is therefore about three-quarters of the recognized force due to the moon, but nearly three hundred times the recognized component in the case of the sun. This last term is more than eighty times the greatest tidal force that can occur on the Newtonian theory.

4. We are forced therefore to the conclusion that upon the hypothesis that there exists an absorption of gravitational force in matter, without change in its inertial mass, the coefficient of absorption cannot exceed one ten-thousandth of that derived by Majorana from his experiments, and must be hopelessly beyond the reach of investigation in the laboratory. There is nothing really new in this conclusion, or in the reasoning by which it has been reached. All depends upon the old and familiar proposition that the motions of the planets prove that their gravitational and inertial masses are strictly proportional to one another, at least within a few parts in a million. Any influence which modifies one must alter the other in the same proportion.

Accepting this, we must assume in section 3 that the accelerations are inversely proportional to the apparent masses, m, instead of the true masses, M. It would then follow that all astronomical motions will take place in accordance with the Newtonian law, but that the apparent masses will everywhere appear in the place of the true masses. The only exceptions occur when one body intervenes directly between two others. The resulting effects are negligible for the planets and small for the moon; but in the case of the tides they are important.

Let the apparent mass of the earth be m_2 and the radius R, and let there be a body B (Fig. 1) of apparent mass m_1, at a distance D from the earth's center C, and D_1 from a point P on its surface. At this point there is a particle of apparent mass μ. The attraction of the earth upon it is

$$g = km_2\mu/R^2.$$

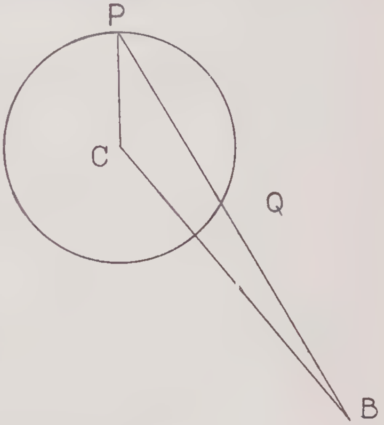

FIG. 1

The horizontal tide-raising force acting upon P will be the sum of the components in this direction of the direct attraction of B and the inertial reaction arising from the acceleration of the system of axes, fixed in the earth, with respect to which the force is measured. (We may suppose that the earth does not rotate.) The force due to the attraction of B is:

$$f = \frac{km_1\mu}{D_1^2} \sin z_1 e^{-h\theta S},$$

where z_1 is the apparent zenith distance of B for an observer at P, S the distance PQ which the line PB traverses inside the earth, and θ the earth's true density (supposed as usual to be constant).

Since $S = -2\ R \cos z_1$, we have by (4):

$$f_1 = \frac{km_1\mu}{D_1^2} \sin z_1\, e^{2p \cos z_1} = \frac{km_1\mu}{D_1^2} \sin z_1\, (1 + 2p \cos z_1)$$

(since p is small).

If $\cos z_1$ is positive, the last factor is to be set equal to unity.

In this case, where the attraction between P and B varies with their direction as well as their distance, the apparent gravitational mass of P will vary according to whether we consider the attraction between it and B, or between it and the earth. (We obviously cannot suppose that the apparent masses of the earth or of B, whose attraction on one another is unaltered, are sensibly affected by the existence of the minute particle P.)

The inertial mass of P may be equal to either of these values of its gravitational mass, or, more probably, to some compromise between them. Let us set it equal to $\mu\,(1-\epsilon)$. The acceleration of the earth, due to the attraction of B, will be $km_1/D^2 \sin z$, where z is the angle PCB (the geocentric zenith distance). We have, rigorously,

$$D \sin z = D_1 \sin z_1 \,,$$

and, neglecting R^2/D^2,

$$D = D_1 + R \cos z_1 \,.$$

The inertial reaction of the particle P, in the horizontal direction, will be, to the first order:

$$f' = \frac{km_1\mu}{D^2}(1-\epsilon) \sin z = \frac{km_1\mu}{D_1^2} \sin z_1 \left(1-\epsilon-\frac{3R}{D} \cos z_1 \;.\;.\;.\;.\;\right) .$$

The deflection of the vertical by the tidal force will be given by

$$\tan \delta = \frac{f_1-f'}{g} = \frac{m_1 R^2}{m_2 D_1^2} \sin z_1 \left(3\frac{R}{D} \cos z_1 + 2p \cos z_1 + \epsilon\right) .$$

The first term in the parenthesis gives the effect on the Newtonian theory.

The quantity ϵ must be very small. If the inertial mass of the pendulum, swinging under the earth's attraction, were $1-\epsilon$ times its gravitational mass, its period would be $1-\epsilon/2$ times that derived from the ordinary theory. When the sun and moon are above the horizon, ϵ must be zero. If it were as great as 0.001 when both are below the horizon, all pendulum clocks would gain at the rate of nearly two seconds an hour. The greatest admissible value must be well below 0.0001. On the other hand, $3R/D$ is 0.050 in the case of the moon, and 0.00013 for the sun, while $2p$, for the earth, is 0.048.

The assumption of an absorption of gravitational force in passing through the earth leads therefore to discrepancies in the case of the tides which cannot be removed by any admissible assumption regarding changes in the inertial mass of the attracted water. The lunar tides should be twice as great, and the solar tides 370 times as great, when the attracting bodies are below the horizon as when they are at the same altitude above.

The most accurate observations of tidal force are undoubtedly those of Michelson and Gale, derived from observations of the displacements of the water level in underground pipes. From their curves[1] it is evident that the Newtonian theory represents the forms of the observed curves within a few per cent. The relative amplitudes of the solar and lunar tides, for a whole year, agree with theory within the probable errors (about 3 per cent for the larger oscillations). This indicates that any absorption of gravitation, in passing through the earth, cannot exceed 1/5000 of the value assigned by Majorana.

5. It appears therefore that the assumption that gravitational force is weakened in passing through matter must be definitely abandoned.

But what then becomes of Professor Majorana's long and careful series of experiments? If their result is accepted, it seems necessary to interpret it as showing that the *mass* of one body (his suspended sphere of lead) was diminished by the presence of another large mass (the surrounding mercury); that the effect was a true change in the mass (since inertial mass and gravitational mass are all the kinds of mass that we know of); and that it depended on the proximity of the larger mass, and not upon any screening action upon the earth's gravitation.

Strange as this notion may seem, it is not inherently absurd. Indeed, if the phenomena of gravitation and inertia may be accounted for by assuming that the four-dimensional "world" possesses certain non-Euclidean properties, or "curvature," both in the presence of matter and remote from it, it is not very surprising if the curvature induced by one mass of matter should be modified to some degree by the superposition of the curvature due to another, so that the effects were not exactly additive.

---

[1] *Astrophysical Journal*, **50**, 342, 1919.

A great variety of assumptions may be made regarding such an influence, and many of these might have the advantage of giving a conservative field of force, which Majorana's did not. Complications are still likely to arise. For example, consider a large spherical mass, alone in space and gradually contracting upon itself while it moves forward in a straight line. Its mass will presumably diminish as its various parts come closer together; but what will happen to its velocity? Presumably this would increase, but it seems obvious that either the conservation of momentum or the conservation of energy would have to be abandoned, if not both. Come next to a planet revolving in an eccentric orbit about the sun. Its mass will diminish at perihelion, and this will probably lead to changes in its orbital velocity. The resulting alterations in the orbit will depend on the law of change of velocity, and it might be possible to invent a law which would lead to conclusions consistent with observation.

Further speculation on such matters seems, however, to be premature, when it is considered that the whole structure would rest upon the observation of a change in weight amounting to one part in 1200 millions. Discussion of the possibility that some undetected systematic error has crept into the results, in spite of the great care taken to eliminate such errors, or to correct them, must be left to those better versed in experimental technique than the present writer; but it is to be hoped that the further experiments which Professor Majorana contemplates will provide the data regarding the reality, magnitude, and laws of variation of the suspected influence which are now evidently desirable.

APPENDIX

The proofs of certain statements made previously are collected here to avoid interruption of the course of the discussion.

Let *P*, Figure 2, be any point at which it is desired to find the gravitational attraction of a mass *M*. Draw through *P* an elementary cone, of solid angle $d\omega$, intersecting *M* between the points

A and B. Let Q be any point inside M at a distance r from P. The element of this cone between the distance r and $r+dr$ from P will have a volume $r^2 dr d\omega$ and a mass $\theta r^2 dr d\omega$, where θ is the true density. Its attraction upon a unit particle at P will be $k\theta dr d\omega$, according to Newton's law. If we set $\theta dr = dn$, n will be the total mass per unit section of a thin cylindrical column extending from Q to A, and the attraction at P will be $k d\omega dn$. Integrating, we find for the attraction of the conical frustum AB the value $kn_1 d\omega$ where n_1 is the value of $\int \theta dr$ between A and B.

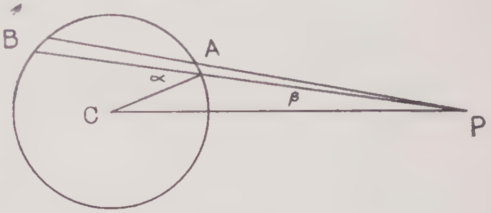

FIG. 2

According to Majorana, we must take the absorption of gravitation into account. In passing through a distance dr, this is $h\theta dr$ or hdn. Hence the transmission through the layer QA is e^{-hn}, and we find easily for the whole attraction at P, due to the frustum,

$$\frac{k}{h}(1-e^{-hn_1})d\omega.$$

Suppose now that M is spherical and that the density depends only on the distance from the center C. Let the angle CPB be β and CAB be α, also let $CP=R$, $CA=R_0$, then

$$\sin\beta = \frac{R}{R_0}\sin\alpha\,.$$

The whole attraction of the sphere at P must obviously be directed toward C. The component in this direction of the attraction of the frustum already considered is $kn_1 d\omega \cos\beta$. If ϕ is the position-angle about the axis CP, we have:

$$d\omega = \sin\beta\, d\beta\, d\phi = \frac{R_0^2}{R^2}\sin\alpha\cos\alpha\sec\beta\, d\alpha\, d\phi\,.$$

The whole attraction of the sphere at P will be

$$F = \frac{2\pi k R_0^2}{R^2}\int_0^{\frac{\pi}{2}} n_1 \sin\alpha\cos\alpha d\alpha, \tag{1}$$

according to Newton, but

$$F' = \frac{2\pi k R_0^2}{hR^2} \int_0^{\frac{\pi}{2}} (1 - e^{-hn_1}) \sin \alpha \cos \alpha d\alpha, \tag{2}$$

according to Majorana.

It is evident that n_1 depends only upon the length of the chord AB, that is, that it is a function of α, and hence that the definite integrals in (1) and (2) depend only upon the distribution of density within the sphere. Therefore the whole attraction of the sphere at an exterior point is inversely proportional to the square of the distance from the center, on Majorana's theory as well as Newton's.

When finally reduced, equation (1) goes over, of course, into the familiar form

$$F = kM/r^2.$$

If the density is uniform, $n_1 = 2R_0\theta \cos \alpha$, and equation (2) gives Majorana's formula for ψ. For other laws of density the integrals will in general be difficult or impracticable to reduce to known forms; but if the total absorption is small, we may write:

$$\frac{1}{h}(1 - e^{-hn_1}) = n_1 - \tfrac{1}{2}hn_1^2 \quad . \; . \; . \; . \; .$$

If the density θ is proportional to $(R_0^2 - S^2),^n$ where S is the distance from the center of the sphere, we find without difficulty that n_1 is proportional to $(R_0^2 - S_0)^{n+\frac{1}{2}}$, where S_0 is the least distance of the chord from the center. But then $S_0 = R_0 \sin \alpha$. We may then write $n_1 = CR_0 \cos^{2n+1} \alpha$ and find on Majorana's theory:

$$F' = \frac{2\pi k C R_0^3}{R^2}\left(\frac{1}{2n+3} - \frac{hCR_0}{8n+8} + \; . \; . \; . \; . \right).$$

The first term equals kM/R^2, or $4k\pi\theta_0 R_0^3/3R^2$, if θ_0 is the true mean density. Hence

$$C = \frac{4n+6}{3}\theta_0,$$

and

$$F = \frac{kM}{R}\left(1 - \frac{(2n+3)^2}{12n+12}h\theta_0 R_0\right),$$

as stated in the text.

Mount Wilson Observatory
July 20, 1921

NOTE

Professor D. L. Webster, in a conversation with the writer, has pointed out that the supposition of a change in velocity of a spherical body which is contracting and hence diminishing in mass (according to the alternative theory suggested in section 5) is inconsistent with the principle of relativity, since, from the magnitude of such a change (no matter whether energy or momentum should be conserved) it would be possible to determine the absolute velocity of the body.

This difficulty makes the theory of an actual change of mass appear very improbable, and the trouble is not diminished when it is asked what becomes of the energy which, on relativistic principles, is equivalent to the mass which has disappeared. Further evidence regarding the reality of the experimental effect appears to be urgently called for.

PRINCETON UNIVERSITY OBSERVATORY
September 27, 1921

Contributions from the Mount Wilson Observatory, No. 217
Reprinted from the *Astrophysical Journal*, Vol. LIV, pp. 293–95, 1921

NOTE ON COOLING BY EXPANSION IN SUN-SPOTS

By HENRY NORRIS RUSSELL[1]

ABSTRACT

Cooling by expansion in sun-spots.—Assuming the low temperature of sun-spots to be due to the expansion of the rapidly rising gases, it is shown that the base of the spot vortex must be a region of very high temperature, probably over 20,000°, and the increase of volume on ascending must be large, probably over 30 times. But only rough estimates can be made.

It is generally accepted that the relatively low temperatures of sun-spots are due to the cooling of the gases by expansion in the upper part of the vortex. The temperature of the spots is probably 2000° to 2500° C. lower than that of the photosphere, so that they may be regarded as the most powerful refrigerating engines known to science.

To estimate the degree of expansion which is necessary to produce this cooling, consider a mass of gas rising in the vortex. It cannot cool faster than the rate given by adiabatic expansion; nor, indeed, nearly as fast, for great quantities of heat are flowing into it by radiation from the hotter regions surrounding the vortex, and, within the gases of the vortex, processes of recombination of electrons with ionized atoms and of formation of chemical compounds are at work on a large scale, and these liberate great quantities of heat. (Formation of TiO_2, 3000 calories per gram of reacting material; neutralization of singly ionized calcium, 3500 calories per gram; most neutralizations give off more heat.)

Meanwhile, the temperature of the surrounding solar gases, through which the vortex column rises, must diminish upward; and this temperature gradient cannot be less than that of radiative equilibrium, for otherwise the observed outward flow of heat from the sun's interior could not be maintained.

In radiative equilibrium, we have

$$T \propto P^{1/4} \propto \rho^{1/3}$$

---

[1] Research Associate of the Mount Wilson Observatory.

where T, P, and ρ represent the temperature, pressure, and density, respectively. In adiabatic expansion:

$$T \propto \rho^{\gamma-1} \propto P^{\frac{\gamma-1}{\gamma}},$$

γ being the ratio of specific heats. The effect of ionization in altering the mean molecular weight of the gases is here ignored.

Suppose that the vortex starts at a depth where the temperature, pressure, and density are T_0, P_0, and ρ_0, and rises to the surface where, outside the spots, these quantities are T_1, P_1, and ρ_1. In the spots, at the visible surface, the temperature will have the lower value T_2. The pressure will be about the same as P_1, for it is probable that we look down through about the same amount of matter per square centimeter, before being stopped by atmospheric scattering, in the spots and in the photosphere; and, of course, the solar gravity is the same.

Hence:

$$P_2 = P_1; \qquad \rho_2 = \frac{T_1}{T_2}\rho_1 .$$

We have then for radiative equilibrium:

$$\frac{T_1}{T_0} = \left(\frac{P_1}{P_0}\right)^{1/4},$$

and for adiabatic equilibrium:

$$\frac{T_2}{T_0} = \left(\frac{P_1}{P_0}\right)^{\frac{\gamma-1}{\gamma}};$$

whence:

$$\frac{T_2}{T_1} = \left(\frac{P_1}{P_0}\right)^{\frac{3\gamma-4}{4\gamma}} = \left(\frac{T_1}{T_0}\right)^{\frac{3\gamma-4}{\gamma}},$$

$$\frac{T_0}{T_1} = \left(\frac{T_1}{T_2}\right)^{\frac{\gamma}{3\gamma-4}}; \quad \frac{P_0}{P_1} = \left(\frac{T_0}{T_1}\right)^4; \quad \frac{\rho_0}{\rho_1} = \left(\frac{T_0}{T_1}\right)^3.$$

Now in the actual case T_1 is about 6000°, T_2 3500° to 4000° C., and T_1/T_2 1.5 or more. The greatest possible value of γ is 5/3 (monatomic gas). This would give:

$$T_0 = 2.0T_1 = 12{,}000°; \qquad P_0 = 16P_1; \qquad \rho_0 = 8\rho_1 = 5.3\rho_2.$$

But, for reasons already stated, this must greatly underestimate the amount of expansion. If, as a rough allowance for the effects of radiation and recombination in the ascending vapor, we assume that, on the average, γ equals 7/5, as for a diatomic gas, we would find:

$$T_0 = 17T_1 = 100{,}000^\circ; \quad P_0 = 80{,}000P_1; \quad \rho_0 = 5000\rho_1 = 3300\rho_2.$$

Assuming $\gamma = 3/2$, we have:

$$T_0 = 3.7T_1 = 22{,}000^\circ; \quad P_0 = 190P_1; \quad \rho_0 = 51\rho_1 = 34\rho_2.$$

It is evident, therefore, that the base of the spot vortex must be in a region of high temperature, and that the increase of volume in ascending must be great; but no numerical estimates can be made.

It may be noticed in conclusion that the very existence of cooling by expansion in sun-spots shows that any general vertical convection in the outer layers of the sun must either reach only to a depth which is small compared with that from which the ascending spot vortex comes, or else be so slow that the cooling by expansion as the gases rise is continuously made up by heating by radiation. Otherwise the temperature gradient would be so nearly adiabatic that no important differential cooling could occur in the spots.

Mount Wilson Observatory
July 27, 1921

Contributions from the Mount Wilson Observatory, No. 218
Reprinted from the *Astrophysical Journal*, Vol. LIV, pp. 323–33, 1921

STUDIES BASED ON THE COLORS AND MAGNITUDES IN STELLAR CLUSTERS

NINETEENTH PAPER: A PHOTOMETRIC SURVEY OF THE PLEIADES

By HARLOW SHAPLEY and MYRTLE L. RICHMOND

ABSTRACT

Survey of photographic and photo-visual magnitudes of 821 stars in four square degrees in the Pleiades.—The photometric study of a region two degrees square, with Alcyone in the center, was undertaken to supplement Trumpler's study of the proper motions. The results of measurement of 30 photographs made with the 60-inch reflector, comprising a total of 290 exposures, are given in Table II. There are no abnormally large color-indices. This is the first star cluster for which *comprehensive data for dwarf stars* have been secured.

A detailed study of the proper motions of over a thousand stars in the neighborhood of the Pleiades by Dr. Trumpler has shown that the cluster contains in the central field of 4 square degrees about 200 members brighter than the fourteenth magnitude. The parallax of the Pleiades is of the order of $0''01$; hence the absolute magnitudes of the main bulk of the cluster stars lie between $+5$ and $+9$. As this is one of the few stellar groups in which the color, frequency, distribution, and motions of dwarf stars can be investigated successfully, a study of the photographic and photovisual magnitudes was begun at Mount Wilson three years ago in order to supplement Dr. Trumpler's work on proper motion.

The comparison of the Mount Wilson magnitudes and colors with the work of other observers will be made in Trumpler's monograph, which will also include a full discussion of the structure of the system of the Pleiades.

For each catalogued magnitude the average number of images measured is approximately four, and the average probable error is of the order of 0.06 mag. Only the final results of the photometric work are given in the present paper. Information relating to the photographs, measures, and reduction for any individual star can be obtained by communicating with the Mount Wilson Observatory.

In order to cover with the 60-inch reflector a region 2 degrees square (Alcyone at the center), it was necessary to divide the area into 36 equal fields, the centers of adjacent fields being separated by about 20′.

TABLE I

PHOTOGRAPHS OF THE PLEIADES

Plate Number	Kind	Date	Fields
4072	S 27	1917 Oct. 12	19, 20, 21, 22, 23, 24
4073	S 27	Oct. 12	25, 26, 27, 28, 29, 30
4183	Iso	Nov. 11	20, 23, N. P.
4184	S 27	Nov. 11	20, 23, N. P.
4185	S 27	Nov. 11	23, 24, N. P.
4300	Iso	Dec. 20	13, 14, 15, 16, 17, 18
4301	S 27	Dec. 20	13, 14, 15, 16, 17, 18
4680	S 27	1918 Sept. 1	31, 32, 33, 34, 35, 36
4681	Iso	Sept. 1	31, 32, 33, 34, 35, 36
4682	S 27	Sept. 1	1, 7, 13, 19, 25, 31
4765	Iso	Nov. 1	12, 10, N. P.
4766	S 27	Nov. 1	12, 10, N. P.
4767	S 27	Nov. 1	10, 7, N. P.
4768	Iso	Nov. 1	7, 8, 9, 10, 11, 12
4769	S 27	Nov. 1	7, 8, 9, 10, 11, 12
4849	Iso	1919 Feb. 25	19, 20, 21, 22, 23, 24
4850	S 27	Feb. 25	1, 2, 3, 4, 5, 6, N. P.
4851	Iso	Feb. 25	6, 3, N. P.
4852	S 27	Feb. 25	6, 3, N. P.
5026	S 30	July 23	6, 12, 18, 24, 30, 36, N. P.
5027	S 30	July 23	36, 33, N. P.
5043	Iso	Aug. 22	25, 26, 27, 28, 29, 30
5056	Iso	Sept. 21	1, 2, 3, 4, 5, 6
5118	Iso	Oct. 31	6, 12, 18, 24, 30, 36
5154	S 30	Dec. 18	15, 16, 22, N. P.
5155	S 30	Dec. 18	21, 22, 27, 28, N. P.
5607	Iso	1920 Sept. 14	28, 22, 21, N. P.
5608	S 30	Sept. 14	22, 21, N. P.
5609	S 30	Sept. 14	21, 15, 16, 22
5610	Iso	Sept. 14	22, 16, 8, 2, 20, 26

The scales of the photographic and photovisual magnitudes were determined by comparison of these fields with the North Polar standards[1] and with each other. The list of photographs in Table I shows how the various fields were intercompared and connected with the Pole. Each plate was given two separate exposures to each of three or more fields, with exposure times of one minute and five minutes, respectively, for photographic and photovisual magnitudes. Yellow filter *C* was used with the isochromatic plates (Cramer Instantaneous). The measures and reductions were made according to the methods generally used for photometry at Mount Wilson.

---

[1] Seares, *Mt. Wilson Contr.*, No. 97; *Astrophysical Journal*, **41**, 206, 1915.

The photometric catalogue, Table II, contains in the first three columns the number in Trumpler's forthcoming catalogue and the abbreviated positions for 1900.0 from the same source. The fourth and fifth columns contain the photographic magnitude and color index determined at Mount Wilson. In the sixth column the first number for each star refers to photographic plates, the second to photovisual plates.

All stars brighter than 11.0 photographic, or 10.0 photovisual, are omitted from our catalogue. Those stars whose magnitudes are disqualified by the proximity of the photographic images of other stars are also omitted. A few of the stars catalogued are probably variable; the data relative to them will be published by Trumpler.

The color indices of 753 stars are given in Table II; five of them are negative; only two exceed +2.00. For 26 stars there are photographic magnitudes, but no color indices; for 42 stars there are photovisual magnitudes only. The total number of stars in our catalogue is 821.

TABLE II

Catalogue of 821 Stars in the Pleiades

Trumpler No.	R.A. 1900	Decl. 1900	Pg. Mag.	C.I.	No. of Plates
	3^h37^m				
1......	$6^s.3$	24°41′.3	14.54	0.35	3,3
3......	7.9	24 29.3	.11.89	......	1,.
4......	8.5	24 47.7	13.17	1.61	1,1
5......	11.0	24 33.0	14.00	0.49	4,1
9......	12.6	23 1.4	14.14	0.63	2,1
10......	16.0	22 50.4	13.61	1.06	2,1
11......	16.8	23 36.8	14.30	0.72	2,2
12......	16.9	23 17.2	....	......	1,1
13......	17.1	23 51.4	13.92	1.07	1,1
14......	17.8	24 46.5	13.73	0.73	3,3
16......	20.1	23 16.0	13.04	1.94	1,1
17......	20.3	24 29.6	14.72	0.47	4,1
18......	21.0	23 14.7	13.67	0.59	1,1
19......	22.7	23 56.1	14.43	1.71	1,1
20......	22.8	24 5.8	12.52	0.38	1,1
21......	23.0	22 55.7	13.24	1.53	2,1
22......	23.2	24 39.9	14.39	0.85	3,3
23......	23.7	23 32.5	14.29	0.54	3,3
24......	24.2	24 22.2	14.55	1.15	1,1
25......	25.3	23 16.7	14.09	0.39	1,2
26......	25.5	24 10.1	....	......	.,1
27......	25.7	23 42.8	13.94	0.54	2,2
28......	26.5	24 31.1	14.27	1.05	4,3
29......	27.5	22 56.8	13.68	0.73	2,1
31......	28.7	24 18.0	14.03	1.01	4,4
32......	28.9	22 58.3	12.12	1.62	2,1
33......	29.7	23 21.2	....	......	.,1
34......	30.4	22 54.5	....	......	2,1
35......	34.2	24 38.6	14.42	0.64	4,3
36......	34.3	24 20.1	12.23	0.47	1,1
37......	36.8	23 21.4	11.04	0.34	1,2
38......	37.4	24 27.8	14.90	1.37	4,4
39......	37.5	24 16.5	14.49	0.62	1,1
40......	37.7	24 16.2	14.52	0.80	1,1
41......	39.0	23 26.7	11.94	0.65	3,3
42......	39.1	24 36.1	12.66	1.26	4,3
43......	40.6	22 52.3	14.63	1.68	1,1
44......	42.0	24 25.4	14.03	0.23	1,1
45......	42.1	24 32.4	12.58	0.43	4,3
46......	42.9	23 13.1	....	......	.,2
48......	44.9	22 56.8	13.15	0.39	2,1
49......	45.1	23 28.3	14.40	0.50	3,3
52......	46.9	24 45.7	14.18	1.80	3,3
54......	49.0	24 39.0	12.18	0.87	4,3
55......	49.5	24 38.4	13.43	0.36	4,3
56......	50.0	24 41.2	12.34	0.67	3,3
57......	52.0	23 43.3	12.16	0.72	2,2
58......	53.3	22 53.7	11.42	1.26	2,1
59......	53.6	24 44.7	14.14	0.45	3,3
60......	54.2	23 55.8	11.76	0.36	1,1
61......	56.5	23 14.6	15.12	1.14	1,2
62......	57.0	22 56.3	13.61	1.56	2,1
63......	57.2	23 2.8	11.70	0.87	2,1
66......	58.2	24 44.4	14.71	0.74	3,3
67......	58.3	23 22.8	13.46	0.54	1,2
	3^h37^m				
68....	$58^s.9$	23°56′.0	11.09	0.99	1,1
69....	59.3	23 26.1	13.24	0.61	3,4
71....	59.8	24 12.9	....	......	.,1
	3^h38^m				
72....	2.0	23 55.8	13.85	0.41	1,1
73....	2.3	24 8.3	12.29	0.27	1,2
76....	3.2	23 49.8	11.62	1.27	2,3
77....	4.1	23 53.1	11.79	0.47	1,1
78....	5.2	22 54.6	13.86	0.81	2,1
79....	5.6	23 13.6	11.32	−0.08	1,2
82....	7.0	23 48.9	14.18	0.54	3,3
83....	7.0	23 55.6	13.07	0.31	1,1
84....	7.1	23 17.0	13.07	0.74	1,2
85....	7.5	23 52.3	13.07	−0.09	1,1
86....	8.1	24 25.9	13.75	0.67	1,1
87....	8.1	24 41.2	13.97	0.69	3,3
88....	8.1	23 45.4	14.34	0.47	3,2
89....	8.2	23 57.6	12.08	0.32	1,1
90....	8.5	24 4.8	14.09	1.37	1,1
91....	9.2	24 1.6	13.95	0.51	1,1
92....	9.7	24 1.2	14.03	0.59	1,1
93....	10.4	24 12.2	....	......	.,1
94....	13.4	23 55.8	....	......	.,1
95....	15.0	24 25.2	11.65	0.41	1,1
96....	15.2	24 18.4	14.63	......	1,.
97....	15.8	24 14.4	....	......	.,1
98....	16.1	24 27.8	....	......	2,2
99....	16.2	24 5.2	11.20	0.70	1,1
100....	16.6	23 3.8	12.15	0.82	2,2
101....	16.6	23 43.0	12.64	0.62	2,2
102....	16.6	24 45.4	12.33	1.09	3,3
103....	17.0	23 42.9	12.28	0.58	2,2
106....	20.0	23 57.4	....	......	1,1
107....	21.5	22 51.3	12.91	0.58	2,1
108....	22.2	24 28.8	11.04	0.31	1,2
111....	22.5	22 49.2	13.80	0.92	2,1
112....	22.5	24 14.5	....	......	.,1
113....	22.7	24 27.4	11.55	0.93	2,2
114....	22.9	23 56.7	12.26	0.06	1,1
115....	24.1	24 27.2	14.14	0.87	2,2
117....	25.6	23 12.1	13.88	1.07	1,1
119....	27.4	24 6.6	13.53	1.39	1,1
120....	28.4	23 21.1	12.13	0.85	1,1
122....	28.9	24 16.4	....	......	1,2
123....	32.0	24 23.9	13.85	0.37	1,1
124....	34.8	23 3.8	14.09	0.17	1,1
124*a*....	34.9	23 3.9	14.89	0.49	1,1
125....	38.4	23 22.4	13.71	0.84	1,2
126....	38.5	24 43.4	14.21	0.49	5,5
127....	39.0	24 38.8	14.41	0.71	5,5
128....	39.1	23 24.4	13.64	0.57	1,1
129....	39.1	23 44.8	13.22	1.80	2,2
129*a*....	39.3	23 41.2	15.68	1.48	2,1
130....	42.2	24 11.7	11.89	0.76	1,1

TABLE II—*Continued*

Trumpler No.	R.A. 1900	Decl. 1900	Pg. Mag.	C.I.	No. of Plates
	3^h38^m				
131....	$42^s.8$	$24^\circ30'.2$	....	......	.,1
132....	44.7	24 5.0	12.42	0.62	2,2
133....	44.9	23 2.9	14.02	0.62	2,1
134....	45.2	23 58.2	13.81	0.55	4,3
135....	45.8	24 35.3	14.64	0.49	5,3
136....	46.2	24 44.6	13.90	0.58	4,3
137....	47.3	23 55.0	12.11	0.64	4,3
138....	48.6	24 24.9	13.41	1.29	2,1
140....	51.9	24 35.8	14.50	1.14	4,3
141....	52.6	24 34.4	14.12	0.62	3,3
142....	52.7	23 50.8	13.24	1.78	3,2
143....	52.9	23 44.3	13.28	......	1,.
144....	53.2	24 6.1	14.95	0.84	3,2
145....	53.3	23 16.4	11.13	......	1,.
146....	55.0	23 4.5	14.11	0.75	2.1
147....	55.7	24 37.7	14.20	0.63	3,3
150....	57.0	24 24.9	14.03	0.91	1,1
151....	57.9	23 36.4	11.62	0.71	2,1
152....	58.7	24 28.4	13.04	1.12	1,3
153....	59.3	24 7.1	11.02	0.60	3,3
154....	59.9	23 3.2	13.95	0.64	3,1
	3^h39^m				
154*a*....	0.7	23 46.5	14.90	1.33	4,2
155....	2.4	23 38.0	14.84	1.11	1,1
156....	3.7	24 16.2	13.52	1.80	1,1
157....	5.3	23 46.6	14.12	0.56	4,2
157*a*....	6.9	23 9.4	14.94	1.26	1,2
158....	7.5	23 31.5	13.11	1.30	1,1
159....	8.4	24 40.3	14.61	0.79	2,2
160....	8.5	23 4.8	13.98	0.53	4,2
161....	9.0	24 43.0	12.82	0.40	2,2
164....	10.4	24 27.4	14.00	0.36	2,3
165....	10.9	24 21.6	13.98	0.54	1,1
167....	12.7	24 10.2	11.56	0.43	2,1
167*a*....	12.8	24 28.9	15.60	1.26	3,2
168....	14.8	24 46.4	14.49	0.74	2,2
169....	15.1	23 34.8	13.44	0.92	1,1
170*a*....	16.0	24 30.7	15.74	1.16	2,2
171....	16.1	23 48.6	12.86	1.26	3,2
172....	16.9	24 43.1	14.36	0.62	2,2
173....	17.1	24 37.2	13.25	0.62	2,2
174....	18.2	22 58.9	13.03	0.85	3,1
175....	18.4	24 9.7	15.00	1.42	2,3
176....	19.3	24 34.4	12.45	0.38	2,2
178....	19.8	24 24.6	12.20	0.36	1,1
179....	22.0	24 33.4	14.02	0.49	2,2
181....	22.6	23 50.3	13.68	0.49	3,2
182....	22.8	24 40.5	14.64	0.69	2,2
183....	23.1	23 51.9	11.23	0.39	3,2
184....	23.5	24 18.4	14.60	0.65	1,1
185....	24.1	23 47.6	14.42	0.71	4,2
186....	25.6	23 24.8	13.22	0.70	2,3
	3^h39^m				
187....	$25^s.9$	$24^\circ34'.3$	....	......	2,2
188....	26.1	24 25.1	14.81	0.84	1,1
189....	27.2	24 24.8	14.66	1.00	1,1
190....	27.2	23 9.5	13.15	0.67	1,2
192....	29.5	23 45.3	14.05	0.59	4,2
193....	29.5	23 10.3	12.58	0.67	1,2
194....	29.7	24 12.6	14.32	0.79	1,1
196....	30.4	24 18.0	14.12	0.72	1,1
197....	31.1	23 7.0	12.90	0.82	4,3
199....	32.5	23 55.8	13.80	1.46	3,2
200....	33.0	22 48.0	13.12	0.94	3,1
201....	33.0	22 56.6	13.82	0.98	3,1
202....	33.2	23 5.1	13.00	0.64	4,3
203....	33.9	23 26.8	14.80	1.22	2,3
204....	35.1	24 42.2	14.09	0.69	2,2
205....	35.8	23 33.4	13.98	1.06	1,1
206....	36.0	23 59.4	14.02	0.96	3,2
207....	36.0	23 18.4	13.83	0.80	1,2
207*a*....	37.0	23 41.5	15.98	1.38	1,1
209....	38.1	22 57.2	13.98	0.58	3,1
210....	38.4	24 35.3	11.84	1.07	2,2
211....	38.8	24 11.2	12.54	0.48	1,1
212....	38.8	23 36.8	13.92	0.64	1,1
213....	39.0	23 46.2	....	......	4,2
214....	39.8	23 2.5	14.18	0.78	3,1
216....	41.2	23 36.0	13.98	0.83	1,1
217....	42.5	24 18.8	....	......	1,1
218....	43.7	24 36.3	14.16	0.63	2,1
220....	43.7	23 26.5	13.38	1.18	2,3
221....	43.8	24 35.6	....	......	2,2
222....	43.8	24 44.6	14.32	1.07	2,2
223.....	44.5	23 58.5	....	......	2,2
224....	44.6	24 7.1	12.12	0.82	4,3
225....	46.5	23 57.4	12.64	0.68	3,2
226....	46.7	24 24.0	12.48	1.45	1,1
227....	47.1	24 40.4	12.84	0.86	3,2
228....	47.7	23 54.4	11.46	0.48	3,2
228*a*....	47.7	23 45.7	15.20	0.69	2,1
229....	50.3	24 33.9	13.59	0.64	2,2
230....	51.2	23 11.2	....	......	1,1
232....	52.5	24 6.8	12.12	1.18	4,2
236....	55.3	23 18.4	13.44	1.14	1,2
237....	56.2	24 41.2	14.94	0.64	3,3
238....	56.3	24 29.3	12.93	0.68	1,2
239....	56.7	23 7.1	12.44	0.24	1,2
241....	57.8	23 56.3	13.75	1.84	3,2
241*a*....	59.9	23 8.6	14.70	1.20	1,2
	3^h40^m				
242....	0.1	22 49.8	13.85	1.01	4,1
243....	0.5	24 3.8	14.11	0.61	3,2
244....	0.7	24 44.3	....	......	2,2
244*a*....	1.8	24 12.8	15.04	0.80	1,1
245....	4.0	24 31.6	12.84	0.50	3,2
246....	4.1	24 6.6	14.29	0.66	1,1
248....	7.7	23 43.9	12.52	......	2,.
249....	7.1	23 25.5	....	......	.,2
250....	7.3	24 40.8	11.10	0.64	2,3
251....	7.6	24 42.3	11.02	0.12	3,3

TABLE II—*Continued*

Trumpler No.	R.A. 1900	Decl. 1900	Pg. Mag.	C.I.	No. of Plates
	$3^{h}40^{m}$				
252....	$7^{s}.9$	$24^{\circ}26'.0$	14.40	1.25	2,1
253....	8.9	24 15.3	14.03	1.41	1,1
254....	9.0	24 34.2	14.30	0.89	3,3
255....	9.1	24 31.7	13.96	0.78	2,2
257....	9.3	24 15.0	14.66	1.19	1,1
258....	9.4	22 59.8	14.11	0.99	4,1
259....	9.4	24 33.3	12.88	0.74	2,3
260....	9.9	22 47.8	14.08	1.04	2,1
261....	10.9	24 36.3	13.98	1.12	3,3
262....	10.9	24 37.1	13.85	0.53	3,3
263....	11.4	24 35.8	14.46	1.08	3,3
264....	11.4	24 19.3	14.07	0.73	1,2
265....	11.6	23 44.9	11.28	......	2,.
266....	11.6	22 54.4	11.25	0.88	4,1
267....	12.9	22 49.2	13.20	1.59	2,1
268....	14.0	24 18.6	12.51	0.70	2,2
269....	15.0	22 59.4	14.64	1.17	2,1
271....	15.7	22 49.4	13.96	......	2,.
272....	16.3	24 43.8	13.74	0.70	3,3
274....	17.2	23 53.3	13.85	0.65	2,4
275....	17.5	24 18.7	14.75	1.28	2,1
276....	17.7	24 45.0	14.19	0.63	3,2
277....	17.8	22 53.8	14.03	0.88	3,1
278....	18.4	22 49.0	....	......	.,1
280....	19.2	23 40.4	13.79	0.61	2,1
282....	20.4	24 33.5	12.30	0.66	1,1
283....	20.7	24 30.6	13.35	0.39	1,1
283*a*....	21.0	23 36.4	15.35	......	3,.
283*b*....	21.9	24 1.2	14.55	0.73	2,2
285....	22.8	23 10.5	11.55	0.65	1,1
287....	23.5	23 43.4	13.58	0.30	2,1
287*a*....	23.5	23 36.3	14.87	0.51	2,1
288....	24.5	23 12.5	13.17	0.76	1,2
289....	25.0	24 15.5	11.00	0.36	1,1
290....	25.1	24 38.4	14.05	0.37	2,2
291....	27.0	24 3.0	13.52	0.71	2,2
292....	27.2	24 42.3	11.80	1.62	2,2
293....	27.5	24 38.1	13.58	0.40	2,2
294....	29.5	23 0.6	11.62	1.20	2,1
296....	31.0	24 7.4	11.51	0.33	1,2
297....	32.4	23 16.9	13.56	0.90	1,2
298....	32.8	23 3.8	14.15	0.59	2,1
299....	33.3	24 44.8	13.68	0.70	2,2
300....	33.7	23 4.0	14.34	0.68	2,1
302....	34.4	22 47.6	14.06	0.54	2,1
303....	34.5	24 1.3	13.74	0.26	2,2
304....	34.7	24 0.7	13.93	0.27	2,2
305....	34.9	24 36.9	14.38	0.06	2,2
305*a*....	35.4	23 58.2	15.36	0.90	2,2
306....	35.6	22 52.3	12.32	0.55	2,1
306*a*....	35.6	23 40.3	14.59	1.03	2,1
307....	36.1	23 33.0	11.41	0.08	2,1
308....	36.4	24 16.6	14.21	0.41	1,1
309....	37.4	23 49.6	12.23	0.32	3,2
310....	37.5	23 32.1	13.41	1.07	2,1
312....	38.7	24 27.5	13.86	0.10	1,2
313....	38.8	23 39.0	11.90	−0.06	2,1
314....	38.8	23 29.3	13.78	0.58	2,2
315....	38.8	23 40.7	13.37	0.62	2,1
316....	39.7	24 26.2	12.70	0.52	1,1
	$3^{h}40^{m}$				
317....	$40^{s}.0$	$22^{\circ}48'.1$	14.35	0.44	2,1
318....	40.1	24 1.9	12.89	0.71	2,2
319....	40.1	24 38.9	11.12	0.69	1,2
321....	40.4	24 37.7	14.20	1.08	2,2
322....	41.3	24 12.6	14.52	0.96	1,1
323....	41.7	24 30.5	13.76	0.61	2,3
324....	41.8	23 28.6	....	......	2,2
325....	42.0	24 35.4	14.04	0.51	2,2
326....	42.3	23 41.0	13.58	0.95	2,1
328....	42.7	24 2.4	13.77	0.26	2,2
329....	42.9	23 43.1	12.80	0.43	2,1
330....	45.0	23 11.2	12.83	0.52	1,1
332....	46.5	24 37.1	13.75	0.63	2,2
333....	46.6	23 56.7	14.20	0.79	2,2
333*a*....	46.7	23 56.7	15.29	1.07	2,2
334....	47.2	24 0.1	10.92	0.28	2,2
335....	47.3	23 1.8	14.06	0.30	2,1
336....	47.5	24 19.0	14.17	0.18	1,1
339....	49.0	24 17.5	14.47	0.74	1,1
340....	49.3	24 35.3	14.28	0.55	2,2
341....	49.6	23 30.9	13.47	0.32	2,1
342....	50.5	24 14.9	13.41	0.19	1,1
343....	52.3	22 50.5	12.48	0.89	2,1
344....	54.5	24 39.2	13.85	0.41	1,2
344*a*....	55.2	24 13.3	14.84	0.42	1,1
345....	55.6	23 51.7	14.43	0.53	2,2
347....	56.6	24 36.6	11.90	0.71	2,2
348....	56.6	24 29.2	....	......	.,3
349....	57.7	22 53.9	11.52	0.99	2,1
350....	58.3	23 16.4	11.00	0.22	1,1
	$3^{h}41^{m}$				
350*a*....	0.3	24 10.5	15.18	0.88	3,3
351....	0.5	23 30.4	13.66	0.51	2,1
352....	1.3	24 46.8	13.45	1.29	1,1
353....	1.6	22 59.8	13.98	0.76	2,1
355....	2.4	23 46.7	12.60	0.34	4,3
356....	2.4	24 4.4	11.30	0.40	2,2
357....	2.6	24 1.2	12.68	1.36	2,2
358....	4.0	23 40.3	12.69	0.85	2,1
359*a*....	5.5	23 33.8	14.41	0.02	2,1
360....	5.8	24 19.5	12.29	1.90	1,1
361....	6.1	23 11.1	12.39	0.96	1,1
362....	6.7	22 57.5	14.12	0.70	2,1
363....	7.0	22 49.6	13.86	0.58	2,1
364....	7.1	23 23.8	14.12	0.32	1,1
366....	10.2	24 33.6	12.67	0.39	1,2
367....	10.4	23 7.4	13.92	0.44	2,2
368....	10.6	24 12.9	14.01	1.07	1,1
369....	11.0	23 24.3	12.87	0.56	1,1
370....	11.9	23 10.2	13.79	0.41	1,1
370*a*....	12.8	23 24.0	14.32	1.10	1,1
371....	12.9	24 46.3	14.79	0.77	1,1
373....	13.2	24 48.4	11.52	0.30	1,2
374....	13.3	24 7.5	14.07	0.56	3,3
375*a* ...	14.3	23 44.0	14.59	0.34	2,2
376....	14.3	23 53.6	14.16	0.34	2,2
377....	16.0	24 29.4	14.75	0.77	2,1
378....	17.7	23 24.2	13.17	0.68	1,1
379....	18.0	23 48.4	13.86	0.48	4,3
380....	18.3	23 53.0	13.03	0.59	2,2
382....	20.4	23 30.5	11.50	0.83	2,1

TABLE II—*Continued*

Trumpler No.	R.A. 1900	Decl. 1900	Pg. Mag.	C.I.	No. of Plates	Trumpler No.	R.A. 1900	Decl. 1900	Pg. Mag.	C.I.	No. of Plates
383....	3^h41^m $20^s.7$	$24^\circ\ 4'.8$	13.62	0.86	2,2	451....	3^h41^m $57^s.0$	$23^\circ 29'.0$	13.85	0.50	3,2
384....	20.9	23 36.2	12.44	1.42	3,2	452....	58.0	23 30.8	13.80	0.78	2,2
385....	21.2	24 8.6	12.96	1.06	3,3	453....	58.3	23 59.6	13.96	0.42	4,5
385*a*....	21.2	23 47.4	15.17	0.83	3,3	454....	58.8	24 42.2	11.77	1.01	4,3
386....	21.4	24 19.9	13.93	0.25	3,2	455....	59.0	22 54.2	14.26	0.40	3,2
388....	21.8	22 56.5	13.99	0.71	4,1	456....	59.0	24 27.2	13.34	0.74	4,3
389....	22.4	24 33.8	13.39	0.68	4,2	457....	59.2	23 22.8	13.72	1.05	2,3
390*a*....	22.6	23 38.4	14.66	0.62	3,1	458....	59.8	23 7.7	....	......	.,4
392....	23.2	23 41.5	13.92	0.72	3,2						
393....	23.5	24 39.3	14.82	0.75	5,3						
394....	24.1	23 0.2	13.87	1.35	4,1	459....	3^h42^m 0.0	23 23.2	11.96	0.23	2,3
396....	24.3	23 46.2	13.75	0.73	3,3	460....	0.1	24 1.2	14.25	0.49	4,5
398....	26.1	24 44.6	13.98	1.15	5,3	461....	0.1	23 26.0	14.13	0.25	3,4
400....	27.5	23 14.6	11.18	0.24	3,3	462....	0.3	23 9.4	11.56	0.17	2,3
401....	27.7	23 36.3	....	......	.,1	463....	0.7	23 17.0	13.43	0.37	3,4
401*a*....	28.1	23 46.8	15.08	1.46	3,3	464....	0.7	24 25.8	13.88	0.67	4,2
403....	28.4	24 21.0	11.40	0.18	2,3	465....	0.8	24 26.0	13.90	0.22	4,2
404*a*....	28.5	23 35.3	14.83	0.81	1,3	466....	1.4	24 25.4	14.51	0.93	3,2
405*a*....	28.7	24 16.6	15.28	0.49	4,1	467....	1.5	23 7.5	12.76	0.28	4.4
406....	29.3	24 37.0	15.06	1.39	5,4	468....	1.5	22 53.0	11.58	......	2,.
407....	29.4	24 11.9	13.82	0.48	3,2	469....	1.6	23 40.8	13.85	0.46	3,3
408....	29.8	23 19.2	13.43	1.24	3,2	470....	1.8	23 16.7	13.94	1.05	3,4
409....	30.4	23 13.9	11.92	1.22	3,3	471....	2.1	22 53.2	13.96	0.73	3,1
411....	31.2	24 14.8	12.30	1.70	4,3	473....	2.7	23 7.0	14.31	0.42	4,4
415....	33.5	23 38.6	13.89	0.96	4,3	475....	4.6	23 34.2	12.49	1.14	2,2
416....	34.0	24 14.9	14.56	0.60	4,2	476....	5.1	23 46.7	13.51	1.53	5,5
417....	34.2	24 46.2	14.32	0.76	4,4	477....	5.6	23 20.1	11.94	0.26	2,3
417*a*....	34.5	24 0.2	15.62	0.96	2,3	478....	6.0	24 17.4	14.60	0.36	4,2
418....	34.7	24 29.1	....	......	1,1	479....	7.0	24 33.4	11.28	−0.12	3,2
419....	34.8	24 17.7	14.76	0.51	4,2	481....	8.1	24 36.0	14.90	0.52	3,2
420....	35.6	24 22.5	13.92	0.96	4,3	482....	8.4	23 45.8	13.52	1.24	3,5
421....	36.2	23 39.4	14.14	0.28	4,3	483....	9.4	24 9.9	12.67	0.59	6,5
422....	36.4	24 11.6	13.80	1.27	4,3	484....	9.5	23 4.4	11.04	0.88	1,2
423....	37.0	23 22.2	13.66	0.49	3,3	485....	9.5	24 8.6	14.54	0.21	6,5
424....	37.9	24 13.6	12.00	1.66	4,3	487....	11.0	24 34.7	13.28	0.36	3,2
425....	38.7	23 54.3	13.57	1.07	5,4	488....	11.2	23 33.4	12.56	0.24	2,2
426....	40.9	22 58.5	13.56	0.57	4,2	489....	11.2	23 25.7	14.21	0.25	3,5
428....	41.6	24 46.4	13.33	0.77	3,3	490....	12.1	23 56.3	13.05	0.45	3,3
428*a*....	42.7	23 9.5	14.42	1.10	3,3	490*a*....	14.2	23 8.1	14.53	0.57	2,4
429....	43.1	24 46.5	13.58	0.90	4,3	491....	14.3	24 47.4	12.99	0.31	3,2
430....	43.1	24 3.3	11.27	0.39	5,4	492....	16.1	23 41.4	13.78	1.88	2,2
431....	43.2	24 22.6	12.98	0.40	4,3	494....	18.6	22 56.6	12.42	0.40	2,1
432....	43.4	23 41.6	11.85	1.06	4,3	495....	18.6	24 44.4	11.22	0.04	3,2
433....	43.6	23 50.4	12.53	0.83	4,4	496....	19.2	23 20.6	12.94	0.99	2,3
434....	44.1	23 49.7	12.58	0.86	4,4	497....	19.5	23 59.1	13.39	0.53	3,3
435....	45.0	23 39.8	14.31	1.02	4,3	498....	19.7	22 51.7	14.12	0.03	2,1
436....	46.0	23 58.3	12.63	0.66	5,5	498*a*....	19.9	23 20.8	14.48	0.57	2,3
437....	46.3	24 21.7	14.56	0.33	4,2	499....	20.8	23 35.0	11.05	0.49	1,2
438....	46.5	22 48.2	12.88	0.22	3,2	500....	21.1	23 19.7	....	......	.,2
440....	46.9	24 22.3	13.38	0.17	4,3	501....	21.3	24 32.3	11.72	0.12	5,3
441....	52.8	24 22.2	14.15	0.32	4,3	502....	21.6	24 28.0	13.54	0.50	5,4
442....	52.9	24 15.7	13.60	0.36	4,3	503....	21.8	24 22.0	13.85	0.40	3,2
443....	53.2	24 33.4	14.68	0.57	3,2	504....	22.5	23 45.2	13.08	1.16	3,5
444....	53.4	22 54.6	11.64	0.28	3,2	505....	23.6	23 24.8	13.43	0.25	3,5
445....	53.7	24 3.4	12.47	1.01	4,5	507....	25.7	24 32.2	13.65	1.13	3,2
446....	55.5	23 6.0	13.48	0.64	4,3	508....	26.2	24 34.2	11.04	0.12	3,2
447....	55.5	24 27.8	14.20	0.59	5,3	509....	27.1	23 17.0	13.30	0.23	2,3
448....	56.1	23 38.0	....	......	1,2	510....	27.4	22 57.6	13.99	0.55	2,1
449....	56.7	24 47.7	13.45	0.39	3,2	511....	28.0	24 41.2	11.84	0.52	3,1
450....	56.9	24 16.0	14.30	0.60	4,3	512....	29.1	23 27.0	13.87	0.79	4.5

TABLE II—*Continued*

Trumpler No.	R.A. 1900	Decl. 1900	Pg. Mag.	C.I.	No. of Plates
	3^h42^m				
513....	$29\overset{s}{.}2$	$24^\circ\ 0\overset{\prime}{.}0$	12.34	0.11	3,3
514....	29.4	23 44.4	....	......	1,3
515....	29.5	23 19.7	11.96	0.25	2,3
516....	31.7	23 47.0	13.84	0.54	5,5
517....	32.1	24 33.9	13.58	0.61	3,2
519....	32.7	24 7.3	13.24	0.11	4,4
520....	33.0	22 59.6	13.50	0.70	2,1
521....	33.5	23 36.4	13.92	0.37	2,2
522....	33.8	23 58.0	12.39	0.94	3,3
523....	34.8	24 21.0	13.18	0.22	3,2
524....	35.6	24 45.5	11.24	0.10	3,2
525....	35.7	23 18.5	13.94	0.99	2,3
526....	36.6	23 36.1	13.42	1.04	2,2
527....	37.2	23 46.3	14.25	0.97	3,5
529....	39.0	24 34.1	14.26	0.52	3,2
530....	39.2	23 7.6	....	......	.,3
531....	39.4	23 30.7	12.76	1.54	2,2
532....	39.6	23 54.7	13.12	−0.03	3,3
533....	39.6	24 28.4	14.47	0.99	4,3
534....	41.4	24 22.5	11.96	0.08	3,2
535....	42.7	24 8.8	12.34	0.45	4,4
536....	42.7	23 14.4	12.50	0.13	2,3
537....	42.8	24 27.9	13.66	0.40	4,3
538....	43.2	23 0.7	13.40	0.63	2,1
539....	43.4	24 37.4	14.12	0.43	3,2
540....	43.4	23 28.2	13.18	1.30	3,5
541....	44.8	22 59.5	12.54	0.27	2,1
542....	45.2	24 1.4	12.26	0.99	3,3
543....	45.2	23 28.4	13.76	0.50	3,5
544....	45.6	24 10.5	13.96	0.18	3,2
545....	45.9	23 31.6	14.27	0.37	2,2
546....	46.0	24 0.9	14.08	0.97	3,3
547....	46.8	24 23.7	14.15	0.33	3,2
548....	47.7	23 34.8	13.40	0.26	2,2
549....	48.6	24 1.2	13.29	0.36	3,3
550....	48.7	22 52.9	14.24	1.01	2,1
552....	49.1	23 50.4	14.18	0.46	3,3
553....	49.4	24 27.4	14.52	0.50	3,2
554....	49.5	23 20.0	14.28	0.94	2,3
555....	49.6	22 53.2	14.23	0.30	3,1
556....	50.0	24 14.2	14.35	0.49	3,2
557....	50.3	23 1.9	14.56	1.12	2,1
558....	50.4	23 13.1	11.22	1.03	2,2
559....	50.5	24 43.0	12.84	0.34	4,3
560....	50.8	24 19.6	....	......	.,3
561....	51.0	24 25.1	14.40	0.50	3,2
562....	51.6	23 57.6	11.75	0.59	2,5
563....	52.7	23 40.2	13.54	0.76	2,3
564....	52.7	23 7.0	13.34	0.33	1,2
565....	53.0	24 28.1	14.37	0.63	2,1
566....	53.2	24 44.2	14.88	1.00	4,3
567....	54.2	23 59.0	13.86	0.44	3,5
568....	55.5	24 28.0	14.65	0.75	2,1
569....	56.4	24 24.3	12.85	......	3,.
569*a*....	57.6	23 34.2	15.50	0.91	1,3
570....	58.1	23 50.0	12.14	0.52	3,4
571....	58.3	23 27.6	12.86	0.00	1,2
572....	58.3	23 31.6	12.98	0.41	3,3
572*a*....	58.7	23 29.1	15.02	0.66	1,2
573....	59.4	23 59.0	12.55	1.19	2,2
	3^h43^m				
575....	$0\overset{s}{.}4$	$24^\circ 44\overset{\prime}{.}9$	14.41	0.58	4,3
576....	0.9	23 21.6	13.98	0.38	2,4
577....	1.7	23 57.6	14.35	0.85	4,5
578....	3.1	23 34.7	13.18	1.39	4,3
579....	3.3	24 24.4	13.74	1.05	2,1
580....	3.6	22 53.7	12.40	0.76	4,2
581....	4.0	23 39.0	14.63	1.11	3,3
581*a*....	5.5	23 47.8	15.32	1.00	1,1
582....	5.8	24 18.1	14.44	0.33	4,3
583....	6.3	23 45.2	13.83	0.90	1,1
584....	7.3	22 56.8	12.46	0.58	4,2
585....	8.5	24 5.4	14.39	0.84	1,3
586....	9.1	23 1.7	13.44	0.59	1,1
586*a*....	9.8	23 43.9	14.49	0.00	1,1
587....	9.8	24 10.3	....	......	.,1
588....	9.9	23 28.5	11.03	0.70	1,1
589....	10.0	23 20.8	13.89	0.97	1,3
590....	10.2	24 26.8	....	......	.,1
591....	10.5	23 39.6	13.83	0.53	4,3
592....	10.9	23 42.2	13.67	1.01	3,3
592*b* ...	11.2	24 1.0	14.49	0.05	1,2
592*c*....	11.5	24 1.0	15.32	0.78	1,2
593....	12.6	23 19.4	14.47	0.48	1,4
595....	13.2	24 28.1	....	......	.,1
596....	13.5	24 19.8	....	......	.,1
597....	13.5	23 33.7	12.58	0.50	2,2
598....	13.7	23 16.2	14.14	0.44	1,4
600....	13.9	22 57.7	14.01	0.38	1,1
601....	14.1	23 18.3	11.13	0.17	2,3
603....	14.5	23 55.8	12.59	0.57	2,3
604....	15.1	23 13.4	12.82	1.38	1,4
605....	15.1	23 45.4	14.33	1.21	1,1
606....	15.4	24 26.6	....	......	.,1
608....	15.8	22 57.6	11.06	......	2,.
609....	16.5	23 8.8	14.44	0.60	1,2
610....	16.8	24 10.3	13.20	0.60	1,1
612....	17.1	23 11.0	14.26	0.28	1,3
612*a*....	18.2	24 2.2	15.51	0.87	1,2
613*a*....	20.2	23 45.7	14.83	1.02	1,1
614....	20.4	24 6.5	12.37	0.59	2,3
614*a*....	21.1	23 50.2	14.90	0.40	1,2
615....	21.9	23 56.8	12.96	0.82	2,3
616....	22.0	24 28.2	13.47	0.89	2,3
617....	23.3	24 43.4	13.88	0.35	2,2
618....	23.3	23 43.2	12.87	0.25	2,1
619....	23.4	23 57.5	14.01	0.44	2,3
620....	23.5	22 59.0	13.97	1.01	2,1
621....	23.5	24 38.1	14.92	0.24	2,2
621*a*....	23.7	23 50.8	15.04	......	1,.
623....	24.2	23 17.3	15.66	1.14	1,3
624....	26.0	24 33.8	13.98	0.30	2,2
625....	26.4	24 28.6	13.84	0.70	3,3
626....	26.7	24 37.9	11.54	0.88	2,2
627....	27.1	24 25.1	13.81	0.75	1,1
628....	27.6	23 32.0	12.07	1.02	2,1
630....	28.7	23 10.2	13.66	0.84	1,3
632....	28.9	23 29.3	14.14	2.19	2,1
633....	29.4	23 30.2	12.76	1.22	2,1
634....	30.4	22 50.8	14.16	0.61	2,1
635....	30.7	24 0.2	13.28	0.74	2,3

TABLE II—*Continued*

Trumpler No.	R.A. 1900	Decl. 1900	Pg. Mag.	C.I.	No. of Plates
	$3^{h}43^{m}$				
636....	$31^{s}.4$	$22^{\circ}48'.4$	13.38	0.58	2,1
637....	32.4	22 55.4	14.27	0.53	2,1
638....	32.6	24 10.0	13.89	0.47	1,2
639....	32.6	24 4.7	14.04	0.42	2,2
640....	32.6	23 24.4	12.13	0.74	1,2
641....	32.7	23 34.7	13.82	2.09	2,1
642....	32.7	23 57.8	13.99	0.43	2,2
643....	33.3	24 10.4	14.41	0.39	1,2
644....	33.6	24 29.0	14.24	0.69	3,3
645....	34.9	24 21.0	13.53	0.53	1,1
646....	35.2	24 19.4	11.40	......	1,.
647....	35.9	22 58.4	13.69	0.69	2,1
648....	36.7	24 20.4	13.57	0.51	1,1
649....	36.8	23 29.4	11.47	0.90	2,1
650....	36.8	23 43.5	13.68	0.62	2,1
650*a*....	36.9	24 3.6	14.66	0.05	2,2
652....	38.2	23 46.4	13.74	0.53	4,3
653....	38.6	24 35.3	14.58	1.38	2,2
654....	38.7	24 11.9	13.75	0.23	1,1
655....	38.8	24 44.6	14.64	0.48	2,2
656....	38.9	23 57.2	13.59	0.36	2,2
657....	39.0	23 59.4	12.52	0.98	2,3
657*a*....	40.5	23 27.2	15.06	0.54	2,1
658....	40.6	23 9.8	13.81	0.15	1,2
659....	41.0	23 10.8	13.60	0.54	1,1
660....	41.2	24 22.6	13.89	0.73	1,1
661....	42.0	23 55.3	13.32	1.14	2,2
662....	42.3	23 39.0	13.88	0.76	2,1
663....	43.6	24 7.6	13.74	0.15	3,3
664....	43.8	24 6.6	12.62	0.65	3,3
665....	43.8	23 43.9	11.96	1.32	2,1
666....	44.0	23 8.6	14.19	0.33	1,1
667....	44.2	22 59.1	12.02	0.63	2,1
668....	44.4	24 9.5	13.01	0.83	3,3
669....	44.6	23 22.6	14.26	0.89	1,2
672....	47.9	24 2.6	12.96	0.88	2,2
673....	48.1	24 13.3	14.00	0.29	1,1
674....	48.6	22 58.0	12.28	0.18	2,1
675. ..	48.6	23 56.4	11.11	1.04	2,1
676....	49.2	24 41.4	13.94	1.08	2.2
677....	49.5	23 28.5	11.70	0.35	2,3
678....	50.0	23 26.4	11.93	0.67	3,3
679....	50.7	23 49.6	13.88	0.40	4,2
680....	54.2	23 24.0	12.30	0.57	2,2
681....	54.4	24 12.2	13.05	0.41	1,1
682....	54.6	23 59.8	13.44	0.39	2,2
683....	55.5	23 25.3	14.98	0.50	2,2
684....	56.6	23 43.4	13.16	0.56	2,1
685....	57.0	24 2.2	13.23	0.69	2,2
687....	57.6	23 13.5	11.50	......	1,1
690....	58.9	24 17.0	13.20	0.24	1,1
691....	59.8	23 32.6	14.67	......	1,.
	$3^{h}44^{m}$				
692....	0.4	23 38.7	14.04	0.88	2,1
696....	1.4	22 54.8	....	......	.,1
698....	2.7	24 3.3	12.66	0.36	2,2
699....	3.7	23 36.6	13.80	0.37	2,1
700....	3.8	23 53.0	14.01	0.57	1,2
	$3^{h}44^{m}$				
701....	$4^{s}.6$	$23^{\circ}\ 6'.7$	14.00	0.94	2,3
702....	5.2	24 23.6	13.60	0.67	1,1
703....	6.0	24 22.0	12.41	0.46	1,1
704....	6.2	24 19.2	13.47	0.63	1,1
705....	8.8	23 54.6	11.98	0.48	2,2
706....	10.0	23 59.6	14.42	0.55	2,3
707....	10.1	23 42.8	13.52	1.03	2,1
708....	11.1	23 49.1	12.30	1.20	3,2
709....	12.6	23 50.4	14.33	0.85	2,2
710....	12.8	23 55.4	12.49	1.28	3,3
711....	13.3	24 36.3	13.90	0.67	4,3
712....	14.2	24 13.7	14.28	1.12	2,1
713....	14.4	23 59.5	14.46	1.10	3,3
714....	14.7	24 19.4	11.32	0.04	2,2
715....	14.7	24 9.9	13.78	0.35	1,1
716....	15.0	22 54.1	14.03	0.52	4,2
717....	15.1	24 29.2	13.90	0.50	2,1
718....	16.0	23 30.9	13.77	0.41	3,2
719....	16.6	24 30.1	14.14	0.52	2,1
720....	17.2	23 34.8	13.93	0.48	4,2
722....	18.0	23 34.8	13.69	0.21	4,2
723....	18.9	23 11.6	14.28	0.56	2,3
725....	19.9	24 46.7	14.40	0.22	5,2
726....	22.8	24 10.2	12.92	0.15	2,1
727....	22.9	24 9.8	11.74	0.86	2,2
728....	23.4	24 0.2	14.54	0.48	3,3
729....	23.4	23 36.1	14.48	0.58	4,2
730....	23.5	23 34.6	13.12	0.24	4,2
731....	23.5	23 38.9	13.02	1.40	4,2
732....	23.6	24 17.8	14.44	0.34	1,2
733....	23.7	23 30.2	14.08	0.48	3,2
734....	24.8	23 55.0	14.22	1.00	3,3
735....	25.2	22 50.6	14.24	0.56	4,2
736....	26.6	23 52.6	14.47	0.72	3,3
736*a*....	27.0	23 3.8	14.86	0.39	2,1
737....	27.1	23 34.2	14.46	0.22	4,2
738....	27.9	24 27.4	13.70	1.14	1,1
739....	28.8	23 52.9	14.66	0.55	2,3
740....	29.1	23 0.4	13.85	0.80	4,2
741....	29.1	24 21.2	14.47	1.12	2,2
742....	29.9	24 11.5	....	......	.,2
743....	30.2	24 2.6	12.67	1.24	3,3
744....	30.5	24 12.8	11.58	0.75	2,2
745....	30.6	23 16.1	11.58	0.38	2,3
746....	31.8	23 35.2	13.98	0.36	4,2
747....	32.2	24 32.0	12.54	0.40	4,2
748....	32.3	23 43.8	13.81	......	3,.
749....	33.5	24 12.3	11.34	0.27	2,2
750....	33.7	24 13.5	14.12	0.96	1,2
752....	35.1	24 33.9	14.20	0.48	5,2
753....	35.1	23 52.6	13.72	0.40	2,2
755....	35.8	24 36.1	11.76	0.49	4,4
757....	36.1	23 57.0	13.56	0.27	2,3
758....	36.3	24 2.6	10.92	0.40	1,1
759....	36.3	23 0.2	14.30	0.86	3,2
760....	36.4	24 12.3	13.96	1.00	2,1
761....	37.9	22 57.1	13.84	0.54	3,1
762....	39.3	23 58.0	14.08	0.63	2,3
763....	39.3	23 29.2	14.75	0.50	2,1
764....	39.9	24 14.4	14.04	0.31	2,1

TABLE II—*Continued*

Trumpler No.	R.A. 1900	Decl. 1900	Pg. Mag.	C.I.	No. of Plates
	$3^{h}44^{m}$				
765	$40^{s}.0$	$24^\circ 37'.1$	15.01	0.89	4,2
766	40.5	23 11.4	13.32	1.37	2,2
767	40.8	23 39.4	14.60	0.95	3,1
768	41.2	22 56.4	13.54	0.37	3,1
769	41.4	23 53.5	12.42	0.37	2,1
770	41.6	23 34.3	13.32	0.52	3,1
771	42.2	22 55.0	13.62	0.55	3,1
772	43.3	23 37.8	10.63	......	1,.
773	44.1	24 17.0	14.16	0.83	2,1
774	44.6	24 43.0	12.34	1.09	4,2
775	46.2	23 15.5	14.26	0.41	2,2
776	46.4	23 2.1	14.21	0.68	2,1
777	46.6	23 0.4	12.18	1.12	3,1
778	46.8	23 33.2	14.52	0.96	3,1
780	48.5	22 56.4	13.77	0.63	4,2
781	48.6	23 4.8	14.10	1.02	3,2
782	50.0	24 8.2	13.71	0.39	2,2
783	50.3	24 23.9	14.22	0.49	1,1
783*a*	50.4	23 12.0	15.20	0.51	1,1
784	51.0	24 7.6	11.42	1.06	2,2
785	51.4	24 16.8	13.41	0.34	1,1
786	51.8	23 33.1	13.20	0.24	2,1
787	53.6	24 24.3	14.03	1.12	1,1
788	53.8	23 7.2	11.77	0.35	2,2
789	54.5	23 25.4	13.46	0.32	2,2
790	54.6	23 26.3	14.62	0.86	3,2
792	55.7	24 29.1	14.34	0.53	4,3
794	57.	23 1.3	14.44	0.68	2,1
795	57.6	23 53.7	12.26	0.58	1,1
796	57.7	23 31.9	12.20	0.73	2,1
797	57.9	23 19.2	13.65	0.31	1,2
798	58.7	23 10.7	13.69	0.46	1,1
799	59.0	24 21.8	14.52	0.76	1,1
800	59.1	24 32.6	12.70	0.52	3,2
801	59.1	24 14.7	13.35	0.39	1,1
803	59.3	23 56.9	14.07	0.71	1,1
804	59.9	24 8.8	13.92	0.52	2,2
	$3^{h}45^{m}$				
805	0.3	23 26.0	14.20	0.74	3,2
806	0.5	24 22.6	13.45	0.49	1,1
807	2.8	24 45.2	14.00	0.82	3,2
808	4.0	24 23.8	14.22	0.89	1,1
809	4.7	24 2.4	13.65	0.35	1,1
810	4.8	23 55.2	14.12	0.70	1,1
811	5.4	24 17.7	14.12	0.39	1,1
812	5.5	23 36.1	11.18	......	2,.
813	5.7	24 38.2	12.46	0.98	3,2
814	5.9	24 39.2	14.48	0.94	3,2
815	6.1	23 39.3	13.34	1.29	2,1
816	6.3	23 54.0	14.00	0.70	1,1
817	6.8	24 26.1	14.74	0.93	1,1
819	7.2	24 22.3	12.13	1.10	1,1
820	7.5	23 48.5	13.79	1.02	3,1
821	9.8	24 3.3	14.03	1.29	1,1
822	9.8	24 45.2	14.39	0.95	3,2
823	11.0	23 35.7	13.62	0.39	2,1
824	12.3	23 55.6	14.00	0.15	1,1
825	12.9	24 26.8	13.70	0.56	2,2
	$3^{h}45^{m}$				
827	$15^{s}.4$	$23^\circ 20'.8$	13.17	0.14	1,1
829	15.6	24 13.0	12.54	0.15	1,1
830	17.1	22 59.1	14.27	0.46	2,1
831	17.3	23 12.7	13.14	0.45	1,1
833	20.2	23 31.5	13.27	0.64	2,1
834	20.3	24 17.2	13.41	0.38	1,1
835	21.5	23 55.1	14.44	0.54	1,1
835*a*	22.	23 22.6	14.74	1.38	1,1
836	22.3	24 4.8	11.43	......	1,1
837	22.3	24 32.0	14.48	0.90	3,2
838	25.0	24 33.6	12.11	0.86	3,2
839	25.0	24 32.0	14.80	0.88	3,2
840	25.3	24 13.4	14.19	0.83	1,1
841	25.7	24 21.8	13.45	0.49	1,1
842	25.9	24 33.5	14.10	0.66	3,2
843	27.1	23 23.6	13.69	0.39	1,1
844	27.1	23 47.2	14.38	1.02	3,1
845	27.2	24 46.5	11.69	0.49	3,2
846	28.3	23 28.9	14.33	1.13	2,1
847	28.5	23 39.4	13.14	0.98	2,1
849	29.1	24 25.0	14.22	0.49	1,1
850	29.5	24 15.7	12.23	0.45	1,1
851	29.6	24 4.5	14.54	0.43	2,1
853	30.3	24 42.8	13.96	0.50	2,1
854	30.5	23 21.1	14.22	......	1,.
855	30.6	23 33.4	14.36	0.71	2,1
856	31.0	24 30.3	14.50	0.24	3,2
857	31.1	23 37.4	12.54	0.69	2,1
859	32.0	22 57.9	11.62	0.59	2,1
861	33.0	23 54.3	14.44	0.63	1,1
862	33.1	23 35.9	14.71	1.01	2,1
863	33.9	24 19.0	14.22	1.17	1,1
865	35.0	24 11.1	14.25	0.40	1,1
866	35.2	24 18.6	13.50	0.40	1,1
867	35.2	23 43.9	12.90	......	2,.
868	35.4	23 20.1	13.69	0.33	1,1
869	35.5	23 5.8	14.69	0.96	2,2
870	35.6	23 36.6	12.66	0.64	2,1
871	35.7	23 49.8	13.73	0.37	1,1
872	35.9	24 41.9	14.05	0.65	3,2
873	37.2	23 42.8	14.68	......	2,.
874	39.2	24 43.6	14.24	0.48	3,1
875	39.5	23 44.7	14.55	......	2,.
877	40.2	24 46.1	14.66	0.62	3,2
878	40.6	24 10.5	14.22	0.57	1,1
879	40.9	24 14.9	12.73	0.49	1,1
880	41.0	24 40.9	11.61	0.57	3,2
881	41.7	23 27.5	14.59	0.68	2,2
882	42.1	23 42.6	14.64	......	2,.
883	42.2	24 22.0	12.73	0.60	1,1
884	42.5	23 20.4	14.22	0.61	1,1
885	42.8	24 40.2	12.45	0.43	3,2
886	42.8	22 52.9	14.26	0.93	2,1
887	44.0	24 40.4	13.68	0.34	3,2
888	44.9	24 15.0	12.90	0.10	1,1

TABLE II—*Continued*

Trumpler No.	R.A. 1900	Decl. 1900	Pg. Mag.	C.I.	No. of Plates	Trumpler No.	R.A. 1900	Decl. 1900	Pg. Mag.	C.I.	No. of Plates
	3^h45^m						3^h45^m				
890....	$46^s.8$	$23°13'.4$	14.52	0.76	1,1	903....	$51^s.2$	$23°41'.1$	14.33	......	2,.
892....	47.4	24 25.5	13.14	1.73	1,1	905....	52.1	24 25.7	14.00	......	1,.
894....	48.0	22 53.4	12.69	0.49	2,1	906....	52.7	24 41.2	13.90	0.28	3,2
895....	49.4	24 46.0	13.84	0.92	3,2	907....	53.2	24 36.5	11.41	0.06	3,2
896....	49.7	24 19.4	13.45	0.15	1,1	908....	53.4	23 19.4	14.12	0.44	1,1
897....	49.7	24 3.6	14.19	0.83	1,1	909....	54.4	24 44.2	11.47	0.21	3,2
898....	49.8	23 55.4	14.07	0.24	1,1	910....	55.0	23 56.0	12.85	0.01	1,1
899....	50.1	22 53.9	12.76	0.33	2,1	915....	57.3	24 23.0	14.22	......	1,.
901....	50.9	24 46.3	13.37	0.47	3,2	....	......	....	....	......	......
902....	51.0	23 27.0	....	......	.,1	....	......	....	....	......	......

Mount Wilson Observatory
March 1921

Contributions from the Mount Wilson Observatory, No. 219
Reprinted from the *Astrophysical Journal*, Vol. LV, pp. 162–164, 1922

THE VACUUM-SPARK SPECTRA OF THE METALS

By EDNA CARTER

ABSTRACT

Vacuum-spark spectrograms of Ca, Mg, Cd, Ti and Fe were obtained *with comparison arc and spark pectra*, on portrait films, using for the most part a 20-cm concave grating spectrograph. The Fe spectrum was also photographed with a dyed film from λ 4000 to λ 6600 A. The new spectra show no striking new characteristics. In the case of Ca and also of Mg (see Plate IX), the vacuum-spark spectrum is practically identical with the spark spectrum in air; in the case of Cd (see Plate X), the arc lines are somewhat more intense; with Ti this tendency to strengthen the arc lines is even greater, and the vacuum-spark spectrum of Fe is more like the arc spectrum than the spark. In general these spectra resemble the luminescence spectra produced by cathode-ray bombardment in a high vacuum, and it is probable that the conditions of emission are very similar in the two sources.

I. INTRODUCTION

The production of a brilliant spark between electrodes very close together in a high vacuum was observed by Rowland[1] and also by Wood.[2] The nature of the discharge was studied by Loving.[3] He concludes in regard to the spectrum produced that it is characteristic of the anode, the cathode having no effect, and that it is not analogous to either the spark or the arc. The spectra which he obtained were not sufficiently intense for an exact determination of their character.

Millikan[4] developed independently a method of producing this discharge; and, by using it as a source in a vacuum spectrograph, succeeded with his co-workers in extending the spectra of various elements into the extreme ultra-violet.

It was of interest to see whether a careful study of this source would disclose any peculiarities of metallic spectra in the usual photographic region. A comparison of the vacuum-spark spectra with the arc and the spark spectra of typical metals was therefore undertaken.

---

[1] Rowland, *Physical Papers*, p. 574.

[2] *Physical Review*, **5**, 1, 1897.

[3] *Astrophysical Journal*, **22**, 285, 1905.

[4] *Ibid.*, **52**, 47, 286, 1920; **53**, 150, 1921; *Physical Review*, **12**, 168, 1918; *Science*, **19**, 138, 1919.

2. EXPERIMENTAL METHOD

The vacuum sparks were produced in a glass bulb about 12 cm in diameter provided with a quartz window, which in the case of the more easily vaporized metals was removed to a distance of 30 cm on account of the sputtering. The iron electrodes consisted of cylinders about one cm long and one cm in diameter, tapering to blunt points. These cylinders were screwed on the ends of aluminum rods, which projected to the outside through side tubes and were sealed in with sealing wax. The iron electrode was retained as cathode throughout the experiments, while anodes of the other metals were made by wedging a piece of the metal into a hole in the end of the aluminum rod. The distance between the electrodes was about 1.5 mm in the case of iron, but it amounted to 3 or 4 mm with some of the other metals, which were largely vaporized during the exposure.

Evacuation was effected with a Langmuir diffusion pump, the mercury vapor being kept away from the discharge by a trap immersed in solid CO_2 and ether.

The discharge was produced with a large induction coil used with an electrolytic interrupter. A current of from 15 to 20 amperes was passed through the primary. To secure the necessary capacity across the secondary, four parallel plate condensers, consisting of copper plates about 56 by 61 cm separated by 5-mm glass plates, were connected in series. The whole was immersed in oil to prevent leakage.

About eight hours were required to obtain a spectrogram of iron, because of the tendency of the discharge to pass over into an ordinary gas discharge, with the liberation of gas from the electrodes, and because it was necessary to keep the sealing wax joints cool. The total duration of the spark discharge was estimated at about thirty-five minutes for iron and not more than ten minutes in the case of cadmium. The iron required a much higher potential gradient between the electrodes for the production of the spark than the other metals.

A spectrograph with concave grating of 20-cm radius and ordinary portrait films were used in obtaining most of the spectrograms. The iron spectrum was photographed in the region 4000–6600 A

PLATE IX

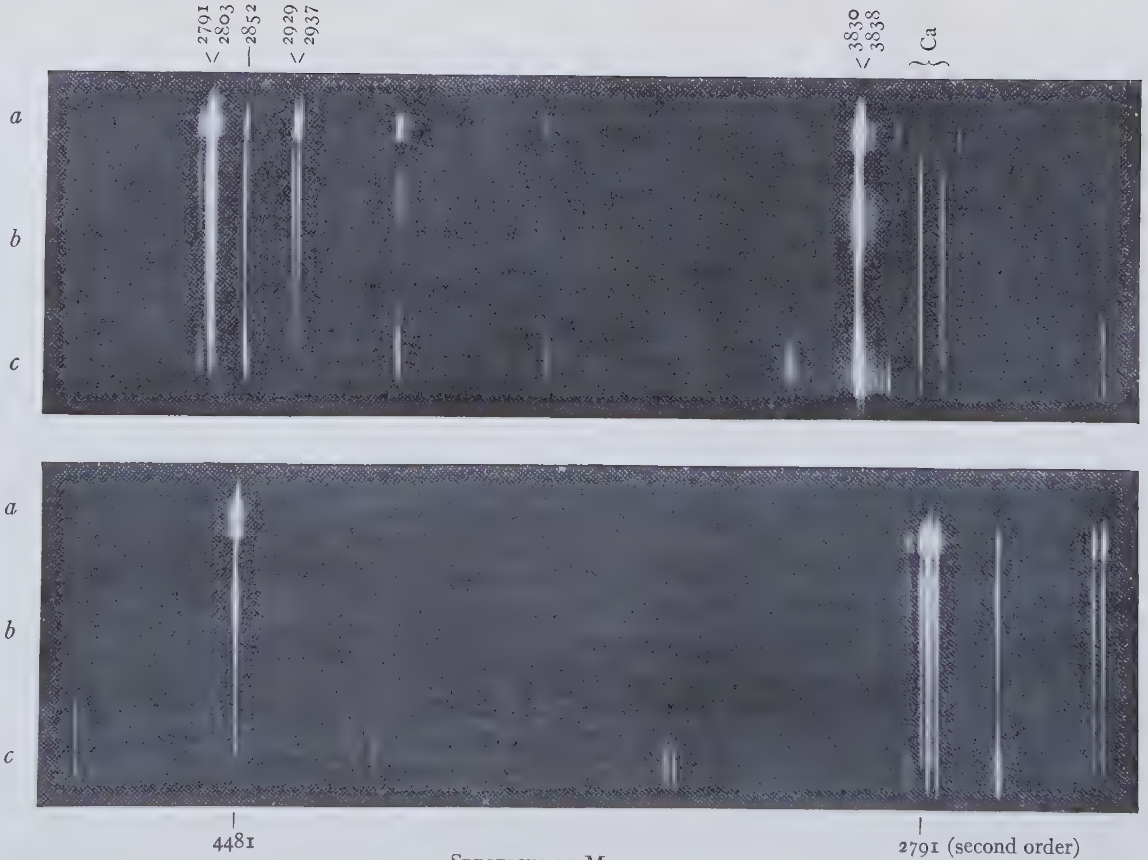

Spectrum of Magnesium

a Spark in air
b Vacuum-spark
c Arc

PLATE X

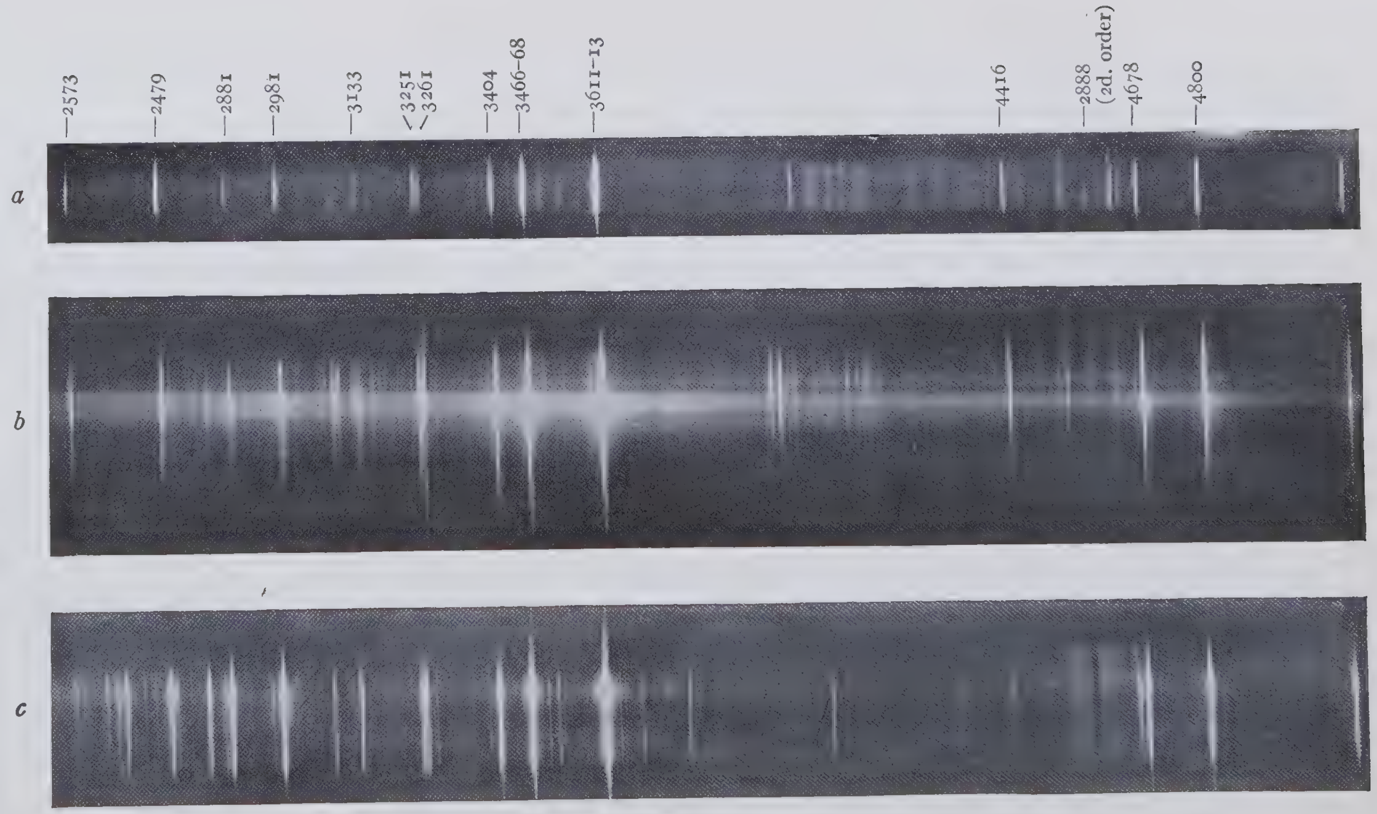

SPECTRUM OF CADMIUM

a Spark in air
b Vacuum-spark
c Arc

by using an aesculin filter and films sensitized with a Wallace three-dye solution. Fairly rich spectra of iron and titanium were obtained also with a one-meter concave grating spectrograph.

The vacuum-spark spectra of magnesium and cadmium with comparison arc and spark spectra are reproduced in Plates IX and X.

3. DISCUSSION OF RESULTS

The vacuum-spark spectra of calcium and magnesium are practically identical with the spark spectra in air.

The cadmium vacuum-spark spectrum retains arc lines in somewhat greater relative intensity than they possess in the ordinary spark. The line λ 3261 is an example. This line came out also with marked intensity in the luminescence spectrum produced by cathode-ray bombardment.[1]

Titanium shows an even greater tendency to retain the arc lines. The spectrum is plainly an enhanced one, however, as is evidenced by the brightness of the lines λλ 4164 and 4172, for example, the ratios of whose intensities in the spark and the arc, as given by Exner and Haschek, are 20:2 and 15:1, respectively.

The vacuum-spark spectrum of iron, on the other hand, seems to resemble more closely the arc spectrum. The low-temperature lines found in the arc are missing, and the lines which are stronger at the poles and in the core of the arc are relatively more intense in this source. Even in this spectrum a close examination reveals the presence of the enhanced lines, such as λλ 4508, 4515, 5018, and 5316. Hα comes out very strongly and sharply in the photographs of the iron spectrum made in this region.

The varying tendency exhibited by these different metals toward the production of enhanced lines suggests a resemblance of the vacuum-spark spectra to the luminescence spectra produced by cathode-ray bombardment in a high vacuum. It is probable that the conditions of emission are very similar in the two sources. The difficulties in the way of obtaining rich spectra are considerably less in the case of the vacuum-spark.

MOUNT WILSON OBSERVATORY
September 1921

---

[1] *Astrophysical Journal*, **44**, 303, 1916; **49**, 224, 1919.

Contributions from the Mount Wilson Observatory, No. 220
Reprinted from the *Astrophysical Journal*, Vol. LV, pp. 11–19, 1922

SYSTEMATIC CORRECTIONS TO SPECTROSCOPIC AND TRIGONOMETRIC PARALLAXES

By GUSTAF STRÖMBERG

ABSTRACT

Systematic corrections to reduce spectroscopic and trigonometric parallaxes to absolute parallaxes.—The fact that the systematic and accidental errors of spectroscopic parallaxes are proportional to the parallaxes themselves, while the errors in trigonometric parallaxes are independent of the values of the parallaxes, makes it possible, theoretically at least, to determine from a comparison of the two systems the true systematic corrections for each system and even for each observer. The basis of grouping the stars must be independent of each system and therefore Kapteyn's mean parallaxes, derived from apparent magnitudes and proper motions, were used. The factorial correction (x) for the spectroscopic parallaxes and the additive correction (s) for the trigonometric parallaxes, connected by the fundamental equation $x\pi_s=\pi_t+s$, were thus determined. For dwarfs x ranges from 0.97 to 1.07 for different spectral types; for giants the range is from 0.89 to 1.13, the extreme values being rather uncertain. The corresponding systematic correction to absolute magnitudes averages only about 0.1 for dwarfs, but may be somewhat larger for the giants. *For the separate observatories*, McCormick, Allegheny, Yerkes, and Mount Wilson, the reductions from relative to absolute parallaxes come out, respectively, $+0\rlap{.}''0053$, $+0\rlap{.}''0076$, $+0\rlap{.}''0084$ and $-0\rlap{.}''0010$ within about $\pm 0\rlap{.}''002$. These values agree well with those obtained by van Maanen and Miss Wolfe. Hence the list of 1646 spectroscopic parallaxes recently published from Mount Wilson probably gives the absolute parallaxes without any appreciable systematic error.

The large number of spectroscopic parallaxes now available enables us to determine fairly accurate values of the systematic corrections for both spectroscopic and trigonometric parallaxes. In the derivation of the reduction tables for converting line intensities into absolute magnitudes used in the recent list of 1646 parallaxes[1] no corrections were applied to the trigonometric parallaxes, but it was found that if the corrections deduced by van Maanen and Miss Wolfe[2] had been used, the effect due to these corrections would have been less than 0.1 magnitude. The method used by van Maanen and Miss Wolfe consisted in comparing the means of the trigonometric parallaxes found by different observers for groups of stars of nearly the same mean apparent magnitude and mean proper motion. Their corrections represent the deviations of the results by individual observers from the mean system defined by all the trigonometric parallaxes. Since the systematic errors of individual observers must compensate each other to a large extent in the mean system, the corrections of van Maanen and Miss Wolfe are presumably close approximations to the true systematic errors.

---

[1] *Mt. Wilson Contr.*, No. 199; *Astrophysical Journal*, **53**, 1, 1921.

[2] *Mt. Wilson Contr.*, No. 189.

Other determinations of systematic corrections of trigonometric parallaxes have been made by Flint[1] and B. Boss,[2] the former reducing his corrections to a system based upon the Yale parallaxes, the latter comparing the spectroscopic parallaxes published in *Mt. Wilson Contribution*, No. 142 (*Astrophysical Journal*, **46**, 313, 1917) with the different series of trigonometric parallaxes.

The comparison of spectroscopic and trigonometric parallaxes enables us, theoretically at least, to determine the true systematic corrections for each observer and for the spectroscopic system as well. This depends upon the fact that the systematic and accidental errors of the spectroscopic parallaxes are proportional to the parallaxes themselves, while the errors in the trigonometric parallaxes are independent of the size of the parallax. Hence, for any series of trigonometric parallaxes, when compared with the spectroscopic system, we have, as shown more in detail below, an equation of the form

$$x\pi_s = \pi_t + s,$$

from which the systematic correction s, and the correction factor x for the spectroscopic parallaxes, can be determined. The successful use of the equation of course presupposes a considerable range in the values of the parallaxes compared. Another important advantage of the method is that any error in the assumed values of the mean parallax of the comparison stars used for the reduction of the relative trigonometric parallaxes to absolute values goes over into s and is determined as a part of the systematic correction. In principle, therefore, the comparison permits us to establish an absolute system of parallaxes.

The principal object of this investigation being to determine systematic corrections of the spectroscopic parallaxes as a whole, taking into account the possibility of constant corrections to the trigonometric parallaxes, only the larger lists of trigonometric parallaxes, viz., those derived at the McCormick, Allegheny, Yerkes, Mount Wilson, Sproul, and Yale observatories, have been discussed.

---

[1] *Astronomical Journal*, **29**, 189 (No. 696), 1916.

[2] *Ibid.*, **33**, 17 (No. 771), 1920.

The following notation has been used:

M = Absolute magnitude as published in *Mt. Wilson Contribution*, No. 199.

ΔM = Systematic correction to M to obtain the most probable absolute magnitude.

T = Accidental error of $M+\Delta M$.

π = True parallax.

π_1 = Spectroscopic parallax based on the absolute magnitude M.

π_0 = Trigonometric parallax.

s = Systematic correction to π_0.

ϵ = Accidental error of π_0+s.

We have then (cf. *Mt. Wilson Contribution*, No. 199, p. 4)

$$\left.\begin{array}{ll} & \pi=10^{0.2(\Delta M+T)}\pi_1=\pi_0+s+\epsilon \\ \text{or} & \sigma\tau\pi_1=\pi_0+s+\epsilon \\ \text{where} & \sigma=10^{0.2\Delta M}, \qquad \tau=10^{0.2T} \end{array}\right\} \qquad (1)$$

Expanding τ in a power series,

$$\left.\begin{array}{l} \tau=1+E+\frac{1}{2}E^2=A+E \\ E=\dfrac{0.2T}{\text{Mod}} \\ A=1+\frac{1}{2}E^2 \end{array}\right\} \qquad (2)$$

Thus

$$\sigma A\pi_1-s-\pi_0=\epsilon-E\sigma\pi_1 \qquad (3)$$

As the right-hand side of this equation must be assumed equal to zero, we cannot group the stars according to the size of π_0 or π_1. If we group the stars according to values of π_0 the quantity $\bar{E}$ could be assumed zero,[1] but $\bar{\epsilon}$ would show a continuous decrease from positive to negative values as $\bar{\pi}_0$ increases. The same holds for $\bar{E}$ if we group the stars according to π_1, and furthermore the weight of the unknown quantity σ would be systematically affected by the accidental errors in π_1. These circumstances correspond to the difference in slope of the two regression lines in the correlation theory. A neutral basis of grouping according to the size of the parallaxes must therefore be used, i.e., one for which we can assume the errors in the parallaxes to be independent of the errors in the measured quantities M and π_0. Such an independent basis of grouping is afforded by Kapteyn's mean parallaxes, which are a function of apparent magnitude and proper motion. For each star the mean parallax was therefore computed from Kapteyn's formula in *Groningen Publication*, No. 8, and groups of stars were then formed having mean parallaxes within certain limits. The mean spectroscopic and trigonometric parallax was then found for each group. Each of these groups then furnished an equation of condition.

---

[1] A bar above a symbol denotes throughout this paper an algebraic mean.

From equation (3) we find

$$\sigma\bar{A}\bar{\pi}_1 - s - \bar{\pi}_0 = \bar{\epsilon} - \sigma\overline{E\pi_1}\,.$$

For a neutral basis of grouping we have $\bar{\epsilon}=0$ and $\bar{E}=0$. The second term on the right-hand side, however, is not quite zero, as E is to some extent dependent on π_1 and thus $\overline{E\pi_1}$ is not exactly equal to $\bar{E}\bar{\pi}_1$.

To reduce the right-hand side of the equation of condition to zero, we multiply equation (1) by

$$\frac{1}{\tau} = 1 - E + \tfrac{1}{2}E^2 = A - E$$

and find

$$\sigma\pi_1 = A(\pi_0 + s + \epsilon) - E(\pi_0 + s + \epsilon).$$

Thus

$$\frac{\sigma}{A}\pi_1 - s - \pi_0 = \epsilon\left(1 - \frac{E}{A}\right) - \frac{E}{A}(\pi_0 + s).$$

For a neutral basis of grouping, we have, including terms of second order of E,

$$\frac{\sigma}{\bar{A}}\pi_1 - s - \bar{\pi}_0 = \bar{\epsilon}(1 - \bar{E}) - \bar{E}(\bar{\pi}_0 + s) = 0.$$

The equations of condition thus become

$$\left.\begin{aligned} x\pi_1 - s - \pi_0 &= 0 \\ \text{Weight} = \frac{1}{\overline{\epsilon^2} + \overline{E^2}\,\overline{\pi^2}} &= \frac{N}{\overline{\epsilon^2} + \overline{E^2}\,\overline{\pi^2}} \end{aligned}\right\} \tag{4}$$

TABLE I

Systematic Corrections—Separate Solution for Each Type

Spectrum	M	x	McCormick s_1	Allegheny s_2	Yerkes s_3	Mount Wilson s_4	Sproul s_5	Yale s_6
A6 to F9....	1.0 to 5.5	1.056 ± .035	+0″.0037 (53) ± .0020	+0″.0020 (92) ± .0015	+0″.0013 (25) ± .0019	−0″.0009 (24) ± .0015	−0″.0068 (35) ± .0021	−0″.0008 (46) ± .0022
G0 to G9....	≦3.0	1.095 ± .134	+0.0012 (35) ± .0033	+0.0011 (69) ± .0031	+0.0052 (10) ± .0055	−0.0040 (13) ± .0036	−0.0114 (11) ± .0062	+0.0085 (11) ± .0082
G0 to G9....	≧3.1	0.975 ± .053	−0.0055 (36) ± .0044	+0.0038 (60) ± .0032	−0.0048 (27) ± .0034	+0.0221 (8) ± .0040	−0.0130 (10) ± .0054	−0.0008 (74) ± .0031
K0 to K9....	≦4.0	1.075 ± .113	−0.0028 (25) ± .0034	+0.0058 (54) ± .0025	+0.0181 (7) ± .0050	−0.0085 (26) ± .0017	−0.0090 (8) ± .0040	+0.0198 (7) ± .0056
K0 to K9....	≧4.1	1.030 ± .064	+0.0040 (39) ± .0061	+0.0069 (27) ± .0062	+0.0109 (30) ± .0052	−0.0012 (7) ± .0092	+0.0133 (20) ± .0067	+0.0054 (70) ± .0050
A6 to K9....	....	....	+ .0012 (188) ± ″.0016	+0.0030 (302) ± ″.0011	+0.0026 (99) ± ″.0014	−0.0024 (78) ± ″.0010	−0.0069 (84) ± ″.0016	+0.0018 (208) ± ″.0016

where $x=\frac{\sigma}{A}$ is the quantity by which the spectroscopic parallaxes must be multiplied in order to obtain the best agreement with π_0+s. N is the number of stars in the group.

Assuming only that the quantities x and s are constant for a certain group of stars, we can determine them separately without introducing any limitation as to their size. The value of s found in this way is the systematic correction which reduces π_0 to *absolute* parallax.

We have assumed that the external accidental probable error in the trigonometric parallaxes determined at the McCormick, Allegheny, Yerkes, and Mount Wilson observatories is $\pm 0''.010$. The probable errors of the spectroscopic parallaxes have been assumed to be $\pm 0.20\ \pi_1$. The weights of the equations of condition are therefore proportional to $N/(0.09\bar{\pi}^2+0.000225)$ where for $\bar{\pi}$ we have used $\frac{1}{2}(\bar{\pi}_1+\bar{\pi}_0)$, x being nearly equal to unity.

The following provisional reductions to absolute parallaxes were applied before the computations were made: For McCormick, Allegheny, and Yerkes observatories, $+0''.005$; for Mount Wilson, $+0''.002$; for Sproul and Yale the reductions were computed from the table given by Kapteyn in *Groningen Publications*, No. 24, page 15. The Sproul and Yale parallaxes were given half-weight.

The value of x was determined separately for giant and dwarf stars of different spectral types. For the first solution the systematic correction s was determined for each of the above-mentioned groups of trigonometric parallaxes. The results are given in Table I. The first column indicates the limits of spectral type, the second the division according to absolute magnitude. The probable errors for x and s are below the numbers to which they belong. The numbers of stars used are given in parentheses. The last line shows the weighted means of s for all types and absolute magnitudes.

Using these mean systematic corrections to the trigonometric parallaxes and recomputing the correction factor of the spectroscopic parallaxes, we find the values of x and ΔM_1, given in Table II. The quantity ΔM_1 is the correction that must be applied to M in

TABLE II

CORRECTION FACTORS FOR SPECTROSCOPIC PARALLAXES

Spectrum	M	x	ΔM_1
A6 to F9	1.0 to 5.5	1.059±.012	+0.12±0.02
G0 to G9	≦3.0	1.121±.040	+0.25±0.08
G0 to G9	≧3.1	0.999±.029	0.00±0.06
K0 to K9	≦4.0	1.001±.059	0.00±0.13
K0 to K9	≧4.1	0.960±.019	−0.09±0.04
F0 to F9	≦0.0	1.149±.103	+0.30±0.20
Ma to Md	<3.0	0.892±.081	−0.25±0.20
Ma to Md	>7.0	1.089±.086	+0.18±0.17

order to obtain the most probable parallax and is determined by the equation

$$\Delta M_1 = 5 \log x = \Delta M - 5 \log \bar{A}.$$

Another solution was made, using all the spectral types, A6 to Md, and solving all the equations as a simultaneous set of conditions, assuming the correction s to be constant for each observer. The results of this solution are given in Table III.

TABLE III

SIMULTANEOUS SOLUTION FOR ALL TYPES

	s		s
McCormick	−0″.0015±0″.0018	Mount Wilson	−0″.0038±0″.0014
Allegheny	+ .0010± .0015	Sproul	− .0085± .0025
Yerkes	+ .0019± .0021	Yale	+ .0004± .0021

Spectrum	M	x	ΔM_1
A6 to F	1.0 to 5.5	1.015±.040	+0.03±0.08
G	≦3.0	1.037±.078	+0.08± .16
G	≧3.1	0.969±.033	−0.07± .07
K	≦4.0	0.922±.074	−0.18± .17
K	≧4.1	0.940±.029	−0.14± .07
F	≦0.0	0.962±.247	−0.08± .57
M	<3.0	0.750±.154	−0.63± .45
M	>7.0	1.082±.045	+0.17± .09

From van Maanen's investigation we know, however, that the Sproul and Yale parallaxes have a considerable magnitude correction. Such an error would affect appreciably the determination of the factor x, and for this reason a final solution was made, omitting the Sproul and Yale parallaxes. The results of this solution, which are given in Table IV, are probably the most trustworthy. They are in good agreement with those found by van Maanen and Miss Wolfe, which, reduced to the same system of corrections for reduction to absolute parallaxes as used here, are given in the last column of Table IV.

TABLE IV

SIMULTANEOUS SOLUTION (SPROUL AND YALE OMITTED)

	s	s (van Maanen)
McCormick	+0″.0003±0″.0021	−0″.0016
Allegheny	+ .0026± .0017	+ .0027
Yerkes	+ .0034± .0022	+ .0036
Mount Wilson	− .0030± .0014	− .0020

Spectrum	M	x	ΔM_1
A6 to F	1.0 to 5.5	1.041±.045	+0.09±0.09
G	≦3.0	1.135±.092	+0.27± .18
G	≧3.1	0.987±.037	−0.03± .08
K	≦4.0	1.012±.086	+0.03± .18
K	≧4.1	0.972±.034	−0.06± .08
F	≦0.0	1.090±.254	+0.19± .52
M	<3.0	0.888±.167	−0.26± .41
M	>7.0	1.068±.052	+0.14± .11

Using the systematic corrections resulting from this final solution, we find the following reductions from *relative* to *absolute* parallax.

McCormick	+0″.0053±0″.0021	Yerkes	+0″.0084±0″.0022
Allegheny	+0″.0076±0″.0017	Mount Wilson	−0″.0010±0″.0014

The systematic corrections to the absolute magnitudes are in general very small except in the case of the giant G and M stars and the very brightest F stars, most of which are Cepheids or pseudo-Cepheids. For these stars, however, the probable errors are rather large on account of the smallness of the parallaxes. In the previous derivation of the reduction tables for the determination of absolute magnitudes it was found that in the case of the giant G stars the results from trigonometric parallaxes and parallactic motion differed considerably. The determination of the mean absolute magnitudes based on parallactic motion would make these stars considerably brighter than the results from the trigonometric parallaxes indicate. A weighted mean was accordingly used. The discordance is now nearly eliminated by the application of the systematic corrections to the trigonometric parallaxes. The same holds for the brightest F stars, for which originally the measured parallaxes were not used at all, the result from parallactic motion having much higher weight. For the giant M stars the original determination was based mainly on the peculiar motion, and the present results seem to indicate that for these stars as a whole the system is nearly correct.

As the final result of this investigation, we may say that the system of spectroscopic parallaxes in *Mt. Wilson Contribution*, No. 199, as a whole, is correct within the errors of the quantities involved, and that there is no need at present to apply corrections to the system. The systematic corrections to the trigonometric parallaxes determined at the McCormick, Allegheny, Yerkes, and Mount Wilson observatories have been found to agree satisfactorily with those of van Maanen and Miss Wolfe, and, as the method used here gives absolute corrections, it can be regarded as probable that after these corrections have been applied there remain no appreciable outstanding constant errors in the resulting absolute parallaxes.

Mount Wilson Observatory
September 1921

Contributions from the Mount Wilson Observatory, No. 221
Reprinted from the *Astrophysical Journal*, Vol. LV, pp. 30–35, 1922

THE ORBITS OF THE SPECTROSCOPIC BINARIES 1 HYDRAE AND 75 CANCRI

By R. F. SANFORD

ABSTRACT

Orbits of the spectroscopic binaries, Boss 2227 = 1 Hydrae and Boss 2447 = 75 Cancri.—These stars are of classes F1 and G2 and of visual magnitudes 5.7 and 6.0, respectively. Twenty-seven spectrograms of each give for the periods, 1.563 and 19.46 days; for e, 0.05 and 0.206; for K, 30.3 and 20.2 km/sec.; and for γ, +71.3 and +12.3 km/sec., respectively. Attention is called to the large γ for Boss 2227, and to the fact that Boss 2447 is a dwarf star. Radial velocity-curves are shown.

A previous paper[1] discusses the orbits of seven spectroscopic binaries; the present note gives the orbits of two additional binaries. The general remarks which precede the discussions of individual stars in the first paper are equally applicable here and need not be repeated.

The data in Table I, except for the last column which gives the number of revolutions of the star in its orbit between the first and last observations, are taken from the list of spectroscopic parallaxes of 1646 stars.[2] Figures 1 and 2 show the radial velocity-curves. In the following pages the derivation of the orbits of these two spectroscopic binaries is discussed.

TABLE I

Name	Vis. Mag.	α (1900)	δ (1900)	Spectral Class	Vis. Abs. Mag.	μ	$\pi_{sp.}$	No. Rev.
Boss 2227–1 Hydrae	5.7	$8^{h}19^{m}.6$	$-3°26'$	F1	+3.6	$0''.216$	$0''.038$	340
Boss 2447–75 Cancri	6.0	9 2.9	+27 3	G2	+4.1	0.404	0.042	59

BOSS 2227

Measures of the first two spectrograms of this star by Professor H. C. Wilson showed that its radial velocity is variable. Accordingly observations were started immediately for the determination of the elements of its orbit. Twenty-seven suitable spectrograms are listed in Table II. The derivation of the correct period presented some difficulty at first because of its shortness. Finally, all observations were gathered into one period in a satisfactory manner when $P = 1.562975$ days was used. Since approximately 340 revolutions of the star in its orbit occurred between the first and last observations it seemed needless to endeavor to correct the period, and therefore the value given above has been taken as final.

---

[1] *Mt. Wilson Contr.*, No. 201; *Astrophysical Journal*, **53**, 201, 1921.

[2] *Mt. Wilson Contr.*, No. 199; *Astrophysical Journal*, **53**, 13, 1921.

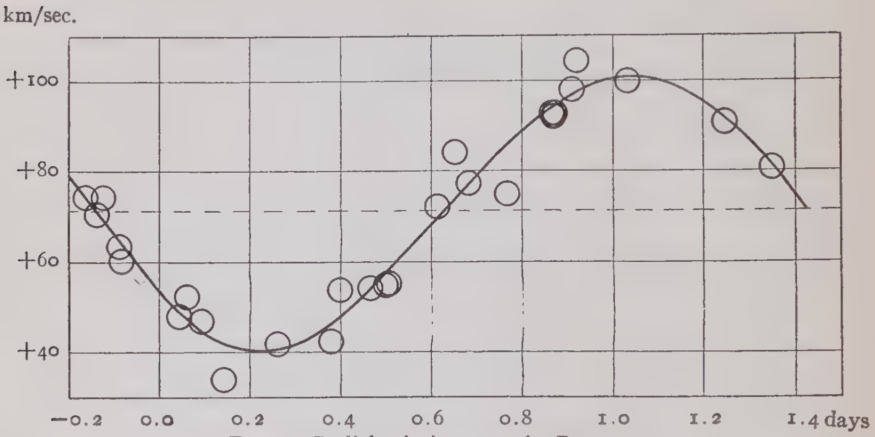

FIG. 1.—Radial velocity-curve for Boss 2227

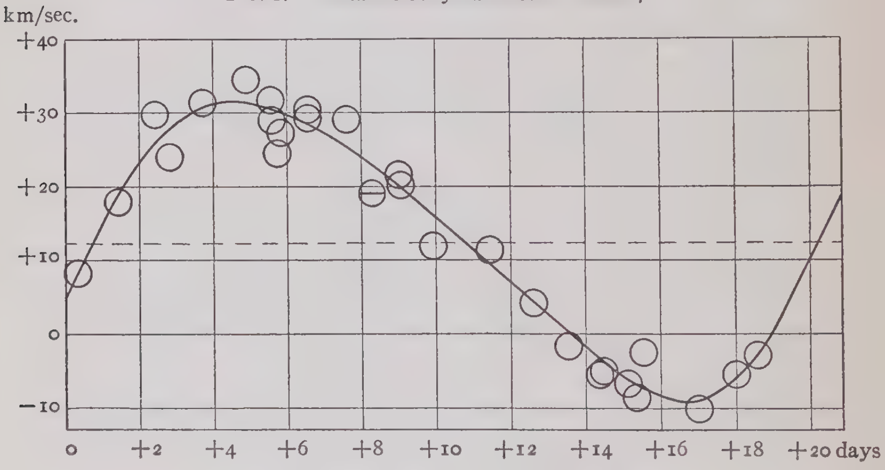

FIG. 2.—Radial velocity-curve for Boss 2447

With preliminary elements derived by Russell's method, an ephemeris was computed and the residuals (O–C) derived. The spectrum is of Class F1, with only one set of lines which at best yields a velocity of only fair precision and which varies so in quality from plate to plate that it has seemed advisable to assign weights to the measures of different plates. The best have been given weight unity and the rest weight 0.75 to 0.50, according to the inherent quality of the lines, or their quality as affected by photographic density, focus, etc., or a combination of these circumstances. The twenty-seven observations were converted into seventeen normal places, assigned proper weights and then used to correct the preliminary elements by the method of least squares. With the elements thus corrected the quantity Σpv^2 is about 75 per cent

TABLE II

OBSERVATIONS OF BOSS 2227

Plate No.	Date	G.M.T.	Phase	Weight	Velocity	O−C
					km/sec.	km/sec.
γ 8860	1919 Nov. 12	$0^h 43^m$	$0^d.062$	0.75	+ 52.2	+ 4.9
9109	1920 Apr. 4	15 11	0.870	0.75	+ 92.6	− 1.8
9666	Oct. 26	0 19	0.501	1.00	+ 54.6	− 2.7
9687	29	0 24	0.380	0.75	+ 42.4	− 3.9
C 741	Nov. 1	0 40	0.262	0.75	+ 41.8	+ 1.3
γ 9705	2	0 13	1.246	1.00	+ 90.6	− 1.2
9723	20	0 36	0.506	0.50	+ 55.0	− 2.8
9732	20	23 58	1.479	0.75	+ 60.3	− 3.6
9738	21	22 47	0.867	1.00	+ 92.8	− 1.4
9747	23	1 06	0.401	0.50	+ 53.7	+ 5.8
C 778	24	1 28	1.416	1.00	+ 70.9	− 0.8
γ 9809	Dec. 22	22 55	0.614	1.00	+ 72.1	+ 2.4
9893	1921 Feb. 15	16 47	0.653	0.50	+ 84.0	+ 9.9
9897	17	15 22	1.031	0.75	+ 99.9	− 0.7
9934	21	18 20	0.466	0.75	+ 54.1	+ 0.4
C 897	22	18 29	1.473	1.00	+ 63.5	− 1.2
γ 9940	23	18 32	0.910	1.00	+ 98.0	+ 1.2
9957	25	19 46	1.400	0.75	+ 74.2	− 0.2
9995	Mar. 16	14 50	1.439	1.00	+ 74.4	+ 5.2
9999	16	18 52	0.045	1.00	+ 48.0	− 0.9
10003	17	14 42	0.871	1.00	+ 92.8	− 1.6
10012	19	15 42	1.349	0.75	+ 80.6	− 0.2
10046	24	15 19	0.095	1.00	+ 46.9	+ 1.8
10091	Apr. 17	16 25	0.682	0.50	+ 77.3	+ 0.1
10099	18	17 03	0.143	0.50	+ 33.9	− 8.0
10124	25	17 40	0.920	1.00	+104.4	+ 7.0
10139	28	17 04	0.768	0.75	+ 75.0	−11.0

of its value when derived with the preliminary elements. The residuals obtained by substitution of the unknowns in the equations of condition agree satisfactorily with the residuals from an ephemeris based on the final elements. In Table III are to be found preliminary elements, corrections, final elements, and their probable errors. The probable error of a single observation of velocity of weight unity is ±2.64 km/sec. The absolute magnitude (+3.6) is very nearly that of Class F stars of greatest frequency and is therefore typical.

TABLE III

Preliminary Elements		Corrections	Final Elements
P		....	1.562975 days
e	0.08	−0.029	0.051 ± .035
ω	119°	$+4\overset{\circ}{.}92$	123.92 $\pm 34\overset{\circ}{.}4$
K	30.5 km/sec.	−0.22 km/sec.	30.28 ± 1.38 km/sec.
T	J.D. 2422650.073	$+0\overset{d}{.}009$	2422650.082 $\pm\ 0\overset{d}{.}132$
γ	+71.7 km/sec.	−0.40 km/sec.	+71.3 km/sec.
$a \sin i$		....	650000 km
$\frac{m^3 \sin^3 i}{(m+m_1)^2}$		....	0.0045 ⊙

BOSS 2447

This was announced as a spectroscopic binary in a list published by Adams and Joy.[1] The single set of lines appearing on its spectrograms, which show that its class is G2 and its absolute magnitude +4.1, is quite satisfactory for measurement on properly exposed plates. Table IV gives the data for the twenty-eight plates which have been obtained. With $P = 19.4589$ days all observations arranged themselves satisfactorily within a single period and furnished the basis for the preliminary elements. Since the observations extend over an interval of approximately sixty revolutions of the star in its orbit, this period was taken as definitive. By the method of least squares the other five elements were corrected, equal weights being given to all of the twenty-seven plates which were used. Plate γ 6662, whose residual stood out as the only large one, was arbitrarily rejected from the least-squares solution, and Plate γ 9997 was obtained after the elements were derived. Data for both plates are given in Table IV, however. The quantity Σpv^2 derived from the elements, corrected as indicated by the solution given above, is 18 per cent less than for the preliminary elements, and substitution of the unknowns into the equations of condition gave residuals comparable with those derived from an ephemeris calculated with the corrected elements, which are therefore adopted as final. The preliminary elements, corrections, final elements, and probable errors are given in Table V. The probable error of a single observation of velocity of weight unity is ±1.74 km/sec. The barred circle in Figure 2 represents the velocity from Plate γ 9997.

---

[1] *Publications of the Astronomical Society of the Pacific*, 31, 41, 1919.

TABLE IV

OBSERVATIONS OF BOSS 2447

Plate No.	Date	G.M.T.	Phase	Velocity	O−C
				km/sec.	km/sec.
γ 6396	1917 Nov. 27	0^h01^m	$9^d.021$	+21.6	+ 1.5
6591	1918 Jan. 22	22 51	7.598	+29.1	+ 3.8
6662*	30	22 19	15.574	+ 4.3	+11.8
6706	Feb. 28	20 43	5.589	+29.0	− 1.4
6894	May 1	16 59	9.057	+20.2	+ 0.3
6943	30	16 43	18.589	− 2.8	− 0.3
C 346	1920 Apr. 3	15 02	11.456	+11.4	+ 1.8
352	4	18 43	12.609	+ 4.2	− 0.1
356	5	17 00	13.537	− 1.6	− 1.8
γ 9123	6	15 22	14.469	− 5.0	− 1.2
9130	7	17 04	15.540	− 2.5	+ 4.9
9179	May 6	15 39	5.563	+31.7	+ 1.2
9186	7	15 35	6.560	+30.4	+ 2.0
C 410	7	15 35	6.560	+29.3	+ 0.9
γ 9255	June 4	16 16	15.130	− 6.7	− 0.5
9266†	6	15 58	17.017	−10.1	− 1.2
9272	7	15 56	18.016	− 5.4	+ 0.6
9667	Oct. 26	0 52	2.813	+24.0	− 3.9
9688	29	1 03	5.821	+27.3	− 2.7
9767	Nov. 26	1 05	14.367	− 5.5	− 2.1
9774	27	0 53	15.359	− 8.6	− 1.8
9876	1921 Jan. 28	20 14	0.326	+ 8.2	− 0.1
9886	29	22 21	1.414	+17.9	− 0.8
9889	30	22 33	2.422	+29.8	+ 3.9
9927	Feb. 20	16 36	3.716	+31.4	+ 0.8
9935	21	20 56	4.896	+34.5	+ 3.3
C 896	22	17 10	5.739	+24.4	− 5.7
γ 9969	26	21 46	9.930	+11.9	− 4.4
9997‡	Mar. 16	17 06	8.277	+19.2	− 3.7

* Not used in least-squares solution.

† Poor plate.

‡ This plate obtained after elements were derived.

TABLE V

	Preliminary Elements	Corrections	Final Elements
P		....	19.4589 days
e	0.200	+ .006	0.206 ± .002
ω	248°.5	+4°.00	252°.5 ± 7°.70
K	20.5 km/sec.	−0.29 km/sec.	20.21 ± 0.49 km/sec.
T	J.D. 2422426.555	$+0^{d}.079$	$2422426.634 \pm 0^{d}.384$
γ	+12.49 km/sec.	−0.16 km/sec.	+12.3 km/sec.
$a \sin i$		....	5295900 km
$\frac{m^3 \sin^3 i}{(m+m_1)^2}$		....	0.0157 ⊙

Mount Wilson Observatory
October 1921

Contributions from the Mount Wilson Observatory, No. 222
Reprinted from the *Astrophysical Journal*, Vol. LV, pp. 48–70, 1922

THE WAVE-LENGTH IN ASTRONOMICAL INTERFEROMETER MEASUREMENTS

By J. A. ANDERSON

ABSTRACT

Effective wave-length in measurements with astronomical interferometer.—The separation of double stars and the diameters of stellar disks are measured by the interferometer in terms of an effective wave-length λ which is such that if the stellar object emitted monochromatic light of wave-length λ the setting of the interferometer would be that actually found. The accuracy of setting obtainable in these measurements is such that in each case λ should be known to a few tenths of 1 per cent. *For any star*, the normal effective wave-length may be computed from the effective temperature corresponding to its spectral type, by combining the Planck radiation law with the mean transmission curve for the atmosphere and with the A.I.S. visibility-curve for the normal eye. The corrections required for variations of atmospheric absorption and of eye sensitivity from the assumed values may best be obtained experimentally by observations on sunlight, since in any case the correction is equal to the difference between the observed and computed effective wave-lengths for sunlight under the same conditions. The method and apparatus used in the *determination of the effective wave-length for sunlight* are described, and the results of some observations on the *variation of λ with zenith distance and atmospheric conditions* are given. On Mount Wilson the values found vary from 5660 A at sunrise and sunset to 5510 A for zenith distances up to 60°; at Pasadena the variation with zenith angle was more rapid. The wave-length was greater on cloudy days and least after a rain.

Astronomical interferometer.—The distribution of intensity in the interference patterns, for both circular and rectangular apertures, is fully discussed, and in the particular case of a double star is given mathematically for all points of the focal plane, for all orientations of the apertures. *The effect of the size of the apertures on the setting* is nil when rotation is used and also when the setting is made for minimum visibility of the fringes; but when the apertures are separated until minimum intensity at the center is obtained, it is found both theoretically and experimentally that for apertures of width a and separation D, the effective separation is very closely equal to $D/[1+K\ (a/D)^2]$ for D/a greater than 3.5, where K is 0.223 instead of 0.765 as given by Hamy.

The interferometer as used in astronomical measurements consists of two apertures alike in shape and size, placed either in front of the objective or in the converging beam a short distance in front of the focal plane. The idea of using a telescope in this manner appears to have originated with Fizeau,[1] and the first actual trials were made by Stephan.[2] Michelson[3] carried both the theory and applications of the method considerably farther than his predecessors; he gave an analytical treatment for the case of a pair of narrow slits, and applied it to the determination of the diameter of Jupiter's satellites. Hamy[1] treated the case of narrow slits, and also that of rectangular apertures whose width cannot be neglected in comparison to their separation, and applied his results to a measurement of the diameter of Jupiter's satellites and of some of the brighter asteroids. Comstock[2] used the method for a determination of the effective wave-length of star light. The work of the past two years is so recent that references to it need not be given here in detail.

---

[1] *Comptes Rendus*, **66**, 934, 1868.

[2] *Ibid.*, **78**, 1008, 1874.

[3] *Philosophical Magazine*, **30**, 1, 1890.

The purpose of the present paper is to call attention to the necessity of knowing quite accurately the effective wave-length of the source which is studied; to describe and illustrate a method for determining this quantity quickly and accurately; and to discuss in some detail the effect of using apertures of different shapes and sizes.

Consider first the determination of the diameter of a star, assumed to appear as a uniformly luminous circular disk. If the apertures are narrow in comparison with their separation, the angular diameter is given by

$$\beta=\frac{1.22\lambda}{D} \tag{1}$$

where β is the angular diameter, D the distance between the centers of the apertures corresponding to the first vanishing of the interference fringes as the distance is increased, and λ the wave-length of light. The two quantities which determine β are λ and D. Experience indicates that the probable error in the determination of D under good conditions is of the order of 1 per cent; and accordingly if the uncertainty of the true value of λ exceeds a few tenths of 1 per cent, the probable error of β will be larger than that of D.

Again, consider a double star whose angular separation is to be measured. This is given by

$$a=\frac{\lambda}{2D} \tag{2}$$

where a is the angular separation, the other quantities being the same as in (1). In this case, under good conditions, the uncertainty in the value of D is considerably less than 1 per cent.

[1] *Bulletin Astronomique*, **16**, 257, 1899.

[2] *Astrophysical Journal*, **5**, 26, 1897.

Other cases might be given, but always the quantity to be measured will be expressed in the form $K\lambda$, where K is determined by the actual observation, while λ in general must be found by some other means, and since λ is always a simple multiplier, it is necessary or at least desirable to know its value with a probable error considerably smaller than that involved in K.

At present all observations with the interferometer are made visually, and hence the value of λ will fall somewhere near the middle of the visibility curve of the eye, at least for sources emitting white light: or, we may say that λ will have a value lying somewhere within the range 5400 A to 6000 A. It follows from what has just been said that, if possible, λ should be known for a given source within 10 A to 20 A.

Definition of the effective visual wave-length.—a) Let an artificial double star be illuminated with the white light whose effective visual wave-length is required; let this double star be viewed with an interferometer, and the latter adjusted so that the interference fringes just disappear according to equation (2). Leaving the interferometer unchanged we now illuminate the double star with the monochromatic light whose known wave-length can be varied at will. The value of λ which just makes the fringes disappear is defined as the effective visual wave-length of the white source in question.

b) Analytically[1] the definition may be given as follows: Take rectangular co-ordinates in the focal plane with the origin on the axis of the telescope. Let the geometrical images of the components of a double star fall at $(+c, 0)$ and $(-c, 0)$. Let the apertures be narrow slits separated by a distance D, and the focal length of the objective be F.

If $I(\lambda)d\lambda$ be the visual effect of the radiation of the source lying between the limits λ and $\lambda+d\lambda$, the intensity along the x-axis is given by

$$J=\int_0^\infty I(\lambda)d\lambda\left[\cos^2\frac{\pi D(x-c)}{F\lambda}+\cos^2\frac{\pi D(x+c)}{F\lambda}\right] \tag{3}$$

---

[1] This statement was first suggested to the writer in a letter from Dr. C. M. Sparrow.

When D is very small, J has a maximum at $x=0$. As D increases, J diminishes for $x=0$, reaching a value of zero when D is somewhere near $F\lambda_0/2c$ where λ_0 is an arbitrary value of λ near the middle of the range for which $I(\lambda)$ has an appreciable value. Both for D small and for D having a value near $F\lambda_0/2c$, J oscillates as x is varied; but for a value of D in the neighborhood of $F\lambda_0/4c$, these oscillations become very small, and in particular at $x=0$, $J(x)$ will have a stationary value for some particular value of D. The condition for this is

$$\frac{\partial^2 J}{\partial D^2}=0; \text{ for } x=0 \tag{4}$$

Solving (4) we have $D=F\lambda_0'/4c$, where λ_0' is the effective visual wave-length required.

For a source such as a given star, $I(\lambda)$ is defined as follows: Let $E(\lambda)$ represent the energy-curve of the star, as determined outside our atmosphere; let $T(\lambda)$ be the transmission-curve of the atmosphere at the time and place of the observation; and let $V(\lambda)$ be the visibility-curve of the eye of the observer; then

$$I(\lambda)=E(\lambda)T(\lambda)V(\lambda).$$

Some questions now naturally arise, among which the following are important enough to state:

1. If in (*a*), instead of using an artificial double star, we use an artificial star disk, would the same value of λ be obtained?

2. If the components of a double star are of different spectral types, or, what amounts to the same thing, if the effective wave-length of the components is not the same, what wave-length is to be used in calculating the angular separation from the data given by an observation with the interferometer?

3. In case of a star disk darkened toward the limb, if this darkening is accompanied by a color change, what value of λ is to be used?

It is important to remember that when the observations are made visually, different observers will not in general find the same effective wave-length for a given source. In (*b*) above this is provided for by the factor $V(\lambda)$, which may differ slightly for different observers. In (*a*) it is automatically provided for by reason of the fact that the same observer is supposed to make both the adjustments. Again, since $T(\lambda)$ enters as a factor in $I(\lambda)$, an observer will not obtain the same value of λ for a given source under different conditions of observations as to time and place.

Only a beginning has thus far been made in the application of the interferometer to astronomical measurements, and it is too early to predict what its future may be; yet it will undoubtedly be valuable in certain restricted fields; for example, in the direct determination of star diameters and in the measurement of very close double stars of particular types. No doubt it will be applied successfully also in other fields. Now, as has already been pointed out, the result of any interferometer measure[1] will be expressed in the form

$$\theta = K\lambda \tag{5}$$

where K is given by the observation, and λ depends upon the object observed. If λ did not depend upon local conditions such as the observer, the time and place of the observation, and the instruments employed, the reduction would be a relatively simple matter; for this case the value of λ could be found, once and for all, for stars of all spectral types. It is clear, however, from what has already been said, that this may involve errors very much larger than the errors of observation. On the other hand, it will obviously be quite impracticable for each observer to determine independently the value of λ for every observation he makes. The following plan will, it is hoped, remove most of the difficulties. We will leave out of account objects such as the planetary nebulae, that is, objects having discontinuous spectra, for in such cases there is no difficulty in determining the value of λ with sufficient accuracy. Consider then only objects like the great majority of the stars, having continuous spectra, more or less similar to spectra of black bodies at various temperatures. The fact that no star radiates exactly like a black body is of little importance, because the black-body temperature will be used merely as an auxiliary in the general scheme. The black-body temperature of stars has been determined for all or nearly all the brighter stars, and these include nearly all of the spectral types that it will be necessary to consider.

---

[1] The position-angle of a double star is an exception.

Using Planck's law, the mean transmission-curve of the atmosphere, and the adopted *A.I.S.* visibility-curve of radiation, we may compute by equation (4) the value of λ_0' for a few temperatures from 3000° to 20,000° absolute. A curve passed through the computed points will enable one to read off λ_0' for any temperature within the range. The absolute value of the wave-lengths thus derived may not be correct, but this does not matter, for their relative values will be sensibly right. To illustrate the use of such a curve in practice, suppose that an observer has made an interferometer measure of a star of spectral type F0; assume also that he has made a determination of the effective wave-length of sunlight by the method given later in this paper. From tables giving the effective temperatures of stars of different spectral types, he reads off the temperature for an F0 star and for a star of the same spectral type as the sun. Let these temperatures be, respectively, T_1 and T_2. From the curve the corresponding wave-lengths are λ_1 and λ_2. If now the measured wave-length of sunlight is λ_0, the proper wave-length for the F0 star will be

$$\lambda=\lambda_0+\lambda_1-\lambda_2 \tag{6}$$

Of course, as the determination of λ_0 is necessarily made in daytime while the observation of the star is made at night, it is probable that the atmospheric conditions will have changed in the interval. But as different determinations of λ_0 will soon show about what correction is required for variations in observing conditions, this difficulty is not very serious.

Experimental determination of effective wave-length.—In Figure 1 let *A* be an artificial double star, consisting of two small pinholes whose linear separation is δ, illuminated by white light such as sunlight. At *B* are two circular apertures separated by the distance *D*, so mounted that they can be rotated about the axis of the telescope *C*. Observations are made through the compound

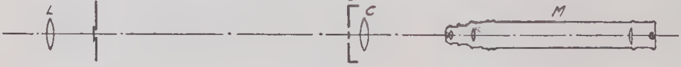

FIG. 1

microscope M. The distance A to B will be denoted by L. The angular separation of the pinholes as viewed from B is δ/L. The value of D for the first disappearance of the interference fringes, if the line joining the pinholes is parallel to that joining the apertures at B, is, by equation (2),

$$\frac{\delta}{L}=\frac{\lambda}{2D}$$

or, if the two lines make an angle θ with each other,

$$\frac{\delta}{L}=\frac{\lambda}{2D\cos\theta} \tag{7}$$

All the quantities in the equation except λ are directly measurable, and hence λ can be determined.

In order to form some idea of the accuracy to be expected in this determination, we will now examine in detail the measurement of each of the quantities entering into equation (7).

In the present experiments δ was of the order of 0.6 mm. The two pinholes were made in tinfoil, as follows: A fine needle was selected and mounted in a mechanics' pin-chuck. A small piece of tinfoil was smoothed out on a flat, smooth piece of soft metal such as brass or aluminum. A small round hole was made by resting the needle point on the tinfoil, the needle and chuck being vertical, and then carefully turning the chuck a few times. By always taking care to have the pressure about the same, holes of very nearly the same diameter may be made, and if care is used in rotating the chuck and in lifting the needle after the operation, the holes will be quite perfectly round. The diameter of the pinholes used was between 0.035 and 0.050 mm. Under a microscope the distance between such a pair of openings can be determined with a probable error of about 0.0002 mm. Since δ is about 0.6 mm, this corresponds to a probable error of the order of 1 in 3000. Before measurement the tinfoil is mounted on a metal plate through which a hole about 2 mm in diameter has been drilled, the apertures in the tinfoil being directly over this hole.

Two sources of error are to be noted in using such an arrangement as an artificial double star:

1. The plane of the apertures will not in general be exactly perpendicular to the line of sight from the observing telescope, but will make an angle ϕ with this line. The apparent separation will then be not δ but $\delta \sin \phi$. With ordinary care in mounting the tinfoil and adjusting the plate, ϕ should not differ from 90° more than a degree, which would at most cause an error of 15 parts in 100,000, which is negligible.

2. When an image of the sun is formed on the apertures, the tinfoil becomes heated somewhat, causing δ to increase. The rise in temperature to be expected may be roughly estimated. The image-forming lens has an area of 16 cm^2, and its focal length was 1 meter, so the diameter of the image was roughly 1 cm. Of this $\frac{1}{25}$ fell on the tinfoil, which is equal to the amount of sunlight falling on $\frac{16}{25}$ cm^2, or 1 calorie per minute. Assuming that the tinfoil reflects 80 per cent of this, we have $\frac{1}{5}$ calorie per minute taken up by the tinfoil or 0.003 calorie per second. When equilibrium is established, the greater part of this energy passes by conduction from the tinfoil to the brass plate, which is so large that its temperature never rose appreciably above room temperature. A temperature gradient of 3° per centimeter in the tinfoil would more than suffice to carry this amount of energy to the brass plate—and hence we may conclude that, within a very few degrees, the tinfoil was always at room temperature, and that the error due to thermal expansion was less than 1 in 10,000, which is negligible.

The value of D was usually between 6 and 7 mm. The apertures were round holes made with a drill in a brass plate; they were always sensibly equal in diameter, and the determination of their distance apart could always be made with an error less than 1 part in 5000. Various diameters were used, from about 1 mm up to 2.5 mm. The effect of using apertures of different sizes will be discussed more fully below.

The value of L was about 900 centimeters, and with a good steel tape this distance could always be measured to a millimeter.

It follows that, as far as the quantities δ, D, and L are concerned, the sum of the errors made in their evaluation should never affect the result by as much as 1 part in 1000; and, since the wave-length of the light used was near 5500 A, the uncertainty arising from the instrumental constants is not more than 5 A.

It remains now to discuss the value of θ, which is the only quantity directly measured in an actual experiment. In order to make the discussion of θ intelligible it is necessary to describe and explain the appearance of the diffraction pattern and its system of interference fringes in some detail.

Consider the distribution of intensity in the focal plane, due to a single distant point source, when the objective is covered by a screen perforated by a single circular aperture of radius r. Denote the focal length by F, and let the origin of rectangular co-ordinates coincide with the optical axis. The intensity is given by

$$I = K \frac{4J_1^2 \dfrac{2\pi r\sqrt{x^2+y^2}}{F\lambda}}{\left(\dfrac{2\pi r\sqrt{x^2+y^2}}{F\lambda}\right)^2} \tag{8}$$

where J_1 is a Bessel function of the first order.

This well-known expression states that at $x=0$, $y=0$, the intensity is a maximum and equal to K; as we move away from the origin, the intensity diminishes at first very slowly, then more rapidly, and reaches a value zero, when the argument of J_1 is equal to about 219°33′. For larger values of the argument the intensity increases, reaching a second maximum whose value is $0.0175\,K$ near 292°, and a second zero value near 401°, etc. This is, of course, simply the ordinary diffraction pattern of a circular aperture, or the so-called spurious star disk. In ordinary telescopic observations with relatively large apertures the entire disk and diffraction rings are apparently very small; but in interferometer work, on account of the small apertures and the very high magnification employed, the pattern may cover the larger part of the field of view.

The appearance is independent of the location of the aperture, as long as this falls entirely within the objective. Hence we will assume that it is placed so that its center is at a distance $D/2$ from the axis. Now let an equal aperture be uncovered, at the same distance from, but on the other side of, the axis. This second aperture alone would give exactly the same intensity as the first, namely that expressed by equation (8); but if we use both apertures together, the result will be the sum, not of the intensities as given by (8), but of the amplitudes formed by taking the square root of the right-hand side of (8), with proper attention to the relative phases of the two disturbances.

Let the apertures be so placed that the line joining their centers is parallel to the x-axis; in this case the amplitudes and phases will be equal at $x=1$. At $x=\pm F\lambda/2D$ the phases will differ by 180°, and since the amplitudes are equal, the resultant amplitude is zero. At $x=\pm F\lambda/D$, the phases differ by 360°, that is, they are in phase, and the amplitude will be the sum of the two, and so on.

It follows that the resultant intensity is now given by

$$I=I_0\frac{4J_1^2\,\frac{2\pi r\sqrt{x^2+y^2}}{F\lambda}}{\left(\frac{2\pi r\sqrt{x^2+y^2}}{F\lambda}\right)^2}\cos^2\frac{\pi D x}{F\lambda} \tag{9}$$

I_0 being the intensity at the origin.

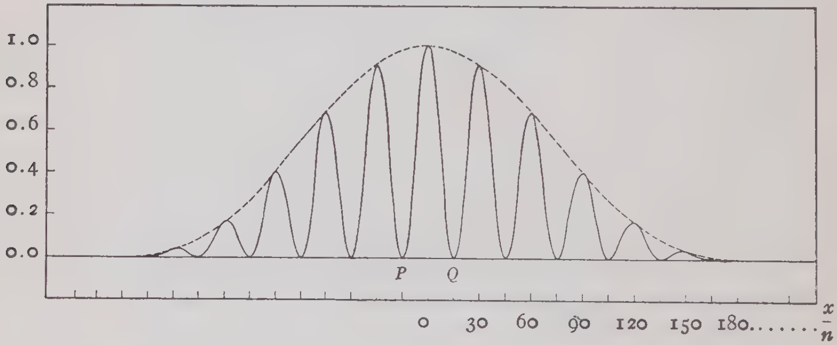

FIG. 2.—Dotted curve; $y=\frac{\sin^2\frac{x}{n}}{\left(\frac{x}{n}\right)^2}$ $(n=6)$

Full curve: $y=\frac{\sin^2\frac{x}{n}}{\left(\frac{x}{n}\right)^2}\cos^2 x$

Hence the general outline of the pattern is the same as that given by a single aperture; we still have the central disk surrounded by diffraction rings; but the effect of using two apertures is to break up the disk and rings into a series of equally spaced interference fringes parallel to the y-axis—that is, perpendicular to the line joining the apertures. Along a line parallel to the y-axis the distribution of relative intensity is exactly the same as that in the pattern given by a single aperture; parallel to the x-axis we have this intensity multiplied by the factor $\cos^2 \pi Dx/F\lambda$.

Figure 2 gives a graphical representation of the intensity along the x-axis. The dotted curve is the intensity due to a single aperture, multiplied by the factor 4.

If we retain the apertures, but use two point-sources separated by an angular distance α, there will be two such patterns, whose centers are separated by the distance $2c=F\alpha$. If the centers fall at $(-c, 0)$ and $(+c, 0)$, respectively, the expression for the intensity becomes

$$I=I_0\left\{\frac{4J_1^2\left(\frac{2\pi r\sqrt{(x-c)^2+y^2}}{F\lambda}\right)}{\left(\frac{2\pi r\sqrt{(x-c)^2+y^2}}{F\lambda}\right)^2}\cos^2\frac{\pi D(x-c)}{F\lambda}\right.$$
$$\left.+\frac{4J_1^2\left(\frac{2\pi r\sqrt{(x+c)^2+y^2}}{F\lambda}\right)}{\left(\frac{2\pi r\sqrt{(x+c)^2+y^2}}{F\lambda}\right)^2}\cos^2\frac{\pi D(x+c)}{F\lambda}\right\} \qquad (10)$$

If the line joining the apertures makes an angle θ with the x-axis, then, letting $m=\tan\theta$, the expression for the intensity will be that given by equation (10), except that we write $x+my$ instead of x in the cosine factors. Figure 3 is a sketch showing the pattern for such a double point-source, the line joining the apertures making the angle θ with x-axis. The centers of the patterns are at P and P' respectively; the pattern centered at P' is shown in dotted lines. The straight lines represent the centers of the bright fringes, AA being the central fringe for P', $A'A'$ that for P'. The angle θ has been so chosen that the fringes due to P' are just midway between those due to P. If θ is diminished, the similarly lettered fringes will approach each other and the visibility will be increased; and similarly, if θ is increased, AA will approach $B'B'$, etc., and the visibility will again increase. The position represented is that of minimum visibility.

Remembering that the intensity in a pattern diminishes from the center outward, it is clear that at all points on the y-axis the intensity of one pattern is the same as that of the other, except for the changes due to the interference, and since the maxima in one pattern fall on the minima of the other, the result is very nearly uniform intensity along this line. To the right of the y-axis the intensity of P' is greater than that of P, and hence the maxima of the P' pattern become more and more prominent as we go to the right. To the left of the y-axis the P pattern is stronger and hence its maxima become increasingly prominent in this direction. The observer will therefore see two sets of fringes meeting just out of step near and along the y-axis. (a) If θ is decreased a certain amount, so that the distance between AA and $A'A'$ becomes smaller than the adjacent intervals, the corresponding bright fringe will start at A' on the right and run in a sensibly straight line to A on the left, crossing the y-axis exactly at the origin. (b) If θ is increased, we shall have a dark fringe running from A on

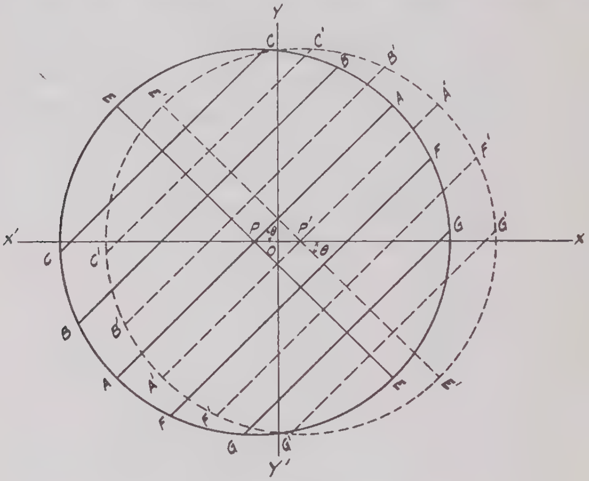

FIG. 3.—Pattern for double star

the right in a nearly straight line to A' on the left, also crossing the y-axis at the origin. The change in θ necessary to pass from condition (a) to condition (b) depends upon the number of fringes in the pattern as here represented, being the smaller, the larger the number of fringes. For a case such as that in Figure 3, with 6 fringes across the central disk, the total required change in θ is about 5°. With 12 to 15 fringes it will be from 2° to 3°. It is evident, therefore, that a setting for the exact bisection can be made quite accurately—in general to a few tenths of a degree.

We can now estimate the probable error in the determination of θ. In one rotation of the aperture plate there are four values of θ which give the appearance just described, and a "set of observations" in the present experiments has consisted of five complete rotations. As a typical example we may take the measures made on Mount Wilson on June 18, 1921. Fourteen sets of observations were made of which only eleven were complete. The probable error of each set was calculated in the usual way, and the sum of these probable errors found to be $0\overset{\circ}{.}48$, or an average of about $0\overset{\circ}{.}035$ for a set. Taking $\theta=45°$, the percentage error of $\cos\theta$ is 0.05 per cent or 1 part in 2000.

Hence the experimental method should be capable of giving λ to at least 1 part in 1000, or to about 5 A.

Effect of the size of the apertures.—Hamy[1] derived a formula for the correction to be applied to observations made with apertures of finite width. The apertures were assumed to be rectangular, of width a and separation D; the source was assumed to be a uniformly luminous circular disk of angular diameter β. The fringes will disappear near the center of the pattern when

$$D=\frac{1.22\,\lambda}{\beta}\left\{1+0.765\left(\frac{a}{D}\right)^2\;.\;.\;.\;.\;\right\}$$

No other cases were treated. It would seem reasonable to assume, however, that if the source is a double star of angular separation α, the corresponding formula would be

$$D=\frac{\lambda}{2\alpha}\left\{1+0.765\left(\frac{a}{D}\right)^2\;.\;.\;.\;.\;\right\}$$

---

[1] *Bulletin Astronomique*, **16**, 257, 1899.

since the correction must depend upon some property of the observing instrument. For circular apertures, a further modification would no doubt be required, and we may reasonably assume that this would be the substitution of $a'/1.22$ for a where a' is the diameter of the circular aperture.

Observations were made on the artificial double star with circular apertures of various sizes, using the method of rotating aperture plate. These gave the *same* value of θ for all sizes of apertures, well within the errors of observation, thus indicating that for this method of observing and with this kind of a source no correction whatever is required. This result was so surprising that it seemed worth while to make a theoretical examination of the problem, using a method somewhat different from that employed by Hamy.

The method adopted, while being very simple, has the advantage of giving a clear physical picture of the phenomenon so that the need for a correction, if required, is made evident.

Let us consider rectangular apertures having a width a, and a length b, and let their centers be separated by a distance D. When the line joining the apertures is parallel to the x-axis the intensity in the focal plane due to a distant point-source is

$$I=I_0\frac{\sin^2\dfrac{\pi ax}{F\lambda}}{\left(\dfrac{\pi ax}{F\lambda}\right)^2}\,\frac{\sin^2\dfrac{\pi by}{F\lambda}}{\left(\dfrac{\pi by}{F\lambda}\right)^2}\cos^2\frac{\pi Dx}{F\lambda} \tag{11}$$

If a double point-source is used, the angular separation being α, we have, writing $2c=F\alpha$

$$I=I_0'\left\{\frac{\sin^2\dfrac{\pi a(x-c)}{F\lambda}}{\left(\dfrac{\pi a(x-c)}{F\lambda}\right)^2}\,\frac{\sin^2\dfrac{\pi by}{F\lambda}}{\left(\dfrac{\pi by}{F\lambda}\right)^2}\cos^2\frac{\pi D(x-c)}{F\lambda}\right.$$
$$\left.+\frac{\sin^2\dfrac{\pi a(x+c)}{F\lambda}}{\left(\dfrac{\pi a(x+c)}{F\lambda}\right)^2}\,\frac{\sin^2\dfrac{\pi by}{F\lambda}}{\left(\dfrac{\pi by}{F\lambda}\right)^2}\cos^2\frac{\pi D(x+c)}{F\lambda}\right\} \tag{12}$$

If circular apertures of radius r be employed, we have equation (10) instead of the foregoing.

These expressions hold for monochromatic light of wave-length λ, and hence by definition (*a*) they are also valid for white light of visual effective wave-length λ. If we limit ourselves to the phenomena on the x-axis, which in no way restricts the generality of the treatment, we can place the factors involving y equal to 1 in equation (11) and write x for $\sqrt{x^2+y^2}$ in equation (10). Writing $D/a=n$, equation (12) may be put in the form

$$I=I'_0\left\{\frac{\sin^2\dfrac{z-c'}{n}}{\left(\dfrac{z-c'}{n}\right)^2}\cos^2(z-c')+\frac{\sin^2\dfrac{z+c'}{n}}{\left(\dfrac{z+c'}{n}\right)^2}\cos^2(z+c')\right\} \qquad (12a)$$

in which $c'=\pi Dc/F\lambda$.

When n is very large, the intensity near the center of the pattern is given very nearly, by

$$I=I'_0\{\cos^2(z-c')+\cos^2(z+c')\}.$$

The visibility will be zero when $z-c'=z+c'-\frac{\pi}{2}$, or, $2c'=\frac{\pi}{2}$, or, applied to equation (12), we find that for a small in comparison to D, the fringes will vanish when

$$\frac{2\pi Dc}{F\lambda}=\frac{\pi}{2}$$

whence $2c=F\lambda/2D$, or, since $2c/F=\alpha$,

$$\alpha=\frac{\lambda}{2D}$$

which is the ordinary formula, equation (2).

In order to form a clear idea of what happens when a is increased, let us refer to Figure 2, and for this purpose we will assume that the dotted curve represents

$$\frac{\sin^2\dfrac{z-c}{n}}{\left(\dfrac{z-c}{n}\right)^2}$$

instead of

$$\frac{4J_1^2\left(\frac{2\pi rx}{F\lambda}\right)}{\left(\frac{2\pi rx}{F\lambda}\right)}$$

which really makes very little difference.

With this understanding, we have then $2n$-loops of the inscribed curve in the central loop of the dotted curve. If n is very large, or a very small, the loops of the inscribed curve near the origin all have very nearly the same height, the dotted curve approaching a straight line parallel to the x-axis, and the inscribed curve approaching a true cosine-square curve more and more closely as n is increased. If, under these conditions, we superpose two patterns displaced in the x direction by one-quarter of a period, the maxima of one will fall upon the minima of the other, and the sum will be a constant, which leads directly to equation (2).

When n is not large, the inscribed curve may be regarded as a distorted cosine-square curve, the distortion becoming more and more pronounced the more the dotted curve deviates from a straight line parallel to the axis. Since with white light the fringes are observable only near the center of the pattern, it follows that we need consider only the loops of the inscribed curve which are near the origin, and when n is small we have to confine our attention to the central fringe only, or to the portion of Figure 2 between the points P and Q. Let the ordinate at $x=0$ be taken as unity, and expressing x in degrees, we have for the undistorted curve ($n=\infty$) the value 0.500 at $\pm 45^\circ$ and the value 0 at 90°. For the distorted curve we have unity at $x=0$, and zero at 90°, but a value less than 0.500 at 45°. Hence if we superpose two such curves, 90° apart, there will be a minimum at 45°, or at the point midway between them, which will disappear only if their distance apart is made less than 90°. This makes it clear why equation (2) requires modification for small values of n, at least if we regard only the center of the pattern. It is necessary to remember, however, that when the minimum at 45° for the superposed curves disappears, the minimum at 135° has been made more prominent, and accordingly the "correction" that we employ to remove the minimum at 45° is really somewhat too large.

In order to calculate the angular displacement necessary to fill up the minimum at the center of the superposed curves, we need only equate the second derivative of (12) with respect to c, equate it to zero, and solve for c on the assumption that $x=0$. The factor in y is of course placed equal to unity. Table I gives the results of this calculation for a few values of n.

Here we have written the formula applicable to double stars in the form

$$D=\frac{\lambda}{2a}(1+K)$$

where K according to Hamy is $0.765\left(\frac{a}{D}\right)^2$.

Experimental verification of the results given in Table I.—In Table I we have applied Hamy's formula to a case which was not considered in his investigation, namely that of double stars. The difference between our calculated values and those given by Hamy's formula as here applied is so great that it seemed worth while to test both the case of double stars and that of a star disk experimentally, to see if there is really any difference between the two.

TABLE I

n	c	K (Calculated)	K by Hamy's Formula	Ratio $\frac{K\text{(Hamy)}}{K\text{(Calc.)}}$
∞	45°000	0	0	....
11.5	44.9234	0.0017	0.00577	3.395
5.75	44.6938	0.0068	0.02314	3.403
4.60	44.5275	0.0106	0.03615	3.411
3.45	44.1721	0.0187	0.06427	3.437

The experimental arrangement was as follows: A screen having a horizontal slot 2 mm in width was placed in front of the objective of the observing telescope. A plate was arranged to slide in a vertical direction directly in front of and in contact with this screen. This plate had two parallel slots 5 mm apart, each tapering from $\frac{1}{2}$ mm in width at one end to $2\frac{1}{2}$ mm at the other end, the length being 55 mm. This arrangement provided two nearly rectangular openings in front of the objective, at a constant distance apart; by sliding the plate up and down the width of each opening could be varied continuously from $\frac{1}{2}$ mm to $2\frac{1}{2}$ mm, or, what amounts to the same thing, n could be varied from $n=2$ to $n=10$ in a continuous manner.

Observations were made both on an artificial double star, and on an artificial star disk. The disk was illuminated with approximately monochromatic green light, in order to avoid the variations in color which are troublesome with white light, especially when the visibility of the fringes is low.

The observations were made by finding the distance between the observing telescope and the source which gave the minimum visibility for $n=10$, and also the distance at which the central minimum for $n=2$ just vanished. Since the results were the same as far as the correction factor is concerned, whether a star disk or a double star was used, we will record only the observations made on the star disk:

Wave-length of green light (mean) 5400 A.
Diameter of artificial star disk (δ) 0.650 mm.
Distance between centers of rectangular apertures (D) $=5.0$ mm.
Minimum visibility $n=10$, at 492 cm $\pm$ 2 cm.
Minimum in central fringe just disappears ($n=2$) at 478 *cm* $\pm$ 2 cm.

Using $L=D\delta/1.22\,\lambda$ for the distance at which fringes should vanish with $n=\infty$ and substituting, we get $L=493.3$ cm, which, considering the uncertainty in the value of λ used, is sufficiently near 492 cm.

From this we find an experimental value of K for $n=2$, namely, $\frac{492}{478}-1$ or $\frac{493.3}{478}-1$, according to whether we use the observed or calculated value of L_∞. The first gives $K=0.0293$, the second $K=0.0320$, while by Hamy's formula, which is strictly applicable to this case, K should equal 0.19125. An extrapolation of the values in Table I to $n=2$ gives a value of K slightly larger than 0.03, which is in good agreement with the observations. We must conclude that the formula given by Hamy is incorrect, and that if the observations are made directly on the vanishing of the minimum in the central fringe, the values given in Table I are correct. It must be borne in mind, however, that if the observations are made simply on the minimum visibility of the pattern as a whole, which on account of seeing, will generally be the case in astronomical work, the simple formulae (1) and (2) are to be used without any corrections. It has already been shown (see p. 13) that, with the method of rotating apertures, no correction to the simple formula is required.

Determination of the effective wave-length of sunlight.—We will first consider some general questions which bear directly on the problem. It may be assumed that the quality of sunlight outside of our atmosphere is constant or very nearly so. In passing through the atmosphere it is modified by selective absorption and scattering to an extent which depends both on the thickness of the air layer and upon its character, such as water-vapor content, smoke, haze, etc. Most of these factors will reduce the intensity of the short wave-lengths more than that of the red end of the spectrum. Water-vapor is, however, an exception. It is very transparent to the short wave-lengths, while absorption begins somewhat below 6000 A and increases rapidly toward the red. Since its absorption lies almost entirely on the red side of the maximum of the sensitivity curve of the human eye, it appears that the effect of water-vapor by itself is to move the value of the effective wave-length toward the violet. Dust, smoke, haze, and increased thickness of the atmosphere due to large zenith distances might be expected to shift the wave-length to the red. A priori, then, a given observer would not expect to find a constant value for the wave-length.

Apparatus.—Figure 1 gives a schematic diagram of the apparatus, and Figure 4 is a drawing of the observing telescope and aperture plate. The lens C is a theodolite objective of 22 mm aperture and of about 20 cm focus. The miscroscope consists of an 8-mm objective and a 7.5-power eyepiece, giving a linear magnification of about 125×. The circle B is graduated in degrees and can be read easily to $0\overset{\circ}{.}1$. It carries the aperture plate AA, and is rotated by a worm DW, so arranged that one revolution of the worm gives a rotation of 10°. The whole instrument is mounted on a solid brass base plate, *K*, which is easily clamped to a table or other convenient support. The slot *S* was designed to hold a plane parallel quartz plate, cut at 45° to the optic axis. Viewed through this plate, a single distant pinhole appears as an artificial double star, whose angular separation depends only on the thickness of the quartz plate. A slight difficulty arises in the use of such a quartz plate, on account of the fact that one of the emergent beams of light is colored, due to the dispersion of the quartz. A great deal of time was spent in the calibration of the plate by the use of monochromatic light, and a few observations were made using it in conjunction with the 100-inch Hooker telescope on some of the brighter stars, but the results were not entirely satisfactory. When the quartz plate is not used the slot *S* is covered by a suitable cap. In the determination of the wave-length of sunlight the source was always a pair of pinholes made and mounted as described above; the sunlight was reflected into the quartz projection lens *L*, Figure 1, by a two-mirror coelostat, the mirrors being freshly silvered and polished every two or three weeks.

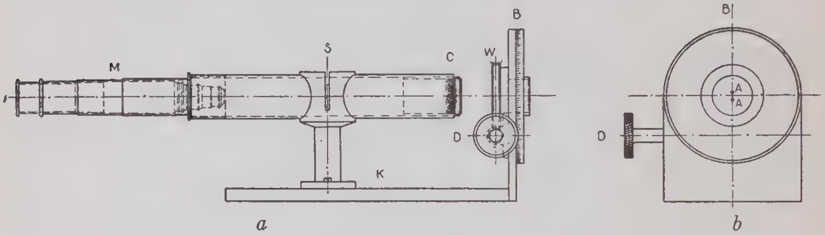

FIG. 4.—Laboratory apparatus
a. Side view. *b*. End view

In Tables II and III are collected the observations which have been made with the apparatus shown in Figure 4. Table II gives the observations made on Mount Wilson, June 15 to June 18, while in Table III are collected all the miscellaneous observations made under all sorts of conditions of sky in Pasadena. The first two columns give the date and hour of the observation. Since each complete observation required about 10 minutes, the time given refers to the middle of the observation. The third column gives the zenith distance of the sun to the nearest degree at the time. The fourth column gives the number of settings in each determination, which was always 20, excepting for the first observation on Mount Wilson which was stopped by fog, and for the three early observations on June 18, when the available time did not permit a complete set. The only observations calling for special comment are those of April 5 and 6 in Pasadena. These were made immediately after a rain, and the abnormally low value for the wave-length may be due to a relatively large amount of water-vapor; this, as mentioned above, would tend to displace the effective wave-length to the violet.

TABLE II

MOUNT WILSON OBSERVATIONS

Date	Mean Time	ζ	No. of Settings	λ	Remarks
June 15.....	8:35 A.M.	45°	16	(5546)	Incomplete. Fog blowing over. Image drifting badly.
June 16.....	5:14 A.M.	85	20	5631	
June 16.....	5:46 A.M.	79	20	5574	
June 16.....	6:35 A.M.	69	20	5542	
June 16.....	7:53 A.M.	53	20	(5535)	Fog coming over. Foggy remainder of day.
June 17.....	6:32 A.M.	69	20	5554	
June 17.....	7:52 A.M.	53	20	5515	
June 17.....	8:34 A.M.	45	20	5519	Faint haze.
June 17.....	9:18 A.M.	35	20	5519	
June 17.....	10:06 A.M.	25	20	5520	
June 17.....	10:49 A.M.	17	20	5515	Clouded over at 11:00 A.M.
June 17.....	4:50 P.M.	65	20	5546	Clouds. Haze as high as mountain tops. Sky blue.
June 17.....	5:22 P.M.	71	20	5579	Clouds. Haze as high as mountain tops. Sky blue.
June 17.....	6:13 P.M.	82	20	5596	Through very thin clouds. Haze.
June 17.....	6:37 P.M.	86	20	5625	Haze only.
June 18.....	4:58 A.M.	87	8	5656	Sky clear all day.
June 18.....	5:06 A.M.	86	8	5629	Sky clear all day.
June 18.....	5:07 A.M.	85	8	5619	Sky clear all day.
June 18.....	5:17 A.M.	83	20	5593	
June 18.....	5:47 A.M.	78	20	5561	
June 18.....	6:12 A.M.	73	20	5546	
June 18.....	6:44 A.M.	67	20	5528	
June 18.....	7:43 A.M.	55	20	5523	
June 18.....	8:12 A.M.	48	20	5512	
June 18.....	9:10 A.M.	37	20	5512	
June 18.....	10:11 A.M.	25	20	5515	
June 18.....	10:56 A.M.	17	20	5513	
June 18.....	11:20 A.M.	14	20	5510	
June 18.....	11:58 A.M.	11	20	5509	

TABLE III

PASADENA OBSERVATIONS

Date	Mean Time	ζ	No. of Settings	λ	Remarks
March 27...	10:11 A.M.	40	20	5537	
March 27...	11:41 A.M.	32	20	5521	
March 28...	9:05 A.M.	48	20	5568	
March 28...	9:57 A.M.	42	20	5531	
March 28...	11:03 A.M.	34	20	5515	
March 28...	2:03 P.M.	42	20	5555	
March 29...	9:19 A.M.	48	20	5556	
March 29...	9:50 A.M.	42	20	5542	
March 29...	10:29 A.M.	36	20	5522	
March 29...	11:30 A.M.	31	20	5525	
March 29...	1:10 P.M.	36	20	5559	Sky very thick.
March 30...	8:30 A.M.	56	20	5562	Sky thick toward east.
March 30...	9:10 A.M.	49	20	5537	
March 30...	9:40 A.M.	45	20	5542	
March 30...	10:03 A.M.	41	20	5547	
March 30...	10:27 A.M.	37	20	5528	Clearing rapidly.
March 30...	11:01 A.M.	33	20	5522	
March 30...	11:25 A.M.	31	20	5515	
March 30...	1:00 P.M.	34	20	5519	
March 30...	1:30 P.M.	38	20	5522	
March 30...	2:05 P.M.	43	20	5526	
March 30...	2:50 P.M.	51	20	5526	Cirrus developing rapidly.
April 2...	10:10 A.M.	28	20	5553	Some fog. Light unsteady.
April 2...	10:38 A.M.	34	20	5547	White sky, haze.
April 2...	11:10 A.M.	31	20	5524	
April 2...	11:30 A.M.	30	20	5524	
April 2...	1:35 P.M.	37	20	5527	
April 4...	8:30 A.M.	55	20	5524	After a rain. Cumulus clouds. Sky clear. Windy.
April 4...	8:56 A.M.	50	20	5527	
April 4...	9:48 A.M.	40	20	5524	
April 4...	10:42 A.M.	34	20	5533	
April 4...	11:17 A.M.	31	20	5531	Observer P.W.M.
April 5...	9:10 A.M.	46	20	5517	Thin cirrus here and there.
April 5...	10:12 A.M.	37	20	5494	Through cirrus.
April 5...	11:13 A.M.	30	20	5503	Clear.
April 6...	8:05 A.M.	59	20	5515	Clear.
April 6...	9:46 A.M.	39	20	5513	Clear.
April 6...	11:22 A.M.	29	20	5506	Clear.
June 21...	8:50 A.M.	40	20	5560	Haze obscuring mountains. White area around sun. Sky blue otherwise.
June 21...	9:26 A.M.	33	20	5545	
June 21...	10:12 A.M.	24	20	5533	
June 21...	11:05 A.M.	14	20	5524	
June 21...	11:40 A.M.	11	20	5522	

Figure 5 gives a graphical representation of the Mount Wilson results. This shows that on clear days for purposes of interferometer measurement the wave-length is sensibly constant if the zenith distance is less than 60°, while for greater zenith distances it rises rapidly. The Pasadena observations in general show that for zenith distances less than 40° there is not much change in the wave-length. For small zenith distances the Pasadena observations indicate a value not far from 5520, while the Mount Wilson observations indicate 5510. The difference of 10 A, though perhaps real, is so small that it may be said to be negligible as far as ordinary astronomical interferometer work is concerned.

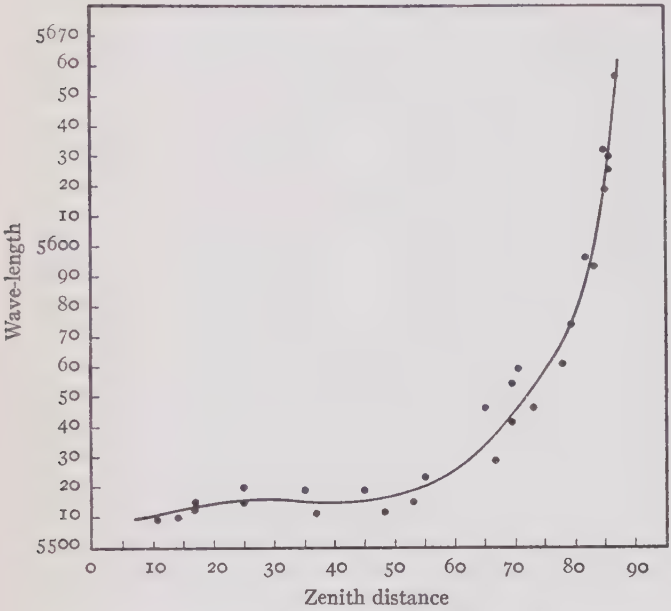

FIG. 5.—Mount Wilson observations June 16–18, 1921

MOUNT WILSON OBSERVATORY
October 1921

Contributions from the Mount Wilson Observatory, No. 223
Reprinted from the *Astrophysical Journal*, Vol. LV, pp. 36–47, 1922

AN INVESTIGATION OF THE CONSTANCY IN WAVE-LENGTH OF THE ATMOSPHERIC AND SOLAR LINES

By CHARLES E. ST. JOHN and HAROLD D. BABCOCK

ABSTRACT

Constancy in wave-length of atmospheric lines in the solar spectrum.—In 1915 Perot reported having found the wave-length of an O line considerably longer at noon than at sunrise and sunset. Since these lines are constantly used as standards of wave-length in solar observations, a study of the *wave-length as a function of the altitude of the sun* was made for a number of atmospheric lines in the B group at λ 6867, in the α group at λ 6276, and in the water-vapor band near λ 5900. Measurements of 25 plates show no indication of a variation greater than the accidental error. Moreover, spectrograms and data accumulated at Mount Wilson since 1911 give wave-lengths, some determined with reference to solar lines and some with reference to arc lines, which agree very closely, the difference from the general mean shown by any plate seldom exceeding 0.001 A. This negative result indicates the absence of high velocity *radial currents in the earth's atmosphere* and justifies the use of atmospheric lines as a reliable standard of reference even in work requiring the highest precision.

Constancy in wave-length of lines from the center of the solar disk.—While Evershed reported in 1919 remarkable variations amounting to several thousandths of an angstrom, the experience at Mount Wilson is that the more carefully the solar wave-lengths are compared with standard arc lines, the smaller the deviations from spectrogram to spectrogram become. Evidence from 13 plates is presented. These results prove that the *radial convection currents in the sun*, while not absent, are remarkably constant, apparently downward at high levels and upward, but small, at low levels.

In spectrographic observations on the solar spectrum for determining wave-lengths and displacements of the Fraunhofer lines with high precision, a desideratum is some means of procuring a simultaneous comparison spectrum under the same conditions of illumination as those obtaining for the spectrum under investigation. Provided their wave-lengths are constant, ideal conditions occur when atmospheric lines are used for reference in solar observations, since in the instrument the path of the light is identical for both classes of lines.

It has been generally assumed that under all practical conditions of solar observation the velocities of terrestrial atmospheric movements are of such an order that no measurable Doppler effect is produced. It would require motion in the line of sight of approximately 125 miles an hour to cause a displacement of 0.001 A at λ 6000. Some observations reported by Perot,[1] however, give very remarkable and surprising results, and if confirmed would show that the atmospheric lines are not constant in wave-length and hence not reliable as standards of reference. He measured with an interferometer the wave-length of an oxygen line in the B group at different hours of the day and concluded that the wave-length increased from morning to noon and decreased from noon to evening. He interprets his results as showing a recession of the absorbing centers from the surface of the earth with a radial velocity of about 3 km per second.

In view of the importance of the atmospheric lines in solar observations we have examined for change in wave-length during the day the atmospheric lines in three spectral regions, namely, in the B group at λ 6867, in the a group at λ 6276, and in the water-vapor band near λ 5900, and have supplemented these observations from spectrograms taken for other purposes through a series of years. For much of the measurement and reduction we are under obligation to Miss Ware, Miss Miller, and Miss Keener.

Oxygen lines in the B group.—On two occasions grating spectrograms of the center of the sun were taken in the first order of the 75-foot spectrograph of the 150-foot tower at intervals from sunrise to sunset. The wave-lengths of eight oxygen lines were obtained from solar lines whose wave-lengths were corrected for the earth's motions. The statistical results are given in Table I. The lines are identified by their Rowland wave-lengths in the first and fourth columns and in the other columns are given the deviations from the mean for the hours of observation. In Figure 1*A* the average deviations from the general mean are plotted against the corresponding altitudes of the sun.

From our investigation on solar wave-lengths in the international system we extract the data given in Table II. These measurements were made during June, 1919, with the interferometer attached to the Snow telescope. Our unpublished international values of solar lines were used as standards. The first column contains the preliminary wave-lengths in the international system of 28 oxygen lines in the B group. In the other columns are shown

---

[1] *Comptes Rendus*, **160**, 549, 1915.

TABLE I

Relative Wave-Lengths of Oxygen Lines of the B Group at Different Hours of the Day. Grating Spectrograms

(Unit for residuals=0.001 A)

λ Rowland	February 25–26, 1919, P.S.T.			λ Rowland	June 5, 1919, P.S.T.						
	7:00	12:00	4:37		6:27	9:12	11:56	2:57	3:02	5:41	5:50
6879.288	+2	−3	0	6877.882	+4	0	−2	−2	0	0	0
6880.172	+6	+2	−7	6880.172	+4	+2	−2	−1	+1	−2	−2
6884.076	0	+2	−3	6884.076	+4	−4	−5	0	+1	+1	0
6886.000	+1	+2	−3	6900.199	+2	−4	−3	+2	+2	−2	+4
6913.448	−7	+5	+1	6905.271	+2	−2	+1	−1	0	−3	0
6914.337	−5	0	+6	6909.676	+1	0	0	−3	+1	−1	−1
6918.370	....	+1	−1	6913.448	+2	0	−1	−3	−1	0	−4
6919.250	....	−1	+2	6918.370	+1	0	+3	0	+2	−2	−1
Mean	−0.5	+1.0	−0.6	Mean	+2.5	−1.0	−1.1	−1.0	+0.6	−1.1	−0.5
Altitude	7°00′	46°40′	10°20′	Altitude	17°40′	51°30′	78°10′	49°40′	48°40′	16°10′	14°20′

the deviations from the mean values for altitudes varying from 12°50′ to 75°40′. The observed mean wave-length at the highest altitude is 0.0012 A less than the general mean.

Oxygen lines of the α group.—On June 7 and 9, 1919, spectrograms of the center of the sun were taken with the 75-foot spectrograph at intervals from 6:00 A.M. to 6:00 P.M. Eight oxygen lines of the α group were measured in terms of solar standards. After correction of the reference lines for the earth's motions, the mean wave-length at noon exceeded the mean for the two lowest altitudes by 0.0016 A. The numerical data are given in Table III; the relative results are plotted in Figure 1*B* against the hours of observation.

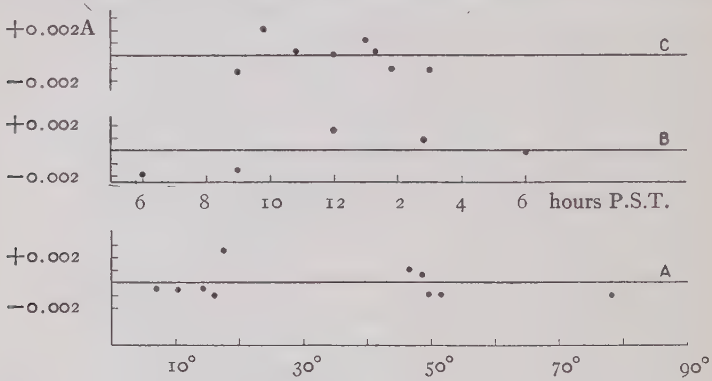

FIG. 1.—*A*. Deviations of oxygen lines in B group from mean wave-length; for different altitudes of sun.

B. Deviations of oxygen lines in α group from mean wave-length; at different hours of the day. Solar standards.

C. Same as *B*, referred to absorption lines of iodine as standards.

In order to eliminate solar standards and obtain an independent determination, spectrograms of sunlight filtered through iodine vapor were taken with an interferometer using two absorption lines of iodine as the fixed references. These observations were made in the Pasadena laboratory in April, 1919, with an etalon of 20 mm separation giving a mean order of interference of 63400 for the eight measured oxygen lines of the α group. The deviations from the mean wave-length at the hours of observation are plotted in Figure 1*C*. The wave-length at noon shows no deviation from the mean of the series.

TABLE II

RELATIVE WAVE-LENGTHS OF OXYGEN LINES OF THE B GROUP AT DIFFERENT HOURS OF THE DAY. INTERFEROMETER SPECTROGRAMS

(Unit for residuals = 0.001 A)

June 6, 15, 16, 1919, P.S.T.

λ I.A.	June 6 9:08	June 6 10:32	June 6 12:36	June 16 3:40	June 15 5:11	June 16 6:03
6872.265	−3	−1	+1	+2	+3	−3
6872.861	+1	−3	−3	+3	0	....
6873.816	−2	0	0	0	+4	−2
6874.671	−2	+1	−3	−2	+5	0
6875.608	0	0	0	0	+3	−5
6876.733	−2	+3	0	−2	−2	+1
6877.655	+2	+2	−2	−3	+1	−1
6879.058	+2	+3	−3	+2	−1	−10
6879.947	+4	0	−3	−1	−1	−5
6883.850	+1	+1	0	−1	+1	−6
6885.772	−1	+1	−1	−1	+4	−4
6886.761	−1	+1	−2	0	+3	−3
6888.967	+1	+1	−1	0	0	−3
6889.921	−2	0	0	+2	−3	....
6892.389	−6	+3	−3	+2	−1	....
6893.328	0	0	−5	−2	+6	−4
6896.056	0	+2	+2	−2	−3	−2
6896.984	+1	0	0	+1	−3	−3
6899.972	−1	0	−1	+2	−1	+2
6900.887	−2	+1	−4	+0	+4	−5
6904.137	−1	+2	−2	−2	0	....
6905.137	−1	+2	−2	−2	0	....
6908.553	+1	+1	−3	−1	+3	−2
6909.450	−1	+2	−2	−1	+1	−3
6913.219	0	+3	+1	−4	+1	....
6914.109	0	+5	0	−4	+1	....
6918.140	−2	+2	−2	+1	−3	....
6919.022	+1	0	−1	−1	+3	....
Mean	−0.4	+1.1	−1.4	−0.5	+1.0	−2.9
Altitude	50°40′	67°20′	75°40′	41°10′	22°30′	12°50′

From spectrograms and data accumulated since 1911, when the *a* band was first studied at Mount Wilson, a yearly record is available. The results for eight lines are given in Table IV. The mean wave-lengths for the eleven-year period are in the first column and those for the separate years in the succeeding columns. The mean wave-length of the group is shown at the bottom of the table. The spectrograms were taken in various months, on various days, and at various hours. It would seem that frequently occurring disturbances should have been detected; but on none of the scores of spectrograms measured is there definite evidence of radial movements of the absorbing regions of the atmosphere. The difference from the general mean shown by any plate seldom exceeds 0.001 A.[1]

TABLE III

WAVE-LENGTHS OF OXYGEN LINES OF THE α GROUP AT DIFFERENT HOURS OF THE DAY. GRATING SPECTROGRAMS

June 7–9, 1919, P.S.T.

λ I.A.	June 7 6:00	June 7 9:00	June 7–9 12:00	June 9 2:50	June 9 6:00
6280.404.........	.403	.402	.406	.404	.403
6281.187.........	.185	.186	.189	.189	.186
6281.964.........	.962	.962	.966	.966	.963
6290.230.........	.229	.230	.232	.230	.229
6295.187.........	.185	.184	.188	.187	.188
6295.969.........	.967	.968	.970	.971	.968
6302.009.........	.006	.006	.010	.009	.010
6302.770.........	.768	.769	.772	770	.771
Mean .215........	.2131	.2134	.2166	.2158	.2148
No. of plates......	2	1	3	2	4
Altitude..........	12°30′	49°10′	78°40′	51°20′	12°40′

Water-vapor lines near λ 5900.—To complete the investigation on atmospheric lines, grating spectrograms of the center of the sun's disk were taken at high and low sun in the region of the rainband near D_1 and D_2. The results of the measures of eleven lines on twenty-four spectrograms are shown in Table V. Solar lines were used as standards. The mean wave-lengths in the international system are in the first column, weighted according to the number of exposures. For the eleven lines the wave-length at high sun exceeds the mean at low sun by 0.001 A.

---

[1] This confirms and extends in time other observations on the α group. Royds, *Annual Report, Kodaikanal Observatory*, 1917; St. John and Babcock, *Publications of the Astronomical Society of the Pacific*, 31, 178, 1919.

TABLE IV

Yearly Record for Atmospheric Lines of the α Group

Mean Wave-Lengths I.A. Units	Standards of Reference										
	Solar Lines Corrected for the Earth's Motions								Iron Arc Lines Used as Standards		
	At Center			At Limb, Corrected for Limb-Center Shift							
	1911	1912	1913	1914	1915	1916	1917	1918	1919	1920	1921
6280.400	.400	.400	.403	.403	.400	.397	.400	.402	.402	.398	.403
6281.186	.183	.185	.185	.186	.184	.183	.185	.185	.186	.187	.188
6281.963	.961	.960	.963	.964	.966	.962	.963	.963	.963	.963	.964
6290.229	.230	.229	.228	.230	.229	.228	.226	.229	.229	.229	.229
6295.186	.187	.183	.184	.186	.185	.184	.187	.182	.187	.185	.185
6295.968	.970	.967	.968	.969	.968	.967	.967	.965	.968	.968	.970
6302.008	.009	.007	.010	.012	.006	.008	.005	.005	.008	.007	.009
6302.771	.771	.771	.769	.776	.772	.768	.771	.767	.770	.772	.772
Mean .214	.214	.213	.214	.216	.214	.212	.213	.212	.214	.214	.215
No. of plates	8	2	2	3	4	2	2	2	22	13	2

TABLE V

WAVE-LENGTHS OF WATER-VAPOR LINES AT DIFFERENT HOURS OF THE DAY
(March and June 1921)

λ I.A.	P.S.T. of Observation			
	7:03	11:40	3:16	5:40
5885.982	.980	.983	.984	.980
5887.227	.226	.227	.230	.226
5887.665	.664	.668	.663	.664
5892.402	.396	.405	.403	.402
5909.001	.998	.000	.004	.002
5913.999	.998	.996	.004	.999
5919.058	.056	.059	.059	.057
5919.646	.644	.647	.646	.646
5924.276	.275	.275	.278	.276
5932.097	.096	.097	.098	.097
5932.788	.788	.788	.788	.788
Mean .4675	.466	.468	.469	.467
Altitude	16°	61°	35°	13°

When the observations on atmospheric lines at high sun are compared with the mean for all altitudes, the residuals, high sun *minus* mean, are as follows:

Source	Lines Observed	Altitude High Sun	Residuals
Table I	B group	78°10′	−0.0010 A
Table II	B group	75 40	−0.0012
Table III	α group	78 30	+0.0016
Table IV	Water-vapor	61 20	+0.0005
Mean			0.0000

We are unable to account for the wide divergence between our measures and those of Perot. Within the error of measurement our series of observations show no variation in the wave-lengths of the terrestrial lines with the altitude of the sun. It will be recalled that Dunér,[1] in his determination of solar rotation in 1887–1889, used the terrestrial line λ6302.209 as a fixed point of reference, and in 1899–1901 the other component of the pair, λ6302.975. If the terrestrial atmosphere in the absorbing region is subject to radial velocities of 3 km per second his consistent values are remarkable, particularly for the highest latitude where the observed rotational velocity was only 0.39 km per second. It must be admitted that radial velocities in the earth's atmosphere of the order of 3 km per second, if they do occur, are extremely rare and very local. It seems to us more probable that a different interpretation should be sought for Perot's observations. His interpretation requires for the absorbing centers a radial velocity of 6700 miles per hour. That such enormous radial velocities occur even in attenuated regions of the earth's atmosphere is open to question, and it is more doubtful still that the radial component would remain constant for a month over a given locality. From our observations we feel justified in using the atmospheric lines as reliable standards of reference, even in work requiring the highest precision.

---

[1] *Über die Rotation der Sonne*, Upsala, 1906.

On constancy of wave-length of solar lines.—Jewell[1] was the first to raise the question of variability in the wave-lengths of the solar lines. He says,

> Another effect of this investigation may be to make the lines of the solar spectrum step down from the commanding position which they have occupied, as standards of reference.

At the period of Jewell's investigation the instability of many lines in the arc spectra of metals had not been recognized. Moreover, the records of the spectrograms taken by Rowland and used by Jewell were not sufficiently detailed to determine corrections depending upon the earth's motions. Under these conditions the conclusion reached by Jewell loses much of its weight. Evershed[2] reports that

> a continuous series of sunlight and Fe spectra was taken to test the constancy of the sun-arc displacement. Confining attention to the region 4337–4531 and to lines not subject to pole-effect in the arc, it was found that some remarkable variations occurred amounting to several thousandths of an angstrom. The variations are of two kinds: a general change for all the lines in the region studied, and a change affecting particular lines or groups of lines.

He says,

> These displacements may be observed at the center of the disk, but up to the present they have not been found very near the limb. It appears therefore that, unlike the displacements in the penumbra of spots, they may be

---

[1] *Astrophysical Journal*, **3**, 113, 1896.

[2] *Annual Report, Director, Kodaikanal and Madras Observatories*, 1919, p. 2.

due to movements normal to the surface or having a component normal to the surface.

At Mount Wilson it has been found that in the determination of solar wave-lengths from arc standards, the more carefully the iron arc is controlled, the more completely instrumental displacements are eliminated, the more accurately the image of the sun is centered,[1] and the more exactly the axes of the light-cones incident upon the grating are made to coincide, the smaller the deviations from spectrogram to spectrogram become.

A comparison of four observations with the grating spectrograph from April to June, 1921, and the mean of measures in 1917 for the 13 solar lines common to all plates gives for the fractional part of the mean wave-length the following:

		1917, Mean	1921, April 21	1921 April 29	1921 May 1	1921 June 1
13 lines..........	λ 4337–λ 4401	0.5545	0.5552	0.5550	0.5565	0.5554

The three April-June observations for the other common lines also show good agreement in the fractional part.

		1921, April 21	April 29	May 1
17 lines..............	λ 4489–λ 4607	0.5574	0.5594	0.5593
15 lines..............	λ 4615–λ 4688	0.3942	0.3941	0.3945
20 lines..............	λ 4707–λ 4784	0.5217	0.5217	0.5216

These wave-lengths are determined from the arc standards, not by measuring the displacements between the center of the sun and arc, but by using the arc lines as standards of reference. Five interferometer spectrograms likewise referred to arc standards, taken on August 5, 1920, at intervals from 10:44 A.M. to 5:03 P.M. P.S.T. and one taken a year later on August 8, 1921, give deviations from the mean of the six as follows for a group of 38 solar lines:

		August 5, 1920					August 8, 1921
		10:44	2:34	3:30	4:22	5:03	4:50
38 lines...	λ 5497–λ 5862	.0000	+.0011	+.0003	−.0020	+.0005	.0000 A

---

[1] *Observatory*, 43, 260, 1920.

The degree of constancy of the solar wave-lengths at the center of the sun shown by these determinations is further evidenced by considering the data in Table IV from this point of view.

The wave-lengths of the oxygen lines in the table, except for the years 1920–1921, were referred to solar standards determined as above. In 1911, 1912, 1913, and 1919 the wave-lengths of the solar lines at the center of the disk were used. For the years 1920–1921 the oxygen lines were referred directly to the iron-arc standards. This completes the cycle: arc–sun–atmospheric lines–arc. The closing of the cycle is practically perfect. Unless it is assumed that continuously compensating changes in the wave-lengths of the solar and terrestrial lines occur, the agreement between the first and last sections of Table IV may be taken as a measure of the constancy in wave-length of the atmospheric lines and of the solar lines at the center of the disk, and also of the accuracy of their determination in terms of the international iron-arc standards. In 1914–1918 the results are less dependable, as the measures were made upon spectrograms of the limb and it was necessary to apply a correction for the limb-center shift, a somewhat uncertain quantity for a single observation. From an extended series the mean limb-center shift for solar lines in this spectral region is 0.007 A with a range of 0.002 to 0.010 A.

In view of the probable existence of radial convection currents on the sun the relative constancy of wave-length at the sun's center is somewhat surprising. At any given level, the radial velocity appears to reach a comparatively steady state, differing from level to level and in widely different levels even opposite in direction. For the strong lines—high-level lines—the motion is apparently downward. The great intensity of these lines at high levels is probably dependent on the increased ionization under the low pressures at the high elevations.[1] As yet too little is known of the ionizing potentials of the elements involved for a definite conclusion. For very low-level lines the motion is small but upward. At both low and high levels we appear, however, to be dealing with remarkably steady states. In this regard there is a marked difference between the center and the limb, the range of deviation from plate to plate at the limb being four- to five-fold that at the center. Though the causes of the motions in the solar and terrestrial atmospheres are different, there may be common characters in the general atmospheric movements due to the similar damping influences. In both cases centrifugal velocities are opposed by gravitation, very powerfully so in the sun, while tangential movements are damped by the smaller forces of friction. Thus through a kind of selective action the tangential components would tend to persist and the radial components to be quenched, so that in both the solar and terrestrial atmospheres the prevalent atmospheric flows would tend to be tangential. In the sun the opposing effects of light-pressure and gravitation may have influence in producing the steady state at any given level, the different levels of the absorbing centers being again a selective result as the equilibrium between light-pressure and gravitation depends upon the ratio between the mass and diameter of the centers.

---

[1] Megh Nad Saha, *Philosophical Magazine*, 40, 472, 1920.

From these observations it is evident that differences between solar wave-lengths at the sun's center and in terrestrial sources may be determined with an accuracy comparable to that for the terrestrial lines. Upon the magnitude of these differences, their variation over the solar disk, from element to element, from line to line, and from wave-length to wave-length, rests the possibility of disentangling the causes of the displacement of solar lines, a formidable but far from hopeless undertaking.

Mount Wilson Observatory
October 1921

Contributions from the Mount Wilson Observatory, No. 224

INVESTIGATIONS ON PROPER MOTION

SIXTH PAPER: THE MOTIONS OF 65 STARS IN THE NEIGHBORHOOD OF α TAURI

By ADRIAAN VAN MAANEN

ABSTRACT

Proper motions of 65 faint stars within 15′ of α Tauri.—In order to test the new stereocomparator and possibly discover some faint members of the Hyades group, two plates taken in 1919 at the 80-foot focus of the 60-inch reflector were compared with two taken in 1914, the first and second of 1919 being paired with the first and second of 1914 respectively. The photographic magnitudes range from 11.3 to 15.4. The plate constants were determined from measurements of 29 selected stars. The results for the relative motions μ_α and μ_δ from the two pairs of plates differ, on the average, by $\pm 0''.014$ per year and the average absolute values of μ_α and μ_δ are only $\pm 0''.011$ except for four or five stars with components over $0''.03$. Only two of the stars, Nos. 45 and 62, can possibly be members of the Hyades group.

Distribution of apparent magnitudes in the Hyades group.—The rapid falling off in the number of group members with increasing magnitude is shown in Table II which analyzes the results of Kapteyn and de Sitter for 395 stars in the region of the Hyades.

New stereocomparator at Mount Wilson is similar in principle to the Zeiss instrument, but it is more rigid and less subject to temperature changes and has other advantages including the provision of slow motions for both plate-holders in both co-ordinates as well as in rotation.

Since 1914 several plates of the region of α Tauri have been taken at the 80-foot focus of the 60-inch reflector, the exposures, under normal conditions, being 25 minutes. Two photographs taken in 1919 have been compared with two secured in 1914, the purpose being twofold: First, the comparison would afford good material to test the accuracy obtainable with the new stereocomparator, recently completed in the instrument shop of the Observatory; and second, the measures might reveal some faint members of the Hyades group.

The new instrument is similar in principle to the Zeiss stereocomparator, but has several advantages over the latter machine: The castings are more rigid; the distance between the centers of the two plates, as well as the tube containing the optical parts, has been reduced by about 25 per cent, which also helps in stabilizing the instrument; the frame work, the plate-carriers, and the tube supporting the optical parts are all made of the same material, thus avoiding the difficulties due to changes in temperature during a long series of measures; the frame holding both plates can be moved both horizontally and vertically, affording a constant position of the eyepiece; both plate-holders have been provided with slow motions in both co-ordinates as well as in rotation; and, finally, the magnification can be changed by moving the two lenses in the eyepiece tube along the optical axis. As now used, the magnification is about two and a half times that of the Zeiss instrument.

The following plates have been measured:

Plate No.	Date	Obs.	Quality	H. A. at Middle of Exposure
265.	1914, Sept. 15	vM	g	−15°0
266.	15	vM	g	− 7.0
2424_1.	1919, Oct. 20	H	g	−13.5
2424_2.	20	vM	g	− 6.5

They are combined in two pairs, 2424_1–265 and 2424_2–266, designated by the numerals 1 and 2, respectively, in Table I. Each pair was measured in four positions, with the directions east, west, north, and south, successively coinciding with the direction of increasing readings of the micrometer screw. The two series of measures in right ascension for each pair of plates were combined into one; the same was done for the measures in declination. Then in order to deal with smaller quantities, the measured distances were reduced to thousandths of a second of arc per year by multiplying by the factor

$$q=\frac{8227}{12251\times 5.10}=0.1285.$$

where

8227 = number of thousandths seconds of arc per mm on plates
12251 = number of parts of micrometer screw per mm
5.10 = interval in years between the two exposures

Designating the measured quantities after this reduction by m_α and m_δ, we have

$$\begin{aligned} m_\alpha &= a+bx+cy+dx^2+exy+fy^2+\mu_\alpha \\ m_\delta &= a'+b'x+c'y+d'x^2+e'xy+f'y^2+\mu_\delta \end{aligned} \qquad (1)$$

where $a, b \ldots a', b' \ldots f'$ are the plate constants, and μ_α and μ_δ the annual proper motions in thousandths of a second of arc. The plate constants were derived by least-squares solutions of the sets of equations, each including six constants, of the form (1) for the comparison stars; for this purpose twenty-nine stars were selected, well distributed over the plates; care was taken to avoid (*a*) the brighter stars, (*b*) the very faintest stars, (*c*) stars showing poor images, and (*d*) stars which after a preliminary reduction seemed to have considerable proper motion. The constants thus derived were substituted into equations (1) applied to each of the sixty-five stars. The resulting proper motions for each of the plates, relative to the mean motions of the twenty-nine comparison stars, are given in the fifth, sixth, seventh, and eighth columns of Table I.

The second column gives the photographic magnitudes, derived from a plate taken of the polar sequence; for No. 44, α Tauri, the magnitude is that given in the *Draper Catalogue.* The third and fourth columns give the co-ordinates of each star with respect to α Tauri.

It was hoped that enough members of the Hyades group would be found to permit a reduction from relative to absolute proper motions. By comparing the motions of these stars with those of the group as given in Boss's *Preliminary General Catalogue*, the motions of all the stars could then have been reduced to the system of that catalogue. But the results show that only two of the stars, Nos. 45 and 62, can possibly be members of the group, and even for these the question of membership is doubtful.

A discussion of the results derived by Kapteyn and de Sitter[1] for 395 stars in the region of the Hyades shows that the lack of members of the group among the stars on our plates is not surprising. Of the 395 stars down to photometric magnitude 10.3, Kapteyn and de Sitter find:

Very probable members.	42
Probable members.	19
Doubtful members.	16

---

[1] *Groningen Publications,* No. 14, 1904.

TABLE I

Proper Motion of Faint Stars near α Tauri

No.	Phot. Mag.	x	y	Relative μ_α		Relative μ_δ		Absolute	
				1	2	1	2	μ_α	μ_δ
1	15.3	−15′.1	− 2′.7	+0″.050	+0″.014	+0″.007	+0″.008	+0″.029	+0″.016
2	13.7	−14.9	+ 8.6	− 14	− 47	− 8	− 19	− 33	− 6
3	14.8	−13.8	+ 6.2	+ 13	+ 16	+ 18	− 10	+ 11	+ 12
4	13.7	−13.7	+ 5.8	+ 12	− 18	− 4	− 8	− 6	+ 2
5	14.8	−13.3	−10.7	− 25	+ 3	+ 8	+ 9	+ 14	+ 16
6	14.8	−13.3	+12.5	− 28	− 30	+ 17	− 7	− 32	+ 13
7	15.3	−13.2	+12.5	+ 9	− 29	+ 44	− 36	− 13	+ 12
8	14.8	−12.6	−10.5	+ 5	− 3	− 22	− 12	− 2	− 9
9	13.1	−12.5	+ 3.7	+ 6	− 2	+ 16	+ 2	− 1	+ 17
10	15.3	−11.9	− 8.2	+ 36	+ 14	+ 2	+ 15	+ 22	+ 16
11	14.8	−11.5	+ 1.1	+ 22	+ 18	− 20	+ 7	+ 17	+ 2
12	12.9	−11.4	+ 0.7	− 37	− 14	+ 10	+ 8	− 29	+ 17
13	15.3	−11.4	−10.0	− 15	− 14	+ 3	− 6	− 17	+ 6
14	11.7	−11.2	− 2.5	+ 4	+ 15	− 30	− 12	+ 7	− 13
15	15.3	− 9.9	− 9.3	− 17	− 14	− 5	+ 4	− 19	+ 8
16	13.8	− 9.2	+ 3.3	− 5	+ 11	+ 12	+ 7	0	+ 18
17	15.3	− 9.0	− 5.6	+ 19	− 18	+ 12	− 4	− 3	+ 12
18	14.9	− 8.2	+ 9.2	− 11	− 2	− 11	− 33	− 9	− 14
19	13.9	− 8.2	+ 6.8	+ 4	+ 4	+ 13	+ 15	+ 1	+ 22
20	15.2	− 8.1	+ 3.6	− 2	+ 15	+ 7	+ 8	+ 3	+ 16
21	14.9	− 8.1	−13.0	+ 15	− 1	− 6	− 24	+ 4	− 7
22	13.9	− 7.9	+ 7.5	− 13	+ 9	+ 4	+ 8	− 5	+ 14
23	15.5	− 7.8	+ 0.7	− 19	− 6	− 19	− 5	− 15	+ 1
24	14.8	− 7.0	− 7.5	− 1	+ 15	+ 4	+ 1	+ 4	+ 10
25	13.8	− 7.0	+10.3	− 8	0	− 1	− 4	− 7	+ 6
26	13.5	− 6.4	0.0	− 7	+ 12	+ 4	+ 17	− 1	+ 18
27	14.9	− 6.3	−10.8	+ 2	+ 1	+ 23	+ 3	− 1	+ 21
28	13.6	− 6.3	+ 4.4	− 9	+ 3	+ 4	+ 4	− 6	+ 12
29	12.5	− 5.8	− 1.6	− 4	+ 12	+ 2	+ 7	+ 1	+ 12
30	14.7	− 5.5	− 9.5	− 36	− 3	− 24	− 27	− 23	− 18

31	14.7	− 5′.3	+ 8′.4	− 15	0	+ 3	+ 7	− 11	+ 6
32	14.9	− 4.5	−11.8	− 12	− 11	− 10	− 18	− 15	− 6
33	14.9	− 4.5	−10.1	+ 9	+ 12	+ 3	+ 13	+ 7	+ 16
34	14.5	− 4.0	+ 8.8	+ 4	− 11	− 8	0	− 7	+ 4
35	15.0	− 4.0	+12.2	+ 7	+ 12	− 6	+ 4	+ 7	+ 7
36	14.8	− 3.6	+ 7.9	− 7	− 15	− 20	− 8	− 14	− 6
37	14.8	− 3.2	−11.4	0	+ 2	0	− 24	− 2	− 4
38	15.2	− 2.9	− 1.4	....	+ 3	....	+ 13	0	+ 21
39	15.3	− 2.5	+ 2.5	− 4	− 4	+ 23	+ 6	− 7	+ 22
40	15.1	− 2.1	− 5.6	− 4	+ 16	− 40	− 9	+ 3	− 16
41	15.0	− 1.5	+12.3	− 2	+ 19	− 2	− 29	+ 5	− 8
42	15.2	− 1.4	− 4.4	− 3	− 12	− 10	+ 8	− 11	+ 7
43	11.3	− 1.1	− 5.8	− 42	− 33	+ 1	− 24	− 41	− 4
44	2.2	0.0	0.0	+ 69	+ 39	− 208	− 161	+ 51	− 176
45	12.1	+ 1.1	+ 1.6	+ 74	+ 77	− 27	− 19	+ 73	− 15
46	14.7	+ 3.2	+ 3.0	+ 7	0	− 6	− 2	+ 1	+ 4
47	14.9	+ 3.6	+ 1.6	− 5	− 20	+ 15	+ 3	− 15	+ 17
48	15.2	+ 3.6	+ 9.9	+ 6	+ 2	− 5	− 7	+ 1	+ 2
49	12.9	+ 3.7	− 2.5	− 27	....	− 60	....	− 30	− 52
50	15.4	+ 4.1	+ 7.9	+ 18	− 25	− 20	− 24	− 7	− 14
51	15.1	+ 4.2	−11.1	+ 8	− 6	+ 7	− 5	− 2	+ 9
52	15.2	+ 4.2	− 2.1	+ 5	− 16	+ 15	+ 10	− 9	+ 20
53	15.2	+ 4.2	+11.6	− 10	+ 8	− 8	− 24	− 4	− 8
54	14.7	+ 4.5	+ 6.8	+ 8	− 12	+ 6	− 2	− 5	+ 10
55	14.7	+ 4.8	+ 7.1	+ 32	+ 26	− 19	− 25	+ 26	− 14
56	13.5	+ 7.4	+ 2.1	+ 13	+ 12	− 8	− 23	+ 9	− 8
57	15.4	+ 8.1	+ 9.3	+ 16	+ 9	− 14	− 14	+ 9	− 6
58	13.1	+ 8.8	− 1.6	− 4	+ 18	− 14	− 8	+ 4	− 3
59	15.3	+ 8.8	− 2.5	− 3	+ 8	− 5	− 30	− 1	− 10
60	12.8	+ 9.5	+ 3.3	− 12	0	+ 11	+ 2	− 9	+ 14
61	14.2	+11.4	+ 1.1	− 7	− 1	− 11	− 2	− 7	+ 2
62	15.2	+12.6	+ 8.6	+ 102	+ 86	+ 29	− 2	+ 91	+ 22
63	14.5	+12.7	+ 2.2	− 3	0	+ 12	+ 16	− 5	+ 22
64	14.1	+13.3	+ 2.9	− 1	0	− 1	+ 3	− 3	+ 9
65	12.3	+13.4	0.0	+0″.053	−0″.110	−0″.075	−0″.006	−0″.031	−0″.032

The striking fact, however, is the rapid falling-off in the number of group-members with increasing magnitude. Table II gives for successive magnitudes the numbers and the percentages of group stars.

TABLE II

Magnitude	Total No. of Stars	Very Probable	Probable	Doubtful
4.0– 4.9......	3	2 or 67%	0 or 0%	0 or 0%
5.0– 5.9......	0	0 or 0	0 or 0	0 or 0
6.0– 6.9......	27	15 or 56	4 or 15	3 or 11
7.0– 7.9......	20	5 or 25	1 or 5	3 or 15
8.0– 8.9......	58	9 or 16	2 or 3	3 or 5
9.0– 9.9......	211	8 or 4	11 or 5	6 or 3
10.0–10.3......	76	3 or 4	1 or 1	1 or 1

As all stars on our plates, with the exception of α Tauri, are fainter than photographic magnitude 11.2, it is clear that only a few of them could well be members of the group.

We must therefore resort to other means of deriving the absolute motions. The following process was used. *Groningen Publications*, No. 14, contains twenty-six stars included in Boss's *Preliminary General Catalogue*. Correcting Boss's proper motions according to the remark on page xxviii of that catalogue and comparing them with the proper motions given in *Groningen*, No. 14, we find

$$\mu_\alpha \textit{ P.G.C.} - \mu_\alpha \textit{ Groningen} = +0''.025$$
$$\mu_\delta \textit{ P.G.C.} - \mu_\delta \textit{ Groningen} = -0''.004.$$

With the help of these differences we can reduce the proper motions in *Groningen*, No. 14, to the system of *P.G.C.* Finally *Groningen*, No. 14, and the present paper contain six stars in common, viz.,

Gron. 14,	Nos.	331,	333,	340,	341,	342,	355
vM	Nos.	14,	29,	43,	44,	45,	65, respectively.

Although the number of stars is hardly sufficient for a satisfactory reduction, it seemed best, at least for the present, to use this roundabout way. For one of the stars, No. 65, unfortunately the measures on the Mount Wilson plates are unreliable, as the images on Plate 2424 are in contact with the trail of α Tauri, which was added to the plate for the purpose of orientation. Omitting this star, we find

μ_α *Groningen* 14 (corrected to *P.G.C.*)$-\mu_\alpha$ vM$=-0\overset{''}{.}003$
μ_δ *Groningen* 14 (corrected to *P.G.C.*)$-\mu_\delta$ vM$=+0\overset{''}{.}008$.

Applying these corrections to the motions in the fifth, sixth, seventh, and eighth columns of Table I, we derive the values of the mean absolute μ_α and μ_δ, which are given in the ninth and tenth columns, respectively.

The probable error of a mean motion in right ascension is $0\overset{''}{.}0042$, in declination $0\overset{''}{.}0044$; the small probable error is an indication of the stability of the measuring machine. Since the measures of the region of α Tauri were made, series of measures with this machine have also been completed on the spiral nebulae M 51 and 81, corroborating the reliability of the new stereocomparator.

As stated above only two stars have proper motions which might indicate that they are members of the group, viz.,

No. 45 $\mu_\alpha=+0\overset{''}{.}073$ $\mu_\delta=-0.015$
No. 62 $\mu_\alpha=+0.091$ $\mu_\delta=+0.022$.

For the first star the motion given by Kapteyn and de Sitter and reduced to the *P.G.C.* system is

$$\mu_\alpha=+0\overset{''}{.}081 \qquad \mu_\delta=-0\overset{''}{.}022.$$

Comstock[1] gives for this star:

$$\mu_\alpha=+0\overset{''}{.}090 \qquad \mu_\delta=-0\overset{''}{.}039.^{2}$$

The star also appears in Burnham's *General Catalogue of Double Stars*, No. 2266, C.D.: Burnham assigns a common motion to the close double, viz., $\mu_\alpha=+0\overset{''}{.}087$, $\mu_\delta=-0\overset{''}{.}035$. All four values are in good agreement. Since on the system of the *P.G.C.* the Hyades cluster has the mean motions $\mu_\alpha=+0\overset{''}{.}115$, $\mu_\delta=-0\overset{''}{.}029$, it is very doubtful if either star No. 45 or No. 62 is a member of the cluster.

MOUNT WILSON OBSERVATORY
October 1921

---

[1] *Publications of the Washburn Observatory*, **12**, 216, 1908.

[2] In a recent note in the *Astronomical Journal*, **34**, 33, 1922, Comstock derives for this star:

$$\mu_\alpha=+0\overset{''}{.}100 \qquad \mu_\delta=-0\overset{''}{.}040.$$

Contributions from the Mount Wilson Observatory, No. 225
Reprinted from the *Astrophysical Journal*, Vol. LV, pp. 119–144, 1922

THE THEORY OF IONIZATION AND THE SUN-SPOT SPECTRUM

By HENRY NORRIS RUSSELL[1]

ABSTRACT

Saha's theory of temperature ionization, assuming the ionization to be due to temperature alone, leads to the relation: $Px^2/(1-x^2)=K$; that is, the ratio of the fraction of atoms ionized (x) to the fraction un-ionized ($1-x$), times the partial pressure of the free electrons [$Px/(1+x)$], is equal to K, a function only of the ionization voltage I and of the absolute temperature T, namely: $\log_{10} K=-5036\, I/T+2.5 \log_{10} T-6.5$. The theory is here *extended to mixtures of elements* by putting the partial pressure of the electrons equal to $Px/(1+\bar{x})$ where $\bar{x}$ is the fraction of ionization for all the atoms present, and P, as before, is the total pressure. Hence, $Px_1\, \bar{x}/(1-x_1)(1+\bar{x})=K_1$; $Px_2\, \bar{x}/(1-x_2)(1+\bar{x})=K_2$; etc.; and the ratio of $x_1/(1-x_1)$ to $x_2/(1-x_2)$ is merely K_1/K_2. Therefore the degree of ionization is always higher for an element of easy than for one of difficult ionization, and the relation between the two depends only on (I_2-I_1) and on T, and not on the pressure or on the relative concentrations. Saha's *formulae for second-stage ionization* are corrected. Only two successive stages of ionization can be present in any considerable proportions at the same time. Strong *evidence in favor of the theory* is afforded by a comparison of the sun-spot and the solar spectrum, since the predictions of the theory with reference to the relative intensity in the hotter and the cooler spectrum, of lines associated with ionized and un-ionized atoms, are found to be in general agreement with the facts. However, discrepancies such as the presence of too large a fraction of ionized Ba atoms, suggest the need of some modification of the theory; and it is evidently incomplete, since it neglects the effects of radiation on ionization.

Relative intensity in solar and sun-spot spectra of series lines.—The lines of the *alkali metals* (all of which are due to the neutral atoms) are *greatly strengthened* in the spot spectrum. Na ($I=5.11$ volts) exhibits its principal and subordinate series, K (4.32) the principal series alone, and Li (5.37) and Rb (4.16) the leading pair of the principal series, and only in the spot spectrum. The corresponding lines of Cs are out of reach in the infra-red.

Among the *alkaline earths* the lines of the *neutral atom* for Ca (6.08 volts) are strengthened in the spots to a degree which is greatest for the principal series and least for the combination series. The corresponding lines of Sr (5.67) are faint in the sun and much strengthened in spots. For Ba (5.12 volts) they are absent both in sun and spots. The *enhanced lines* arising from the ionized atoms (Ca+, Sr+, Ba+) are strong in both spectra.

For Mg (7.65 volts) the lines of the *neutral atom* are little affected, except that the fundamental line $1S-2p_2$ is stronger, while for Zn (9.4 volts) the arc lines are much weaker in the spot spectrum.

These results are all in agreement with Saha's theory. The lines of Li and Ba, however, are much weaker than the theory indicates.

Relative intensity of arc and enhanced lines.—It is pointed out that enhanced lines of easily ionized elements can be produced with less excitation than arc lines of difficultly ionized elements. This fact explains many apparent anomalies in astrophysical spectra.

Ionization potential of the elements as a function of atomic number.—Since from the relative behavior in sun, spot, and furnace spectra, of the lines of *Ca, Sc, Ti, V, Cr, Mn, Fe, Co, Ni, Cu, and Zn*, the elements as arranged in the order of their atomic numbers, are progressively more difficult to excite spectroscopically, the ionization

---

[1] Research Associate of the Mount Wilson Observatory.

potential probably increases regularly from 6 volts for Ca to 9.4 volts for Zn, and this result combined with other data suggests that, *in general*, the ionization potential is a periodic function of the atomic number.

Identification of certain solar lines.—Lines of Rb have been detected in the sun for the first time. Also several faint Na lines have been identified and Datta's identifications of Na and K lines have been partly confirmed, partly not.

Tables of the series lines of Li, Na, K, Rb, Cs, Ca, Sr, Ba, Mg, and Zn are given with intensities in sun and spot, and wave-lengths in international units to 0.01 A.

Dr. Megh Nad Saha, in an important series of papers,[1] has shown the great importance of the modern thermodynamic theory of ionization in astrophysical and spectroscopic researches. In particular, he makes certain predictions about the behavior of the lines of the alkali metals in the spectra of sun-spots. The present communication deals with certain points connected with the theory, especially when many kinds of atoms are present at the same time, and with the observational verification of the predictions, which has been complete.

I. THE THEORY OF IONIZATION WHEN ATOMS OF SEVERAL KINDS ARE PRESENT

The equation of the "reaction isobar" as given by Saha[2] in the case of the ionization of a gas consisting of atoms of but a single kind is

$$\log \frac{x^2}{1-x^2} P = \log K = -\frac{U}{4.571\, T} + 2.5 \log T - 6.5 \qquad (1)$$

where the logarithms are to the base 10, P is the pressure of the gas, x the fraction of all the atoms which are ionized, T the absolute temperature centigrade, and U the "heat of ionization" in calories per gram-molecule. For the gas in question, the latter is proportional to the ionization potential, I being 23,020 calories if I is one volt, so that we may also write

$$\frac{x^2}{1-x^2} = \frac{K}{P}, \qquad \log K = -\frac{5036\, I}{T} + 2.5 \log T - 6.5. \qquad (2)$$

---

[1] "Ionization in the Solar Atmosphere," *Philosophical Magazine*, **40**, 472, 1920; "Elements in the Sun," *ibid.*, **40**, 809, 1920; "On the Temperature Radiation of Gases," *ibid.*, **41**, 267, 1921; "On a Physical Theory of Stellar Spectra," *Proceedings of the Royal Society*, A, **99**, 135, 1921.

[2] *Philosophical Magazine*, **40**, 479, 1920.

If atoms of several different kinds, all capable of ionization, are present, the situation is somewhat more complicated. To use equation (1), introducing for P the value of the partial pressure of the vapor of each element separately, is inadmissible, since one of the products of the reaction—free electrons—is produced by all the ionizations. But if p' is the partial pressure of the ionized atoms of any sort, p that of the corresponding non-ionized atoms, and p'' that of the free electrons, we will always have

$$\frac{\mathrm{p}'\mathrm{p}''}{\mathrm{p}}=K \tag{3}$$

when K is given by (2).

If now atoms of several kinds are present in the relative numbers a_1, a_2, a_3 . . . . and the fractions x_1, x_2, x_3 . . . . of these are ionized, the whole number of atoms and free electrons present will be $a_1(1+x_1)+a_2(1+x_2)$ . . . . and the partial pressures for element 1 will be

$$\mathrm{p}_1'=\frac{a_1x_1}{\Sigma a+\Sigma ax}P \qquad \mathrm{p}_1=\frac{a_1(1-x_1)}{\Sigma a+\Sigma ax}P$$

(P being as before the whole pressure of the gas), while for the free electrons we will have

$$\mathrm{p}''=\frac{\Sigma ax}{\Sigma a+\Sigma ax}P=\frac{\bar{x}}{1+\bar{x}}P$$

where

$$\bar{x}=\frac{\Sigma ax}{\Sigma a}\,. \tag{4}$$

$\bar{x}$ is therefore the fraction of all the atoms present which are ionized, and may be regarded as a weighted mean of the values of x for the individual elements.

Equation (3) then becomes for the various elements

$$\frac{x_1}{1-x_1}\,\frac{\bar{x}}{1+\bar{x}}=\frac{K_1}{P}, \qquad \frac{x_2}{1-x_2}\,\frac{\bar{x}}{1+\bar{x}}=\frac{K_2}{P}, \quad . \ . \ . \ . \tag{5}$$

where K_1, K_2 are given by (2) with the ionization potentials for the elements concerned.

We then have

$$\frac{x_1}{1-x_1}=\frac{K_1}{K_2}\,\frac{x_2}{1-x_2}, \qquad \log\frac{K_1}{K_2}=5036\,\frac{I_2-I_1}{T} \tag{6}$$

or, expressed verbally: *The ratios of the number of ionized atoms to that of non-ionized atoms for any two elements in a gaseous mixture bear a fixed proportion to one another, which depends only on the temperature, and is independent of the pressure, the relative abundance of the two elements, or the presence of other elements.*

These latter conditions affect the amount of ionization, without modifying this proportion. The element of lower ionization potential is always the more highly ionized.

We may write (5) in the form

$$\frac{x_1^2}{1-x_1^2}=\frac{K_1}{P_1},$$

where

$$P_1=P\frac{\bar{x}}{x_1}\frac{1+x_1}{1+\bar{x}}. \qquad (7)$$

If $x_1>\bar{x}$, that is, if the element is more easily ionized than the average, P_1 will be less than P, and the percentage of ionization will be greater than it would be if this element alone were present, with the same total pressure. For elements ionized with more difficulty than the average, the reverse will be the case.

The ionization will in all cases be less than if this element were present alone with its actual partial pressure, for p'', in equation (3), will always be greater than the partial pressure p_1' of the electrons arising from the dissociation of this one component of the mixture.

When ionization is just beginning all the x's will be small, and we will have approximately

$$x_2=\frac{K_2}{K_1}x_1,\ \text{etc.} \qquad \bar{x}=\frac{x_1\Sigma aK}{K_1\Sigma a}$$

$$P_1=P\frac{\bar{x}}{x_1}=P\frac{a_1}{\Sigma a}\left(1+\frac{K_2a_2}{K_1a_1}+\frac{K_3a_3}{K_1a_1}+\dots\right).$$

The factor outside the parentheses is the partial pressure of constituent 1. It follows that at the beginning of ionization the constituent of lowest ionization potential behaves very nearly as if it alone were present at its actual partial pressure. For constituents more difficult of ionization the initial ionization is less, and may be very much smaller.

When the ionization of any element is nearly complete, we may set $x_1=1$ in (7) and find

$$P_1=P\frac{2\bar{x}}{1+\bar{x}}.$$

The effective pressure for this element is therefore nearly equal to the total pressure (unless a large proportion of atoms of more difficult ionization is present).

For an element of easy ionization the range of temperature or pressure within which both ionized and uncharged atoms will be present in sensible proportions is therefore extended by the presence of other constituents in the mixture.

For an element of difficult ionization, x_1 will be much less than $\bar{x}$ and P_1 greater than P, when ionization is beginning. The range within which both phases are present will in this case be reduced.

If we set

$$\frac{\bar{x}^2}{1-\bar{x}^2}=\frac{\bar{K}}{P}$$

we find easily

$$\bar{K}\frac{1-\bar{x}}{\bar{x}}=K_1\frac{1-x_1}{x_1}=K_2\frac{1-x_2}{x_2}\;\ldots\;=\frac{\Sigma aK(1-x)}{\Sigma ax}$$

$$\bar{K}=\frac{\Sigma aK(1-x)}{\Sigma a(1-x)}$$

so that $\bar{K}$ is the mean of the individual K's, weighted in proportion to the number of non-ionized atoms remaining. At low temperatures, the atoms of easy ionization, which have the largest values of K, will contribute most to this mean; but at high temperatures these will be ionized, and the atoms of difficult ionization will contribute most. The effective mean ionization potential, corresponding to the value of $\bar{K}$, will therefore increase with the temperature.

Successive ionization.—Consider now atoms of the same kind, which are susceptible of the loss of two successive electrons. Let the ionization potential for the removal of the first be I and the additional potential for the second be I'. If x is the proportion of singly-ionized and y of doubly-ionized atoms, that of free electrons will be $x+2y$, and we will have[1]

$$\left.\begin{aligned}\frac{x(x+2y)}{(1-x-y)(1+x+2y)}&=\frac{K}{P}\\ \frac{y(x+2y)}{x(1+x+2y)}&=\frac{K'}{P}\end{aligned}\right\}. \tag{8}$$

The first of these equations may be written

$$\frac{(x+y)^2}{1-(x+y)^2}=\frac{K}{P}\,\frac{(x^2+2xy+y^2)(1+x+2y)}{(x^2+2xy)(1+x+y)}>\frac{K}{P}$$

also

$$\frac{x^2}{1-x^2}=\frac{K}{P}\left(1-\frac{y(2-x+x^2+2xy)}{(1-x^2)(x+2y)}\right)<\frac{K}{P}$$

while the second may be written

$$\frac{y^2}{1-y^2}=\frac{K'}{P}\,\frac{x}{1-y}\,\frac{2y^2+xy+y}{2y^2+xy+2y+x}<\frac{K'}{P}\,.$$

It follows that the numbers of both neutral and singly-ionized atoms are less than they would be if the second ionization did not occur—the draft upon the singly-ionized atoms being partly made up by fresh ionization of neutral ones; but the number of doubly-ionized atoms is less than it would be if the second ionization was the only one which occurred.

Dividing the second of the equations (8) by the first we find

$$\frac{y(1-x-y)}{x^2}=\frac{K'}{K}. \tag{9}$$

Now

$$\log\frac{K'}{K}=-5036\frac{I'-I}{T}$$

and in all cases which have so far been investigated $I'-I$ is positive, and equal to at least five volts.

---

[1] These equations differ from Saha's (*Proceedings of the Royal Society*, A, **99**, 143, 1921) which contain x^2 and y^2 in the numerators; but the latter formula would appear to involve the inadvertent assumption that an atom can combine only with an electron previously liberated by another atom which happens to be in the same state of ionization.

Hence K'/K is usually a small quantity, and it is impossible for y and $1-x-y$ to be considerable at the same time; that is, there will not simultaneously be any noticeable proportion of atoms in all three states of ionization. When the temperature is high K'/K increases; but in this case x is small and the number of neutral atoms very small.

At low temperatures we may set $y=0$, when the ordinary equation for single ionization is obtained; at high temperatures we may set $x+y=1$ and have

$$\frac{y^2+y}{2-y^2-y}=\frac{K'}{P}.$$

One or the other of these formulae will always give a good first approximation, provided that a third electron is not lost.

In a mixed gas, containing other constituents, we will have

$$\frac{x\bar{x}}{(1-x-y)(1+\bar{x})}=\frac{K}{P}; \quad \frac{y\bar{x}}{x(1+\bar{x})}=\frac{K'}{P}; \quad \bar{x}=\frac{\Sigma a(x+2y)}{\Sigma a}. \tag{10}$$

Since the potential for the second ionization is always high, the presence of other elements will in general diminish its amount; but equation (9) will hold in all cases.

Instead of equation (6) we will have

$$\frac{x}{1-x-y}=\frac{K}{K_2}\frac{x_2}{1-x_2} \qquad \frac{y}{x}=\frac{K'}{K_2}\frac{x_2}{1-x_2} \tag{11}$$

where x_2 is the percentage of ionization for any singly ionized element.

2. THE ALKALIES AND ALKALINE EARTHS IN THE SUN-SPOT SPECTRUM

Saha has shown[1] that sodium should be considerably ionized in the reversing layer, potassium almost completely, and rubidium and caesium entirely. As the familiar lines of these elements are absorbed by the neutral atoms only, the faintness of the lines of potassium in the solar spectrum and the absence of those of rubidium and caesium is immediately explained. At the lower temperatures which prevail in the spots he predicts that the lines of potassium should be strengthened, and that those of rubidium should show faintly.

---

[1] *Philosophical Magazine*, 40, 812–815, 1920.

Observations upon the behavior of sodium in sun-spots have been published by Adams[1] and the presence of lithium has been determined by King.[2] The study of the other alkali metals, which have their lines principally in the red, has been made very easy by the publication of extensive and accurate tables of wave-lengths in the red and infra-red, both in the solar spectrum[3] and in the arc,[4] and by the existence at Mount Wilson of an excellent series of plates of the spot spectrum, extending to λ 8200, taken by Mr. Brackett with the 150-foot tower telescope and 75-foot spectrograph, in the first order, with nicol prism and compound quarter-wave plate. All the available lines of the alkali metals were examined on these plates (or on the photographic map of the spot spectrum for the wave-lengths less than 6600 A) and some additions to the data for sodium and lithium were made.

The results, including those of the earlier observers, are given in Table I. In this table the first column gives the element and series designation of the line (after Sommerfeld). The leading pair of the principal series is denoted by 1s–2p, the next pair by 1s–3p, and so on. The corresponding pairs for the diffuse series are 2p–3d, 2p–4d, and for the sharp series 2p–3s, etc. Lines lying too far in the infra-red to be observed, or too far in the ultra-violet to be observable in spots, are in general omitted, as are also the fainter members of a series when the stronger earlier members are invisible.

The second column gives the wave-lengths found in the laboratory by Datta or by Meggers (or, in one or two cases, by others); and the third, the wave-length of the corresponding solar line derived from Rowland's tables, from Meggers, or from measurements made at Mount Wilson. All wave-lengths are given in

---

[1] *Mt. Wilson Contr.*, No. 40; *Astrophysical Journal*, **30**, 108, 1909.

[2] *Mt. Wilson Contr.*, No. 122; *Astrophysical Journal*, **44**, 169, 1916.

[3] W. F. Meggers, "Solar and Terrestrial Absorption in the Sun's Spectrum from 6500 A to 9000 A," *Publications of the Allegheny Observatory*, **6**, 12–44, 1919.

[4] W. F. Meggers, "Wave-Length Measurements in Spectra from 5600 A to 9600 A," *Bulletin of the Bureau of Standards*, **14**, 371–397, 1916; S. Datta, "The Vacuum Arc Spectra of Sodium and Potassium," *Proceedings of the Royal Society*, A, **99**, 69–78, 1921.

TABLE I

Lines of the Alkali Metals

Element	Wave-Lengths		Intensity		Authority	Notes
	Arc	Sun	Sun	Spot		
Lithium						
1s–2p.........	6707.82	07.83	abs	5	King	1
2p–2s.........	8126.52	....	abs	abs	Russell	
2p–3d.........	6103.53	....	abs	abs	King	
Sodium						
1s–2p.........	5895.94	95.94	20	60	Adams	
	5889.97	89.97	30	90	Adams	
2p–3d.........	8194.82	94.84	2	7	Russell	
	8183.30	83.27	3	10	Russell	
2p–4d.........	5688.22	88.22	6	12	Adams	
	5682.67	82.65	5	12	Adams	
2p–5d.........	4982.86	82.82	2	4	Russell	2
	4978.61	78.56	0	1	Russell	3
2p–6d.........	4668.60	68.57	1*N*	3	Russell	4
	4664.86	....	....	....	Russell	5
2p–7d.........	4497.72	97.73	abs	0	Wilson	6
	4494.27	....	abs	abs	Russell	7
2p–4s.........	6160.72	60.75	3	8	Adams	
	6154.21	54.23	2	9	Adams	
2p–5s.........	5153.85	....	abs	abs	Russell	8
	5149.27	....	abs	abs	Russell	9
2p–6s.........	4751.89	51.83	00	2	Adams	
	4748.02	47.98	000	0	Adams	
Potassium						
1s–2p.........	7699.00	99.01	5	13	Russell	
	7664.92	64.92	6	15	Russell	10
1s–3p.........	4047.20	47.19	00*Nd*	0	Russell	11
	4044.14	44.14	0	2	Russell	
2p–4d.........	6965.0	....	abs	abs	Russell	12
	6936.0	....	abs	abs	Russell	
2p–5d.........	5832.31	....	abs	abs	Russell	
	5812.71	....	abs	abs	Russell	
2p–4s.........	6939.50	....	abs	abs	Russell	13
	6911.80	....	abs	abs	Russell	
2p–5s.........	5802.16	....	abs	abs	Russell	
	5782.77	....	abs	abs	Russell	

TABLE I—*Continued*

Element	Wave-Lengths In		Intensity In		Authority	Notes
	Arc	Sun	Sun	Spot		
Rubidium						
1s–2p.........	7947.64	47.63	abs	0	Russell	14
	7800.29	00.29	abs	1	Russell	
1s–3p.........	4215.57	....	abs	abs	Russell	
	4199.85	....	abs	abs	Russell	
2p–4d.........	7757.80	....	abs	abs	Russell	
	7619.12	....	abs	abs	Russell	
Caesium						
1s–2p.........	8943.46	....	abs	Unknown	....	15
	8521.12	....	abs	Unknown	....	
1s–3p.........	4593.22	....	abs	abs	Russell	
	4555.31	....	abs	abs	Russell	
	8079.4	....	abs	abs	Russell	16
	8016.2	....	abs	abs	Russell	

NOTES TO TABLE I

1. Much widened in the spot, and showing strong Zeeman effect.

2. Rowland's line 4982.994, for which he gives no origin. Identified by Datta.

3. Rowland 4978.732. Shows, like the last, a conspicuous Zeeman effect. Clearly separated from the iron line 4978.785 which is erroneously identified by Datta as the sodium line.

4. Rowland 4668.749. Shows Zeeman effect. Identified by Datta.

5. Masked by the chromium line 4664.965 (Rowland).

6. A faint line, visible only in the spot, and showing conspicuous Zeeman effect. Measured by Wilson (unpublished) 4497.900 on Rowland's scale. Datta identifies this with Rowland 4497.842, a titanium line which is clearly separated.

7. Datta identifies this with Rowland 4494.356 (00) which is not strengthened in the spot, and is probably not the sodium line. No trace of the latter could be seen. The character of the foregoing lines, and their strong intensification in the spots, support their identification as sodium lines. It is very difficult to get these lines sharp in the laboratory, and Datta's measures, though much superior to earlier ones, demanded long exposures.

8. Datta identifies as Rowland 5153.848 (000). This is a band line showing no Zeeman effect.

9. Datta identifies as 5149.267 (000) Rowland C. This is very little strengthened in the spot and shows no Zeeman effect. No trace of the sodium lines could be found in this vicinity.

10. Practically coincident with a strong atmospheric line in the tail of the A band, but identified by Meggers by means of the sun's rotation. The intensification of this line in the spot spectrum and the Zeeman effect are conspicuous in spite of this blending, which has been allowed for in the estimates of intensity.

11. Identification by Rowland and Datta confirmed.

12. Wave-lengths from Saunders. These lines are abnormally faint in the arc spectrum. Datta identifies as Rowland 6965.320 (000 N) which shows no Zeeman effect and 6926.290 (0000) which is invisible both in sun and spot on the Mount Wilson plates.

13. Identified by Datta as 5832.490 (000) and 5812.942 (0000). These lines are too faint to be visible on the Mount Wilson plates, either in sun or spot.

14 Typical spot lines, diffuse and showing strong Zeeman effect, and greatly resembling the lithium line at λ 6708. Measured by the writer, the first on one plate, the second on two. Probable error of measurement about ±0.01 A. One of the Zeeman components of 7947.63 is clearly separated from the atmospheric line at 7947.766 (Meggers). The other is blended with it.

15. These lines, which are the first pair of the principal series, lie beyond the limits of the region so far photographed at Mount Wilson, and attempts to secure plates showing the spot spectrum in this region have not yet been successful. They are not present in the solar spectrum (Meggers). The absence of the second pair of this series might have been anticipated.

16. This relatively narrow pair is strong in the arc, but does not belong to the known series. There are no strong lines of the subordinate series of caesium in favorable positions for investigation.

International units and Rowland's values have been reduced to this standard with the aid of a correction-curve which was kindly furnished by St. John.

The fourth and fifth columns give the intensity of the lines in sun and spot. The values in the former are taken from Rowland or Meggers; the latter, for the lines previously observed, from Adams or King. For lines newly observed, estimates have been made on the original plates, as nearly as possible upon the same scale as that used by Rowland or Meggers. Cases in which a line is certainly invisible are denoted by "abs." The sixth column gives the authority for the data concerning the spot spectrum (including measures of wave-length when the line does not appear in the spectrum of the photosphere), and the last provides references to the notes which follow.

These results may be summarized as follows:

Sodium is represented in the sun by the principal, diffuse, and sharp series, and all its lines are much strengthened in the spot spectrum. Some of Datta's identifications of faint lines have been confirmed and others modified. The absence of the pair λλ 5153, 5149 in both sun and spot is remarkable, since the following and fainter pair of the series appears to be present.

Potassium is represented by the principal series only. Its lines are greatly strengthened in the spots. Datta's identifications of faint solar lines as belonging to the subordinate series of this element are not confirmed.

Lithium shows in the spot spectrum alone, and only through the leading line of the principal series.

Rubidium, previously undetected in the sun, is definitely proved to be present by the appearance of both members of the leading pair of the principal series in the spot spectrum.

The corresponding lines of caesium lie far in the infra-red, and satisfactory photographs of the spot spectrum have not yet been obtained in this region.

The alkaline earths (for which the ionization potentials are likewise known) are of special interest, because the fundamental members 1s–2p, of the series of enhanced lines, absorbed by the ionized atoms, lie within the accessible portion of the solar spectrum

TABLE II

Lines of Alkaline Earths in Sun-Spots

Elements	Wave-Length	Intensity in		Notes
		Sun	Spot	
Mg				
1S–2P	2852.13	....	....	Out of reach
1S–2P$_2$	4571.11	5	7	1
2P–4D	5528.47	8	8	1
2P–5D	4703.07	10	10	1
2P–6D	4351.94	5	4	1
2P–4S	5711.13	6	6	1
2p–3s	5183.62	30	30	1
	5172.68	20	22	1
	5167.33	15	17	1
2p–4d	3838.28	25	....	
	3832.31	15	....	7
	3829.36	10	....	
Mg+				
1s–2p	2802.70	....	....	Out of reach
	2795.52	....	....	
Ca				
1S–2P	4226.73	20	25	2
1S–2p$_2$	6572.78	1	10	3
2P–3D	7326.10	2	5	4
2P–4D	5188.85	3	4	4
2P–4S	5512.98	4	5	4
2P–5S	4847.29	0	1	4
3D–4F	4878.13	3	3	4
3D–2P	6717.19	5	8	4
2p–4d	4556.61	2	4	2
	4555.88	3	5	2
	4554.77	5	7	2
	4535.67	4	6	2
	4534.95	5	7	2
	4525.43	4	6	2
2p–2s	6162.18	15	25	2
	6122.22	10	20	2
	6102.72	9	20	2
3d–4f	4585.92 4585.87 }	4	6	4
		....	....	
	4581.41	4	6	4
	4578.57	3	6	4
Ca+				
1s–2p	3968.08	700	700	3
	3933.68	1000	1000	3
2p–3d	8662.42	15	....	
	8542.48	16	....	
	8498.32	12	....	
2p–2s	3736.92	5	....	7
	3706.03	6	....	7
Sr				
1S–2P	4607.35	1	3	4
1S–2p$_2$	6892.36	abs	abs	4
2p–3s	7070.7	abs	abs	4
	6878.8	abs	abs	4
	6791.4	abs	abs	4

TABLE II—*Continued*

Elements	Wave-Length	Intensity in		Notes
		Sun	Spot	
Sr				
2p–4d	4971.68	abs	abs	4
	4967.94	…………	…………	5
	4962.28	000	00	4
	4876.06	abs	abs	4
	4872.49	abs	000	4
	4852.06	abs	abs	4
Sr+				
1s–2p	4215.50	8	8	2
	4077.73	5	5	2
2p–4d	10915.0	…………	…………	
	10328.3	…………	…………	Out of reach
	10038.7	…………	…………	Out of reach
2p–2s	4305.44	(3)	(5)	5
	4161.79	1	00	2
Ba				
1S–2P	5535.53	abs	abs	6
1S–$2p_2$	7911.36	abs	abs	4
Ba+				
1s–2p	4934.07	7	7	4
	4554.04	8	10	4
2p–4d	4166.01	0	0	4
	4130.65	2	2	4
	3891.83	…………	…………	5
2p–2s	4899.97	(2)	(2)	5
	4524.95	0	0	4
Zn				
1S–2P	2139.33	…………	…………	Out of reach
1S–$2p_2$	3075.90	1	…………	7, 8
2P–3D	6362.35	1	0	9
2p–2s	4810.54	3	0	4
	4722.16	3	0	4
	4680.14	1	00	4
2p–4d	3346.02	0	…………	7
	3345.58	1	…………	7
	3345.12	2	…………	7
	3303.37	…………	…………	5
	3303.59	1	…………	7
	3282.33	…………	…………	5

NOTES

1. Adams, *Mt. Wilson Contr.*, No. 40, p. 20; *Astrophysical Journal*, **30**, 105, 1909.
2. Adams, *Mt. Wilson Contr.*, No. 22; *Astrophysical Journal*, **27**, 45–55, 1908.
3. Adams, *Mt. Wilson Contr.*, No. 40, p. 7; *Astrophysical Journal*, **30**, 93, 1909.
4. From examination of the map of the sun-spot spectrum or of original plates for wave-lengths greater than 6600. Many of these lines have previously been studied at Mount Wilson, but they have been re-examined because the later plates are probably better.
5. Masked by other lines.
6. This line (according to the accurate measures of Schultz (*Zeit. für Wiss. Phot.*, **11**, 209, 1912) lies at 5535.755 on Rowland's scale, and falls in a very confused region between the iron line 5535.644 (intensity 2) and the line 5535.778 (intensity 0), for which Rowland gives no origin. Between these two there is a faint line which is confined to the spot, in which it is of intensity 0 and shows Zeeman effect. It was measured and found to be at 5535.703. There is also a faint band line close by showing no Zeeman effect, but nothing which can be identified as the barium line. It is either absent, or masked by 5535.778.
7. Too far to the violet to show changes in the spot spectrum.
8. Rowland's line 3076.002, for which he gives no origin. Kayser and Runge find 3075.99 in the arc; Exner and Haschek, 3076.02.
9. But little weakened in the photographic map. Weakening confirmed on an original negative. Zeeman effect stronger over penumbra of spot than over umbra. May be blended with a band line. These are numerous in this region.

(except for magnesium) which is not known to be the case for any other elements. They are also noteworthy for possessing two radiation potentials, corresponding to the shift of an electron from its normal position in the neutral atom to the position corresponding to the limits of the subordinate series of single lines and of triplets.

These lines afford the most delicate tests for the presence of the ionized or neutral atoms of these elements. Their behavior in spots is indicated in Table II. Various other lines of these elements and the observable lines of zinc are included.

This table exhibits the well-known fact that the strongest lines of the alkaline earths (except magnesium) are enhanced lines.

The series of calcium and magnesium, both of triplets and of single lines, are conspicuous in the solar spectrum, and only some of the more prominent lines are given in the table. The calcium lines are considerably strengthened in the spot spectrum; those of magnesium are not, with one exception.

In the case of strontium, only the strongest lines of the neutral atom appear in the sun; these are very faint, but are intensified in spots, while not one of the strong low-temperature lines of barium appears either in the sun or the spots. This has been confirmed by examining a number of those which did not belong to known series and are therefore not given in the table.

3. APPLICATION OF THE THEORY OF IONIZATION TO THESE DATA

The ionization potentials of a number of elements of astrophysical importance are as follows:

	Volts		Volts		Volts
Caesium	3.81	Barium	5.12	Ba+	9.86
Rubidium	4.16	Strontium	5.67	Sr+	10.70
Potassium	4.32	Calcium	6.08	Ca+	11.86
Sodium	5.11	Magnesium	7.65	Mg+	15.02
Lithium	5.37	Zinc	9.4	Zn+	18.20
Hydrogen	13.54	Helium	25.2	He+	53.4

The last column gives the potentials corresponding to the additional energy required to remove a second electron after the first is already gone.

We may now proceed to calculate the percentages of the atoms of various elements which are neutral, singly-ionized, and doubly-ionized, in a gaseous mixture at the temperature of the reversing layer and of a sun-spot—which we will take in round numbers as 6000° and 4000° respectively—and at various pressures.

Since the pressure in the solar atmosphere is unknown within very wide limits (except that it is probably small) we may save trouble by computing for assigned values of the "effective pressure" P_1, for sodium, using equations (2) and (7). The difference between the effective pressure and the true pressure will be much less than the range of uncertainty of the latter. We may then find the percentages of ionization of other elements by (5) or (11).

The results are given in Table III. Neutral atoms are denoted as usual by Ca; singly-ionized, by Ca+; and doubly-ionized, by Ca++ (taking calcium as an example). The percentage of atoms in the highest stage of ionization for each element is not given, except for hydrogen, since it can easily be found by subtracting the sum of the others from 100, and also because atoms of the elements given in the table, when in these states, absorb no known lines in the visible spectrum.

It should be remembered that the equations from which these tables have been calculated are based upon certain assumptions, as yet unverified, namely, that the chemical constant for the electron may be derived by an extrapolation of the Sackur-Tetrode relation (which gives this constant as a function of the atomic weight of an element) to the electron, considered as having an atomic weight of 0.00055, and also that the chemical constant is the same for the neutral and ionized atoms of any element.[1] An error in the former assumption could be corrected by multiplying all the tabular pressures by a constant factor; one in the second, by multiplying the pressure for each element by an appropriate factor before entering the table.

What is more important, the tabular numbers depend on the assumption that temperature alone is effective in producing ionization. This is certainly not the case in the solar atmosphere, where the absorption of radiation, though it does not completely ionize the absorbing atoms, must undoubtedly get them into a state in which ionization by some other stimulus becomes easier.[1] This should operate to increase the ionization in the reversing layer to a considerable degree.

---

[1] See Saha, *Philosophical Magazine*, **40**, 479, 1920.

TABLE III

PERCENTAGES OF NEUTRAL AND IONIZED ATOMS

ELEMENT	P IN ATMOSPHERES						
	1	10^{-1}	10^{-2}	10^{-3}	10^{-4}	10^{-5}	10^{-6}
	Reversing Layer—Temperature 6000° C.						
Cs......	22.6	6.1	0.87	0.09	0.01	0.001	0.0001
Rb......	37.2	12.3	1.7	0.18	0.02	0.002	0.0002
K.......	44.7	14.8	2.2	0.19	0.02	0.002	0.0002
Na......	79.3	44.4	9.6	1.1	0.11	0.011	0.0011
Li.......	86.1	57.0	15.0	1.9	0.19	0.019	0.002
Ba......	79.1	45.0	9.7	1.1	0.10	0.005	0.0001
Ba+....	20.9	55.0	90.2	98.0	91.3	48.3	9.6
Sr.......	91.7	70.2	23.8	3.2	0.3	0.03	0.001
Sr+.....	8.3	29.8	76.2	96.4	97.9	84.6	35.8
Ca......	96.1	84.0	41.0	6.8	0.7	0.07	0.007
Ca+....	3.9	16.0	59.0	93.2	99.1	98.0	83.6
Mg......	99.8	99.1	93.5	60.4	13.2	1.5	0.15
Mg+....	0.2	0.9	6.5	39.6	86.8	98.5	99.8
Zn......	99.99	99.96	99.7	96.9	75.6	23.7	3.1
Zn+....	0.01	0.04	0.3	3.1	24.4	76.3	96.9
H+.....	2×10^{-6}	1×10^{-5}	8×10^{-5}	8×10^{-4}	0.008	0.08	0.76
	Sun-Spot—Temperature 4000° C.						
Cs......	54.9	27.0	9.3	2.2	0.30	0.032	0.003
Rb......	77.0	50.0	21.9	5.7	0.83	0.089	0.009
K.......	84.2	61.5	30.9	8.8	1.3	0.14	0.014
Na......	98.1	94.1	81.5	48.9	11.6	1.37	0.14
Li.......	99.2	97.1	90.3	66.9	21.8	2.95	0.29
Ba......	98.2	94.1	81.8	49.5	11.8	1.42	0.14
Ba+....	1.8	5.9	18.2	50.5	88.2	98.58	99.86
Sr.......	99.63	98.76	95.8	82.9	40.0	6.6	0.72
Sr+.....	0.37	1.24	4.2	17.1	60.0	93.4	99.28
Ca......	99.89	99.62	98.7	94.1	68.5	18.7	2.3
Ca+....	0.11	0.38	1.3	5.9	31.5	81.3	97.7
Mg.....	99.999	99.996	99.975	99.93	99.52	95.6	69.0
Mg+....	0.001	0.004	0.025	0.07	0.48	4.4	31.0
Zn......	100.00	100.00	100.00	100.00	99.995	99.95	99.51
Zn+....	1.3×10^{-5}	4.3×10^{-5}	1.6×10^{-4}	7.2×10^{-4}	0.005	0.05	0.49
H.+....	4.7×10^{-11}	1.6×10^{-10}	5.7×10^{-10}	2.6×10^{-9}	1.9×10^{-8}	1.8×10^{-7}	1.8×10^{-6}

In applying these results to the interpretation of the spot spectrum, it is probably safe to work on the assumption that the

[1] The existence of such an effect for iodine has been experimentally proved by Smythe and Compton (*Physical Review*, 16, 501, 1920). Its importance in the solar atmosphere was suggested to the writer, in conversation, by Dr. Lindblad.

more abundant elements in the solar atmosphere are present in amounts much greater than is necessary to produce strong lines and that, for the principal lines of these elements (at least) the absorption is substantially "saturated" so that a considerable change in the amount of element would produce little change in these lines, except in the strength of the wings. It is also important to remember that, according to modern theory, the atoms of a given element, in their normal state, are ready to absorb certain fundamental lines (those of the principal series, denoted by 1s–2p, etc., above) while, in order that they may absorb other lines (such as those of the subordinate series) they must first have absorbed energy enough to shift the electrons within them to some other definite state, less stable than the normal one. Saha, who has discussed this matter in detail, states that the relative numbers of atoms which are in condition to absorb lines of these various groups probably depend upon the temperature alone—high temperature favoring the absorption of the subordinate lines. It is obvious that "high" temperature must here be a relative term, the scale for any element being roughly proportional to the temperature at which ionization becomes large.

The main features of the behavior of the lines of the alkali metals in spots, as Saha has shown, may be accounted for by the relative ease of ionization, sodium being considerably ionized, potassium still more, and rubidium completely so, except in spots. But the fact that lithium, like rubidium, appears only in the spots, cannot be explained on the basis of ionization potentials alone, for it is harder to ionize than sodium, and the percentage of neutral atoms should be greater.

A solution may be found in the probable difference in the relative abundance of the elements. Sodium and potassium are among the most abundant of terrestrial metals, being present in the earth's crust in nearly equal amount (each about 2 per cent of the whole). Lithium is relatively rare on the earth, and, if the proportion present in the solar atmosphere is sufficiently small, it may well be that the number of neutral atoms which remain is insufficient to produce perceptible absorption lines, except in the spots, where the ionization is less. Among the far more numerous sodium atoms the number which escape ionization, though a smaller percentage of the whole, is so great that there are enough of them in a condition to absorb the subordinate series fairly strongly, and the principal series heavily. In potassium the percentage of neutral atoms is much less, and only the lines of the principal series appear, with moderate intensity, but much strengthened in the spots.

It remains somewhat puzzling, however, why rubidium, which is much easier to ionize than lithium, should show nearly the same behavior in the spot spectrum. According to Table III the percentage of neutral rubidium atoms should be less than one-tenth as great as in the case of lithium. The increase in this percentage in spots is great enough for both elements to account for the appearance of their lines there, and not on the disk, provided that we assume that the pressure in the region where the lines are absorbed is 0.01 atmospheres or less (which seems reasonable). But it is hard to see why the rubidium lines should appear at all, unless it is considerably more abundant in the sun than lithium is, which does not at all seem to be the situation on the earth.

Passing to the alkaline earths we find improved opportunities. While the ionized atoms of the alkali metals give no recognized lines in the visible spectrum, those of calcium and its congeners are unique in that the fundamental lines of the ionized atom lie within the region accessible to astrophysics. The great importance of these lines (H and K of calcium and λλ 4078, 4215 of strontium) is thus explained. They enable us to detect the ionization of these easily ionized atoms as soon as it occurs. The ionized atom of calcium is at once capable of absorbing the H and K lines.

From Table III it appears that, under the pressures which probably prevail in the reversing layer, the greater part of the calcium is in the singly-ionized condition.

H and K, therefore, are the lines which the atoms of one of the most abundant constituents of the solar atmosphere absorb most powerfully, when in that state in which under solar conditions they are most likely to occur. There are no other lines in the visible spectrum, so far as known, for which these three maximal conditions are all satisfied.

It is not surprising, therefore, that they are exceptionally conspicuous, and that few other lines play so important a part throughout almost the whole of the sequence of stellar spectra. A great deal of the calcium must be ionized, even in the spots, and this, coupled with the fact that the absorption in the H and K lines is probably far more than saturated, makes it easy to understand why these lines are not perceptibly weakened in the spots. The same remark applies, with even greater force, to the corresponding enhanced lines of strontium and barium.

Magnesium should also be considerably ionized in the reversing layer; but the only line by which we can detect the presence of ionized magnesium (λ 4481) is absorbed only by atoms which have undergone two internal changes subsequent to ionization, corresponding to the shifting of an electron from its normal position to the states denoted symbolically by 2p and 3d, and demanding the absorption of large amounts of energy. The temperature of the reversing layer, compared with that at which a considerable percentage of these Mg+ atoms would lose a second electron, is undoubtedly low. Hence very few such atoms indeed should be in a state to absorb λ 4481, and it is not surprising that it is excessively faint in the solar spectrum, if it appears at all, or that it becomes conspicuous only in the hotter stars.

If the earth's atmosphere transmitted light of short enough wave-length, we would probably find that the fundamental pair of enhanced magnesium lines near λ 2800 were rivals of H and K in intensity and astrophysical importance.

The very strong infra-red lines of calcium at λλ 8498, 8542, 8662, belong to the diffuse series and represent a stage of excitation intermediate between H and K and λ 4481. King[1] has found that they cannot be produced in the furnace, at temperatures at which H and K appear strongly. It may safely be predicted that they are weakened in the spot spectrum, and the matter will be investigated when suitable photographs can be obtained. The corresponding group for strontium is hopelessly far in the infra-red; but the leading pair of the sharp series of enhanced lines is accessible. One line is concealed by a blend; the other is greatly weakened in spots.

---

[1] *Mt. Wilson Contr.*, No. 150; *Astrophysical Journal*, 48, 13, 1918.

For barium, which is easier to ionize a second time, the enhanced lines of the diffuse series are not perceptibly weakened in spots.

The behavior of the lines due to the neutral atoms is also in accordance with this theory. Beginning with zinc, which has the highest ionization potential, we find that the prominent triplet in the blue is greatly weakened in spots, and the line in the red is also weakened, though to a less degree. These lines belong to the sharp series of triplets and the diffuse series of single lines, both of which are absorbed by atoms in which the electron has been shifted one step from its normal position (to 2p or 2P). Measured by a scale appropriate to the zinc atom, the temperature of the photosphere must be low and that of the spots very low; hence the weakening of these subordinate lines is just what should be expected.

It is of interest to note that the lines of hydrogen, which also belong to a subordinate series and to an element for which the ionization potential is high, are much weakened in the spot spectrum.[1]

The lines of magnesium are very little affected in spots. In this case the effects of higher excitation and greater ionization at the higher temperature of the reversing layer appear very nearly to balance one another except in the case of λ 4571, which is a characteristic low-temperature line, and is the easiest of all magnesium lines to excite in the laboratory.[2] This line, as might be expected, is strengthened in the spots, but only to a moderate degree.

For calcium, all the important lines of the neutral atom are strengthened in spots, indicating that the controlling factor is the diminution of ionization at the lower temperature, which increases the number of neutral atoms. Where allowance is made for the general increase toward the red of the degree to which lines are affected in spots, it appears that the strengthening is greatest for the lines absorbed by atoms in which the electron is in the normal state, 1S; less for those of the subordinate series, in which the electron starts from the state 2P (for single lines) or 2p (for triplets); and least of all for those of the Bergmann or combination series in which it starts from 3D or 3d. According to Saha[1] the ratio of the number of atoms which are in any one of these states to the number which are in the preceding stage should increase with the temperature. Hence the effect of the diminished number of neutral atoms in the hotter regions is almost neutralized for the lines of the "outer" series (3D–4F and 3D–2P) and increased for the fundamental lines (1S–2P), and 1S–2p.[2] The first of these, λ 4227, is so far to the violet that the effect in spots is not conspicuous, though great for a line in this region. This is very prominent in the cooler stars. The second, λ 6573, is one of the most remarkable of all sun-spot lines. It is an exact analogue of λ 4571 of magnesium, which likewise shows the greatest strengthening of any line of the element to which it belongs.

---

[1] Adams, *Mt. Wilson Contr.*, No. 40, p. 10; *Astrophysical Journal*, **30**, 95, 1909.

[2] Foote and Mohler, *Philosophical Magazine*, **37**, 40, 1919.

For strontium, the ionization is still greater, and the amount of the element present in the solar atmosphere probably much less, if we may judge by the earth's crust, in which strontium and barium are much rarer than calcium and magnesium. It is not surprising, therefore, that only the strongest lines of the neutral atom appear in the solar spectrum, or that these should be strengthened in the spots, especially the fundamental line λ 4607. λ 6892, which is analogous to λ 6573 of calcium, is absent even in the spot spectrum.

The probable reason for this is that the temperature, even in the spots, is high on the scale which it is necessary to use for the neutral strontium atom, and that, under this high excitation, the proportion of atoms in which the electron undergoes the corresponding change is small.

For barium the final stage appears to have been reached. The lines of the neutral atom do not appear at all either in the spectrum of the sun or of the spots. Even the fundamental line 1S–2P (λ 5535) is gone. This can be explained only on the assumption that barium is completely ionized in the sun, leaving not a trace of the neutral atoms, for the element is abundant enough, as is shown by the strength of its enhanced lines.

---

[1] *Proceedings of the Royal Society*, A, **99**, 142, 1921.

From the qualitative standpoint this explanation is quite satisfactory, but a quantitative study brings out difficulties. The ionization potentials for sodium and barium, as determined from their spectral series, should be practically identical. Hence, by the theory developed above, the atoms of both should be ionized to the same degree. But the direct spectroscopic evidence indicates that barium is ionized to a much greater extent than sodium. The absence of the flame lines even in spots, and the fact that the enhanced lines of the diffuse series are not sensibly weakened, would indicate a decidedly lower ionization potential both for Ba and Ba+.

A similar discrepancy, though less marked, exists in the case of strontium.

As the theory of the subject is still in an early stage of development, these facts may be taken as the results of an experiment performed by nature upon a grand scale, which may be used in improving our theories; but speculation as to the exact form of this improvement would at present be premature.

4. GENERAL COMMENTS

The data detailed above cover all the cases in which elements, for which the ionization potentials and spectral series are known, possess lines of any notable strength within the region in which the sun-spot spectrum can be satisfactorily investigated. It is evident that they are all in striking agreement with Dr. Saha's theory of ionization and that they confirm it in a very conclusive fashion, both in the matters in regard to which he has made predictions, and in various others which are here discussed for the first time.

There are many other elements whose lines show conspicuous changes in the spots; but no data are at present available regarding the ionization potentials. Most of these elements have spectra rich in lines, for which the series relations are known very incompletely or not at all.

The behavior of these lines in the spot spectrum,[1] coupled with that in the furnace, arc, and spark, makes it possible to arrange them in a decidedly definite order.

[1] Adams, *Mt. Wilson Contr.*, No. 40, pp. 6–26; *Astrophysical Journal*, **30**, 91–111, 1909.

A few of the elements already discussed are added for comparison. Lines which are relatively strong at the lowest temperatures (King's Class I) are called flame lines for brevity.

Calcium.—All lines strong in sun. Flame lines much strengthened in spots. Arc lines considerably strengthened in spots. Enhanced lines produced at medium temperature in furnace,[2] very strong in arc, and not weakened in spots.

Scandium.[1]—Flame lines very faint or absent in sun, greatly strengthened in spots. Arc lines faint in sun, much strengthened in spots. Enhanced lines produced in furnace at high temperature, strong in arc, and slightly weakened in spots.

Titanium[2] *and vanadium*[3]—These elements behave in a very similar fashion, both in the laboratory and in sun-spots. The furnace lines are greatly strengthened in spots and the arc lines strengthened. Practically all the arc lines may be obtained in the furnace. The enhanced lines can be obtained in the furnace only with great difficulty, and are weakened in spots.

Iron,[4] *manganese,*[5] *and chromium.*[3]—These again are similar in their behavior. The flame lines are strengthened in the spot spectrum, the arc lines little affected, and the enhanced lines much weakened. Many arc lines are very hard to produce in the furnace, and the enhanced lines cannot be produced there at all, and are faint in the arc. The percentage of lines which are strengthened in the spot spectrum is greater for chromium than for manganese and still smaller in the case of iron.

Cobalt and nickel.[6]—The number of lines weakened in spots is nearly as great as that of the strengthened lines in the case of cobalt, and much greater for nickel. The number of arc lines which cannot be obtained in the furnace is greater for nickel than for cobalt.

---

[1] King, *Mt. Wilson Contr.*, No. 211; *Astrophysical Journal*, **54**, 28, 1921.

[2] King, *Mt. Wilson Contr.*, No. 76; *Astrophysical Journal*, **39**, 139, 1914.

[3] King, *Mt. Wilson Contr.*, No. 94; *Astrophysical Journal*, **41**, 86, 1915.

[4] King, *Mt. Wilson Contr.*, No. 66; *Astrophysical Journal*, **37**, 239, 1913.

[5] King, *Mt. Wilson Contr.*, No. 198; *Astrophysical Journal*, **53**, 133, 1921.

[6] King, *Mt. Wilson Contr.*, No. 108; *Astrophysical Journal*, **42**, 344, 1915.

A number of cobalt lines and one nickel line described by Lockyer as enhanced appear in the furnace, but King gives good reason for supposing that these are not enhanced lines of the regular type.

Copper reveals itself in the sun by the first pair of the principal series, λλ 3274, 3247, which are produced when mere traces of the metal are present. They are recorded as of intensity 10 by Rowland, yet no trace of the lines of the subordinate series appears; although λλ 5782, 5700 are furnace lines.[1] The limit of the principal series, 1605 A,[2] corresponds to an ionization potential of 7.7 volts.

For *zinc*, as has already been noted, the arc lines are fairly strong in the sun, but greatly weakened in the spots. Finally, at the end of the series, come *silicon*, for which all the solar lines are greatly weakened in spots, and *oxygen*. The triplet of the latter in the extreme red, λλ 7772–7775, is faintly present in the arc, stronger in the spark, and, though fairly strong in the sun, is completely obliterated in the spot spectrum.[3] Yet the series relations of these lines, which belong to a combination series 2s–mp, show conclusively that they are produced by the neutral atom.

Part of the effect observed in the spots, however, is probably due to the formation of titanium oxide, which must diminish considerably the amount of free oxygen in the solar atmosphere.

The foregoing list shows a definite sequence in the behavior of the elements, alike in furnace, arc, and sun-spots, which suggests strongly that we have to do with a series in which the ionization potential steadily increases (except perhaps in the case of copper, for which the data are very meager). It cannot be a matter of chance that the list, from calcium, and, indeed, from potassium to zinc in order of increasing difficulty of spectroscopic excitation, is a complete list of the intervening elements in the order of their atomic numbers. It appears highly probable that in this region at least the ionization potential increases with the interval in the periodic table which separates the element from the preceding noble gas. Whether this relation holds good more generally cannot be known until further data become available, but it is of interest to note that silicon and oxygen, which are evidently decidedly hard to ionize, fit in very well, since, in the known cases, the ionization potential falls steadily for corresponding elements in each successive period of the periodic table.

---

[1] King, *Astrophysical Journal*, **21**, 250, 1904.

[2] Konen, *Das Leuchten der Gase* (Braunschweig, 1913), p. 146.

[3] Merrill, *Mt. Wilson Contr.*, No. 183, p. 7; *Astrophysical Journal*, **51**, 247, 1920.

The behavior in the spot spectrum of most of the elements in this list is intermediate between that of calcium and that of zinc. It may therefore be surmised that the ionization potentials for these metals lie between six and nine volts, as Saha has suggested[1] without specifying his reasons.

One further comment may be made on the foregoing. It is evident that the enhanced lines of an easily ionized element, such as barium or calcium, may be produced with a weaker excitation than the arc lines of an element of difficult ionization, such as zinc or silicon; the intervening elements present all degrees intermediate between these extremes. The mere fact that an enhanced line appears in a given spectrum is therefore not a proof that the temperature, for example, is high on an absolute scale, but only that it is high relative to the scale appropriate for the element in question. It would probably be fairly safe to assume that temperatures proportional to the various ionization potentials produce similar effects upon different atoms, but further knowledge is necessary before we can be sure of this.

The principles of the ionization theory will evidently be of great importance throughout the whole field of astrophysics, and Dr. Saha[2] has made an application of the highest interest to the question of the physical meaning of the sequence of stellar spectra. The writer hopes to present a discussion of many features of this problem at some time in the not distant future.

The possibilities of the new method appear to be very great. To utilize it fully, years of work will be required to study the behavior of the elements mentioned above and of others, in the stars, in laboratory spectra, and by the direct measurement of ionization, but the prospect of increase of our knowledge, both of atoms and of stars, as a result of such researches, makes it urgently desirable that they should be carried out.

---

[1] *Philosophical Magazine*, **40**, 822, 1920.

[2] *Proceedings of the Royal Society*, A, **99**, 135, 1921.

Mount Wilson Observatory
August 1, 1921

Note.—An admirable summary of the theory of ionization by Mr. E. A. Milne, in the *Observatory* for September (44, 261, 1921), has appeared since the completion of the foregoing discussion. He points out the influence of the free electrons resulting from the dissociation of easily ionized atoms in diminishing the ionization of other atoms, and gives the correct equation for second-stage ionization. Section 1 of the present paper was prepared independently and carries the analysis somewhat further, so that it appears sufficient to call attention here to Mr. Milne's prior publication.

Contributions from the Mount Wilson Observatory, No. 226
Reprinted from the *Astrophysical Journal*, Vol. LV, pp. 165–237, 1922

THE MASSES AND DENSITIES OF THE STARS

By FREDERICK H. SEARES

ABSTRACT

Mean magnitudes and masses of visual binaries and dwarf stars of the different spectral types.—A statistical comparison of the absolute magnitudes (M_b) of 105 visual binaries, the hypothetical magnitudes (M_c) of these and 400 other visual binaries (computed by Jackson and Furner, assuming the combined mass, $\mu=\mu_1+\mu_2$, of each binary to be 2), and the absolute magnitudes (M_s) of 1152 single stars (including some binaries) by Kapteyn and Adams, gives the mean difference $(\overline{M}_b-\overline{M}_c)=(\overline{M}_s-\overline{M}_c)-0.3\pm0.1$ for each type; that is, $\overline{M}_b=\overline{M}_s-0.3\pm0.1$. This indicates that the selection used is sufficiently homogeneous, also that the variation of the mean magnitude of binary star components with spectral type is the same as that of single stars. The values of $\overline{M}_s$ (Table IV and Fig. 1) for dwarf stars of types B0, A0, F0, G0, K0, and Ma are -1.60, $+0.70$, 2.40, 4.35, 5.90, and 9.80 respectively. The geometric mean mass for each spectral type of visual binary was next computed from the formula $\log\mu=\log 2-0.6\,(\overline{M}_s-0.3-\overline{M}_c)$. The values of μ, slightly corrected for the effect of selection as determined by a study of the binaries of known parallax, give, when multiplied by $\frac{4}{7}$ to reduce to single stars, a first approximation to the geometric mean masses of single stars along the dwarf branch of Russell's diagram, the values for types B0, A0, F0, G0, K0, and Ma, coming out 10, 6.0, 2.5, 1.0, 0.68, and 0.59, respectively, in terms of the sun's mass (Table IV). The data for visual binaries of known parallax indicate that the distribution of $\log\mu$ is approximately Gaussian and that the *dispersion in mass* is small, probably half the stars of each type having masses between 0.7 and 1.5 times the mean (Table VIII).

Mean velocity and energy of dwarf stars of different spectral types.—The mean square space-velocity corresponding to the mean magnitude was determined from the available data for each type, and these values were multiplied by the corresponding mean masses. The mean energy for each type so obtained is practically the same for all types from A0 to Ma, in spite of a 10 to 1 variation in mass (Table IX). The logarithm of the *mean kinetic energy constant* is 3.27 ± 0.036 (average deviation per type) in terms of sun's mass and km/sec., corresponding to 3.5×10^{46} ergs. The mean radial energy is also approximately constant for all except the B-type stars, which seem to be abnormal in this as in other respects. Whatever the cause may be, the distribution of energy among these stars seems to approximate equipartition.

Masses of stars as functions of magnitude and spectral type were then computed from the values of the mean velocity for each magnitude and type, assuming the mean energy independent of magnitude as well as of type (Table X). In Figure 2, curves are given showing M as a function of type for various constant values of the mass. To get more reliable data for the giants, the masses of 28 Cepheids were computed from the period, magnitude, and surface brightness of each, using a formula based on the pulsation theory (Table XVI), and Figure 2 was revised to agree with these values, giving Figure 3. If the masses computed in accordance with Eddington's theory of Cepheids (Table XIX) are adopted, a further slight revision will be necessary. The constant mass lines would be less irregular if bolometric magnitudes were used instead of visual. For the Cepheids, the probable *dispersion in mass* for a given M and type is only about 20 per cent. This result taken with the data for visual binaries indicates that in general the luminosity of a star is very closely determined by its spectral type (temperature) and its mass.

Effective temperature, color index, and surface brightness of stars of different spectral types.—The effective or black-body temperatures of the giants as determined from

Wilsing's spectrophotometric measures of c/T for 199 stars, vary from 2890° for Mc to 10,500° for Bo, while those of the dwarfs as determined from Mount Wilson color indices (provisional values, hitherto unpublished, also given for the giants) reduced to the same system, vary from 3330° for Ma to 6080° for F5 (Table XII). The difference between dwarfs and giants of the same type is too great to be neglected, the later-type dwarfs being considerably hotter. The surface brightness j as a function of temperature may be computed (1) from the difference between visual and bolometric magnitudes as determined by Eddington ($j=M-M_B-10 \log T+\text{const.}$) and (2) from Hertzsprung's formula derived from Planck's radiation law ($j=2.3\ (c/T)^{0.93}+\text{const.}$), both formulae giving practically the same results (Table XI). Combining these values with the temperatures of the stars of various types, we get the surface brightness as a function of spectral type, the results varying from 4.81 for $T=2890°$ to -2.28 for $T=10,500°$, expressed in magnitudes, sun $=0$ (Table XII). As a check on these values, the surface brightness of three stars, α Orionis, α Boötis, and α Scorpii, whose diameters have been determined directly by Pease, were computed and found to agree with the interpolated values within $\pm 0^{\mathrm{M}}.2$ in each case (Table XIII).

Diameter and density of stars as a function of magnitude and spectral type were readily computed from the surface brightness, absolute magnitude, and mass (Table XIV). For dwarfs the diameter decreases from 6.8 to 0.54 (sun $=1$) and the density increases from 0.045 to 5.4 (water $=1$) as the type changes from Bo to Ma, while for giants of zero magnitude the corresponding changes of diameter and density are from 3.2 to 66 and from about 0.3 to 10^{-5}. When M is plotted as a function of type for various constant values of the density (Fig. 2), the equidensity lines are straight and nearly parallel and quite regularly spaced, so that the equation: $\log \rho=-1.22\,S+0.57\,M+1.11$, where S is the type number beginning with 0 for Bo, represents the results quite closely for a wide range of density. For dwarfs of types B to F, the values agree satisfactorily with the values found by Shapley for the densities of eclipsing variables of these types. The giant part of the diagram, however, is less reliable, and is later modified in Figure 3 to agree with the values for 28 Cepheids (Table XVI) computed from their periods by the use of the theoretical formula: $\log \rho=-2 \log P+\text{const.}$ Adoption of Eddington's formula for Cepheids would lead to only a slight further modification (see Table XVII).

Relation of the observed variation of mean mass and of M with spectral type to the problem of stellar evolution.—For the dwarf branch, the decrease in mass from 10 for Bo to 0.6 for Ma may be partly, and perhaps wholly, accounted for by selection, the earlier and brighter stars being observed throughout a larger volume; further, only massive stars can attain high temperatures. The possibility that *mass may decrease with loss of energy by radiation* is also suggested, a possibility which agrees with the theory of relativity and does not necessarily conflict with Newtonian mechanics. For the giants, the observed change in M with spectral type (mass constant) is difficult to account for. Probable changes in mean atomic weight are insufficient. Changes in the opacity are doubtless involved, and likely also the source of energy, which almost certainly is not wholly gravitational and probably not independent of the time; for instance, the probable degree of ionization involves an amount of energy greater than seems to be available from gravitational forces. The intersection of equal-mass lines with the dwarf branch at large angles (Figs. 2, 3), however, does not conflict with the gravitational contraction hypothesis.

Eddington's radiative equilibrium theory of giants.—Although this involves the assumption that the ratio of the energy flow to the gravitational acceleration is constant throughout a star, whereas the ratio probably decreases considerably from center to outside surface, the calculated variation of magnitude with mass for a given spectral type is in fair agreement with observed values (Table XXII), but for a given mass the absolute magnitude is not constant as required by theory. *For Cepheids*, the theory gives the formula: $\log \rho=-2 \log P-2 \log (\gamma a)^{\frac{1}{2}}+\text{const.}$, and this combined with the empirical relation, mass is proportional to radius, which Eddington's results suggest as a *condition for Cepheid variation*, gives: $M=-5 \log P+j-5 \log (\gamma a)^{\frac{1}{2}}+\text{const.}$, which agrees with the observed variation of M with P for $P>2$ days, quite closely (Table XVIII and Fig. 5). This shows the consistency of Eddington's theory of Cepheids with his theory of radiative equilibrium

and tends to confirm the relation of mass to radius, which is equivalent to the condition that the average heat content per unit mass is constant. Various consequences of this condition are given. The theoretical values of mass and density given by the pulsation theory are close to those indicated by Figure 3 (Table XVII).

Ionization and mean atomic mass inside stars.—Theoretical computations indicate that the temperature and pressure at various points inside a star change in such a way as to keep the degree of ionization of the same order throughout (Table XX); hence the mean atomic mass is also about constant. When we consider giant stars of constant mass but of increasing temperature, we find that while the densities change very greatly, the high degree of ionization in the earliest stages is maintained with but little change (Table XXI), so that the mean atomic mass should decrease but slowly as development proceeds.

Comparison of spectroscopic parallaxes of visual binaries with the hypothetical parallaxes of Jackson and Turner shows systematic differences for their Table II (Table III).

Information on the masses of stars has its origin in what can be learned of the masses of binary systems, spectroscopic and visual. Any discussion of spectroscopic binaries from the standpoint of mass is complicated by lack of definite information on the inclination of orbital planes, while in the case of visual binaries the lack is that of accurate knowledge of stellar distances. Approached from either standpoint, the problem, with rare exceptions, must be treated by statistical methods whose application presupposes an abundance of data. Any solution is therefore involved in some uncertainty, which is not lessened by the fact that a transfer of results thus obtained to the stars at large involves assumptions of comparability: we do not know, for example, how the mass of an average binary is related to that of an average single star of the same type and luminosity, or even that the relation is the same for all classes of stars. The uncertainty, however, is probably not great; at any rate, we can proceed only by making such assumptions.

The following discussion is based on the visual binaries. These lead to values of the masses of stars along the dwarf branch of the Russell diagram, including those of B-type spectra. The average mass decreases continuously with advancing spectral type. The combination of these results with the space velocities of large numbers of stars recently published by Adams, Strömberg, and Joy shows that the mean kinetic energy of translation of the A's and the dwarfs is approximately constant. The principle of equipartition is then used to derive values of the masses of stars of other luminosities. The distribution curves thus obtained for mass as a function of spectral type and absolute magnitude are a first approximation in so far as they concern stars of highest luminosity, but in the vicinity of the dwarf branch they should be reliable within a moderate percentage.

Valuable information on density has at various times been obtained from the eclipsing variables, but it has been difficult to correlate these results with other stellar characteristics, except loosely, because here again the distances, and hence the luminosities, of individual stars are inadequately known. Density, however, depends in a simple way on mass, total luminosity, and surface brightness. The surface brightness can be computed from radiation formulae, the results being checked in part by their agreement with Pease's measures of angular diameters. Hence with mass once known as a function of spectral type and absolute magnitude, the values of the density follow as a matter of course. The results thus found for mass and density are subject to control and readjustment with the aid of the Cepheid variables, whose relative densities and masses can be calculated directly from their periods, spectra, and surface brightness.

The lines of equal mass for the giant stars in Russell's diagram are irregular curves, considerably inclined to the axis of zero absolute magnitude. If therefore a giant star in its evolutionary development follows an equal-mass line, its luminosity does not remain constant during the giant stage as has often been supposed. The curves of equal density are approximately linear and parallel to the line of maximum frequency for the dwarfs. The correlation of mass with spectral type along the dwarf branch can be explained, in part at least, as a consequence of selection, although other factors may also enter. The concluding sections of the paper discuss the relation of these results to certain phases of Eddington's theory.

I. THE METHOD

The mean masses of the visual binaries of different spectral types may be found by a statistical comparison of the absolute magnitudes corresponding to their hypothetical parallaxes with the absolute magnitudes of stars of known parallax. The relation

$$\mu=\mu_1+\mu_2=\frac{a^3}{\pi^3P^2} \qquad (1)$$

leads at once to

$$\log \mu = k - 0.6M \qquad (2)$$

where

$$k = 3 \log a - 2 \log P + 0.6m + 3$$

and where the absolute magnitude is defined by

$$M = m + 5 + 5 \log \pi . \qquad (3)$$

For a hundred systems of known orbital elements Jackson and Furner[1] have used equation (1) to calculate the hypothetical parallax π_c corresponding to an assumed mass $\mu = 2$. For about 450 systems of unknown elements they have calculated hypothetical parallaxes from a formula depending on changes in position angle and distance, the assumption for the mass again being $\mu = 2$. The absolute magnitudes M_c corresponding to the hypothetical parallaxes for the two groups of stars are given in Tables I and II of their paper.

For any system of known elements, by (2),

$$0.30 = k - 0.6\, M_c$$

and by combination with (2) itself,

$$\log \mu = 0.30 - 0.6\, \Delta M \qquad (4)$$

where $\Delta M = M - M_c$. Hence for a group of stars[2]

$$\left.\begin{aligned} \overline{\log \mu} = \log \underline{\mu} &= 0.30 - 0.6\, \overline{\Delta M} \\ \overline{\Delta M} &= \overline{M} - \overline{M}_c \end{aligned}\right\} \qquad (5)$$

in which $\underline{\mu}$ represents the geometrical mean mass.

Equations (4) and (5) are the basis of the present discussion. Since the hypothetical parallaxes derived from changes in position angle and distance involve the mean inclination of the orbit-planes, the individual values of π_c thus found will differ from those obtained with the rigorous relation (1). Equation (4) therefore holds for individual stars only in the case of systems of known elements. Formulae (5), however, are valid for any representative group of stars, whether their elements are known or not, and can therefore be applied to objects in both the lists of Jackson and Furner.

---

[1] *Monthly Notices*, **81**, 2, 1920.

[2] Upon re-reading Russell's address, "Relations between the Spectra and Other Characteristics of the Stars," *Publications of the American Astronomical Society*, **3**, 22; *Popular Astronomy*, **22**, 275, 331, 1914, I find that in principle the method is essentially one used by him.

To determine the mass from equations (4) and (5), the values of M, or at least of $\overline{M}$, must be known for the various spectral types. For a certain number of systems direct determinations of distance are available. Hence, M is known, and the use of (4) gives at once values of μ for the individual stars. These results will be affected by large uncertainties, but the means for groups of stars should be accurate within a small percentage. For most of the binaries, however, only the hypothetical absolute magnitude M_c is known; no other approximation for M is available, and we must proceed indirectly. This we might do by using values of $\overline{M}$ derived from single stars of known parallax whose selection with respect to the stars as a whole presents the same characteristics as those of the binaries themselves. Similarity of selection in the two lists of stars—binaries and single stars—is, however, difficult to attain in practice. It will be sufficient if we can find a list of single stars whose differences in selection as compared with the binaries are the same for all spectral types.

Let $\overline{M}_s$ represent the mean absolute magnitude for a given spectral type of the single stars of known parallax, and let $\overline{M}$ be the corresponding magnitude of the binaries of the same type. We may then write

$$\overline{M}=\overline{M}_s+\delta M \qquad (6)$$

where δM indicates the influence of difference in selection. If this difference is the same for all types, δM will be constant, and we shall then speak of the selection as homogeneous.

The second of (5) then becomes

$$\overline{\Delta M}=\overline{M}_s-\overline{M}_c+\delta M=\overline{\Delta M}_s+\delta M \qquad (7)$$

where $\overline{M}_c$ is the mean hypothetical absolute magnitude of the binaries of the spectrum under consideration. The value of $\overline{\Delta M}_s=\overline{M}_s-\overline{M}_c$ is found by comparing the two lists of stars for which it is presupposed that the selection for different spectral types is homogeneous, while the constant δM is given by

$$\delta M=\overline{\Delta M}-\overline{\Delta M}_s=\overline{M}-\overline{M}_c-\overline{\Delta M}_s \qquad (8)$$

applied to the systems of independently determined parallax referred to above. M represents here the magnitude corresponding to the measured parallax of a binary whose hypothetical absolute magnitude is M_c. In other words, we derive δM by (8) from the hundred or more binaries of measured parallax, calculate $\overline{\Delta M}_s$ for each type by comparing the five hundred and fifty-odd stars in the lists of Jackson and Furner with the homogeneously selected single stars of known parallax, form $\overline{\Delta M}$ by (7), and, finally, solve for μ by means of the first of equations (5). Since the question of homogeneity of selection can be put to a direct test, the only assumption underlying this procedure is that the relation of mass to luminosity is the same for both binaries and single stars, which may be accepted as plausible at least.

The values of $\overline{M}_s$ and $\overline{M}_c$, whose difference is $\overline{\Delta M}_s$, are readily found by a graphical process. Plotting the values of M_c against spectral type, we find for the binaries a frequency diagram similar to that first given by Russell. The late-type giants are not numerous, but the dwarf branch is well defined. The points of maximum frequency for the dwarfs define a curve which joins smoothly with the line of modal values of the B- and A-type stars. This curve expresses the variation of $\overline{M}_c$ with spectral type, the giants of late type being disregarded altogether for the present. For $\overline{M}_s$ a similar curve was found from the data in the list of spectroscopic parallaxes,[1] supplemented by those for about 430 helium stars whose parallaxes have been determined by Kapteyn.[2] These two curves are shown in the central part of Figure 1. Their ordinates and differences in ordinates are given in the second, third, and fourth columns of Table IV. The data for the $\overline{M}_s$ curve could have been greatly increased by including results from trigonometric parallaxes. Little would have been gained in precision, however, for, as it is, the number of stars entering into the $\overline{M}_s$ curve is more than twice that for the $\overline{M}_c$ curve.

If we may assume that the selection for different spectral types is homogeneous, the differences in the ordinates of the two curves

---

[1] Adams, Joy, Strömberg, and Burwell, *Mt. Wilson Contr.*, No. 199; *Astrophysical Journal*, **53**, 13, 1921.

[2] *Mt. Wilson Contr.*, Nos. 82, 147; *Astrophysical Journal*, **40**, 43, 1914; **47**, 146, 255, 1918.

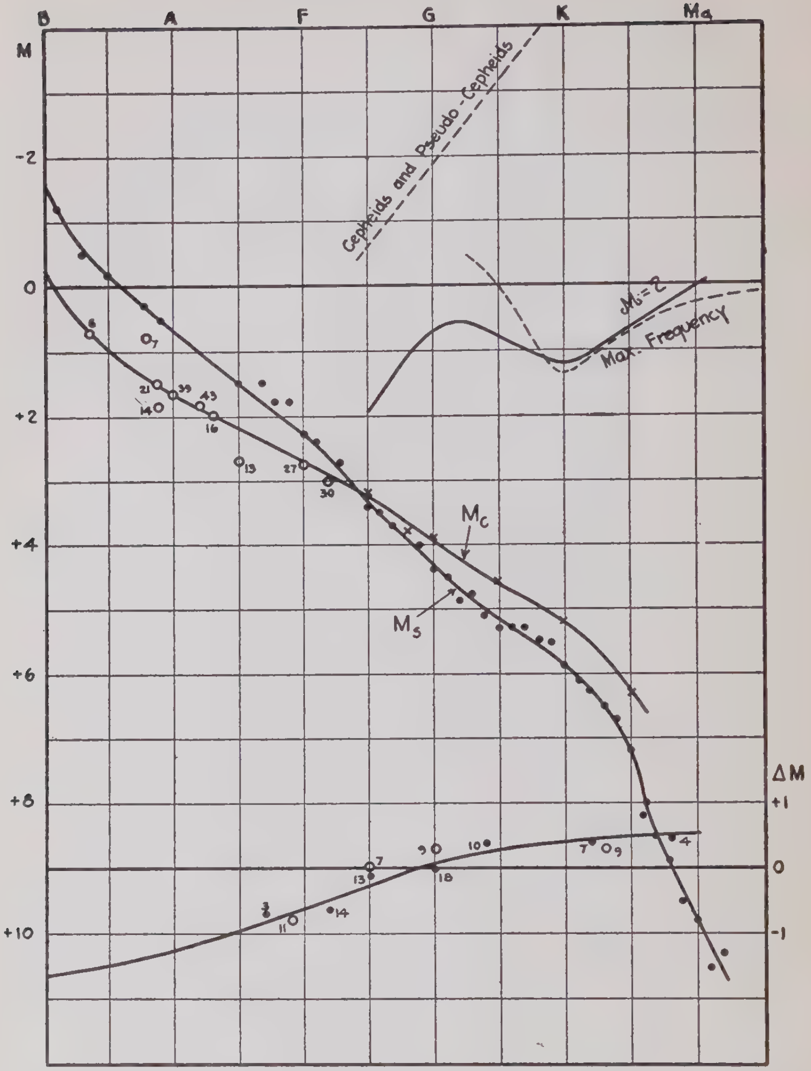

FIG. 1.—The curve M_s is the line of maximum frequency of M for the B stars of Kapteyn and the dwarfs from the list of spectroscopic parallaxes. M_c is the similar curve for the hypothetical absolute magnitudes of Jackson and Furner. The differences in the ordinates, corrected for zero point, are shown by the curve below (ΔM). The remaining curves refer to the discussion in section 16.

represent the values $\overline{\Delta M}_s$ as a function of spectrum. Irregularities of selection, or a progressive change in selection with type, will produce deformations or a tilt of the curve for $\overline{\Delta M}_s$. The curve for $\overline{\Delta M}$, formed directly from the curves for M_c and $\overline{M}_s$ and corrected for δM, is shown in the lower part of Figure 1 (the points are explained later). Since the curve is smooth, we conclude that there are no marked irregularities of selection, or at least that their influence has been minimized in drawing the curves for M_s and M_c.

2. INFLUENCE OF SELECTION ON THE STATISTICAL COMPARISON

To examine the question of selection more closely, consider the numbers of binaries and single stars of known parallax in each interval of apparent magnitude. Excluding the late-type giants and a few scattering stars at the ends of the sequence of apparent magnitudes, we find the data in the first two divisions of Table I. If the selection for the two lists were the same (not merely homogeneous), the ratios of the corresponding numbers for each type would not vary with the magnitude. Difference in selection for the binaries and single stars of any type implies a change in ratio with increasing magnitude; and, if the selection is homogeneous, the ratios for different types will show the same change. Absolute values of the ratios are of no significance, and for ease of comparison the ratios for each type have been multiplied by a constant factor which reduces that for median magnitude 6.5 to unity. Further, the numbers for the G5–K5 binaries have been combined with the mean numbers for single stars of F0–F9 and K0–K9 types.

The results in the third division of Table I indicate a satisfactory degree of homogeneity. The irregularities affecting the bright G5–K5 stars are unimportant, since the individual groups include only two or three stars each. The only deviations requiring comment are those shown by the faint G5–K5 stars and the faint B's. The latter arise from the fact that Kapteyn's lists of B stars include none fainter than the 6th magnitude. The binaries involved are ten in number, all of the 7th magnitude or fainter, and all but one or two of types B8 or B9. Any error in the corresponding $\overline{\Delta M_s}$ must be small, for there is no pronounced irregularity in the curve. The value of $\overline{M}_s$ for Kapteyn's earlier B's

TABLE I

Numbers of Stars—Influence of Selection

Spectrum	Median Apparent Magnitude								Total No.
	2.5	3.5	4.5	5.5	6.5	7.5	8.5	9.5	
	Binaries—Jackson and Furner								
Oe5–B9	1	1	7	7	7	8	2	0	33
A0 –A9	4	3	12	32	42	25	15	1	134
F0 –G0($M>+1$)	0	6	15	36	66	78	54	2	257
G5 –K5($M>+3$)	0	1	3	4	9	24	39	1	81
Total	......	......	......	......	......	......	......	......	505
	Single Stars*—Kapteyn and Adams								
Oe5–B9	23	42	137	194	30	0	0	0	426
A0 –A9	0	7	11	11	8	3	(2)	(1)	43
F0 –F9($M>+1$)	2	14	48	105	63	50	29	3	314
G0 –G9($M>+3$)	0	5	10	35	57	54	40	8	209
K0 –K9($M>+4$)	0	1	2	14	26	43	62	12	160
Total	......	......	......	......	......	......	......	......	1,152
	Ratio—Binaries/Single Stars								
B	......	0.1	0.2	0.2	1.0	∞	∞	......	......
A	......	0.1	0.2	0.6	1.0	1.6	1.5	0.2	......
F	......	0.4	0.3	0.3	1.0	1.5	1.8	0.7	......
G5–K5	......	1	3	0.8	1.0	2.2	3.5	0.5	......
	Ratio—Jackson and Furner/Pickering								
B	......	......	7	2	1.0	0.52	0.08	0.00	......
A	......	......	3	2	1.0	0.29	0.04	0.00	......
F	......	......	3	2	1.0	0.38	0.10	0.01	......
G5–K5	......	......	3	2	1.0	0.80	0.54	0.02	......
	Ratio—Kapteyn and Adams/Pickering								
B	......	......	34	13	1.0	0.00	0.00	0.00	......
A	......	......	17	4	1.0	0.18	0.03	0.02	......
F	......	......	12	6	1.0	0.25	0.05	0.01	......
G	......	......	3	4	1.0	0.33	0.08	0.02	......
K	......	......	0.4	1.5	1.0	0.46	0.34	0.12	......

* The "single stars" include the brighter members of a few binaries.

can scarcely have been affected by the limitation in apparent magnitude, for these stars are all so luminous that the limitation is of little consequence.

Among the stars fainter than $m=7.0$ there is an excess of G5–K5 binaries which represents a considerable fraction of the total number of G5–K5 stars. The corresponding $\overline{M}_c$ may be slightly too large. But, if appreciable, this effect must also be small, for as the stars actually observed in the intervals of fainter apparent magnitude are successively added, the value of $\overline{M}_c$ increases very slowly. A direct test is afforded by the binaries of measured parallax considered in a later paragraph.

The number of A stars in the spectroscopic list is small, but this does not seriously interfere with the determination of the curve of modal values because there are well-determined points for the early B's and for the F's. It does suggest, however, the advisability of an independent test of the selection of the much larger group of A's among the binaries, whose numbers can be considerably changed without greatly affecting the ratios in the middle section of Table I. To cover this point and as a further general test, both groups of stars have been compared with the counts of W. H. Pickering.[1] Using means of his values for the galactic poles and the galaxy itself (except for the B's, for which the galactic counts alone have been employed), we find the ratios in the last two sections of Table I. There is here some progression with type due to the fact that Pickering's counts include the late-type giants; but the ratios for the A-type binaries are in general agreement with those of the adjacent classes, which answers the question as to the selection of the A's. The large ratios for the bright B's in the last section of the table show merely what appears directly from the counts, namely, that Kapteyn's lists are not complete beyond the 6th magnitude. There seems also to be a defect of fainter A's in the spectroscopic list, a conclusion apparently confirmed by the fact that the points for these stars lie above the smooth $\overline{M}_s$ curve shown in Figure 1. It seems clear that none of the questions raised is serious and that we may accept the values of $\overline{\Delta M_s}$ found in the manner described and proceed to the determination of δM.

---

[1] *Publications of the Astronomical Society of the Pacific*, **33**, 140, 1921.

3. ZERO POINT OF THE CURVE FOR MASS AND SPECTRUM

It will be noted that the values of $\overline{\Delta M_s}$ determine the rate of change of mass with spectral type, while the constant, δM, determines the zero point. For the calculation of δM only the spectroscopic parallaxes have been used, since these are based on a homogeneous system and are sufficiently numerous to afford an excellent determination. In forming values of $M-M_c$ for individual stars to be substituted into (8), two points must be borne in mind: First, the values of M given in the spectroscopic list correspond to the most probable values of the parallaxes, and, because of the logarithmic relation connecting absolute magnitude and parallax, are not the most probable magnitudes themselves. To obtain the latter, a small constant correction of +0.08 mag. must be applied to the tabular values.[1] Second, the values of M_c given by Jackson and Furner usually represent the total luminosity of the system. To make them comparable with values of M in the spectroscopic list, they must be reduced to the brighter component.

A summary of the results for δM is given in Table II, the two lists of Jackson and Furner being treated separately. The values of $\overline{\Delta M_s}$ required for equation (8) were interpolated from the fourth column of Table IV. The adopted result is $\delta M = -0.3$, whence equation (7) becomes

$$\overline{\Delta M} = \overline{\Delta M_s} - 0.3. \qquad (9)$$

It will be noted that there is no marked progression in the values of δM with type, which confirms, in part at least, the foregoing conclusion as to homogeneity of selection. This is also shown by the lower part of Figure 1, in which the curve is that representing equation (9), while the points correspond to the values of $M-M_c$ in Table II. With the exception of the constant term, the curve depends wholly upon the statistical comparison, while the points are derived from values of M and M_c referring to the same star and are uninfluenced by any possible dissimilarity in selection. The agreement of the points with the curve is, however, within the uncertainty affecting their positions.

---

[1] *Mt. Wilson Contr.*, No. 199, p. 15; *Astrophysical Journal*, **53**, 27, 1921.

TABLE II

ZERO POINT OF CURVE FOR $\overline{\Delta M}_s$

J and F, Table I					J and F, Table II				
Sp.	$\overline{M-M}_c$	$\Delta\overline{M}_S$	δM	No. Stars	Sp.	$\overline{M-M}_c$	$\Delta\overline{M}_S$	δM	No. Stars
A7.....	−0.7	−0.5	−0.2	3	A9....	−0.8	−0.4	−0.4	11
F2.....	−0.6	−0.2	0.4	14	F5....	0.0	0.0	0.0	7
F5.....	−0.1	0.0	0.1	13	G0....	+0.3	+0.4	−0.1	9
G0....	0.0	+0.4	0.4	18	K3....	+0.3	+0.8	−0.5	9
G4....	+0.4	+0.6	0.2	10					
K2....	+0.4	+0.7	0.3	7					
K8....	+0.5	+0.8	−0.3	4					
Mean and total......			−0.29	69	Mean and total			−0.27	36

A further detail bearing on the question of selection is the circumstance that the constant δM arises almost wholly from the use of the tabular values of M_c for the derivation of the curve for $\overline{M}_c$. Since these generally represent total luminosity, the reduction to the brighter component appears in δM, and in the mean is nearly equal to the value found for this constant. The effect upon $\overline{\Delta M}_s$ of the obvious differences in selection shown in Table I is therefore very small. Consequently, the influence of small deviations from homogeneity in selection in passing from type to type may be regarded as altogether negligible.

4. SYSTEMATIC DIFFERENCES IN THE HYPOTHETICAL PARALLAXES

Although the two mean values of δM given in Table II are practically identical, this was not the case when the calculation was originally made, the difference then amounting to several tenths of a magnitude. This discordant result has been traced to a systematic difference between the parallaxes of the two lists of Jackson and Furner, the character of which may be seen from the comparisons shown in Table III. For systems of known elements (J and F, Table I) the agreement of the mean hypothetical parallaxes with the spectroscopic results is excellent; the one large difference, +0″.014, is only 7 per cent of the corresponding π_c and would be reduced to +0″.004 by the rejection of a single star, Bu 2109.

TABLE III

COMPARISON OF SPECTROSCOPIC AND HYPOTHETICAL PARALLAXES

π_c	J AND F, TABLE I			J AND F, TABLE II			J AND F, TABLE I—TABLE II		
	Mean π_c	$\pi-\pi_c$	No.	Mean π_c	$\pi-\pi_c$	No.	Mean π_c*	$\pi-\pi_c$	No.
<0″.020	0″.016	+0″.001	7	0″.015	−0″.002	8	0″.015	−0″.001	6
0.020–0.049	0.030	−0.001	28	0.036	−0.009	16	0.024	−0.007	12
0.050–0.099	0.065	−0.003	22	0.064	−0.012	13	0.043	−0.012	8
>0.100	0.198	+0.014	10	0.209	−0.071	1	......	....	....

* The intervals for π_c are $\leqq$0″.020, 0″.021–0″.029, and $\geqq$0″.030.

For the stars in the second list, however, the agreement for the first group alone is within the uncertainty; for the others the differences are systematic and an important percentage of the parallaxes themselves. Further, the same difference is shown by a direct comparison of the hypothetical parallaxes of twenty-six stars which occur in both the lists of Jackson and Furner. The means, arranged in three groups, are in the last division of Table III. For half of these stars no spectroscopic parallaxes are available, and to that extent the second comparison is independent of the first.

The difference, which is about 20 per cent of the parallax, corresponds to a difference of 0.4 mag. in the two values of δM and fully accounts for the discordance. For the final determination of δM, the hypothetical parallaxes from the second list were reduced to the spectroscopic system in accordance with the indications of Table III, in order that all the results may refer consistently to this system. The resulting value of δM is that given in the right-hand division of Table II.[1]

---

[1] I am greatly indebted to Mr. Adams for the spectroscopic parallaxes of nineteen binaries in the first list of Jackson and Furner (six stars also occur in the second list) which have been obtained since the reductions described in the text were finished. These reductions have not been revised, but I have satisfied myself that the inclusion of the new data would not change the results in section 4 or the following sections

5. PROVISIONAL MASSES—EFFECT OF SELECTION

The derivation of values of the masses now requires only the substitution of $\overline{\Delta M}$ from (9) into the first of (5). The results for log $\underline{\mu}$ are in the fifth column of Table IV. The first and last values depend upon extrapolations, and it is possible that those for B5 and A0 are also affected by considerable uncertainty. So far as the statistical comparison is concerned, the remaining values should be dependable within 5 or 10 per cent.

TABLE IV

Adopted Geometrical Mean Mass ($\odot = 1$), Spectral Type and Absolute Magnitude

Sp.	M_s	M_c	$\overline{\Delta M}_s$	Provisional Log $\underline{\mu}$	Corr. for Selection	Vis. Binaries		Single Stars	
						Log $\underline{\mu}$	$\underline{\mu}$	Log $\mathcal{M}$	$\mathcal{M}$
B0	−1.60	(−0.25)	(−1.35)	1.29	−0.04	1.25	18	1.01	10
B5	−0.20	+1.00	1.20	1.20	− 4	1.16	14	0.92	8.3
A0	+0.70	1.65	0.95	1.05	− 3	1.02	10.5	0.78	6.0
A5	1.50	2.15	0.65	0.87	− 3	0.84	6.9	0.60	4.0
F0	2.40	2.70	−0.30	0.66	− 2	0.64	4.4	0.40	2.5
F5	3.32	3.27	+0.05	0.45	− 2	0.43	2.7	0.19	1.5
G0	4.35	3.95	0.40	0.24	− 1	0.23	1.7	9.99	1.0
G5	5.20	4.60	0.60	0.12	0	0.12	1.3	9.88	0.76
K0	5.90	5.20	0.70	0.06	+ 1	0.07	1.2	9.83	0.68
K5	7.10	6.30	0.80	0.00	+ 3	0.03	1.1	9.79	0.62
Ma	+9.80	(+8.95)	(+0.85)	9.97	+0.04	0.01	1.0	9.77	0.59

These results can be accepted, however, only with some reservation, for it is easily seen that the visual binaries are a selected class of stars in the characteristic of mass itself, and especially is this true of the more distant objects. Since motion is detected only with difficulty, or not at all, in case the period is very long, equation (1) shows that the selection of large masses is favored to an increasing degree as more and more distant stars are considered. For a given value of a the factor a^3/π^3 increases rapidly with increasing distance; the smaller masses are therefore excluded in succession because they correspond to periods so long that motion has not been observed. For large values of π a wide range in mass

---

in any essential particular. Thus the first two differences in the first division of Table III would be +0″002 and −0″002 for seventeen and thirty-seven stars, respectively. The differences in the third division would not be changed by the inclusion of the six stars also occurring in the second list.

will be included, but since there is a practicable lower limit to *a*, only the most massive among the more distant stars will appear in our lists.

Another and perhaps even more important form of selection arises from the fact that only the most luminous of the distant stars get into our lists; the others are too faint to be seen. This, too, excludes in succession the smaller masses with increasing distance, and is related to the correlation of mass with spectral type discussed in section 16.

The influence of distance on the selection of mass seems to be shown by the data now available. To test the matter, consider the sixty-nine binaries of known parallax[1] in the first list of Jackson and Furner. For these, the individual masses, μ, can be calculated by (4). Comparing these values with the mean mass for stars of the same spectrum, as interpolated from Table IV, we obtain a series of residuals $\Delta \log \mu = \log \mu - \log \underline{\mu}$. When grouped according to parallax, these lead to the mean systematic deviations shown in Table V. A progression with increasing parallax, in the direction anticipated, is evident, the negative sign of the differences associated with the more distant stars indicating that the corresponding

TABLE V

DEPENDENCE OF MASS ON PARALLAX

π_s	Mean Sp.	No. Stars	$\overline{\Delta \log \mu}$	Curve
0″.018	F2	10	−0.08	−0.11
.026	F6	10	−0.12	−0.08
.032	G1	10	−0.08	−0.07
.046	F7	10	+0.03	−0.03
.061	G3	10	−0.04	0.00
.102	G1	10	+0.04	+0.04
0.270	G8	9	+0.12	+0.12

---

[1] The thirty-six stars of known parallax in the second list are not included because of the systematic difference in the parallaxes of the two lists. In the preparation of Table II, where only a mean result for all the stars was finally used, the systematic difference can be corrected with sufficient precision. Here, however, we are concerned with individual stars, or at most with small groups, and it is not certain that the mean correction is applicable. Then, too, the fact that the second list of Jackson and Furner is based on a statistical formula, renders these data unsuitable for the present discussion.

mean masses in Table IV are too large. The character of the progression is best seen from the smoothed values of the differences given in the last column of Table V. Considered as corrections, these differences are such as would reduce the masses to values representing the selection for $\pi = 0''.06$. Even at this moderate distance the smallest masses will still be excluded; hence some further correction, a constant, is required. This cannot be accurately specified; but in general it may be said that, if we regard the selection for the two nearest groups in Table V as approximately representative of the visual binaries as a whole, the data of this table would indicate that the mean masses of the binaries actually observed at distances corresponding to $\pi = 0''.02$ are roughly 50 per cent larger than those of a representative collection.

This result at once suggests that the variation of log $\underline{\mu}$ with spectral type found above has been influenced by selection, for in general the mean parallax of the earlier-type stars, which are all highly luminous, is less than that of the late-type dwarfs. Forming the mean parallax for each of the spectral groups in the first half of Table II, we find in fact a progression in distance as shown in Table VI. If the data of Table V may be accepted, the values of log $\underline{\mu}$ in Table IV must be corrected as indicated in the last column of Table VI, in order to obtain the true variation of log $\underline{\mu}$ with spectral type. To make the results fully representative, the additional constant correction referred to above must also be applied. This seems to be of the order of −0.08.

TABLE VI

CORRECTIONS TO LOG $\underline{\mu}$

(To Eliminate Selection in Mass)

Sp.	$\bar{\pi}_s$	No. Stars	Correction to log $\underline{\mu}$
A7	($0''.133$)	3	−0.03
F2	0.051	14	−0.02
F5	0.038	13	−0.05
G0	0.055	18	−0.01
G4	0.069	10	0.00
K2	0.114	7	+0.06
K8	0.229	4	+0.11

Unfortunately, however, the results in Table V are not as reliable as could be wished. The individual values of the masses are affected by large uncertainties, and the number of stars in the separate groups is small. Further, the residuals $\log \mu - \log \underline{\mu}$ depend upon the ordinates of the curve for ΔM shown in Figure 1. Any error in the curve, in the nature of a tilt with respect to the axis, must therefore have introduced a progression in the residuals which only partially disappears when they are grouped according to parallax, because such a grouping, in part at least, is also a grouping with respect to spectral type. This uncertainty is probably not very serious, for Table V shows that the relative effect on the corrections to $\log \mu$, for the two extremes of distance, is the differential error in the ordinates of the ΔM curve for F2 and G8. Since these ordinates are not widely separated, the influence of incorrect slope in the curve cannot be great.

6. ADOPTED MASSES

On the basis of the evidence in Table VI, the corrections given in the sixth column of Table IV were finally adopted. These are the smoothed values of the results in Table VI, extrapolated to B0 and slightly modified in the case of type K because of the small number of these stars. The small constant correction referred to above is ignored, because of its uncertainty and relative unimportance. It merges with the uncertainty involved in the assumptions of comparability which must be made in extending the results for the masses of the binaries to the stars at large.

The differential correction, affecting the relative values of the masses as it does, is of more interest. The present determination is to be considered as only a first approximation; the results are at least in the right direction, and it is believed that they do not represent an over-correction.

We have, finally, as adopted values of the geometrical mean masses of the visual binaries, the data in the seventh and eighth columns of Table IV. These results refer mainly to dwarf stars and correspond to the mean absolute magnitudes given in the second column of the table.

Owing to the small number of late-type giants in the lists of visual binaries, it is not possible to use the statistical method for a determination of the masses of these stars. Some indication of their values is afforded, however, by the application of equation (4) to such of these objects as occur in the spectroscopic list. For 14 G and K stars, with a mean absolute magnitude of 0.0,

$$\log \underline{\mu}=0.47\pm 0.16$$

whence $\underline{\mu}=3.0$ with an uncertainty of about 40 per cent.

The use of the geometrical mean makes it difficult to compare the masses thus found with other results,[1] for which the arithmetical mean has usually been employed. For a Gaussian distribution of the logarithms of the mass, which seems to be that indicated by the available data, the conversion formula would be[2]

$$\log \bar{\mu}=\log \underline{\mu}+2.53\, r^2$$

where $\bar{\mu}$ is the arithmetical mean, and r the probable dispersion, i.e., the median value of the differences $\log \mu-\log \underline{\mu}$, arranged in order without regard to sign. The value of r is difficult to determine. For the dwarf stars it is certainly small, probably not larger than 0.15 (see page 21), whence, approximately, $\bar{\mu}=1.14\,\underline{\mu}$.

Applied to the present data, this relation would lead to arithmetical mean masses a little larger than those previously found, but close comparisons are not possible. The change in mass with spectral type is of the general character of that resulting from other investigations and is certainly well established, although the variation given here is not as large as that derived by Ludendorff[3] from a discussion of spectroscopic binaries.

Strictly speaking, the present results refer only to the particular group and class of stars upon which the conclusions are based.

---

[1] Russell, *loc. cit.; Publications of the American Astronomical Association*, **3**, 327; *Popular Astronomy*, **25**, 666, 1917. Aitken, *The Binary Stars*, pp. 206 ff., 1918. Van Maanen, *Publications of the Astronomical Society of the Pacific*, **31**, 231, 1919. Ludendorff, *Astronomische Nachrichten*, **189**, 145, 1911; **211**, 105, 1920.

[2] Adams, Strömberg, and Joy, *Mt. Wilson Contr.*, No. 210, p. 17; *Astrophysical Journal*, **54**, 25, 1921. Although derived for use in another connection the formula is generally applicable.

[3] *Loc. cit.*

Their applicability to any other class of stars presupposes some assumption. Thus in passing from the combined masses of the visual binaries to those of single stars, we can make use of the average mass-ratio of the two components and associate the resulting average values for the central stars with that for the non-binaries of the same spectra; but it is by no means certain that the stars so associated are strictly comparable. For the further discussion we make this assumption. Presumably the uncertainty is not large, for we thus arrive at a mean mass for the solar-type stars which is the same as that of the sun itself. To give this conclusion force it must be added that the average deviation of the mass of a dwarf star from the mean mass for the type in question is small (see next section).

There is some evidence that the mass-ratio varies with the type.[1] Adopting, however, the mean value 0.75 for the ratio of secondary to principal component, we find for the stars at large the geometrical mean masses ($\mathcal{M}$) in the last two columns of Table IV.

7. DISPERSION IN MASS

The residuals in log μ for the sixty-nine stars discussed above throw some light on the dispersion in mass. Freeing the individual residuals from the influence of selection in mass, we find the frequencies shown in Table VII. In spite of the small numbers of

TABLE VII

DISTRIBUTION OF Δ LOG μ

INTERVAL OF Δ LOG μ	NO. RESIDUALS		TOTAL	
	+	−	Obsd.	Theor.
0.00–0.09	8	4	12	17
0.10–0.19	10	8	18	15
0.20–0.29	6	7	13	12
0.30–0.39	5	7	12	10
0.40–0.49	5	5	10	6
0.50–0.59	0	1	1	4
0.60–0.69	1	1	2	3
0.70–0.79	0	0	0	1
0.80–0.89	1	0	1	0
Sums	36	33	69	68

---

[1] Aitken, *The Binary Stars*, pp. 206, 216, 1918.

stars, it is seen from the second and third columns that the frequency curve is approximately symmetrical. Further, the last two columns show that, within the uncertainty of the data, the values of log μ follow a Gaussian distribution.

The probable dispersion (dwarfs F0 to M) is

$$r(\Delta \log \mu) = \pm 0.22. \tag{10}$$

This, however, is not a true measure of the dispersion in log μ, for the result has been derived with the aid of equation (4) and includes, therefore, the influence of errors in M and M_c. Those in M_c arise from the factor a^3/P^2 and are relatively small. Bearing on the accuracy of M are the data in *Contribution* No. 199, p. 15, from which for the spectral types and luminosities involved, $r(M) = \pm 0.36$ mag. By (4), the contribution to the calculated dispersion in log μ arising from errors in M is therefore ± 0.22, which is the same as the calculated value of $r(\Delta \log \mu)$ itself. Since the dispersion in the masses presumably is not zero, the adopted value of $r(M)$ is probably too large. This unfortunately makes it impossible to gain any definite information as to the dispersion, and we can only indicate, as in the second column of Table VIII, the probable values corresponding to various assumed values of $r(M)$. The last column of the table gives the limits within which it is an even chance that the mass of any visual binary will be found. Thus, if we assume that the true probable error of the spectroscopic absolute magnitude is ± 0.25, the masses of one-half of the stars should be between 0.7 and 1.5 times the mean mass.

TABLE VIII

PROBABLE DISPERSION IN MASS

$r(M)$	Probable Dispersion in Log μ	Limits for Prob. = ½
±0.35	±0.07	0.85μ–1.18μ
0.30	0.13	0.74 –1.35
0.25	0.16	0.69 –1.45
0.20	0.18	0.66 –1.51
±0.15	±0.20	0.63 –1.58

Apparently the range in the masses of the dwarf stars from F0 on must be small. Further evidence is given on page 50. These results are in general agreement with the earlier findings of Russell and Eddington.[1]

8. EQUIPARTITION OF ENERGY

A possible analogy between the dynamical behavior of the stars and that of the molecules of a gas has frequently been mentioned.[2] Applicability of the kinetic theory would imply an equipartition of the energy of translation such that

$$\mu_1\overline{v_1^2}=\mu_2\overline{v_2^2}= \ . \ . \ . \ =\mu_n\overline{v_n^2} \qquad (11)$$

where the individual values in $\overline{v_n^2}$ include all the velocities associated with a definite class of masses μ_n. In a gas this final state is brought about very quickly; in a collection of stars the period of relaxation, if the term has any meaning at all, obviously must be enormously long.

As a matter of fact, the theory for a collection of stars is much simpler than that of a gas, because the occurrence of collisions and close encounters is so rare that they may be neglected.[3] The effective agency for the transfer of energy is therefore only that arising from the attraction of the great mass of stars as a whole upon the individual members of the group. But this simplification of the theory and the consequent restriction of the mechanism for the redistribution of energy so enormously lengthens the interval required for the attainment of statistical equilibrium that Eddington[1] rejects altogether the analogy with a gas and proceeds on the principle that the motions of the stars do not mutually interfere.

---

[1] *Monthly Notices*, **77**, 30, 1916; **604**, 1917. Russell, in this connection, makes the important suggestion that the real dispersion in mass may be largely concealed in a discussion based upon spectroscopic data. This would be the case if the spectral characteristics used for the determination of a star's absolute magnitude are functions of its surface brightness (temperature) and density alone. For Russell's discussion of this interesting point see the following *Contribution*, No. 227.

[2] See for example Poincaré, *Hypothèses Cosmogoniques*, p. 257, 1911; Halm, *Monthly Notices*, **71**, 634, 1911; Eddington, *Stellar Movements*, pp. 159, 247, 1914; Jeans, *Problems of Cosmogony and Stellar Dynamics*, pp. 224 ff., 1919.

[3] Jeans, *op. cit.*, p. 229.

As far as the present state of the universe is concerned, Jeans[2] concurs in this opinion, but points out that the conditions of an earlier stage in its history may have been entirely different. Following his conjecture that the system has evolved from a rotating nebula of dimensions much less than those of its present configuration, he shows that the earlier stages of development would be favorable to a rapid redistribution of energy, and that the system may have proceeded far on the way toward equipartition before its gradual expansion reduced the rate of transfer to its present negligible amount. The fact that readjustments are now inappreciable does not therefore demonstrate the absence of equipartition, which must be put to an observational test.

Although a certain type of systematic motion is not incompatible with a steady state, the phenomenon of star-streaming shows that equipartition has not been completely attained. Within the individual streams, however, there may be an approach to this state, just as in the case of two intermingling streams of gas. Further, if the stream motion is small as compared with the peculiar velocities of the stars, it will have little influence on the statistical averages in (11). For a decade or more some correlation of mass with velocity of the type hereby implied has been suspected, for it has been known that in general the most massive stars are the most luminous, and the most luminous stars have on the average the smallest velocities.[3] Now, however, we are in possession of data which admit of a more definite test.

For the B and A stars, whose extreme range in luminosity is small, we have the determinations of mean radial velocity by

---

[1] Eddington, *loc. cit.*, p. 254. See also *Astronomische Nachrichten, Jubiläumsnummer*, p. 9, 1921.

[2] *Op. cit.*, p. 237.

[3] Campbell, *Stellar Motions*, p. 207, 1913. Kapteyn, *Mt. Wilson Contr.*, No. 45; *Astrophysical Journal*, **31**, 258, 1910. Russell, *Observatory*, **37**, 174, 1914. Kapteyn and Adams, *Mt. Wilson Comm.*, No. 1; *Proc. Nat. Acad. of Science*, **1**, 14, 1915. Adams and Strömberg, *Mt. Wilson Contr.*, No. 131; *Astrophysical Journal*, **45**, 293, 1917.

Campbell.[1] For the remaining types, within which the differences in luminosity are much greater, we have the recent Mount Wilson results,[2] giving both radial and space velocities for each of these types as a function of absolute magnitude. Since the values of the masses in the last column of Table IV are probably representative of the stars at large, they may be combined with the mean velocities of the different types, in conformity with (11), to determine the degree to which the condition of equipartition is satisfied.

The values of the velocities have not been corrected for stream motion and thus subject the hypothesis of equipartition to a severe test. The Mount Wilson results for radial and space velocities include the K-term. For the late-type dwarfs, this is small, and negligible for the present discussion. Campbell, on the other hand, has freed his results from this term, which for the B stars is two-thirds of the mean radial velocity itself. If one prefers to regard the K-term as a real velocity, and not merely a systematic correction, its contribution to the energy can be found as indicated below.

It has been shown that the distribution of the space velocities for types F to M is not in accordance with Maxwell's law,[3] but agrees well with the assumption that the logarithms of the velocities follow a Gaussian distribution. Nevertheless, Campbell's theorem to the effect that the arithmetical mean space velocity equals twice the mean radial velocity, holds for the giants with close approximation.[4] We assume that a similar state of affairs exists for the B and A stars, and thus obtain for these types the arithmetical means of their space velocities. The square of the arithmetical mean space velocity could have been used directly for a test of equipartition; but to evaluate the influence of the K-term, considered as a velocity, it is simpler to use the mean-square space velocity.

---

[1] *Lick Observatory Bulletins*, **6**, 101, 1911; **7**, 19, 1912.

[2] Adams, Strömberg, and Joy, *Mt. Wilson Contr.*, No. 210; *Astrophysical Journal*, **54**, 9, 1921. These results are vital for the remainder of the discussion. Without them it could not have been undertaken.

[3] Kapteyn and Adams, *Mt. Wilson Comm.*, No. 1; *Proc. Nat. Acad. of Sciences*, **1**, 14, 1915. Adams, Strömberg, and Joy, *op. cit.*, p. 15.

[4] *Ibid.*, p. 13.

For a Gaussian distribution of the logarithms of the space velocities, the relation of the mean square velocity to the arithmetical and geometrical means is expressed by[1]

$$\left.\begin{aligned}\log \overline{v^2} &= 2\log \bar{v} + \frac{1}{2h^2\,\text{Mod.}} = 2\log \bar{v} + 0.148\\ \log \overline{v^2} &= 2\log \underline{v} + \frac{1}{h^2\,\text{Mod.}} = 2\log \underline{v} + 0.296\end{aligned}\right\} \qquad (12)$$

where h is the modulus of the distribution function. It is assumed that the value of h for types F to M given in *Contribution* No. 210 applies also to the B and A stars.

The mean radial velocities taken from Campbell's papers[2] are

B3, 6.2; B8.5, 6.7; A0, 10.3; A2, 11.4; A5, 12.6.

The corresponding mean square velocities were obtained by doubling the radial velocities, as indicated above, and substituting the results into the first of (12). For the later types the values of $\log \overline{v^2}$ were derived from the data for $\underline{v}$ given in *Contribution* No. 210. These were plotted—$\underline{v}$ against corresponding M—thus giving four curves, which refer to the approximate mean types F5, G5, K3, and Ma+. The mean absolute magnitudes of the dwarf stars of these types were then interpolated from Table IV and used as arguments to read from the curves values of $\underline{v}$ corresponding to the average dwarf of each of the four types. Graphical interpolation and an extrapolation to F0, followed by substitution into the second of (12), gave finally the required values of $\log \overline{v^2}$ for every

---

[1] The second equation is found by applying the mean value theorem to the frequency function

$$F(v) = \frac{h\,\text{Mod.}}{\sqrt{\pi}} e^{-h^2(\log v - \log \underline{v})^2}$$

The first results from the combination of the second with

$$\log \bar{v} = \log \underline{v} + \frac{1}{4h^2\,\text{Mod.}}$$

which is given by Adams, Strömberg, and Joy, *op. cit.*, p. 17.

[2] *Lick Observatory Bulletins*, **6**, 127, 1911; **7**, 28, 1912.

half-interval of spectral type from F0 to Ma. These mean-square velocities are not affected by any smoothing from type to type, since the interpolation card was drawn *through* the points derived from the four curves giving $\underline{v}$ the function of M.

The results, including those for log $\mathcal{M}\overline{v^2}$, are in the first six columns of Table IX. With the exceptions of the B stars, the values of the energy show close accordance. For a range of 10 to 1 in the masses the average deviation in $\mathcal{M}\overline{v^2}$ is 9 per cent, and, by a moderate amount of smoothing, is easily reduced to 3 per cent. The large divergence for the B stars seems to be real. It cannot be supposed that the adopted values for their masses are in error by 50 per cent, nor does it seem permissible to assume that the velocities could by any chance be increased by the 2 or 3 km necessary to bring the energy up to the mean for the other types. It is more likely that the velocities are already too large, because of undetected spectroscopic binaries among the stars combined in the means.

TABLE IX

THE ENERGY CONSTANT

Sp.	$\overline{M}$	Log $\mathcal{M}$	Log $\overline{v^2}$	Log $\mathcal{M}\overline{v^2}$	Residual	Log θ^2	Log $\mathcal{M}\theta^2$	Residual
B3	−0.6	0.95	2.34	(3.29)	(+0.28)	1.74	(2.69)	(+0.07)
B8.5	+0.4	0.81	2.40	(3.21)	(+ .36)	1.62	(2.43)	(+ .33)
A0	0.7	0.78	2.78	3.56	+ .01	2.00	2.78	− .02
A2	1.0	0.70	2.87	3.57	.00	2.10	2.80	− .04
A5	1.5	0.60	2.95	3.55	+ .02	2.19	2.79	− .03
F0	2.4	0.40	3.11	3.51	+ .06	2.36	2.76	.00
F5	3.3	0.19	3.36	3.55	+ .02	2.56	2.75	+ .01
G0	4.4	9.99	3.62	3.61	− .04	2.76	2.75	+ .01
G5	5.2	9.88	3.78	3.66	− .09	2.84	2.72	+ .04
K0	5.9	9.83	3.80	3.63	− .06	2.84	2.67	+ .09
K5	7.1	9.79	3.74	3.53	+ .04	2.92	2.71	+ .05
Ma	9.8	9.77	3.78	3.55	+0.02	3.06	2.83	−0.07
Means, average deviations				3.57	±0.036	......	2.76	±0.036

The inclusion of the K-term as a velocity removes only a small part of the divergence. Thus, for any radial direction, the resultant mean-square velocity $\overline{r^2}$ would be

$$\overline{r^2}=\overline{v^2}+K^2-\overline{2vK\cos\alpha}=\overline{v^2}+K^2$$

where α is the inclination of the space velocities to the given line of sight. Extending this to all radial directions, we have for the entire group of B3 stars,

$$\overline{r^2}=(14.8)^2+(4.7)^2=241.1;\ \log \mathcal{M}\overline{v^2}=3.33,$$

an increase of only 0.04 in the logarithm of the energy.

The foregoing results depend upon the assumptions that the mean space velocities of the B and A stars may be found by doubling the mean radial velocities, and that the modulus h applies equally to all types. We may avoid these assumptions by restricting the test to the mobility in the line of sight. For this comparison the K-term has been included throughout. The mean radial velocities from Campbell's data thus become[1]

B3, 7.45; B8.5, 6.50; A0, 10.1; A2, 11.3; A5, 12.5 km/sec.

For the remaining types *Contribution* No. 210 was again used, the values being read from curves for radial velocity θ as a function of absolute magnitude as in the case of $\underline{v}$. The values of $\log \mathcal{M}\theta^2$ (eighth column, Table IX) show about the same degree of accordance as those of $\log \mathcal{M}\overline{v^2}$, the average deviations, without smoothing, again being 9 per cent. The inclusion of the K-term as a part of the radial velocity has brought the B3 stars into agreement with the mean for types A to Ma, and only the B8–B9 stars are now divergent.[2] But this improved agreement is not to be taken very seriously, and perhaps the most satisfactory point of view is that since the B stars are peculiar in many particulars, the abnormality shown by Table IX should not be looked upon as surprising, especially when it is remembered that they form a local aggregation[1] and that their masses are among the largest known.

---

[1] *Ibid.*, **6**, 108. The means for the B stars are those found by correcting Campbell's values V_1 by 4.7 (B0–B5) and 4.1 (B8–B9). For the A stars the mean of V_2, *Lick Observatory Bulletin*, **7**, 20, has been used without correction.

[2] Freundlich, *Physikalische Zeitschrift*, **20**, 561, 1919, has attempted to show that the K-term may be identified with the displacement of spectral lines toward the red required by the theory of relativity. This displacement may be involved, but results given later in this paper indicate that other factors must also play a part. See footnote p. 48.

There are suggestions of systematic divergencies in both sets of residuals, but by forming the means of the two series of values of the energy constant, these disappear, and the average deviation is reduced to 5 per cent.

Were the condition of equipartition exactly satisfied, we should have

$$\overline{v^2} = 3\,\overline{\theta^2}\,.$$

For a Gaussian distribution of the radial velocities

$$\overline{\theta^2} = \frac{\pi}{2}\,\bar{\theta}^2$$

where $\bar{\theta}^2$ is the square of the arithmetical mean radial velocity used in Table IX. For unit mass, $\log \overline{v^2} = 3.57$; and since $\log \pi/2 = 0.20$, $\log \overline{\theta^2} = 2.96$. The mean-square velocities therefore appear to have a ratio of 4 to 1 instead of 3 to 1. It is known, however, that the radial velocities do not follow a Gaussian distribution closely.

Approaching the matter from another direction, we have for a random distribution in direction, irrespective of the form of the frequency function of the magnitudes of the velocities,

$$\bar{v} = 2\,\bar{\theta}.$$

Substituting into the first of equations (12), we find the condition

$$\log \overline{v^2} = \log \theta^2 + 0.75$$

where θ^2 denotes the square of the arithmetical mean. The difference in the two members of this equation is 0.06 in the logarithm, or 11 per cent, a much better agreement than before. The remaining difference is doubtless to be attributed to the fact that the velocity distribution is not random; stream motion produces a preferential drift parallel to the galactic plane.

---

[1] This result follows directly from an analysis of star counts. Seares, *Publications of the Astronomical Society of the Pacific*, **30**, 114, 115, 1918. Shapley in recent papers has accumulated much additional evidence: *Mt. Wilson Contr.*, Nos. 157, 161; *Astrophysical Journal*, **49**, 311, 1918, and **50**, 107, 1919; *Mt. Wilson Communications*, Nos. 54, 64; *Proceedings of the National Academy of Sciences*, **4**, 224, 1918; **5**, 434, 1919.

In spite of the known departures from Maxwell's law, there is, with the exception of the B stars, a surprisingly close approach to a state of equipartition. That the deviations are no larger is remarkable,[1] and suggests that for the stars considered (dwarfs) there is little difference between the different spectral types in the average contribution of stream motion to the total energy of translation. Since the unit of mass—that of the sun—is 1.9×10^{33} grams, and since the velocities are expressed in kilometers per second, the mean kinetic energy of translation is of the order of 3.5×10^{46} ergs.

9. DERIVATION OF MASS FROM THE ENERGY-CONSTANT

The constancy of the energy is apparently such as to justify an attempt to evaluate the masses of stars having luminosities and velocities different from those appearing in Table IX. Thus by reading from the curves referred to above the values of $\underline{v}$ and θ corresponding to different values of M and combining them with the energy-constant, more or less hypothetical values of the corresponding masses can be obtained.

This procedure assumes that equipartition holds for the stars of high luminosity as well as the dwarfs, for which alone a direct test has been possible. The behavior of the B stars suggests caution in an extension of the principle to other giants; but since the translatory energy of the B's is of the same order as that found for the dwarfs, it is perhaps not too much to expect that the use of the energy constant will lead to masses for later-type giants which will also be of the right order of magnitude.

The results obtained in this manner are given in Table X. The values of log $\mathcal{M}$ are the means of the two values found with the aid of $\underline{v}$ and θ from the two energy constants, log $\mathcal{M}\overline{\underline{v}^2}$ and log $\mathcal{M}\theta^2$. To indicate the agreement between the masses derived with the aid of the two velocities, the differences log $\mathcal{M}_v -$ log $\mathcal{M}_\theta$ are also given in the table. In general these are reasonably small, although for the group of Ma stars the extreme values correspond to a two-to-one ratio in the masses. The data of Table X express, with more detail and precision, the correlation between mass and luminosity found by van Maanen.[1]

---

[1] In this connection see Jeans, *Problems of Cosmogony*, p. 238, 1919.

TABLE X

MASS AND LUMINOSITY

M	F5		G5		K3		Ma+	
	log $\mathcal{M}$	Diff.	log $\mathcal{M}$	Diff.	log $\mathcal{M}$	Diff.	log $\mathcal{M}$	Diff.
−3	......	......	0.74	−0.08	......	......	0.98	−0.36
−2	0.78	−0.02	.62	+ .02	......	......	.64	− .02
−1	.74	− .02	.51	+ .08	0.72	−0.10	.41	+ .16
0	.68	− .02	.38	+ .10	.45	+ .08	.23	+ .24
+1	.62	+ .02	.28	+ .14	.28	+ .14	0.08	+ .30
2	.51	.00	.17	+ .11	.17	+ .12	......	......
3	.30	− .02	0.06	+ .06	.07	+ .08	......	......
4	0.01	−0.04	9.96	− .02	0.01	+ .04	......	......
5	9.77	......	9.88	− .11	9.94	− .02	......	......
6	......	......	9.81	−0.21	9.89	− .04	......	......
7	......	......	......	......	9.84	− .06	......	......
8	......	......	......	......	9.81	−0.08	......	......
10	......	......	......	......	......	......	9.68	+0.14

The general relation of these results to spectral type and absolute magnitude is best seen by means of the diagram in Figure 2. This was prepared by plotting the data in Table X and reading from the resulting curves the values of M coresponding to integral values of the mass $\mathcal{M}$. These values of M were then plotted in the diagram of Figure 2, along with similar points on the dwarf branch, whose co-ordinates were derived from the second and last columns of Table IV. Through these points were drawn the full-line curves of the figure, which thus represent lines of equal mass.

The curves are highly irregular, the maximum near G0 followed by the minimum at K0–K5 being particularly noteworthy. Much of this disappears, however, when the ordinary visual absolute magnitude is replaced by the bolometric magnitude, which measures the total radiation and is therefore the quantity of physical significance. The reductions to bolometric magnitude (see following section) of interest here are

G0, −0.09; G5, −0.30; K0, −0.73; K5, −1.30; Ma, −1.60 mag.

[1] *Publications of the Astronomical Society of the Pacific*, **31**, 231, 1919.

The application of these corrections would practically remove the minima from the curves for all but the largest masses, and these

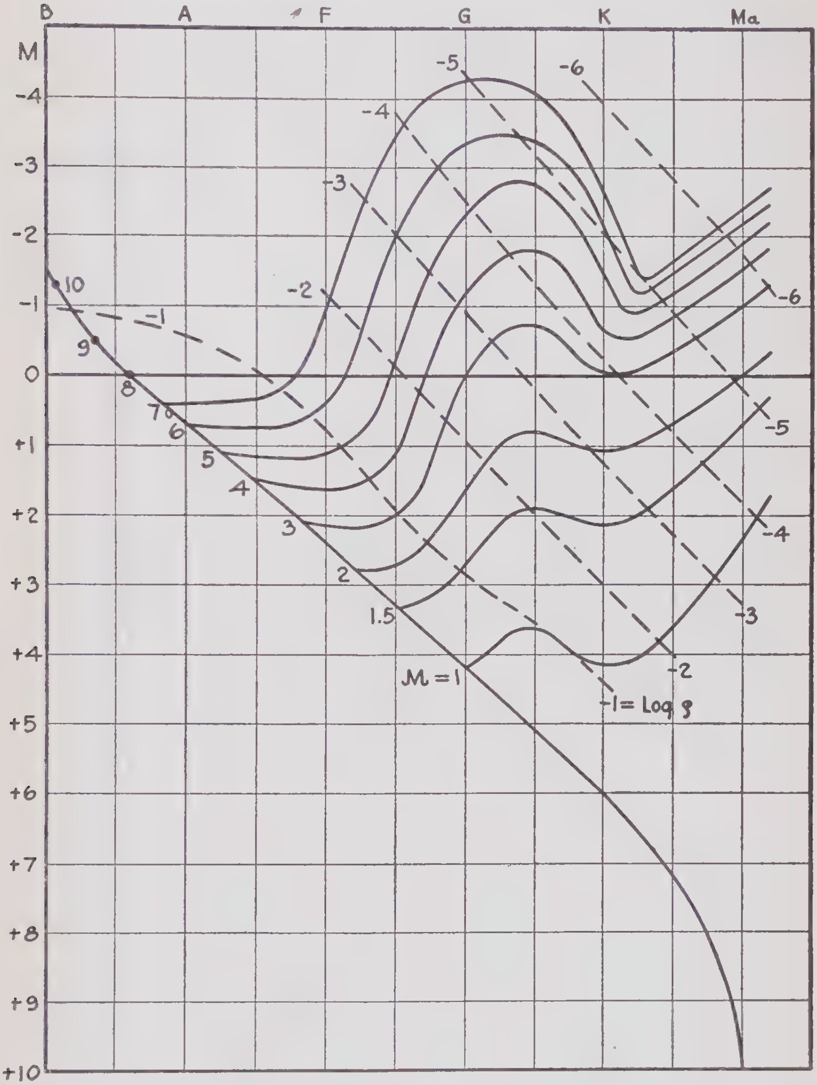

FIG. 2.—Distribution of mass (full-line) and mean density (broken curves) derived from the principle of equipartition. The full-line curve running downward to the right is the line of the maximum frequency of the dwarfs.

are relatively uncertain because they depend more or less upon extrapolations of the data in Table X.

To explain the derivation of the lines of equal density, which are also shown in Figure 2, it is necessary to consider the question of surface brightness.

10. SURFACE BRIGHTNESS

To derive values of surface brightness we may start from Stefan's law

$$E=\sigma T^4 \tag{13}$$

where E represents the total energy radiated per unit area of the surface of a star whose effective temperature is T. Let J be the integrated visual intensity, referred to the same unit of surface, and write $J=\alpha E$, whence

$$2.5 \log E=2.5 \log J-2.5 \log \alpha$$

and, by substitution into (13),

$$2.5 \log J-2.5 \log \alpha=2.5 \log \sigma+10 \log T.$$

Further, let M_B and j represent the total energy and surface brightness, respectively, expressed in magnitudes. The former is the bolometric absolute magnitude, while $M=-2.5 \log (J\times \text{Area})$ is the ordinary visual absolute magnitude. Since α is also the ratio of the visual energy to total energy received from the entire surface of the star,

$$-2.5 \log \alpha=M-M_B$$

and

$$j=M-M_B-10 \log T+\text{const.} \tag{14}$$

where the constant involves $\log \sigma$ and an additional constant depending on the zero point chosen for M_B. Eddington[1] has calculated values of the difference between the visual and bolometric absolute magnitudes $M-M_B$ for a range of temperatures including the normal classes of spectra. Through these values, which are based upon Nutting's measures of visual sensibility for the normal eye, j, by (14), becomes a simple function of T.

---

[1] *Monthly Notices*, **77**, 605, 1917. Nutting's measures of visual sensibility, which are the basis of Eddington's calculation, are practically identical with the A.I.E. visibility-curve.

Results found by this equation may be checked by an equivalent formula derived by Hertzsprung in 1906. Starting from Planck's law and the visibility measurements of Langley, Abney, and others, he found[1]

$$j_H = +2.3\left(\frac{c}{T}\right)^{0.93} + \text{const.} \qquad (15)$$

in which c is the second constant in Planck's formula, for which the value adopted is 14300. Both (14) and (15) involve quadratures, and, starting as they do from entirely different observational data, independently discussed, provide an excellent numerical control. How close the agreement is may be seen from Table XI.

TABLE XI

SURFACE BRIGHTNESS AND TEMPERATURE

T	$M-M_B$	j	j_H	$j-j_H$
2540°	+2.59	+6.32	+6.32	0.00
3000	+1.71	+4.72	+4.68	+ 4
3600	+0.95	+3.17	+3.16	+ 1
4500	+0.35	+1.60	+1.58	+ 2
6000	0.00	0.00	0.00	0
7500	+0.02	−0.95	−0.93	− 2
9000	+0.12	−1.64	−1.62	− 2
10500	+0.31	−2.12	−2.09	− 3
12000	+0.53	−2.48	−2.45	−0.03

The values of $M-M_B$ have been taken directly from Eddington's table. The maximum difference between the results from the two formulae is only 0.04 mag., which is ample.

To connect these results with spectral type, Wilsing's spectral-photometric measures of the reciprocal temperature, c/T, of 199 stars[2] were plotted against their respective types. The ordinates (c/T) of the curve thus obtained are in the second column of Table XII. The corresponding effective temperature, T, and the surface brightness, j, calculated by the foregoing formulae and expressed in magnitudes ($\odot = 0.00$), are in the third and fourth columns, respectively.

[1] *Zeitschrift für wissenschaftliche Photographie*, **4**, 43, 1906.

[2] *Potsdam Publikationen*, No. 74, 1919.

With few exceptions, the stars in Wilsing's list are all giants whose mean absolute magnitudes, with sufficient approximation, may be assumed to be zero. To extend the results to other luminosities, use was made of the Mount Wilson color indices,[1] whose values are in the fifth and last columns of Table XII, those for the dwarfs corresponding to the mean absolute magnitudes in the column immediately preceding. The color indices were reduced to Schwarzschild's absolute system,[2] whose relation to effective temperature is known. This gave the relation between the Mount Wilson values and the temperature for both giants and dwarfs. Owing to various necessary assumptions the temperatures thus found for the giant stars differ slightly from the adopted values given in the first half of Table XII, and this systematic difference was made the basis for reducing the calculated temperatures for the dwarfs to the adopted system of Wilsing. The results, in

TABLE XII

SPECTRUM, EFFECTIVE TEMPERATURE, AND SURFACE BRIGHTNESS

Sp.	Giants, $M = 0$				Dwarfs				
	c/T	T	j	MW CI	c/T	T	j	M	MW CI
B0	1.36	10500°	−2.28	−0.32	......	......	......	......	....
B5	1.43	10000	2.14	−0.17	......	......	......	......	....
A0	1.55	9230	1.89	0.00	......	......	......	......	....
A5	1.76	8110	1.45	+0.19	......	......	......	......	....
F0	2.04	7000	0.88	0.38	......	......	......	......	....
F5	2.35	6080	−0.26	0.62	2.35	6080	−0.26	+3.3	+0.62
G0	2.70	5300	+0.44	0.86	2.48	5770	0.00	4.4	0.72
G5	3.10	4610	1.24	1.15	2.60	5500	+0.25	5.2	0.83
K0	3.70	3860	2.41	1.48	2.93	4880	0.90	5.9	0.99
K5	4.37	3270	3.71	1.84	3.47	4120	1.96	7.1	1.26
Ma	4.65	3080	4.25	1.88	4.30	3330	+3.58	+9.8	+1.76
Mb	4.82	2960	4.58	+1.88	......	......	......	......	....
Mc	4.94	2890	+4.81	......	......	......	......	......	....

---

[1] These results, which have not hitherto been published, are still to be regarded as provisional. They take account of the important difference in color between giants and dwarfs, which cannot be disregarded in any discussion of the surface brightness of late-type stars. See *Mt. Wilson Comm.*, No. 59; *Proc. Nat. Acad. of Sciences*, 5, 232, 1919.

[2] *Göttingen Aktinometrie*, B, 29, 1912.

the sixth column of Table XII, were then used to compute the corresponding values of j as before.[1]

The difference in surface brightness between giants and dwarfs is large, and cannot be neglected. Unfortunately, the change in j with absolute magnitude is not well determined, for this must be inferred from the behavior of the color indices, and the data available at present do not extend to stars of the highest luminosity. This means that extrapolation will be necessary, and, in view of the consequent uncertainty, a simple linear relation of surface brightness to absolute magnitude has been used in the calculation of j for all values of M not appearing directly in Table XII.

The reliability of the foregoing results depends upon the possibility of representing the energy distribution in the spectra of stars of different types by means of the black-body radiation formula. It should be noted that it is not at all a question of agreement of the effective temperature, calculated from the radiation formula, with the true mean temperature of the radiating layers in the star's atmosphere. In general these will not agree. The stars are not perfect radiators; further, general and selective absorption deforms the energy-curve to such an extent that effective temperature cannot be an accurate measure of true temperature; but in the visible region the resultant curve seems to agree[2] approximately with a black-body curve, although not with the curve corresponding to the true mean temperature. That being the case, the surface brightness is immediately calculable by the foregoing formulae, provided the effective temperature corresponding to the deformed curve is employed for the computation; and it is of course just this temperature which is given by Wilsing's observations.

[1] The values of j in Table XII may be compared with Öpik, *Astrophysical Journal*, **44**, 296, 1916; Russell, *Publications of the Astronomical Society of the Pacific*, **32**, 307, 1920. Related questions are discussed by Wilsing, *Potsdam Publikationen*, No. 76, 1920; *Astronomische Nachrichten*, **214**, 185, 1921.

[2] See, for example, Wilsing, *Potsdam Publikationen*, No. 74, pp. 17, 18. The mean systematic deviations of the observed values of the energy at different points in the visual spectrum from Planck's formula are small. Further, Milne, *Monthly Notices*, **81**, 378, 1921, finds that the theoretical spectrum for non-selective absorption is practically identical with that corresponding to black-body radiation, the principal difference being a bodily displacement of the energy-curve, corresponding to a reduction of 3 per cent in the constant of Wien's displacement law.

The possibility of systematic error in the values of the temperature is more serious. Those for the B stars given in Table XII are almost certainly too small. The early-type stars in Wilsing's list are not numerous, and the dispersion in the values of c/T is large. In fact, the data would be almost equally well represented by assigning a temperature of 12,000° to B0, which would change j from -2.28 to -2.67. The value for B5 would also be slightly changed, but that for A0 can scarcely be modified without violence to the data.[1]

It will be noted that T for a G0 giant is nearly 500° lower than that for a dwarf of the same spectrum. Some question as to the reliability of Wilsing's measures has been felt because of the low value found for G0 stars as compared with the probable temperature of the sun. But the objects observed by him are giants; with proper allowance for the sun's absolute magnitude (4.85), the corresponding temperature from Wilsing's data would be about 5820°, which is not far from the values usually assigned, and indeed, agrees well with that derived by Abbot[2] from the solar constant (5860°).

A partial control of the values of j in Table XII is afforded by Pease's recent measures of the angular diameters of stars with the interferometer. In this connection, and for later use, it is convenient to insert at this point the following formulae, all easily derived, expressing relations between the various physical constants of a star: angular diameter (d), linear diameter (D), mass ($\mathcal{M}$), density (ρ), apparent (m) and absolute (M) magnitude, and surface brightness (j).

$$\log d = 0.2\,(j-m) - 2.061 \tag{16}$$

$$\log D = 0.2\,(j-m) - \log \pi - 0.030 \tag{17}$$

$$\log D = 0.2\,(j-M) + 0.970 \tag{18}$$

$$D = 107.4\,d/\pi \tag{19}$$

$$j = 5 \log d + m + 10.30 \tag{20}$$

$$\log \rho = \log \mathcal{M} - 3 \log R + 0.14 \tag{21}$$

$$\log \rho = \log \mathcal{M} + 0.6\,(M-j) - 2.77 \tag{22}$$

---

[1] See also Rosenberg, *Abhandlungen der Kaiserl. Leop.-Karol. deutschen Akademie der Naturforscher*, 150, No. 2, 1914.

[2] *Op. cit.*, p. 114.

These formulae give d in seconds of arc, D and $\mathcal{M}$ in terms of the solar diameter and mass, and j in magnitudes, the value for the sun being 0; the unit for ρ is the density of water. The numerical constants depend upon the following data for the sun: $D = 865{,}000$ miles, $d = 1920''$, distance from earth 92,930,000 miles, $m = -26.72$, $M = +4.85$. Equations (16) and (17) are the equivalent of formulae already given by Russell.[1]

Proceeding now to a comparison with the results of Pease's measures, we have the data in Table XIII. The "observed" values of j derived from the angular diameter by (20) are in the sixth line of the table. Immediately below are the calculated results interpolated from Table XII. It seems unlikely that the mean systematic difference for O−C will exceed one- or two-tenths of a magnitude. The effect of darkening at the limb has not been taken into account, either in the measures of d or in the calculation of j. Nor has the question of a possible differential effect from this source upon the observed and calculated values of j been considered, for it is evident that this cannot be large.

TABLE XIII

COMPARISON WITH MEASURED ANGULAR DIAMETERS*

	α Orionis	α Boötis	α Scorpii
Sp.	Ma	Ko	Map
m	+0.9	+0.2	+1.2
π	0.″020	0.″095	0.″0085
M	−2.6	+0.1	−4.2
d (Pease)	0.″047	0.″022	0.″040
Obs. j, equation (20)	+4.6	+2.2	+4.5
Cal. j, Table XII	+4.4	+2.4	+4.5
O–C	+0.2	−0.2	0.0
Obs. D, equation (19)	252	25	506
Cal. D, equation (18)	235	27	513
Approx. $\mathcal{M}$ (Fig. 3)	8	3	15
Approx. log ρ (Fig. 3)	−6.2	−3.8	−6.6

* Michelson and Pease, *Mt. Wilson Contr.*, No. 203; *Astrophysical Journal*, **53**, 249, 1921. Pease, *Publications Astronomical Society of the Pacific*, **33**, 171, 204, 1921. The parallax of α Scorpii assumes it to be a member of the Scorpius group. The other two parallaxes are weighted mean values.

It is of interest, further, to compare the values for the linear diameters calculated from the measured angular diameter by (19) with those derived from (17) or (18) with the aid of the adopted values of j. The results are in the third and fourth lines from the bottom of table. On the whole, Pease's measures afford an excellent confirmation of the surface brightness found for late-type stars of high luminosity, and at present there seems to be no observational evidence which would justify a modification of the values adopted.[1]

---

[1] *Publications of the Astronomical Society of the Pacific*, **32**, 307, 1920.

11. DISTRIBUTION OF DENSITY

The densities are now easily calculated by equation (22) with the aid of values of j from Table XII. The results for stars on the dwarf branch, including the B's, are in the fourth column of Table XIV, which also gives values for the mean linear diameters D found by (18).

TABLE XIV

LUMINOSITY, MASS, MEAN DENSITY, AND DIAMETER

(Units for $\mathcal{M}$ and D are values for sun; for ρ, that of water)

Sp.	Dwarf Branch				Giants, $M=0$			Giants, $\mathcal{M}=10$		
	M	$\mathcal{M}$	ρ	D	$\mathcal{M}$	ρ	D	M	ρ	D
B0	−1.60	10	0.04^5	6.8	.....	....	3.2	−1.2	0.08	6
B5	−0.20	8.3	0.20	3.8	8.2	0.26	3.5	−1.8	0.03	8
A0	+0.70	6.0	0.36	2.8	7.0	0.16	3.9	−2.4	0.008	12
A5	+1.50	4.0	0.40	2.4	5.6	0.071	4.8	−3.1	0.002	20
F0	+2.40	2.5	0.40	2.0	4.3	0.025	6.2	−3.6	0.0004	32
F5	+3.35	1.5	0.39	1.8	3.2	0.0078	8.3	−4.0	0.0001	52
G0	+4.35	1.0	0.68	1.26	2.6	0.0025	11.5	−3.9	0.00002	83
G5	+5.20	0.76	1.2	0.96	2.8	0.00087	17	−3.3	0.00001	102
K0	+6.00	0.68	1.3	0.89	3.0	0.00018	28	−2.3	0.00001	107
K5	+7.20	0.62	1.4	0.83	2.6	0.000026	51	−2.2	0.000002	182
Ma	+9.80	0.59	5.4	0.54	2.0	0.0000096	66	−3.0	0.0000006	288

For the determination of the equal-density lines (dotted) shown in Figure 2, values of M were read from each mass line in the diagram for every half-interval of spectrum. The use of (22) then gave the values of log ρ corresponding to each of these points in the sequence of spectral type. Plots of these results—log ρ against spectrum—then led to a series of curves, one for each integral value of the mass (also one for $\mathcal{M}=1.5$), from which were read spectral types corresponding to integral values of log ρ. The corresponding points were marked on the diagram and connected by the dotted lines shown in the figure.

---

[1] Mr. Pease has kindly placed at my disposal provisional results for three other stars. The observed and theoretical values of j and d, or D, are here also in excellent agreement, although the accidental deviations are larger than those shown in Table XIII.

Within the limits considered, and with the exception of that for $\log \rho = -1$, the curves of equal density are sensibly linear; the regularity of their spacing is remarkable. Including the line for $\log \rho = -1$ from A5 onward through the later types, the mean density corresponding to any given spectrum and absolute magnitude is represented by the formula

$$\left.\begin{array}{c}\log \rho = -1.22\,S + 0.57\,M + 1.11 \\ (S = 0 \text{ for B0, 1 for A0, etc.})\end{array}\right\} \qquad (23)$$

with a probable error of about 15 per cent, over a range in ρ extending from 0.1 to 0.000001.

The question now arises as to what means can be found for testing the validity of these results. Some control is obviously necessary, for with the exception of the masses and densities along the dwarf branch, the whole scheme of mass and density distribution depends upon the assumed applicability of the principle of equipartition. In this connection, the eclipsing variables, many of which are known to be of exceptionally low density, immediately suggest themselves as suitable for a test. The weak point, however, is that we do not know their absolute magnitudes, except in a very few cases. Any attempt to use hypothetical absolute magnitudes fails, because it involves an assumption for the mass, and this, as shown by (22), is equivalent to a direct assumption for the density.

Some general indications, however, can be obtained. With slight revisions of spectral classification, Shapley's data[1] for the densities of eclipsing variables give the following mean values:

Sp.	ρ	No. Stars
B6	0.12	15
A0+	0.20	48
F(dwarfs)	0.35	9

For these groups of B and A stars the values of $\log \rho$ are -0.9 and -0.7, respectively. From Figure 2 the corresponding values of M are seen to be -0.6 and $+0.2$. These are of the order to be expected, and are obviously possible values. The value $\rho=0.35$ for the F-type dwarfs agrees closely with that found here for F5, namely, 0.39. For the dwarfs the dispersion in absolute magnitude is so small that lack of knowledge of the luminosities gives rise to no appreciable error.

---

[1] *Contributions from Princeton University Observatory*, No. 3, p. 124, 1915.

These results are all satisfactory, as far as they go, but they do not reach that part of the diagram which is involved in the greatest doubt, namely the region of very high luminosity and exceptionally low density. On the other hand, if the validity of the mass and density distribution can once be established, the densities of the eclipsing variables should give a reliable determination of their distances. Fortunately, the uncertainty can be removed to a large extent with the aid of the Cepheid variables.

12. REVISION OF MASSES AND DENSITIES BY MEANS OF CEPHEID VARIABLES

There are still difficulties connected with the pulsation hypothesis as a means of explaining Cepheid variation, although there seems little doubt that, in some form or other, it must be used to account for the changes in brightness of these stars. That being the case, the mean density must vary inversely as the square of the period. Hence[1]

$$\log \rho = -2 \log P + \text{const.} \tag{24}$$

Further, the period-luminosity relation[2]

$$M = f\,(P) \tag{25}$$

---

[1] The exact form of the relation of density to period as applied to Cepheids is possibly open to some question. Emden, *Gaskugeln*, p. 451, 1907, finds for ellipsoidal oscillations of a polytropic gas sphere

$$P \propto (m\,\rho)^{-\frac{1}{2}}$$

where m is the order of the harmonic oscillation; the important vibration corresponds to $m=2$. Eddington, *Monthly Notices*, **79,** 2, 1918; 177, 1919, discusses pulsations which are symmetrical about the star's center and finds a result equivalent to (24), with the exception that the constant is replaced by a slowly varying function of the specific heats and the ratio of radiation-pressure to gravitation, the latter increasing with the mass. For a first approximation we may adopt (24).

[2] Shapley, *Mt. Wilson Contr.*, No. 151; *Astrophysical Journal*, **48,** 89, 1918.

determines the absolute magnitude. With M and the spectral type as arguments, $\log \rho$ and $\mathcal{M}$ can be interpolated from the mass-density diagram. Then,

a) The interpolated values of $\log \rho$ may be compared with those calculated by (24), the constant being adjusted to give the best representation of the densities of the entire group of stars. Since the range in ρ as determined by (24) is from about 0.1 to 0.00001, the control on the densities should be effective.

b) Having determined the constant in (24), we may write (22) in the form

$$\log \mathcal{M} = -2 \log P - 0.6\,(M - j) + \text{const.} \tag{26}$$

which expresses the mass of a Cepheid variable as a function of its period and surface brightness, for, by (25), M is a function of the period alone. The values of $\mathcal{M}$ interpolated from the diagram may be compared with those calculated by (26). This checks the distribution of mass.

c) Finally, with spectral type and $\log \rho$ calculated from (24), we may interpolate M from the diagram. The absolute magnitudes thus found may then be compared with the period-luminosity relation (25). This is not an independent test, but exhibits the results of (*a*) in a different form.

Because of the enormous range in the density, the application of these tests will mean little except in the case of stars of accurately determined spectra. This makes trouble at once, for the type of a Cepheid, in so far as determined from the hydrogen lines at least, varies with its brightness, as was first clearly shown by Pease's[1] observations of RS Boötis. Isolated determinations of spectrum based on the appearance of these lines are therefore unsuitable for the comparisons. Adams and Joy,[2] on the other hand, have shown that many spectral characteristics change little or not at all as the light of the star varies; their "estimated" spectral classes are practically independent of phase.

---

[1] *Publications of the Astronomical Society of the Pacific*, **26**, 256, 1914.

[2] *Mt. Wilson Comm.*, No. 53; *Proceedings of the National Academy of Sciences*, **4**, 129, 1918.

The list of spectroscopic parallaxes[1] includes twenty-nine Cepheids for which estimated types are available. One of these, RY Boötis, although usually classed as a Cepheid, does not show Cepheid spectral characteristics and has an absolute magnitude at variance with that derived from the period-luminosity relation. Further, three cluster-type Cepheids, SU Aurigae (8.7), SU Draconis (9.2), and SW Draconis (10.0), and the long-period Cepheid V Vulpeculae (8.6) are so faint that the types assigned are less certain than the others. The classification of faint stars, observed with low dispersion, is likely to be influenced to some extent by the hydrogen lines. The case of V Vulpeculae, moreover, is peculiar. The light-curve is irregular; and the period-luminosity relation leads to a value of M which not only differs widely from that derived from the spectrum, but falls outside the limits of the mass-density diagram. These five stars were therefore excluded,[2] leaving a total of twenty-four.

These data are supplemented by Shapley's[3] results for twenty Cepheids, based on systematic observations of spectral characteristics that do vary with the changes in light. The median value of the type, which was used for the discussion, is about 0.3 of a spectral interval earlier than the estimated spectrum.

This difference will lead to different values of the constants in the foregoing formulae, unless the value of M and the spectral type are referred to the same phase. Thus, the estimated type agrees with the hydrogen-line type at, or very near, the time of minimum brightness (estimated *minus* hydrogen-line type at minimum $= -0.1$ spectral interval). Hence for the comparisons, the minimum, and not the median M (the period-luminosity relation gives the latter), should be associated with the estimated spectra. The simplest procedure, however, is to use the median M and subtract 0.3 of an interval from the estimated spectra before making interpolations from the diagram. Sixteen stars are common to the two lists, but owing to the different methods of classification used, the duplicate observations have been treated as separate stars.

---

[1] *Mt. Wilson Contr.*, No. 199; *Astrophysical Journal*, **53**, 13, 1921.

[2] It was not noted until after the comparisons had been finished that, on the criterion of brightness, W Serpentis (9.0) should also have been excluded.

[3] *Mt. Wilson Contr.*, No. 124; *Astrophysical Journal*, **44**, 273, 1916. In general the means of the limiting values of the type as given by Shapley have been adopted. Deviations from this rule occur in a few cases where the distribution of the observations is such that the mean does not correspond to median brightness of the variable.

The results of the application of tests (*a*), (*b*), and (*c*) are summarized in Table XV, which gives the range in log ρ, log $\mathcal{M}$, and M over which the comparisons were made, and the average differences resulting therefrom. Thus, on the basis of estimated spectra, formula (24) represents the density distribution in Figure 2 over a range in log ρ from -1.1 to -4.8, with an average difference of ± 0.15. Similarly, the values of M interpolated from the diagram in the interval -0.3 to -4.7 agree with those from the period-luminosity relation within ± 0.30 mag. We conclude at once that the masses and densities derived with the aid of the principle of equipartition are of the right order of magnitude, at least as far as type G3, which is the latest occurring among the Cepheids used.

TABLE XV

REPRESENTATION OF MASSES AND DENSITIES
EQUATIONS (24) TO (26) AND FIGURE 2

TEST	RANGE	AVERAGE DIFFERENCE	
		Est. Sp.	H.L. Sp.
(*a*) log ρ	-1.1 to -4.8	± 0.15	± 0.18
(*b*) log $\mathcal{M}$	0.46 to 1.28	0.15	0.16
(*c*) M	-0.3 to -4.7	± 0.30	± 0.32

A classification of the differences in log ρ and log $\mathcal{M}$ according to M, which is also more or less a classification according to spectrum, revealed, however, the presence of systematic divergences. These run from about -0.18 (at $M = -0.7$, A8) to $+0.18$ (at $M = -3.8$, F8) in the logarithms of both quantities. The algebraic signs mean that the range of mass in Figure 2, for a given interval in M, is too small, that the masses of the most luminous Cepheids are larger, and those of less luminous stars smaller, than the values given by the diagram. The density lines, on the other hand, are too closely spaced.

These differences were made the basis of a readjustment of the lines of mass and density. The percentage divergence in ρ and $\mathcal{M}$

is the same, as it must be by (22), but since the scale for $\mathcal{M}$ is much larger than that for ρ (in passing from one curve to the next the mass changes by one unit while ρ changes tenfold), the adjustments were made in the mass-curves, the densities being computed by (22) as before. The masses and densities along the dwarf branch, of course, remain unchanged.

The result of several trials is the diagram shown in Figure 3. A repetition of tests (*a*), (*b*), and (*c*) gave the differences shown in the last six columns of Table XVI, the first column under each of the headings log ρ, log $\mathcal{M}$, and M referring to estimated spectra, the second to those based on the hydrogen lines. The average differences have been reduced to about two-thirds their original values, while the run in the differences has disappeared. Thus for four groups of eleven stars each, the mean systematic values are:

M	−1.0	−2.1	−2.7	−3.6
Sp	F0	F6	F7	F8
log ρ	−0.01	−0.03	+0.02	+0.02
log $\mathcal{M}$	−0.02	−0.01	−0.04	0.00

The comparison of the interpolated values of M with the period-luminosity relation is shown graphically in Figure 4.

In this connection it will be noted that values of M interpolated from the diagram with log ρ and the type as arguments are sensitive to uncertainties in the spectra. The relations are such that the average difference ± 0.2 in M (Table XVI) corresponds to 0.1 of a spectral interval (see equation [23]). The normal uncertainty of classification therefore accounts for nearly all the deviation shown by individual stars in Figure 4.

The principal change in the diagram has been the depression of the mass-curves near G0 and the change in their curvature in the region of the early types. Since the data for the Cepheids do not extend beyond G3, the lines through types G to M have been left much as in the original diagram. As will be seen later, there is some evidence favoring the reality of the minimum near K0. If the reductions to bolometric magnitude given on page 30 be applied, the variation of mass with spectrum becomes fairly

TABLE XVI

Masses and Densities of Cepheid Variables

Star	Spectrum		P	Calculated				Calculated *minus* Fig. 3					
	Est.	H.L.		*M*	log ρ	ℳ		log ρ		log ℳ		*M*	
α Ursae Minoris	F9	....	3.97	−1.8	−3.10	5.0		+0.01		+0.03		0.0	
TU Cassiopeiae	....	F4.5	2.14	−1.2	−2.56		5.5		+0.08		+0.11		−0.1
SU Cassiopeiae	F4	F1.5	1.95	−1.2	−2.48	3.0	2.9	−0.17	−0.09	−0.22	−0.24	+0.4	+0.3
SZ Tauri	F8p	F6	3.15	−1.6	−2.90	4.6	4.4	+0.01	+0.09	0.00	−0.01	0.0	−0.3
RX Aurigae	F9p	....	11.63	−3.4	−4.04	5.2		−0.18		−0.21		+0.3	
T Monocerotis	G1p	F8.5	27.01	−4.7	−4.76	13.8	13.2	0.00	+0.03	+0.06	+0.04	0.0	−0.1
RT Aurigae	F8p	F5	3.73	−1.8	−3.04	5.0	4.8	−0.03	−0.05	+0.02	−0.01	0.0	+0.1
W Geminorum	G0p	F6.5	7.92	−2.8	−3.70	5.8	5.5	+0.01	−0.06	−0.07	−0.09	0.0	+0.1
RS Boötis	....	A4	0.38	−0.3	−1.06		9.6		+0.18		+0.17		−0.2
ζ Geminorum	G0p	....	10.15	−3.2	−3.92	6.0		−0.06		−0.12		0.0	
X Sagittarii	F9p	F5	7.01	−2.6	−3.60	4.8	4.6	−0.14	−0.21	−0.12	−0.15	+0.3	+0.5
Y Ophiuchi	....	F9	17.11	−4.0	−4.36		14.4		+0.13		+0.16		−0.2
W Sagittarii	G0p	F6	7.60	−2.7	−3.66	5.5	5.2	0.00	−0.12	−0.07	−0.10	0.0	+0.3
Y Sagittarii	G2p	F9	5.77	−2.3	−3.42	9.6	9.1	+0.24	+0.27	+0.24	+0.22	−0.5	−0.5
U Sagittarii	G0p	....	6.74	−2.5	−3.56	6.0		0.00		0.00		0.0	
YZ Sagittarii	G1p	....	9.55	−3.1	−3.86	9.1		+0.05		+0.08		−0.2	
TT Aquilae	G2p	....	13.75	−3.6	−4.18	11.5		+0.13		+0.11		−0.3	
RR Lyrae	F0p	A5.5	0.57	−0.4	−1.42	6.6	6.3	+0.09	+0.02	+0.09	+0.03	−0.2	−0.1
U Aquilae	G0p	F9	7.02	−2.6	−3.60	5.5	5.2	+0.01	+0.19	−0.05	−0.07	0.0	−0.4
XZ Cygni	....	A3	0.47	−0.3	−1.24		5.5		−0.10		−0.08		+0.2
U Vulpeculae	G0p	F7	7.99	−2.8	−3.70	5.8	5.5	+0.01	−0.01	−0.07	−0.09	0.0	0.0
SU Cygni	F7p	F4	3.85	−1.8	−3.08	3.5	3.3	−0.17	−0.19	−0.16	−0.18	+0.3	+0.4
η Aquilae	F9p	F7	7.18	−2.6	−3.62	4.6	4.4	−0.11	−0.03	−0.14	−0.15	+0.3	+0.1
S Sagittae	G1p	F8.5	8.38	−2.9	−3.74	7.9	7.6	+0.12	+0.15	+0.06	+0.04	−0.2	−0.3
X Cygni	G3p	....	16.38	−3.9	−4.32	19.0		+0.24		+0.28		−0.5	
T Vulpeculae	F9	F5	4.44	−2.0	−3.20	5.2	5.0	+0.01	−0.11	+0.02	−0.02	0.0	+0.2
δ Cephei	G0	F6	5.37	−2.2	−3.36	6.3	6.0	+0.05	−0.07	+0.08	+0.05	−0.1	+0.1
W Serpentis	F9p	....	14.15	−3.7	−4.20	6.3		−0.19		−0.16		+0.4	
Average difference	....	....	....	....	....	....		±0.08^5	±0.11	±0.10	±0.10	±0.17	±0.22

regular, the course of the topmost line ($\mathcal{M} = 10$) being indicated by the dotted curve in Figure 3.

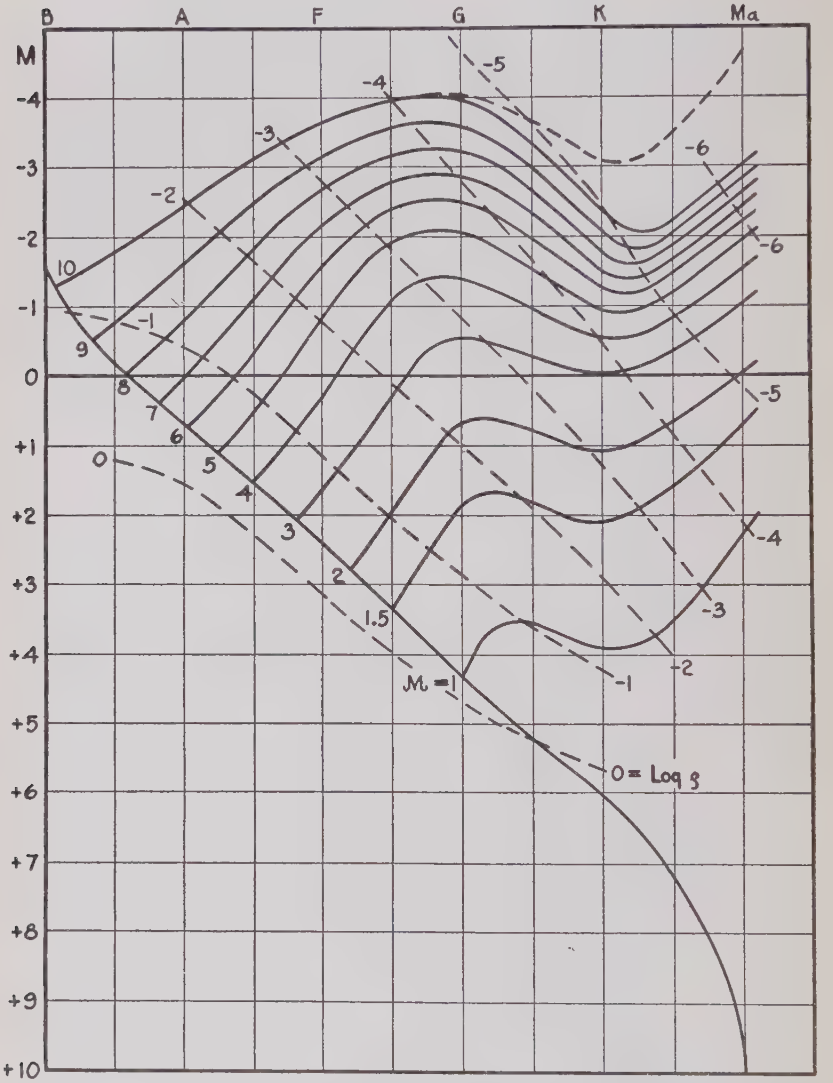

FIG. 3.—Distribution of mass and mean density, revised with the aid of Cepheid variables. The dotted curve at the top indicates the reduction to bolometric absolute magnitude for late-type stars of mass 10.

The curves of equal density are little changed. They still remain sensibly linear, but are no longer so closely parallel. Formula (23) has not wholly lost its applicability, for it still expresses approximately the relation of density to spectrum and absolute magnitude, though less accurately than before.

It will be noted that the densities along the dwarf branch are consistent with the values demanded by the density-distribution defined by the lines $\log \rho = 0, -1, -2$, etc. In other words, if we interpolate, say, for the value $\log \rho = -0.4$ ($\rho = 0.4$) along the line $\mathcal{M} = 6$, we find the point where it belongs, namely, on the dwarf branch. This detail is of some importance because it shows that the constants in the formulae for $\log \rho$ and $\log \mathcal{M}$ have been correctly determined. The spacing of the lines is fixed by the periods of the variables; their position as a group, by the condition that they must be consistent with the densities adopted for the dwarfs, whose values are independent of any assumption as to equipartition.

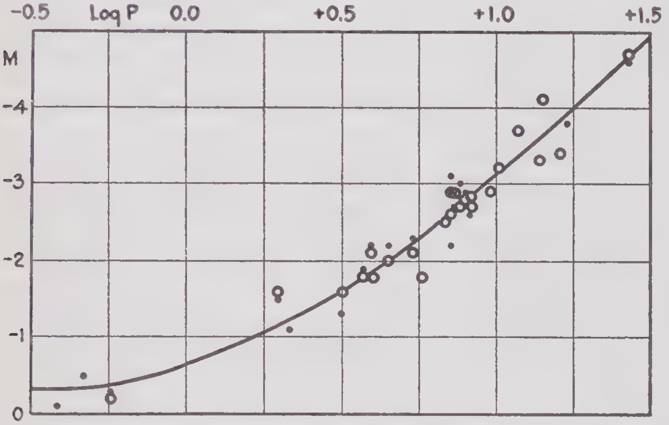

FIG. 4.—Absolute magnitudes of Cepheids interpolated from Fig. 3 with spectral type and $\log \rho$ from equation (24) as arguments. Circles, "estimated" spectra by Adams; points, hydrogen-line spectra by Shapley. The curve is Shapley's period-luminosity relation.

Presumably the diagram in Figure 3 is to be preferred to that in Figure 2. Certainly that is the case when Cepheid variables are concerned; and it seems likely that this holds also for the stars at large. The mass lines in Figure 2 pass *through* the points defined by the energy-constant and the velocities; no allowance for observational uncertainty by smoothing between the types was attempted; and with the exception of the terminal points on the dwarf branch everything preceding F5 is an extrapolation. On the other hand, an assumption of comparability is here involved, and it is perhaps worth remarking that if we reject the original diagram, we may thereby exclude relations between mass, density, luminosity, temperature, etc., which differentiate stars of constant light from Cepheid variables.

In view of the tentative character of the results, a detailed tabulation of the mass and density relations is unnecessary; Figure 3 will answer all practical purposes to which the results can be adapted. The data for the dwarf branch given in the first part of Table XIV, which are the most reliable, have already been referred to. To these have been added, by way of numerical illustration, results for the giants of zero absolute magnitude and for those whose masses are equal to 10.[1]

As a further illustration, the masses and densities corresponding to the spectra and absolute magnitudes of the individual stars measured by Pease with the interferometer have been given in the last lines of Table XIII. As a source of error, the values of M for these stars are probably as serious in respect to mass and density as the uncertainties of Figure 3 itself. Equation (22) shows that an error of 0.5 in M means an uncertainty factor of 2 in the density, whereas it seems unlikely that values from the diagram should be in error by so large an amount. In the case of an individual star, dispersion may of course enter, since the diagram gives mean values; but the probability of the occurrence of large deviations from the mean is small.

---

[1] Since the displacement of spectral lines required by relativity is proportional to $\mathcal{M}/R$ (R=radius of star) the results in Table XIV have a direct bearing on this question. The values of $\mathcal{M}/R$ do not run parallel to those of the K-term. Hence this term cannot be wholly identified with the relativity displacement, although the latter may of course be involved. As an illustration, the K-term for the B stars is about four times that for the A's. The ratio of the displacements on the other hand would be about 1.3. The most extreme deviation, however, is found by comparing the B's with the giant M stars. Their K-terms are of the same order of magnitude, whereas the red-displacement of the lines in M stars should be of the order of 0.01 that of the B's. See footnote No. 2, p. 27.

13. ON DISPERSION IN THE MASSES OF CEPHEIDS

From Shapley's work it appears that, for the variables in globular clusters at least, the deviations in M from the values determined by the period-luminosity relation are of the same order as the observational errors in the apparent magnitudes,[1] which of course must be used for any comparison. Practically, therefore, M is uniquely determined by P. Hence, by (26), the dispersion in the mass is related to that arising from such differences in j as may be associated with the same value of P, and it is an observational fact that the latter are small.

Direct evidence is also afforded by the comparison of the values of $\mathcal{M}$ for the Cepheids calculated by (26) with those interpolated from Figure 3. The average difference in log $\mathcal{M}$ is ±0.10, corresponding to about 25 per cent in $\mathcal{M}$. But what part of this may be attributed to uncertainty in the spectrum?

With proper allowance for the systematic difference of 0.3 between the hydrogen line and estimated spectra, the internal agreement is such as to indicate an average uncertainty of 0.05 of an interval. Assume an adopted value of the type to be too late by this amount. From (26)

$$\text{Mod.}\,\frac{d\mathcal{M}}{\mathcal{M}}=+0.6\,dj. \tag{27}$$

For the region F0–G0, j increases about 0.07 for the assumed increase in the spectrum. Hence, the calculated $\mathcal{M}$ will be 10 per cent too large. On the other hand, we find from Figure 3, for F5, $M=-2.5$, as an average, that the same error in the spectrum leads to an interpolated $\mathcal{M}$ about 3 per cent too small. The resulting errors are in opposite directions; whence, in the difference, the uncertainty becomes 13 per cent.

This average percentage error, combined with the dispersion and the errors of interpolation, must equal the average deviation of 25 per cent from the mean masses of the diagram. Neglecting the interpolation errors, whose inclusion would make the dispersion still smaller, we find the probable dispersion $r(\mathcal{M}) = 19$ per cent. As far as the evidence goes, we should therefore expect one-half the Cepheids to have masses lying between 0.8 and 1.2 times the mean mass. Since the Cepheids are a very special class of objects, it would be too much to assume that this result holds for all classes of stars (see Section 7).

---

[1] *Mt. Wilson Contr.*, No. 151, p. 26; *Astrophysical Journal*, 48, 114, 1918.

14. MASSES AND DENSITIES OF CEPHEID VARIABLES

The calculated values of the masses and densities used for the comparisons with the diagram of Figure 3 have been collected in the sixth and seventh columns of Table XVI, while their deviations from the adopted distribution are in the following columns. The formulae used are:

$$\log \rho = -2 \log P - 1.90 \tag{29}$$

$$\log \mathcal{M} = -2 \log P - 0.6\,(M - j) + 0.87 \tag{30}$$

in which the constants are the means for the two sets of data, the individual values differing by only 0.02. In case the spectral type is the median value derived from the hydrogen lines, the median value of M, given directly by the period luminosity relation, is to be used. For estimated spectra, the minimum M is required, although it is simpler to subtract 0.3 from the estimated spectrum and use the median M.

The values of both density and mass depend upon the assumed constancy of the numerical term in (29), but this assumption apparently leads to results of the right order, although for stars of short period the percentage deviation may be considerable.

For individual stars the calculated values are probably to be preferred to those interpolated from Figure 3. This follows not merely because of the dispersion in mass, but also because the differences for stars having determinations based on both estimated and hydrogen-line spectra are almost always of the same sign. This indicates real deviations from the mean distribution, in addition to those arising from the unavoidable errors of spectral classification. In such cases the values from (29) and (30) are likely to be nearer the truth than those derived from the diagram.

The results in Table XVI, both calculated and interpolated, may be compared with the masses and densities derived by Eddington[1] for certain Cepheids on the basis of his theory of radiative equilibrium. The agreement shown by Table XVII is remarkable when it is considered that the two methods approach the problem from entirely different directions. There are a few cases of serious discordance, and some systematic divergence, but nothing so large as might have been expected. The agreement with (29) has been commented upon by Eddington himself.

TABLE XVII

Comparison with Eddington's Results for Cepheid Variables

Star	Mass			Mean Density		
	Eddington	Eq. (30)	Fig. 3	Eddington	Eq. (29)	Fig. 3
Y Ophiuchi	13.0	14.4	10	0.000080	0.000044	0.000032
ζ Geminorum	7.4	6.0	7.9	.00046	.00012	.00014
S Sagittae	6.1	7.8	6.9	.00019	.00018	.00013
W Sagittarii	5.5	5.4	6.5	.00041	.00022	.00025
η Aquilae	5.2	4.5	6.2	.00033	.00024	.00028
X Sagittarii	5.1	4.7	6.4	.00025	.00025	.00038
Y Sagittarii	4.3	9.4	5.5	.00027	.00038	.00021
δ Cephei	4.0	6.2	5.3	.00052	.00044	.00045
T Vulpeculae	3.6	5.1	5.1	.00072	.00063	.00071
SU Cygni	3.1	3.4	5.0	.00160	.00083	.0013
RT Aurigae	3.0	4.9	4.8	.00110	.00091	.0010
SZ Tauri	2.8	4.5	4.5	.0015	.0013	.0011
SU Cassiopeiae	2.3	3.0	5.0	.0028	.0033	.0045
RR Lyrae	1.7	6.4	5.6	0.015	0.038	0.033

The geometrical mean mass of the twenty-four Cepheids in Table XVI is 6.2, which happens to agree almost exactly with that derived from the principle of equipartition. This can scarcely be more than accidental, however, for the velocities of only fifteen of these stars are available.

---

[1] *Monthly Notices*, **79**, 5, 1918.

15. AVERAGE HEAT CONTENT AND CEPHEID VARIATION

On the basis of the theory of radiative equilibrium Eddington[1] finds for the central temperature of a star

$$T_c \propto \rho^{\frac{1}{3}} \mathcal{M}^{\frac{2}{3}} \beta m \tag{31}$$

where ρ is the mean density, β the ratio of radiation pressure to gas pressure, and m the atomic weight which is here assumed to be constant. The formula may also be written

$$T_c \propto \frac{\beta \mathcal{M}}{R} \tag{32}$$

R being the radius. $R = D/2$ is given by (18) or an equivalent expression; β is a function of $\mathcal{M}$, and $\mathcal{M}$ in turn appears in his formulae as a function of the luminosity alone, which can be obtained from (25). T_c can therefore be calculated for any star. For thirteen Cepheids with periods ranging from 2 to 17 days Eddington[2] finds that T_c/β is sensibly constant. There are accidental deviations, but no progressive change. Moreover, for two theoretical stars with periods of 4.5 and 30.8 days the values of T_c/β are practically identical. This suggests as a possible condition for Cepheid variation

$$\frac{\mathcal{M}}{R} = \text{const., or } \rho \mathcal{M}^2 = \text{const.} \tag{33}$$

Since $\mathcal{M}^2/R$ is proportional to the total heat-content of a star,[3] the physical significance of (33) is that the average heat-content per unit mass is a constant, or, in another form, that the gravitational potential at the surface of the star is constant for the Cepheids. Shapley[4] has discussed this condition from the standpoint of the relation of period to absolute magnitude and finds agreement with the observed period-luminosity relation (25). We may proceed somewhat differently by combining (24) and (26) in accordance with (33). This gives the theoretical period-luminosity relation

$$M = -5 \log P + j + \text{const.} \tag{34}$$

---

[1] *Monthly Notices*, **77**, 601, 1917.

[2] *Ibid.*, **79**, 5, 1918; 181, 1919.

[3] Jeans, *Problems in Cosmogony*, p. 191, 1919.

[4] *Mt. Wilson Contr.*, No. 190, p. 7; *Astrophysical Journal*, **52**, 79, 1920.

A comparison of the values of M from (34) for the twenty-eight stars in Table XVI with those from the observed relation, (25) above, gives results which are shown graphically in Figure 5. The agreement is not good, the divergence amounting to about a magnitude between $\log P = 0.25$ and 1.5, with even larger differences for the cluster-type Cepheids, which are not shown in the diagram.

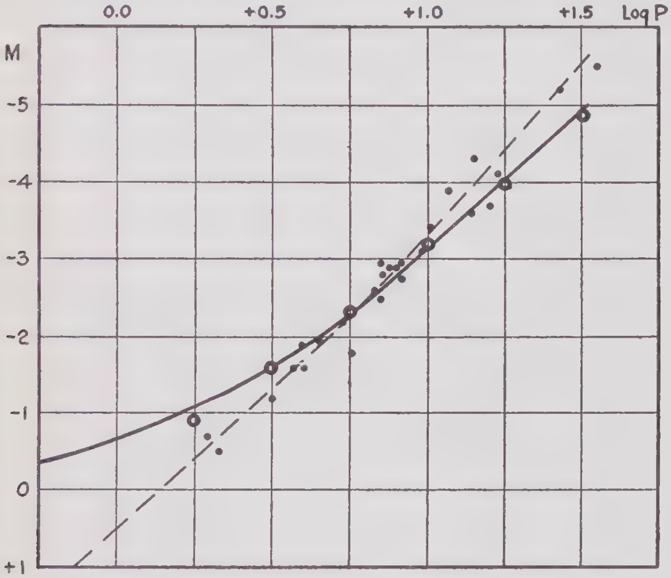

FIG. 5.—Absolute magnitudes of Cepheids based on the assumption of constant average heat content. The points are values for individual stars from equation (34). The circles, from equation (36), show the agreement with Shapley's period-luminosity relation when the term involving the specific heats in Eddington's expression for the density is included.

It will be noted that (33) is an empirical result which follows from an application to Cepheids of the period-luminosity relation (25) and the general theory of radiative equilibrium, but its derivation does not in any way involve the theory of Cepheid variation itself. If valid, it ought, however, in combination with the latter theory, to lead back to relation (25). But the comparison, as made, does not give complete agreement. Since the theory of Cepheids has entered only through (24), the difficulty presumably lies with that equation, which has been assumed to be applicable. If instead we use the corresponding relation derived by Eddington[1] himself, the difficulty disappears. For (24) we must substitute

$$\log \rho = -2 \log P - 2 \log (\gamma\alpha)^{\frac{1}{2}} + \text{const.} \qquad (35)$$

where $(\gamma\alpha)^{\frac{1}{2}}$ is a function of β and of the ratio of the specific heats, and changes slowly with the mass. With this emendation, (34) becomes

$$M = -5 \log P + j - 5 \log (\gamma\alpha)^{\frac{1}{2}} + \text{const.} \qquad (36)$$

The factor depending on the specific heats enters to the fifth power and thus becomes important. Its neglect in (34) causes the divergence shown by Figure 5.

The necessary corrections are easily calculated, however, with the aid of Table V of Eddington's paper. The values of $1-\beta$ required for the interpolation of $(\gamma\alpha)^{\frac{1}{2}}$ are given in *M.N.*, **77**, 602, 1917, under the heading "Molecular Weight 2," with the mass as argument. For $\mathcal{M}$ we may use the values in Table XVI, or more consistently with the present procedure, we may calculate $\mathcal{M}$ from

$$\log \mathcal{M} = -0.2\,(M - j) + \text{const.} \qquad (37)$$

which follows at once from (18) and the condition $\mathcal{M} \propto R$ given by (33). The latter method was adopted, the constant in (37) being determined so that the mean $\mathcal{M}$ from (37) agrees with that from the diagram in Figure 3. We are interested only in the variation of $(\gamma\alpha)^{\frac{1}{2}}$, which is practically the same for all possible values of the ratio of specific heats. $\Gamma = 1\frac{4}{9}$ was used, however, since Eddington's results show that this agrees well with the data of observation. With the constant in (36) equal to 1.48, the values of $-5 \log (\gamma\alpha)^{\frac{1}{2}}$ are as shown in the third column of Table XVIII. The sums of the remaining terms on the right of (36) are given in the second column under the heading M_0. These are the co-ordinates of the dotted curve in Figure 5 and were read directly from a large-scale diagram. The calculated values of M from (36) (fourth column) when compared with those from (25) give the residuals in the last column of the table. For values of P between 3 and 30 days the agreement is very close. For $P<2$ days there is still a large divergence, but that is to be expected. For all but the cluster-type Cepheids, therefore, the theoretical relation (36) is practically the equivalent of the observed period-luminosity relation (25).

---

[1] *Monthly Notices*, **77**, 15, 1918.

TABLE XVIII

THEORETICAL AND OBSERVED PERIOD-LUMINOSITY RELATION

Log P	M_0	$-5 \log (\gamma\alpha)^{\frac{1}{2}}$	M		O−C
			(36)	(25)	
0.25	−0.45	−0.45	−0.90	−1.08	−0.18
0.50	−1.30	−0.29	−1.59	−1.58	+0.01
0.75	−2.25	−0.08	−2.33	−2.26	+0.07
1.00	−3.34	+0.15	−3.19	−3.15	+0.04
1.25	−4.43	+0.45	−3.98	−4.05	−0.07
1.50	−5.54	+0.68	−4.86	−4.95	−0.09

Shapley's discussion referred to above starts with the assumption of constant heat-content and leads to a theoretical relation which agrees well with (25), but does not involve Eddington's theory of Cepheids because his comparison is based on equation (24) instead of (35). The close agreement found by Shapley is due partly to the fact that his final formula neglects $2.5 \log (\gamma\alpha)^{\frac{1}{2}}$ instead of $5 \log (\gamma\alpha)^{\frac{1}{2}}$, which by itself would lead to a divergence from (25) equal to one-half that shown in Figure 5, and partly to his readjustment of the mean atomic weight.

The matter is of interest from two or three points of view: First, because it shows the consistency of Eddington's theory of Cepheid variation with the general theory of radiative equilibrium, in that it is necessary to include the term depending on the specific heats in order to work back to the observed period-luminosity relation which was one of the premises; and second, because it exhibits the empirical result (33) in another form and possibly gives weight to the suggestion that constant average heat-content may be a determining circumstance in Cepheid variation.

The fact that the term which has been under discussion enters to so high a power subjects Eddington's theory of Cepheid variation to a severe test. Something of the sort is also true of the empirical condition (33). Assume for a moment that the relation $\mathcal{M} \propto R$ is not exact, and suppose that all the variations which occur are thrown into the mass. The maximum systematic deviation in log $\mathcal{M}$, by (18), (22), and (37), will then be equal to 0.4 of that shown by the differences in the last column of Table XVIII, which is well within the uncertainty of the comparison.

This close agreement justifies the mention of other relations which follow at once from the assumption of constant average heat-content, combined with the following equations of radiative equilibrium:[1]

$$\left.\begin{aligned} T_e^4 &\propto g(1-\beta) \propto \mathcal{M}^{\frac{1}{3}}\rho^{\frac{2}{3}}(1-\beta) \\ T_c &\propto \mathcal{M}^{\frac{2}{3}}\rho^{\frac{1}{3}}\beta \\ 1-\beta &\propto \mathcal{M}^2\beta^4 \end{aligned}\right\} \tag{38}$$

where T_e and T_c are the effective and central temperatures, respectively, g the acceleration due to gravity, and $1-\beta$ the ratio of radiation pressure to gravitational attraction. Assuming $\mathcal{M} \propto R$ we find then

$$\left.\begin{aligned} &\mathcal{M}^2\rho = c_1;\ \mathcal{M}g = c_2;\ Rg \propto c_3;\ \rho \propto g^2 \\ &T_c \propto \beta;\ T_e \propto T_c\mathcal{M}^{\frac{1}{4}} \propto \mathcal{M}^{\frac{1}{4}}\beta \propto T_c\rho^{-\frac{1}{8}} \end{aligned}\right\} \tag{39}$$

where c_1, c_2, and c_3 are constants. Further, with the aid of (35)

$$\mathcal{M} \propto (\gamma a)^{\frac{1}{2}}P;\ T_e \propto T_c(\gamma a)^{\frac{1}{8}}P^{\frac{1}{4}} \propto \beta(\gamma a)^{\frac{1}{8}}P^{\frac{1}{4}}. \tag{40}$$

The relation $T_e \propto \mathcal{M}^{\frac{1}{4}}\beta$ is of special interest. Since β diminishes faster than $\mathcal{M}^{\frac{1}{4}}$ increases, T_e must decrease with increasing $\mathcal{M}$. The change for the range in $\mathcal{M}$ shown above corresponds to an increase of about one spectral interval, which agrees well with the observed range in spectral type. At the same time M decreases from -1.2 to -5.1.

The formulae of radiative equilibrium admit of no dispersion in the case of individual stars. This is also true of the relations (39) and (40) for the Cepheids. In the case of the masses and densities, we have already found reasons for believing that this is not strictly in accordance with the facts. Although the dispersion is small, it is in part undoubtedly real, for at present the theory necessarily neglects the modifications of gravitational acceleration produced by the rotation of the stars on their axes, which must influence the relation of radiation to other stellar characteristics.

---

[1] Eddington, *Monthly Notices*, **79**, 180, 1919.

16. RELATION TO RUSSELL'S FREQUENCY DIAGRAM—REMARKS ON THE DISTRIBUTION OF MASS AND DENSITY

The justification for the discussion of Eddington's theory of Cepheids in this place is the light thrown upon the distribution of mass and density. Equations (35) and (37), for example, afford a basis for a further revision of the mass- and density-curves; but an additional approximation seems scarcely justified at present. Table XVII shows already a surprisingly good agreement between his results and those in Figure 3. Further modification would affect mainly the stars of masses 10 or larger, and these are not numerous. Moreover, Eddington himself has repeatedly emphasized the fact that his theory is but a first approximation, in that certain simplifying assumptions had to be introduced in order to make a beginning. Figure 3 is therefore allowed to stand as it is for the present, although the data in Table XIX are added to show, in a general way, what would result, for the Cepheids at least, from rigorous application of the theory. The values of M and the spectrum may be regarded as co-ordinates for the location of corresponding values of $\mathcal{M}$ in a diagram similar to Figure 3.

TABLE XIX

Mass, Absolute Magnitude, and Spectrum, Eddington's Theory of Cepheids

$\mathcal{M}$	M	Sp.	$\mathcal{M}$	M	Sp.
2	−0.9	F1.0	10	−3.4	F8.0
3	−1.4	F4.0	12	−3.6	F8.4
4	−1.9	F5.2	15	−4.0	F9.0
6	−2.5	F6.5	20	−4.6	F9.3
8	−3.0	F7.5	25	−5.1	F9.6

The values of the masses are adjusted to give a mean value equal to that derived from Figure 3.

It is, of course, not to be supposed that the stars are uniformly distributed along the mass-curves of Figure 3. In general they cluster about certain lines of maximum frequency which, with one exception, bear little relation to the lines of equal mass. The most conspicuous of the frequency lines is that defined by the dwarfs, which continues through the A's and joins smoothly with the line of maximum frequency of the B stars. Along this line we have found a regular decrease in the average mass with increasing spectral type and absolute magnitude.

The number of A stars of very high luminosity seems to be relatively small.[1] If this is really the case, there must be a region of low frequency in the diagram between the most luminous B's and the very bright giants of the later types. Beyond F0 the giants fall into two groups, the Cepheids and pseudo-Cepheids, and a large group of G, K, and M stars whose absolute magnitudes lie mainly between $M=-0.5$ and $+2.5$. The Cepheids and pseudo-Cepheids attain very high luminosities and show a rather definite correlation line running approximately from $M=-0.4$, F4, to $M=-4$, G8, which in general cuts the mass lines obliquely. For the Cepheids alone, its course is determined by the intersections of the mass lines of Figure 3 with those defined by equation (37), which, empirically at least, is a condition of Cepheid variability.

The frequency line for the second and more numerous group of giants seems, on the other hand, to be definitely related to the distribution of mass. It has a clearly marked minimum at K0 and coincides approximately[2] with the mass line $\mathcal{M}=2$ as shown in Figure 3. The chief difference is a steeper descent from G0 to K0 and an even more pronounced minimum than is shown by the mass line. The coincidence is probably significant, for Eddington[3] finds on theoretical grounds that, among the giants, masses of this order of magnitude may be expected to have the highest frequency.

---

[1] The frequency diagram of Russell for the helium stars of Kapteyn and the stars in the list of spectroscopic parallaxes is illustrated in Annual Report, Mt. Wilson Observatory, *Year Book Carnegie Institution of Washington*, 1921.

[2] The position of this correlation line and of the line of maximum frequency for the G, K, and M giants is shown in Fig. 1. This figure also shows the course of the equal-mass line $\mathcal{M}=2$. The correlation of spectral type with absolute magnitude for the most luminous stars of our own immediate system is essentially that found by Shapley for the brightest stars in globular clusters; and it now appears from results not yet published that in some of the galactic clouds a similar correlation with apparent magnitude is to be found. It should be possible in such cases to estimate roughly the distances of the clouds. Provisional results indicate values of the order of 20,000 to 50,000 light years. See *Annual Report, loc. cit.*

[3] *Report of the British Association for the Advancement of Science*, 1920, p. 43.

These circumstances seem to afford justification for the peculiar course of the mass lines for the late-type giants, which otherwise must depend solely upon the applicability of the principle of equipartition.

The minimum itself, or what remains of it after the reduction of the visual absolute magnitudes to bolometric values in the manner indicated above, must not be taken too seriously, however, for the residual irregularity in the mass lines is little in excess of the small systematic uncertainties affecting the absolute magnitudes of the different spectral types.[1]

In this connection the result of page 19 for the masses of fourteen giant visual binaries may be recalled. Divided by 1.75 to reduce to the central component, the mean mass becomes 1.7±0.9. For the same stars we find by interpolation from Figure 3, with spectral type and absolute magnitude as arguments, the mean value $\mathcal{M}=2.7\pm0.2$ The agreement is not good, but falls within the limits of uncertainty incident upon the small number of stars available for the comparison.

The decrease in mass along the dwarf branch from $\mathcal{M}=10$ at Bo to $\mathcal{M}=0.6$ at Ma raises a question of much interest, especially when it is recalled that the dispersion in mass is certainly small.[2] Practically, large masses are not to be found in our lists of dwarf stars. And yet the large-mass early-type stars are numerous. Why, therefore, do we not find more large masses among the dwarfs?

Several possibilities must be considered. Thus we might assume that the stars now on the dwarf branch (including the B's, as usual) began their development at much the same time, and that those of largest mass have only partially run their course and are now in the B stage. The assumption would seem less arbitrary could we suppose that all the stars began their evolutionary careers at the same time; but this apparently is not the case, for numerous objects with only moderate masses of 2 or 3 are still in an early stage of development. The most serious objection to this explanation, however, is that it takes no account of a peculiar kind of selection.

---

[1] Strömberg, *Mt. Wilson Contr.*, No. 220; *Astrophysical Journal*, **55**, 11, 1922.

[2] Russell has also discussed this correlation., *Observatory*, **37**, 173, 1914.

Let us therefore make the contrary assumption and suppose that stellar development has continued so long that all possible masses really occur among the dwarfs of late type. Among these, the large masses, say of the order of 10, will be of very low frequency as compared with the modal value for all types together. Kapteyn and van Rhijn place the maximum of the frequency-curve of absolute magnitudes at $M=+7.7$. The modal value of the mass therefore should be about 0.7, and since the dispersion is small, the large masses must be very infrequent.

Consider now only the stars in our lists of data. The dwarfs among these will all be included in a restricted region of space near the sun. The small masses will greatly predominate and the mean mass will be low. The giants, on the other hand, will be scattered through a large volume of space, and their average mass will be large, because only stars of large mass can attain high luminosity. The B's among them will form the collection at the upper end of the dwarf branch whose mean mass we have found to be 10. The total number of these in our catalogues will be considerable, because they represent those present in a large volume, whereas the large masses among the dwarfs will be absolutely as well as relatively infrequent, because we can see only those which are near us.

The stars of intermediate luminosity fill in the gap, and we must therefore expect to find a correlation of mass with absolute magnitude and spectral type very similar to that actually observed. The average mass decreases with advancing type; at the same time the number of stars of large mass in our catalogues decreases rapidly and the smaller masses appear in succession and in increasing numbers because they can attain the temperatures corresponding to the later spectral types.

One other possibility should also be borne in mind, namely, a decrease in mass through loss of energy by radiation. From the standpoint of relativity[1] any change dE in the total energy of a system implies a corresponding change of dE/c^2 in the inertial mass, where c is the velocity of light. A similar conclusion follows also on the basis of the Newtonian mechanics[1] from the phenomenon of radiation pressure, for, unless we attribute mass to radiation, there are certain cases, at least, in which neither the energy nor the motion of the center of gravity will be conserved. Since the principles of mechanics are inductions, we cannot be sure that they apply to physical phenomena with the degree of precision implied by assuming that mass actually changes with changes in the energy. But considerations of consistency are sufficient to give the matter importance, and it derives added interest from the fact that a decrease in mass has been invoked as a means of accounting for the enormous unknown supply of energy which is now generally recognized as an essential feature of stellar phenomena. The suggestion that the packing of electrons and the nuclei of hydrogen atoms to form nuclei of heavier elements, with an accompanying loss in mass which reappears in the form of great quantities of radiant energy, attaches itself naturally to the relation between mass and energy that harmonizes with fundamental mechanical principles, whether of Einstein or of Newton.

---

[1] Einstein, *Annalen der Physik*, 18, 639, 1905.

Of these three factors which may affect the correlation of mass and spectral type, selection certainly enters in the manner indicated, but its quantitative evaluation is at present impossible. This leaves the operation of the other two factors entirely speculative. If, however, there is any appreciable change in the mass of the stars during their development, they will not follow the mass lines of Figure 3, but cut across them obliquely; and this leads to a peculiarity of these lines that immediately attracts attention.

The equal-mass lines do not meet the dwarf branch tangentially, as one might expect on the basis of a simple gravitational contraction with its accompanying changes of temperature, but intersect the frequency line at large angles. A comparison of Figures 2 and 3 shows that in this particular there is a large element of uncertainty; and yet the evidence seems to exclude the possibility of tangential intersections, unless we are prepared to abandon the principle of equipartition at the point where it seems to be best justified, namely, in the vicinity of the dwarf branch.

---

[1] *Ibid.*, **20**, 627, 1906. This result seems also to have been pointed out by others—Planck, for one, I believe—although I have been unable to locate the source.

The space-velocities of stars of any given type, say F5, show a definite correlation with absolute magnitude, the mean velocity increasing continuously as the brightness decreases. If equipartition holds for the stars of a given type which are near the frequency line of the dwarfs, as it does in the mean for the stars of different types scattered along the frequency line, there must be a continuous decrease in mass downward along the vertical lines of Figure 3. The data of Table X give a numerical expression to this relationship of mass to luminosity, which, quantitatively, should be most exact for values of *M* near the frequency line of the dwarfs. Now on this line, for spectral type F5, as an illustration, we find a mean mass of 1.5. Above this point in the diagram, that is, for more luminous stars, the masses are larger; below they are smaller. If the decrease in mass downward is really continuous, it follows at once, since the mass also decreases continuously along the dwarf frequency line, that curves connecting equal masses cannot meet the frequency line tangentially, but must intersect it at a considerable angle. In fact Figure 2 shows that the strict application of the principle of equipartition leads to angles in excess of 90°, counting as 0° the tangential junction required by gravitational contraction. The evolutionary path of any given star, however, when once it has joined the dwarf branch, must lie in the general direction of the frequency line.

The explanation of the contradiction lies in the peculiar selection which determines the decrease in mass along the dwarf branch. Consider for example two dwarf stars of Type F5, one a large mass which in its development has followed the dwarf branch downward from some earlier type, the other a star of mass so small that it has been unable to attain the high temperatures of the very early types and joins the dwarf branch at Type F5. The star of large mass will be the brighter of the two. Hence the path of the small star must intersect the line of maximum frequency at some point a little in advance of F5 in order that it may swing into position below the larger star. The path of the larger star, on the other hand, will lie above the frequency line. Similar reasoning applies to stars of intermediate mass and it is evident that the entire group of F5 dwarfs will show a correlation of mass with absolute magnitude similar to that found from the principle of equipartition. In their further evolution these stars will move as a group along paths approximately parallel to the line of maximum frequency. But these paths do not and cannot coincide with the equal mass lines of Figure 3, for when the group in question is at F5, there is at G0 another group, whose luminosities show a similar correlation with mass, but whose masses, because of selection, are systematically smaller than those at F5. If the points in the diagram corresponding to equal masses in these two simultaneously observed groups be connected, the lines of equal mass will cut the frequency line at high angles as shown in Figure 3. Hence there is no conflict between the mass-distribution shown by this diagram and the gravitational theory of stellar development. The only point is that in the vicinity of the dwarf branch the stars do not follow the equal mass lines.

17. IONIZATION AND MEAN ATOMIC WEIGHT

The final equations of Eddington's theory[1] are

$$L=\frac{4\pi cG\mathcal{M}}{k}(1-\beta) \tag{41}$$

$$1-\beta=0.0026\ \mathcal{M}^2\beta^4m^4 \tag{42}$$

where c and G are constants. These formulae refer to the giant stage and assume that the mean atomic weight is independent of the temperature. Variations in m during the star's development would affect the relation between luminosity and spectral type. The absolute value of m fixes the relation between mass and radiation-pressure β, and hence determines the values of the mass which are most likely to occur.

It is unnecessary to repeat here Eddington's arguments in favor of a small value of m. In general these seem to be only strengthened by the results of recent investigations of ionization phenomena. Eggert,[2] for example, has considered the behavior of the iron atom when subjected to pressures and temperatures comparable with those at the center of a typical giant star and finds that 16 of the

---

[1] *Astrophysical Journal*, **48**, 208, 210, 1918.

[2] *Physikalische Zeitschrift*, **20**, 570, 1919.

26 electrons would be stripped from the atom, thus reducing the mean "atomic" weight to 3.3.

It is easy to extend this result to other parts of the star. Using the reaction isobar of Nernst and basing the calculation of the energy of dissociation on the dynamical relations of the Bohr atom, Eggert finds as the condition for the removal of 8 electrons from 99 per cent of the atoms[1]

$$2.68+0.4 \log P=\frac{-2\times 10^5}{T_i}+\log T_i \tag{43}$$

in which the pressure P is measured in atmospheres. For the separation of 16 electrons the corresponding condition is approximately the same as (43) except for the appearance of an additional factor of 10 in the first term on the right.

Equation (43) and its alternate may be used to calculate the values of T_i corresponding to the pressures at different points along the radius. The comparison of the ionization temperatures thus found with the corresponding stellar temperatures should then give some indication as to the variation in ionization throughout the star.

The total pressure P is given by the ordinary gas equation, divided by β, the factor arising from radiation-pressure.

$$P=\frac{p}{\beta}=\frac{\mathfrak{R}}{\beta m}\rho T \tag{44}$$

T and ρ may be found from Emden's[2] formulae, or we may use the values given by Eddington[3] for his typical star ($\mathcal{M}=1.5$, $\rho_m=0.002$), taking care to modify those for T, which contain the factor m, to make them conform with the degree of ionization expressed by (43) and its alternate. Since T contains both m

---

[1] Professor Paul Epstein of the California Institute of Technology calls my attention to an error in Eggert's expression for K (*op. cit.*, p. 573). A factor 8^8 has been omitted. It has little effect, however, on equation (43), the absolute term being increased from 2.32 to 2.68.

[2] *Gaskugeln*, p. 97, 1907. Eddington has called attention to the misprint in the formula for θ^3. The last factor in the denominator should be squared.

[3] *Astrophysical Journal*, 48, 213, 1918. Unless I am in error, Eddington's values for the temperature have been computed with $m=2$, whereas the text seems to imply that 2.8 has been used. If so, the tabular values should be increased by 40 per cent.

and β as factors, the total pressure P depends upon neither the value of the radiation-pressure nor the degree of ionization. T, however, depends upon both, and, moreover, β also depends upon m (see equation [42]).

For the removal of 8 and 16 electrons, respectively, the values of m become 6.2 and 3.3. Corresponding to these, for $\mathcal{M}=1.5$, $\beta=0.496$ and 0.766. With these data we find the values of P and T given in the second, third, and fifth columns of Table XX

TABLE XX

IONIZATION AND STELLAR TEMPERATURES, IRON IN EDDINGTON'S TYPICAL STAR

r	LOG P (ATM)	−8 ELECTRONS $m=6.2$		−16 ELECTRONS $m=3.3$		PERCENTAGE OF MASS OUTSIDE r
		T	T_i	T	T_i	
0.......	7.40	8.7×10^6	8.0×10^5	7.1×10^6	2.6×10^6	100
1.......	7.13	7.4	6.7	6.1	2.4	88
2.......	6.47	5.0	4.9	4.1	2.0	48
3.......	5.63	3.1	3.4	2.5	1.6	18
4.......	4.69	1.8	2.5	1.5	1.3	5
5.......	3.59	0.96	1.8	0.79	1.1	0.7
6.......	1.98	0.39	1.2	0.32	0.8	0.005

Radius of star $=6.9$, $\mathcal{M}=1.5$, $\rho_m=0.002$.

for various points along the radius. The unit for r is such that the distance from the center to the surface is 6.9. Substituting the values of P into Eggert's formula, we find the ionization temperatures given in the fourth and sixth columns of the table. These temperatures, required for the removal of 8 and 16 electrons, respectively, may be compared with the corresponding stellar temperatures. The latter, which change little with the assumed change in m, are approximately ten times the temperature required to separate 8 electrons from the nucleus, and of the same order as the ionization temperatures corresponding to the removal of 16 electrons. The decrease in pressure toward the surface compensates for the fall in temperature to such an extent that the ionization should be nearly constant throughout the star. It is only within a thin shell near the surface, which contains an insignificant fraction of the mass (see last column, Table XX), that m can rise much above the value 3.3.

Eggert's formula is an extrapolation and involves assumptions which cannot at present be directly controlled; but its general indications are in close agreement with Eddington's conclusions. Even admitting the various underlying assumptions, the result applies only to a star consisting wholly of iron; but one can scarcely doubt that the mean values of m for all the elements actually present must be small and nearly constant for all points within the star except those close to the surface.

It seems worth while also to consider the relation of ionization to stellar temperature in giant stars of constant mass but differing spectral types, in order to gain some idea of the permanence of this relation as a star contracts under the action of gravitation.

Consider stars of Eddington's critical mass $\mathcal{M}=2$, which, as we have seen, are those occurring most frequently among the late-type giants. It will be sufficient to calculate the central temperatures and pressures, and in view of the preceding results it is clear that we may use $m=3.3$. The corresponding value of β is 0.70. Using Emden's formula as before (remembering that for the type of equilibrium considered $\rho_c=54.25\ \rho_m$), we find the results for T_c and P_c given in Table XXI. The values of M and $\log \rho_m$ in the second and third columns were read from the diagram of Figure 3. The ionization temperatures for the removal of 16 electrons are in the last column of the table.

TABLE XXI

CENTRAL TEMPERATURES AND PRESSURES, AND IONIZATION TEMPERATURES FOR IRON
($\mathcal{M}=2$, $m=3.3$)

Sp.	M	Log ρ_m	Log T_c	Log P, (Atm)	T_c	T_i
Ma............	0.0	−5.1	6.10	4.3	1.3×10^6	1.2×10^6
K5............	+0.7	−4.1	6.43	5.6	2.7	1.5
K0............	+1.1	−3.1	6.77	7.0	5.9	2.1
G5............	+0.8	−2.7	6.90	7.5	7.9	2.6
G0............	+0.7	−2.2	7.07	8.2	11.7	3.3
F5............	+2.0	−1.0	7.47	9.8	29.5	7.0

These data represent the sequence of changes from an early stage of development, on the basis of Russell's theory, through to the dwarf stage, where the density is so large that Boyle's law is no longer accurately obeyed. The increases in T_c, ρ and P_c are approximately 20, 10,000, and 300,000 fold, respectively. In spite of these extraordinary changes, the ionization temperatures remain of the same general order as those at the center of the star throughout its development. Initially, the two temperatures are sensibly equal, and the gain in T_c over T_i is so slight that any further decrease in m must be small. The complete removal of the third sheath of electrons, for example, would give $m=2.2$.

Even for stars of the lowest density, such as Antares or Betelgeuse, conditions are very similar to those illustrated by the first line of Table XXI. Low density means relatively low central temperature and pressure, but this factor is compensated by the large masses which characterize the very luminous giants, so that the relation of ionization to stellar temperatures is much the same as for the objects already examined.

It may be remarked incidentally that the values of T_c in Table XXI throw some light upon the behavior of the effective radiating layers in stars of different types. The increase in T_c is approximately ten times that in the effective temperature. But for the type of equilibrium in question the temperature gradient is independent of the density, that is, the temperature increase for homologous points along the radius should be constant. The explanation must be that the thickness of the radiating layer in an Ma giant, because of the enormous difference in density, is very much greater than that for an F5 dwarf. As development progresses, radiation from the deeper and hotter strata is absorbed as a result of increasing density, and, in consequence, the increase in effective temperature is less rapid than would otherwise be the case.

On the basis of the preceding evidence we must expect a high degree of ionization at the earliest stages of stellar development with which we are familiar, and comparatively little decrease in the value of m as the development proceeds. The Bohr atom affords the only foundation we have for estimates such as have been made, and it is not certain that the results are of the right order of magnitude. One consequence of their acceptance, however, should not be overlooked, and that is the total amount of energy required for ionization. For the removal of 8 electrons this equals 1.8×10^7 calories per gram atom,[1] corresponding to an ionizing potential of about 800 volts. The mass of Eddington's typical star is approximately 2.9×10^{33} grams. The removal of 8 electrons from all the atoms in this mass would therefore require

$$U_0=\frac{2.9\times10^{33}\times1.8\times10^7\times4.2\times10^7}{56}=4\times10^{46}\text{ ergs,}\tag{45}$$

while for the removal of the second sheath of 8 electrons a quantity of the order of ten times this amount, or

$$U_0=4\times10^{47}\text{ ergs}\tag{46}$$

would be necessary.

Now the total energy generated by gravitational contraction of the star from a state of infinite diffusion is[2]

$$\Omega=\frac{3(\gamma-1)}{5\gamma-6}\,\frac{G\mathcal{M}^2}{R}\tag{47}$$

where γ is the ratio of specific heats, G the gravitational constant, 6.66×10^{-8} cm³/grams sec.², and R the radius, 7×10^{11} cm; γ lies between the limits 4/3 and 5/3, whence the fractional coefficient on the right has the limiting values 3/2 and 6/7. At a maximum, therefore, which also corresponds to Eddington's model,

$$\Omega=\tfrac{3}{2}\cdot\tfrac{2}{3}\cdot\frac{10^{-7}\times9\times10^{66}}{7\times10^{11}}=1.3\times10^{48}\text{ ergs.}\tag{48}$$

Of this total the ethereal energy alone,[3] namely,

$$(1-\beta)\Omega=0.234\,\Omega=3.0\times10^{47}\text{ ergs,}\tag{49}$$

---

[1] Eggert, *loc. cit.*

[2] Emden, *Gaskugeln*, p. 125, 1907.

[3] Eddington, *Monthly Notices*, **79**, 23, 1918. Anderson, with whom I have had much stimulating discussion during the preparation of this paper, calls my attention to the fact that ionization cannot be produced by the collision of electrons with atoms without violating the Nernst formula of equilibrium, which is well established on thermodynamical grounds. This equation depends upon the pressure, whereas the hypothesis of ionization by collisions alone leads to a condition for equilibrium which is independent of pressure. If the effective energy is assumed to be partly radiant and partly kinetic, the pressure would enter, but not in the manner required by Nernst's equation. Since the internal kinetic energy of the atoms is not available, the radiant energy alone can be operative (as in the case of the photoelectric effect, for example). See also Milne, *Observatory*, **44**, 269, 1921.

seems to be available for ionization. This is of the same order as U_o, the energy of dissociation given in (46). Admitting, therefore, the validity of Bohr's theory and the applicability of the Nernst formula of equilibrium, the insufficiency of the gravitational theory presents itself in a new form. As an alternative, the question is perhaps raised as to whether the giant stars, even in their very earliest stages of development, are ever in a state other than one of high dissociation.

The calculation of the stellar temperatures in Tables XX and XXI neglects altogether the depletion of the available supply of energy by ionization. Were gravitation the only source, we could expect neither the temperatures nor the degree of ionization indicated by the discussion; but, instead, an equilibrium state which would be established for something less than the extremes of temperature and ionization shown by the tables.

18. COMPARISONS WITH EDDINGTON'S FORMULAE

The assumption concerning m which underlies equations (41) and (42) has been discussed in the preceding section. These formulae also assume that the outflow of energy across any surface of unit area is proportional to the gravitational acceleration at that point ($H \propto g$), and that the mass coefficient of absorption, k, is a constant. The energy assumption can also be stated in the form that the outflow throughout the star per unit of mass is constant. The source of the energy is not specified; it may be derived from gravitational contraction or any other source capable of providing an adequate supply. Assuming further that the transfer of energy is by radiation and not by convection, the conditions for equilibrium are found to be the same as those for adiabatic equilibrium with a ratio of specific heats equal to 4/3. It then follows through (41) and (42) that the bolometric magnitude of a star remains constant so long as it behaves as a perfect gas.[1]

A giant star in its development, however, presumably follows closely one of the equal-mass lines in the upper part of Figure 1, for the selection which enters along the dwarf branch has comparatively little influence on the average mass of the giants which come under observation. Observations indicate, therefore, that the absolute magnitude is not independent of the stage of development. The change is even larger than shown in Figure 3, for, as already stated, the visual absolute magnitudes must be corrected by the quantities given on page 30 to make them comparable with the bolometric magnitudes calculated by (41).

---

[1] As Jeans points out, *Monthly Notices*, **79**, 319, 1919, this general result follows at once, by simple considerations, from the assumption H/g=const. The nature of the dependence of radiation on mass and other characteristics is, however, another matter, less easily disposed of.

The question now arises as to the particulars in which the underlying assumptions must be modified in order to effect a closer agreement with observations. Such consideration as can be given here may be prefaced by the remark that Jeans,[1] starting from the assumptions of radiative conduction, gravitational contraction, and constant k and m, finds that the radiation of a star will remain constant as long as Boyle's law is obeyed. This is also the case if the star has sources of energy other than gravitational contraction, provided the rate of generation per unit mass is independent of the time. This is Eddington's result without his assumption that $H \propto g$; but the functional dependence of radiation upon the mass cannot be specified. Jeans also finds that H/g will be constant throughout the mass of gas only when the mass is so large that radiation-pressure predominates and β may be put equal to zero. For the ordinary run of stellar masses, however, H/g will not be constant within the star, but for a given point will be independent of the time, provided the only source of energy is gravitational.

Eddington[2] himself points out that H/g cannot be rigorously constant within the star, for, assuming gravitational contraction through a series of homologous states and a temperature- and pressure-distribution corresponding to adiabatic equilibrium with $\gamma = 4/3$, the outflow of energy per unit mass would increase about 70 per cent from the surface to the center.

In view of a probable variation of H/g of the order indicated, the original assumption gives close agreement with observations. The matter can be tested by comparing the calculated values of M corresponding to different values of $\mathcal{M}$ with that shown by Figure 3 for stars of the same spectral type. By proceeding in this manner we avoid disturbances arising from variations in k and m, since for stars of the same type these quantities should be less subject to change.

---

[1] *Loc. cit.*

[2] *Monthly Notices*, 77, 599, 1917.

The results are shown in Table XXII. This table gives the deviations of the observed values of M (Fig. 3) from those calculated by Eddington, which are in the second column of the table. Zero point corrections have been applied to the latter to make the mean O−C for each type equal to zero. There is a large progressive change for the F stars, but the agreement improves with advancing type and, with the exception of one difference, is practically perfect for the K and M stars. From this comparison it is clear that the error in the assumption $H/g=$const. is not very serious when we consider stars of a specified type.

TABLE XXII

OBSERVED AND CALCULATED (EDDINGTON) VARIATION OF ABSOLUTE MAGNITUDE WITH MASS

$\mathcal{M}$	CAL. M	O−C			
		Fo	Go	Ko	Ma
1.5	−0.3	.....	+1.5	+0.7	+0.3
2	−0.9	.....	+0.9	+0.3	+0.2
3	−1.7	.....	+0.5	0.0	0.0
4	−2.2	+1.4	+0.1	0.0	0.0
5	−2.6	+0.7	−0.1	0.0	0.0
6	−2.9	+0.3	−0.3	−0.1	0.0
7	−3.1	−0.1	−0.5	−0.1	0.0
8	−3.3	−0.5	−0.6	−0.2	0.0
9	−3.5	−0.7	−0.8	−0.3	0.0
10	−3.7	−1.0	−0.9	−0.3	0.0

The lack of parallelism of the equal-mass lines with the axis $M=0$ is difficult to account for because the assumption of constancy for both k and m enters here, as well as that concerning the flow of energy. In general the luminosity for any given mass decreases with increasing temperature. For mass 4, as an illustration, the bolometric absolute magnitude increases from −3.1 at Ma to +0.3 at Fo. This is in the direction corresponding to decreasing values of m, and one might expect much of the change to be accounted for by increasing ionization. The evidence of section 17, however, is against any considerable variation in m. Even in the earliest visible stages of development we should not anticipate a value much in excess of 3.3, and unless there is a large amount of nuclear disintegration, which seems improbable, the value of m cannot fall below 2. It is easily shown that a decrease from $4\sqrt{2}$ to 2 would cause an increase in M of about one magnitude, which is only a third of the amount required. The admission of much larger initial values of m is insufficient to bridge the gap, for (42) shows that $1-\beta$, and hence the luminosity, are not much affected as m is increased.

The behavior of k is obscure. Although the conditions within the star which determine the degree of absorption must be analogous to those governing the absorption of X-rays, it should be borne in mind that the effective value of k is that corresponding to the outermost layers of the star where the temperature is very much lower than in the interior. Even near the surface the opacity is large, but we have no data as to its variations that are certainly applicable.

This leaves the larger part of the increase in the absolute magnitude unaccounted for, and it is not clear as to how the discrepancy is to be explained. If the contraction is homologous and the energy gravitational, or gravitational plus a source independent of the time, we should not expect variations in outflow with advancing development other than those caused by changes in k and in m.

As an explanation, changes in m that would be sufficient seem to be excluded; those of k are in doubt. There remain, however, the assumptions underlying the outflow of energy. The source of energy almost certainly is not wholly gravitational, and if not, with almost equal certainty, is not independent of the time. The outstanding questions therefore lead directly into the realm of atomic physics, and it seems more than ever likely that the problem of the stars will find its solution in the solution of the problem of the atom.

In conclusion, attention may be directed to the relation of mass to luminosity along the dwarf branch. Here Boyle's law is in general no longer obeyed. It will be noted, however, that the density increases slowly until the late types are reached, which suggests that the departure from the conditions of a perfect gas may affect the behavior of stars of different spectral types much alike, so that a formula giving the relation of luminosity to mass for the giants, with the exception of a constant, would also hold approximately for the dwarfs.

The matter is easily tested by calculating $\mathcal{M}$ from (41) for the values of L corresponding to the absolute magnitudes given in the second column of Table IV. Choosing the constant factor so that the mean of the values thus calculated agrees with the observed mean mass, we have the results in Table XXIII. With the exception of a spectral interval at either end of the series, where the deviations from the average density are large, the agreement is good.

TABLE XXIII

VALUES OF MASS ON DWARF BRANCH

Sp.	Obs.	Cal.	Sp.	Obs.	Cal.
B0	10	18	G0	1.0	1.0
B5	8.3	10.5	G5	0.76	0.76
A0	6.0	6.6	K0	0.68	0.62
A5	4.0	4.1	K5	0.62	0.48
F0	2.5	2.5	Ma	0.59	0.26
F5	1.5	1.5			

I must express my grateful acknowledgments to Miss Joyner and Miss Richmond, of the Computing Division, for their efficient assistance in the extensive tabulations and calculations involved in the preceding discussion.

MOUNT WILSON OBSERVATORY
December 1921

Contributions from the Mount Wilson Observatory, No. 227
Reprinted from the *Astrophysical Journal*, Vol. LV, pp. 238–241, 1922

ON THE CALCULATION OF MASSES FROM SPECTROSCOPIC PARALLAXES

By HENRY NORRIS RUSSELL[1]

ABSTRACT

Calculation of masses of stars from spectroscopic parallaxes.—It appears probable that the line intensities upon which spectroscopic parallaxes are based are functions of the temperature and density of the star's atmosphere. If this were exactly true, all stars of the same surface brightness and density would have the same spectroscopic absolute magnitude, and the masses, computed from the spectroscopic parallaxes, would come out the same for all the stars of such a group (whatever the dispersion among their actual masses) and equal to the geometrical mean of the latter. To obtain a reliable measure of the dispersion in mass among binary stars, parallaxes must be determined in some other way.

Spectroscopic and dynamical parallaxes.—It follows that the spectroscopic parallaxes and the dynamical parallaxes (derived on the assumption that the mass of a binary system is equal to the mean value for stars of its spectral type and absolute magnitude) are systematically equivalent to one another, and really rest on the same physical relationships and assumptions.

Dispersion of mass among visual binaries (dwarf stars).—By an indirect method, depending on Strömberg's comparisons of spectroscopic and trigonometric parallaxes, Seares's conclusion that the dispersion is small is confirmed. The probable error of dispersion of log $\mathcal{M}$ appears to be less than ±0.2, but cannot be exactly determined.

The very small values obtained by Seares in the preceding paper[2] for the dispersion in mass among dwarf stars suggest the following explanation.

It appears very probable, from physical considerations, that the spectral type of a star is determined by the temperature T of its outer atmosphere, while the characteristics associated with the absolute magnitude depend also, and mainly, upon the density of the atmosphere, ρ'. If M_s is the absolute magnitude, determined spectroscopically, we may then write

$$M_s = F(T, \rho') . \qquad (1)$$

It is also probable that the surface brightness j depends almost entirely on the temperature, and that the density of the atmosphere above the visible surface is a function of the mean density ρ (though not necessarily proportional to it). We have then

---

[1] Research Associate of the Mount Wilson Observatory.

[2] *Mt. Wilson Contr.*, No. 226.

$$M_s = f(j, \rho). \qquad (2)$$

It may be that M_s depends to some degree on other variables, but it is probable that their influence is slight. The form of the function f cannot be predicted by theory, but can be found empirically when sufficient data regarding stellar masses and densities are available.

Assuming the relation for the moment to be exact, and introducing it into equation (22) of Seares's paper, we have

$$\log \mathcal{M}_s = \log \rho + 0.6j - 0.6f(j, \rho) + 2.77. \qquad (3)$$

Hence $\mathcal{M}_s$ the mass corresponding to the spectroscopic parallax is itself a function of ρ and j alone. Like (22) this is a general result, holding good no matter how the mass is calculated, so long as the formula involves the absolute magnitude and our assumptions about the latter are correct.

Stated in words, this signifies: *If the spectroscopic absolute magnitude of a star depends only on its surface brightness and density, the masses computed from the spectroscopic parallaxes will be identical for all stars which have the same density and surface brightness, no matter how different their actual masses may be.*

In still other words, the spectroscopic parallax (on our assumptions) will be correct only in the case of stars having a certain average value of the mass. For larger or smaller masses there will be a systematic error in the absolute magnitudes, making the former too faint and the latter too bright, which will alter the spectroscopic parallax to just such a degree as to conceal entirely the real differences in mass.

If the spectroscopic calibration curves are adjusted so as to give a correct value for the mean absolute magnitude of the stars, the "spectroscopic mass" will be the geometrical mean of the individual masses, since, if j and ρ are constant, M varies proportionally to $\log \mathcal{M}$.

To determine the dispersion in mass among visual binaries, it is therefore necessary to have recourse in some way to parallaxes other than spectroscopic. One way of doing this is through Strömberg's[1] discussion of the errors of the spectroscopic parallaxes—which he has determined by comparison of individual spectroscopic and trigonometric parallaxes, allowing for the errors of the latter. Let the probable error thus found for log π be $\pm r$. Three sources contributory to this error may be distinguished: (1) the error just discussed, arising from differences between the masses of individual stars of the same surface brightness and density; (2) the error arising from other physical causes, on account of which the functional relation (2) is not exactly true; and (3) errors of observation. If we call the amounts of these, expressed as probable errors of log π, respectively, r_m, r_p, and r_e, we will have

$$r^2 = r_m^2 + r_p^2 + r_e^2 .$$

If, on the other hand, we compute individual masses as Seares has done, the error r_m will be without influence on these masses, while r_p and r_e will affect log $\mathcal{M}$ by 0.6 of their amounts, and there will be an additional source of error, due to the imperfections of the orbits and also to errors in the assumed ratio of the masses of the components, which we may call $\pm r_c$. If then r' is the probable error of distribution, which Seares calls $r(\Delta \log \mu)$, we have

$$\begin{aligned} r_m^2 + r_p^2 + r_e^2 = r^2 &= (0.36)^2 \\ 0.36(r_p^2 + r_e^2) + r_c^2 = r'^2 &= (0.22)^2 \\ r_m^2 &= 2.78\, r_c^2 - 0.004. \end{aligned}$$

This would indicate that the actual dispersion in log $\mathcal{M}$ (which corresponds to the probable error $\pm 0.6\, r_m$) is very small—being substantially equal to the spurious dispersion which arises from errors in the orbital elements of the binaries.

The observed values of r and r' are, however, subject to some uncertainty, and it is possible that some other concealed correlation may still be making the agreement appear better than it should.

It is obvious, however, that a better way of determining the dispersion in mass among visual binaries of the same spectral type will be a direct comparison of "hypothetical" or dynamical parallaxes, computed with a mean value of the mass, with trigonometric parallaxes. In this case there seems to be no reason to fear a correlation of the sort discussed above.

---

[1] *Mt. Wilson Contr.*, No. 199, p. 15; *Astrophysical Journal*, **53**, 27, 1921.

It may be noticed that the dynamical parallax of a binary, calculated on the assumption that the principal star has the mass $\mathcal{M}_s$ derived from spectroscopic parallaxes of stars of similar kind, and the spectroscopic parallax itself, must agree exactly in every case (barring the effects of errors of observation and the small uncertainty arising in the estimate of the ratio of the mass of the system to that of the brighter component), so that it may fairly be said that spectroscopic and dynamical parallaxes are systematically equivalent to one another, so long as the mass used in computing the dynamical parallaxes is taken as a function of both absolute magnitude and spectral type. The two then rest essentially on the same physical assumptions—though this is far from obvious at first sight. If this conclusion is correct, spectroscopic parallaxes are unfitted by their very nature to give us information about the differences in mass between systems which have similar spectra (with regard to the "absolute magnitude lines" as well as other characteristics).

When a direct determination of the dispersion in mass among visual binaries has been made—for example, from the trigonometric parallaxes—it will be possible to obtain a valuable control upon the theory which atttributes the spectroscopic phenomena in question to differences in density.

Mount Wilson Observatory
February 16, 1922

END OF VOL. X

INDEX TO VOLUME X

Nos. 200 to 227

AUTHORS

PAGE

Adams, Walter S., Gustaf Strömberg, and Alfred H. Joy—
  The Relationship of Absolute Magnitude to Space-Velocity . . . 181

Anderson, J. A.—
  The Wave-Length in Astronomical Interferometer Measurements . 297

Babcock, Harold D. *See* St. John, Charles E.

Carter, Edna—
  The Vacuum-Spark Spectra of the Metals 277

Duncan, John C.—
  Bright and Dark Nebulae near ζ Orionis Photographed with the 100-Inch Hooker Telescope 175
  The Spectroscopic Binary Boss 3644 Virginis 217

Hopper, F. L. *See* Merrill, Paul W.

Joy, Alfred H. *See* Adams, Walter S.

Keith, Clyde R. *See* Merrill, Paul W.

King, Arthur S.—
  The Electric Furnace Spectrum of Scandium 199

Merrill, Paul W.—
  Characteristic Behavior of the Bright Lines in Stellar Spectra of Class Md 1
  Observations of the Nebular Lines in the Spectrum of the Long-Period Variable Star R Aquarii 155

Merrill, Paul W., F. L. Hopper, and Clyde R. Keith—
  Identification of Air Lines in Spark Spectra from λ 5927 to λ 8683 161

Michelson, A. A., and Francis G. Pease—
  Measurement of the Diameter of α Orionis with the Interferometer 81

Nicholson, Seth B. *See* St. John, Charles E.

Pease, Francis G. *See* Michelson, A. A.

Richmond, Myrtle L. *See* Shapley, Harlow

PAGE

Russell, Henry Norris—
  Note on Cooling by Expansion in Sun-Spots 261
  On Majorana's Theory of Gravitation 247
  On the Accuracy with which Mean Parallaxes Can Be Determined from Parallactic and Peculiar Motions 241
  On the Calculation of Masses from Spectroscopic Parallaxes . . 441
  The Theory of Ionization and the Sun-Spot Spectrum . . . 341

St. John, Charles E., and Harold D. Babcock—
  An Investigation of the Constancy in Wave-Length of the Atmospheric and Solar Lines 321
  Wave-Lengths of Lines in the Iron Arc from Grating and Interferometer Measures λ 3370–λ 6750 41

St. John, Charles E., and Seth B. Nicholson—
  On Systematic Displacements of Lines in Spectra of Venus . . 163

Sanford, R. F.—
  The Orbits of Seven Spectroscopic Binaries. 17
  The Orbits of the Spectroscopic Binaries 1 Hydrae and 75 Cancri 291

Seares, Frederick H.—
  The Masses and Densities of the Stars 367

Shapley, Harlow, and Myrtle L. Richmond—
  Studies Based on the Colors and Magnitudes in Stellar Clusters. Nineteenth Paper: A Photometric Survey of the Pleiades . 265

Strömberg, Gustaf—
  Systematic Corrections to Spectroscopic and Trigonometric Parallaxes 281

Strömberg, Gustaf. *See also* Adams, Walter S.

van Maanen, Adriaan—
  Investigations on Proper Motion.
    Third Paper: The Proper Motions of Stars in and near the Double Cluster in Perseus 125
    Fourth Paper: Internal Motion in the Spiral Nebula Messier 51 221
    Fifth Paper: The Internal Motion in the Spiral Nebula Messier 81 231
    Sixth Paper: The Motions of 65 Stars in the Neighborhood of α Tauri 333
    The Photographic Determination of Stellar Parallaxes with the 60-Inch Reflector: Fifth Series 93

SUBJECTS

Absolute magnitude, relation to space-velocity, 181
Air lines in spark spectra, 161
Betelgeuse, measurement of diameter with the interferometer, 81
Binaries, spectroscopic, Boss 3644 Virginis, 217
———, orbits of Boss 373, OΣ 82, Lalande 29330, Companion to α Herculis, 205 Draconis, Boss 5591, Lalande 46867; 17
———, orbits of 1 Hydrae and 75 Cancri, 291
Clusters, photometric study of the Pleiades, 265
———, studies based on their colors and magnitudes, 265
Colors and magnitudes in stellar clusters, 265
Densities, of the stars, 367
Electric furnace spectrum, of scandium, 199
Furnace, electric. *See* Electric furnace
Gravitation, Majorana's theory, 247
Interferometer measurements, astronomical, effective wave-lengths, 297
———, of diameter of α Orionis, 81
Ionization and the sun-spot spectrum, 341
Iron arc lines, wave-length from grating and interferometer measures, 41
Magnitude, absolute, relationship to space-velocity, 181
Magnitudes in stellar clusters, 265
Majorana's theory of gravitation, 247
Masses, calculated from spectroscopic parallaxes, 441
———, of the stars, 367
Messier 51, 81, internal motion, 221, 231
Nebulae, bright and dark, near ζ Orionis, 175
———, spiral, internal motion, 221, 231
Parallaxes, mean, accuracy of determination from parallactic and peculiar motions, 241
———, spectroscopic, used to calculate masses, 441
———, spectroscopic and trigonometric, systematic corrections, 281
———, trigonometric, determined with the 60-inch reflector, 93
Pleiades, photometric study, 265
Proper motion, in the spiral nebulae Messier 51, 81; 221, 231
———, of 65 stars in the neighborhood of α Tauri, 333
———, of stars in and near the double cluster in Perseus, 125
Scandium, electric furnace spectrum, 199
Space-velocity, relationship to absolute magnitude, 181
Spark spectra. *See* Spectra

Spectra, of Venus, systematic displacement of lines, 163
———, spark, air lines from λ 5927 to λ 8683; 161
———, stellar, of class Md, behavior of bright lines, 1
———, vacuum-spark, of metals, 277
Spectroscopic binaries. *See* Binaries
Spectroscopic parallaxes, used to calculate masses, 441
Spectrum, electric furnace, of scandium, 199
———, of long-period variable R Aquarii, 155
———, of sun-spots, and theory of ionization, 341
Stars, masses and densities, 367
———, Md, behavior of bright lines in their spectra, 1
Sun-spot spectrum and ionization, 341
Sun-spots, low temperatures due to cooling by expansion, 261
Systematic displacements of lines in spectra of Venus, 163
Vacuum-spark spectra of metals, 277
Variable stars, nebular lines in spectrum of long-period variable, R Aquarii, 155
Velocity, space, relationship to absolute magnitude, 181
Venus, displacements of lines in spectra, 163
Wave-length, in astronomical interferometer measurements, 297
———, of atmospheric and solar lines, constancy, 321
———, of lines in iron arc from grating and interferometer measures, 41

522.19 C28 V10

a39001 006937224b

#201
hecke

BARCO
Contr
3900
Contr
3900

12-1